Supplemental Information-I

Table of Contents

Abbreviations

AM	Amphidinol
BLAST	The basic local alignment search tool
CIP	Cahn–ingold–prelog
2D *J*RES	2D *J*-resolved spectroscopy
DEPT	Distortionless enhancement by polarization transfer
DFT-NMR	Density functional theory-nuclear magnetic resonance
DTX	Dinophysistoxin
ECD	Electronic circular dichroism
H2BC	Heteronuclear two-bond correlation
HETLOC	Sensitivity- and gradient-enhanced hetero (ω1) half-filtered TOCSY
^{1}H–^{1}H COSY	Proton–proton correlation spectroscopy
HMBC	Heteronuclear multiple bond correlation
HPLC	High performance liquid chromatography
HR-ESIMS	High resolution-electrospray ionization-mass spectrometry
HSQC	Heteronuclear single quantum coherence
HSQC-TOCSY	Heteronuclear single quantum coherence-total correlation spectroscopy
INADEQUATE	Incredible natural abundance double quantum transfer experiment
*J*BCA	*J*-based configuration analysis
KmTx	Karlotoxin
LFPs	Ladder-frame polyethers
LR-ESIMS	Low resolution-electrospray ionization-mass spectrometry
Me	Methyl
MTPA	α-Methoxy-α-trifluoromethylphenylacetic acid
NCBI	National center for biotechnology information
NMR	Nuclear magnetic resonance
NOE	Nuclear Overhauser effect
PCA	Principal component analysis
PCR	Polymerase chain reaction
PPCs	Polyol-polyene compounds
SCCCs	Super-carbon-chain compounds
18S rDNA	18S ribosomal DNA
TOCSY	Total correlation spectroscopy
UPLC-MS	Ultra performance liquid chromatography-mass spectrometry

Supplemental Figures

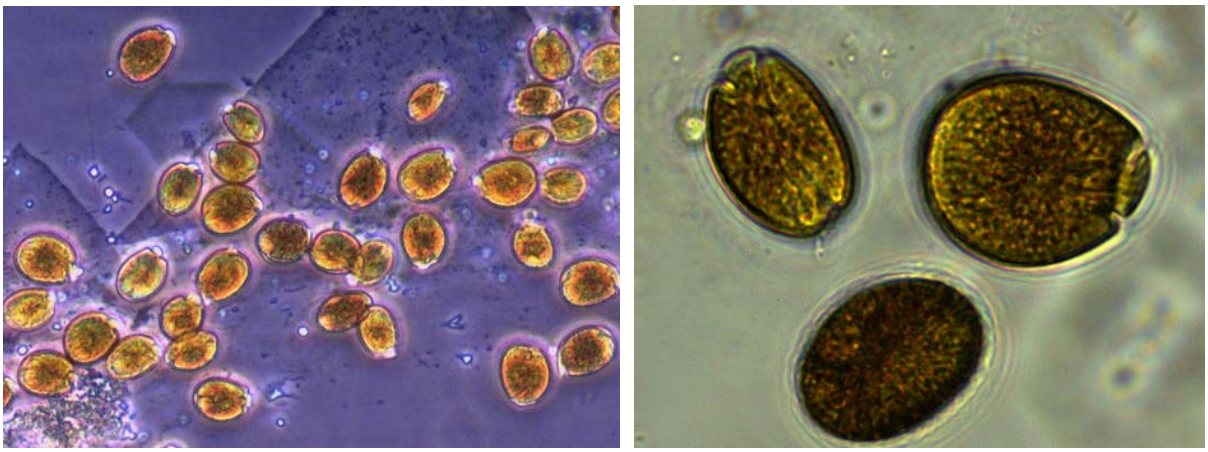

Figure S1. Micrographs of the dinoflagellate strain (MDRC-02)

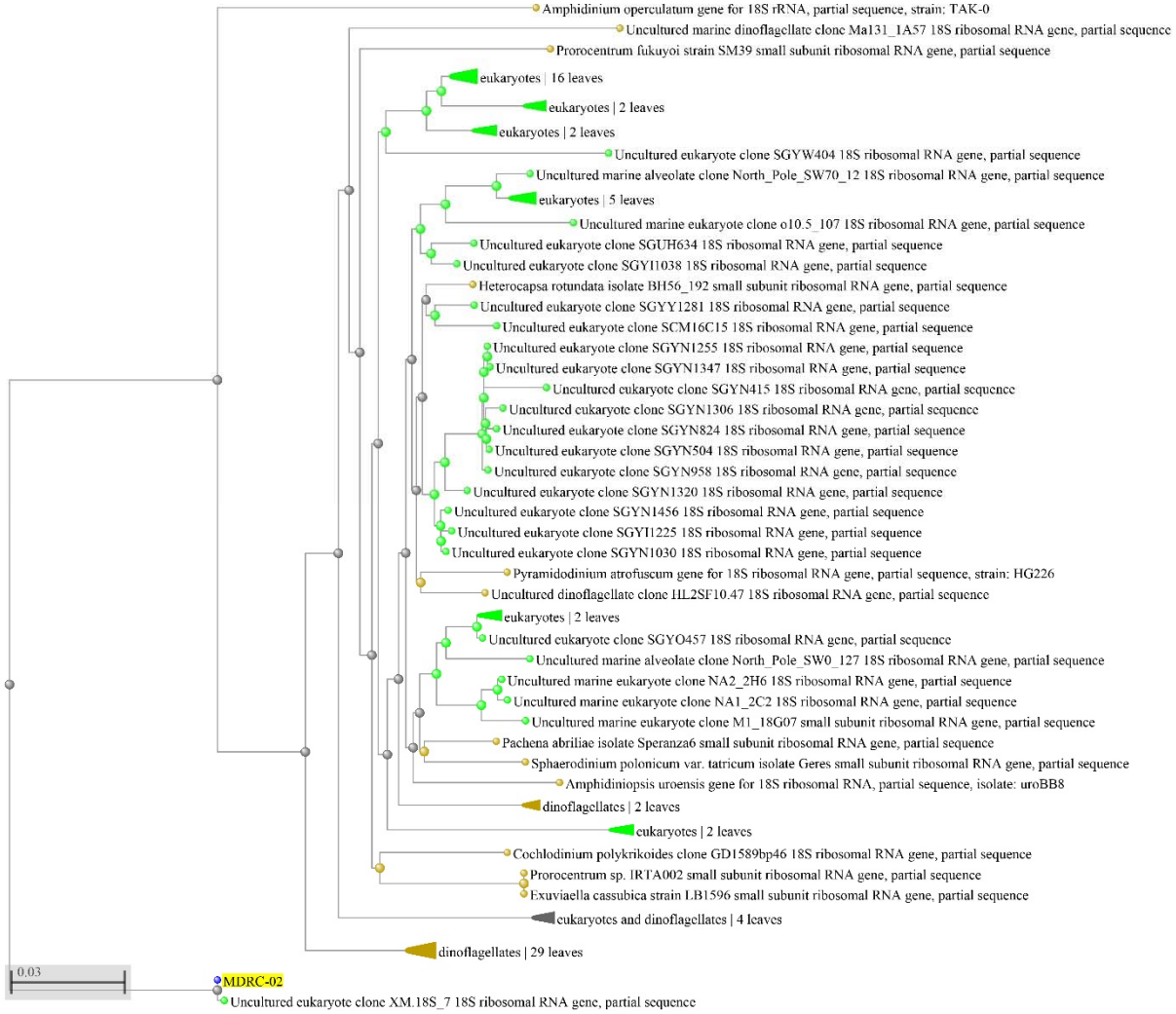

Figure S2. Phylogenetic tree of selected dinoflagellates inferred from the 18S rDNA sequence alignment using the BLAST algorithm.

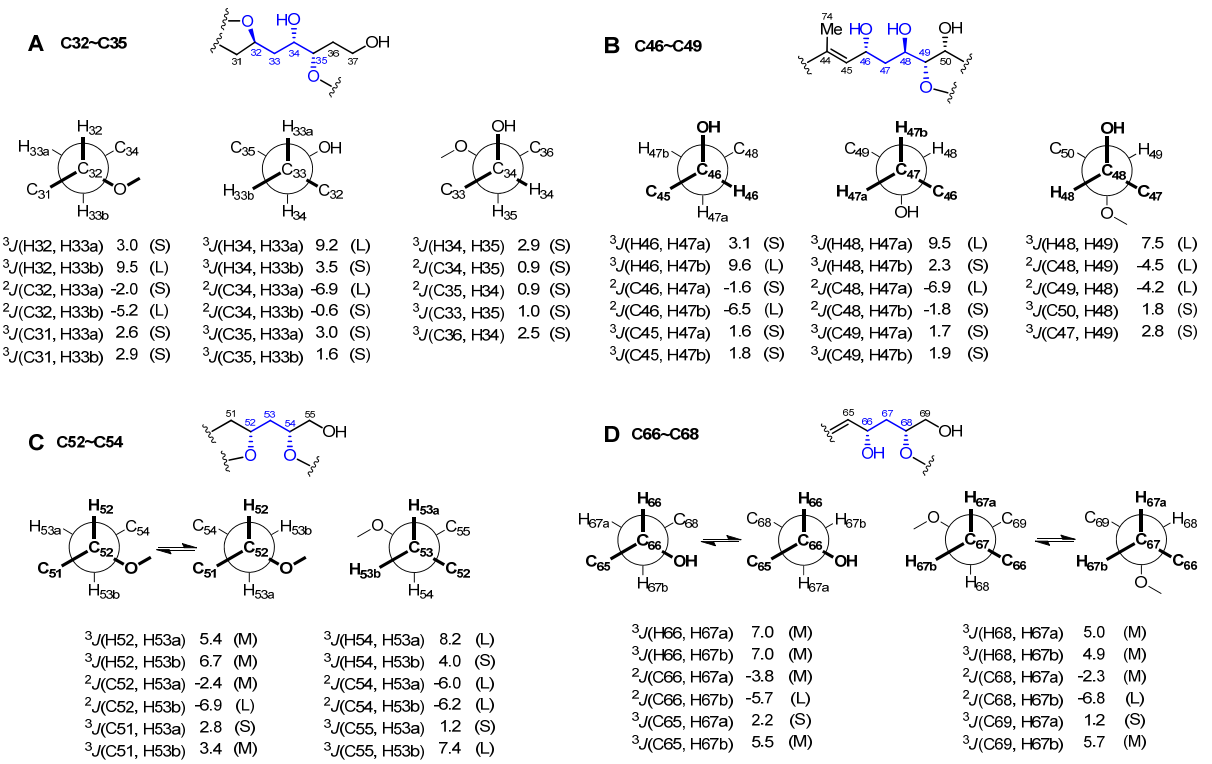

A C32~C35					
^3J(H32, H33a)	3.0	(S)	^3J(H34, H33a)	9.2	(L)
^3J(H32, H33b)	9.5	(L)	^3J(H34, H33b)	3.5	(S)
^2J(C32, H33a)	-2.0	(S)	^2J(C34, H33a)	-6.9	(L)
^2J(C32, H33b)	-5.2	(L)	^2J(C34, H33b)	-0.6	(S)
^3J(C31, H33a)	2.6	(S)	^3J(C35, H33a)	3.0	(S)
^3J(C31, H33b)	2.9	(S)	^3J(C35, H33b)	1.6	(S)

^3J(H34, H35)	2.9	(S)			
^2J(C34, H35)	0.9	(S)			
^2J(C35, H34)	0.9	(S)			
^3J(C33, H35)	1.0	(S)			
^3J(C36, H34)	2.5	(S)			

B C46~C49					
^3J(H46, H47a)	3.1	(S)	^3J(H48, H47a)	9.5	(L)
^3J(H46, H47b)	9.6	(L)	^3J(H48, H47b)	2.3	(S)
^2J(C46, H47a)	-1.6	(S)	^2J(C48, H47a)	-6.9	(L)
^2J(C46, H47b)	-6.5	(L)	^2J(C48, H47b)	-1.8	(S)
^3J(C45, H47a)	1.6	(S)	^3J(C49, H47a)	1.7	(S)
^3J(C45, H47b)	1.8	(S)	^3J(C49, H47b)	1.9	(S)

^3J(H48, H49)	7.5	(L)			
^2J(C48, H49)	-4.5	(L)			
^2J(C49, H48)	-4.2	(L)			
^3J(C50, H48)	1.8	(S)			
^3J(C47, H49)	2.8	(S)			

C C52~C54					
^3J(H52, H53a)	5.4	(M)	^3J(H54, H53a)	8.2	(L)
^3J(H52, H53b)	6.7	(M)	^3J(H54, H53b)	4.0	(S)
^2J(C52, H53a)	-2.4	(M)	^2J(C54, H53a)	-6.0	(L)
^2J(C52, H53b)	-6.9	(L)	^2J(C54, H53b)	-6.2	(L)
^3J(C51, H53a)	2.8	(S)	^3J(C55, H53a)	1.2	(S)
^3J(C51, H53b)	3.4	(M)	^3J(C55, H53b)	7.4	(L)

D C66~C68					
^3J(H66, H67a)	7.0	(M)	^3J(H68, H67a)	5.0	(M)
^3J(H66, H67b)	7.0	(M)	^3J(H68, H67b)	4.9	(M)
^2J(C66, H67a)	-3.8	(M)	^2J(C68, H67a)	-2.3	(M)
^2J(C66, H67b)	-5.7	(L)	^2J(C68, H67b)	-6.8	(L)
^3J(C65, H67a)	2.2	(S)	^3J(C69, H67a)	1.2	(S)
^3J(C65, H67b)	5.5	(M)	^3J(C69, H67b)	5.7	(M)

Figure S3. Rotamers and coupling constants for selected segments in **1A** and **1B**. (A) The C32−C35 segment in **1A**. (B) The C46−C49 segment in **1B**. (C) The C52−C54 segment in **1B**. (D) The C66−C68 segment in **1B**.

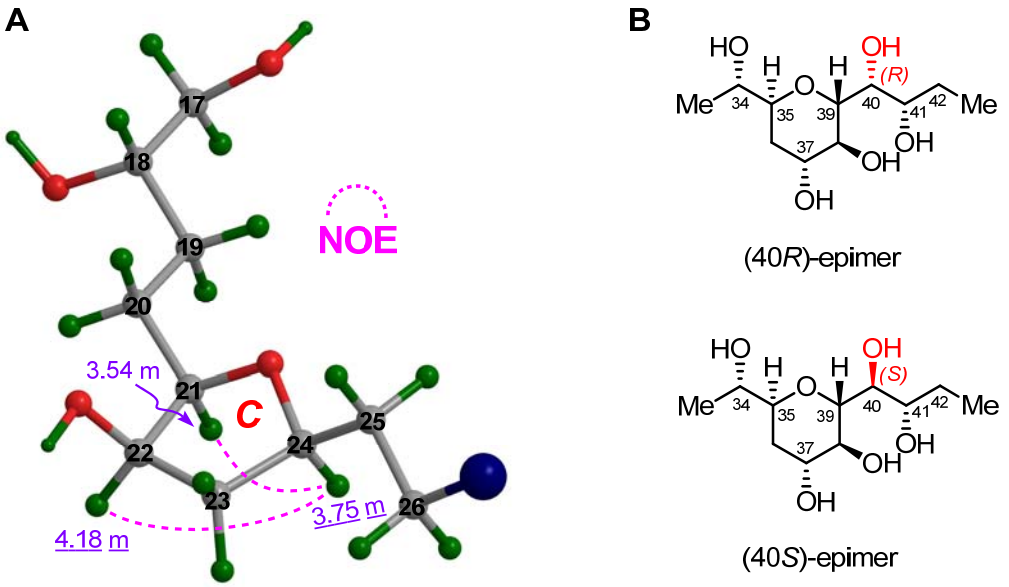

Figure S4. The relative configuration of the ring C in **1b** and model compounds for DFT-NMR calculations

(A) The relative configuration of the ring C in **1b** assigned by diagnostic NOE interactions (The C27 to C44 moiety in **1b**, including Me-74, is omitted for clarity).

(B) The absolute configurations of model compounds, viz., (34*S*,35*S*,37*R*,38*S*,39*R*,40*R*,41*S*)-**1b′** and (34*S*,35*S*,37*R*,38*S*,39*R*,40*S*,41*S*)-**1b′**, representing the C34–C41 region of **1b** for the DFT-NMR ^{13}C chemical-shift calculations.

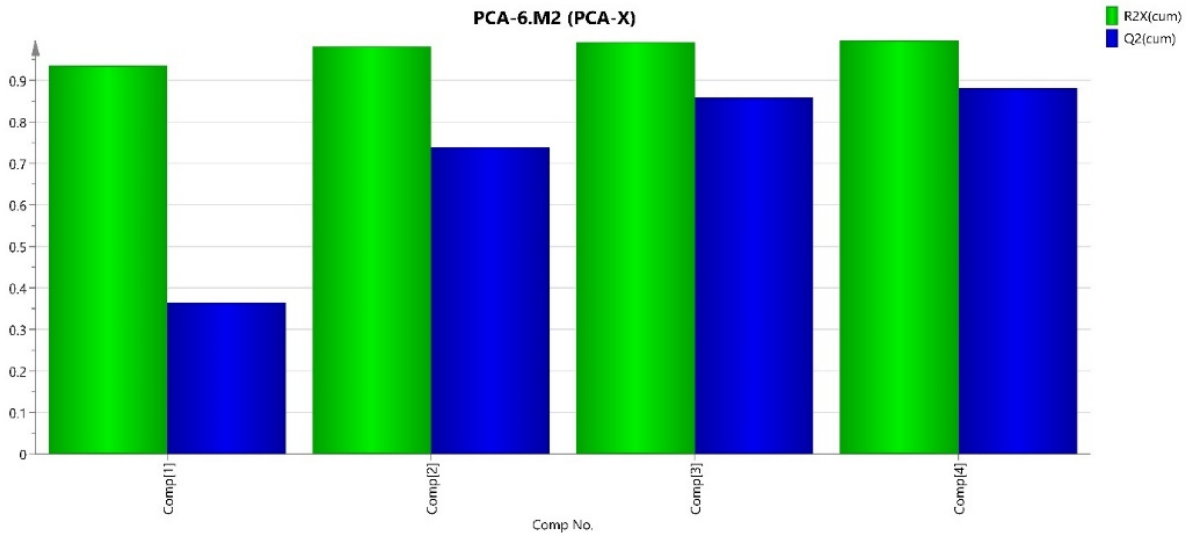

Figure S5. The summary of fit report for PCA

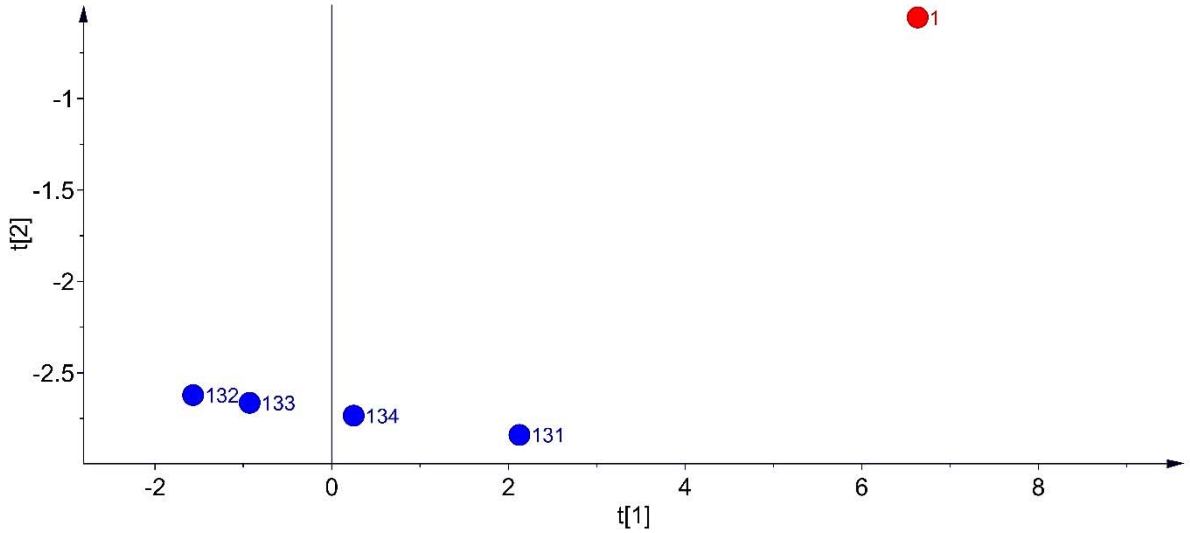

Figure S6. Partial enlarged view of PCA score plot.

The number **1** (the red dot) is benthol A, whereas **131**–**134** are DTX-4, DTX-5a, DTX-5b, and DTX-5c, respectively.

Supplemental Tables

Table S1. The criteria of $^{3}J_{H,H}$ and $^{2,3}J_{C,H}$ values (Hz) for anti and gauche orientations in acyclic systems.

	$^{3}J_{H,H}$*		$^{2}J_{C,H}$*		$^{3}J_{C,H}$*	
	anti	gauche	gauche[a]	anti[b]	anti	gauche
oxygenation	large	small	large	small	large	small
none	9 to 12	2 to 4	——	——	6 to 8	1 to 3
mono	8 to 11	1 to 4	– 5 to – 7	0 to – 2	6 to 8	1 to 3
di	7 to 10	0 to 3	– 4 to – 6	2 to 0	5 to 7	1 to 3

*Our manuscript refers to the criteria proposed in the reference as follows.

Matsumori, N., Kaneno, D., Murata, M., Nakamura, H., Tachibana, K. (1999). Stereochemical determination of acyclic structures based on carbon-proton spin-coupling constants. A method of configuration analysis for natural products. J. Org. Chem. *64*, 866–876.

Table S2. Cartesian coordinates and energies of the low-energy conformers calculated at the B3LYP/6-31+G(d,p) level.

(34*S*,35*S*,37*R*,38*S*,39*R*,40*R*,41*S*)-**1b′**, Conf A

C	-4.350076	-1.222276	-0.722706
C	5.093765	-0.787205	-0.899366
C	3.846664	-1.220818	-0.122989
C	-2.832064	-1.275051	-0.595157
O	-2.462794	-2.653280	-0.507524
C	-2.302400	-0.534833	0.649765
C	-2.530325	0.979738	0.691597
C	-1.586054	1.722708	-0.246251
C	-0.133296	1.347715	0.047504
C	0.047422	-0.180663	-0.038573
O	-0.896421	-0.843152	0.831907
C	1.398572	-0.761367	0.427542
O	-1.789853	3.119318	-0.071475
O	0.654935	2.041189	-0.912110
C	2.655135	-0.273413	-0.316157
O	1.621994	-0.492298	1.812551
O	2.989815	1.064521	0.099247
H	-2.775171	-1.002181	1.520773
H	-0.109091	-0.489394	-1.083543
H	-4.702094	-0.211935	-0.950072
H	-4.664612	-1.883681	-1.534702
H	-4.829182	-1.567771	0.199888
H	5.421870	0.210099	-0.593433
H	5.919255	-1.485621	-0.728345
H	4.898918	-0.758881	-1.978103
H	4.068763	-1.294070	0.949023
H	3.538816	-2.223987	-0.446745
H	-2.385942	-0.840198	-1.503617
H	-1.581211	-2.688470	-0.106902
H	-3.568289	1.222268	0.445613
H	-2.352928	1.339065	1.711816
H	-1.793207	1.452217	-1.294445
H	0.108748	1.684495	1.066080
H	1.321087	-1.848469	0.274270
H	-1.082399	3.566164	-0.560804
H	1.588190	1.987474	-0.624779
H	2.427190	-0.193280	-1.385178
H	0.799152	-0.697944	2.280927
H	2.966669	1.066509	1.070272

B3LYP Energy = -883.820678514 a.u.

(34*S*,35*S*,37*R*,38*S*,39*R*,40*R*,41*S*)-**1b′**, Conf B

C	-4.147052	-1.551302	-0.581083
C	4.077497	-2.074343	-0.778038
C	4.048168	-0.677573	-0.144189
C	-2.629016	-1.457776	-0.480449
O	-2.132713	-2.789723	-0.327089
C	-2.150439	-0.606558	0.712839
C	-2.525998	0.878254	0.689635
C	-1.681927	1.661834	-0.308013
C	-0.192839	1.447258	-0.035421
C	0.139696	-0.057826	-0.049546
O	-0.717093	-0.767040	0.873439
C	1.550263	-0.475393	0.417150
O	-2.020088	3.038658	-0.196251
O	0.499740	2.163707	-1.050220
C	2.741038	0.097163	-0.371845
O	1.766234	-0.113534	1.782717
O	2.931123	1.485272	-0.038128
H	-2.556469	-1.073974	1.616864
H	-0.001781	-0.434022	-1.074231
H	-4.580135	-1.880170	0.369905
H	-4.592810	-0.593354	-0.863295
H	-4.410335	-2.288130	-1.344934
H	3.878645	-2.028194	-1.855453
H	5.062228	-2.533057	-0.644474
H	3.342807	-2.752045	-0.330219
H	4.849528	-0.065598	-0.572742
H	4.239714	-0.746227	0.933678
H	-2.237926	-1.034736	-1.419168
H	-1.242458	-2.721714	0.049404
H	-3.588580	1.005965	0.462683
H	-2.361216	1.303505	1.686385
H	-1.883277	1.318687	-1.335907

H	0.037997	1.858481	0.958061
H	1.575032	-1.570493	0.322199
H	-1.370523	3.527359	-0.724310
H	1.439440	2.218269	-0.784404
H	2.498947	0.086824	-1.440487
H	0.976998	-0.380288	2.277229
H	2.930201	1.541754	0.931236

B3LYP Energy = -883.819920345 a.u.

(34*S*,35*S*,37*R*,38*S*,39*R*,40*R*,41*S*)-**1b′**, Conf C

C	-4.311329	-1.337375	-0.516103
C	4.628475	-1.295671	0.420755
C	3.864372	-0.959687	-0.865770
C	-2.787131	-1.324623	-0.524460
O	-2.353480	-2.686663	-0.547208
C	-2.179602	-0.626465	0.709072
C	-2.468289	0.870508	0.857491
C	-1.644816	1.709287	-0.112787
C	-0.157593	1.386805	0.030154
C	0.077701	-0.124555	-0.166626
O	-0.749926	-0.876585	0.747568
C	1.494199	-0.655674	0.137016
O	-1.890750	3.082128	0.164998
O	0.514735	2.175206	-0.944562
C	2.629026	-0.055697	-0.718753
O	1.832167	-0.433359	1.506868
O	2.988021	1.246069	-0.221141
H	-2.549845	-1.161803	1.590367
H	-0.164252	-0.383828	-1.208681
H	-4.690344	-1.755280	0.422913
H	-4.725256	-0.334136	-0.652400
H	-4.668876	-1.967745	-1.334948
H	4.009793	-1.844284	1.135914
H	5.504722	-1.908565	0.185298
H	4.989307	-0.389157	0.918078
H	3.540310	-1.886155	-1.359516
H	4.539459	-0.455599	-1.567713
H	-2.442326	-0.822763	-1.442433
H	-1.438139	-2.700854	-0.229546
H	-3.533649	1.075322	0.716565
H	-2.217625	1.183344	1.877653
H	-1.934794	1.489827	-1.153379
H	0.159465	1.671164	1.044054
H	1.457413	-1.737886	-0.060820
H	-1.247790	3.589573	-0.353405
H	1.470064	2.158723	-0.736615
H	2.232499	0.123127	-1.724023
H	1.061209	-0.688647	2.035874
H	3.052449	1.170137	0.744653

B3LYP Energy = -883.817998807 a.u.

(34*S*,35*S*,37*R*,38*S*,39*R*,40*R*,41*S*)-**1b′**, Conf D

C	2.558197	3.092299	-0.493741
C	-4.835842	0.727338	0.600951
C	-3.845151	-0.420218	0.378072
C	1.437046	2.055566	-0.478048
O	0.215810	2.777132	-0.525521
C	1.490591	1.164818	0.789473
C	2.680193	0.186470	0.881609
C	2.501093	-1.038738	-0.026302
C	1.128324	-1.669820	0.189338
C	0.046591	-0.599304	0.001194
O	0.265208	0.431986	0.959561
C	-1.394717	-1.111271	0.171147
O	3.456403	-2.073701	0.251494
O	0.896618	-2.730577	-0.742669
C	-2.392351	0.053833	0.264178
O	-1.763787	-1.898821	-0.961470
O	-2.207694	0.951186	-0.847279
H	1.508189	1.840054	1.651261
H	0.118909	-0.206784	-1.022074
H	3.547490	2.627741	-0.547910
H	2.436664	3.741447	-1.364960
H	2.511023	3.718959	0.403617
H	-4.788543	1.452615	-0.216678
H	-5.862038	0.350040	0.662838
H	-4.619901	1.263295	1.532935
H	-4.107811	-0.985326	-0.524084
H	-3.904940	-1.132220	1.212428
H	1.534510	1.429440	-1.380410
H	-0.540146	2.162584	-0.562413
H	3.622042	0.695940	0.646894
H	2.756770	-0.170677	1.914845
H	2.575197	-0.754784	-1.086301
H	1.074001	-2.056936	1.217841
H	-1.469340	-1.705846	1.095724
H	4.334840	-1.790043	-0.032802
H	1.646710	-3.340471	-0.688981
H	-2.129959	0.649316	1.142419
H	-1.047075	-2.531059	-1.134936
H	-2.340893	0.439233	-1.659420

B3LYP Energy = -883.817582424 a.u.

(34*S*,35*S*,37*R*,38*S*,39*R*,40*R*,41*S*)-**1b′**, Conf E

C	-2.755156	-2.888590	-0.218138
C	5.004710	-0.709711	-0.891459
C	3.764007	-1.170679	-0.120712
C	-3.023642	-1.391374	-0.367544
O	-2.571335	-0.905596	-1.639651
C	-2.368402	-0.557943	0.749334
C	-2.647411	0.953324	0.690887
C	-1.695518	1.705064	-0.233041
C	-0.242450	1.355304	0.087624
C	-0.042167	-0.170151	0.002987
O	-0.965328	-0.831179	0.899368
C	1.317253	-0.736954	0.457902
O	-1.923919	3.101806	-0.049517
O	0.550685	2.065858	-0.857885
C	2.565167	-0.226766	-0.284921
O	1.545170	-0.479813	1.846899
O	2.896693	1.102830	0.159609
H	-2.802679	-0.945573	1.678717
H	-0.224216	-0.490174	-1.030597
H	-3.129404	-3.258380	0.742880
H	-3.263877	-3.450856	-1.010039
H	-1.683267	-3.094741	-0.274144
H	5.836454	-1.405999	-0.742320

H	4.804113	-0.655049	-1.968246
H	5.326441	0.282170	-0.561938
H	3.991865	-1.268884	0.948164
H	3.461027	-2.167625	-0.467928
H	-4.107667	-1.209670	-0.277535
H	-2.992074	-1.420171	-2.340560
H	-3.682957	1.133500	0.382440
H	-2.533588	1.371933	1.697866
H	-1.884904	1.430505	-1.278103
H	-0.020848	1.695930	1.110264
H	1.251212	-1.823484	0.297473
H	-1.223682	3.558948	-0.539058
H	1.480331	2.020460	-0.559972
H	2.328884	-0.124691	-1.350263
H	0.711357	-0.664699	2.305119
H	2.843396	1.086161	1.129673

B3LYP Energy = -883.817271483 a.u.

(34*S*,35*S*,37*R*,38*S*,39*R*,40*R*,41*S*)-**1b′**, Conf F

C	2.506896	3.144354	-0.452441
C	-4.825222	0.772136	0.574286
C	-3.834226	-0.388713	0.441292
C	1.467118	2.024271	-0.477595
O	0.146222	2.560457	-0.673604
C	1.522057	1.147388	0.804023
C	2.712874	0.173664	0.874180
C	2.515764	-1.040112	-0.036893
C	1.140170	-1.678577	0.173923
C	0.058981	-0.594599	0.033356
O	0.299307	0.430615	0.999663
C	-1.382044	-1.087159	0.243107
O	3.564850	-1.964286	0.232178
O	1.022940	-2.719386	-0.792159
C	-2.392482	0.076562	0.233067
O	-1.689459	-2.046236	-0.782484
O	-2.314986	0.755334	-1.029846
H	1.565498	1.827283	1.664864
H	0.113342	-0.185774	-0.986380
H	3.525452	2.746995	-0.404138
H	2.419656	3.753066	-1.356320
H	2.358944	3.796011	0.418128
H	-4.812513	1.399021	-0.321752
H	-5.845261	0.399969	0.716355
H	-4.579862	1.406682	1.434809
H	-4.124758	-1.036496	-0.393577
H	-3.864589	-1.012761	1.344044
H	1.630951	1.410318	-1.367946
H	-0.083559	3.114179	0.086541
H	3.654965	0.671754	0.623041
H	2.806272	-0.185244	1.904925
H	2.565626	-0.735403	-1.094965
H	1.093838	-2.094939	1.193269
H	-1.455359	-1.625926	1.194988
H	3.374154	-2.768084	-0.273741
H	0.075792	-2.899756	-0.926553
H	-2.113634	0.761969	1.042615
H	-1.918450	-1.536597	-1.577462
H	-1.556809	1.366446	-1.012537

B3LYP Energy = -883.817211876 a.u.

(34*S*,35*S*,37*R*,38*S*,39*R*,40*R*,41*S*)-**1b′**, Conf G

C	2.546451	3.093115	-0.501625
C	-4.837446	0.720088	0.601543
C	-3.845627	-0.426378	0.378075
C	1.425676	2.056197	-0.478529
O	0.203097	2.775978	-0.513587
C	1.489737	1.164140	0.787740
C	2.687480	0.193759	0.867197
C	2.505719	-1.032148	-0.035870
C	1.132328	-1.669907	0.186676
C	0.046577	-0.602328	0.003583
O	0.268965	0.424715	0.966214
C	-1.394239	-1.115151	0.172324
O	3.541962	-2.009857	0.129721
O	0.905617	-2.733945	-0.739815
C	-2.393088	0.048926	0.266413
O	-1.761958	-1.901400	-0.961585
O	-2.207961	0.948149	-0.843333
H	1.510114	1.839004	1.649594
H	0.118778	-0.206746	-1.018325
H	2.507919	3.717343	0.397889
H	3.534933	2.628925	-0.568232
H	2.415300	3.744614	-1.369617
H	-4.623028	1.254804	1.534571
H	-4.789851	1.446576	-0.214966
H	-5.863357	0.341795	0.661629
H	-4.106889	-0.990307	-0.525222
H	-3.905841	-1.139710	1.211260
H	1.516666	1.431529	-1.382271
H	-0.552078	2.161160	-0.559693
H	3.627072	0.697828	0.621212
H	2.769166	-0.149552	1.908181
H	2.576058	-0.747759	-1.091909
H	1.072891	-2.055448	1.218343
H	-1.469233	-1.711173	1.096098
H	3.691350	-2.152721	1.075541
H	1.708903	-3.274739	-0.776229
H	-2.131890	0.643274	1.145861
H	-1.042888	-2.528406	-1.143069
H	-2.343275	0.438703	-1.656727

B3LYP Energy = -883.817154641 a.u.

(34*S*,35*S*,37*R*,38*S*,39*R*,40*R*,41*S*)-**1b′**, Conf H

C	-3.188661	-2.603541	-0.273570
C	4.466116	0.192112	1.263973
C	3.874598	-0.584821	0.080519
C	-1.866891	-1.843874	-0.361557
O	-0.839410	-2.820948	-0.423226
C	-1.653028	-0.910113	0.857018
C	-2.594304	0.309334	0.949120
C	-2.203971	1.422935	-0.031945
C	-0.717548	1.746908	0.089921
C	0.096006	0.459374	-0.088306
O	-0.289814	-0.458944	0.930848
C	1.620384	0.652480	-0.000647
O	-2.895375	2.653938	0.229478
O	-0.312762	2.692264	-0.905041

C	2.345469	-0.699057	0.103474
O	2.097338	1.304010	-1.178376
O	1.887778	-1.586552	-0.934670
H	-1.768523	-1.527040	1.754267
H	-0.110979	0.050644	-1.086435
H	-4.052090	-1.932013	-0.305429
H	-3.262626	-3.296729	-1.115693
H	-3.230790	-3.189571	0.651024
H	4.133950	-0.223305	2.223087
H	5.559674	0.143567	1.245058
H	4.186281	1.250240	1.238321
H	4.266400	-1.608562	0.077122
H	4.183848	-0.115710	-0.860888
H	-1.871890	-1.250449	-1.290811
H	0.030225	-2.391138	-0.522684
H	-3.635868	0.009462	0.785355
H	-2.533305	0.719584	1.963465
H	-2.395802	1.115684	-1.070388
H	-0.526396	2.155196	1.093705
H	1.858887	1.249136	0.893118
H	-3.829241	2.556744	0.002812
H	-0.910341	3.452137	-0.850268
H	2.026125	-1.176681	1.033009
H	1.524461	2.069171	-1.351125
H	2.106952	-1.180927	-1.786735

B3LYP Energy = -883.816990901 a.u.

(34*S*,35*S*,37*R*,38*S*,39*R*,40*S*,41*S*)-**1b′**, Conf A

C	-4.223351	-1.310376	-0.803822
C	5.161877	-0.582279	-0.676426
C	3.926360	-0.940391	0.160792
C	-2.709258	-1.275850	-0.629590
O	-2.266927	-2.634811	-0.610956
C	-2.271987	-0.572642	0.673114
C	-2.601819	0.919705	0.778391
C	-1.695155	1.751519	-0.118840
C	-0.219621	1.464482	0.170063
C	0.073381	-0.047213	0.083224
O	-0.858598	-0.778663	0.907740
C	1.449536	-0.515708	0.627835
O	-1.986423	3.127401	0.098533
O	0.506687	2.221188	-0.790368
C	2.679580	-0.135090	-0.218461
O	1.441459	-1.939096	0.708462
O	2.899708	1.278618	0.000495
H	-2.742555	-1.116160	1.499501
H	-0.016378	-0.366940	-0.966560
H	-4.632585	-0.311843	-0.980338
H	-4.705825	-1.740901	0.080490
H	-4.471118	-1.938339	-1.663955
H	6.001950	-1.232514	-0.413986
H	4.969893	-0.707968	-1.748823
H	5.507253	0.446730	-0.510853
H	4.133283	-0.787170	1.227366
H	3.690803	-1.999516	0.032365
H	-2.265823	-0.764654	-1.497834
H	-1.334798	-2.640374	-0.350722
H	-3.649654	1.108630	0.527532
H	-2.456739	1.243008	1.815426
H	-1.874279	1.505545	-1.177759
H	0.004091	1.813059	1.190714
H	1.586265	-0.082669	1.631567
H	-1.311124	3.633130	-0.378379
H	1.456299	2.142505	-0.574295
H	2.451775	-0.298341	-1.282832
H	0.623949	-2.171548	1.174080
H	3.730807	1.532275	-0.421631

B3LYP Energy = -883.815052527 a.u.

(34*S*,35*S*,37*R*,38*S*,39*R*,40*S*,41*S*)-**1b′**, Conf B

C	4.232896	-1.279443	0.799220
C	-5.139940	-0.587319	0.740104
C	-3.936054	-0.933954	-0.143534
C	2.718674	-1.266447	0.623235
O	2.297394	-2.632008	0.597704
C	2.272631	-0.564105	-0.676774
C	2.588431	0.931411	-0.778976
C	1.679366	1.751375	0.126398
C	0.203882	1.455096	-0.155885
C	-0.077491	-0.060087	-0.083386
O	0.860362	-0.781371	-0.910024
C	-1.448353	-0.534608	-0.632569
O	1.957807	3.130582	-0.085379
O	-0.519301	2.198894	0.815991
C	-2.682671	-0.125610	0.201345
O	-1.441821	-1.957484	-0.703340
O	-2.933368	1.289647	0.043823
H	2.746612	-1.101424	-1.505222
H	0.010178	-0.386109	0.964536
H	4.627197	-0.275952	0.981469
H	4.722795	-1.698259	-0.086627
H	4.488673	-1.908097	1.656445
H	-6.012163	-1.181852	0.450303
H	-4.926427	-0.802207	1.793514
H	-5.411213	0.470146	0.667341
H	-4.180256	-0.769122	-1.204584
H	-3.692105	-1.995323	-0.053866
H	2.266539	-0.766013	1.493200
H	1.362712	-2.650962	0.348082
H	3.635719	1.129129	-0.532920
H	2.435272	1.256689	-1.814305
H	1.865229	1.501317	1.183074
H	-0.024945	1.812189	-1.173100
H	-1.566341	-0.114862	-1.647698
H	1.289338	3.627962	0.409691
H	-1.470024	2.143062	0.599425
H	-2.456957	-0.242443	1.267294
H	-0.618441	-2.197121	-1.155326
H	-3.328194	1.445316	-0.825991

B3LYP Energy = -883.815009485 a.u.

(34*S*,35*S*,37*R*,38*S*,39*R*,40*S*,41*S*)-**1b′**, Conf C

C	-4.233332	-1.336298	-0.539672
C	4.601164	-0.802488	0.874271
C	3.968180	-0.841124	-0.521315

C	-2.710076	-1.276543	-0.534057
O	-2.245647	-2.624509	-0.631298
C	-2.141630	-0.625878	0.745225
C	-2.480940	0.852588	0.959088
C	-1.693553	1.745038	0.008893
C	-0.190979	1.474941	0.116678
C	0.114605	-0.024576	-0.073926
O	-0.707437	-0.813152	0.812375
C	1.550888	-0.483751	0.292022
O	-1.979189	3.102342	0.327956
O	0.412566	2.289470	-0.880682
C	2.665835	-0.043627	-0.675584
O	1.581366	-1.909362	0.305888
O	2.900658	1.362635	-0.419464
H	-2.508677	-1.216990	1.591181
H	-0.084883	-0.299155	-1.121547
H	-4.676933	-0.339455	-0.613339
H	-4.604520	-1.824355	0.368132
H	-4.566576	-1.923276	-1.399874
H	5.568712	-1.314597	0.865006
H	4.768002	0.224132	1.215807
H	3.966176	-1.308824	1.606718
H	3.763968	-1.875426	-0.812712
H	4.677293	-0.445294	-1.264349
H	-2.374950	-0.715736	-1.420124
H	-1.290768	-2.620789	-0.473939
H	-3.553071	1.031810	0.836040
H	-2.226289	1.130277	1.988235
H	-1.988078	1.547858	-1.034306
H	0.139048	1.781567	1.121829
H	1.788087	-0.091390	1.292638
H	-1.372244	3.645659	-0.197004
H	1.381527	2.222201	-0.774777
H	2.305532	-0.159594	-1.707770
H	0.821309	-2.184242	0.840657
H	3.667836	1.646533	-0.934434

B3LYP Energy = -883.814365135 a.u.

(34*S*,35*S*,37*R*,38*S*,39*R*,40*S*,41*S*)-**1b′**, Conf D

C	2.320779	3.206586	-0.241737
C	-4.265089	1.102213	-0.813492
C	-2.901499	0.418563	-0.963546
C	1.157364	2.222770	-0.297122
O	-0.035953	2.992232	-0.124485
C	1.225822	1.138188	0.797191
C	2.479256	0.255496	0.796715
C	2.454177	-0.789385	-0.315092
C	1.172886	-1.604542	-0.190105
C	-0.059542	-0.686118	-0.261464
O	0.019952	0.323823	0.769211
C	-1.371724	-1.483605	-0.097000
O	3.605421	-1.612736	-0.176224
O	1.163724	-2.564863	-1.252802
C	-2.641896	-0.635300	0.119047
O	-1.272610	-2.450789	0.946572
O	-2.635060	-0.092693	1.446812
H	1.153220	1.660731	1.757298
H	-0.080768	-0.205298	-1.250802
H	2.116389	4.037612	-0.922206
H	3.261124	2.739133	-0.546048
H	2.436922	3.616404	0.767540
H	-4.353158	1.589787	0.161551
H	-4.410927	1.859229	-1.590512
H	-5.079822	0.373744	-0.896899
H	-2.106401	1.174130	-0.950924
H	-2.838227	-0.072504	-1.944555
H	1.140534	1.749530	-1.291440
H	-0.761426	2.377881	0.053898
H	3.380882	0.868734	0.715746
H	2.540874	-0.274257	1.754040
H	2.466820	-0.305510	-1.305616
H	1.175248	-2.115105	0.778722
H	-1.497314	-2.050303	-1.027224
H	3.498913	-2.353423	-0.791410
H	0.663782	-3.339428	-0.963668
H	-3.483437	-1.339058	0.120197
H	-1.604457	-2.026739	1.754653
H	-1.805777	0.405730	1.544610

B3LYP Energy = -883.813632620 a.u.

(34*S*,35*S*,37*R*,38*S*,39*R*,40*S*,41*S*)-**1b′**, Conf E

C	2.285085	3.134118	-0.595630
C	-4.326152	0.384198	-1.429219
C	-2.988737	-0.311143	-1.148304
C	1.192601	2.088693	-0.390484
O	0.010752	2.790900	-0.032646
C	1.556090	1.070629	0.716170
C	2.715843	0.103986	0.414822
C	2.305056	-1.021240	-0.543802
C	1.025477	-1.710100	-0.068203
C	-0.066125	-0.652845	0.135222
O	0.392192	0.311634	1.091875
C	-1.398790	-1.197273	0.681585
O	3.300194	-2.051734	-0.627509
O	0.556812	-2.643283	-1.034341
C	-2.613707	-0.310950	0.333876
O	-1.319743	-1.378086	2.098074
O	-2.407877	1.058771	0.727869
H	1.787293	1.650057	1.616445
H	-0.258031	-0.177003	-0.834738
H	2.502107	3.651903	0.344980
H	1.940081	3.878118	-1.318584
H	3.209615	2.689828	-0.976777
H	-4.557658	0.364165	-2.499217
H	-5.147553	-0.113379	-0.900260
H	-4.299088	1.427988	-1.104712
H	-2.195574	0.179522	-1.726177
H	-3.029076	-1.352351	-1.492012
H	1.035319	1.559960	-1.345480
H	-0.700101	2.159753	0.186062
H	3.577462	0.649235	0.012179
H	3.039113	-0.357023	1.355059
H	2.111634	-0.624256	-1.551412
H	1.226500	-2.213885	0.889171
H	-1.570946	-2.185703	0.242212
H	4.069432	-1.722247	-1.109774
H	1.291104	-3.240337	-1.237358
H	-3.456401	-0.720484	0.910832

H	-0.649953	-0.758010	2.427558
H	-2.303746	1.080100	1.689233

B3LYP Energy = -883.813101937 a.u.

(34*S*,35*S*,37*R*,38*S*,39*R*,40*S*,41*S*)-**1b′**, Conf F

C	2.280693	3.131853	-0.601003
C	-4.329710	0.379726	-1.424110
C	-2.991999	-0.315233	-1.143847
C	1.187936	2.088091	-0.389865
O	0.008897	2.790198	-0.022770
C	1.556929	1.069072	0.714113
C	2.719339	0.108105	0.402259
C	2.305962	-1.016098	-0.553702
C	1.025608	-1.708997	-0.073726
C	-0.066946	-0.653704	0.135989
O	0.396728	0.306230	1.094936
C	-1.399063	-1.198733	0.683243
O	3.349366	-1.976841	-0.761810
O	0.560054	-2.644756	-1.036859
C	-2.614494	-0.312140	0.337802
O	-1.315667	-1.384193	2.098948
O	-2.406581	1.058468	0.728057
H	1.791056	1.648154	1.613714
H	-0.258959	-0.175386	-0.832563
H	2.505955	3.647620	0.338839
H	1.930621	3.877735	-1.319502
H	3.200707	2.686615	-0.991265
H	-4.562404	0.357838	-2.493771
H	-5.150543	-0.116923	-0.893397
H	-4.302159	1.424120	-1.101623
H	-2.199614	0.174010	-1.723959
H	-3.033025	-1.357070	-1.485455
H	1.024550	1.560453	-1.344203
H	-0.704086	2.159553	0.190039
H	3.578754	0.646340	-0.009083
H	3.045730	-0.341298	1.350652
H	2.113033	-0.616713	-1.556020
H	1.220708	-2.212576	0.888329
H	-1.572533	-2.186477	0.242831
H	3.692636	-2.259172	0.098404
H	1.324791	-3.158027	-1.336959
H	-3.456164	-0.719865	0.917351
H	-0.660246	-0.749815	2.430145
H	-2.316695	1.086377	1.690552

B3LYP Energy = -883.812865704 a.u.

(34*S*,35*S*,37*R*,38*S*,39*R*,40*S*,41*S*)-**1b′**, Conf G

C	-2.882808	2.722403	0.384237
C	3.377341	0.659157	1.986388
C	2.856805	1.149170	0.627717
C	-1.536525	2.008226	0.329579
O	-0.551027	3.016315	0.088561
C	-1.458550	0.942856	-0.782188
C	-2.488987	-0.189678	-0.707763
C	-2.153957	-1.210467	0.376324
C	-0.740645	-1.729258	0.141651
C	0.266826	-0.565955	0.136183
O	-0.108771	0.405140	-0.865542
C	1.703172	-1.060102	-0.139894
O	-3.108754	-2.262121	0.305052
O	-0.443259	-2.664488	1.185326
C	2.738194	0.046691	-0.432646
O	1.738319	-2.020028	-1.194534
O	2.506932	0.574955	-1.745903
H	-1.575183	1.475041	-1.732521
H	0.259816	-0.093479	1.129970
H	-2.805049	3.574397	1.064959
H	-3.676158	2.064766	0.749434
H	-3.162519	3.103354	-0.604059
H	4.337427	0.141434	1.877491
H	3.531541	1.503240	2.665573
H	2.680398	-0.030145	2.475159
H	3.542327	1.900653	0.220304
H	1.892479	1.653653	0.765883
H	-1.343999	1.541398	1.308246
H	0.273179	2.575559	-0.160709
H	-3.492410	0.213520	-0.546189
H	-2.508746	-0.715069	-1.669199
H	-2.194150	-0.746083	1.375374
H	-0.706821	-2.228910	-0.832254
H	2.014716	-1.595016	0.763903
H	-2.801009	-2.964255	0.897237
H	0.184394	-3.315950	0.846040
H	3.710114	-0.455713	-0.510878
H	1.899857	-1.527663	-2.015838
H	1.587088	0.888832	-1.769132

B3LYP Energy = -883.812812136 a.u.

(34*S*,35*S*,37*R*,38*S*,39*R*,40*S*,41*S*)-**1b′**, Conf H

C	2.494106	-2.918161	0.327606
C	-5.049465	-0.469108	0.720091
C	-3.850398	-0.866682	-0.148291
C	2.894110	-1.444950	0.409268
O	2.467303	-0.859872	1.647257
C	2.345269	-0.610086	-0.763133
C	2.723709	0.879063	-0.746420
C	1.799806	1.714915	0.130514
C	0.328228	1.456279	-0.202548
C	0.017480	-0.050685	-0.123015
O	0.934784	-0.776856	-0.976722
C	-1.360368	-0.513101	-0.657019
O	2.119583	3.089448	-0.086046
O	-0.407685	2.229784	0.738214
C	-2.588906	-0.055103	0.158652
O	-1.376449	-1.938613	-0.681024
O	-2.829664	1.353750	-0.063121
H	2.788026	-1.062249	-1.658698
H	0.133061	-0.386327	0.915235
H	2.972962	-3.489843	1.131260
H	2.810294	-3.358542	-0.624419
H	1.411062	-3.030588	0.424229
H	-5.929332	-1.065370	0.457459
H	-4.837057	-0.639970	1.781887
H	-5.307466	0.587478	0.601105
H	-4.095251	-0.746311	-1.215132
H	-3.615670	-1.925242	-0.012207
H	3.991825	-1.367411	0.334473

H	2.808464	-1.388771	2.380098
H	3.760377	1.004658	-0.415508
H	2.660444	1.268000	-1.769502
H	1.947825	1.459458	1.186247
H	0.138150	1.808117	-1.229946
H	-1.471214	-0.126580	-1.686828
H	1.456266	3.603218	0.398433
H	-1.351918	2.191769	0.494226
H	-2.362627	-0.124110	1.228478
H	-0.509345	-2.201490	-1.027657
H	-3.183285	1.474703	-0.955916

B3LYP Energy = -883.812130630 a.u.

(34*S*,35*S*,37*R*,38*S*,39*R*,40*S*,41*S*)-**1b′**, Conf I

C	2.121249	3.275392	-0.216704
C	-4.226040	1.004188	-0.863915
C	-2.826629	0.383154	-0.947151
C	1.010932	2.223477	-0.274773
O	-0.272557	2.823479	-0.052996
C	1.155332	1.148866	0.821751
C	2.468097	0.349441	0.792180
C	2.481839	-0.696718	-0.321223
C	1.242650	-1.577605	-0.201781
C	-0.025951	-0.709042	-0.235959
O	0.032270	0.247917	0.835389
C	-1.315666	-1.539263	-0.095572
O	3.676485	-1.460059	-0.197596
O	1.279178	-2.511701	-1.288572
C	-2.601943	-0.707246	0.106443
O	-1.209909	-2.504058	0.948630
O	-2.632517	-0.194860	1.444798
H	1.074037	1.676142	1.778511
H	-0.072329	-0.189122	-1.204524
H	3.093919	2.857536	-0.491468
H	2.193815	3.711276	0.785744
H	1.907644	4.085997	-0.923304
H	-4.348391	1.797232	-1.609393
H	-5.005304	0.253907	-1.043524
H	-4.400377	1.436861	0.125571
H	-2.067296	1.163851	-0.821367
H	-2.677470	-0.058240	-1.943201
H	1.020543	1.752030	-1.268819
H	-0.371840	3.575394	-0.651416
H	3.335706	1.008188	0.697037
H	2.573029	-0.176289	1.747585
H	2.462602	-0.209613	-1.310588
H	1.276437	-2.110609	0.754758
H	-1.420800	-2.105885	-1.028897
H	3.596725	-2.207190	-0.809084
H	0.785919	-3.301620	-1.031541
H	-3.436385	-1.418764	0.068857
H	-1.542562	-2.071169	1.752492
H	-1.864435	0.396470	1.529577

B3LYP Energy = -883.812080125 a.u.

(34*S*,35*S*,37*R*,38*S*,39*R*,40*S*,41*S*)-**1b′**, Conf J

C	3.052754	2.406581	-0.919017
C	-3.820706	-0.666796	-1.563297
C	-2.995697	0.566410	-1.172610
C	1.712099	1.747096	-0.607932
O	0.785541	2.794376	-0.359666
C	1.792071	0.809236	0.619981
C	2.624123	-0.476797	0.456230
C	1.894331	-1.543891	-0.369520
C	0.480516	-1.778983	0.162207
C	-0.261189	-0.438554	0.220810
O	0.467726	0.461425	1.065023
C	-1.686170	-0.515170	0.799242
O	2.553342	-2.817431	-0.314687
O	-0.251607	-2.646933	-0.695689
C	-2.604954	0.623076	0.306703
O	-1.645970	-0.517388	2.229907
O	-2.005417	1.915142	0.523916
H	2.194866	1.402727	1.447590
H	-0.323556	-0.045110	-0.801556
H	3.421164	2.956618	-0.046221
H	2.922236	3.120240	-1.736839
H	3.808229	1.674756	-1.220643
H	-4.709386	-0.767349	-0.929199
H	-4.163278	-0.581120	-2.599432
H	-3.243700	-1.593507	-1.485127
H	-3.570704	1.476866	-1.375684
H	-2.097708	0.631895	-1.799555
H	1.394192	1.173081	-1.494251
H	-0.079901	2.423341	-0.104604
H	3.598457	-0.250808	0.007472
H	2.818304	-0.895191	1.450387
H	1.804138	-1.229484	-1.419993
H	0.546142	-2.203268	1.175306
H	-2.128195	-1.467967	0.494366
H	3.379401	-2.778116	-0.813673
H	0.279495	-3.447221	-0.815351
H	-3.520394	0.552666	0.912459
H	-0.821196	-0.078553	2.492356
H	-1.860589	2.018718	1.474976

B3LYP Energy = -883.811958378 a.u.

(34*S*,35*S*,37*R*,38*S*,39*R*,40*S*,41*S*)-**1b′**, Conf K

C	2.463574	-2.930060	0.341831
C	-5.071049	-0.465004	0.662930
C	-3.843594	-0.866616	-0.166211
C	2.882262	-1.461714	0.416362
O	2.465113	-0.866078	1.652905
C	2.342490	-0.625347	-0.759216
C	2.736986	0.859846	-0.747112
C	1.818245	1.709395	0.122252
C	0.346862	1.462724	-0.217842
C	0.020393	-0.039590	-0.123812
O	0.930954	-0.779178	-0.973458
C	-1.363357	-0.491078	-0.655833
O	2.153639	3.079617	-0.099311
O	-0.390691	2.251310	0.710079
C	-2.587013	-0.058976	0.174436
O	-1.381525	-1.917616	-0.690860
O	-2.794801	1.345932	-0.107985
H	2.781545	-1.085114	-1.652756
H	0.135070	-0.369462	0.916444

H	2.773905	-3.378733	-0.608257
H	1.379171	-3.028233	0.438781
H	2.935534	-3.504063	1.147979
H	-5.919806	-1.115279	0.429346
H	-4.874359	-0.552598	1.738369
H	-5.406002	0.561067	0.461404
H	-4.055281	-0.752342	-1.236760
H	-3.616600	-1.922138	0.001384
H	3.980761	-1.398230	0.339827
H	2.801951	-1.396326	2.386758
H	3.773710	0.975517	-0.412704
H	2.681432	1.245328	-1.771865
H	1.959425	1.457779	1.179997
H	0.163041	1.805554	-1.248696
H	-1.490865	-0.089001	-1.673966
H	1.484646	3.603064	0.366559
H	-1.333948	2.193125	0.464834
H	-2.358137	-0.176124	1.244523
H	-0.516694	-2.176138	-1.045852
H	-3.614799	1.628968	0.316967
H	-3.437429	-1.415619	0.070840
H	-1.554404	-2.096289	1.734602
H	-1.837486	0.362536	1.541098

B3LYP Energy = -883.811924888 a.u.

B3LYP Energy = -883.811915482 a.u.

(34*S*,35*S*,37*R*,38*S*,39*R*,40*S*,41*S*)-**1b′**, Conf L

C	2.116313	3.296249	-0.207953
C	-4.232970	1.014404	-0.839882
C	-2.834919	0.392496	-0.938078
C	1.025837	2.224412	-0.289568
O	-0.274456	2.820614	-0.250174
C	1.162393	1.151036	0.817803
C	2.473392	0.346730	0.795717
C	2.483338	-0.700744	-0.316733
C	1.239437	-1.575025	-0.197997
C	-0.026287	-0.702035	-0.236359
O	0.035820	0.254699	0.838675
C	-1.317429	-1.532181	-0.104437
O	3.673441	-1.469975	-0.188674
O	1.273603	-2.511980	-1.281456
C	-2.603246	-0.703840	0.107392
O	-1.210854	-2.512051	0.926553
O	-2.624756	-0.201591	1.452076
H	1.090029	1.675762	1.779943
H	-0.069417	-0.177347	-1.201811
H	3.108765	2.894086	-0.430331
H	2.151591	3.749435	0.791597
H	1.899009	4.085313	-0.932948
H	-4.357486	1.813217	-1.578320
H	-5.015120	0.266892	-1.018980
H	-4.400421	1.440383	0.153914
H	-2.073980	1.172975	-0.823461
H	-2.697502	-0.046603	-1.936777
H	1.067310	1.754215	-1.277194
H	-0.375033	3.309881	0.578829
H	3.342129	1.003592	0.698318
H	2.576980	-0.178229	1.751780
H	2.469224	-0.214975	-1.306656
H	1.268855	-2.105346	0.760177
H	-1.421693	-2.086172	-1.045252
H	3.593018	-2.215890	-0.801594
H	0.775518	-3.298559	-1.023218

Table S3. Comparison of the ^{13}C NMR experimental data of **1b** with the mPW1PW91/6-311+G(2d,p) //B3LYP/6-31+G(d,p) ^{13}C NMR calculation data of the (34*S*,35*S*,37*R*,38*S*,39*R*,40*R*,41*S*)-**1b′** and (34*S*,35*S*,37*R*,38*S*,39*R*,40*S*,41*S*)-**1b′** stereoisomers. For better comparison, the Δ*δ* values over 3 ppm were underlined.

No.	Exp.	Calc.$_{40R}$	Calc.$_{40S}$	$\Delta\delta_{40R}$	$\Delta\delta_{40S}$
C-34	67.10	65.42	65.34	1.68	1.76
C-35	77.80	82.44	82.16	<u>4.64</u>	<u>4.36</u>
C-36	34.10	31.58	31.73	2.52	2.37
C-37	71.10	68.96	69.25	2.14	1.85
C-38	72.70	71.46	74.61	1.24	1.91
C-39	73.07	76.81	78.03	<u>3.74</u>	<u>4.96</u>
C-40	73.03	75.20	77.19	2.17	<u>4.16</u>
C-41	73.13	73.14	76.89	0.01	<u>3.76</u>
C-42	31.20	30.05	28.26	1.15	2.94
Average	N/A	N/A	N/A	2.14	3.12

Table S4. The structural characteristics of 188 SCCCs for principal component analysis (PCA).

No.	Compound Name	Group	Molecular Weight	Carbon Numbers of the Backbone Chain	Ring Numbers of the Backbone Chain	Hydroxy Numbers of the Backbone Chain	Carbon–Carbon Double Bond Numbers of the Backbone Chain	Chiral Carbon Numbers of the Backbone Chain	Spiroketal Carbon Numbers of the Backbone Chain	The Ratio of Backbone Carbons to Ether Rings	The First Reported Year	References
1	Benthol A	1	1506	72	8	22	4	35	1	9.0		
2	Amdigenol A	*Amphidinium*	2169	98	3	36	11	44	0	32.7	2012	[1]
3	Amdigenol D	*Amphidinium*	2223	101	4	36	12	46	0	25.3	2020	[2]
4	Amdigenol E	*Amphidinium*	1811	78	2	29	8	38	0	39.0	2014	[3]
5	Amdigenol G	*Amphidinium*	1277	57	2	19	7	24	0	28.5	2014	[3]
6	Amphezonol A	*Amphidinium*	1243	60	3	21	2	28	0	20.0	2006	[4]
7	Amphidinol 1	*Amphidinium*	1489	69	2	20	8	27	0	34.5	1991	[5]
8	Amphidinol 2	*Amphidinium*	1375	65	3	22	7	30	0	21.7	1995	[6]
9	Amphidinol 3	*Amphidinium*	1327	67	2	21	9	25	0	33.5	1999	[7]
10	Amphidinol 4	*Amphidinium*	1301	65	2	21	8	25	0	32.5	2001	[8]
11	Amphidinol 5	*Amphidinium*	1371	69	2	22	9	26	0	34.5	1997	[9]
12	Amphidinol 6	*Amphidinium*	1345	67	2	22	8	26	0	33.5	1997	[9]
13	Amphidinol 7	*Amphidinium*	1231	55	2	17	7	23	0	27.5	2005	[10]
14	desulfo-Amphidinol 7	*Amphidinium*	1129	55	2	18	7	23	0	27.5	2006	[11]
15	Amphidinol 9	*Amphidinium*	1327	67	2	21	9	25	0	33.5	2005	[12]
16	Amphidinol 10	*Amphidinium*	1273	63	2	21	8	25	0	31.5	2005	[12]
17	Amphidinol 11	*Amphidinium*	1477	65	3	21	7	30	0	21.7	2005	[12]
18	Amphidinol 12	*Amphidinium*	1403	65	2	20	8	25	0	32.5	2005	[12]
19	Amphidinol 13	*Amphidinium*	1429	67	2	20	9	25	0	33.5	2005	[12]

20	Amphidinol 14	*Amphidinium*	1265	55	2	19	6	24	0	27.5	2006	[11]
21	Amphidinol 15	*Amphidinium*	1163	55	2	20	6	24	0	27.5	2006	[11]
22	Amphidinol 17	*Amphidinium*	1283	59	2	18	6	24	0	29.5	2010	[13]
23	Amphidinol 18	*Amphidinium*	1359	67	2	21	7	26	0	33.5	2014	[14]
24	Amphidinol 19	*Amphidinium*	1461	67	2	20	7	26	0	33.5	2014	[14]
25	Amphidinol 20	*Amphidinium*	1629	80	2	25	9	32	0	40.0	2017	[15]
26	Amphidinol 21	*Amphidinium*	1775	86	2	28	9	36	0	43.0	2017	[15]
27	Amphidinol 22	*Amphidinium*	1645	78	4	26	8	38	0	19.5	2019	[16]
28	Amphidinol A	*Amphidinium*	1339	65	2	21	3	26	0	32.5	2017	[17]
29	Amphidinol B	*Amphidinium*	1441	65	2	20	3	26	0	32.5	2017	[17]
30	Carteraol E	*Amphidinium*	1399	69	3	19	7	27	0	23.0	2009	[18]
31	Colopsinol A	*Amphidinium*	1427	56	1	6	4	15	0	56.0	1999	[19]
32	Colopsinol B	*Amphidinium*	1385	53	2	7	4	15	0	26.5	1999	[20]
33	Colopsinol C	*Amphidinium*	1223	53	2	7	4	15	0	26.5	1999	[20]
34	Colopsinol D	*Amphidinium*	1409	56	2	4	4	15	0	28.0	2000	[21]
35	Colopsinol E	*Amphidinium*	1265	56	1	6	4	15	0	56.0	2000	[21]
36	Gibbosol A	*Amphidinium*	1555	69	2	30	3	37	0	34.5	2020	[22]
37	Gibbosol B	*Amphidinium*	1595	71	2	30	4	37	0	35.5	2020	[22]
38	Gibbosol C	*Amphidinium*	1567	70	2	30	4	36	0	35.0	2020	[23]
39	Karatungiol A	*Amphidinium*	1457	69	2	25	4	30	0	34.5	2006	[24]
40	Karatungiol B	*Amphidinium*	1439	69	2	24	5	29	0	34.5	2006	[24]
41	Lingshuiol	*Amphidinium*	1351	65	2	22	5	27	0	32.5	2004	[25]
42	Lingshuiol A	*Amphidinium*	1273	63	2	21	8	25	0	31.5	2004	[26]
43	Lingshuiol B	*Amphidinium*	1243	57	2	17	8	22	0	28.5	2004	[26]
44	Luteophanol A	*Amphidinium*	1255	57	2	19	7	24	0	28.5	1997	[27]
45	Luteophanol B	*Amphidinium*	1321	64	2	23	7	27	0	32.0	1998	[28]
46	Luteophanol C	*Amphidinium*	1321	64	2	23	7	27	0	32.0	1998	[28]
47	Luteophanol D	*Amphidinium*	1307	63	2	23	7	27	0	31.5	2005	[29]

48	Symbiopolyol	*Amphidinium*	1243	57	2	17	8	22	0	28.5	2010	[30]
49	CTX4B	*Gambierdiscus*	1061	55	13	3	6	31	1	4.2	1990	[31]
50	CTX4A	*Gambierdiscus*	1061	55	13	3	6	31	1	4.2	1997	[32]
51	M-seco-CTX4B	*Gambierdiscus*	1079	55	12	5	6	31	0	4.6	2000	[33,34]
52	M-seco-CTX4A	*Gambierdiscus*	1079	55	12	5	6	31	0	4.6	2000	[33,34]
53	CTX1B	*Gambierdiscus*	1111	55	13	6	5	33	1	4.2	1990	[31]
54	52-epi-CTX1B	*Gambierdiscus*	1111	55	13	6	5	33	1	4.2	2000	[33,34]
55	54-epi-CTX1B	*Gambierdiscus*	1111	55	13	6	5	33	1	4.2	2000	[33,34]
56	54-epi-52-epi-CTX1B	*Gambierdiscus*	1111	55	13	6	5	33	1	4.2	2000	[33,34]
57	7-oxo-CTX1B	*Gambierdiscus*	1127	55	13	6	4	33	1	4.2	2000	[33,34]
58	7-hydroxy-CTX1B	*Gambierdiscus*	1129	55	13	7	4	34	1	4.2	2000	[33,34]
59	4-hydroxy-7-oxo-CTX1B	*Gambierdiscus*	1145	55	13	7	3	34	1	4.2	2000	[33,34]
60	54-deoxy-50-hydroxy CTX1B	*Gambierdiscus*	1111	55	13	6	5	32	1	4.2	2000	[33,34]
61	52-epi-54-deoxy-CTX1B	*Gambierdiscus*	1095	55	13	5	5	32	1	4.2	1991	[35]
62	54-deoxy-CTX1B	*Gambierdiscus*	1095	55	13	5	5	32	1	4.2	1991	[35]
63	CTX3C	*Gambierdiscus*	1023	52	13	3	4	30	1	4.0	1993	[36]
64	CTX3B	*Gambierdiscus*	1023	52	13	3	4	30	1	4.0	2000	[33,34]
65	M-seco-CTX3C	*Gambierdiscus*	1041	52	12	5	4	30	0	4.3	2000	[33,34]
66	M-seco-CTX3C methyl acetal	*Gambierdiscus*	1055	52	12	4	4	30	0	4.3	2000	[33,34]
67	51-hydroxy-CTX3C	*Gambierdiscus*	1039	52	13	4	4	31	1	4.0	1998	[37]
68	51-hydroxy-3-oxo-CTX3C	*Gambierdiscus*	1055	52	13	4	3	31	1	4.0	2000	[33,34]
69	A-seco-51-hydroxy-CTX3C	*Gambierdiscus*	1057	52	12	6	4	31	1	4.3	2000	[33,34]
70	2,3-dihydroxy-CTX3C	*Gambierdiscus*	1055	52	13	5	4	32	1	4.0	1998	[37]
71	2,3-dihydro-2-hydroxy-	*Gambierdiscus*	1041	52	13	4	3	31	1	4.0	2000	[33,34]

	CTX3C											
72	2,3-dihydro-51-hydroxy-2-oxo-CTX3C	*Gambierdiscus*	1055	52	13	4	3	31	1	4.0	2000	[33,34]
73	2,3-dihydro-2,3-dihyroxy-CTX3C	*Gambierdiscus*	1057	52	13	5	3	32	1	4.0	2000	[33,34]
74	2,3-dihydro-2,3,51-trihydroxy-CTX3C	*Gambierdiscus*	1073	52	13	6	3	33	1	4.0	2000	[33,34]
75	A-seco-2,3-dihydro-51-hydroxy-CTX3C	*Gambierdiscus*	1059	52	12	6	3	31	1	4.3	2000	[33,34]
76	2,3,51-trihydroxy-CTX3C	*Gambierdiscus*	1071	52	13	6	4	33	1	4.0	2000	[33,34]
77	2-hydroxy-CTX3C	*Gambierdiscus*	1039	52	13	4	4	31	1	4.0	2000	[33,34]
78	C-CTX-1	*Gambierdiscus*	1141	57	14	5	3	31	0	4.1	1998	[38]
79	C-CTX-2	*Gambierdiscus*	1141	57	14	5	3	31	0	4.1	1998	[38]
80	C-CTX-3	*Gambierdiscus*	1143	57	13	6	3	31	0	4.4	2020	[39]
81	C-CTX-4	*Gambierdiscus*	1143	57	13	6	3	31	0	4.4	2020	[39]
82	MTX-1	*Gambierdiscus*	3424	142	32	27	3	97	0	4.4	1993	[40]
83	MTX-3	*Gambierdiscus*	1038	46	9	5	3	23	0	5.1	2019	[41]
84	Gambieric acid A	*Gambierdiscus*	1057	49	10	4	2	27	0	4.9	1992	[42,43]
85	Gambieric acid B	*Gambierdiscus*	1071	49	10	4	2	27	0	4.9	1992	[42,43]
86	Gambieric acid C	*Gambierdiscus*	1185	49	10	3	2	27	0	4.9	1992	[42,43]
87	Gambieric acid D	*Gambierdiscus*	1199	49	10	3	2	27	0	4.9	1992	[42,43]
88	Gambieroxide	*Gambierdiscus*	1195	52	12	5	1	32	0	4.3	2013	[44]
89	Gambierone	*Gambierdiscus*	1024	46	9	5	3	23	0	5.1	2015	[45]
90	Brevisulcenal-F (KBT-F)	*Karenia*	2052	95	24	13	3	61	0	4.0	2012	[46,47]
91	KBT-H	*Karenia*	2068	95	24	13	3	61	0	4.0	2018	[46,48]
92	KBT-G	*Karenia*	2082	95	24	14	3	63	0	4.0	2018	[46,48]
93	KBT-I	*Karenia*	2098	95	24	14	3	63	0	4.0	2018	[46,48]
94	KBT-A1	*Karenia*	2154	95	24	12	3	61	0	4.0	2021	[46]

95	KBT-A2	*Karenia*	2184	95	24	13	3	63	0	4.0	2021	[46]
96	BTX-B1	*Karenia*	1017	42	11	1	2	23	0	3.8	1995	[49,50]
97	BTX-B2	*Karenia*	1017	42	11	1	2	24	0	3.8	1998	[49,51]
98	Gymnocin-B	*Karenia*	1148	56	15	4	1	33	0	3.7	2005	[52,53]
99	Gymnocin-A	*Karenia*	1028	52	14	3	1	31	0	3.7	2002	[52,54]
100	Karmitoxin	*Karlodinium*	1386	70	2	20	7	26	0	35.0	2017	[55]
101	Karlotoxin-2 (KmTx2)	*Karlodinium*	1345	63	2	22	4	28	0	31.5	2010	[56]
102	4,5-dihydro-KmTx-2	*Karlodinium*	1347	63	2	22	3	28	0	31.5	2016	[57]
103	4,5-dihydro-dechloro-KmTx-2	*Karlodinium*	1313	63	2	22	3	28	0	31.5	2016	[57]
104	KmTx-3	*Karlodinium*	1325	64	2	22	4	28	0	32.0	2010	[58]
105	44-hydroxy-KmTx-2	*Karlodinium*	1361	63	2	23	4	29	0	31.5	2012	[59]
106	KmTx-4	*Karlodinium*	1209	59	2	20	4	25	0	29.5	2012	[59]
107	59-E-chloro-KmTx-4	*Karlodinium*	1243	59	2	20	4	25	0	29.5	2012	[59]
108	KmTx-5	*Karlodinium*	1303	61	2	21	3	27	0	30.5	2012	[59]
109	6-oxo-KmTx-2	*Karlodinium*	1345	63	2	21	3	27	0	31.5	2012	[59]
110	KcTx-1	*Karlodinium*	1317	61	2	21	3	27	0	30.5	2012	[59]
111	KmTx-1	*Karlodinium*	1339	65	2	22	4	28	0	32.5	2008	[60]
112	KmTx-6	*Karlodinium*	1373	65	2	22	4	28	0	32.5	2013	[61]
113	KmTx-7	*Karlodinium*	1419	65	2	21	4	28	0	32.5	2013	[61]
114	KmTx-8	*Karlodinium*	1335	63	2	21	3	27	0	31.5	2015	[62]
115	KmTx-9	*Karlodinium*	1317	61	2	21	3	27	0	30.5	2015	[62]
116	65-E-chloro-KmTx-1	*Karlodinium*	1373	65	2	22	4	28	0	32.5	2010	[63]
117	10-O-sulfo-KmTx-1	*Karlodinium*	1418	65	2	21	4	28	0	32.5	2010	[63]
118	64-E-chloro-KmTx-3	*Karlodinium*	1359	64	2	22	4	28	0	32.0	2010	[63]
119	10-O-sulfo-KmTx-3	*Karlodinium*	1404	64	2	21	4	28	0	32.0	2010	[63]
120	Ostreocin D	*Ostreopsis*	2634	115	10	40	6	61	0	11.5	1995	[64,65]
121	Ovatoxin-a	*Ostreopsis*	2645	115	10	39	6	62	0	11.5	2008	[66,67]

122	Ostreol-A	*Ostreopsis*	1312	41	2	13	5	18	0	20.5	2013	[68]
123	Ostreol-B	*Ostreopsis*	1144	56	1	21	3	24	0	56.0	2018	[69]
124	Ovatoxin-a-IK2	*Ostreopsis*	2645	115	10	39	6	62	0	11.5	2013	[70]
125	Ovatoxin-d-IK2	*Ostreopsis*	2661	115	10	40	6	63	0	11.5	2013	[70]
126	Ovatoxin-e-IK2	*Ostreopsis*	2661	115	10	40	6	63	0	11.5	2013	[70]
127	Ostreocin-B	*Ostreopsis*	2649	115	10	41	6	62	0	11.5	2013	[71,72]
128	Ostreocin-A	*Ostreopsis*	2649	115	10	39	6	62	0	11.5	2019	[73]
129	Ostreocin-E1	*Ostreopsis*	2615	115	10	39	7	60	0	11.5	2019	[73]
130	Palytoxin	*Ostreopsis*	2677	115	10	41	6	64	0	11.5	2003	[73,74]
131	DTX-4	*Prorocentrum*	1472	38	7	4	2	14	3	5.4	1995	[75]
132	DTX-5a	*Prorocentrum*	1391	38	7	4	2	14	3	5.4	1995	[76]
133	DTX-5b	*Prorocentrum*	1405	38	7	4	2	14	3	5.4	1995	[76]
134	DTX-5c	*Prorocentrum*	1431	38	7	4	2	14	3	5.4	2006	[77,78]
135	Belizeanolide	*Prorocentrum*	1424	66	3	13	4	28	0	22.0	2009	[79]
136	Prorocentrol	*Prorocentrum*	1474	65	3	30	7	36	0	21.7	2011	[80]
137	Prorocentroic acid	*Prorocentrum*	1400	60	5	23	5	35	0	12.0	2021	[81]
138	Prorocentrolide B	*Prorocentrum*	1075	49	4	7	5	21	0	12.3	1996	[82]
139	YTX	*Protoceratium*	1142	47	11	2	2	26	0	4.3	1997	[83]
140	45-hydroxy-YTX	*Protoceratium*	1158	47	11	3	2	27	0	4.3	1997	[83]
141	45,46,47-trinorYTX	*Protoceratium*	1102	45	11	2	2	26	0	4.1	1997	[83]
142	HomoYTX	*Protoceratium*	1156	48	11	2	2	26	0	4.4	1997	[83]
143	45-hydroxy-homoYTX	*Protoceratium*	1172	48	11	3	2	27	0	4.4	1997	[83]
144	1-desulfoYTX	*Protoceratium*	1062	47	11	2	2	26	0	4.3	1999	[84]
145	CarboxyYTX	*Protoceratium*	1174	47	11	2	2	26	0	4.3	2003	[85]
146	CarboxyhomoYTX	*Protoceratium*	1188	48	11	2	2	26	0	4.4	2003	[85]
147	noroxoYTX	*Protoceratium*	1048	42	11	1	0	24	0	3.8	2003	[85]
148	noroxohomoYTX	*Protoceratium*	1062	43	11	1	0	24	0	3.9	2003	[85]
149	Adriatoxin	*Protoceratium*	1050	37	10	2	0	24	0	3.7	2003	[85]

150	KetohomoYTX	*Protoceratium*	1062	43	11	1	0	25	0	3.9	2004	[86]
151	KetoYTX	*Protoceratium*	1048	42	11	1	0	25	0	3.8	2004	[86]
152	40-epi-ketoYTX	*Protoceratium*	1048	42	11	1	0	25	0	3.8	2004	[86]
153	YTX-enone	*Protoceratium*	1048	42	11	1	1	24	0	3.8	2004	[86]
154	9-Methyl-41a-homoYTX	*Protoceratium*	1170	47	11	2	2	26	0	4.3	2004	[86]
155	Heptanor-41-oxoYTX	*Protoceratium*	1048	42	11	1	0	25	0	3.8	2004	[87]
156	40-epi-heptanor-41-oxoYTX	*Protoceratium*	1048	42	11	1	0	25	0	3.8	2004	[87]
157	45-hydroxy-carboxy YTX	*Protoceratium*	1190	47	11	3	2	28	0	4.3	2005	[88]
158	Protoceratins I	*Protoceratium*	1200	48	11	1	2	26	0	4.4	2004	[89]
159	Protoceratins II	*Protoceratium*	1464	48	11	1	2	26	0	4.4	2004	[89]
160	Protoceratins III	*Protoceratium*	1310	48	11	1	2	26	0	4.4	2004	[89]
161	Protoceratins IV	*Protoceratium*	1574	48	11	1	2	26	0	4.4	2004	[89]
162	41a-homoYTX	*Protoceratium*	1156	48	11	2	2	26	0	4.4	2005	[90]
163	YTX 32-O-[β-L-arabino furanoside]	*Protoceratium*	1274	47	11	1	2	26	0	4.3	2006	[91]
164	YTX 32-O-[β-L-arabino furanosyl-(5'→1")-β-L-arabinofuranoside]	*Protoceratium*	1406	47	11	1	2	26	0	4.3	2006	[91]
165	1-homoYTX 32-O-[β-L-arabinofuranosyl-(5'→1")-β-L-arabinofuranoside]	*Protoceratium*	1420	48	11	1	2	26	0	4.4	2006	[91]
166	GlycoYTXA (G-YTXA)	*Protoceratium*	1274	47	11	1	2	25	0	4.3	2006	[92]
167	45,46,47-trinor-1-homoYTX	*Protoceratium*	1116	47	11	2	1	26	0	4.3	2007	[93]
168	heptanor-41-oxoYTX enone	*Protoceratium*	1048	42	11	1	1	24	0	3.8	2007	[93]

169	furanoYTX	*Protoceratium*	1142	46	11	2	1	26	0	4.2	2007	[94]
170	tri-glycosilYTX	*Protoceratium*	1538	47	11	1	2	26	0	4.3	2008	[95]
171	nor-ring A-YTX	*Protoceratium*	1072	45	10	2	2	24	0	4.5	2004	[86]
172	44,55-dihydroxy-9-methyl-41a-homo-YTX	*Protoceratium*	1218	48	11	3	2	27	0	4.4	2005	[95,96]
173	9-methyl-41-keto-YTX-1,3-enone	*Protoceratium*	1076	42	11	1	1	24	0	3.8	2006	[95,97]
174	9-methyl-41a-homo-YTXamide	*Protoceratium*	1319	49	11	3	1	27	0	4.5	2005	[90,95]
175	1-desulfocarboxyhomo-YTX	*Protoceratium*	1108	48	11	2	2	26	0	4.4	2007	[95,98]
176	4-desulfocarboxyhomo-YTX	*Protoceratium*	1108	48	11	2	2	26	0	4.4	2007	[95,98]
177	41a-homo-44-oxotrinor-YTX	*Protoceratium*	1132	46	11	2	1	26	0	4.2	2006	[95,97]
178	44-oxotrinor-YTX	*Protoceratium*	1118	45	11	2	1	26	0	4.1	2006	[95,97]
179	45-hydroxy-dinor-YTX	*Protoceratium*	1132	45	11	3	1	26	0	4.1	2006	[95,97]
180	44,55-dihydroxy-41a-Homo-YTX	*Protoceratium*	1190	48	11	3	2	27	0	4.4	2005	[95,96]
181	44,55-dihydroxy-YTX	*Protoceratium*	1176	47	11	3	2	27	0	4.3	2005	[95,96]
182	41-keto-YTX-1,3-enone	*Protoceratium*	1048	42	11	1	1	24	0	3.8	2004	[95,86]
183	41a-homo-YTX amide	*Protoceratium*	1291	48	11	3	1	27	0	4.4	2005	[95,90]
184	Symbiodinolide	*Symbiodinium*	2835	104	5	35	10	61	1	20.8	2007	[99]
185	Zooxanthellamides C_1-C_5	*Symbiodinium*	2698	78	4	26	7	52	1	26.2	2005	[100]
186	Zooxanthellatoxin A	*Symbiodinium*	2831	104	5	35	11	60	1	20.8	1995	[101]
187	Symbiospirols A-C	*Symbiodinium*	1206	67	5	8	1	18	2	13.4	2009	[102]
188	Zooxanthellamide D	*Symbiodinium*	1049	21	2	9	2	12	0	10.5	2007	[103]

Supplemental Experimental Procedures

1.1 General Experimental Procedures

HR-ESIMS was obtained on a Bruker maXis ESI-QTOF mass spectrometer in the positive-ion mode. LR-ESIMS was recorded on a Bruker amaZon SL mass spectrometer in both positive- and negative-ion modes or a Waters ACQUITY QDa mass detector in the positive-ion mode. UPLC-MS was measured on a Waters ACQUITY UPLC H-Class PLUS system combined with a Bruker amaZon SL mass spectrometer. 1D and 2D NMR spectra were measured on a Bruker AV-400, 600, or 700 MHz NMR spectrometer. UV spectra were recorded on a Waters 2998 photodiode array detector and optical rotations determined on an MCP200 modular circular polarimeter (Anton Paar GmbH) with a 0.5 cm cell at 25 °C. HPLC was performed on a Waters 2535 pump equipped with a 2998 photodiode array detector, coupled with a 2424 evaporative light scattering detector, and C_{18} reversed-phase columns (YMC, Kyoto, Japan; 250 mm × 4.6 mm, length × i.d., 5 μm, for analysis; 250 mm × 10 mm, length × i.d., 5 μm, for preparation). For column chromatography, C_{18} reversed-phase silica gel (ODS-A-HG 12 nm, 50 μm, YMC, Japan) was employed.

1.2 Dinoflagellate Isolation and Culture

The dinoflagellate cells of *Amphidinium* sp. (strain: MDRC-02, Figure S1) were isolated using capillary pipettes under microscope observation from the sand sample, collected in October 2013 on the sea floor at the Lingshui Bay, Hainan Province, PR China. The unialgal strain was grown in a 500 mL flask containing sterilized seawater (34‰ salinity), enriched with K medium,[104] and cultured at 27.0 ± 1 °C, with a 12 : 12 h light : dark photocycle and an irradiance of 45 μmol photons·m^{-2}·s^{-1}.

Amplification of 18S rDNA from the dinoflagellate cells was performed three times. The PCR amplified 18S rDNA sequence of the title dinoflagellate (sequence ID: SRP311747) was compared with those in the NCBI databases using the BLAST algorithm. The 18S ribosomal RNA gene, partial sequence of an uncultured eukaryote clone (XM.18S_7; ENV 01-JUL-2015, Xiamen, PR China; sequence ID: KT201583.1) was found to be the closest relative (percent identity: 99.65%), whereas that of *Amphidinium operculatum* (strain: TAK-0; PLN 08-AUG-2012, Taketomi Island, Okinawa, Japan; sequence ID: AB704006.1)[105] was discovered to be the closest dinoflagellate strain (percent identity: 80.95%). Phylogenetic tree inferred from the 18S rDNA sequence alignment in the NCBI databases suggested that the benthic MDRC-02 strain ought to be a new taxon of dinoflagellate (Figure S2). The voucher specimen and 18S rDNA gene were deposited at Marine Drugs Research Center, School of Pharmaceutical Sciences, Southern Medical University, PR China.

Large-scale culture of the title dinoflagellate was kept in plastic buckets (20.0 L × 40), each containing 15.0 L of culture medium. 21 days later, 500.0 L culture medium were separated from cells by filtration using filter paper. According to the same procedure, 100.0 L culture medium enriched with $NaH^{13}CO_3$ (50 mg/L)[106] were also separated from cells.

1.3 Isolation of Benthol A

The filtrate (500.0 L) was loaded onto a macroporous resin column (DIAION, HP-20, 120 cm × 15 cm i.d.), eluted with freshwater to remove sea salt. Then, the loaded sample was successively eluted with 25%, 50%, 75%, and 95% aqueous ethanol. All the eluates were concentrated under vacuum to afford the resultant solid (3.8 g), which was separated by a C_{18} reversed-phase column (45.0 × 5.0 cm i.d.), eluted with aqueous methanol (20% to 100%), to yield 63 fractions. UPLC-MS (Waters ACQUITY UPLC BEH C_{18} 150 × 2.1 mm i.d., 1.7 μm, MeCN/H_2O, from 5:95 to 98:2) was employed for the detection of SCCCs in fractions. The resultant fractions 32 and 33 were combined (116.5 mg) and further purified by preparative HPLC (YMC-Pack 250 × 10 mm i.d., MeOH/H_2O, 50:50) to afford benthol A (**1**) (20.0 mg, t_R = 22.8 min). According to the same procedure, ^{13}C-enriched **1** (4.0 mg) was obtained from 100.0 L

filtrates that were enriched with $NaH^{13}CO_3$.

Benthol A (**1**):
Colorless solid, $[\alpha]_D^{25}$ = + 60.0 (*c* = 0.1, methanol); UV (MeCN) λ_{max} (log *ε*) 194.5 (4.2) nm (Figure S4); HR-ESIMS *m*/*z* $[M + Na]^+$ (calcd for $C_{75}H_{126}NaO_{30}$, 1529.8226, found 1529.8234).

^1H NMR (CD_3OD, 700 MHz) data for **1**: *δ* 5.69 (m, 1H, H-16), 5.65 (m, 1H, H-64), 5.54 (dd, 1H, *J* = 15.4, 7.0 Hz, H-17), 5.50 (dd, 1H, *J* = 15.4, 7.0 Hz, H-65), 5.29 (br d, 1H, *J* = 9.1 Hz, H-45), 5.21 (br d, 1H, *J* = 8.4 Hz, H-61), 4.81 (br s, 1H, H-73b), 4.72 (br s, 1H, H-73a), 4.67 (td, 1H, *J* = 9.1, 3.5 Hz, H-46), 4.45 (m, 1H, H-50), 4.37 (m, 1H, H-62), 4.25 (m, 1H, H-66), 4.18 (m, 1H, H-22), 4.18 (m, 1H, H-30), 4.18 (m, 1H, H-34), 4.11 (m, 1H, H-52), 4.10 (m, 1H, H-48), 4.08 (m, 1H, H-32), 4.05 (m, 1H, H-18), 4.01 (m, 1H, H-56), 4.00 (m, 1H, H-70), 3.90 (m, 1H, H-2), 3.90 (m, 1H, H-14), 3.87 (m, 1H, H-12), 3.86 (m, 1H, H-58), 3.83 (ddd, 1H, *J* = 9.1, 9.1, 4.9 Hz, H-6), 3.76 (m, 1H, H-37), 3.75 (m, 1H, H-24), 3.69 (m, 1H, H-39), 3.69 (m, 1H, H-72b), 3.67 (m, 1H, H-4), 3.63 (m, 1H, H-41), 3.62 (m, 1H, H-40), 3.62 (m, 1H, H-35), 3.61 (m, 1H, H-72a), 3.59 (m, 1H, H-54), 3.56 (m, 1H, H-29), 3.56 (m, 1H, H-68), 3.53 (m, 1H, H-21), 3.49 (m, 1H, H-38), 3.48 (m, 1H, H-1a), 3.48 (m, 1H, H-1b), 3.42 (dd, 1H, *J* = 7.7, 4.2 Hz, H-49), 3.27 (dd, 1H, *J* = 8.4, 2.1 Hz, H-55), 3.22 (dd, 1H, *J* = 9.1, 2.8 Hz, H-69), 3.01 (t, 1H, *J* = 9.1 Hz, H-5), 2.42 (m, 1H, H-31b), 2.38 (m, 1H, H-23b), 2.36 (m, 1H, H-51b), 2.27 (m, 1H, H-43b), 2.26 (m, 1H, H-63b), 2.24 (m, 1H, H-9a), 2.24 (m, 1H, H-9b), 2.22 (m, 1H, H-11b), 2.21 (m, 1H, H-15a), 2.21 (m, 1H, H-15b), 2.20 (m, 1H, H-63a), 2.18 (m, 1H, H-59b), 2.15 (m, 1H, H-3b), 2.11 (m, 1H, H-43a), 2.10 (dd, 1H, *J* = 12.6, 4.9 Hz, H-7b), 2.04 (m, 1H, H-59a), 2.03 (m, 1H, H-36b), 1.99 (m, 1H, H-42b), 1.99 (m, 1H, H-53b), 1.98 (m, 1H, H-11a), 1.96 (m, 1H, H-67b), 1.88 (m, 1H, H-47b), 1.88 (m, 1H, H-53a), 1.83 (m, 1H, H-71b), 1.82 (m, 1H, H-33b), 1.82 (m, 1H, H-57b), 1.74 (m, 1H, H-71a), 1.72 (m, 1H, H-36a), 1.72 (d, 3H, *J* = 1.4 Hz, H_3-74), 1.71 (m, 1H, H-20b), 1.71 (m, 1H, H-25b), 1.70 (d, 3H, *J* = 1.4 Hz, H_3-75), 1.67 (m, 1H, H-13b), 1.64 (m, 1H, H-20a), 1.64 (m, 1H, H-28a), 1.64 (m, 1H, H-28b), 1.64 (m, 1H, H-51a), 1.63 (m, 1H, H-19a), 1.63 (m, 1H, H-19b), 1.63 (m, 1H, H-67a), 1.58 (m, 1H, H-47a), 1.56 (m, 1H, H-25a), 1.55 (m, 1H, H-31a), 1.52 (m, 1H, H-33a), 1.51 (m, 1H, H-57a), 1.50 (m, 1H, H-42a), 1.50 (m, 1H, H-7a), 1.49 (m, 1H, H-23a), 1.48 (m, 1H, H-26b), 1.48 (m, 1H, H-27b), 1.46 (m, 1H, H-3a), 1.40 (m, 1H, H-27a), 1.38 (m, 1H, H-26a).

$^{13}C\{^1H\}$ NMR (CD_3OD, 175 MHz) data for **1**: *δ* 143.1 (qC, C-10), 138.1 (qC, C-44), 137.0 (CH, C-17), 136.3 (CH, C-65), 135.9 (qC, C-60), 130.9 (CH, C-61), 129.6 (CH, C-45), 129.1 (CH, C-64), 128.8 (CH, C-16), 111.2 (CH_2, C-73), 99.8 (qC, C-8), 86.1 (CH, C-49), 84.7 (CH, C-29), 84.5 (CH, C-21), 79.1 (CH, C-24), 77.8 (CH, C-35), 77.3 (CH, C-5), 76.5 (CH, C-52), 75.4 (CH, C-32), 75.0 (CH, C-68), 74.3 (CH, C-54), 73.8 (CH, C-18), 73.54 (CH, C-4), 73.49 (CH, C-50), 73.33 (CH, C-69), 73.30 (CH, C-30), 73.22 (CH, C-22), 73.22 (CH, C-39), 73.15 (CH, C-55), 73.1 (CH, C-40), 73.0 (CH, C-2), 72.8 (CH, C-38), 72.5 (CH, C-41), 71.8 (CH, C-66), 71.1 (CH, C-37), 70.96 (CH, C-58), 70.1 (CH, C-6), 69.2 (CH, C-62), 68.9 (CH, C-56), 68.7 (CH, C-12), 68.3 (CH, C-14), 68.2 (CH, C-48), 68.1 (CH, C-70), 67.1 (CH, C-34), 67.0 (CH_2, C-1), 66.2 (CH, C-46), 62.6 (CH_2, C-72), 46.6 (CH_2, C-59), 44.9 (CH_2, C-9), 44.0 (CH_2, C-7), 43.8 (CH_2, C-13), 43.3 (CH_2, C-47), 42.70 (CH_2, C-31), 42.66 (CH_2, C-15), 42.4 (CH_2, C-23), 41.9 (CH_2, C-63), 41.73 (CH_2, C-33), 41.73 (CH_2, C-51), 41.2 (CH_2, C-11), 41.0 (CH_2, C-67), 39.63 (CH_2, C-57), 39.61 (CH_2, C-53), 37.4 (CH_2, C-25), 36.8 (CH_2, C-43), 36.4 (CH_2, C-3), 35.1 (CH_2, C-19), 34.2 (CH_2, C-36), 33.8 (CH_2, C-71), 33.5 (CH_2, C-42), 30.2 (CH_2, C-28), 27.68 (CH_2, C-26), 27.64 (CH_2, C-27), 26.2 (CH_2, C-20), 17.5 (CH_3, C-75), 16.8 (CH_3, C-74).

1.4 Periodate Degradation

A solution of benthol A (**1**, 10.0 mg, 0.0066 mM) of ^{13}C natural abundance in 1.0 mL water was added with $NaIO_4$ (7.2 mg, 0.03 mM). The reaction mixture was stirred at room temperature for 30.0 min. When the solution was cooled to 0 °C, excess amount of $NaBH_4$ was added and kept for 1.0 h. The reaction mixture was separated by a C_{18} reversed-phase silica gel column (Daisogel, SP-120-50-ODS-

B, 5g, 6.5 cm × 1.0 cm i.d.), eluted with 15.0 mL of water, followed by 20.0 mL of MeOH, to yield three fractions. The second fraction was purified by HPLC (YMC-Pack 250 cm × 4.6 mm i.d., MeCN/H_2O, 15:85) to afford two products, viz., fragments **1A** (1.5 mg, t_R = 28.8 min) and **1B** (2.0 mg, t_R = 22.5 min).

1A: Colorless oil; HR-ESIMS *m*/*z* [M + Na]$^+$ (calcd for $C_{40}H_{70}NaO_{16}$, 829.4556, found 829.4566).
^{1}H NMR (CD_3OD, 700 MHz) data for **1A**: δ 5.68 (m, 1H, H-16), 5.53 (dd, 1H, *J* = 15.4, 7.0 Hz, H-17), 4.77 (br s, 1H, H-73b), 4.69 (br s, 1H, H-73a), 4.17 (m, 1H, H-22), 4.16 (m, 1H, H-30), 4.04 (m, 1H, H-18), 4.01 (m, 1H, H-32), 3.90 (m, 1H, H-14), 3.84 (m, 1H, H-34), 3.81 (m, 1H, H-6), 3.80 (m, 1H, H-12), 3.73 (m, 1H, H-24), 3.73 (m, 1H, H-37b), 3.68 (m, 1H, H-2a), 3.68 (m, 1H, H-2b), 3.68 (m, 1H, H-37a), 3.62 (m, 1H, H-38b), 3.62 (m, 1H, H-39), 3.60 (m, 1H, H-40a), 3.60 (m, 1H, H-40b), 3.59 (m, 1H, H-35), 3.58 (m, 1H, H-38a), 3.57 (m, 1H, H-4), 3.53 (m, 1H, H-29), 3.52 (m, 1H, H-21), 2.99 (t, 1H, *J* = 9.1 Hz, H-5), 2.40 (m, 1H, H-31b), 2.37 (m, 1H, H-23b), 2.22 (m, 1H, H-9a), 2.22 (m, 1H, H-9b), 2.20 (m, 1H, H-15a), 2.20 (m, 1H, H-15b), 2.18 (m, 1H, H-11b), 2.10 (m, 1H, H-3b), 2.08 (dd, 1H, *J* = 12.6, 4.8 Hz, H-7b), 1.97 (t, 1H, *J* = 11.9 Hz, H-11a), 1.88 (ddd, 1H, *J* = 14.0, 9.1, 2.1 Hz, H-33b), 1.84 (m, 1H, H-36b), 1.70 (m, 1H, H-20b), 1.70 (m, 1H, H-25b), 1.66 (m, 1H, H-28b), 1.65 (m, 1H, H-13b), 1.65 (m, 1H, H-33a), 1.64 (m, 1H, H-20a), 1.64 (m, 1H, H-36a), 1.62 (m, 1H, H-19a), 1.62 (m, 1H, H-19b), 1.60 (m, 1H, H-28a), 1.55 (m, 1H, H-25a), 1.55 (m, 1H, H-31a), 1.53 (m, 1H, H-3a), 1.48 (m, 1H, H-7a), 1.47 (m, 1H, H-23a), 1.46 (m, 1H, H-26b), 1.46 (m, 1H, H-27b), 1.44 (m, 1H, H-13a), 1.40 (m, 1H, H-27a), 1.37 (m, 1H, H-26a) .

^{13}C{^{1}H} NMR (CD_3OD, 175 MHz) data for **1A**: δ 143.1 (qC, C-10), 136.9 (CH, C-17), 128.8 (CH, C-16), 110.6 (CH_2, C-73), 99.2 (qC, C-8), 84.6 (CH, C-29), 84.5 (CH, C-21), 82.3 (CH, C-39), 81.0 (CH, C-35), 79.1 (CH, C-24), 77.2 (CH, C-5), 75.8 (CH, C-32), 73.8 (CH, C-18), 73.3 (CH, C-22), 73.2 (CH, C-30), 71.9 (CH, C-34), 71.1 (CH, C-4), 70.5 (CH, C-6), 68.4 (CH, C-14), 68.3 (CH, C-12), 63.4 (CH_2, C-40), 63.2 (CH_2, C-38), 60.5 (CH_2, C-2), 59.7 (CH_2, C-37), 44.8 (CH_2, C-9), 44.2 (CH_2, C-7), 43.9 (CH_2, C-13), 42.8 (CH_2, C-31), 42.39 (CH_2, C-15), 42.39 (CH_2, C-23), 41.3 (CH_2, C-11), 40.4 (CH_2, C-33), 37.4 (CH_2, C-25), 35.7 (CH_2, C-3), 35.1 (CH_2, C-19), 34.6 (CH_2, C-36), 30.1 (CH_2, C-28), 27.7 (CH_2, C-26), 27.6 (CH_2, C-27), 26.2 (CH_2, C-20).

1B: Colorless oil; HR-ESIMS *m*/*z* [M + Na]$^+$ (calcd for $C_{34}H_{62}NaO_{13}$, 701.4083, found 701.4088).
^{1}H NMR (CD_3OD, 400 MHz) data for **1B**: δ 5.66 (m, 1H, H-64), 5.51 (dd, 1H, *J* = 15.2, 7.2 Hz, H-65), 5.26 (dd, 1H, *J* = 8.4, 1.2 Hz, H-45), 5.23 (d, 1H, *J* = 8.8 Hz, H-61), 4.67 (td, 1H, *J* = 9.6, 3.2 Hz, H-46), 4.42 (m, 1H, H-50), 4.36 (m, 1H, H-62), 4.17 (m, 1H, H-66), 4.12 (ddd, 1H, *J* = 9.2, 7.6, 2.8 Hz, H-48), 3.97 (m, 1H, H-52), 3.83 (m, 1H, H-58), 3.73 (m, 1H, H-71b), 3.68 (m, 1H, H-69b), 3.65 (m, 1H, H-55b), 3.65 (m, 1H, H-56a), 3.65 (m, 1H, H-56b), 3.63 (m, 1H, H-71a), 3.61 (m, 1H, H-54), 3.60 (m, 1H, H-72b), 3.54 (m, 1H, H-55a), 3.54 (m, 1H, H-69a), 3.53 (m, 1H, H-41a), 3.53 (m, 1H, H-41b), 3.52 (m, 1H, H-72a), 3.41 (m, 1H, H-68), 3.40 (dd, 1H, *J* = 7.6, 4.0 Hz, H-49), 2.38 (m, 1H, H-51b), 2.36 (m, 1H, H-59b), 2.24 (m, 1H, H-63a), 2.24 (m, 1H, H-63b), 2.06 (m, 1H, H-43a), 2.06 (m, 1H, H-43b), 2.06 (m, 1H, H-59a), 1.91 (m, 1H, H-53b), 1.87 (m, 1H, H-47b), 1.77 (m, 1H, H-57b), 1.76 (m, 1H, H-70a), 1.76 (m, 1H, H-70b), 1.75 (m, 1H, H-53a), 1.75 (m, 1H, H-67b), 1.72 (d, 3H, *J* = 1.2 Hz, H_3-75), 1.70 (d, 3H, *J* = 1.2 Hz, H_3-74), 1.65 (m, 1H, H-42a), 1.65 (m, 1H, H-42b), 1.62 (m, 1H, H-67a), 1.59 (m, 1H, H-51a), 1.54 (m, 1H, H-57a), 1.53 (m, 1H, H-47a).

^{13}C{^{1}H} NMR (CD_3OD, 100 MHz) data for **1B**: δ 137.5 (qC, C-44), 136.6 (CH, C-65), 136.0 (qC, C-60), 131.7 (CH, C-61), 129.8 (CH, C-45), 129.0 (CH, C-64), 86.6 (CH, C-49), 79.2 (CH, C-68), 77.2 (CH, C-54), 76.3 (CH, C-52), 75.3 (CH, C-58), 73.2 (CH, C-50), 71.2 (CH, C-66), 69.0 (CH, C-62), 68.0 (CH, C-48), 67.6 (CH_2, C-69), 66.0 (CH, C-46), 65.2 (CH_2, C-55), 64.6 (CH_2, C-72), 62.6 (CH_2, C-41), 60.3 (CH_2, C-56), 59.8 (CH_2, C-71), 46.4 (CH_2, C-59), 43.3 (CH_2, C-47), 42.4 (CH_2, C-51), 41.7 (CH_2, C-63), 40.3 (CH_2, C-67), 40.0 (CH_2, C-53), 37.9 (CH_2, C-57), 36.9 (CH_2, C-43), 34.1 (CH_2, C-70), 31.8 (CH_2, C-42),

17.6 (CH_3, C-75), 16.6 (CH_3, C-74).

1.5 Ozonolysis

Benthol A (**1**) (4.0 mg, 0.0027 mM) of ^{13}C-enriched abundance was dissolved in the mixture of CH_2Cl_2-MeOH (1:1, each 7.5 mL). Ozone was bubbled into the above solution at –78 °C for 5.0 min. Excess amount of $NaBH_4$ was then added and stirred at –78 °C for 3.0 h. The reaction mixture was purified by a C_{18} reversed-phase silica gel column (Daisogel, SP-120-50-ODS-B, 5g, 6.5 cm × 1.0 cm i.d.), eluted with 15.0 mL of water followed by 20.0 mL of MeOH, to afford three fractions. The second fraction was purified by HPLC (YMC-Pack 250 cm × 4.6 mm i.d., MeCN/H_2O, linear-gradient elution from 5% to 100% MeCN within 35 min) to afford five products, viz., fragments **1a** (0.8 mg, t_R = 14.9 min), **1b** (1.4 mg, t_R =17.1 min), **1c** (0.9 mg, t_R = 15.8 min), **1d** (0.2 mg, t_R = 3.0 min), and **1e** (0.4 mg, t_R = 6.1 min).

1a: Colorless oil; LR-ESIMS *m*/*z* 389.2 $[M + Na]^+$.

^1H NMR (CD_3OD, 600 MHz) data for **1a:** δ 4.31 (dddd, 1H, *J* = 9.9, 9.8, 5.0, 2.0 Hz, H-12), 4.04 (m, 1H, *J* = 5.4, 2.5 Hz, H-10), 4.03 (m, 1H, H-14), 3.92 (m, 1H, H-2), 3.82 (ddd, 1H, *J* = 9.0, 9.0, 5.2 Hz, H-6), 3.74 (td, 1H, *J* = 9.6, 9.6, 2.0 Hz, H-4), 3.71 (m, 1H, H-16b), 3.70 (m, 1H, H-16a), 3.47 (dd, 1H, *J* = 10.8, 6.0 Hz, H-1b), 3.42 (dd, 1H, *J* = 10.8, 5.4 Hz, H-1a), 2.97 (dd, 1H, *J* = 9.3, 9.3 Hz, H-5), 2.17 (dt, 1H, *J* = 14.4, 4.8 Hz, H-3b), 1.97 (dd, 1H, *J* = 12.6, 4.8 Hz H-7b), 1.81 (dt, 1H, *J* = 14.4, 2.4 Hz, H-9b), 1.69 (m, 1H, H-15b), 1.66 (m, 1H, H-11b), 1.64 (m, 1H, H-9a), 1.64 (m, 1H, H-15a), 1.59 (m, 1H, H-13b), 1.50 (m, 1H, H-11a), 1.49 (m, 1H, H-13a), 1.48 (m, 1H, H-7a), 1.42 (m, 1H, H-3a).

$^{13}C\{^1H\}$ NMR (CD_3OD, 150 MHz) data for **1a**: δ 99.1 (qC, C-8), 77.3 (CH, C-5), 74.3 (CH, C-4), 73.6 (CH, C-2), 69.9 (CH, C-6), 67.5 (CH_2, C-1), 66.0 (CH, C-14), 65.3 (CH, C-10), 61.9 (CH, C-12), 60.2 (CH_2, C-16), 44.7 (CH_2, C-13), 44.5 (CH_2, C-7), 42.1 (CH_2, C-15), 40.6 (CH_2, C-9), 39.2 (CH_2, C-11), 36.3 (CH_2, C-3).

1b: Colorless oil; LR-ESIMS *m*/*z* 611.3 $[M + H]^+$.

^1H NMR (CD_3OD, 600 MHz) data for **1b:** δ 4.18 (m, 1H, H-22), 4.17 (m, 1H, H-30), 4.17 (m, 1H, H-34), 4.07 (m, 1H, H-32), 3.76 (m, 1H, H-37), 3.75 (m, 1H, H-24), 3.75 (m, 1H, H-44), 3.75 (m, 1H, H-44'), 3.69 (dd, 1H, *J* = 9.6, 1.2 Hz, H-39), 3.62 (m, 1H, H-40), 3.62 (m, 1H, H-41), 3.61 (m, 1H, H-18), 3.60 (m, 1H, H-35), 3.55 (m, 1H, H-29), 3.54 (m, 1H, H-21), 3.49 (dd, 1H, *J* = 11.4, 4.2 Hz, H-17b), 3.48 (dd, 1H, *J* = 9.6, 9.6 Hz, H-38), 3.44 (dd, 1H, *J* = 11.4, 6.6 Hz, H-17a), 2.40 (m, 1H, H-31b), 2.37 (m, 1H, H-23b), 2.03 (ddd, 1H, *J* = 12.3, 5.0, 1.4 Hz, H-36b), 1.98 (m, 1H, H-42b'), 1.94 (m, 1H, H-42b), 1.82 (m, 1H, H-33b), 1.81 (m, 1H, H-20b), 1.70 (m, 1H, H-25b), 1.70 (m, 1H, H-36a), 1.67 (m, 1H, H-19b), 1.67 (m, 1H, H-43b), 1.67 (m, 1H, H-43b')1.65 (m, 1H, H-20a), 1.64 (m, 1H, H-28a), 1.64 (m, 1H, H-28b), 1.56 (m, 1H, H-25a), 1.54 (m, 1H, H-31a), 1.52 (m, 1H, H-43a), 1.52 (m, 1H, H-43a'), 1.52 (m, 1H, H-33a), 1.49 (m, 1H, H-42a'), 1.49 (m, 1H, H-23a), 1.48 (m, 1H, H-26b), 1.48 (m, 1H, H-27b), 1.47 (m, 1H, H-42a), 1.43 (m, 1H, H-19a), 1.40 (m, 1H, H-27a), 1.38 (m, 1H, H-26a), 1.17 (d, 3H, *J* = 6.6 Hz, H_3-74), 1.17 (d, 3H, *J* = 6.6 Hz, H_3-74').

$^{13}C\{^1H\}$ NMR (CD_3OD, 150 MHz) data for **1b**: δ 84.7 (CH, C-29), 84.6 (CH, C-21), 79.0 (CH, C-24), 77.8 (CH, C-35), 75.3 (CH, C-32), 73.5 (CH, C-18), 73.3 (CH, C-30), 73.13 (CH, C-39), 73.13 (CH, C-22), 73.07 (CH, C-40), 73.0 (CH, C-41), 72.7 (CH, C-38), 71.1 (CH, C-37), 68.9 (CH, C-44), 68.7 (CH, C-44'), 67.3 (CH_2, C-17), 67.1 (CH, C-34), 42.6 (CH_2, C-31), 42.3 (CH_2, C-23), 41.7 (CH_2, C-33), 37.3 (CH_2, C-25), 36.5 (CH_2, C-43'), 36.4 (CH_2, C-43), 34.1 (CH_2, C-36), 31.54 (CH_2, C-42), 31.54 (CH_2, C-42'), 31.2 (CH_2, C-19), 30.1 (CH_2, C-28), 27.62 (CH_2, C-26), 27.59 (CH_2, C-27), 26.1 (CH_2, C-20), 23.7 (CH_3, C-74'), 23.4 (CH_3, C-74).

1c: Colorless oil; LR-ESIMS *m*/*z* 381.2 $[M + H]^+$.
^{1}H NMR (CD_3OD, 600 MHz) data for **1c:** δ 4.43 (m, 1H, H-50), 4.13 (ddd, 1H, *J* = 9.5, 7.0, 2.4 Hz, H-48), 4.03 (m, 1H, H-52), 3.99 (ddd, 1H, *J* = 5.8, 3.2, 2.0 Hz, H-56), 3.95 (m, 1H, H-60), 3.89 (m, 1H, H-46), 3.88 (m, 1H, H-58), 3.64 (td, 1H, *J* = 9.6, 9.6, 2.4 Hz, H-54), 3.51 (dd, 1H, *J* = 11.4, 4.8 Hz, H-45b), 3.47 (dd, 1H, *J* = 11.4, 6.6 Hz, H-45a), 3.43 (dd, 1H, *J* = 7.2, 4.2 Hz, H-49), 3.25 (dd, 1H, *J* = 9.8, 3.2 Hz, H-55), 2.37 (m, 1H, H-51b), 2.05 (ddd, 1H, *J* = 15.0, 6.0, 2.4 Hz, H-53b), 1.81 (m, 1H, H-53a), 1.81 (m, 1H, H-57b), 1.80 (m, 1H, H-47b), 1.63 (m, 1H, H-47a), 1.62 (m, 1H, H-51a), 1.60 (m, 1H, H-59b), 1.56 (m, 1H, H-57a), 1.44 (dt, 1H, *J* = 14.4, 4.8 Hz, H-59a), 1.14 (d, 3H, *J* = 6.0 Hz, H_3-75).

$^{13}C\{^1H\}$ NMR (CD_3OD, 150 MHz) data for **1c**: δ 86.6 (CH, C-49), 77.7 (CH, C-52), 75.4 (CH, C-54), 73.2 (CH, C-50), 72.9 (CH, C-55), 71.8 (CH, C-58), 70.2 (CH, C-46), 68.6 (CH, C-56), 68.2 (CH, C-48), 68.1 (CH_2, C-45), 67.6 (CH, C-60), 45.4 (CH_2, C-59), 42.4 (CH_2, C-51), 40.0 (CH_2, C-57), 39.6 (CH_2, C-53), 39.0 (CH_2, C-47), 23.3 (CH_3, C-75).

1d: Colorless oil; HR-ESIMS *m*/*z* $[M + Na]^+$ (calcd for $C_4H_{10}NaO_3$, 129.0522, found 129.0525).
^{1}H NMR (CD_3OD, 600 MHz) data for **1d:** δ 3.75 (m, 1H, H-62), 3.69 (m, 1H, H-64a), 3.69 (m, 1H, H-64b), 3.53 (dd, 1H, *J* = 10.8, 5.4 Hz, H-61b), 3.47 (dd, 1H, *J* = 10.8, 4.8 Hz, H-61a), 1.73 (m, 1H, H-63b), 1.60 (m, 1H, H-63a).
$^{13}C\{^1H\}$ NMR (CD_3OD, 150 MHz) data for **1d**: δ 70.8 (CH, C-62), 67.5 (CH_2, C-61), 60.0 (CH_2, C-64), 37.2 (CH_2, C-63).

1e: Colorless oil; LR-ESIMS *m*/*z* 215.1 $[M + Na]^+$.
^{1}H NMR (CD_3OD, 600 MHz) data for **1e:** δ 4.00 (dd, 1H, *J* = 5.8, 2.8 Hz, H-70), 3.87 (m, 1H, H-66), 3.73 (ddd, 1H, *J* = 12.4, 9.6, 2.4 Hz, H-72b), 3.66 (td, 1H, *J* = 9.6, 9.6, 3.0 Hz, H-68), 3.62 (ddd, 1H, *J* = 12.4, 5.4, 1.5 Hz, H-72a), 3.53 (dd, 1H, *J* = 11.4, 4.8 Hz, H-65b), 3.45 (dd, 1H, *J* = 11.4, 6.0 Hz, H-65a), 3.24 (dd, 1H, *J* = 9.6, 3.0 Hz, H-69), 2.02 (ddd, 1H, *J* = 14.4, 5.4, 3.0 Hz, H-67b), 1.84 (dddd, 1H, *J* = 12.4, 9.8, 5.4, 2.6 Hz, H-71b), 1.75 (dddd, 1H, *J* = 12.4, 5.6, 3.8, 2.0 Hz, H-71a), 1.53 (ddd, 1H, *J* = 14.4, 9.0, 6.6 Hz, H-67a).

$^{13}C\{^1H\}$ NMR (CD_3OD, 150 MHz) data for **1e**: δ 75.5 (CH, C-68), 73.4 (CH, C-69), 71.8 (CH, C-66), 68.1 (CH, C-70), 66.9 (CH_2, C-65), 62.7 (CH_2, C-72), 37.1 (CH_2, C-67), 33.8 (CH_2, C-71).

1.6 Mosher's MTPA Esters 1As/r, 1Bs/r, 1as/r, 1bs/r, 1cs/r, and 1es/r

The fragment **1A** (0.5 mg) was treated with (*R*)-MTPACl (16.0 μL) in dried pyridine (0.6 mL) at room temperature for 12h. The reaction mixture was concentrated and purified by HPLC (YMC-Pack 250 cm × 4.6 mm i.d., MeCN/H_2O, 99:1) to afford the 2,5,6,14,18,22,30,34,37,38,40-*O*-undeca- (*S*)-MTPA ester of **1A**, namely **1As** (1.7 mg, t_R = 18.2 min). The 2,5,6, 14,18,22,30,34,37,38,40-*O*- undeca-(*R*)-MTPA ester of **1A**, namely **1Ar** (1.8 mg, t_R = 18.3 min) was prepared in the same way. Similarly, fragments **1B**, **1b**, and **1c** were esterified with (*R*)- and (*S*)-MTPACl, respectively, to yield **1Bs** (1.5 mg)/**1Br** (1.6 mg), **1bs** (1.4 mg)/**1br** (1.3 mg), and **1cs** (0.9 mg)/**1cr** (1.0 mg).

The fragment **1a** (0.4 mg) was dissolved in pyridine (0.6 mL) and then added with pivaloyl chloride (6.0 μL) at 0 °C. The reaction mixture was stirred for 30.0 min and then added with water (50.0 μL). The mixture was concentrated and dried under vacuum for 8h, and then treated with (*R*)-MTPACl (8.0 μL) in dried pyridine (0.6 mL) at room temperature for 2h. The reaction mixture was concentrated and purified by HPLC (YMC-Pack 250 cm × 4.6 mm i.d., MeCN/H_2O, 92:8) to afford the 2,6,10,14-*O*-tetra-(*S*)-MTPA ester of **1a**, namely **1as** (1.0 mg, t_R = 15.3 min). The 2,6,10,14-*O*-tetra-(*R*)-MTPA ester of **1a**, namely **1ar** (1.1 mg, t_R = 15.2 min) was prepared in the same way. Similarly, the fragment **1e** was esterified with pivaloyl chloride and then treated with (*R*)- and (*S*)-MTPACl, respectively, to yield **1es** (0.5 mg) and **1er**

(0.5 mg). With the aid of key ^{1}H–^{1}H COSY or ^{1}H–^{1}H TOCSY correlations, ^{1}H NMR spectroscopic data of the above products were assigned.

1As: White, amorphous solid; HR-ESIMS *m*/*z* [M + Na]$^+$ calcd for $C_{150}H_{147}F_{33}NaO_{38}$ 3205.8936, found 3205.8930.

^{1}H NMR ($CDCl_3$, 700 MHz) data for **1As**: *δ* 5.60 (m, 1H, H-16), 5.54 (m, 1H, H-6), 5.40 (m, 1H, H-17), 5.38 (m, 1H, H-14), 5.26 (m, 1H, H-30), 5.23 (m, 1H, H-18), 5.23 (m, 1H, H-34), 5.21 (m, 1H, H-22), 5.11 (t, 1H, *J* = 9.8 Hz, H-5), 4.79 (br s, 1H, H-73b), 4.75 (br s, 1H, H-73a), 4.35 (m, 1H, H-2b), 4.26 (m, 1H, H-37b), 4.26 (m, 1H, H-38b), 4.26 (m, 1H, H-40b), 4.18 (dd, 1H, *J* = 11.2, 7.0 Hz, H-40a), 4.14 (m, 1H, H-37a), 4.12 (m, 1H, H-2a), 4.03 (dd, 1H, *J* = 11.9, 4.9 Hz, H-38a), 3.86 (m, 1H, H-4), 3.81 (m, 1H, H-39), 3.65 (m, 1H, H-24), 3.59 (m, 1H, H-35), 3.52 (m, 1H, H-21), 3.49 (m, 1H, H-29), 3.48 (m, 1H, H-12), 3.38 (m, 1H, H-32), 2.47 (dd, 1H, *J* = 12.6, 5.6 Hz, H-7b), 2.44 (m, 1H, H-23b), 2.38 (m, 1H, H-15b), 2.30 (m, 1H, H-15a), 2.22 (d, 1H, *J* = 13.3 Hz, H-9b), 2.18 (m, 1H, H-31b), 2.16 (m, 1H, H-9a), 2.10 (d, 1H, *J* = 12.6 Hz, H-11b), 1.83 (t, 1H, *J* = 12.6 Hz, H-11a), 1.73 (m, 1H, H-3b), 1.73 (m, 1H, H-13b), 1.72 (m, 1H, H-36b), 1.71 (m, 1H, H-3a), 1.67 (m, 1H, H-13a), 1.66 (m, 1H, H-33b), 1.63 (m, 1H, H-19b), 1.63 (m, 1H, H-33a), 1.60 (m, 1H, H-7a), 1.57 (m, 1H, H-19a), 1.57 (m, 1H, H-36a), 1.48 (m, 1H, H-20b), 1.48 (m, 1H, H-25b), 1.47 (m, 1H, H-23a), 1.47 (m, 1H, H-28b), 1.37 (m, 1H, H-31a), 1.36 (m, 1H, H-28a), 1.35 (m, 1H, H-20a), 1.32 (m, 1H, H-25a), 1.24 (m, 1H, H-26b), 1.24 (m, 1H, H-27b), 1.12 (m, 1H, H-26a), 1.12 (m, 1H, H-27a).

1Ar: White, amorphous solid; HR-ESIMS *m*/*z* [M + Na]$^+$ calcd for $C_{150}H_{147}F_{33}NaO_{38}$ 3205.8936, found 3205.8926.

^{1}H NMR ($CDCl_3$, 700 MHz) data for **1Ar:** *δ* 5.64 (m, 1H, H-16), 5.55 (m, 1H, H-6), 5.46 (dd, 1H, *J* = 14.7, 6.3 Hz, H-17), 5.38 (m, 1H, H-18), 5.29 (m, 1H, H-14), 5.29 (m, 1H, H-30), 5.25 (m, 1H, H-22), 5.16 (m, 1H, H-34), 5.10 (t, 1H, *J* = 9.8 Hz, H-5), 4.69 (br s, 1H, H-73a), 4.69 (br s, 1H, H-73b), 4.43 (m, 1H, H-2b), 4.18 (m, 1H, H-37b), 4.17 (m, 1H, H-38b), 4.17 (m, 1H, H-40a), 4.17 (m, 1H, H-40b), 4.10 (m, 1H, H-2a), 4.10 (m, 1H, H-38a), 3.99 (m, 1H, H-37a), 3.86 (m, 1H, H-39), 3.73 (m, 1H, H-4), 3.69 (m, 1H, H-32), 3.65 (m, 1H, H-24), 3.63 (m, 1H, H-29), 3.60 (m, 1H, H-21), 3.60 (m, 1H, H-35), 3.37 (m, 1H, H-12), 2.45 (m, 1H, H-15b), 2.40 (m, 1H, H-23b), 2.37 (m, 1H, H-15a), 2.37 (m, 1H, H-31b), 2.32 (m, 1H, H-7b), 2.16 (d, 1H, *J* = 13.3 Hz, H-9b), 2.08 (d, 1H, *J* = 13.3 Hz, H-9a), 1.90 (d, 1H, *J* = 12.6 Hz, H-11b), 1.77 (m, 1H, H-19b), 1.74 (m, 1H, H-11a), 1.71 (m, 1H, H-19a), 1.69 (m, 1H, H-3b), 1.65 (m, 1H, H-20b), 1.64 (m, 1H, H-13b), 1.62 (m, 1H, H-3a), 1.60 (m, 1H, H-13a), 1.56 (m, 1H, H-28b), 1.52 (m, 1H, H-20a), 1.49 (m, 1H, H-7a), 1.46 (m, 1H, H-28a), 1.46 (m, 1H, H-33b), 1.45 (m, 1H, H-36b), 1.43 (m, 1H, H-33a), 1.42 (m, 1H, H-31a), 1.38 (m, 1H, H-23a), 1.33 (m, 1H, H-36a), 1.32 (m, 1H, H-25b), 1.20 (m, 1H, H-26b), 1.20 (m, 1H, H-27b), 1.18 (m, 1H, H-25a), 1.09 (m, 1H, H-26a), 1.09 (m, 1H, H-27a).

1Bs: White, amorphous solid; HR-ESIMS *m*/*z* [M + Na]$^+$ calcd for $C_{134}H_{132}F_{30}NaO_{33}$ 2861.8064, found 2861.8070.

^{1}H NMR ($CDCl_3$, 700 MHz) data for **1Bs**: *δ* 5.71 (m, 1H, H-46), 5.70 (m, 1H, H-64), 5.56 (m, 1H, H-62), 5.49 (dd, 1H, *J* = 15.4, 7.7 Hz, H-65), 5.43 (m, 1H, H-66), 5.29 (m, 1H, H-48), 5.21 (m, 1H, H-50), 5.04 (br d, 1H, *J* = 8.4 Hz, H-61), 4.94 (br d, 1H, *J* = 9.1 Hz, H-45), 4.44 (dd, 1H, *J* = 11.9, 3.5 Hz, H-69b), 4.34 (m, 1H, H-56b), 4.33 (m, 1H, H-70b), 4.28 (m, 1H, H-41b), 4.25 (m, 1H, H-55a), 4.25 (m, 1H, H-55b), 4.25 (m, 1H, H-70a), 4.20 (m, 1H, H-41a), 4.08 (m, 1H, H-56a), 3.92 (dd, 1H, *J* = 11.9, 5.6 Hz, H-69a), 3.88 (m, 1H, H-52), 3.69 (dd, 1H, *J* = 7.0, 2.8 Hz, H-49), 3.61 (m, 1H, H-54), 3.53 (m, 1H, H-58), 3.34 (m, 1H, H-72b), 3.24 (m, 1H, H-68), 3.20 (m, 1H, H-72a), 2.43 (m, 1H, H-51b), 2.42 (m, 1H, H-63b), 2.28 (m, 1H, H-63a), 2.26 (m, 1H, H-47b), 2.19 (dd, 1H, *J* = 14.0, 4.2 Hz, H-59b), 1.96 (m, 1H, H-43a), 1.96 (m, 1H, H-43b), 1.94 (m, 1H, H-47a), 1.89 (m, 1H, H-67b), 1.88 (m, 1H, H-59a), 1.78 (m, 1H, H-71a), 1.78 (m, 1H, H-71b), 1.76 (m, 1H, H-53b), 1.74 (m, 1H, H-42b), 1.71 (m, 1H, H-42a), 1.64 (m, 1H, H-57b), 1.64 (m, 1H, H-67a), 1.63 (br s, 3H, H_3-75), 1.62 (br s, 3H, H_3-74), 1.55 (m, 1H, H-53a), 1.47

(m, 1H, H-51a), 1.44 (m, 1H, H-57a).

1Br: White, amorphous solid; HR-ESIMS *m*/*z* [M + Na]$^+$ calcd for $C_{134}H_{132}F_{30}NaO_{33}$ 2861.8064, found 2861.8057.
^{1}H NMR ($CDCl_3$, 700 MHz) data for **1Br**: *δ* 5.70 (m, 1H, H-46), 5.57 (m, 1H, H-64), 5.54 (m, 1H, H-62), 5.40 (m, 1H, H-66), 5.30 (dd, 1H, *J* = 15.4, 7.7 Hz, H-65), 5.15 (m, 1H, H-48), 5.14 (m, 1H, H-50), 5.11 (m, 1H, H-45), 5.10 (m, 1H, H-61), 4.46 (dd, 1H, *J* = 11.9, 3.5 Hz, H-69b), 4.31 (m, 1H, H-70b), 4.31 (m, 1H, H-70a), 4.27 (m, 1H, H-56b), 4.26 (m, 1H, H-41b), 4.23 (m, 1H, H-41a), 4.12 (dd, 1H, *J* = 11.9, 2.8 Hz, H-55b), 4.08 (dd, 1H, *J* = 11.9, 4.9 Hz, H-55a), 4.04 (m, 1H, H-56a), 4.02 (dd, 1H, *J* = 11.9, 5.6 Hz, H-69a), 3.86 (m, 1H, H-52), 3.71 (m, 1H, H-49), 3.43 (m, 1H, H-58), 3.42 (m, 1H, H-72b), 3.36 (m, 1H, H-68), 3.34 (m, 1H, H-54), 3.25 (m, 1H, H-72a), 2.37 (m, 1H, H-63b), 2.26 (m, 1H, H-51b), 2.21 (m, 1H, H-47b), 2.19 (m, 1H, H-59b), 2.19 (m, 1H, H-63a), 2.00 (m, 1H, H-43a), 2.00 (m, 1H, H-43b), 1.87 (m, 1H, H-47a), 1.87 (m, 1H, H-67b), 1.86 (m, 1H, H-59a), 1.82 (m, 1H, H-71a), 1.82 (m, 1H, H-71b), 1.76 (m, 1H, H-42a), 1.76 (m, 1H, H-42b), 1.64 (m, 1H, H-67a), 1.60 (m, 1H, H-57b), 1.59 (br s, 3H, H_3-74), 1.59 (br s, 3H, H_3-75), 1.42 (m, 1H, H-53b), 1.41 (m, 1H, H-57a), 1.26 (m, 1H, H-51a), 1.14 (m, 1H, H-53a).

1as: Colorless oil; HR-ESIMS *m*/*z* [M + H]$^+$ calcd for $C_{66}H_{75}F_{12}O_{19}$ 1399.4705, found 1399.4731.
^{1}H NMR (CD_3OD, 600 MHz) data for **1as**: *δ* 5.48 (m, 1H, H-2), 5.38 (m, 1H, H-14), 5.35 (m, 1H, H-10), 5.28 (m, 1H, H-6), 4.40 (dd, 1H, *J* = 12.6, 1.8 Hz, H-1b), 3.99 (m, 1H, H-12), 3.96 (m, 1H, H-1a), 3.96 (m, 1H, H-16b), 3.80 (m, 1H, H-16a), 3.64 (m, 1H, H-4), 3.28 (t, 1H, *J* = 9.6 Hz, H-5), 2.14 (dd, 1H, *J* = 12.0, 4.8 Hz, H-7b), 2.00 (m, 1H, H-15b), 1.98 (m, 1H, H-11b), 1.91 (m, 1H, H-3b), 1.90 (m, 1H, H-9b), 1.86 (m, 1H, H-15a), 1.83 (m, 1H, H-3a), 1.80 (m, 1H, H-13a), 1.80 (m, 1H, H-13b), 1.73 (m, 1H, H-11a), 1.72 (m, 1H, H-9a), 1.51 (t, 1H, *J* = 12.0 Hz, H-7a).

1ar: Colorless oil; HR-ESIMS *m*/*z* [M + H]$^+$ calcd for $C_{66}H_{75}F_{12}O_{19}$ 1399.4705, found 1399.4719.
^{1}H NMR (CD_3OD, 600 MHz) data for **1ar**: *δ* 5.44 (m, 1H, H-2), 5.37 (m, 1H, H-10), 5.28 (m, 1H, H-6), 5.19 (m, 1H, H-14), 4.09 (m, 1H, H-16a), 4.09 (m, 1H, H-16b), 3.91 (dd, 1H, *J* = 12.6, 1.8 Hz, H-1b), 3.86 (dd, 1H, *J* = 12.6, 4.8 Hz, H-1a), 3.68 (m, 1H, H-12), 3.50 (m, 1H, H-4), 3.38 (t, 1H, *J* = 9.6 Hz, H-5), 2.08 (dd, 1H, *J* = 12.0, 4.8 Hz, H-7b), 2.07 (m, 1H, H-3b), 2.06 (m, 1H, H-15b), 1.96 (m, 1H, H-9b), 1.90 (m, 1H, H-15a), 1.88 (m, 1H, H-3a), 1.86 (m, 1H, H-9a), 1.78 (m, 1H, H-13a), 1.78 (m, 1H, H-13b), 1.75 (m, 1H, H-11b), 1.57 (m, 1H, H-11a), 1.50 (t, 1H, *J* = 12.0 Hz, H-7a).

1bs: White, amorphous solid; HR-ESIMS *m*/*z* [M + H]$^+$ calcd for $C_{119}H_{118}F_{27}O_{31}$ 2555.7220, found 2555.7216.
^{1}H NMR ($CDCl_3$, 700 MHz) data for **1bs**: *δ* 5.33 (m, 1H, H-30), 5.26 (m, 1H, H-34), 5.25 (m, 1H, H-22), 5.21 (m, 1H, H-18), 5.19 (m, 1H, H-37), 5.11 (m, 1H, H-38'), 5.09 (m, 1H, H-38), 4.92 (m, 1H, H-44'), 4.89 (m, 1H, H-44), 4.81 (m, 1H, H-41'), 4.80 (m, 1H, H-41), 4.48 (dd, 1H, *J* = 11.9, 2.1 Hz, H-17b), 4.18 (dd, 1H, *J* = 11.9, 5.6 Hz, H-17a), 4.08 (m, 1H, H-35), 3.68 (m, 1H, H-24), 3.66 (m, 1H, H-39'), 3.58 (m, 1H, H-39), 3.53 (m, 1H, H-29), 3.51 (m, 1H, H-21), 3.50 (m, 1H, H-40'), 3.48 (m, 1H, H-40), 3.47 (m, 1H, H-32), 2.48 (m, 1H, H-23b), 2.36 (m, 1H, H-31b), 1.90 (m, 1H, H-36b), 1.79 (m, 1H, H-33b), 1.73 (m, 1H, H-36a), 1.70 (m, 1H, H-19b), 1.65 (m, 1H, H-33a), 1.59 (m, 1H, H-42a'), 1.59 (m, 1H, H-42b'), 1.58 (m, 1H, H-42a), 1.58 (m, 1H, H-42b), 1.54 (m, 1H, H-19a), 1.50 (m, 1H, H-31a), 1.49 (m, 1H, H-23a), 1.47 (m, 1H, H-28b), 1.43 (m, 1H, H-25b), 1.42 (m, 1H, H-20b), 1.41 (m, 1H, H-28a), 1.38 (m, 1H, H-43a), 1.38 (m, 1H, H-43b), 1.33 (m, 1H, H-20a), 1.33 (m, 1H, H-25a), 1.29 (m, 1H, H-43a'), 1.29 (m, 1H, H-43b'), 1.28 (m, 1H, H-27b), 1.25 (m, 1H, H-26b), 1.16 (d, 3H, *J* = 6.3 Hz, H_3-74), 1.15 (m, 1H, H-26a), 1.13 (m, 1H, H-27a), 1.06 (d, 3H, *J* = 6.3 Hz, H_3-74').

1br: White, amorphous solid; HR-ESIMS *m*/*z* [M + H]$^+$ calcd for $C_{119}H_{118}F_{27}O_{31}$ 2555.7220, found 2555.7240.
^{1}H NMR ($CDCl_3$, 700 MHz) data for **1br**: *δ* 5.32 (m, 1H, H-30), 5.31 (m, 1H, H-18), 5.24 (m, 1H, H-22), 5.21(dd, 1H, *J* = 9.8, 4.9 Hz, H-38), 5.20 (dd, 1H, *J* = 9.8, 4.9 Hz, H-38'), 5.12 (m, 1H, H-37), 5.02 (m, 1H, H-34), 5.00 (m, 1H, H-44'), 4.96 (m, 1H, H-44), 4.83 (m, 1H, H-41), 4.78 (m, 1H, H-41'), 4.50 (dd, 1H, *J* = 11.9, 2.1 Hz, H-17b), 4.17 (dd, 1H, *J* = 11.9, 5.6 Hz, H-17a), 3.67 (m, 1H, H-39), 3.67 (m, 1H, H-24), 3.66 (m, 1H, H-35), 3.66 (m, 1H, H-39'), 3.63 (m, 1H, H-32), 3.61 (m, 1H, H-29), 3.56 (m, 1H, H-21), 3.16 (m, 1H, H-40), 3.12 (m, 1H, H-40'), 2.50 (m, 1H, H-31b), 2.42 (m, 1H, H-23b), 1.76 (m, 1H, H-19b), 1.73 (m, 1H, H-36b), 1.71 (m, 1H, H-19a), 1.67 (m, 1H, H-42a), 1.67 (m, 1H, H-42b), 1.64 (m, 1H, H-42a'), 1.64 (m, 1H, H-42b'), 1.63 (m, 1H, H-33b), 1.59 (m, 1H, H-20b), 1.59 (m, 1H, H-28b), 1.54 (m, 1H, H-43a'), 1.53 (m, 1H, H-43a), 1.52 (m, 1H, H-33a), 1.49 (m, 1H, H-20a), 1.48 (m, 1H, H-28a),1.47 (m, 1H, H-31a), 1.46 (m, 1H, H-36a), 1.41 (m, 1H, H-43b'), 1.39 (m, 1H, H-23a), 1.39 (m, 1H, H-43b), 1.29 (m, 1H, H-25b), 1.29 (m, 1H, H-27b), 1.25 (d, 3H, *J* = 6.3 Hz, H_3-74'), 1.23 (m, 1H, H-25a), 1.22 (m, 1H, H-26b), 1.16 (d, 3H, *J* = 6.3 Hz, H_3-74), 1.13 (m, 1H, H-26a), 1.12 (m, 1H, H-27a).

1cs: Colorless oil; HR-ESIMS *m*/*z* [M + H]$^+$ calcd for $C_{87}H_{82}F_{21}O_{23}$ 1893.4906, found 1893.4936.
^{1}H NMR (CD_3OD, 400 MHz) data for **1cs**: *δ* 5.55 (m, 1H, H-56), 5.40 (m, 1H, H-46), 5.26 (m, 1H, H-48), 5.26 (m, 1H, H-50), 5.12 (dd, 1H, *J* = 10.4, 2.8 Hz, H-55), 5.09 (m, 1H, H-60), 4.54 (dd, 1H, *J* = 12.8, 2.8 Hz, H-45b), 4.12 (dd, 1H, *J* = 12.8, 5.2 Hz, H-45a), 4.05 (m, 1H, H-52), 3.74 (dd, 1H, *J* = 7.2, 3.2 Hz, H-49), 3.67 (m, 1H, H-54), 3.10 (m, 1H, H-58), 2.54 (m, 1H, H-51b), 2.18 (m, 1H, H-47b), 2.06 (m, 1H, H-47a), 1.87 (m, 1H, H-53b), 1.80 (m, 1H, H-57b), 1.80 (m, 1H, H-59b), 1.68 (m, 1H, H-53a), 1.44 (m, 1H, H-51a), 1.43 (m, 1H, H-57a), 1.42 (m, 1H, H-59a), 1.00 (d, 3H, *J* = 6.4 Hz, H_3-75).

1cr: Colorless oil; HR-ESIMS *m*/*z* [M + H]$^+$ calcd for $C_{87}H_{82}F_{21}O_{23}$ 1893.4906, found 1893.4932.
^{1}H NMR (CD_3OD, 400 MHz) data for **1cr**: *δ* 5.61 (m, 1H, H-56), 5.32 (m, 1H, H-46), 5.20 (m, 1H, H-60), 5.13 (m, 1H, H-50), 5.12 (m, 1H, H-48), 4.96 (dd, 1H, *J* = 10.4, 2.8 Hz, H-55), 4.54 (dd, 1H, *J* = 12.8, 2.8 Hz, H-45b), 4.17 (dd, 1H, *J* = 12.8, 5.2 Hz, H-45a), 3.78 (m, 1H, H-52), 3.74 (dd, 1H, *J* = 7.2, 3.2 Hz, H-49), 3.51 (m, 1H, H-58), 3.41 (m, 1H, H-54), 2.38 (m, 1H, H-51b), 2.04 (m, 1H, H-47b), 2.00 (m, 1H, H-47a), 1.86 (m, 1H, H-57b), 1.77 (m, 1H, H-59b), 1.67 (m, 1H, H-57a), 1.59 (m, 1H, H-59a), 1.26 (d, 3H, *J* = 6.4 Hz, H_3-75), 1.24 (m, 1H, H-53b), 1.16 (m, 1H, H-51a), 0.96 (m, 1H, H-53a).

1es: Colorless oil; LR-ESIMS *m*/*z* 956.6 [M + Cl]$^-$.
^{1}H NMR (CD_3OD, 600 MHz) data for **1es**: *δ* 5.56 (m, 1H, H-70), 5.47 (m, 1H, H-66), 5.03 (dd, 1H, *J* = 9.6, 2.4 Hz, H-69), 4.39 (dd, 1H, *J* = 12.6, 2.4 Hz, H-65b), 4.10 (dd, 1H, *J* = 12.6, 6.0 Hz, H-65a), 3.76 (td, 1H, *J* = 10.2, 2.4 Hz, H-68), 3.55 (ddd, 1H, *J* = 12.0, 4.8, 1.2 Hz, H-72b), 3.05 (td, 1H, *J* = 12.0, 2.4 Hz, H-72a), 2.01 (m, 1H, H-71b), 1.96 (m, 1H, H-67b), 1.84 (m, 1H, H-67a), 1.75 (m, 1H, H-71a).

1er: Colorless oil; LR-ESIMS *m*/*z* 956.6 [M + Cl]$^-$.
^{1}H NMR (CD_3OD, 600 MHz) data for **1er**: *δ* 5.75 (m, 1H, H-70), 5.30 (m, 1H, H-66), 5.04 (dd, 1H, *J* = 9.6, 2.4 Hz, H-69), 4.08 (dd, 1H, *J* = 12.6, 2.4 Hz, H-65b), 3.82 (dd, 1H, *J* = 12.6, 6.0 Hz, H-65a), 3.76 (ddd, 1H, *J* = 12.0, 4.8, 1.2 Hz, H-72b), 3.63 (td, 1H, *J* = 10.2, 2.4 Hz, H-68), 3.50 (td, 1H, *J* = 12.0, 2.4 Hz, H-72a), 2.18 (m, 1H, H-71b), 1.97 (m, 1H, H-71a), 1.72 (m, 1H, H-67b), 1.53 (m, 1H, H-67a).

1.7 Relative Configurations of Segments Established by *J*BCA.

For the C32−C34 segment in **1A**, the anti orientations between H32/H33b and H34/H33a were suggested by the large $^3J_{H32,H33b}$ (9.5 Hz) and $^3J_{H34,H33a}$ (9.2 Hz), respectively, while the gauche orientations between H32/H33a and H34/H33b were provided by the small $^3J_{H32,H33a}$ (3.0 Hz) and $^3J_{H34,H33b}$ (3.5 Hz), respectively (Figure S3A). The anti orientations between 32-*O*/H33a and 34-OH/H33b

were deduced from the small $^{2}J_{C32,H33a}$ (-2.0 Hz) and $^{2}J_{C34,H33b}$ (-0.6 Hz), respectively, whereas the gauche orientations between 32-*O*/H33b and 34-OH/H33a were assigned by the large $^{2}J_{C32,H33b}$ (-5.2 Hz) and $^{2}J_{C34,H33a}$ (-6.9 Hz), respectively. The gauche orientations between C31/H33a and C31/H33b were assigned by the small $^{3}J_{C31,H33a}$ (2.6 Hz) and $^{3}J_{C31,H33b}$ (2.9 Hz), respectively. Similarly, the gauche orientations between C35/H33a and C35/H33b were established by the small $^{3}J_{C35,H33a}$ (3.0 Hz) and $^{3}J_{C35,H33b}$ (1.6 Hz), respectively. Thus, the relative configuration between 32-*O* and 34-OH was concluded to be anti (Figure S3A). For the C34−C35 segment in **1A**, the gauche orientation between H34/H35 was supported by the small $^{3}J_{H34,H35}$ (2.9 Hz). The anti orientations between 34-OH/H35 and 35-*O*/H34 were indicated by the small $^{2}J_{C34,H35}$ (0.9 Hz) and $^{2}J_{C35,H34}$ (0.9 Hz), respectively, whereas the gauche orientations between C33/H35 and C36/H34 were established by the small $^{3}J_{C33,H35}$ (1.0 Hz) and $^{3}J_{C36,H34}$ (2.5 Hz), respectively. Therefore, the relationship between 34-OH and 35-*O* was assigned as *syn*. Finally, the relative configuration of the C32−C35 segment in **1A** was determined to be (anti/*syn*) along the direction of the wedge-shaped carbon chain (Figure S3A).

For the C46−C49 segment in **1B**, the anti orientations between H46/H47b and H48/H47a were indicated by the large $^{3}J_{H46,H47b}$ (9.6 Hz) and $^{3}J_{H48,H47a}$ (9.5 Hz), respectively, while the gauche orientations between H46/H47a and H48/H47b were assigned by the small $^{3}J_{H46,H47a}$ (3.1 Hz) and $^{3}J_{H48,H47b}$ (2.3 Hz), respectively. The gauche orientations between 46-OH/H47b and 48-OH/H47a were elucidated by the large $^{2}J_{C46,H47b}$ (-6.5 Hz) and $^{2}J_{C48,H47a}$ (-6.9 Hz), respectively, whereas the anti orientations between 46-OH/H47a and 48-OH/H47b were indicated by the small $^{2}J_{C46,H47a}$ (-1.6 Hz) and $^{2}J_{C48,H47b}$ (-1.8 Hz), respectively. The gauche orientations between C-27/H-29a, C-27/H-29b, C-31/H-29a, C-31/H-29b were supported by the small $^{3}J_{C45,H47a}$ (1.6 Hz), $^{3}J_{C45,H47b}$ (1.8 Hz), $^{3}J_{C49,H47a}$ (1.7 Hz), and $^{3}J_{C49,H47b}$ (1.9 Hz), respectively. Thus, the orientation between 46-OH and 48-OH was assigned as anti (Figure S3B). Similarly, the anti orientation between H48/H49 was indicated by the large $^{3}J_{H48,H49}$ (7.5 Hz), while the gauche orientations between 48-OH/H49 and 49-*O*/H48 were assigned by the large $^{2}J_{C48,H49}$ (-4.5 Hz) and $^{2}J_{C49,H48}$ (-4.2 Hz), respectively. The gauche orientations between C50/H48 and C47/H49 were suggested by the small $^{3}J_{C50,H48}$ (1.8 Hz) and $^{3}J_{C47,H49}$ (2.8 Hz), respectively. Therefore, the orientation between 48-OH and 49-*O* was assigned as anti. Based on the above results, the (anti/anti) relationship was concluded for the relative configuration of the C46−C49 segment in **1B** (Figure S3B).

For the C52−C54 segment in **1B**, the moderate $^{3}J_{H52,H53a}$ (5.4 Hz) and $^{3}J_{H52,H53b}$ (6.7 Hz) suggested two interconverting conformations for both H52/H53a and H52/H53b. Similarly, the $^{2}J_{C52,H53a}$ (-2.4 Hz) and $^{3}J_{C51,H53b}$ (3.4 Hz) indicated two alternating conformations for both 52-*O*/H53a and C51/H53b. The large $^{2}J_{C52,H53b}$(-6.9 Hz) and the small $^{3}J_{C51,H53a}$ (2.8 Hz) revealed that both 52-*O*/H53b and C51/H53a remained in a gauche orientation. Thus, two alternating conformers were assigned for the C52−C53 segment (Figure S3C). The anti orientations between H54/H53a and C55/H53b were determined by the large $^{3}J_{H54,H53a}$ (8.2 Hz) and $^{3}J_{C55,H53b}$ (7.4 Hz), respectively, whereas the gauche orientations between H54/H53b, C55/H53a, 54-*O*/H53a, and 54-*O*/H53b were supported by the small $^{3}J_{H54,H53b}$ (4.0 Hz) and $^{3}J_{C55,H53a}$ (1.2 Hz), and the large $^{2}J_{C54,H53a}$ (-6.0 Hz) and $^{2}J_{C54,H53b}$ (-6.2 Hz), respectively. Finally, the relative configuration between 52-*O* and 54-*O* in **1B** was assigned as *syn* (Figure S3C).

For the C66−C68 segment in **1B**, the intermediate $^{3}J_{H66,H67a}$ (7.0 Hz) and $^{3}J_{H66,H67b}$ (7.0 Hz) suggested two interconverting conformations for both H66/H67a and H66/H67b. Similarly, the moderate $^{2}J_{C66,H67a}$ (-3.8 Hz) and $^{3}J_{C65,H67b}$ (5.5 Hz) indicated two alternating conformations for both 66-OH/H67a and C65/H67b. The large $^{2}J_{C66,H67b}$ (-5.7 Hz) and the small $^{3}J_{C65,H67a}$ (2.2 Hz) revealed that both 66-OH/H67b and C65/H67a remained in a gauche orientation. Thus, two alternating conformers were assigned for the C66−C67 segment (Figure S3D). Similarly, the intermediate $^{3}J_{H68,H67a}$ (5.0 Hz) and $^{3}J_{H68,H67b}$ (4.9 Hz) indicated two interconverting conformations for both H68/H67a and H68/H67b. The $^{2}J_{C68,H67a}$ (-2.3 Hz) and $^{3}J_{C69,H67b}$ (5.7 Hz) suggested two alternating conformations for both 68-*O*/H67a and C69/H67b. The large $^{2}J_{C68,H67b}$ (-6.8 Hz) and the small $^{3}J_{C69,H67a}$ (1.2 Hz) revealed that both 68-*O*/H67b and C69/H67a were in a gauche orientation. Therefore, two alternating conformers were

assigned for the C67−C68 segment. Based on the above results, the relative configuration between 66-OH and 68-*O* in **1B** was determined as *syn* (Figure S3D). To sum up, the relative configurations of the C32−C35 segment in **1A**, and the C46−C49, C52−C54, and C66−C68 segments in **1B** were assigned as (anti/*syn*), (anti/anti), *syn*, and *syn*, respectively, by application of *J*BCA.

In conclusion, the relative configurations of the C32−C35 segment in **1A**, and the C46−C49, C52−C54, and C66−C68 segments in **1B** were assigned as (anti/*syn*), (anti/anti), *syn*, and *syn*, respectively, by application of *J*BCA (Figure S3).

1.8 Computational Details

Mixed torsional/low-mode conformational searches were carried out by means of the Macromodel 10.8.011 software using the MMFF with an implicit solvent model for $CHCl_3$ applying a 21 kJ/mol energy window.[107] Geometry re-optimizations of the resultant conformers [B3LYP/6-31+G(d,p) level in vacuo] and DFT-NMR calculations [mPW1PW91/6-311+G(2d,p)] were performed with Gaussian 09 package.[108] Computed NMR shift data were corrected with I = 185.6277 and S = −1.0175 for MeOH.[109,110] Boltzmann distributions were estimated from the B3LYP energies. Model compounds for DFT-NMR calculations were shown in Figure S5B.

1.9 Principal Component Analysis (PCA)

The structural characteristic data of SCCCs were imported into the SIMCA-P software package (v14.1, Umetric, Umea°, Sweden) for PCA analysis.[111,112] The normalized data were used to categorize benthol A (**1**) and previously reported 187 known SCCCs from marine dinoflagellates of eight genera, viz., *Amphidinium*, *Gambierdiscus*, *Karenia*, *Karlodinium*, *Ostreopsis*, *Prorocentrum*, *Protoceratium*, and *Symbiodinium*. The summary of fit report was shown in Figure S6, whereas partial enlarged view of PCA score plot of **1** and previously reported 187 SCCCs was shown in Figure S7.

1.10 Bioassay

1.10.1 *In vitro* Antiplasmodial Assay

P. falciparum 3D7 (drug-sensitive) was cultured according to the method described by Trager and Jensen.[113] Parasites were maintained in fresh human erythrocytes at 2% hematocrit in complete culture medium (Thermo Fisher Scientific Cat# 22400089) containing 0.5% AlbuMAX II (Thermo Fisher Scientific Cat# 11021045). *In vitro* drug screening was performed using the SYBR green I fluorescence assay.[114] Synchronous ring-stage parasites (> 80%) were plated in triplicate at 2% hematocrit and 0.5% parasitemia in 100.0 µL and treated with serial dilutions of compounds at 37°C for 72 h. *In vitro* antiplasmodial activity was expressed as the compound concentration that inhibited parasite growth by 50%. The experiments were repeated three times.

1.10.2 *In vitro* HIV-1-Inhibitory Assay

293 T cells (2×10^5) were co-transfected with 0.6 µg of pNL-Luv-E^--Vpu^- and 0.4 µg of pHIT/G. After 48h, the VSV-G pseudotyped viral supernatant (HIV-1) was harvested by filtration through a 0.45 µm filter and the concentration of viral capsid protein was determined by p24 antigen capture ELISA (Biomerieux). SupT1 cells were exposed to VSV-G pseudotyped HIV-1 (MOI = 1) at 37 °C for 48 h in the absence or presence of the test compounds. Efavirenz was used as the positive control. The inhibition rates were determined by using a firefly Luciferase Assay System (Promega).[115]

References

1. Inuzuka, T., Yamamoto, Y., Yamada, K., and Uemura, D. (2012). Amdigenol A, a long carbon-backbone polyol compound, produced by the marine dinoflagellate *Amphidinium* sp.. Tetrahedron Lett. *53*, 239–242.
2. Matsuda, M., Kubota, Y., Funabiki, K., Uemura, D., and Inuzuka, T. (2020). Amdigenol D, a long carbon-chain polyol, isolated from the marine dinoflagellate *Amphidinium* sp.. Tetrahedron Lett. *61*, 152376.
3. Inuzuka, T., Yamada, K., and Uemura, D. (2014). Amdigenols E and G, long carbon-chain polyol compounds, isolated from the marine dinoflagellate *Amphidinium* sp.. Tetrahedron Lett. *55*, 6319–6323.
4. Kubota, T., Sakuma, Y., Shimbo, K., Tsuda, M., Nakano, M., Uozumi, Y., and Kobayashi, J. (2006). Amphezonol A, a novel polyhydroxyl metabolite from marine dinoflagellate *Amphidinium* sp.. Tetrahedron Lett. *47*, 4369–4371.
5. Satake, M., Murata, M., Yasumoto, T., Fujita, T., and Naoki, H. (1991). Amphidinol, a Polyhydroxypolyene Antifungal Agent with an Unprecedented Structure, from a Marine Dinoflagellate, *Amphidinium klebsii*. J. Am. Chem. Soc. *113*, 9859–9861.
6. Paul, G.K., Matsumori, N., Murata, M., and Tachibana, K. (1995). Isolation and Chemical Structure of Amphidinol 2, a Potent Hemolytic Compound from Marine Dinoflagellate *Amphidinium klebsii*. Tetrahedron Lett. *36*, 6279–6282.
7. Murata, M., Matsuoka, S., Matsumori, N., Paul, G.K. and Tachibana, K. (1999). Absolute Configuration of Amphidinol 3, the First Complete Structure Determination from Amphidinol Homologues: Application of a New Configuration Analysis Based on Carbon-Hydrogen Spin-Coupling Constants. J. Am. Chem. Soc. *121*, 870–871.
8. Houdai, T., Matsuoka, S., Murata, M., Satake, M., Ota, S., Oshima, Y., and Rhodes, L.L. (2001). Acetate labeling patterns of dinoflagellate polyketides, amphidinols 2, 3 and 4. Tetrahedron *57*, 5551–5555.
9. Paul, G.K., Matsumori, N., Konoki, K., Murata, M., and Tachibana, K. (1997). Chemical structures of amphidinols 5 and 6 isolated from marine dinoflagellate *Amphidinium klebsii* and their cholesterol-dependent membrane disruption. J. Mar. Biotechnol. *5*, 124–128.
10. Morsy, N., Matsuoka, S., Houdai, T., Matsumori, N., Adachi, S., Murata, M., Iwashita, T., and Fujita, T. (2005). Isolation and structure elucidation of a new amphidinol with a truncated polyhydroxyl chain from *Amphidinium klebsii*. Tetrahedron *61*, 8606–8610.
11. Morsy, N., Houdai, T., Matsuoka, S., Matsumori, N., Adachi, S., Oishi, T., Murata, M., Iwashita, T., and Fujita, T. (2006). Structures of new amphidinols with truncated polyhydroxyl chain and their membrane-permeabilizing activities. Bioorg. Med. Chem. *14*, 6548–6554.
12. Echigoya, R., Rhodes, L., Oshima, Y., and Satake, M. (2005). The structures of five new antifungal and hemolytic amphidinol analogs from *Amphidinium carterae* collected in New Zealand. Harmful Algae *4*, 383–389.
13. Meng, Y., Van Wagoner, R.M., Misner, I., Tomas, C., and Wright, J.L.C. (2010). Structure and Biosynthesis of Amphidinol 17, a Hemolytic Compound from *Amphidinium carterae*. J. Nat. Prod. *73*, 409–415.
14. Nuzzo, G., Cutignano, A., Sardo, A., and Fontana, A. (2014). Antifungal Amphidinol 18 and Its 7-Sulfate Derivative from the Marine Dinoflagellate *Amphidinium carterae*. J. Nat. Prod. *77*, 1524–1527.
15. Satake, M., Cornelio, K., Hanashima, S., Malabed, R., Murata, M., Matsumori, N., Zhang, H., Hayashi, F., Mori, S., Kim, J.S., Kim, C.-H., and Lee, J.-S. (2017). Structures of the Largest Amphidinol Homologues from the Dinoflagellate *Amphidinium carterae* and Structure-Activity Relationships. J. Nat. Prod. *80*, 2883–2888.
16. Martínez, K.A., Lauritano, C., Druka, D., Romano, G., Grohmann, T., Jaspars, M., Martín, J., Díaz, C., Cautain, B., de la Cruz, M., Lanora, A., and Reyes, F. (2019). Amphidinol 22, a New Cytotoxic and Antifungal Amphidinium from the Dinoflagellate *Amphidinium carterae*. Mar. Drugs *17*, 385.
17. Cutignano, A., Nuzzo, G., Sardo, A., and Fontana, A. (2017). The Missing Piece in Biosynthesis of Amphidinols: First Evidence of Glycolate as a Starter Unit in New Polyketides from *Amphidinium carterae*. Mar. Drugs *15*, 157.
18. Huang, S.-J., Kuo, C.-M., Lin, Y.-C., Chen, Y.-M., and Lu, C.-K. (2009). Carteraol E, a potent polyhydroxyl ichthyotoxin from the dinoflagellate *Amphidinium carterae*. Tetrahedron Lett. *50*, 2512–2515.
19. Kobayashi, J., Kubota, T., Takahashi, M., Ishibashi, M., Tsuda, M., and Naoki, H. (1999). Colopsinol A, a Novel Polyhydroxyl Metabolite from Marine Dinoflagellate *Amphidinium* sp.. J. Org. Chem. *64*,

1478–1482.
20. Kubota, T., Tsuda, M., Takahashi, M., Ishibashi, M., Naoki, H., and Kobayashi, J. (1999). Colopsinols B and C, new long chain polyhydroxy compounds from cultured marine dinoflagellate *Amphidinium* sp.. J. Chem. Soc. Perkin Trans. 1, 3483–3487.
21. Kubota, T., Tsuda, M., Takahashi, M., Ishibashi, M., Oka, S., and Kobayashi, J. (2000). Colopsinols D and E, New polyhydroxyl Linear Carbon Chain Compounds from Marine Dinoflagellate *Amphidinium* sp.. Chem. Pharm. Bull. *48*, 1447–1451.
22. Li, W., Yan, R., Yu, Y., Shi, Z., Mándi, A., Shen, L., Kurtán, T., and Wu, J. (2020). Determination of the absolute configuration of super-carbon-chain compounds by a combined chemical, spectroscopic, and computational approach: Gibbosols A and B. Angew. Chem. Int. Ed. *59*, 13028–13036.
23. Li, W., Luo, Z., Zhu, Y., Yu, Y., Wu, J., Shen, L. (2020). A Polyol-Polyol Super-Carbon-Chain Compound Containing Thirty-Six Carbon Stereocenters from the Dinoflagellate *Amphidinium gibbosum*: Absolute Configuration and Multi-Segment Modification. Mar. Drugs *18*, 590.
24. Washida, K., Koyama, T., Yamada, K., Kita, M., and Uemura, D. (2006). Karatungiols A and B, two novel antimicrobial polyol compounds, from the symbiotic marine dinoflagellate *Amphidinium* sp.. Tetrahedron Lett. *47*, 2521–2525.
25. Huang, X.-C., Zhao, D., Guo, Y.-W., Wu, H.-M., Lin, L.-P., Wang, Z.-H, Ding, J., and Lin, Y.-S. (2004). Lingshuiol, a novel polyhydroxyl compound with strongly cytotoxic activity from the marine dinoflagellate *Amphidinium* sp.. Bioorg. Chem. Lett. *14*, 3117–3120.
26. Huang, X.-C., Zhao, D., Guo, Y.-W., Wu, H.-M., Trivellone, E., and Cimino, G. (2004). Lingshuiols A and B, two new polyhydroxy compounds from the Chinese marine dinoflagellate *Amphidinium* sp.. Tetrahedron Lett. *45*, 5501–5504.
27. Doi, Y., Ishibashi, M., Nakamichi, H., Kosaka, T., Ishikawa, T., and Kobayashi, J. (1997). Luteophanol A, a New Polyhydroxyl Compound from Symbiotic Marine Dinoflagellate *Amphidinium* sp.. J. Org. Chem. *62*, 3820–3823.
28. Kubota, T., Tsuda, M., Doi, Y., Takahashi, A., Nakamichi, H., Ishibashi, M., Fukushi, E., Kawabata, J., and Kobayashi, J. (1998). Luteophanols B and C, New Polyhydroxyl Compounds from Marine Dinoflageilate *Amphidinium* sp.. Terahedron *54*, 14455–14464.
29. Kubota, T., Takahashi, A., Tsuda, M., and Kobayashi, J. (2005). Luteophanol D, New Polyhydroxyl Metabolite from Marine Dinoflagellate *Amphidinium* sp.. Mar. Drugs *3*, 113–118.
30. Hanif, N., Ohno, O., Kitamura, M., Yamada, K., and Uemura, D. (2010). Symbiopolyol, a VCAM-1 Inhibitor from a Symbiotic Dinoflagellate of the Jellyfish *Mastigias papua*. J. Nat. Prod. *73*, 1318–1322.
31. Murata, M., Legrand, A.M., Ishibashi, Y., Fukui, M., and Yasumoto, T. (1990). Structures and configurations of ciguatoxin from the moray eel *Gymnothorax javanicus* and its likely precursor from the dinoflagellate *Gambierdiscus toxicus.* J. Am. Chem. Soc. *112*, 4380–4386.
32. Satake, M., Morohashi, A., Oguri, H., Oishi, T., Hirama, M., Harada, N., and Yasumoto, T. (1997). The absolute configuration of ciguatoxin. J. Am. Chem. Soc. *119*, 11325–11326.
33. Yasumoto, T., Igarashi, T., Legrand, A.-M., Cruchet, P., Chinain, M., Fujita, T., and Naoki, H. (2000). Structural elucidation of ciguatoxin congeners by fast-atom bombardment tandem mass spectroscopy. J. Am. Chem. Soc. *122*, 4988–4989.
34. Soliño, L., and Costa, P.R. (2018). Differetial toxin profiles of ciguatoxins in marine organisms : chemistry, fate and global distribution. Toxicon *150*, 124–143.
35. Lewis, R.J., Sellin, M., Poli, M.A., Norton, R.S., MacLeod, J.K., and Sheil, M.M. (1991). Purification and characterization of ciguatoxins from moray eel (*Lycodontis javanicus*, Muraenidae). Toxicon *29*, 1115–1127.
36. Satake, M., Murata, M., and Yasumoto, T. (1993). The structure of CTX3C, a ciguatoxin congener isolated from cultured *Gambierdiscus toxicus.* Tetrahedron Lett. *34*, 1975–1978.
37. Satake, M., Fukui, M., Legrand, A.-M., Cruchet, P., and Yasumoto, T. (1998). Isolation and structures of new ciguatoxin analogs, 2, 3-dihydroxy CTX3C and 51-hydroxy CTX3C, accumulated in tropical reef fish. Tetrahedron Lett. *39*, 1197–1198.
38. Lewis, R.J., Vernoux, J.-P., and Brereton, I.M. (1998). Structure of Caribbean ciguatoxin isolated from *Caranx latus.* J. Am. Chem. Soc. *120*, 5914–5920.
39. Kryuchkov, F., Robertson, A., Miles, C.O., Mudge, E.M., and Uhlig, S. (2020). LC-HRMS and Chemical Derivatization Strategies for the Structure Elucidation of Caribbean Ciguatoxins: Identification of C-CTX-3 and -4. Mar. Drugs *18*, 182.
40. Murata, M., Naoki, H., Iwashita, T., Matsunaga, S., Sasaki, M., Yokoyama, A., and Yasumoto, T. (1993). Structure of maitotoxin. J. Am. Chem. Soc. *115*, 2060–2062.
41. Boente-Juncal, A., Álvarez, M., Antelo, Á., Rodríguez, I., Calabro, K., Vale, C., Thomas, O.P., and

Botana, L.M. (2019). Structure Elucidation and Biological Evaluation of Maitotoxin-3, a Homologue of Gambierone, from *Gambierdiscus belizeanus.* Toxins *11*, 79.
42. Morohashi, A., Satake, M., Nagai, H., Oshima, Y., and Yasumoto, T. (2000). The Absolute Configuration of Gambieric Acids A-D, Potent Antifungal Polyethers, Isolated from the Marine Dinoflagellate *Gambierdiscus toxicus*. Tetrahedron *56,* 8995–9001.
43. Murata, M., Torigoe, K., Statake, M., and Yasumoto, T. (1992). Gambieric Acids, New Potent Antifungal Substances with Unprecedented Polyether Structures from a Marine Dinoflagellate *Gambierdiscus toxicus.* J. Org. Chem. *57*, 5448–5453.
44. Watanabe, R., Uchida, H., Suzuki, T., Matsushima, R., Nagae, M., Toyohara, Y., Satake, M., Oshima, Y., Inoue, A., and Yasumoto, T. (2013). Gambieroxide, a novel epoxy polyether compound from the dinoflagellate *Gambierdiscus toxicus* GTP2 strain. Tetrahedron *69*, 10299–10303.
45. Rodríguez, I., Genta-Jouve, G., Alfonso, C., Calabro, K., Alonso, E., Sánchez, J.A., Alfonso, A., Thomas, O.P., and Botana, L.M. (2015). Gambierone, a ladder-shaped polyether from the dinoflagellate *Gambierdiscus belizeanus*. Org. Lett. *17*, 2392–2395.
46. Satake, M., Irie, R., Holland, P.T., Harwood, D.T., Shi, F., Itoh, Y., Hayashi, F., and Zhang, H. (2021). Brevisulcenals-A1 and A2, Sulfate Esters of Brevisulcenals, Isolated from the Red Tide Dinoflagellate *Karenia brevisulcata.* Toxins *13*, 82.
47. Hamamoto, Y., Tachibana, K., Holland, P.T., Shi, F., Beuzenberg, V., Itoh, Y., and Statake, M. (2012). Brevisulcenal-F: A Polycyclic Ether Toxin Associated with Massive Fish-kills in New Zealand. J. Am. Chem. Soc. *134*, 4963–4968.
48. Satake, M., Irie, R., Hamamoto, Y., Tachibana, K., Holland, P.T., Harwood, D. T., Shi, F., Beuzenberg, V., Itoh, Y., Hayashi, F., and Zhang, H. (2018). Brevisulcenal-G, -H, and -I, Polycyclic Ether Marine Toxins From the Dinoflagellate *Karenia Brevisulcata*. Heterocycles *96*, 2096–2105.
49. Abraham, A., El Said, K.R., Wang, Y., Jester, E.L.E., Plakas, S.M., Flewelling, L.J., Henry, M.S., and Pierce, R.H. (2015). Biomarkers of brevetoxin exposure and composite toxin levels in hardclam (*Mercenaria* sp.) exposed to *Karenia brevis* blooms. Toxicon *96*, 82–88.
50. Ishida, H., Nozawa, A., Totoribe, K., Muramaatsu, N., Nukaya, H., Tsuji, K., Yamaguchi, K., Yasumoto, T., Kaspar, H., Berkett, N., and Kosuge, T. (1995). Brevetoxin B1, A New Polyether Marine Toxin From The New Zealand Shellfish, *Austrovenus stutchburyi*. Terahedron Lett. *36*, 725–728.
51. Murata, K., Satake, M., Naoki, H., Kaspar, H. F., and Yasumoto, T. (1998). Isolation and Structure of a New Brevetoxin Analog, Brevetoxin B2, from Greenshell Mussels from New Zealand. Tetrahedron *54*, 735–742.
52. Tsukano, C., and Sasaki, M. (2006). Structure–activity relationship studies of gymnocin-A. Tetrahedron Lett. *47*, 6803–6807.
53. Satake, M., Tanaka, Y., Ishikura, Y., Oshima, Y., Naoki, H., and Yasumoto, T. (2005). Gymnocin-B with the largest contiguous polyether rings from the red tide dinoflagellate, *Karenia* (formerly *Gymnodinium*) *mikimotoi.* Tetrahedron Lett. *46*, 3537–3540.
54. Satake, M., Shoji, M., Oshima, Y., Naoki, H., Fujita, T., and Yasumoto, T. (2002). Gymnocin-A, a cytotoxic polyether from the notorious red tide dinoflagellate, *Gymnodinium mikimotoi.* Tetrahedron Lett. *43*, 5829–5832.
55. Rasmussen, S. A., Binzer, S. B., Hoeck, C., Meier, S., de Medeiros, L. S., Andersen, N. G., Place, A., Nielsen, K. F., Hansen, P. J., and Larsen, T. O. (2017). Karmitoxin: An Amine-Containing Polyhydroxy-Polyene Toxin from the Marine Dinoflagellate *Karlodinium armiger*. J. Nat. Prod. *80*, 1287–1293.
56. Peng,J., R. Place, A., Yoshida, W., Anklin, C., and Hamann, M. T.(2010). Structure and Absolute Configuration of Karlotoxin-2, an Ichthyotoxin from the Marine Dinoflagellate *Karlodinium veneficum*. J. Am. Chem. Soc. *132*, 3277–3279.
57. Cai, P., He, S., Zhou, C., Place, A. R., Haq, S., Ding, L., Chen, H., Jiang, Y., Guo, C., Xu, Y., Zhang, J., and Yan, X. (2016). Two new karlotoxins found in *Karlodinium veneficum* (strain GM2) from the East China Sea. Harmful Algae. *58*, 66–73.
58. Wang, R., Wu, J., Zhou, S., Cao, R., and Chan, L. (2020). A preliminary study on the allelopathy and toxicity of the dinoflagellate *Karlodinium veneficum.* Mar. Pollut. Bull. *158*, 111400.
59. Place, A. R., Bowers, H. A., Bachvaroff, T. R., Adolf, J. E., Deeds, J. R., and Sheng, J. (2012). *Karlodinium veneficum*-The little dinoflagellate with a big bite. Harmful Algae. *14*, 179–195.
60. Van Wagoner, R. M., Deeds, J. R., Satake, M., Ribeiro, A. A., Place, A. R., and Wright, J. L. C. (2008). Isolation and characterization of karlotoxin 1, a new amphipathic toxin from *Karlodinium veneficum.* Tetrahedron Lett. *49*, 6457–6461.
61. Roy, J. S., Poulson-Ellestad, K. L., Sieg, R. D., Poulin, R. X., and Kubanek, J. (2013). Chemical ecology of the marine plankton. Nat. Prod. Rep. *30*, 1364–1379.

62. Waters, A. L., Oh, J., Place, A. R., and Hamann, M. T. (2015). Stereochemical Studies of the Karlotoxin Class Using NMR Spectros-copy and DP4 Chemical-Shift Analysis: Insights into their Mechanism of Action. Angew. Chem. Int. Ed. *54*, 15705–15710.
63. Van Wagoner, R. M., Deeds, J. R., Tatters, A. O., Place, A. R., Tomas, C. R., and Wright, J. L. C. (2010). Structure and Relative Potency of Several Karlotoxins from *Karlodinium veneficu.* J. Nat. Prod. *73*, 1360–1365.
64. Ukena, T., Satake, M. Usami,, M., Oshima, Y., Naoki, H., Fujita, T., Kan, Y., and Yasumoto, T. (2001). Structure Elucidation of Ostreocin D, a Palytoxin Analog Isolated from the Dinoflagellate *Ostreopsis siamensis.* Bios. Biotechnol. Biochem. *65*, 2585–2588.
65. Usami, M., Satake, M., Ishida, S., Inoue, A., Kan, Y., and Yasumoto, T. (1995). Palytoxin Analogs from the Dinoflagellate *Ostreopsis siamensis.* J. Am. Chem. Soc. *117*, 5389–5290.
66. Ciminiello, P., Dell'Aversano, C., Iacovo, E. D., Fattorusso, E., Forino, M., Grauso, L., and Tartaglione, L. (2012) Isolation and Structure Elucidation of Ovatoxin-a, the Major Toxin Produced by *Ostreopsis ovata.* J. Am. Chem. Soc. *134*, 1869–1875.
67. Ciminiello, P., Dell'Aversano, C., Fattorusso, E., Forino, M., Tartaglione, L., Grillo, C., and Melchiorre, N. (2008). Putative Palytotxin and Its New Analogue Ovatoxin-a, in *Ostreopsis ovata* Collected Along the Ligurina Coasts During the 2006 Toxic Outbreak. J. Am. Soc. Mass Spectrom. *19*, 111–120.
68. Hwang, B. S., Yoon, E. Y., Kim, H. S., Yih, W., Park, J. Y., Jeong, H. J., and Rho, J.-R. (2013). Ostreol A: A new cytotoxic compound isolated from the epiphytic dinoflagellate *Ostreopsis* cf*. ovata* from the coastal waters of Jeju Island, Korea. Bioorg. Med. Chem. Lett. *23*, 3023–3027.
69. Hwang, B. S., Yoon, E. Y., Jeong, E. J., Park, J., Kim, E.-H., and Rho, J.-R. (2018). Determination of the Absolute Configuration of Polyhydroxy Compound Ostreol B Isolated from the Dinoflagellate *Ostreopsis* cf*. Ovata.* J. Org. Chem. *83*, 194–202.
70. Uchida, H., Taira, Y., and Yasumoto, T. (2013). Structural elucidation of palytoxin analogs produced by the dinoflagellate *Ostreopsis ovata* IK2 strain by complementary use of positive and negative ion liquid chromatography/quadrupole time-of-flight mass spectrometry. Rapid Commun. Mass Spectrom. *27*, 1999–2008.
71. Terajima, T., Uchida, H., Abe, N., and Yasumoto, T. (2018). Simple structural elucidation of ostreocin B, a new palytoxin congener isolated from the marine dinoflagellate *Ostreopsis siamensis* using complementary positive and negative ion liquid chromatography/quadrupole time-of-flight mass spectrometry. Rapid Commun. Mass Spectrom. *32*, 1001–1007.
72. Ciminiello, P., Dell'Aversano, C., Iacovo, E. D., Fattorusso, E., Forino, M., Tartaglione, L., Yasumoto, T., Battocchi, C., Giacobbe, M., Amorim, A., and Penna, A. (2013). Investigation of toxin profile of Mediterranean and Atlantic strains of *Ostreopsis* cf. *siamensis* (Dinophyceae) by liquid chromatography-high resolution mass spectrometry. Harmful Algae. *23*, 19–27.
73. Terajima, T., Uchida, H., Abe, N., and Yasumoto, T. (2019). Structure elucidation of ostreocin-A and ostreocin-E1, novel palytoxin analogs produced by the dinoflagellate *Ostreopsis siamensis*, using LC/Q-TOF MS. Bios. Biotechnol. Biochem. *83*, 381–390.
74. Taniyama, S., Arakawa, O., Terada, M., Nishio, S., Takatani, T., Mahmud, Y., and Noguchi, T. (2003). *Ostreopsis* sp., a possible origin of palytoxin (PTX) in parrotfish *Scarus ovifrons.* Toxicon. *42*, 29–33.
75. Hu,T., Curtis, J. M., Walter, J. A., and Wright, J. L. C. (1995). Identification of DTX-4, a new water-soluble phosphatase inhibitor from the toxic dinoflagellate *Prorocentrum lima.* J. Chem. Soc., Chem. Commun. 597–599.
76. Hu, T., Curtis, J.M., Walter, J.A., McLachlan, J.L., and Wright, J.L.C. (1995). Two new water-soluble DSP toxin derivatives from the dinoflagellate *Prorocentrum maculosum*: Possible storage and excretion products. Tetrahedron Lett. *36*, 9273–9276.
77. Cruz, P.G., Daranas, A.H., Fernández, J.J., Souto, M.L., and Norte, M. (2006). DTX5c, a new OA sulphate ester derivative from cultures of *Prorocentrum belizeanum*. Toxicon *47*, 920–924.
78. Paz, B., Daranas, A.H., Cruz, P.G., Franco, J.M., Napolitano, J.G., Norte, M., and Fernández, J.J. (2007). Identification and characterization of DTX-5c and 7-hydroxymethyl-2-methylene-octa-4,7-dienyl okadaate from *Prorocentrum belizeanum* cultures by LC-MS. Toxicon *50*, 470–478.
79. Napolitano, J.G., Norte, M., Padrón, J.M., Fernández, J.J., and Daranas, A.H. (2009). Belizeanolide, a cytotoxic macrolide from the dinoflagellate *Prorocentrum belizeanum*. Angew. Chem. Int. Ed. *48*, 796–799.
80. Sugahara, K., Kitamura, Y., Murata, M., Satake, M., and Tachibana, K. (2011). Prorocentrol, a Polyoxy Linear Carbon Chain Compound Isolated from the Toxic Dinoflagellate *Prorocentrum hoffmannianum*. J. Org. Chem. *76*, 3131–3138.
81. Domínguez, H.J., Cabrera-García, D., Cuadrado, C., Novelli, A., Fernández-Sánchez, M.T.,

Fernández, J.J., and Daranas, A.H. (2021). Prorocentroic Acid, a Neuroactive Super-Carbon-Chain Compound from the Dinoflagellate *Prorocentrum hoffmannianum*. Org. Lett. *23*, 13–18.
82. Hu, T., deFreitas, A.S.W., Curtis, J.M., Oshima, Y., Walter, J.A., and Wright, J.L.C. (1996). Isolation and structure of prorocentrolide B, a fast-acting toxin from *Prorocentrum maculosum*. J. Nat. Prod. *59*, 1010–1014.
83. Satake, M., MacKenzie, L., and Yasumoto, T. (1997). Identification of *Protoceratium reticulatum* as the Biogenetic Origin of Yessotoxin. Nat. Toxins *5*, 164–167.
84. Satake, M., Ichimura, T., Sekiguchi, K., Yoshimatsu, S., and Oshima, Y. (1999). Confirmation of Yessotoxin and 45,46,47-Trinoryessotoxin Production by *Protoceratium reticulatum* Collected in Japan. Nat. Toxins *7*, 147–150.
85. Ciminiello, P., Dell'Aversano, C., Fattorusso, E., Forino, M., Magno, S., Guerrini, F., Pistocchi, R., and Boni, L. (2003). Complex yessotoxins profile in *Protoceratium reticulatum* from north-western Adriatic sea revealed by LC–MS analysis. Toxicon *42*, 7–14.
86. Miles, C.O., Wilkins, A.L., Jensen, D.J., Cooney, J.M., Quilliam, M.A., Aasen, J., and MacKenzie, A.L. (2004). Isolation of 41a-Homoyessotoxin and the Identification of 9-Methyl-41a-homo yessotoxin and Nor-ring A-yessotoxin from *Protoceratium reticulatum*. Chem. Res. Toxicol. *17*, 1414–1422.
87. Miles, C.O., Wilkins, A.L., Hawkes, A.D., Selwood, A., Jensen, D.J., Aasen, J., Munday, R., Samdal, I.A., Briggs, L.R., Beuzenberg, V., and MacKenzie, A. L. (2004). Isolation of a 1,3-enone isomer of heptanor-41-oxoyessotoxin from *Protoceratium reticulatum* cultures. Toxicon *44*, 325–336.
88. Aasen, J., Samdal, I.A., Miles, C.O., Dahl, E., Briggs, L.R., and Aune, T. (2005). Yessotoxins in Norwegian blue mussels (*Mytilus edulis*): uptake from *Protoceratium reticulatum*, metabolism and depuration. Toxicon *45*, 265–272.
89. Konishi, M., Yang, X., Li, B., Fairchild, C.R., and Shimizu, Y. (2004). Highly Cytotoxic Metabolites from the Culture Supernatant of the Temperate Dinoflagellate *Protoceratium reticulatum*. J. Nat. Prod. *67*, 1309–1313.
90. Miles, C.O., Wilkins, A.L., Hawkes, A.D., Selwood, A.I., Jensen, D.J., Munday, R., Cooney, J.M., and Beuzenberg, V. (2005). Polyhydroxylated amide analogs of yessotoxin from *Protoceratium reticulatum*. Toxicon *45*, 61–71.
91. Miles, C.O., Wilkins, A.L., Selwood, A.I., Hawkes, A.D., Jensen, D.J., Cooney, J.M., Beuzenberg, V., and MacKenzie, A.L. (2006). Isolation of Yessotoxin 32-*O*-[β-L-arabinofuranosyl- (5'→1")-β-L-arabinofuranoside] from *Protoceratium reticulatum*. Toxicon, *47*, 510–516.
92. Paz, B., Riobó, P., Souto, M.L., Gil, L.V., Norte, M., Fernández, J.J., and Franco, J.M. (2006). Detection and identification of glycoyessotoxin A in a culture of the dinoflagellate *Protoceratium reticulatum*. Toxicon *48*, 611–619.
93. Suzuki, T., Horie, Y., Koike, K., Satake, M., Oshima, Y., Iwataki, M., and Yoshimatsu, S. (2007). Yessotoxin analogues in several strains of *Protoceratium reticulatum* in Japan determined by liquid chromatography–hybrid triple quadrupole/linear ion trap mass spectrometry. J. Chromatogr. A. *1142*, 172–177.
94. Loader, J.I., Hawkes, A.D., Beuzenberg, V., Jensen, D.J., Cooney, J.M., Wilkins, A.L., Fitzgerald, J.M., Briggs, L.R., and Miles, C.O. (2007). Convenient large-scale purification of Yessotoxin from *Protoceratium reticulatum* culture and isolation of a novel furanoyessotoxin. J. Agric. Food Chem. *55*, 11093–11100.
95. Paz, B., Daranas, A.H., Norte, M., Riobó, P., Franco, J.M., and Fernández, J.J. (2008). Yessotoxins, a Group of Marine Polyether Toxins: an Overview. Mar. Drugs *6*, 73–102.
96. Finch, S.C., Wilkins, A.L., Hawkes, A.D., Jensen, D.J., MacKenzie, L., Beuzenberg, V., Quilliam, M.A., Olseng, C.D., Samdal, I.A., Aasen, J.A.G., Selwood, A.I., Cooney, J.M., Sandvik, M., and Miles, C.O. (2005). Isolation and identification of (44-R, S)-44,55-dihydroxyyessotoxin from *Protoceratium reticulatum,* and its occurrence in extracts of shellfish from New Zealand, Norway and Canada. Toxicon *46*, 160–170.
97. Miles, C.O., Wilkins, A.L., Allan, D.H., Selwood, A.I., Jensen, D.J., Cooney, J.M., Beuzenberg, V., and MacKenzie, A.L. (2006). Identification of 45-hydroxy-46,47-dinoryessotoxin, 44-oxo-45,46,47-trinoryessotoxin, and 9-methyl-42,43,44,45,46,47,55-heptanor-38-en-41-oxoyessotoxin, and partial characterization of some minor yessotoxins, from *Protoceratium reticulatum*. Toxcin *47*, 229–240.
98. Ciminiello, P., Dell'Aversano, C., Fattorusso, E., Forino, M., Grauso, L., Magno, S.G., Poletti, R., and Tartaglione, L. (2007). Desulfoyessotoxins from Adriatic Mussles: A New Problem for Seafood Safety Control. Chem. Res. Toxicol. *20*, 95–98.
99. Kita, M., Ohishi, N., Konishi, K., Kondo, M., Koyama, T., Kitamura, M., Yamada, K., Uemura, D. (2007). Symbiodinolide, a novel polyol macrolide that activates N-type Ca^{2+} channel, from the

symbiotic marine dinoflagellate *Symbiodinium* sp.. Tetrahedron *63*, 6241–6251.
100. Onodera, K., Nakamura, H., Oba, Y., Ohizumi, Y., and Ojika, M. (2005). Zooxanthellamide Cs: Vasoconstrictive Polyhydroxylated Macrolides with the Largest Lactone Ring Size from a Marine Dinoflagellate of *Symbiodinium* sp.. J. Am. Chem. Soc. *127*, 10406–10411.
101. Nakamura, H., Asari, T., Murai, A., Kan, Y., Kondo, T., Yoshida, K., and Ohizumi, Y. (1995). Zooxanthellatoxin-A, a Potent Vasoconstrictive 62-Membered Lactone from a Symbiotic Dinoflagellate. J. Am. Chem. Soc. *117*, 550–551.
102. Tsunematsu, Y., Ohno, O., Konishi, K., Yamada, K., Suganuma, M., and Uemura, D. (2009). Symbiospirols: Novel Long Carbon-Chain Compounds Isolated from Symbiotic Marine Dinoflagellate *Symbiodinium* sp.. Org. lett. *11*, 2153–2156.
103. Fukatsu, T., Onodera, K., Ohta, Y., Oba, Y., Nakamura, H., Shintani, T., Yoshioka, Y., Okamoto, T., Lohuis, M.T., Miller, D.J., Kawachi, M., and Ojika, M. (2007). Zooxanthellamide D, a Polyhydroxy Polyene Amide from a Marine Dinoflagellate, and Chemotaxonomic Perspective of the *Symbiodinium* Polyols. J. Nat. Prod. *70*, 407–411.
104. Keller, M., and Guillard, R.R.L. (1985). Proceedings of the 3rd international conference on toxic dinoflagellates. In Toxic Dinoflagellates, D.M. Anderson, A.W. White, and D.G. Baden, eds. (Elsevier), pp. 113–116.
105. Horiguchi, T., Tamura, M., Katsumata, K., and Yamaguchi, A. (2012). *Testudodinium* gen. nov. (Dinophyceae), a new genus of sand-dwelling dinoflagellates formerly classified in the genus *Amphidinium*. J. Phycol. Res. *60*, 137–149.
106. Satake, M., Murata, M., Yasumoto, T., Fujita, T., and Naoki, H. (1991). Amphidinol, a polyhydroxypolyene antifungal agent with an unprecedented structure, from a marine dinoflagellate, *Ampbidnium klebsii*. J. Am. Chem. Soc. *113*, 9859–9861.
107. Schrödinger, L.L.C. (2015). MacroModel. http://www.schrodinger.com/MacroModel.
108. Frisch, M. J., Trucks, G. W., Schlegel, H. B., Scuseria, G. E., Robb, M. A., Cheeseman, J. R., Scalmani, G., Barone, V., Mennucci, B., Petersson, G. A., Nakatsuji, H., Caricato, M., Li, X., Hratchian, H. P., Izmaylov, A. F., Bloino, J., Zheng, G., Sonnenberg, J. L., Hada, M., Ehara, M., Toyota, K., Fukuda, R., Hasegawa, J., Ishida, M., Nakajima, T., Honda, Y., Kitao, O., Nakai, H., Vreven, T., Montgomery, J. A., Jr., Peralta, J. E., Ogliaro, F., Bearpark, M., Heyd, J. J., Brothers, E., Kudin, K. N., Staroverov, V. N., Kobayashi, R., Normand, J., Raghavachari, K., Rendell, A., Burant, J. C., Iyengar, S. S., Tomasi, J., Cossi, M., Rega, N., Millam, J. M., Klene, M., Knox, J. E., Cross, J. B., Bakken, V., Adamo, C., Jaramillo, J., Gomperts, R., Stratmann, R. E., Yazyev, O., Austin, A. J., Cammi, R., Pomelli, C., Ochterski, J. W., Martin, R. L., Morokuma, K., Zakrzewski, V. G., Voth, G. A., Salvador, P., Dannenberg, J. J., Dapprich, S., Daniels, A. D., Farkas, Ö., Foresman, J. B., Ortiz, J. V., Cioslowski, J., Fox, D. J. (2013). Gaussian 09, Revision E. 01; Gaussian: Wallingford, CT, USA.
109. CHESHIRE CCAT, the Chemical shift repository for computed NMR scaling factors, http://cheshirenmr.info/index.htm.
110. Pierens, G.K. (2014). ^{1}H and ^{13}C NMR scaling factors for the calculation of chemical shifts in commonly used solvents using density functional theory. J. Comput. Chem. *35*, 1388–1394.
111. Ivosev, G., Burton, L., and Bonner, R. (2008). Dimensionality reduction and visualization in principal component analysis. Anal. Chem. *80,* 4933–4944.
112. Yu, M., Zhou, C., Tian, D., Jia, H.M., Li, Z.Q., Yang, C., Ba, Y.M., Wu, H.K., and Zou, Z.M. (2021). Molecular classification and clinical diagnosis of acute-on-chronic liver failure patients by serum metabolomics. J. Pharm. Biomed. Ana. *198*, 114004.
113. Trager, W., and Jensen, J.B. (1976). Human malaria parasites in continuous culture. Science *193*, 673–675.
114. Smilkstein, M., Sriwilaijaroen, N., Kelly, J.X., Wilairat, P., and Riscoe, M. (2004). Simple and inexpensive fluorescence-based technique for high-throughput antimalarial drug screening. Antimicrob. Agents Chemother. *48*, 1803–1806.
115. Zhang, Q., Liu, Z.L., Mi, Z.Y., Li, X.Y., Jia, P.P., Zhou, J.M., Yin, X., You, X.F., Yu, L.Y., Guo, F., et al. (2011). High-throughput assay to identify inhibitors of Vpu-mediated down-regulation of cell surface BST-2. Antiviral. Res. *91*, 321-329.

Supporting Information-II

Supplemental Figures S7–S222, including copies of HR-ESIMS for compound **1** and fragments **1A**, **1B**, **1d**, **1As/r**, **1Bs/r**, **1as/r**, **1bs/r** and **1cs/r**; LR-ESIMS for fragments **1a**–**1c**, **1e**, and **1es/r**; and 1D and 2D NMR spectra for compound **1** and fragments **1A**, **1B**, **1a**–**1e**, **1As/r**, **1Bs/r**, **1as/r**, **1bs/r**, **1cs/r**, and **1es/r**.

(**1A**, **1B**, **1As/r**, and **1Bs/r** are chemical entities of ^{13}C natural abundance, whereas **1a**–**1e** and **1as/r**–**1es/r** are those of ^{13}C-enriched abundance, except for MTPA ester groups)

Table of Contents:

Generic Display Report

Analysis Info

		Acquisition Date	9/25/2015 2:55:50 AM
Analysis Name	D:\Data\MS\data\201509\jiangzhongping_AX_pos_13_01_476.d		
Method	LC_Direct Infusion_pos_100-1000mz.m	Operator	SCSIO
Sample Name	jiangzhongping_AX_pos	Instrument	maXis
Comment			

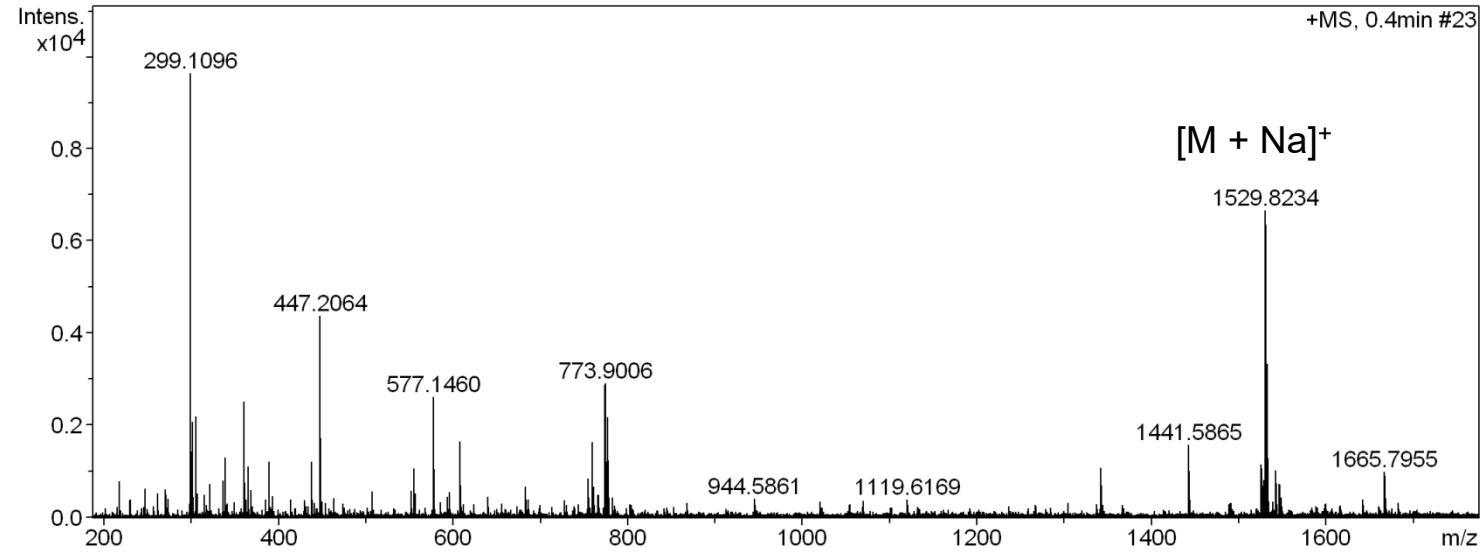

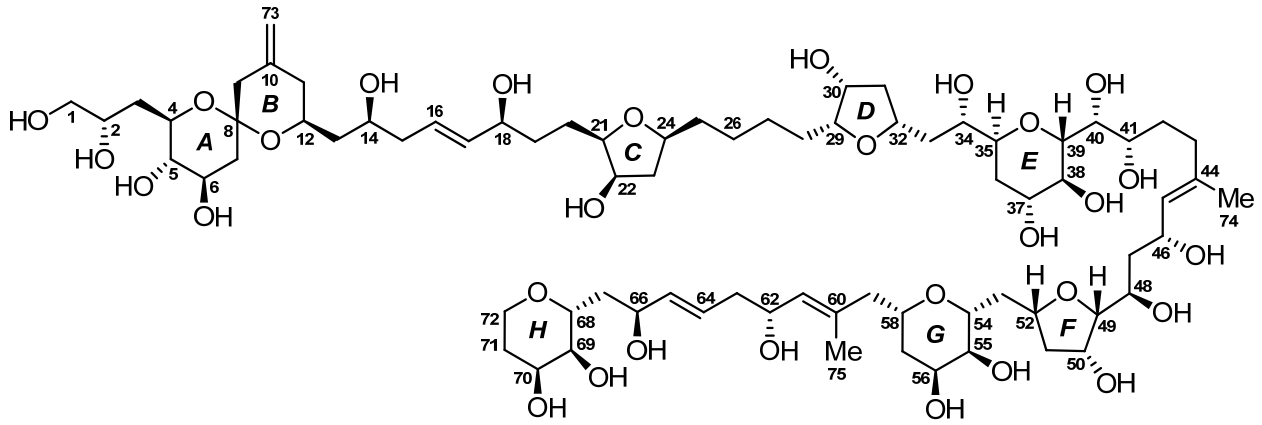

Figure S7. HR-ESIMS for compound **1**

Mass Spectrum SmartFormula Report

Analysis Info

Analysis Name	D:\Data\MS\data\201509\jiangzhongping_AX_pos_13_01_476.d	Acquisition Date	9/25/2015 2:55:50 AM
Method	LC_Direct Infusion_pos_100-1000mz.m	Operator	SCSIO
Sample Name	jiangzhongping_AX_pos	Instrument / Ser#	maXis 29
Comment			

Acquisition Parameter

Source Type	ESI	Ion Polarity	Positive	Set Nebulizer	0.4 Bar
Focus	Active	Set Capillary	4500 V	Set Dry Heater	180 °C
Scan Begin	100 m/z	Set End Plate Offset	-500 V	Set Dry Gas	4.0 l/min
Scan End	2000 m/z	Set Collision Cell RF	800.0 Vpp	Set Divert Valve	Waste

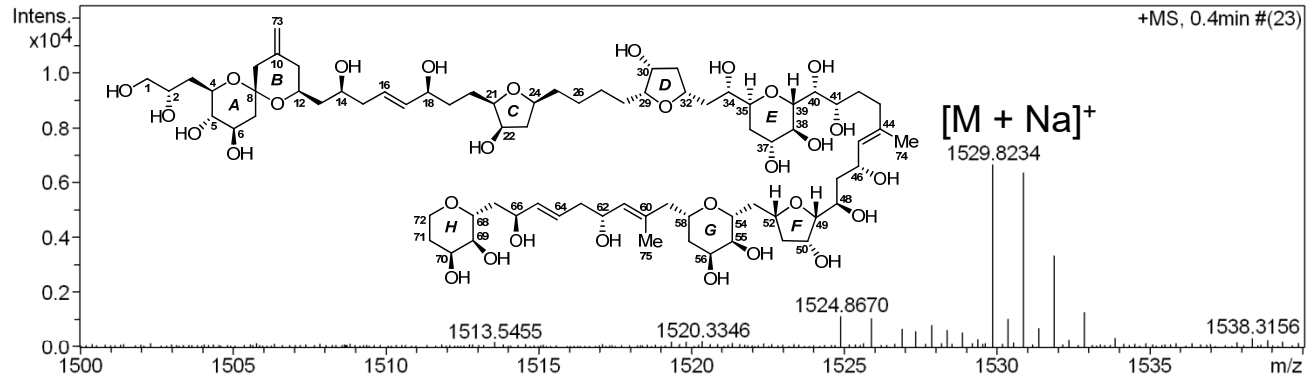

Meas. m/z	#	Formula	Score	m/z	err [ppm]	err [mDa]	mSigma	rdb	e⁻ Conf	N-Rule
1529.8234	1	C 83 H 118 N 4 Na O 21	2.66	1529.8181	-3.5	-5.3	16.2	26.5	even	ok
	2	C 82 H 118 N 6 Na O 20	1.00	1529.8293	3.9	5.9	19.4	26.5	even	ok
	3	C 82 H 122 Na O 25	0.24	1529.8167	-4.4	-6.7	26.3	21.5	even	ok
	4	C 81 H 122 N 2 Na O 24	5.68	1529.8280	3.0	4.6	29.4	21.5	even	ok
	5	C 77 H 118 N 8 Na O 22	59.78	1529.8253	1.2	1.9	44.2	22.5	even	ok
	6	C 76 H 122 N 4 Na O 26	100.00	1529.8240	0.4	0.5	54.2	17.5	even	ok
	7	C 73 H 114 N 14 Na O 20	62.96	1529.8226	-0.5	-0.8	64.2	23.5	even	ok
	8	C 75 H 126 Na O 30	62.70	1529.8226	-0.5	-0.8	64.5	12.5	even	ok
	9	C 72 H 118 N 10 Na O 24	22.38	1529.8213	-1.4	-2.1	68.5	18.5	even	ok
	10	C 71 H 122 N 6 Na O 28	4.43	1529.8199	-2.3	-3.5	78.3	13.5	even	ok
	11	C 70 H 126 N 2 Na O 32	0.57	1529.8186	-3.1	-4.8	88.3	8.5	even	ok

Figure S8. HR-ESIMS for compound **1**

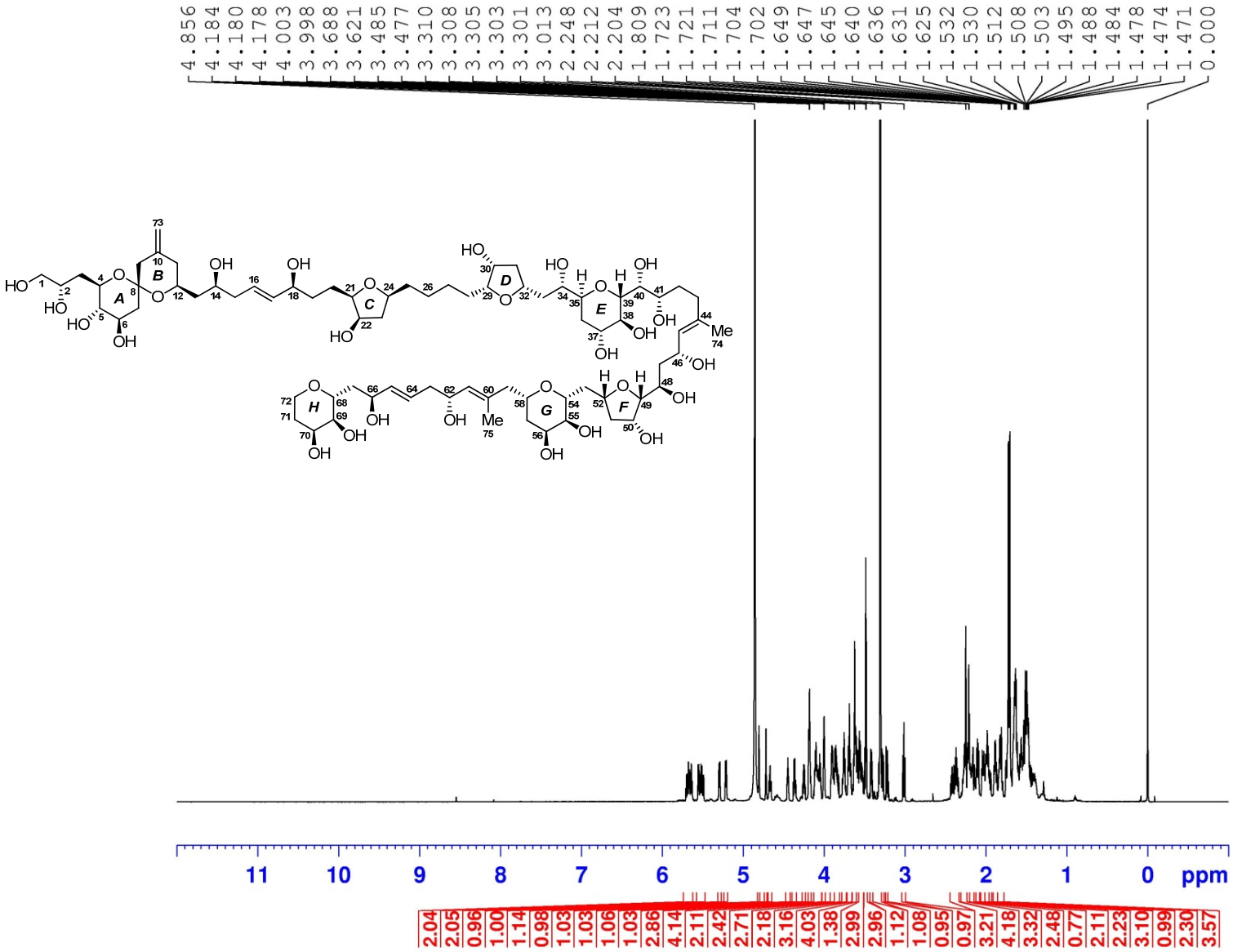

Figure S9. ^{1}H (700 MHz) NMR spectrum of compound **1** in CD_3OD

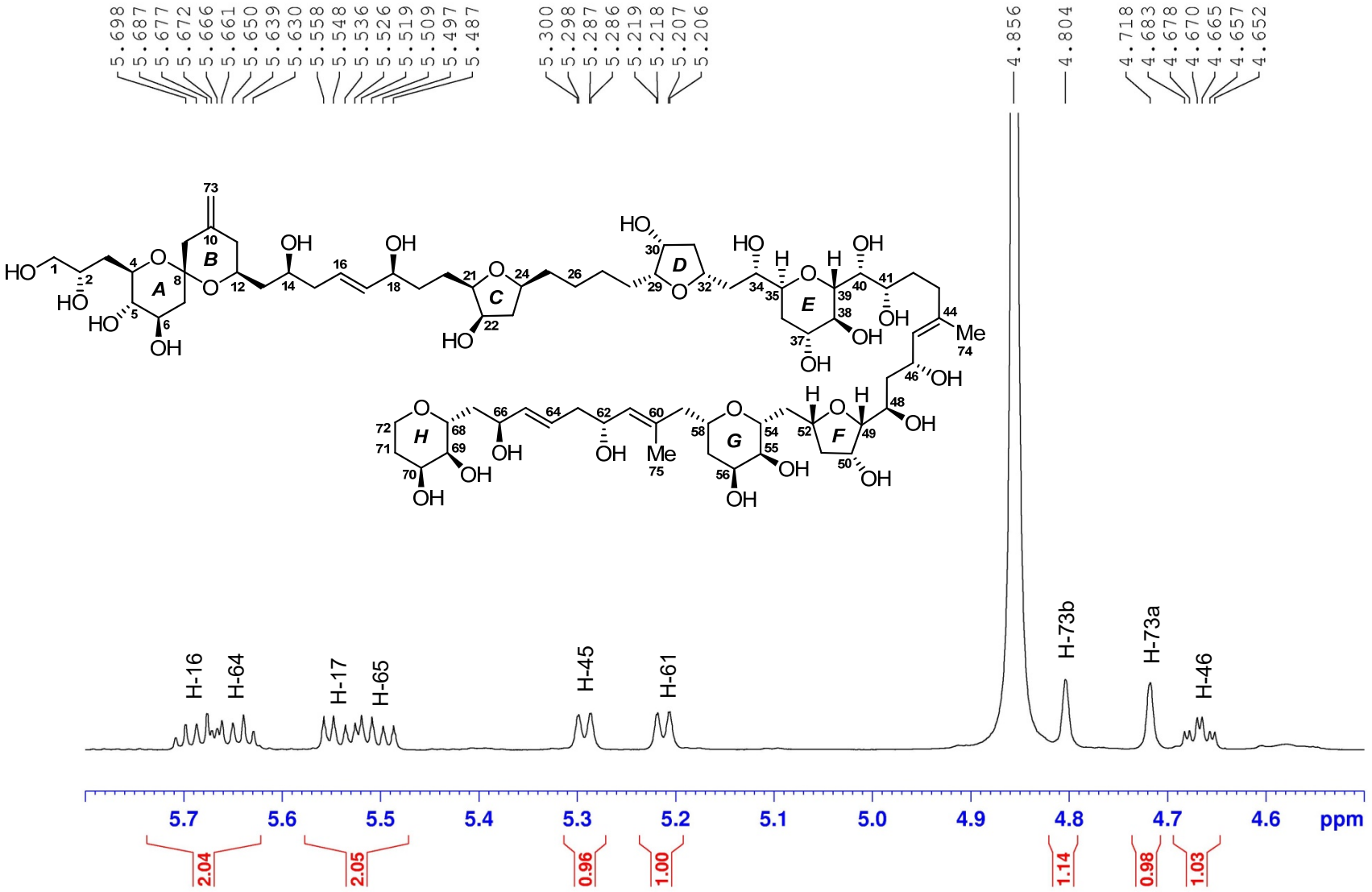

Figure S10. ^{1}H (700 MHz) NMR spectrum of compound **1** in CD_3OD

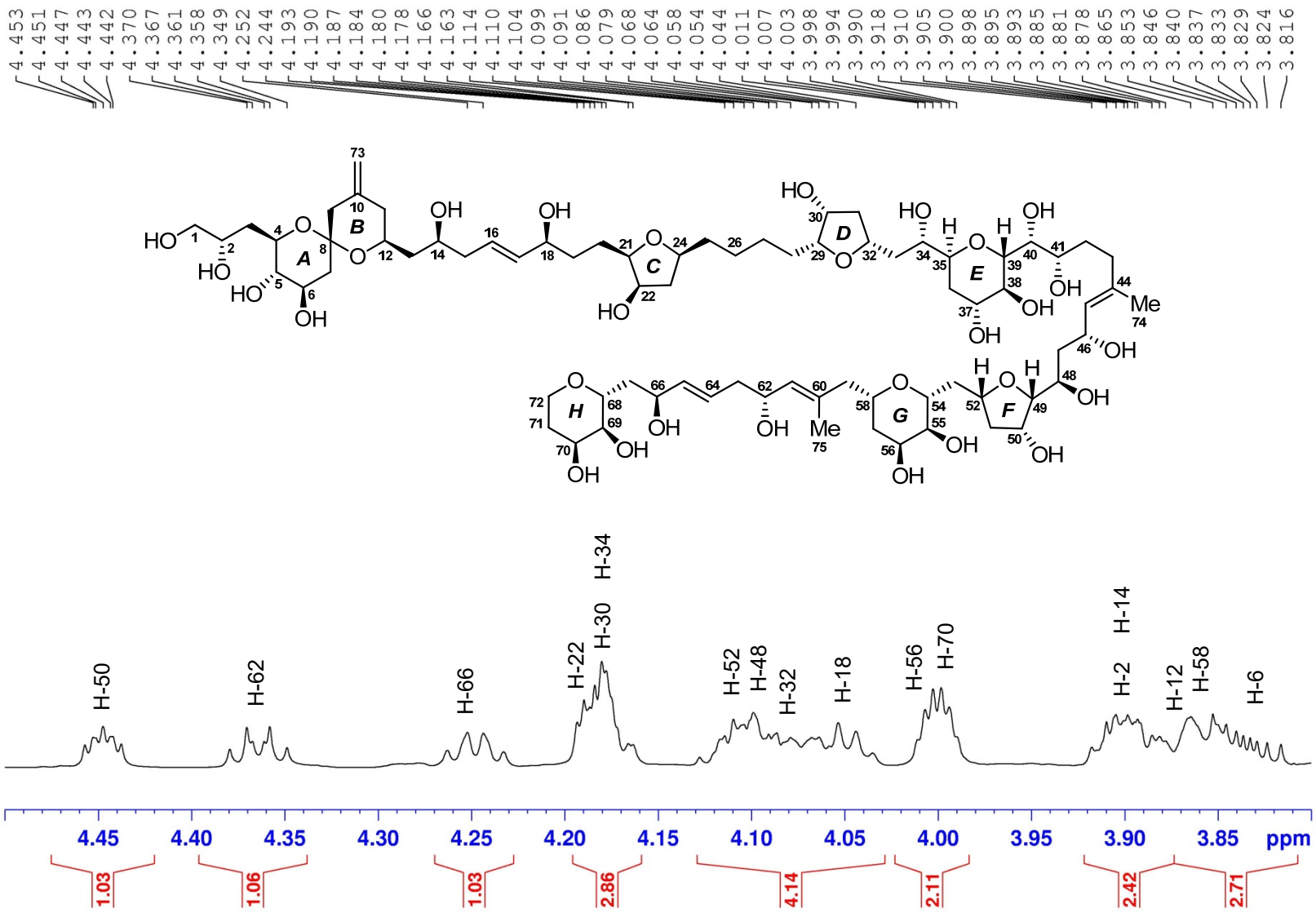

Figure S11. ^{1}H (700 MHz) NMR spectrum of compound **1** in CD_3OD

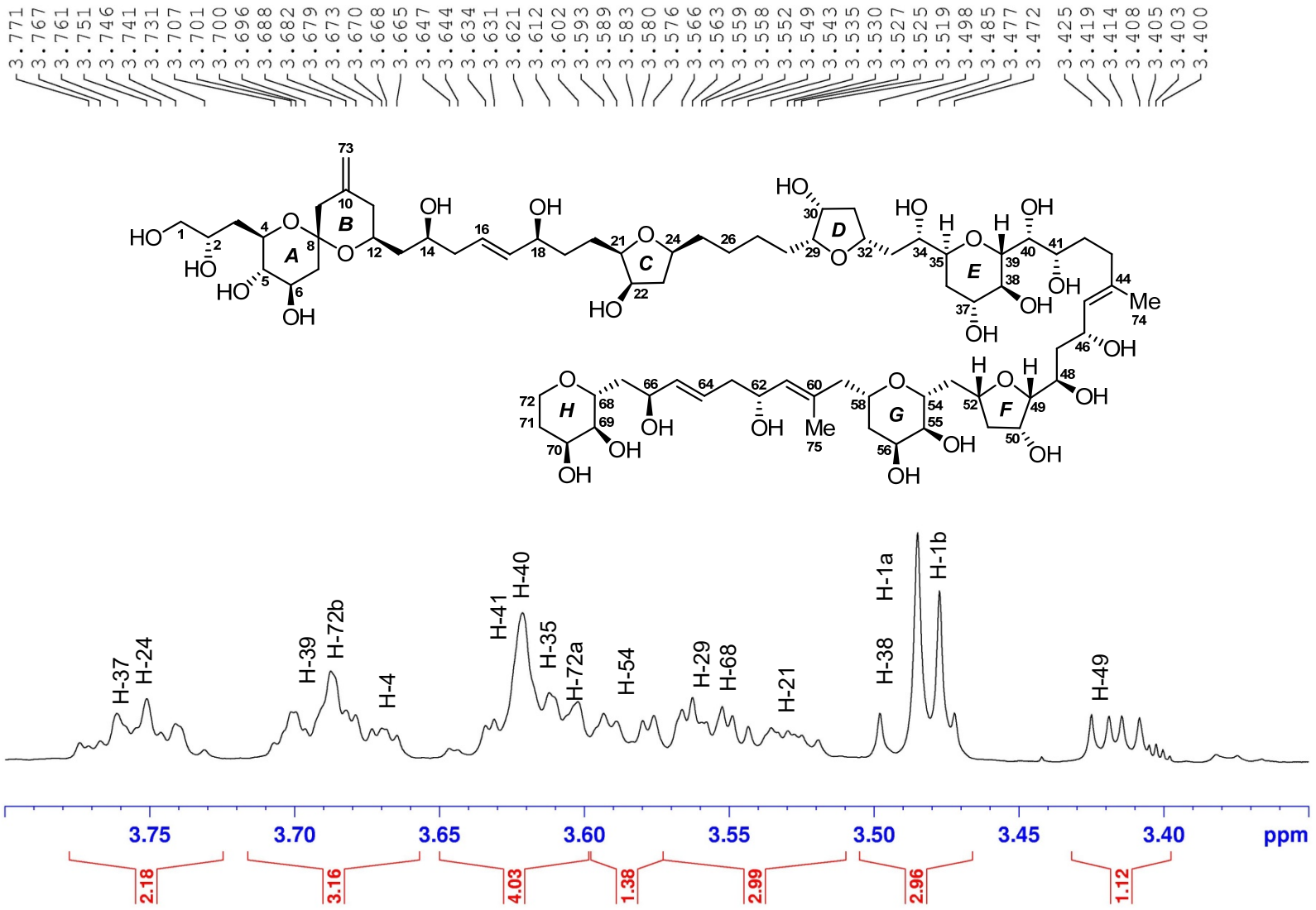

Figure S12. ^{1}H (700 MHz) NMR spectrum of compound **1** in CD_3OD

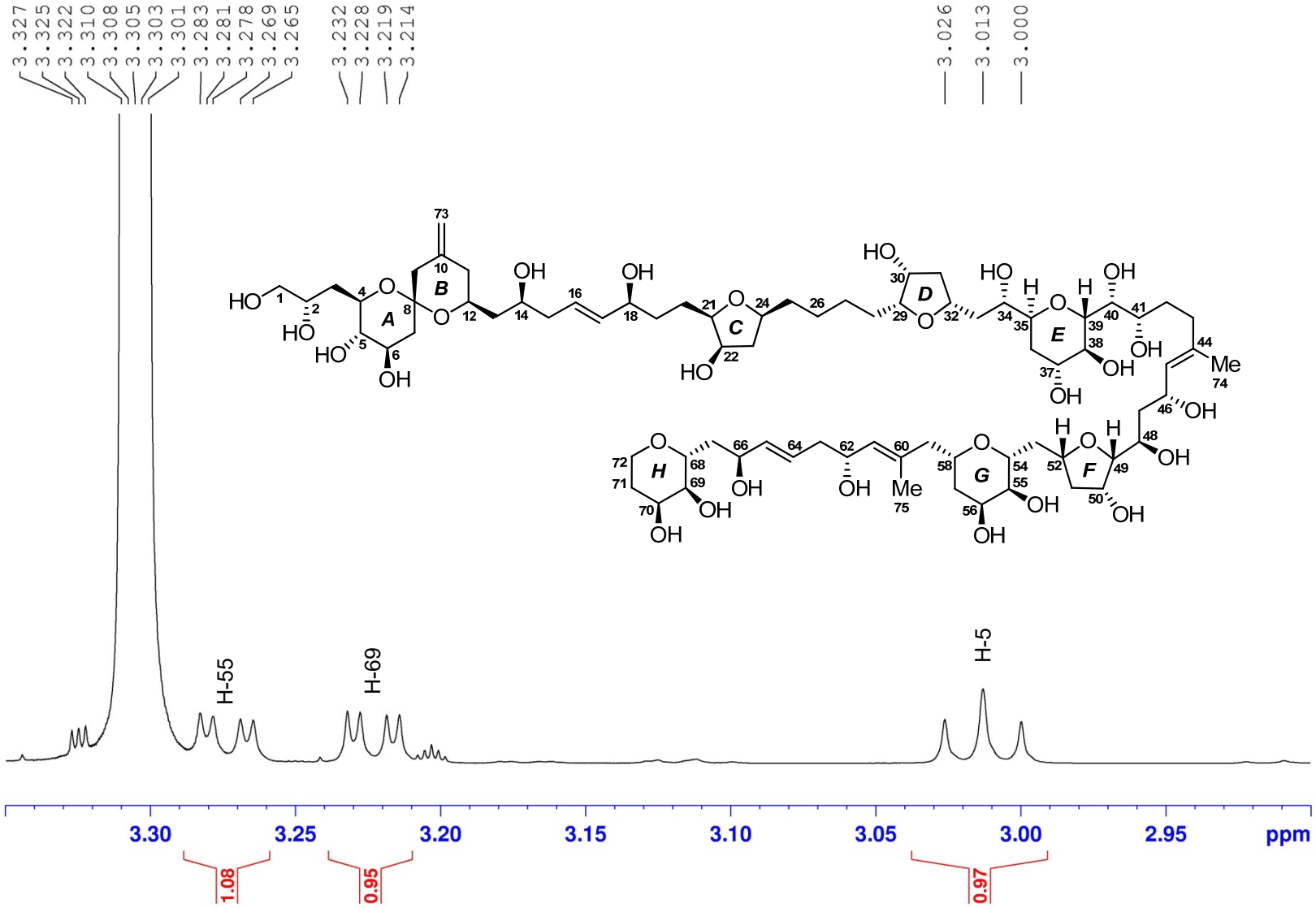

Figure S13. ^{1}H (700 MHz) NMR spectrum of compound **1** in CD_3OD

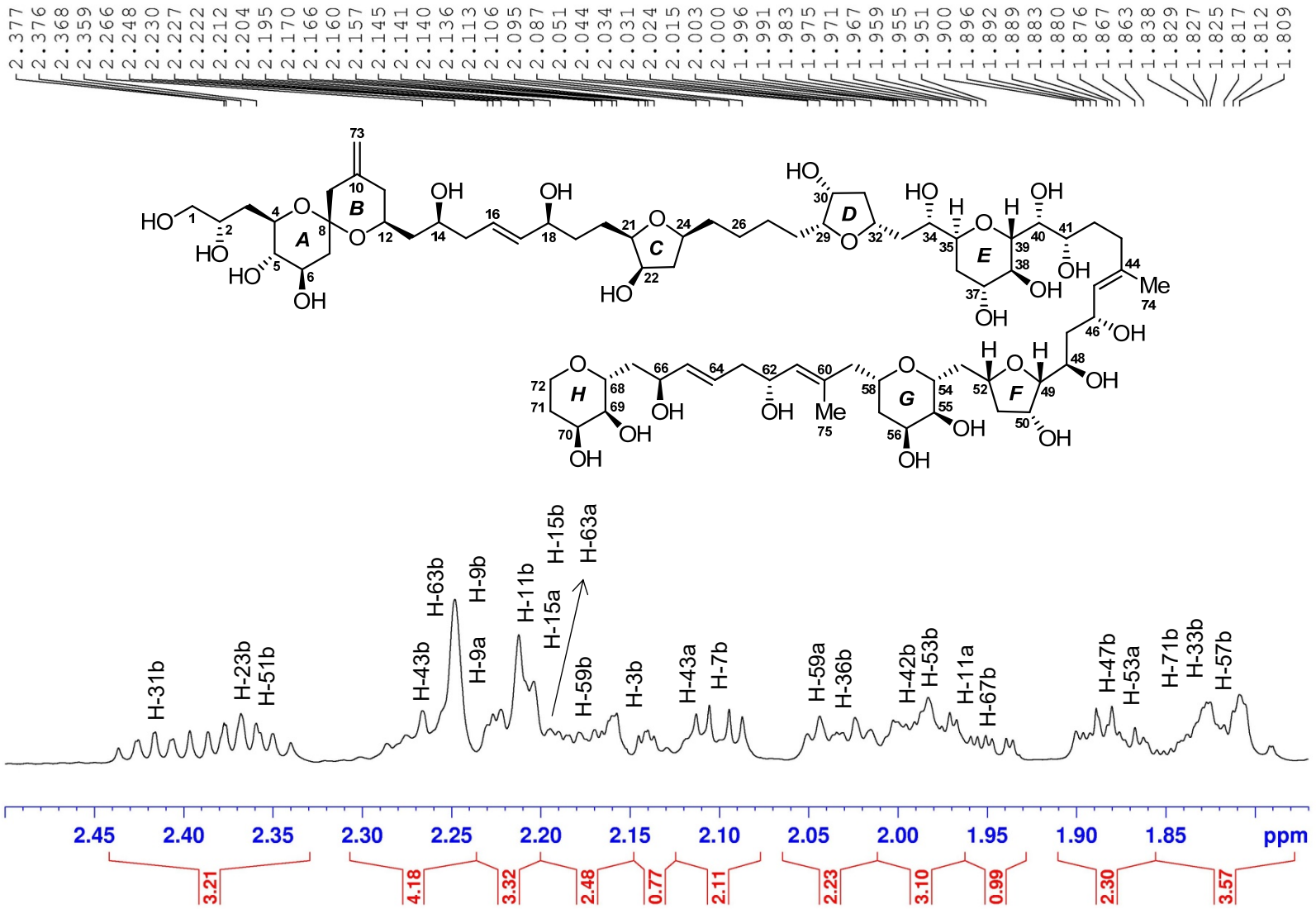

Figure S14. ^{1}H (700 MHz) NMR spectrum of compound **1** in CD_3OD

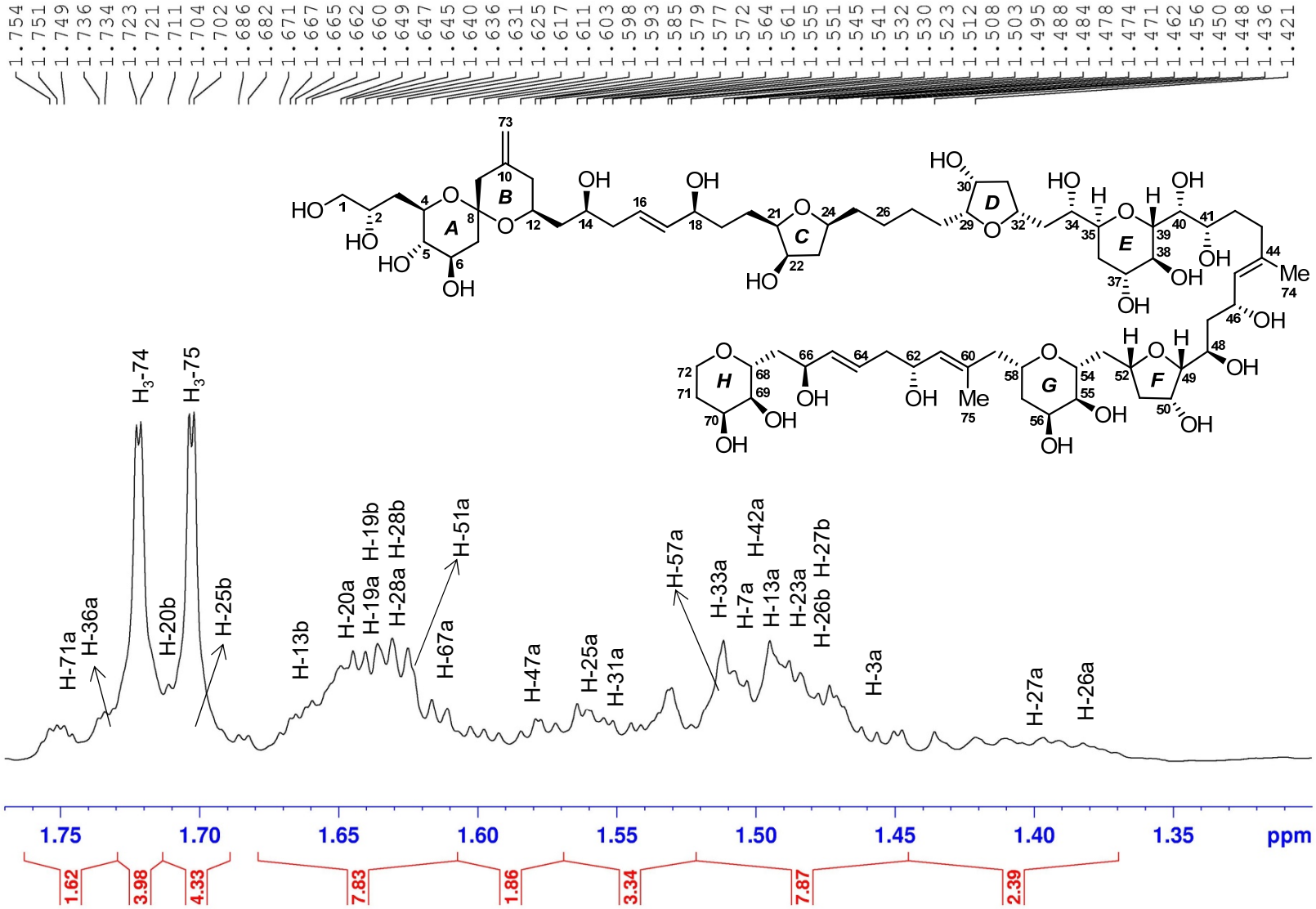

Figure S15. ^{1}H (700 MHz) NMR spectrum of compound **1** in CD_3OD

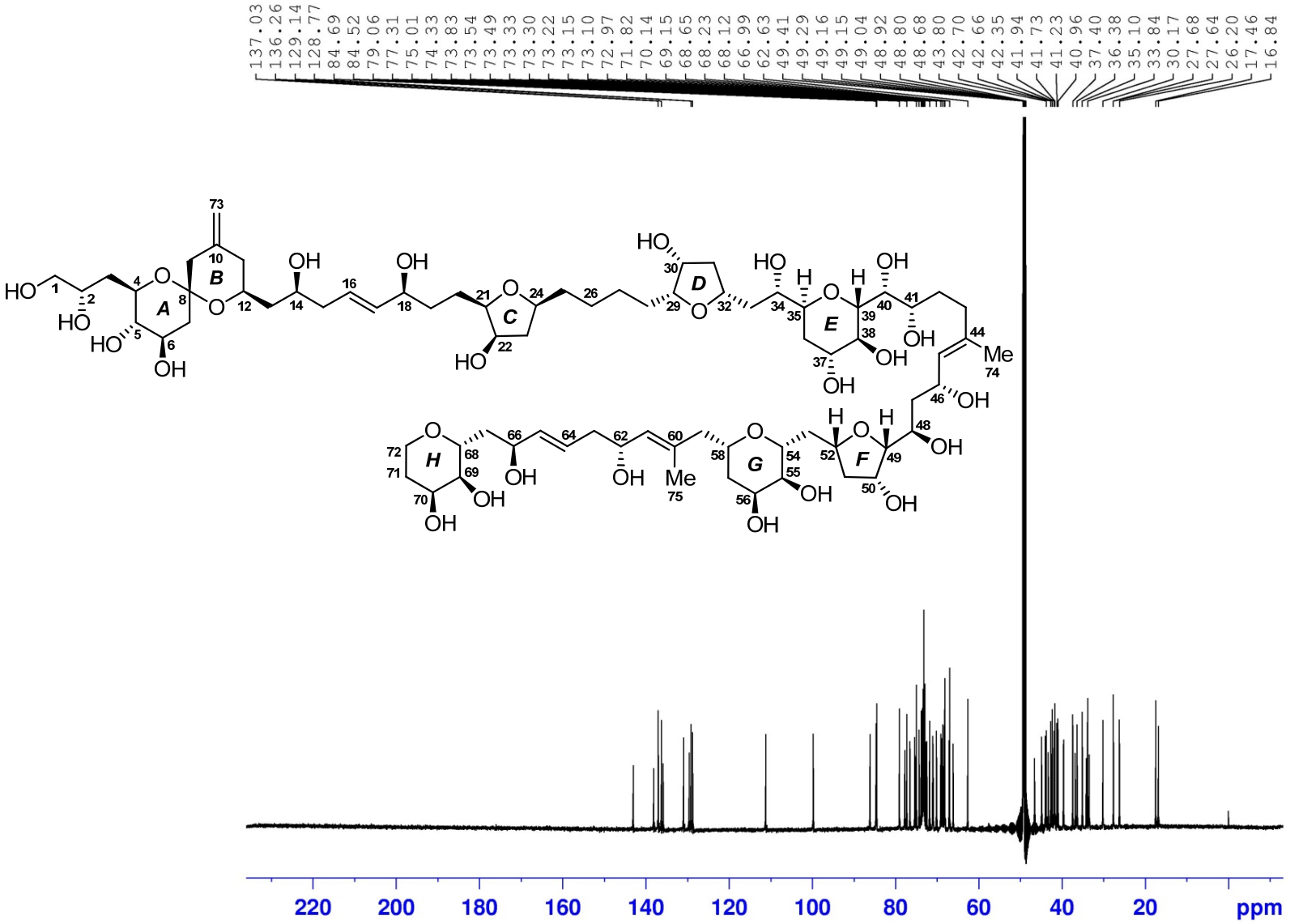

Figure S16. ^{13}C (175 MHz) NMR spectrum of compound **1** in CD_3OD

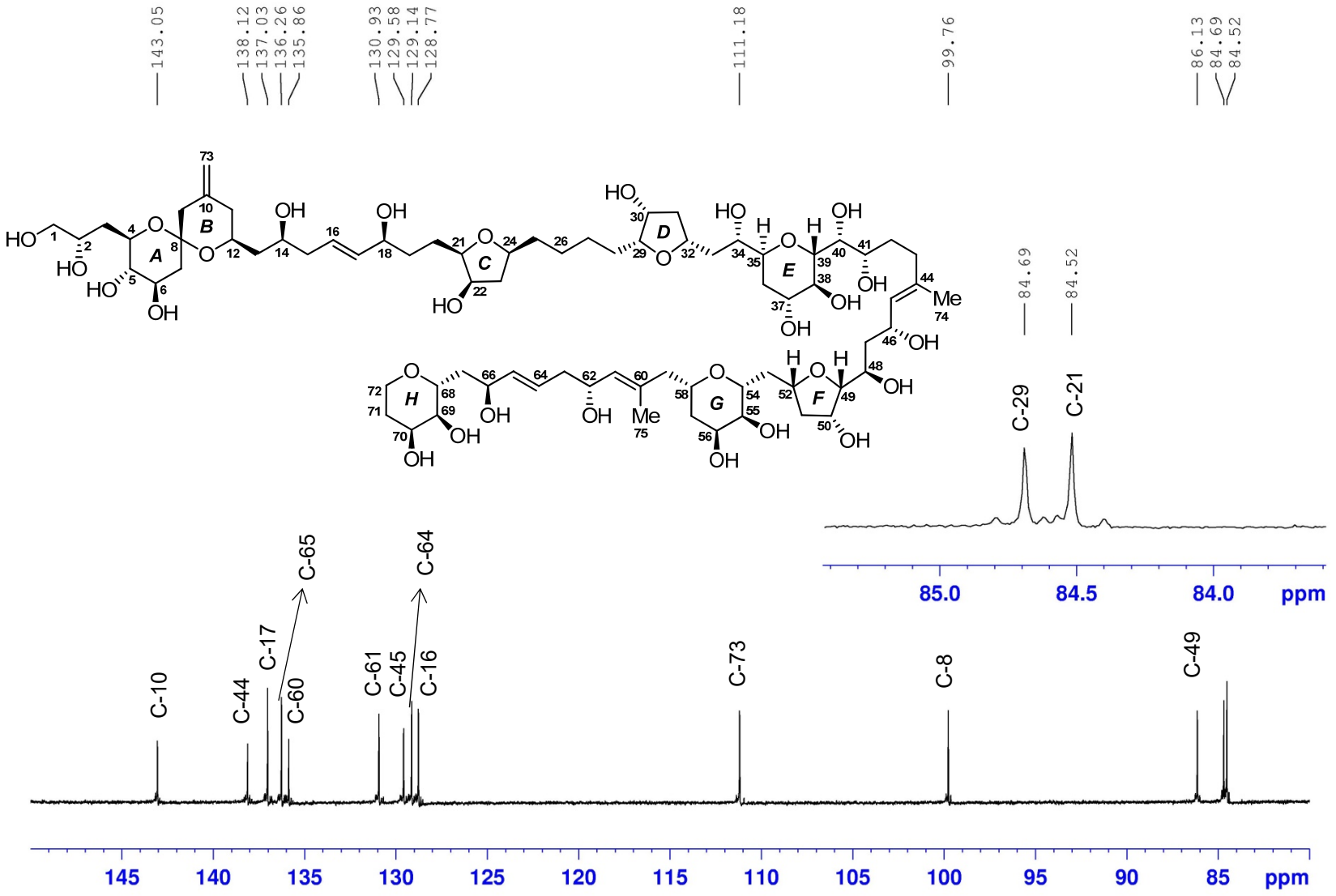

Figure S17. ^{13}C (175 MHz) NMR spectrum of compound **1** in CD_3OD

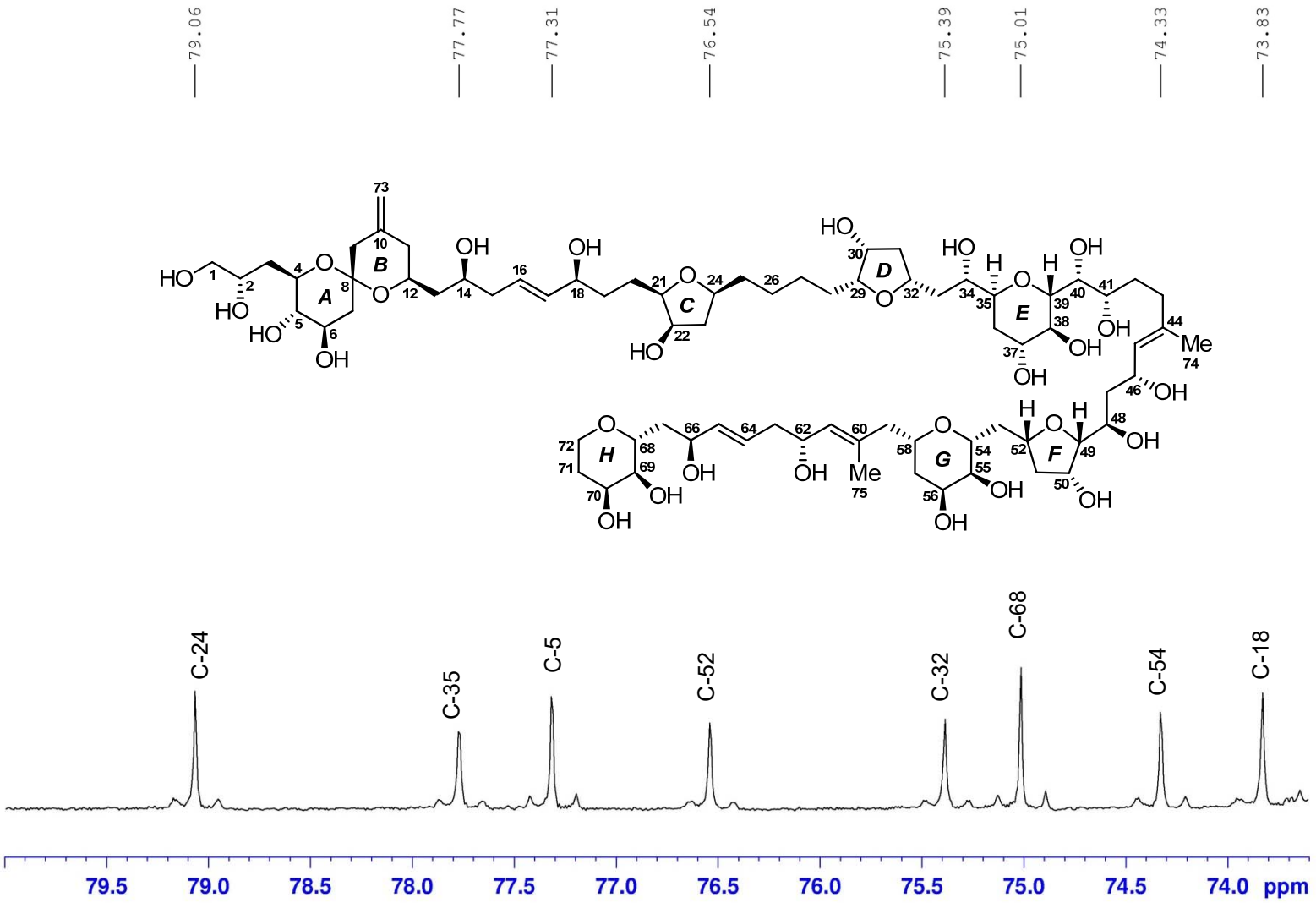

Figure S18. ^{13}C (175 MHz) NMR spectrum of compound **1** in CD_3OD

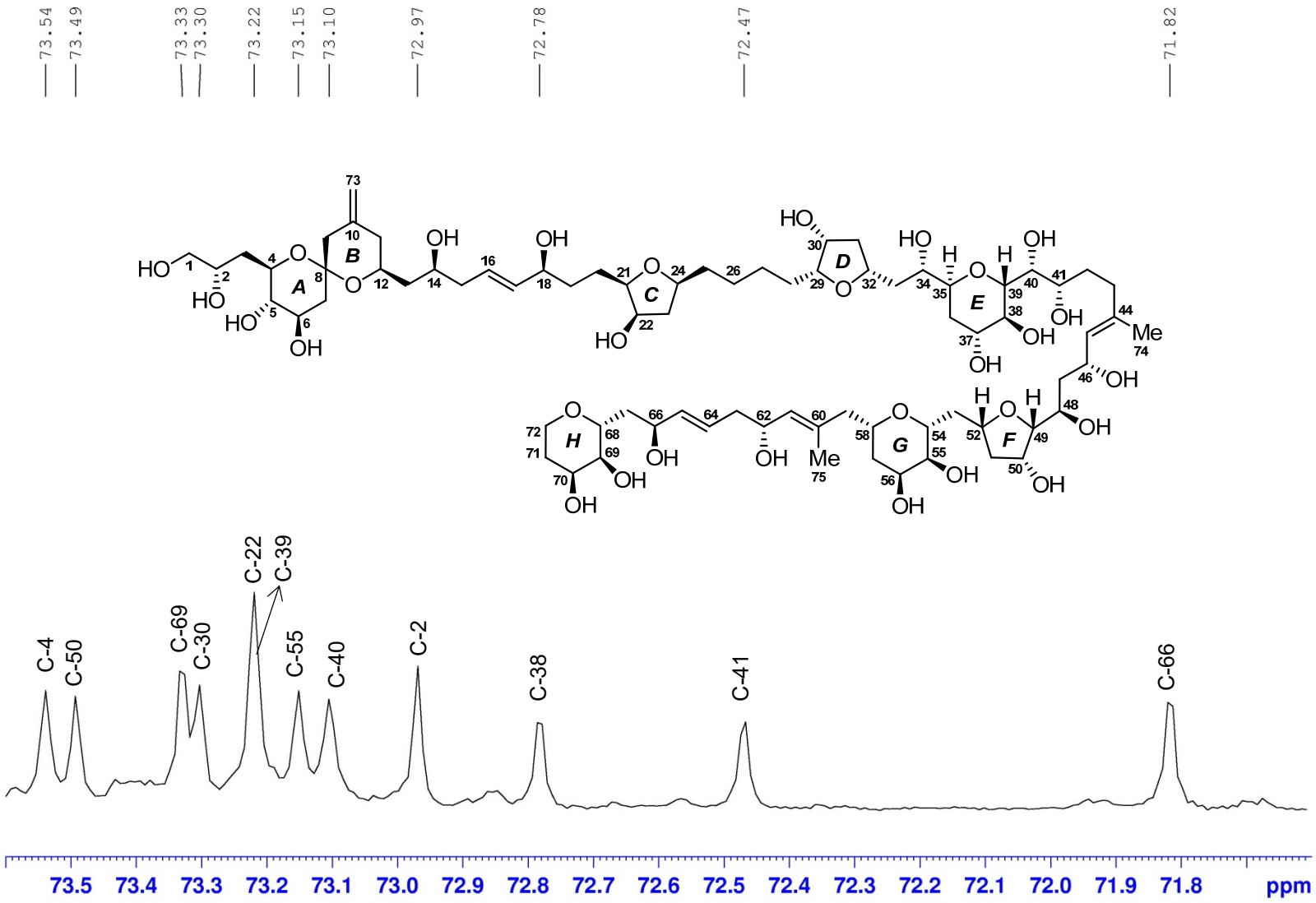

Figure S19. ^{13}C (175 MHz) NMR spectrum of compound **1** in CD_3OD

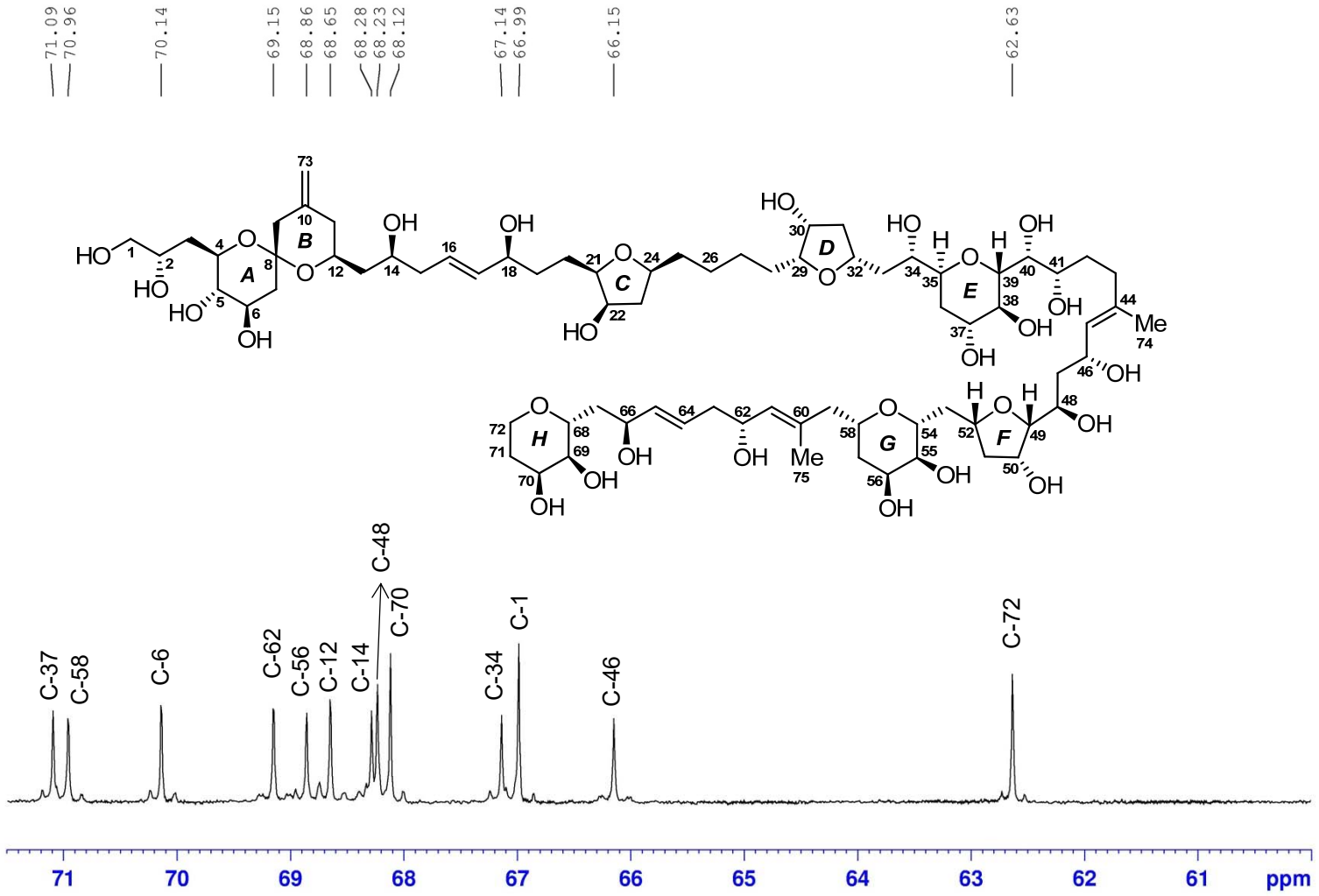

Figure S20. ^{13}C (175 MHz) NMR spectrum of compound **1** in CD_3OD

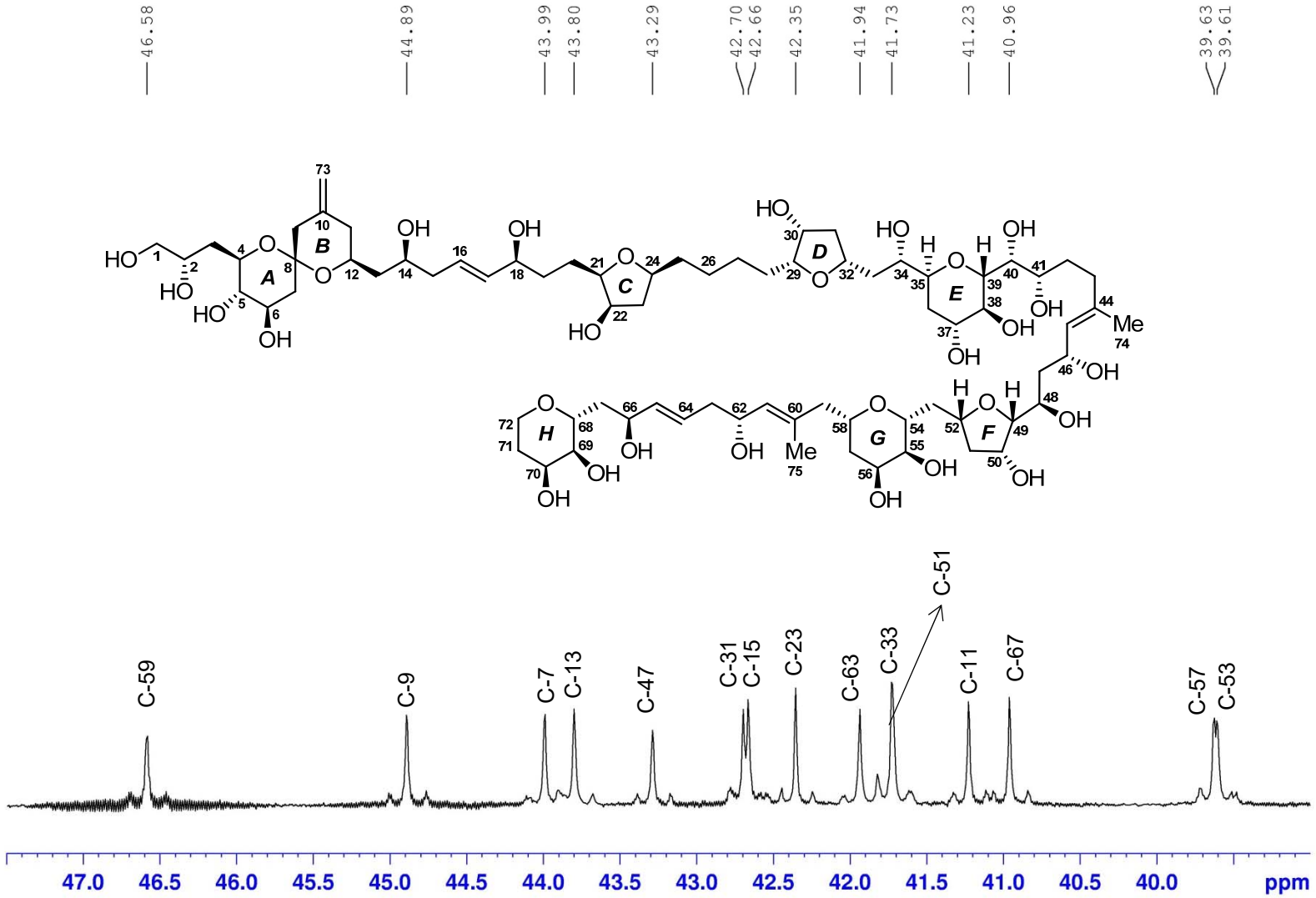

Figure S21. ^{13}C (175 MHz) NMR spectrum of compound **1** in CD_3OD

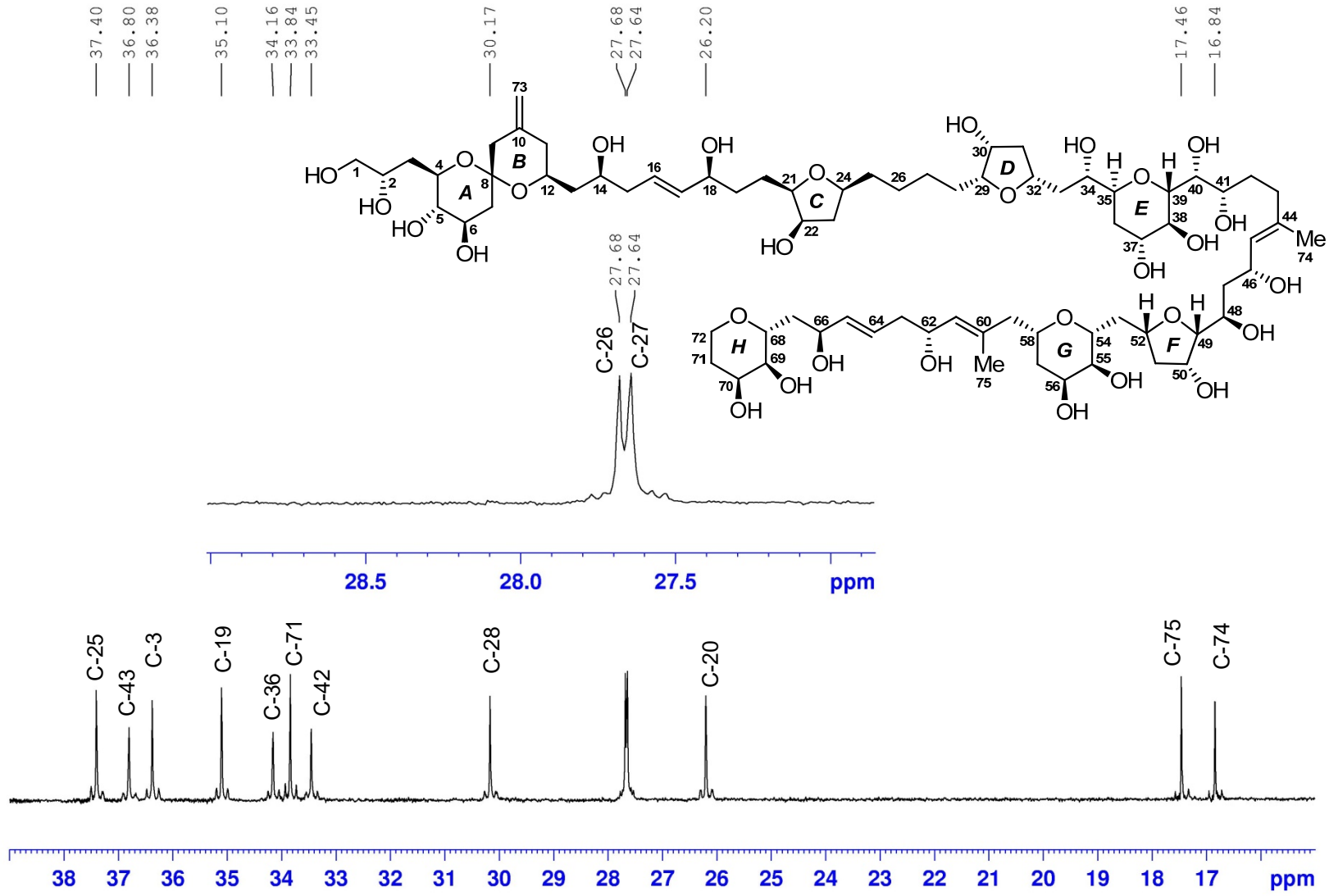

Figure S22. ^{13}C (175 MHz) NMR spectrum of compound **1** in CD_3OD

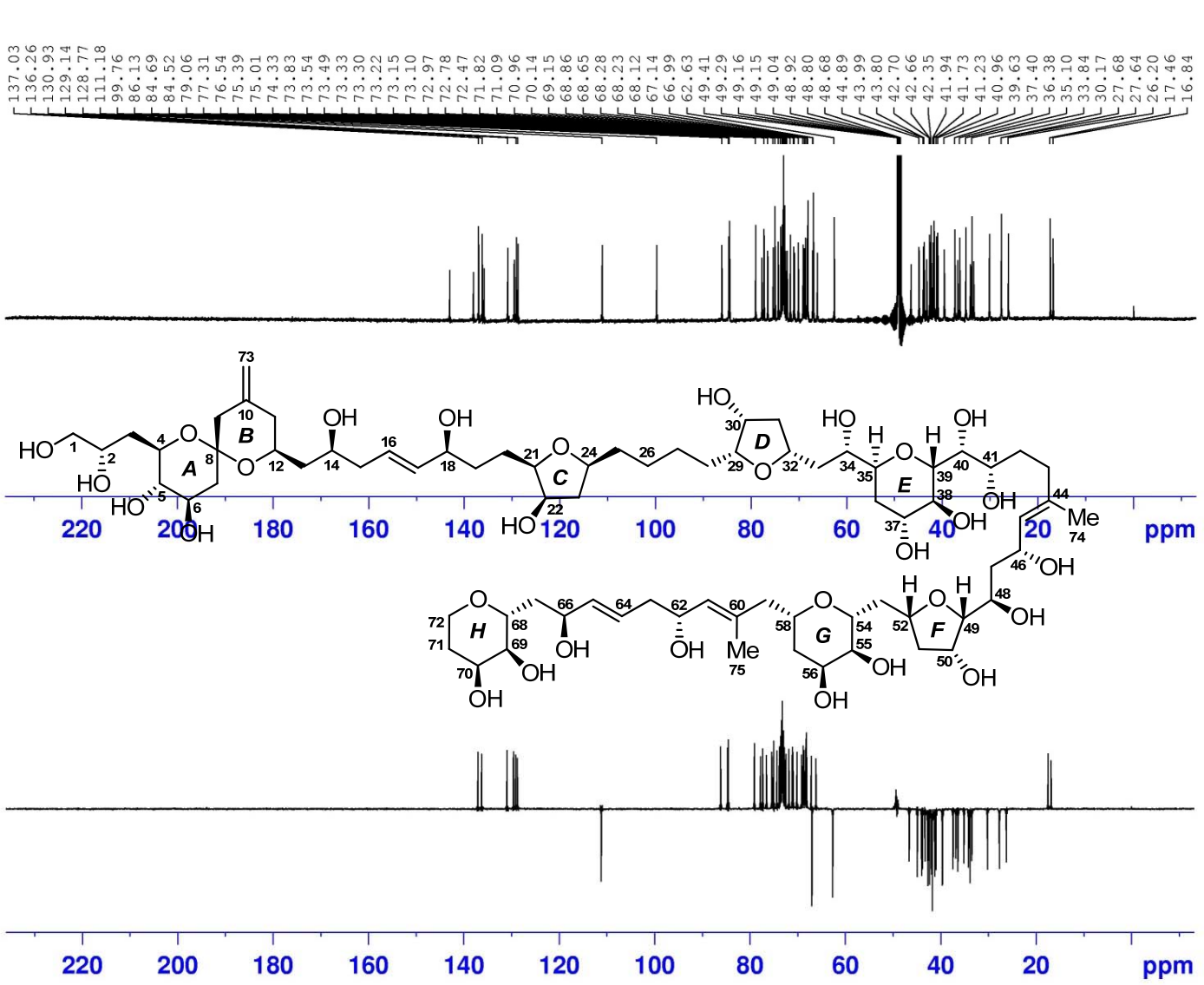

Figure S23. DEPT135 (175 MHz) spectrum of compound **1** in CD_3OD

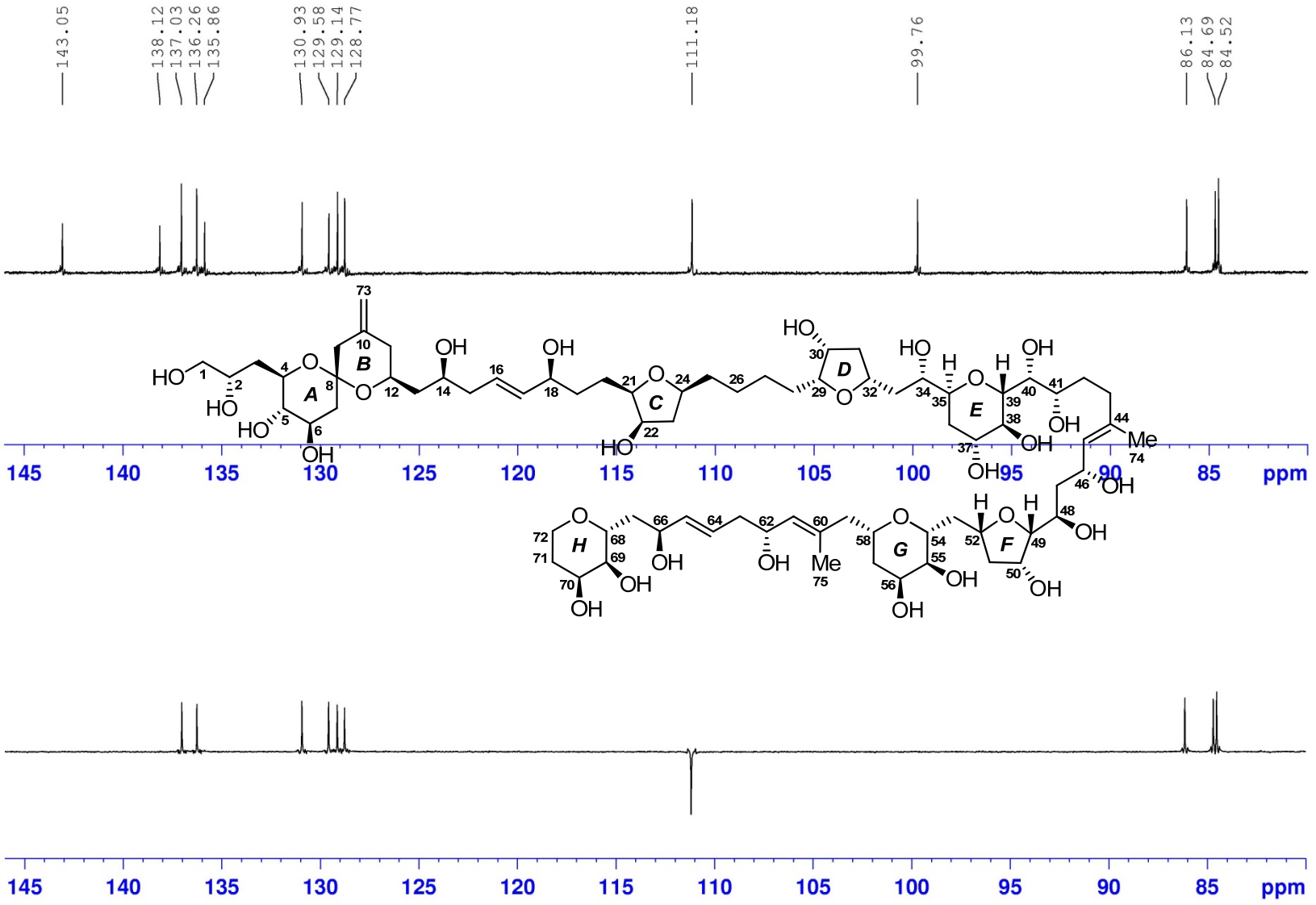

Figure S24. DEPT135 (175 MHz) spectrum of compound **1** in CD_3OD

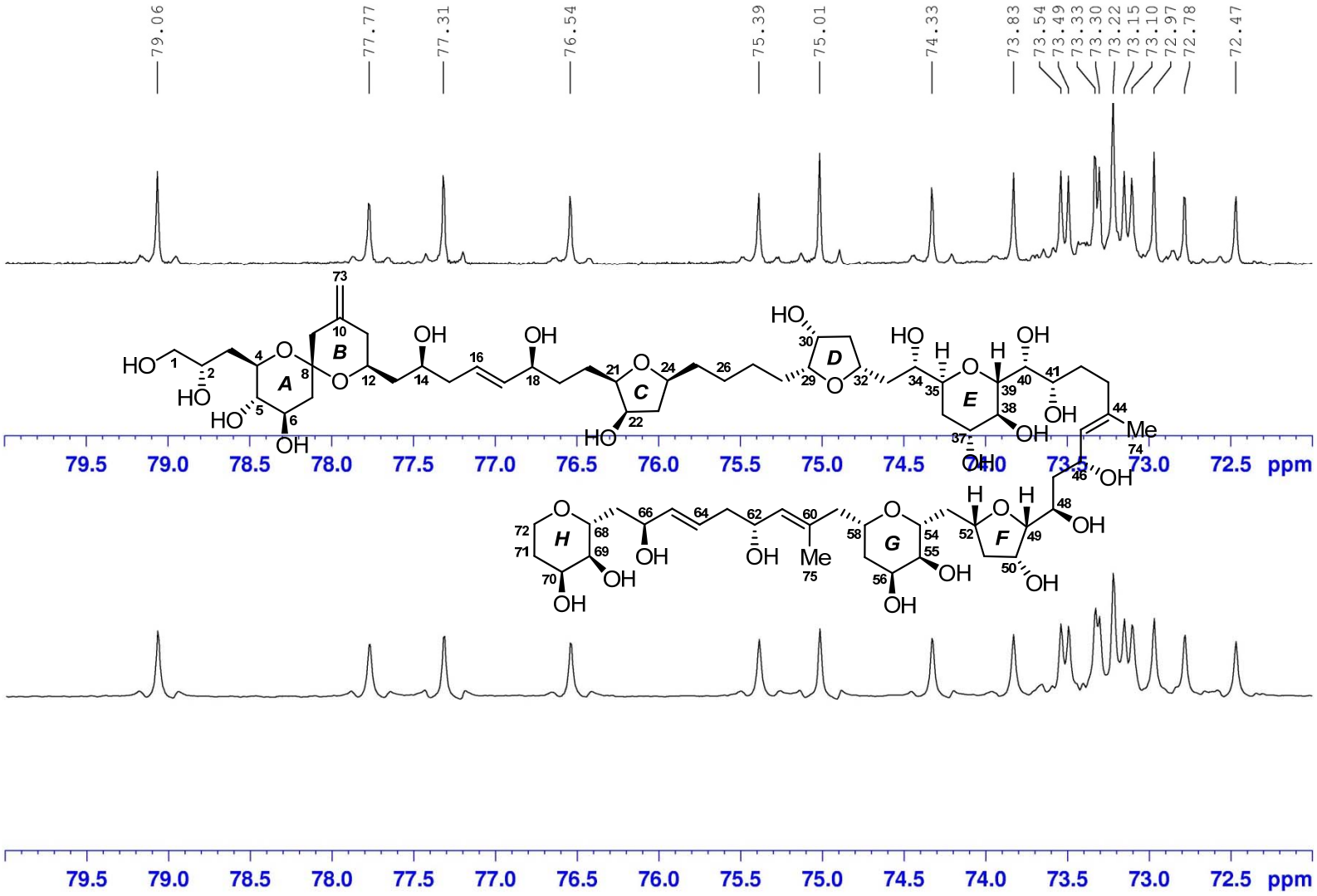

Figure S25. DEPT135 (175 MHz) spectrum of compound **1** in CD_3OD

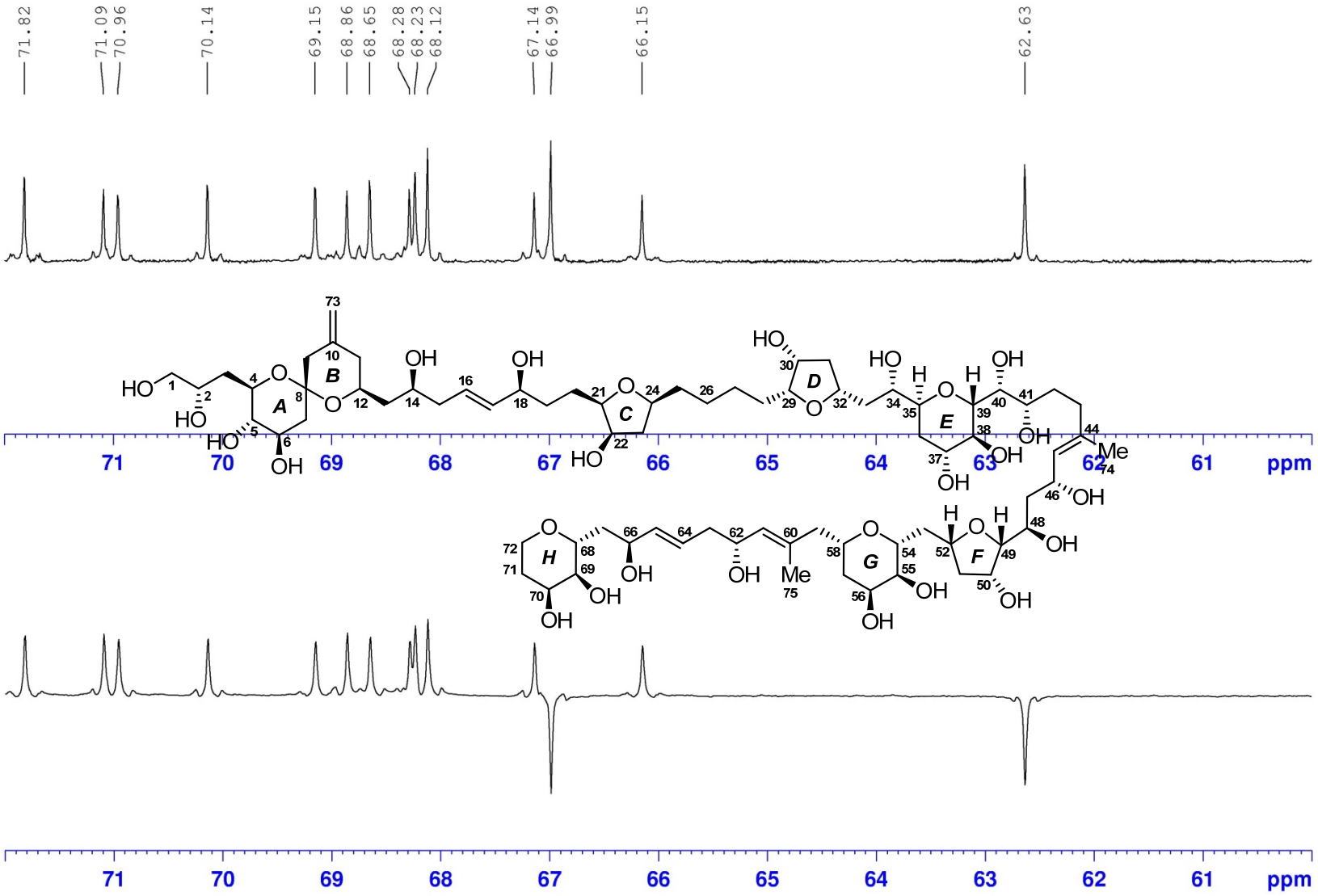

Figure S26. DEPT135 (175 MHz) spectrum of compound **1** in CD_3OD

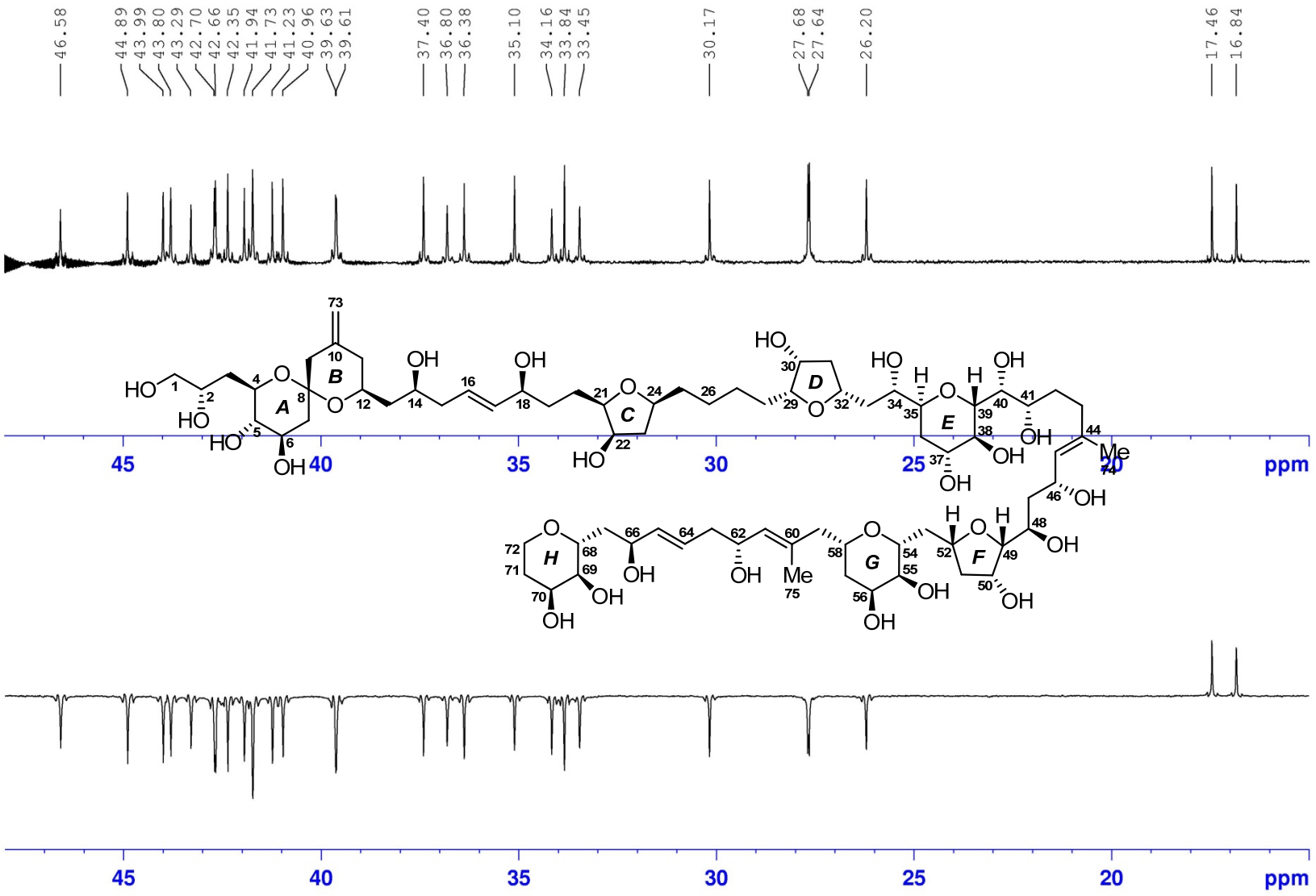

Figure S27. DEPT135 (175 MHz) spectrum of compound **1** in CD_3OD

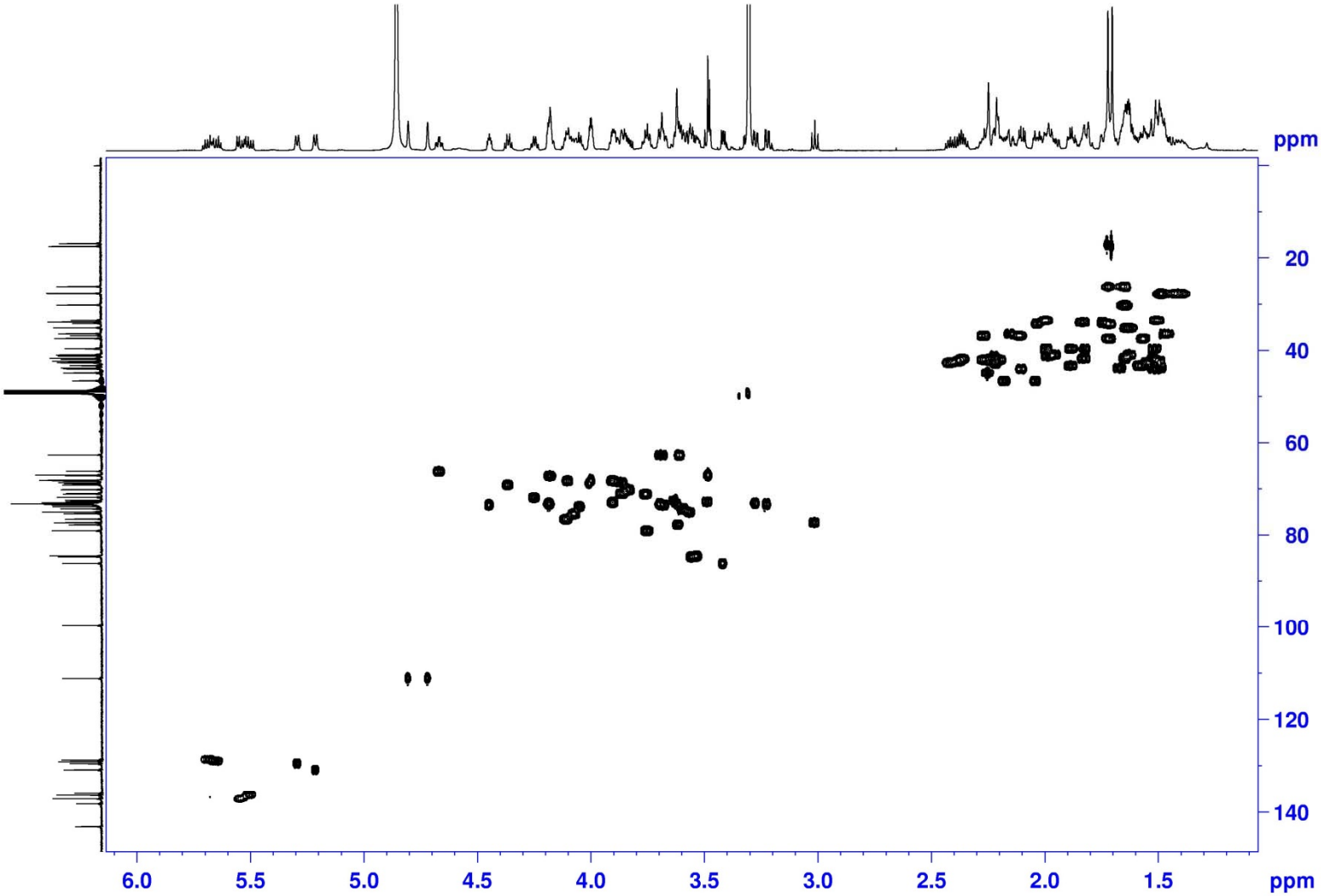

Figure S28. HSQC (700 MHz) spectrum of compound **1** in CD_3OD

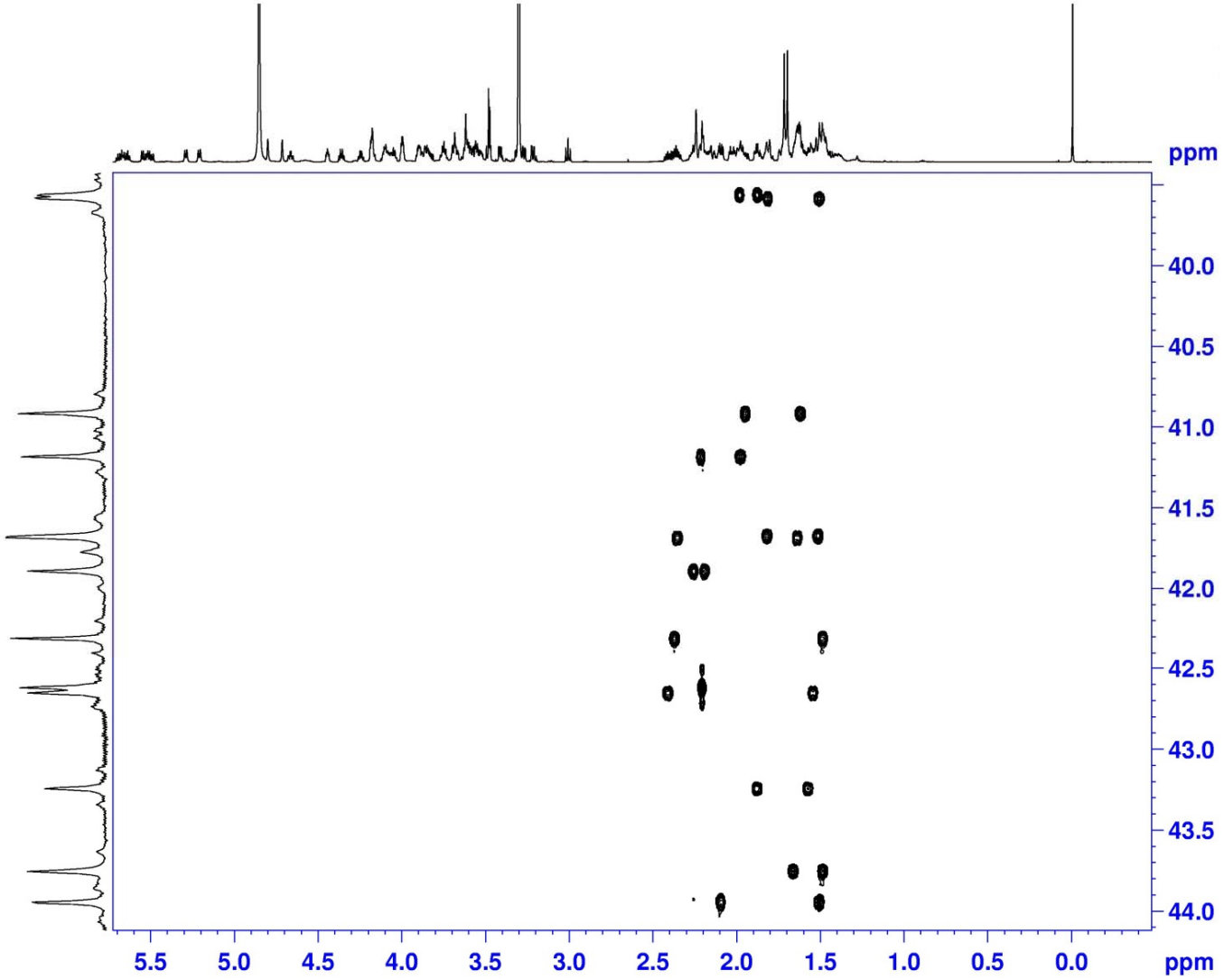

Figure S29. Selective-HSQC (700 MHz) spectrum of compound **1** in CD_3OD

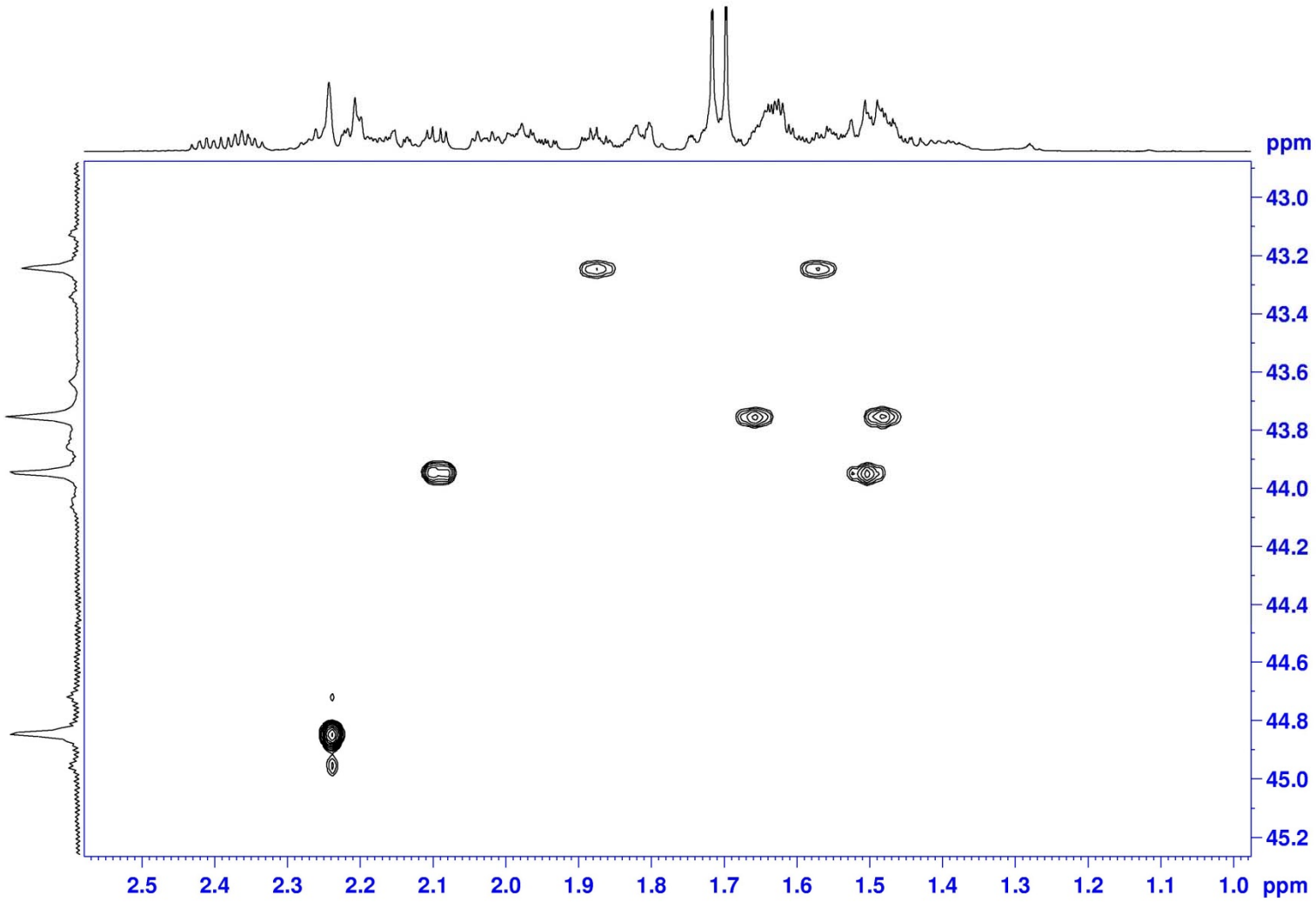

Figure S30. Selective-HSQC (700 MHz) spectrum of compound **1** in CD_3OD

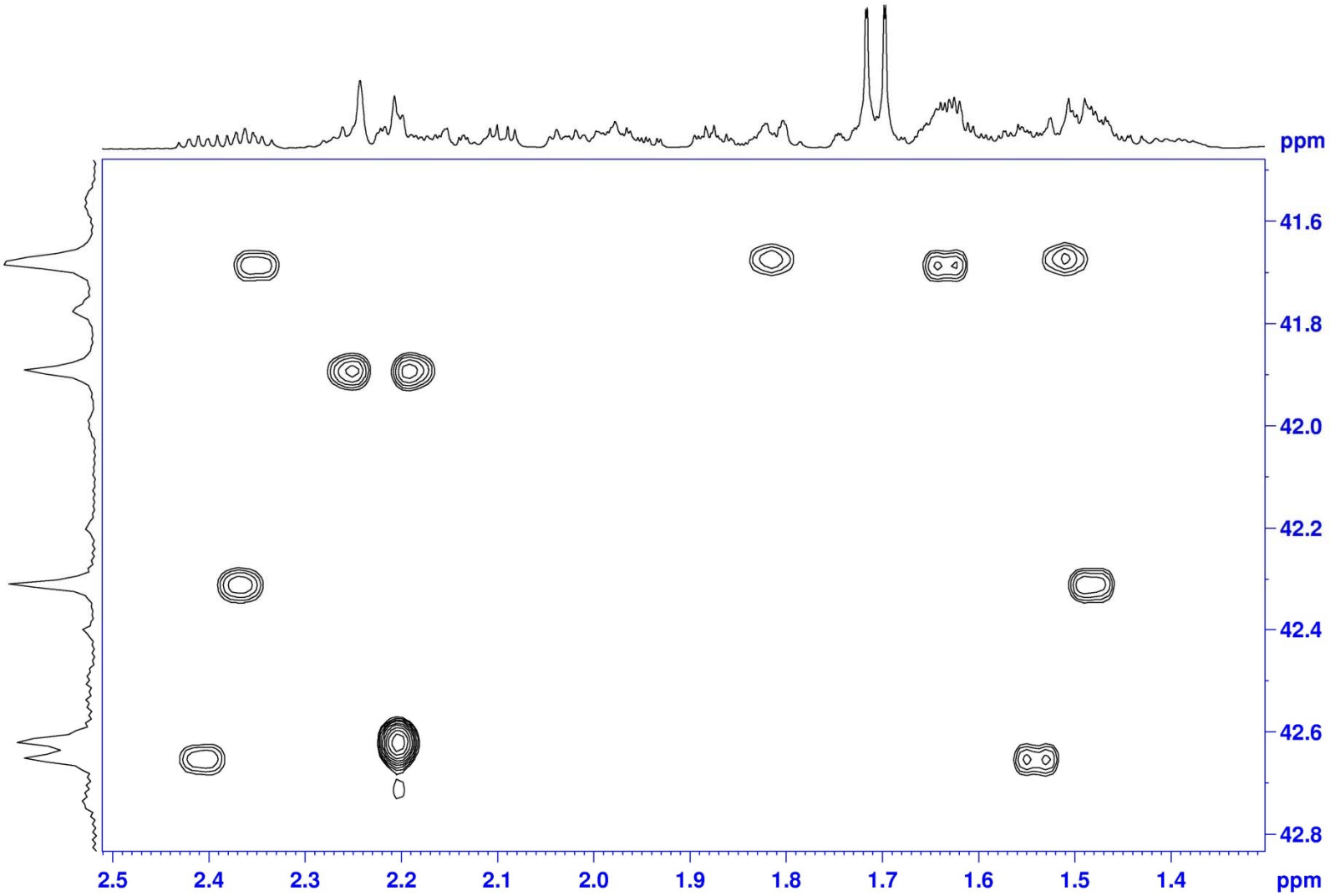

Figure S31. Selective-HSQC (700 MHz) spectrum of compound **1** in CD_3OD

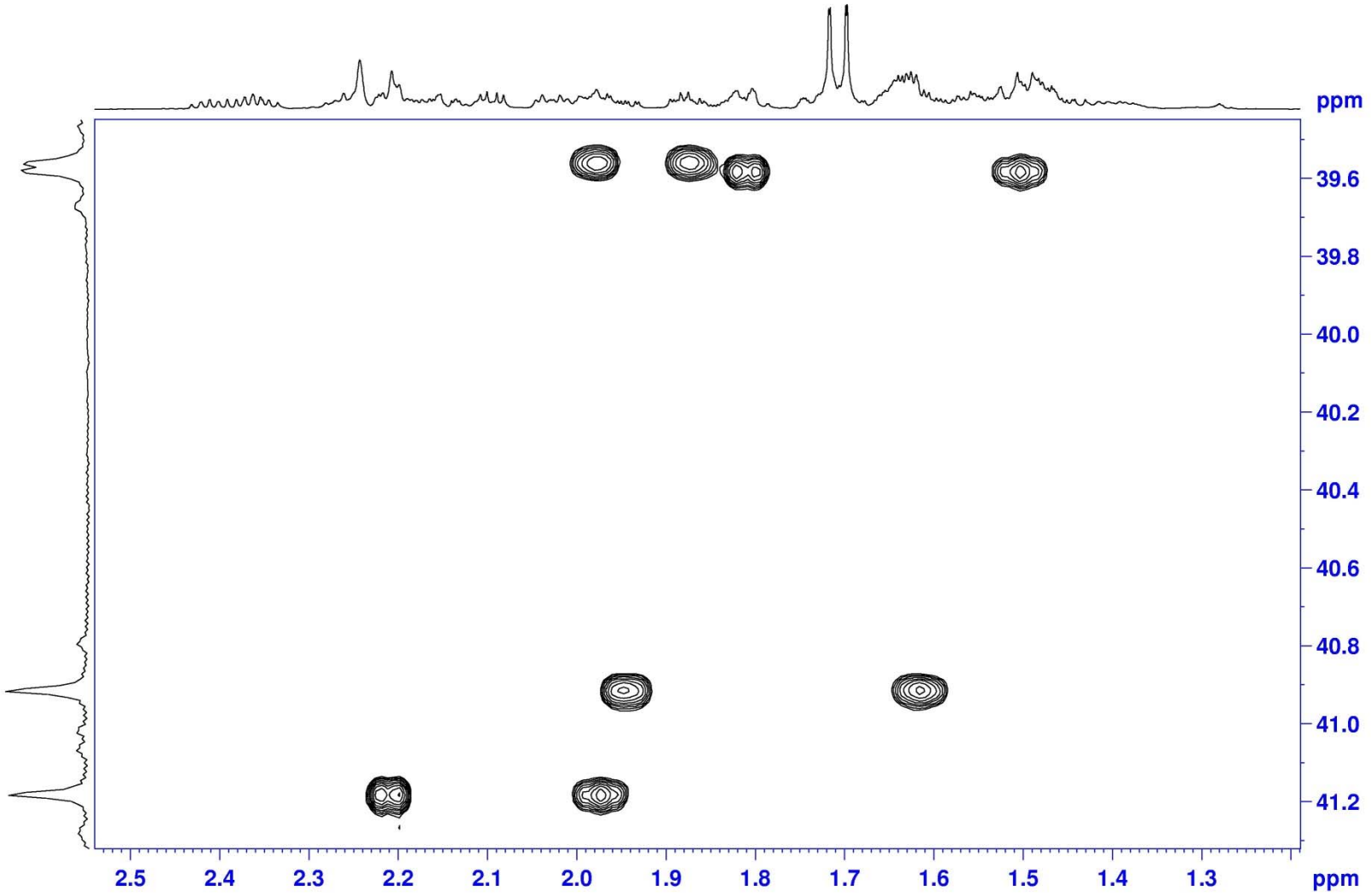

Figure S32. Selective-HSQC (700 MHz) spectrum of compound **1** in CD_3OD

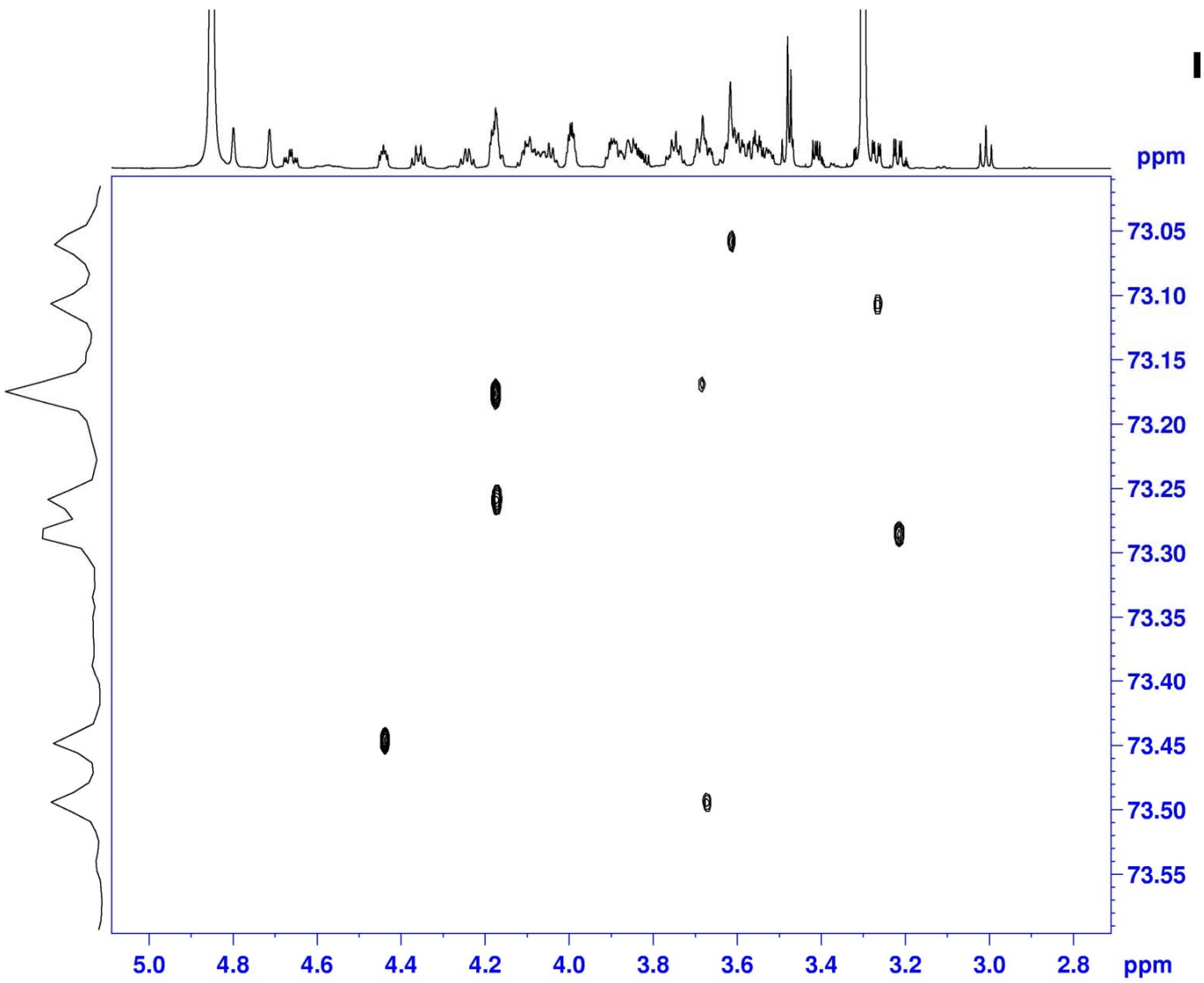

Figure S33. Selective-HSQC (700 MHz) spectrum of compound **1** in CD_3OD

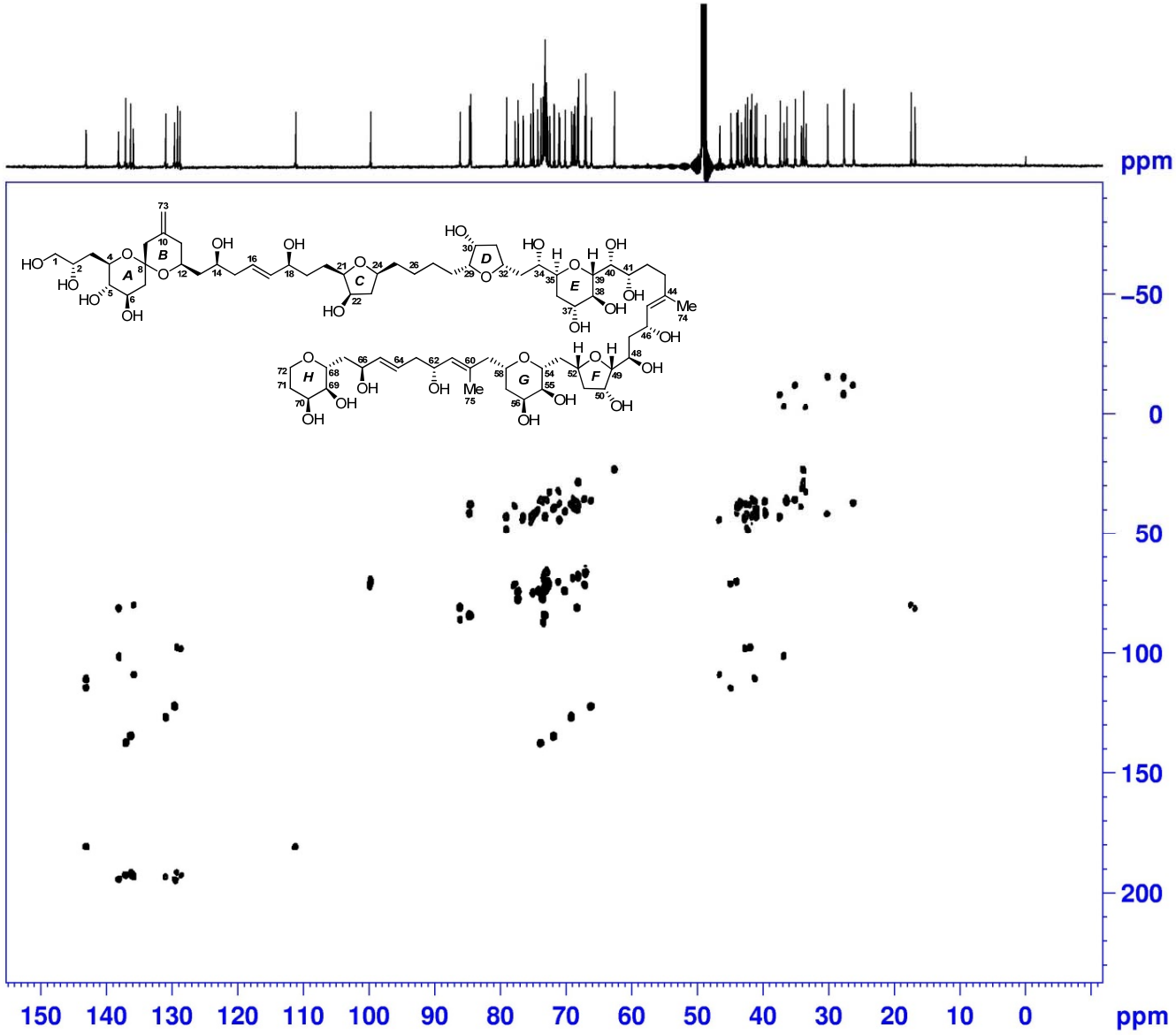

Figure S34. 2D INADEQUATE (175 MHz) spectrum of compound **1** in CD_3OD

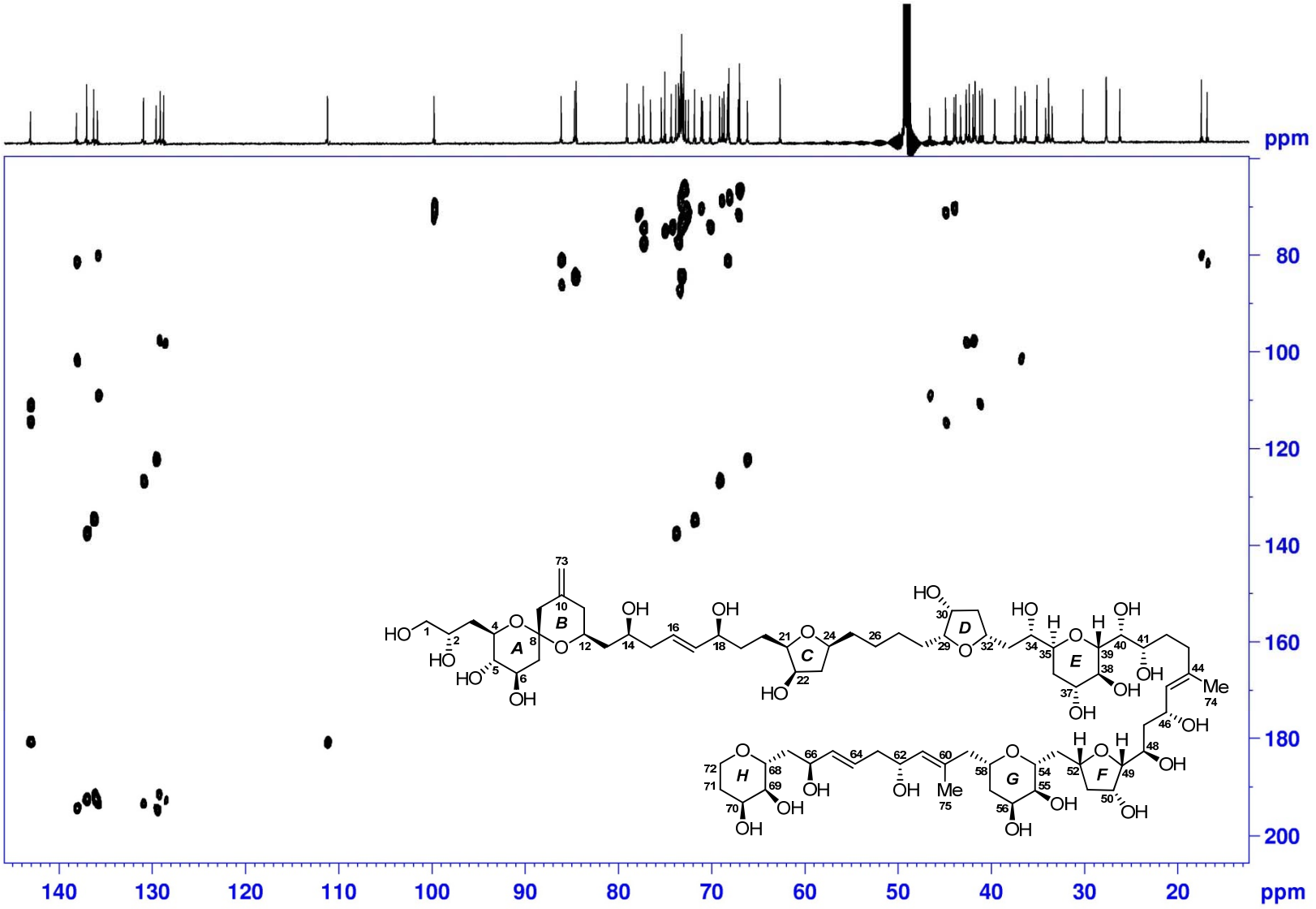

Figure S35. 2D INADEQUATE (175 MHz) spectrum of compound **1** in CD_3OD

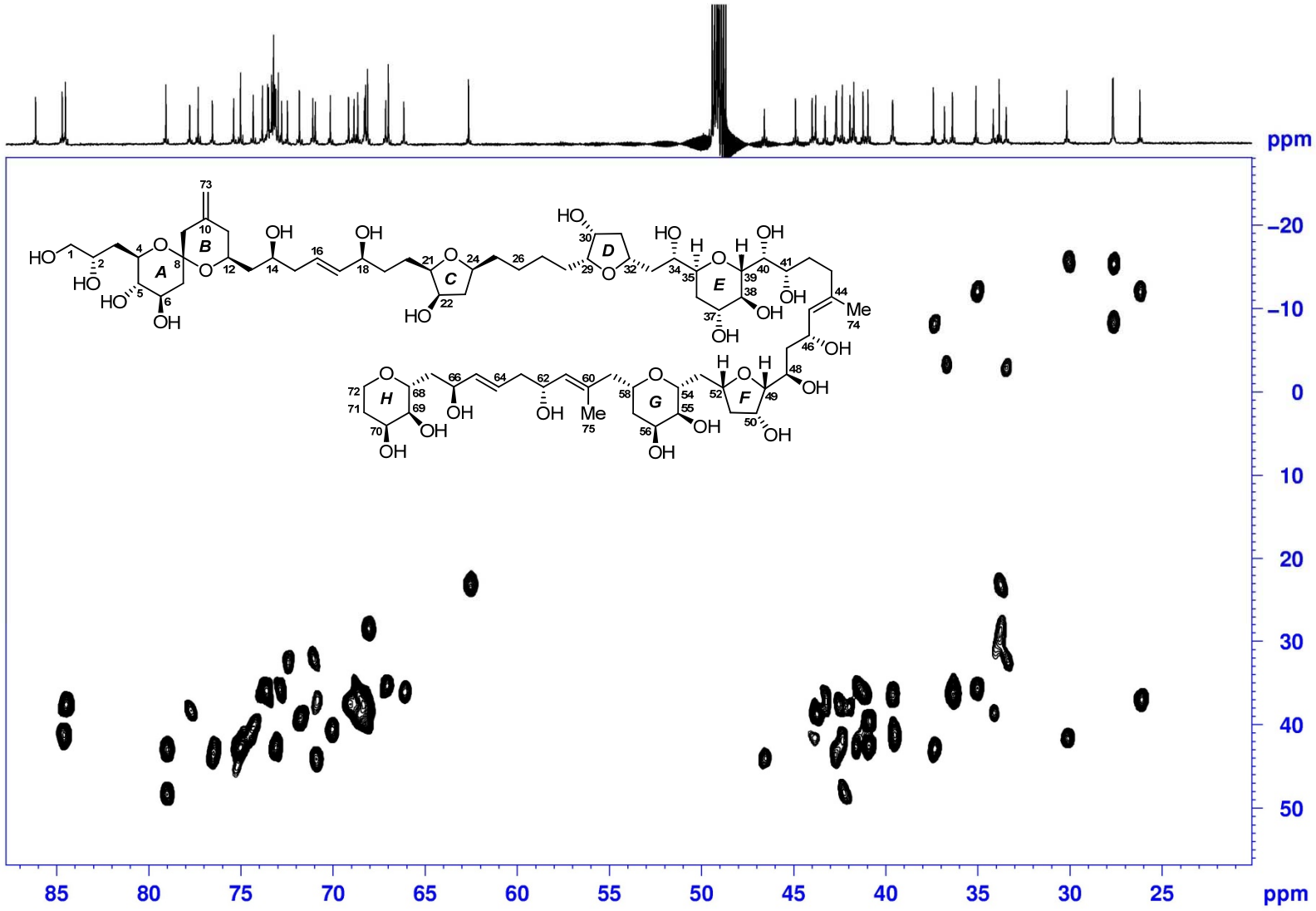

Figure S36. 2D INADEQUATE (175 MHz) spectrum of compound **1** in CD_3OD

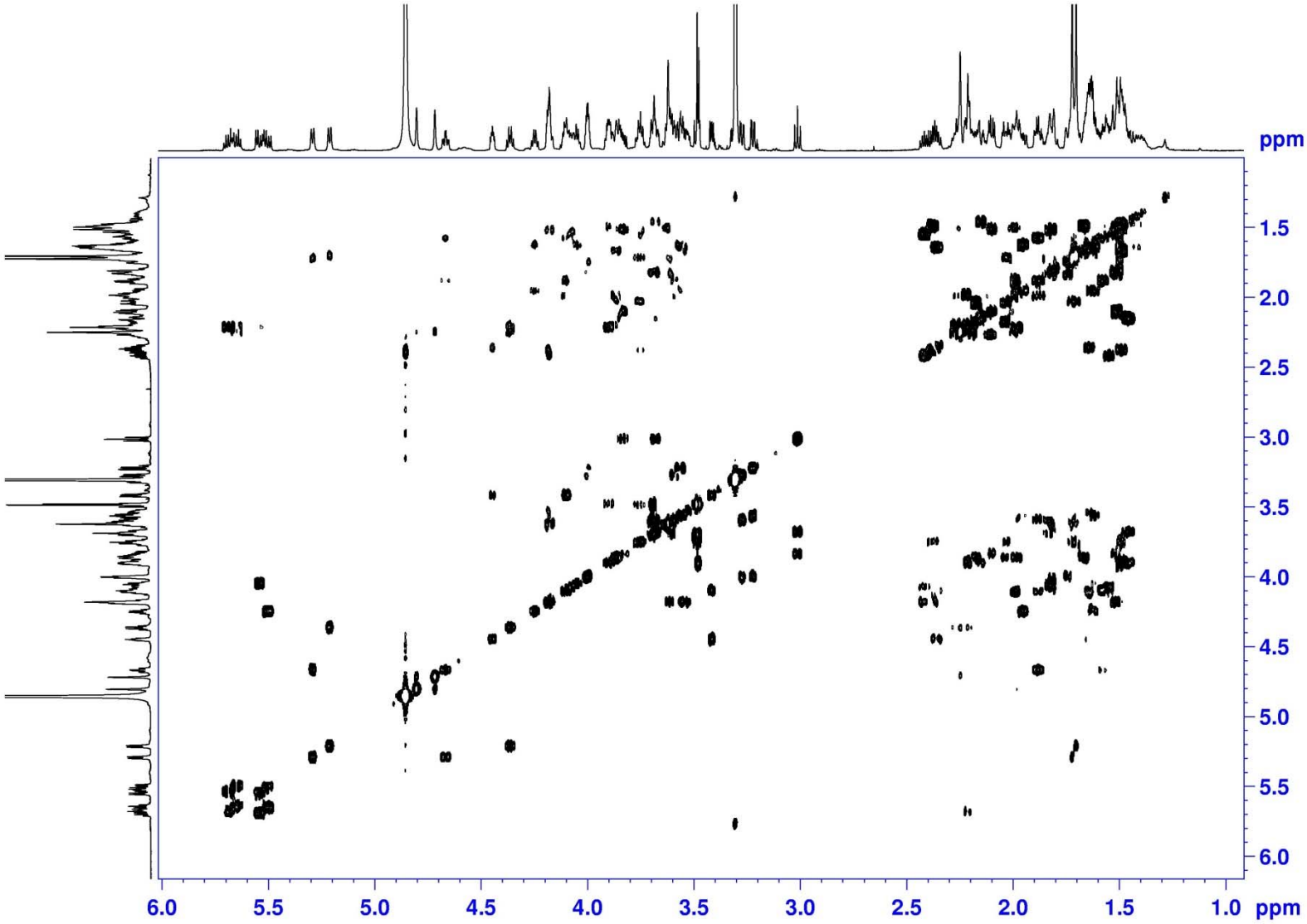

Figure S37. ^{1}H–^{1}H COSY (700 MHz) spectrum of compound **1** in CD_3OD

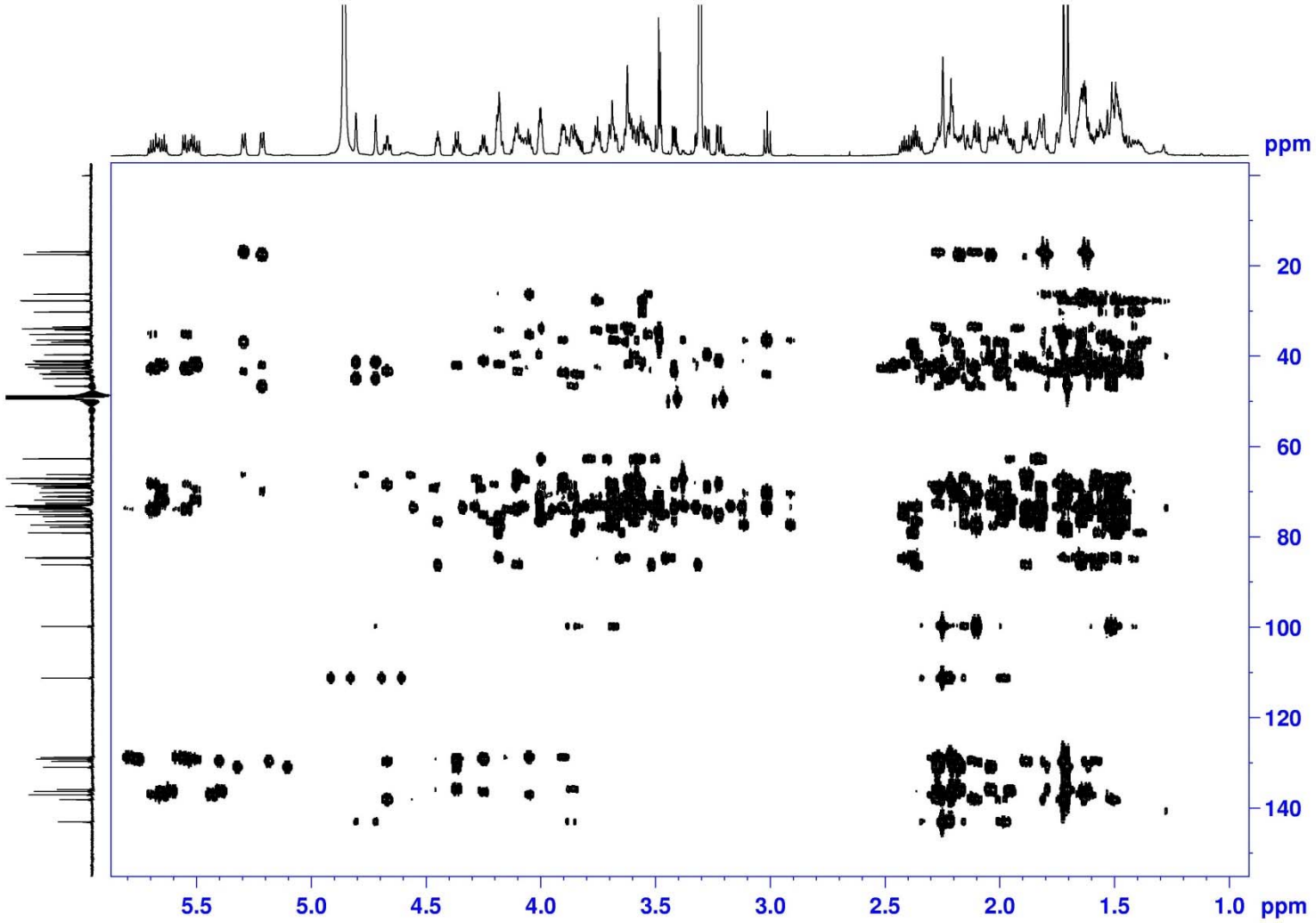

Figure S38. HMBC (700 MHz) spectrum of compound **1** in CD_3OD

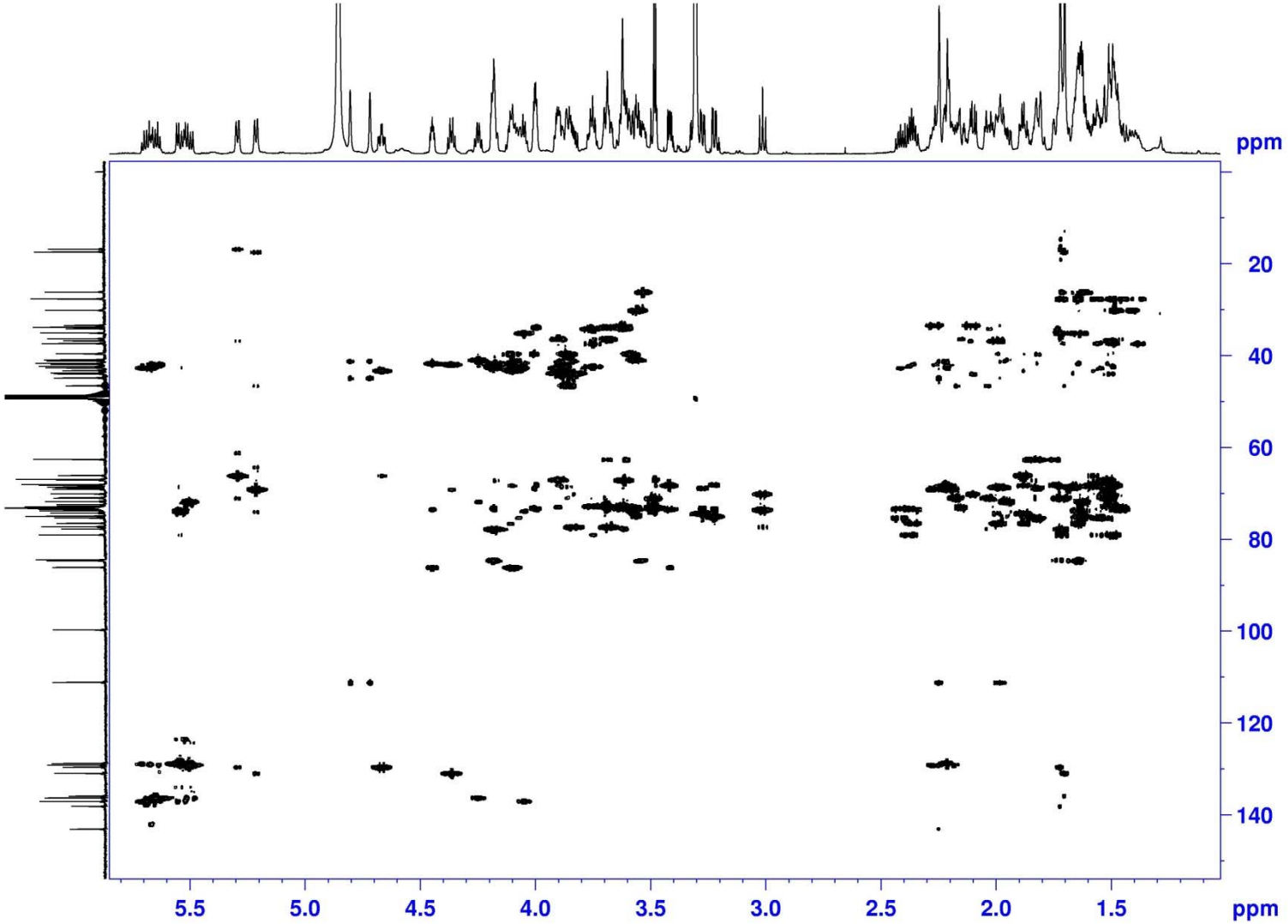

Figure S39. H2BC (700 MHz) spectrum of compound **1** in CD_3OD

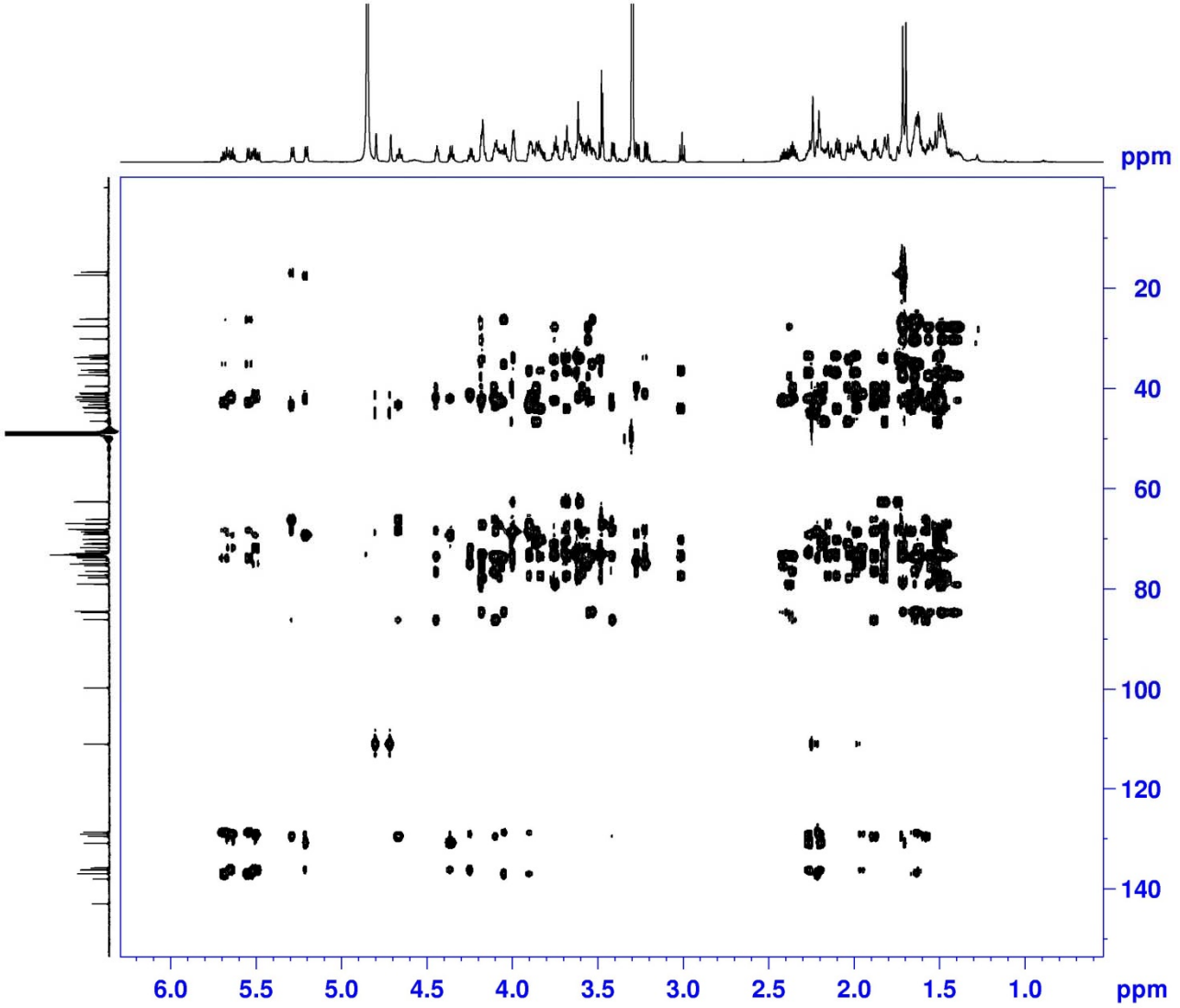

Figure S40. HSQC-TOCSY (700 MHz) spectrum of compound **1** in CD_3OD

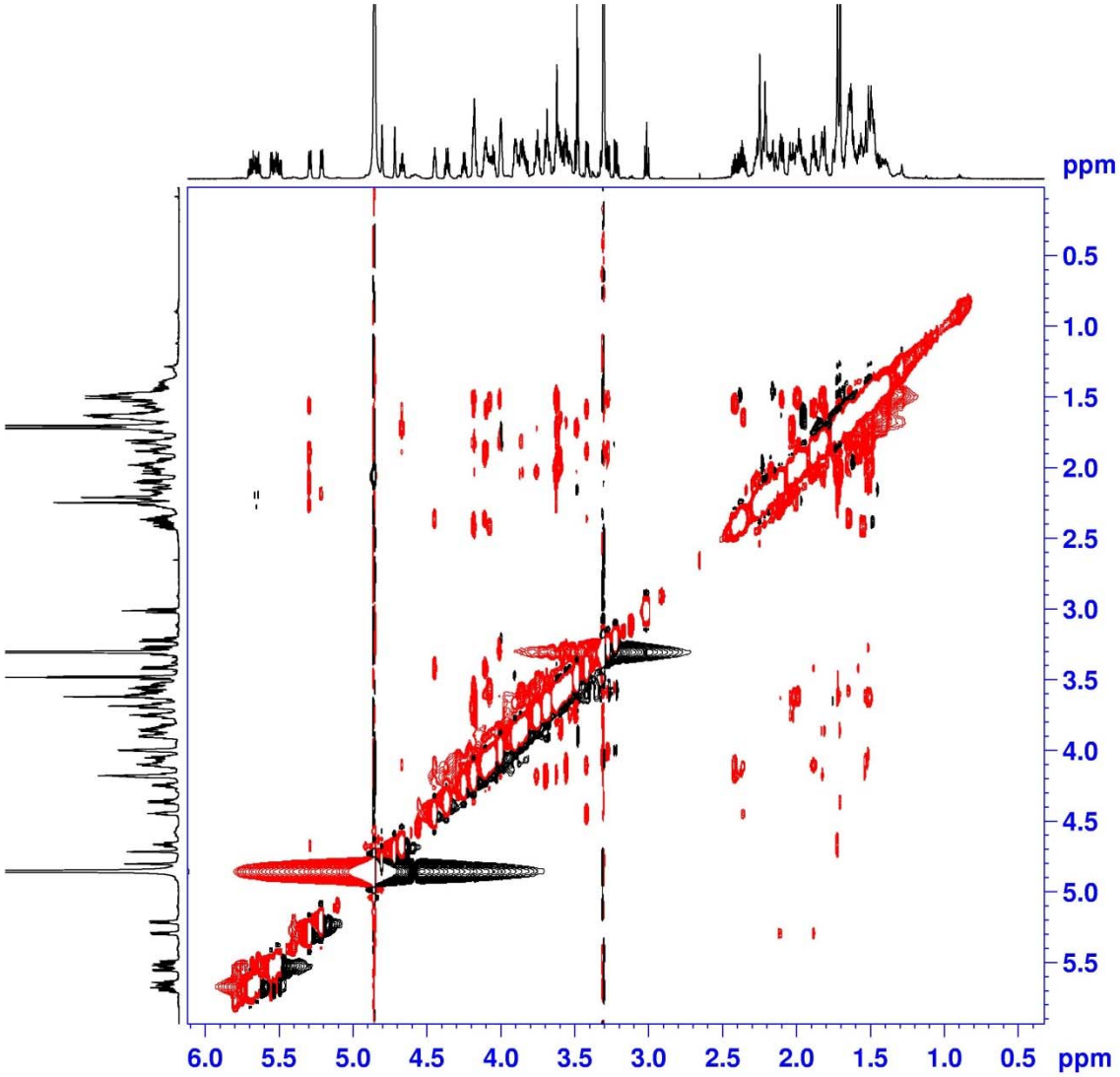

Figure S41. NOESY (700 MHz) spectrum of compound **1** in CD_3OD

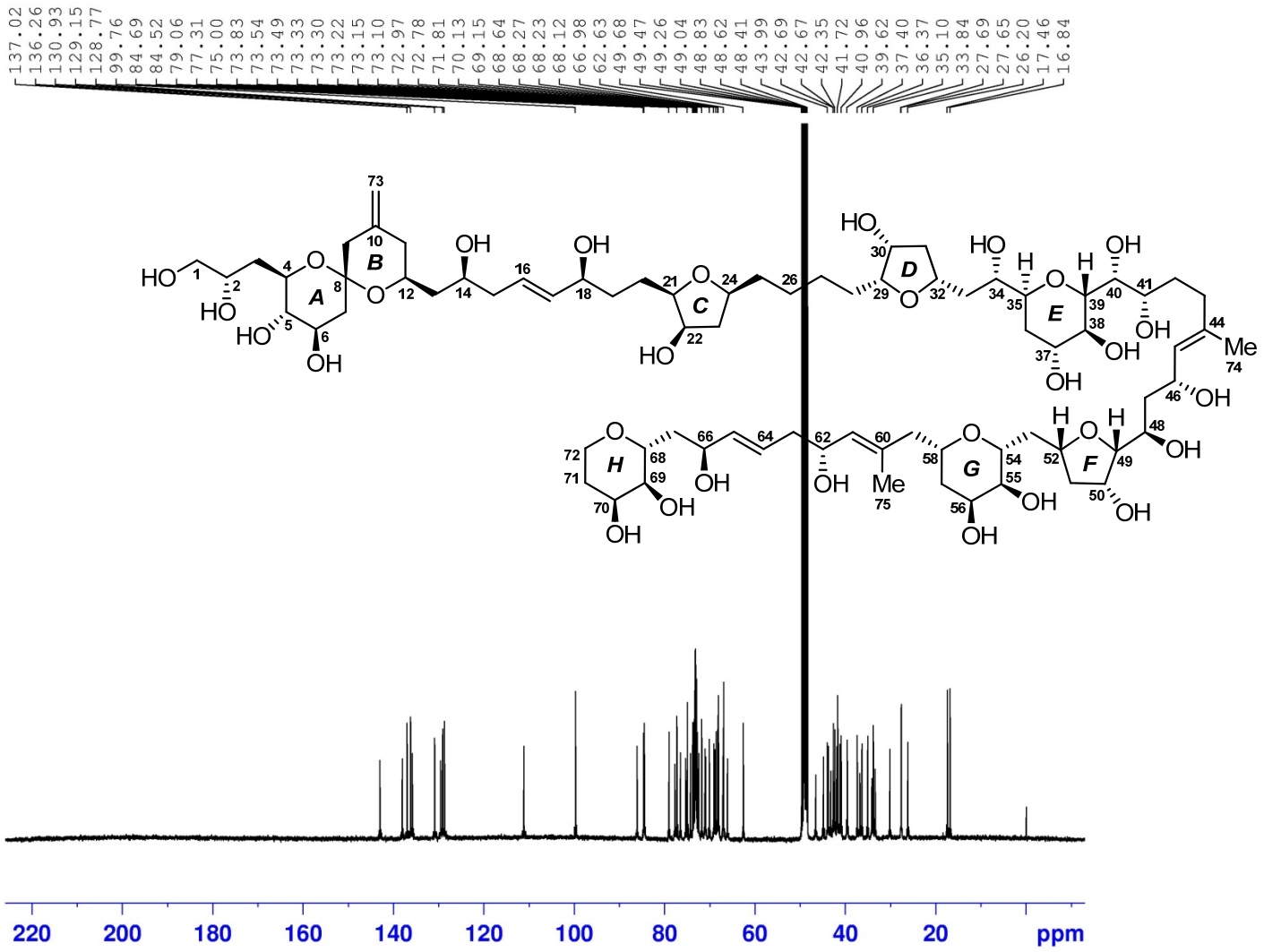

Figure S42. ^{13}C (100 MHz) NMR spectrum of compound **1** in CD_3OD

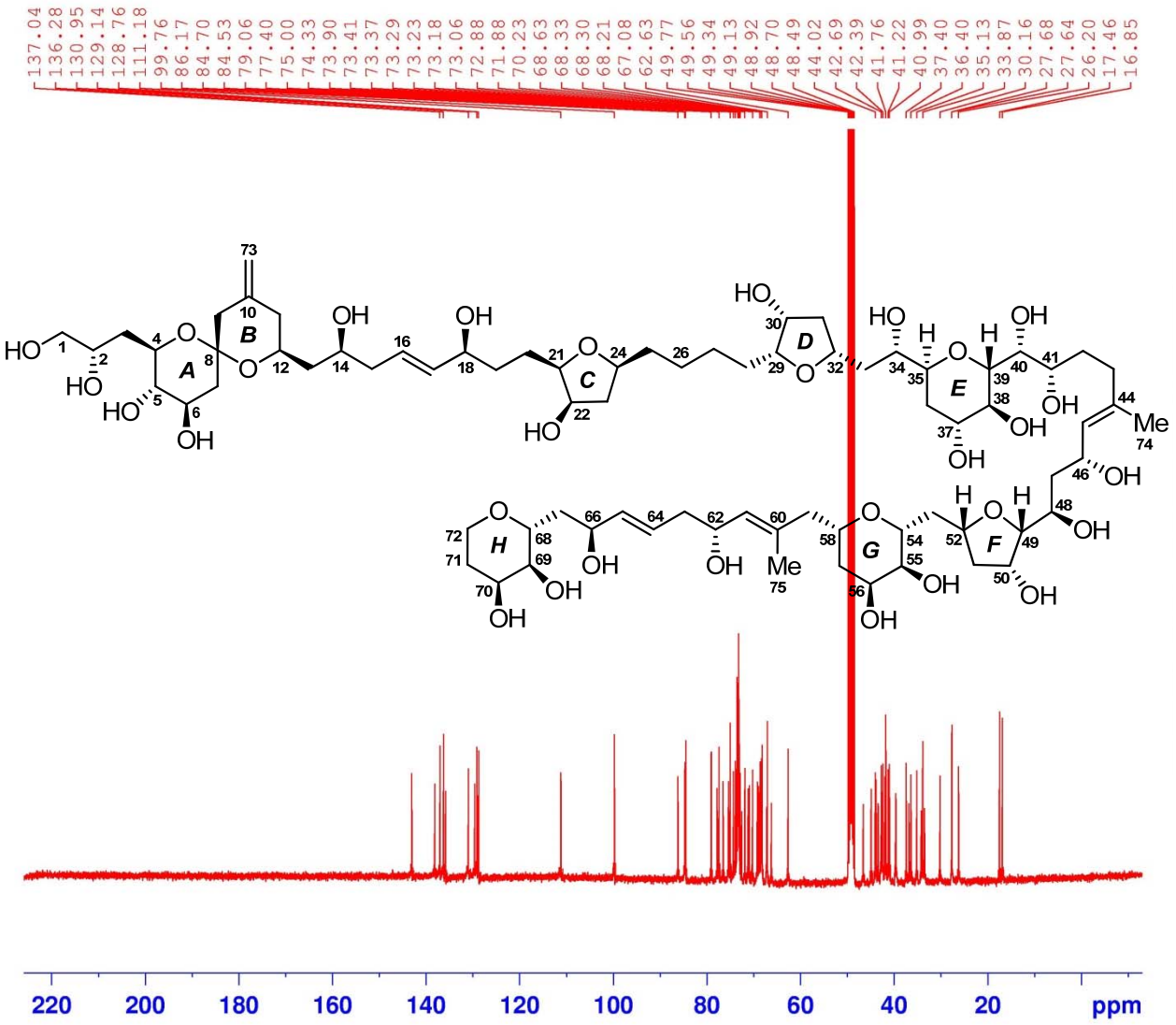

Figure S43. ^{13}C (100 MHz) NMR spectrum of compound **1** in CD_3OH

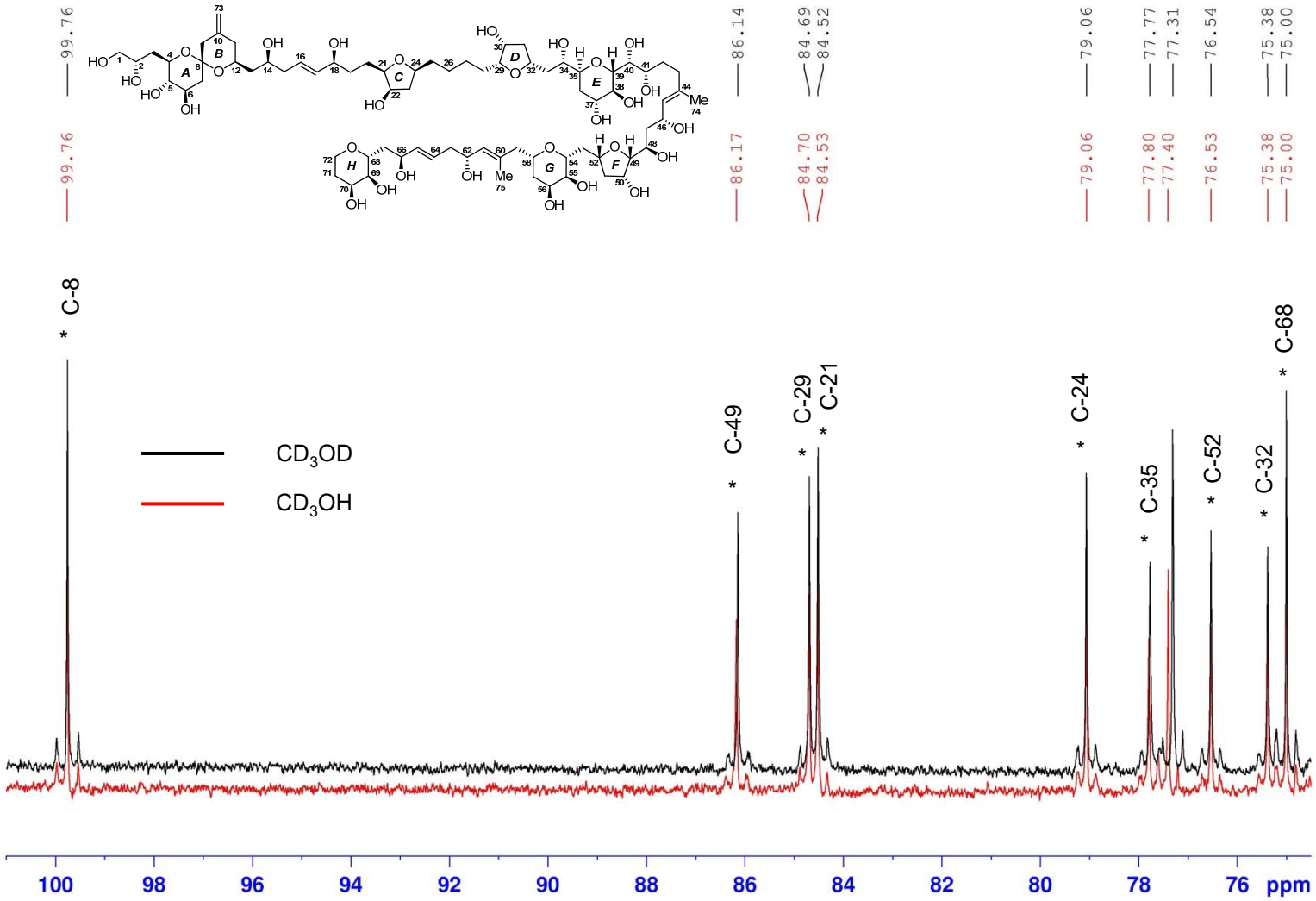

Figure S44. Comparison of ^{13}C (100 MHz) NMR spectrum of compound **1** in CD_3OH with that in CD_3OD

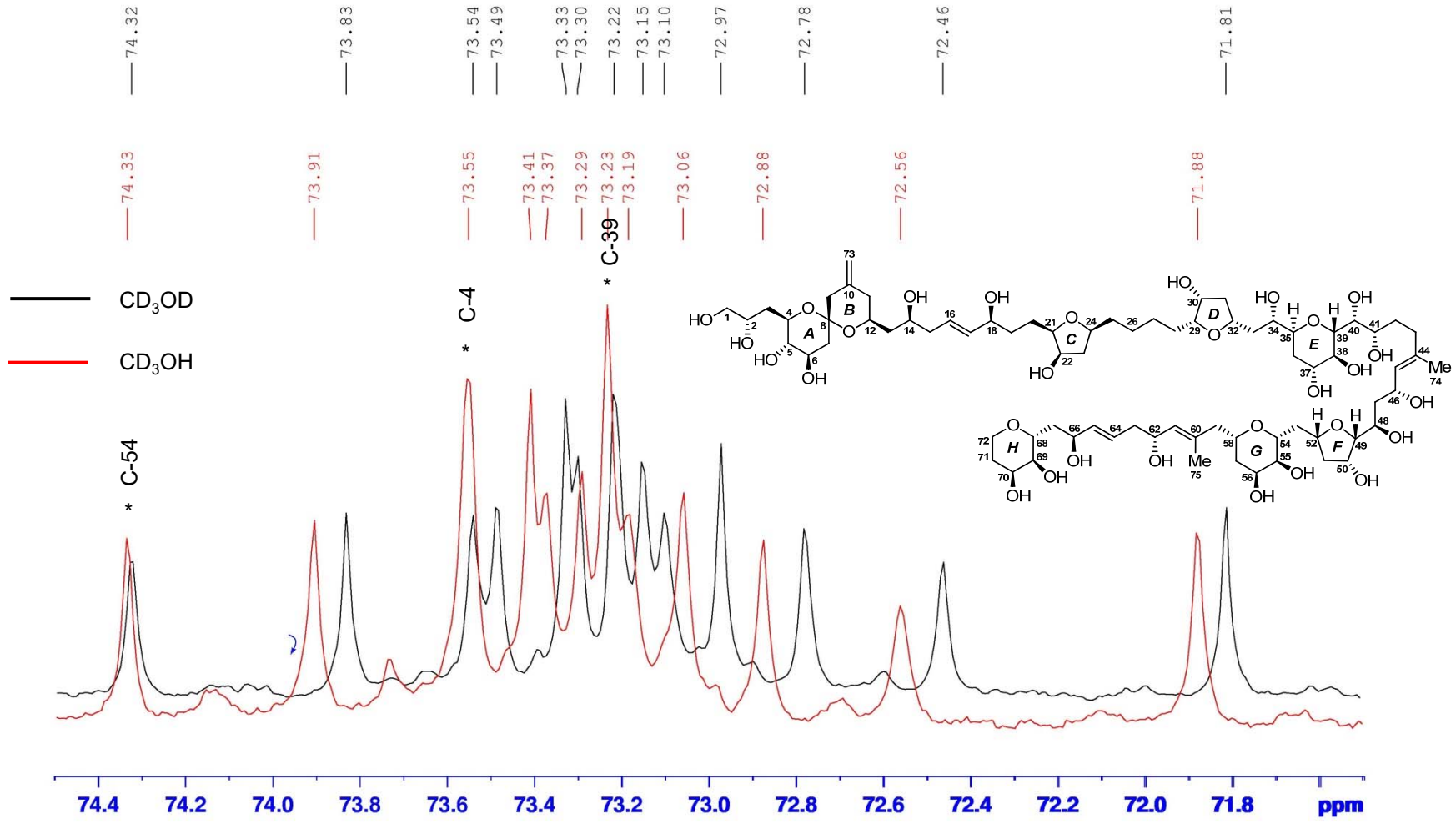

Figure S45. Comparison of ^{13}C (100 MHz) NMR spectrum of compound **1** in CD_3OH with that in CD_3OD

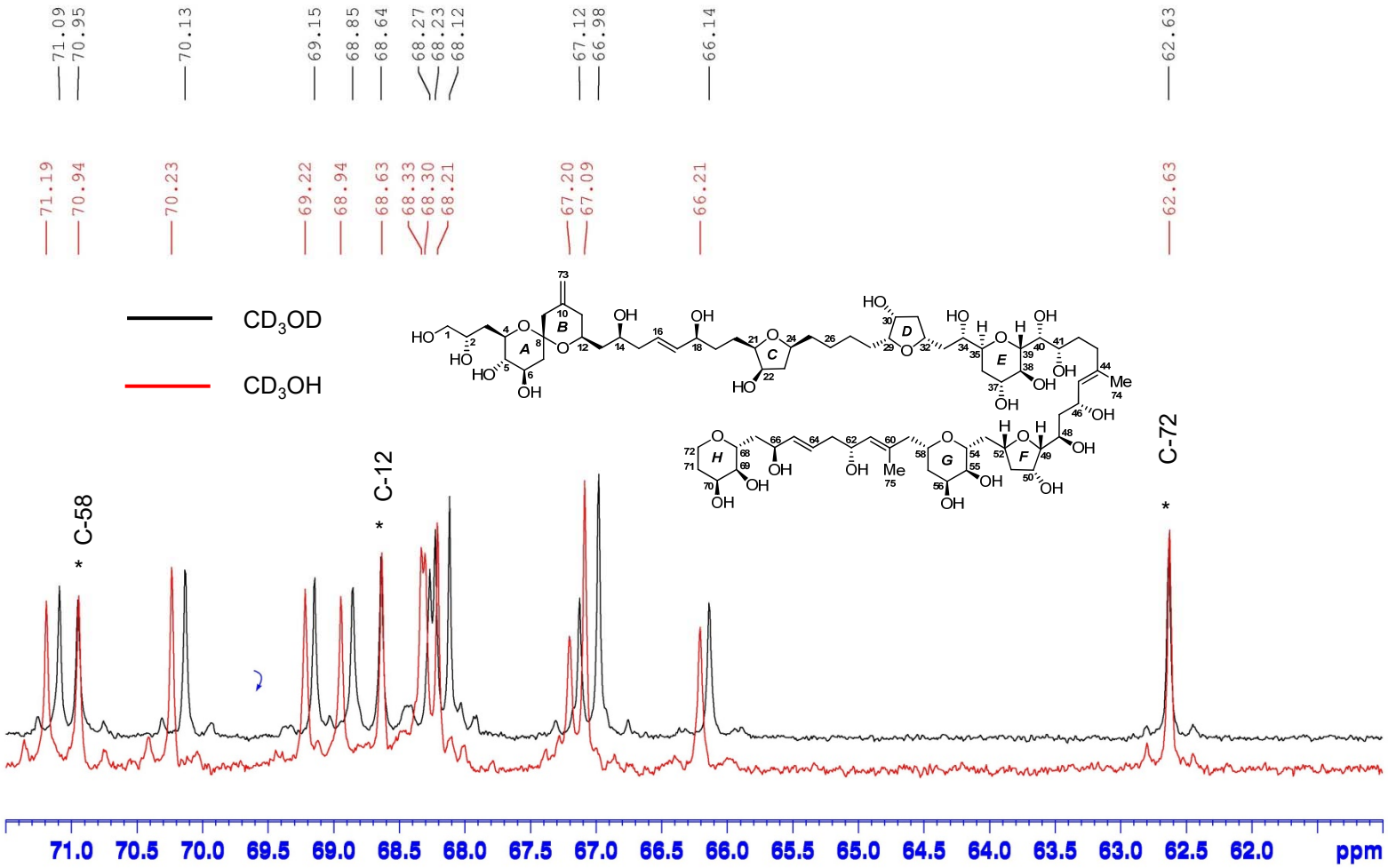

Figure S46. Comparison of ^{13}C (100 MHz) NMR spectrum of compound **1** in CD_3OH with that in CD_3OD

Mass Spectrum SmartFormula Report

Analysis Info

Analysis Name	H:\data2015-2017\201703\liwanshan_AX-1-a_pos_32_01_2761.d	Acquisition Date	3/23/2017 4:22:47 PM
Method	LC_Direct Infusion_pos_70-500mz.m	Operator	SCSIO
Sample Name	liwanshan_AX-1-a_pos	Instrument	maXis 255552.00029
Comment			

Acquisition Parameter

Source Type	ESI	Ion Polarity	Positive	Set Nebulizer	0.4 Bar
Focus	Active	Set Capillary	4500 V	Set Dry Heater	180 °C
Scan Begin	70 m/z	Set End Plate Offset	-500 V	Set Dry Gas	4.0 l/min
Scan End	1500 m/z	Set Charging Voltage	0 V	Set Divert Valve	Waste
		Set Corona	0 nA	Set APCI Heater	0 °C

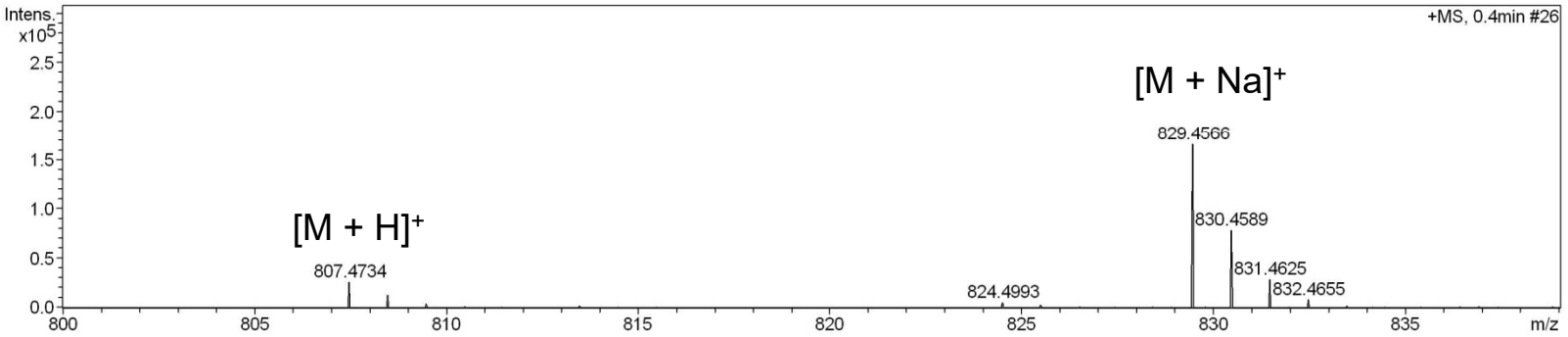

Meas. m/z	#	Ion Formula	Score	m/z	err [ppm]	err [mDa]	mSigma	rdb	e⁻ Conf	N-Rule
807.4734	1	C40H71O16	100.00	807.4737	0.4	0.3	24.7	5.5	even	ok
829.4566	1	C40H70NaO16	100.00	829.4556	1.2	1.0	24.1	5.5	even	ok

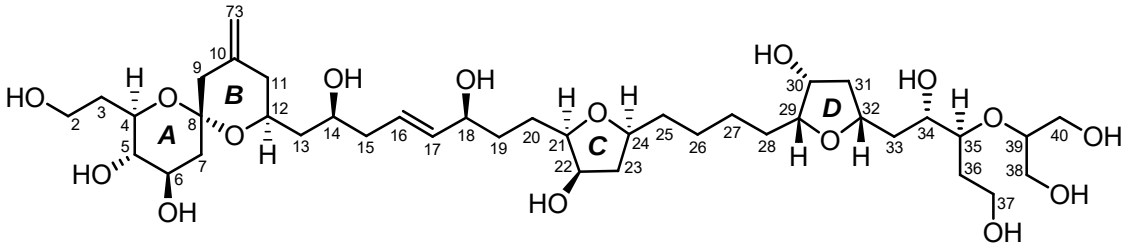

Figure S47. HR-ESIMS for the fragment **1A**

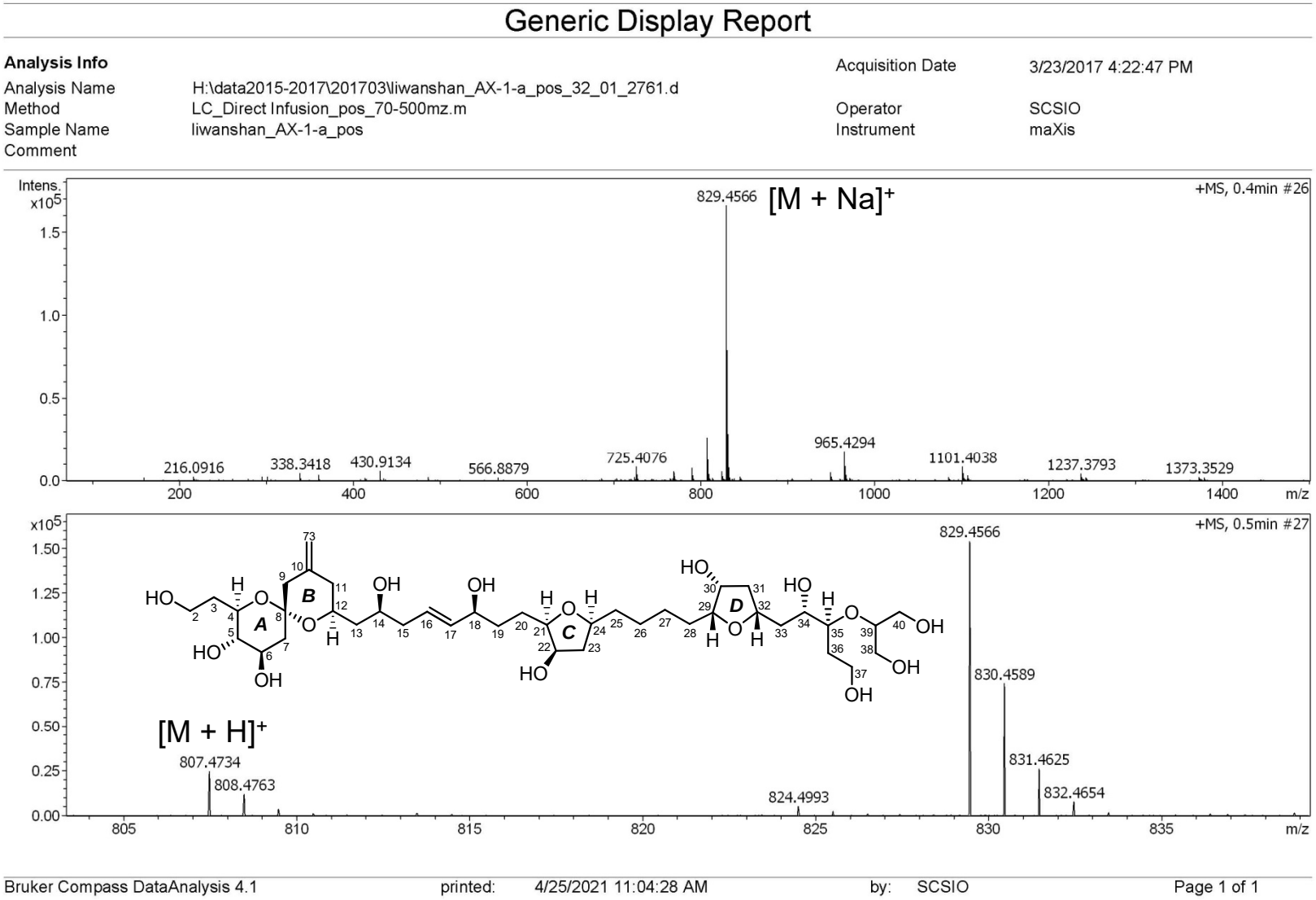

Figure S48. HR-ESIMS for the fragment **1A**

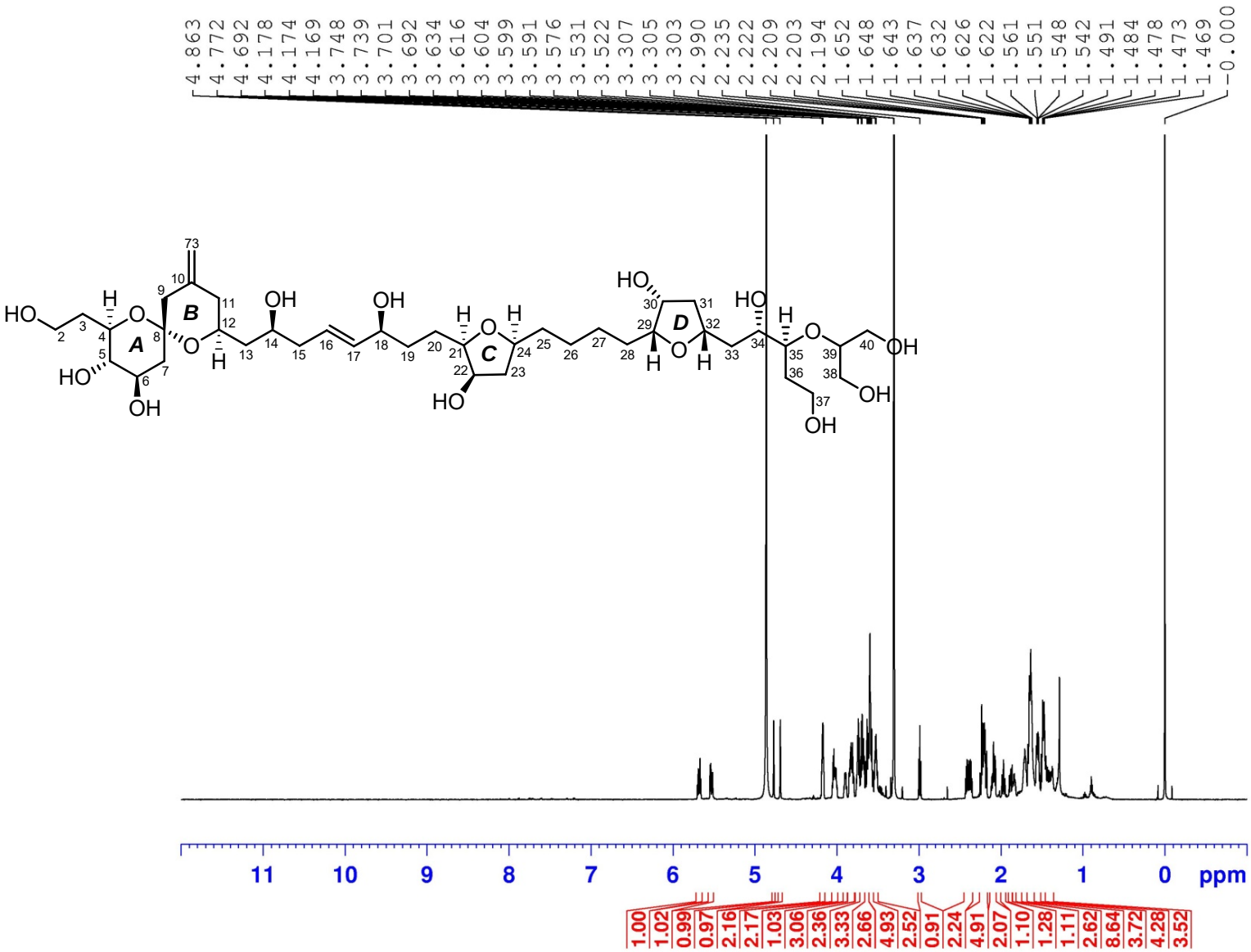

Figure S49. ^{1}H (700 MHz) NMR spectrum of the fragment **1A** in CD_3OD

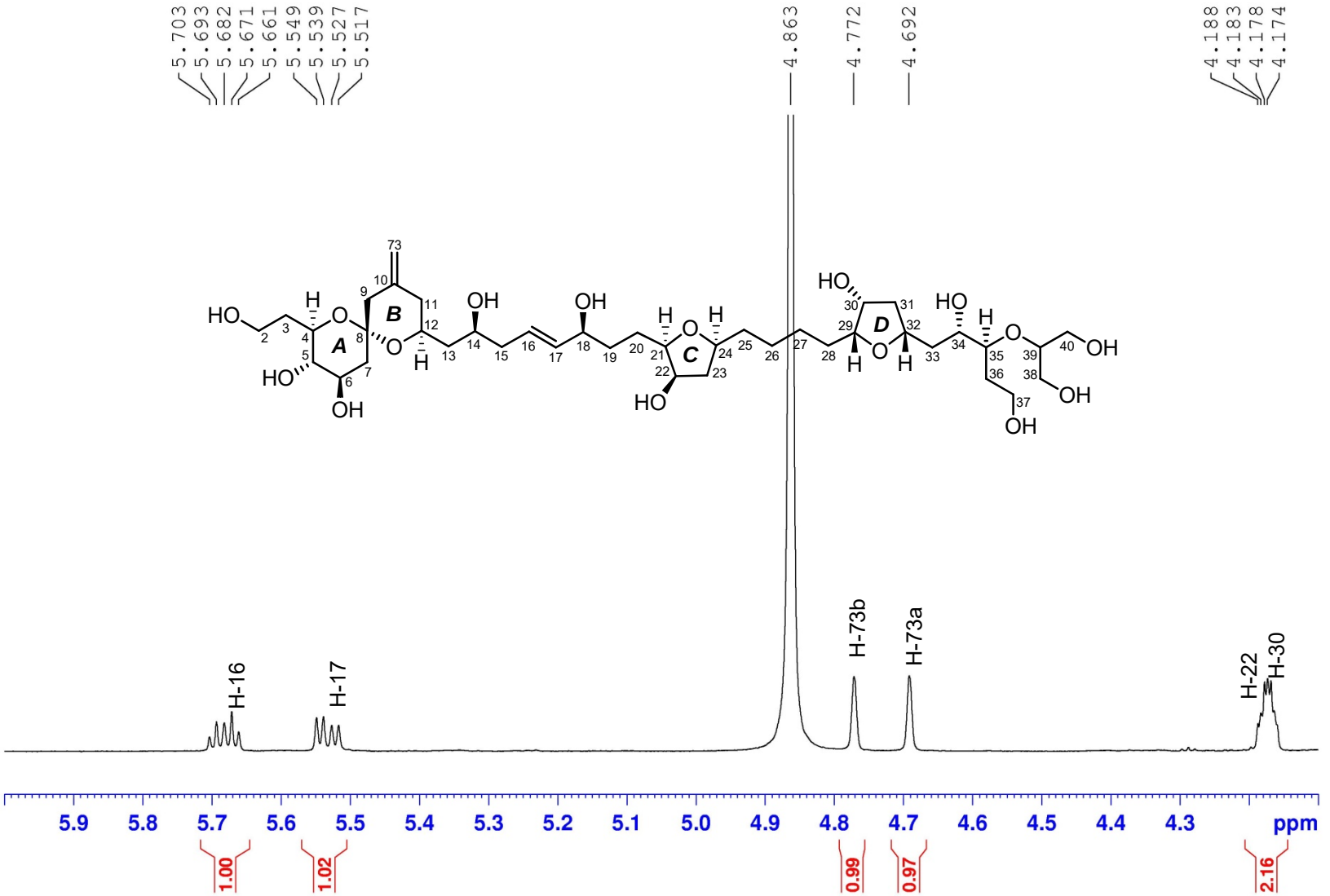

Figure S50. ^{1}H (700 MHz) NMR spectrum of the fragment **1A** in CD_3OD

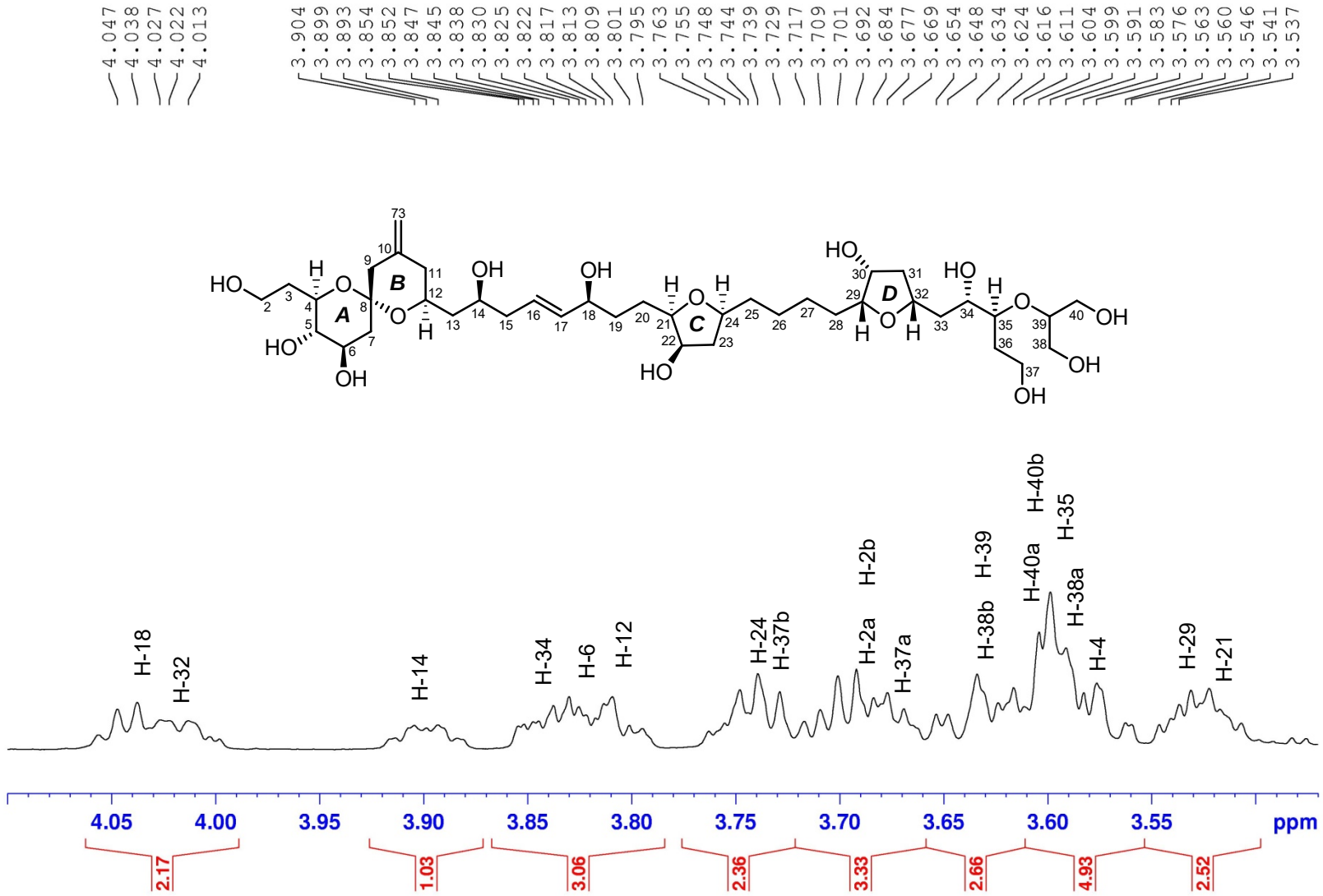

Figure S51. ^{1}H (700 MHz) NMR spectrum of the fragment **1A** in CD_3OD

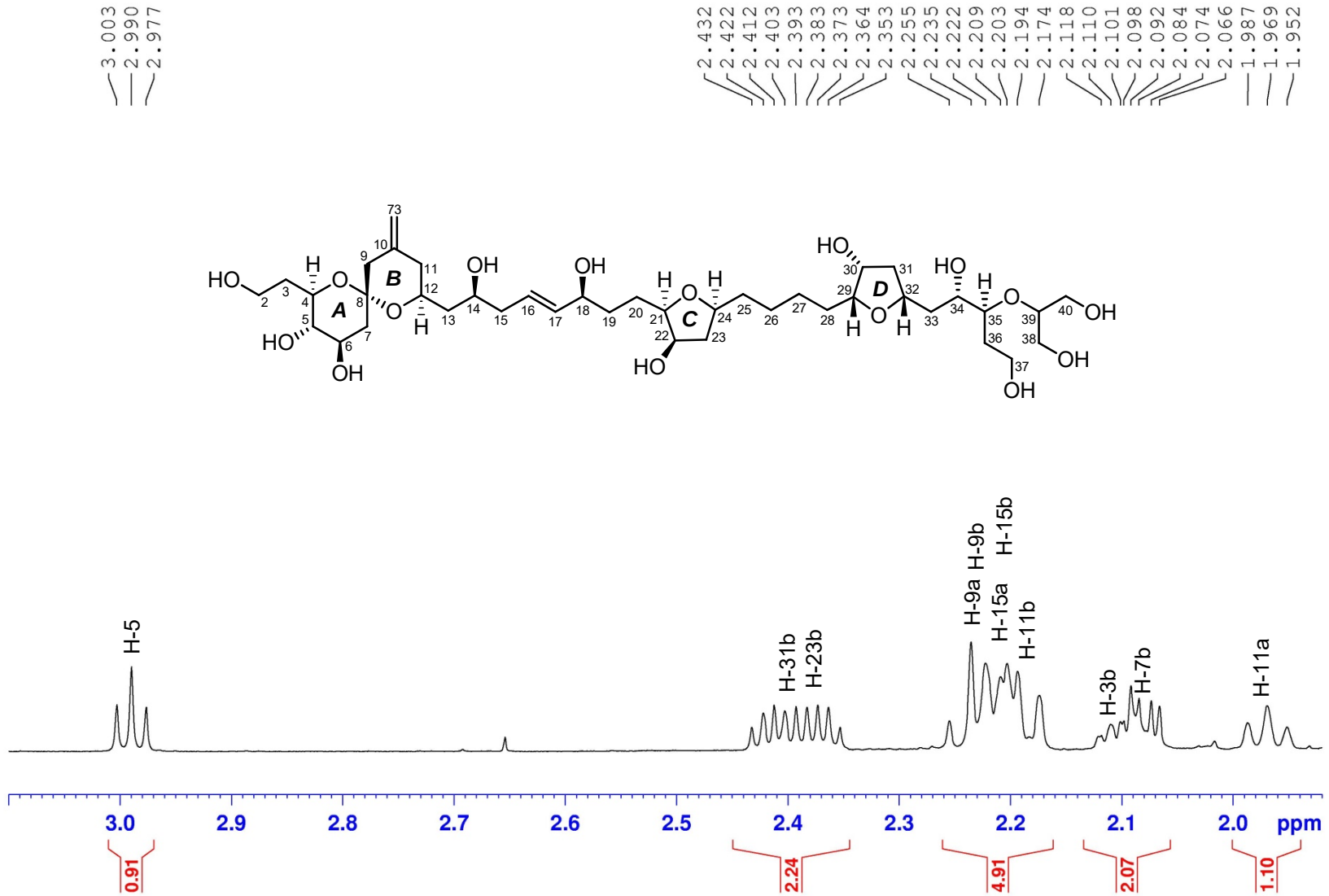

Figure S52. ^{1}H (700 MHz) NMR spectrum of the fragment **1A** in CD_3OD

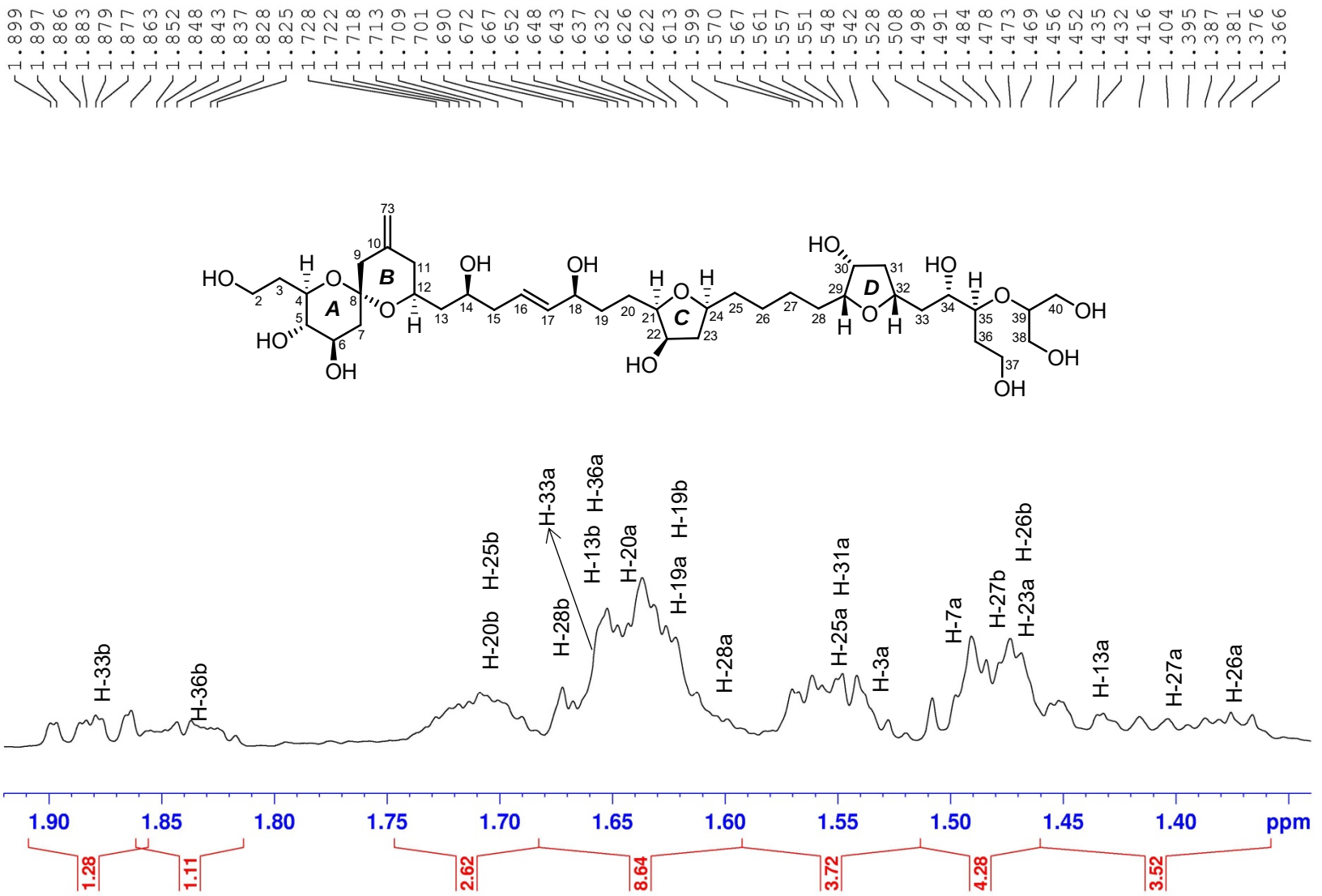

Figure S53. ^{1}H (700 MHz) NMR spectrum of the fragment **1A** in CD_3OD

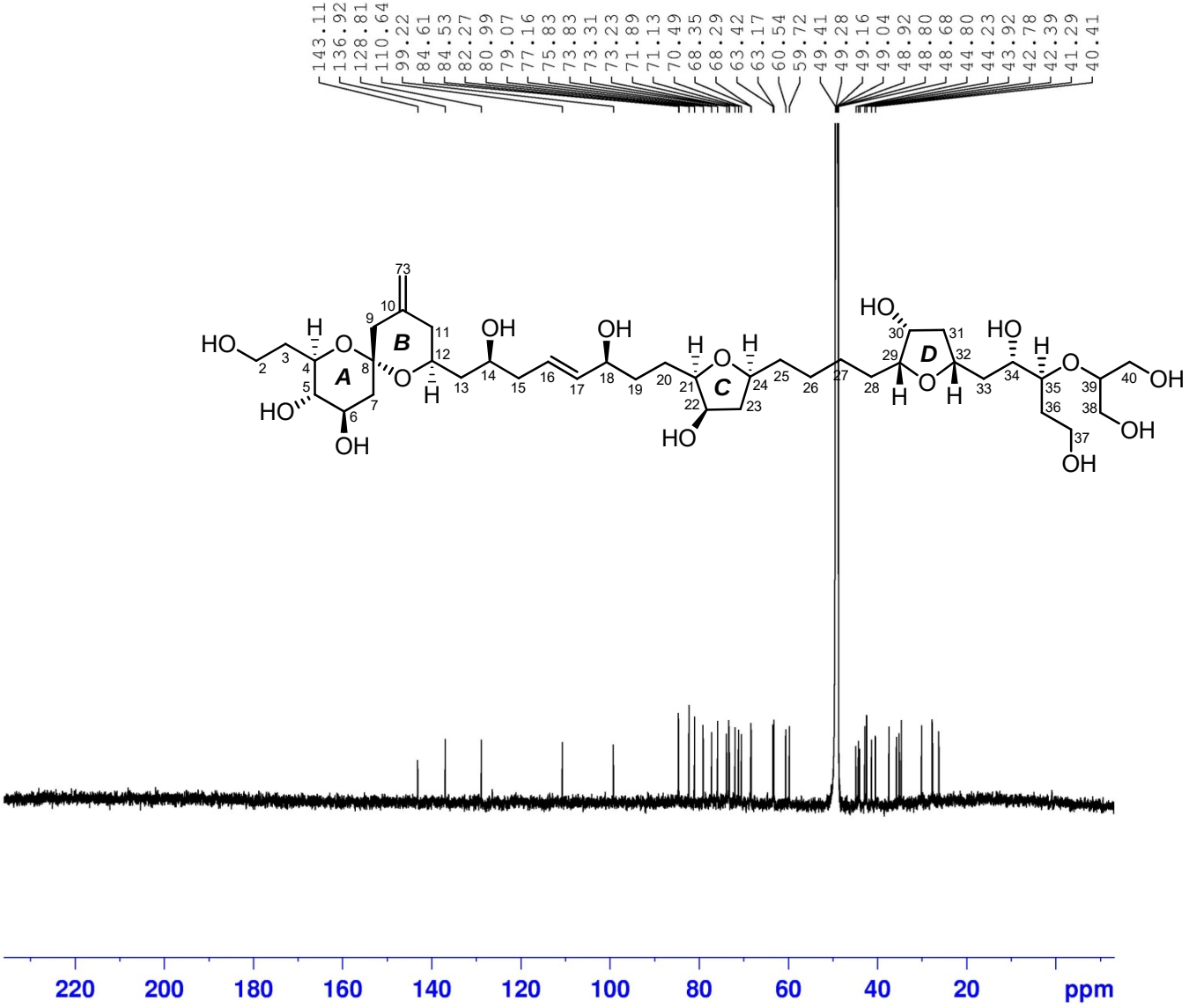

Figure S54. ^{13}C (175 MHz) NMR spectrum of the fragment **1A** in CD_3OD

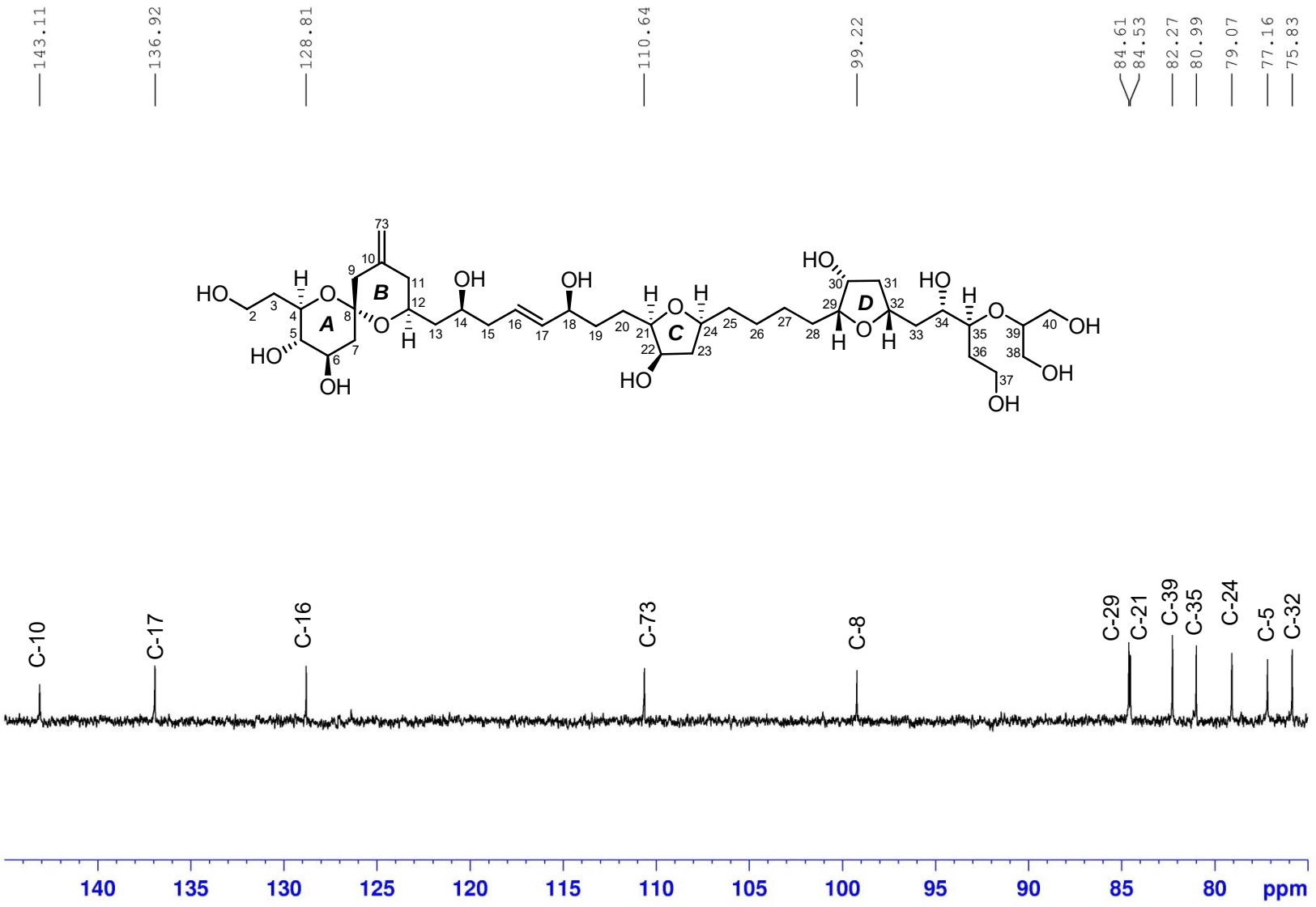

Figure S55. ^{13}C (175 MHz) NMR spectrum of the fragment **1A** in CD_3OD

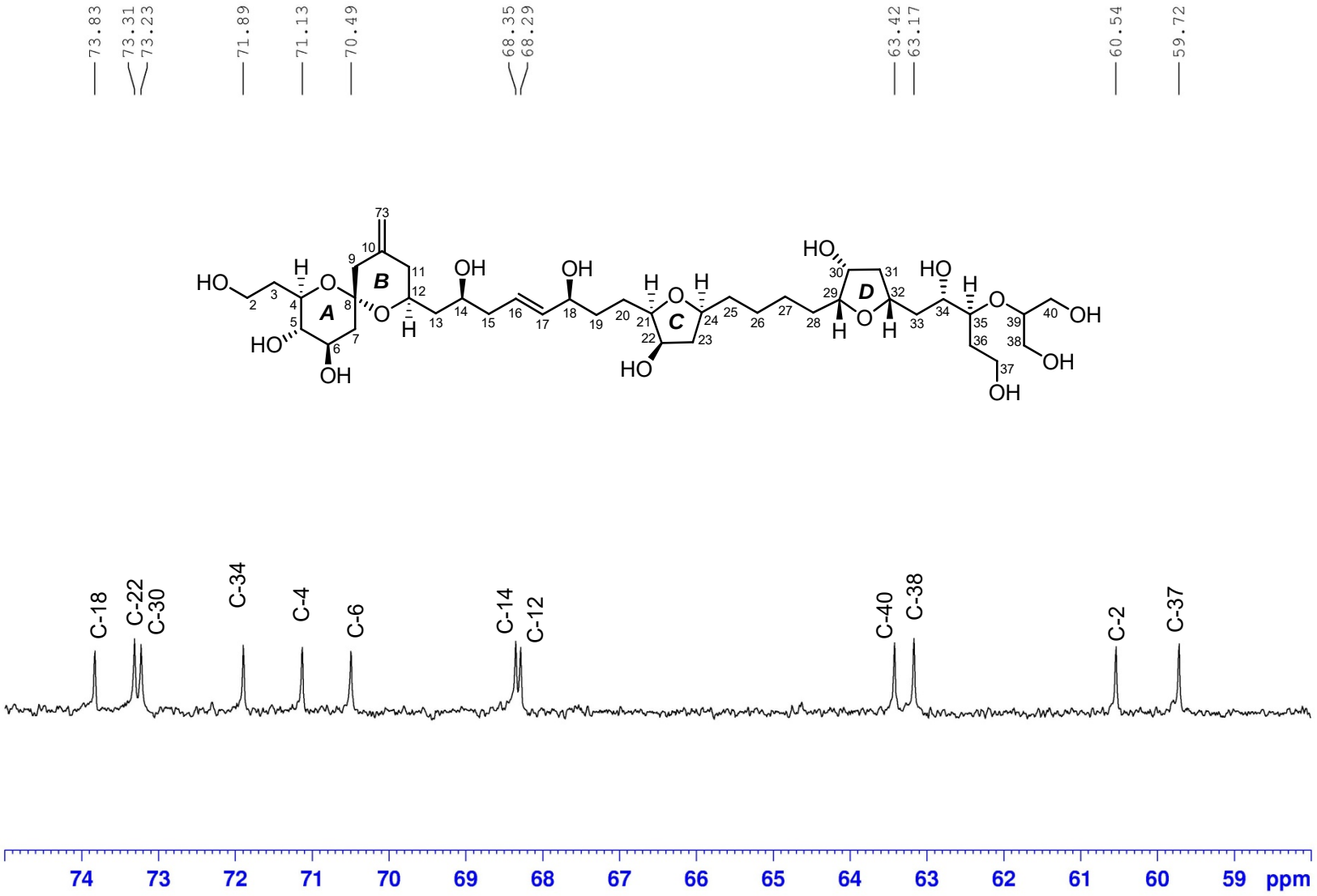

Figure S56. ^{13}C (175 MHz) NMR spectrum of the fragment **1A** in CD_3OD

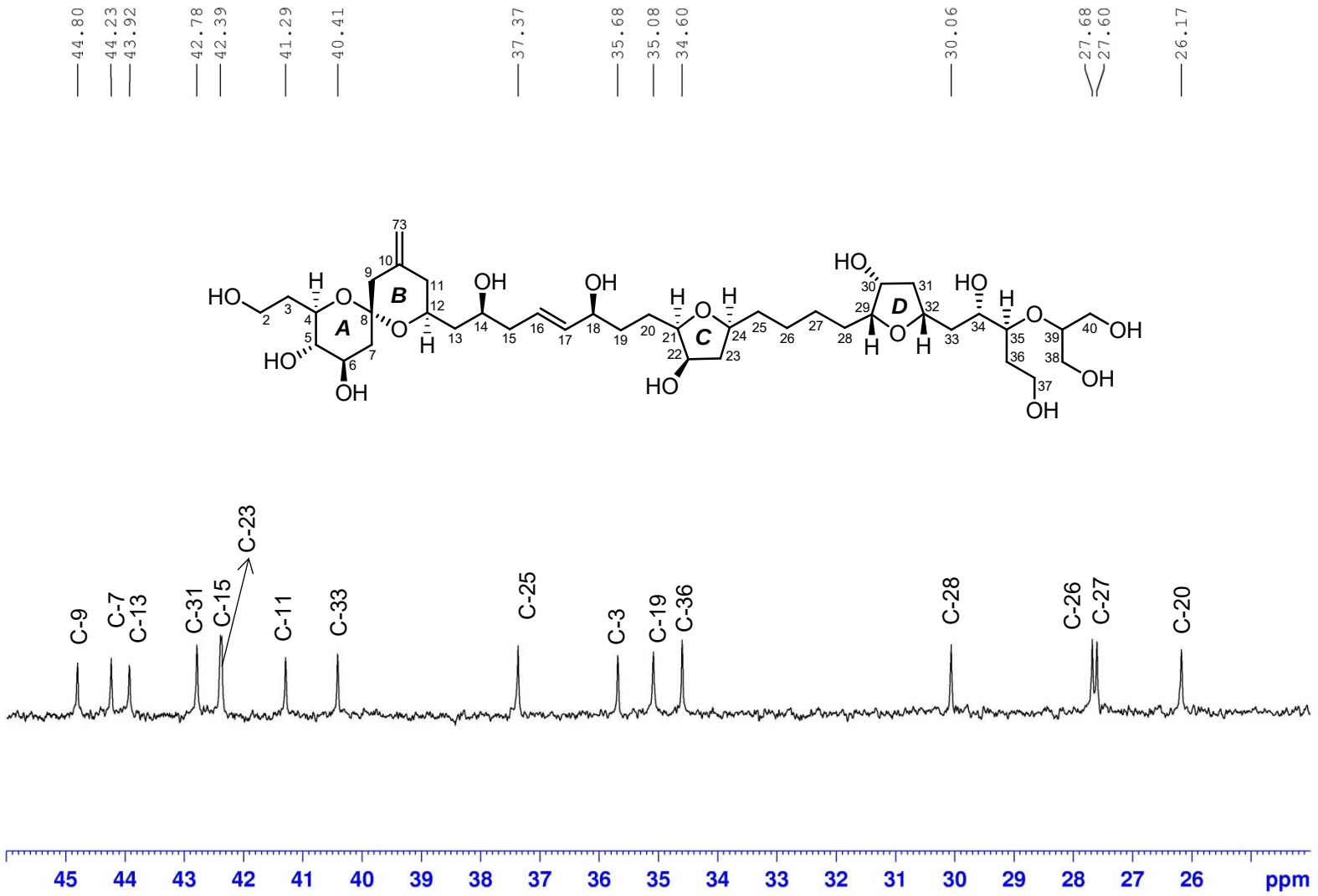

Figure S57. ^{13}C (175 MHz) NMR spectrum of the fragment **1A** in CD_3OD

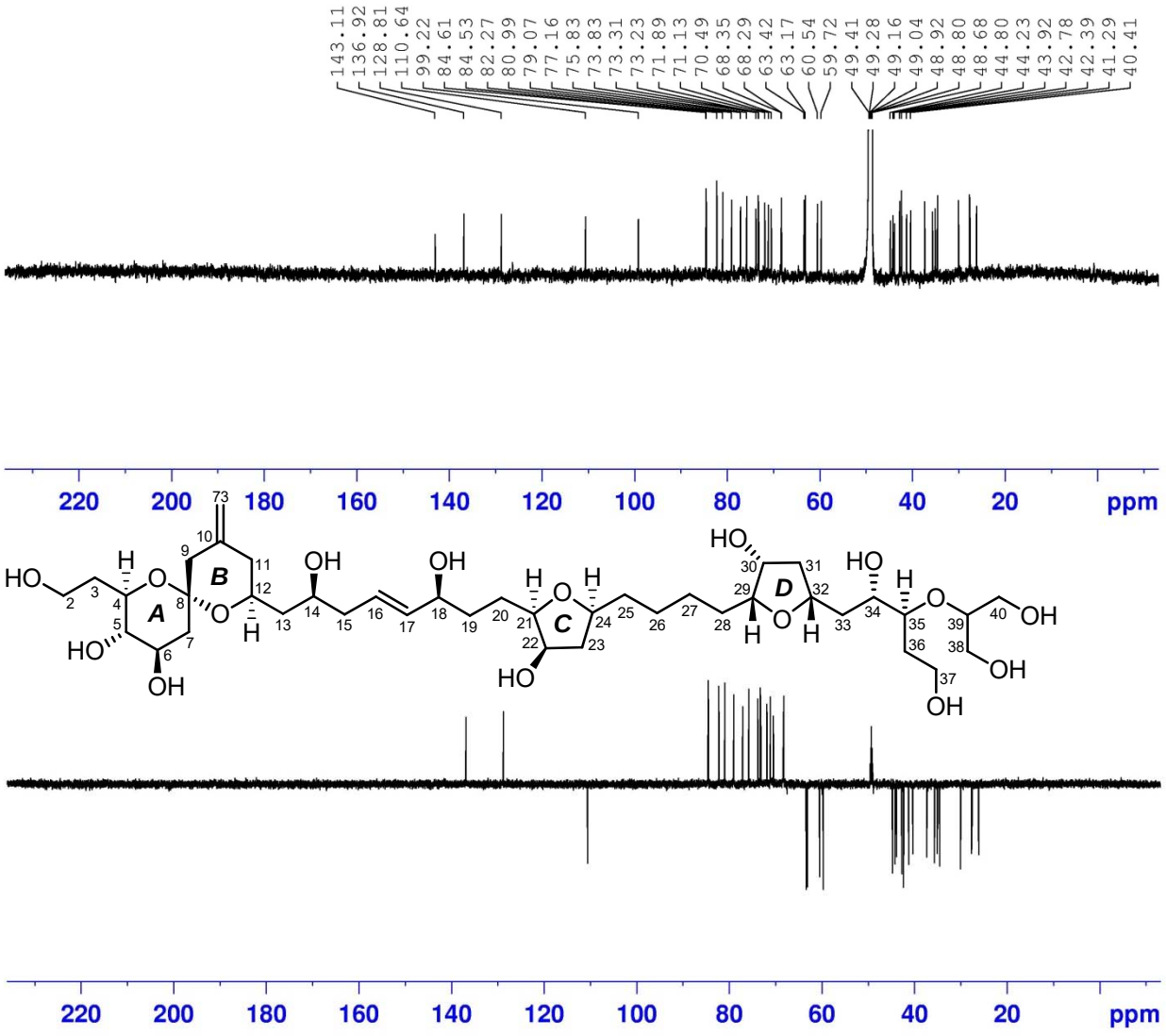

Figure S58. DEPT135 (175 MHz) spectrum of the fragment **1A** in CD_3OD

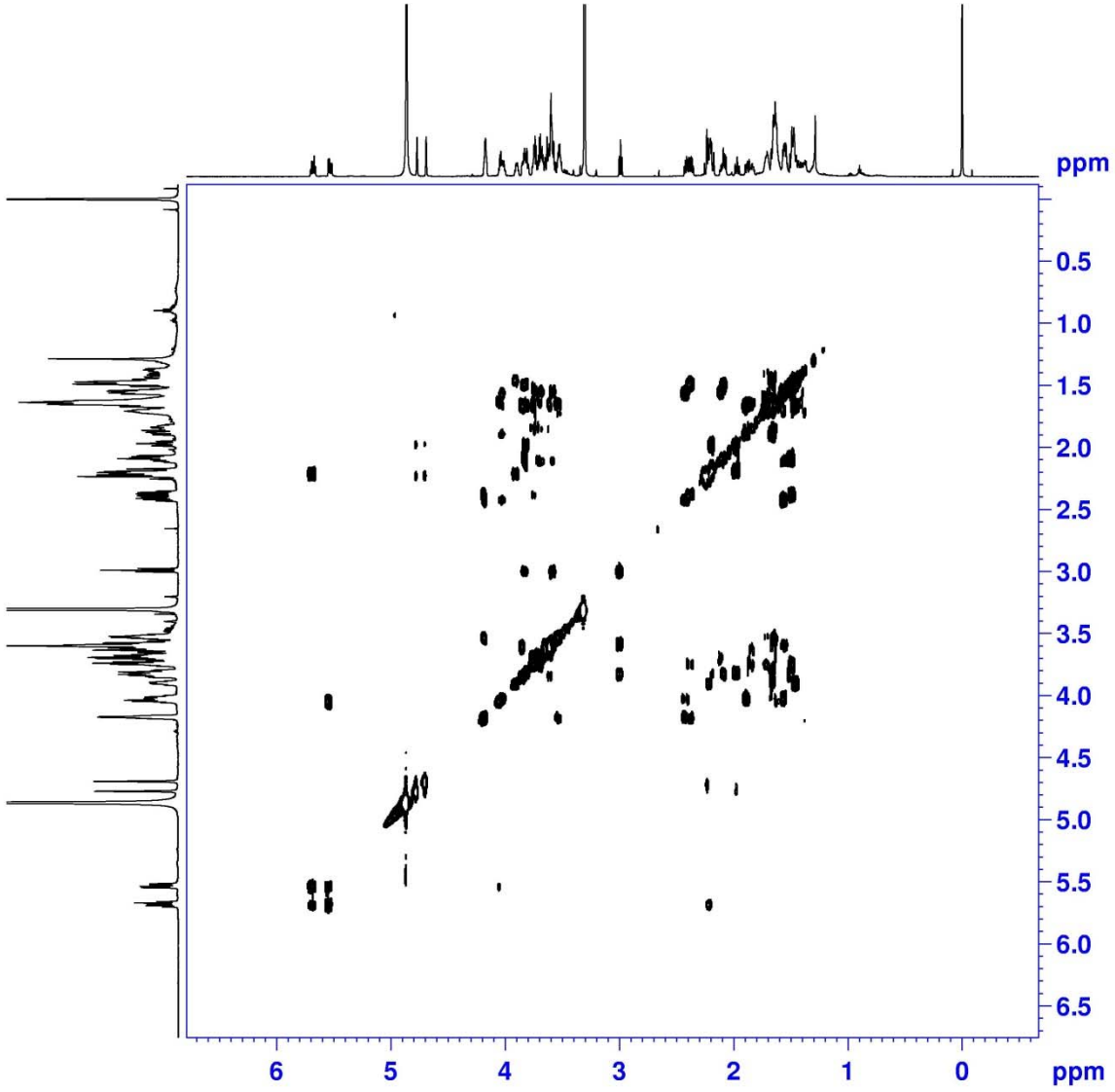

Figure S59. ^{1}H–^{1}H COSY (700 MHz) spectrum of the fragment **1A** in CD_3OD

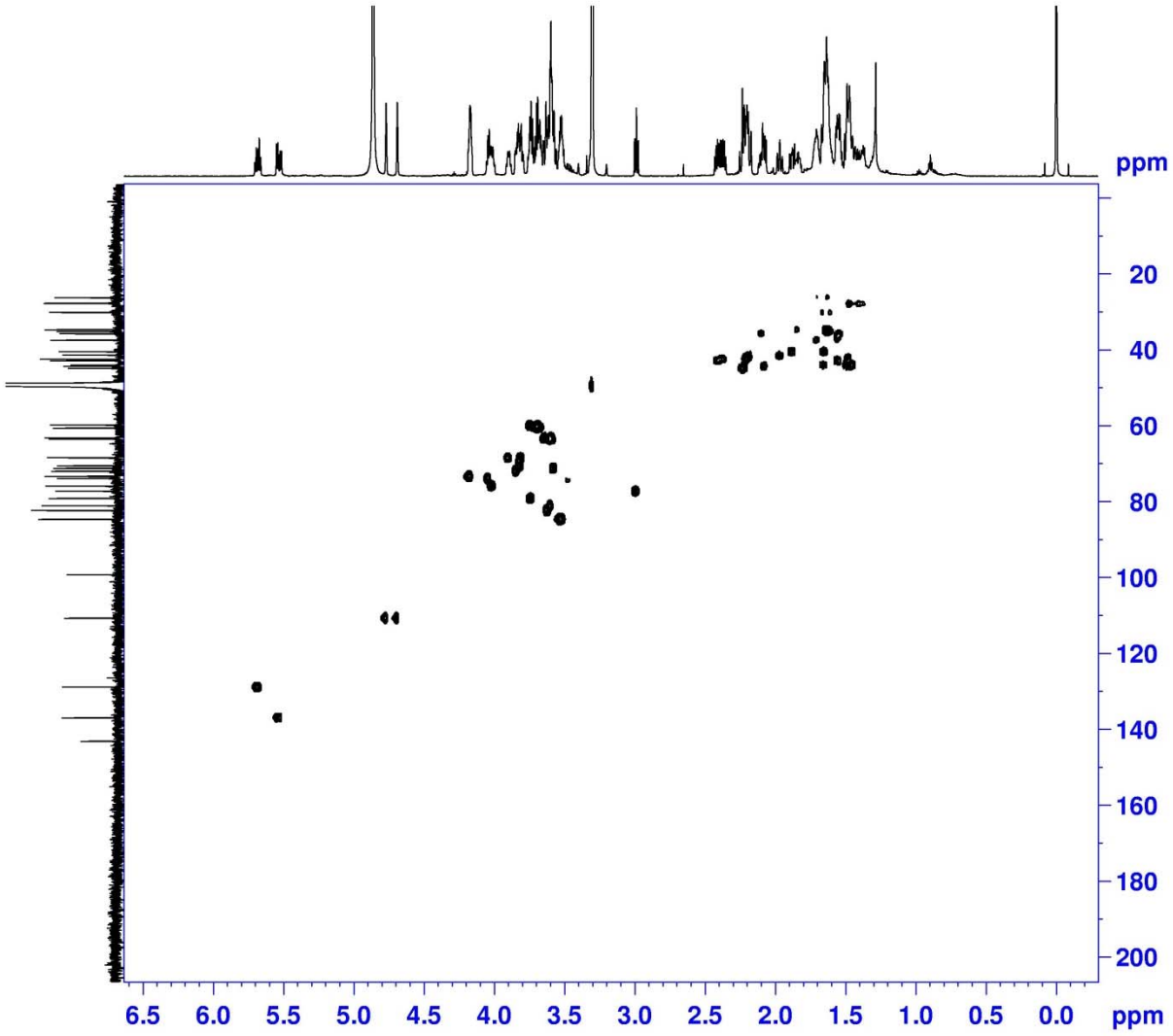

Figure S60. HSQC (700 MHz) spectrum of the fragment **1A** in CD_3OD

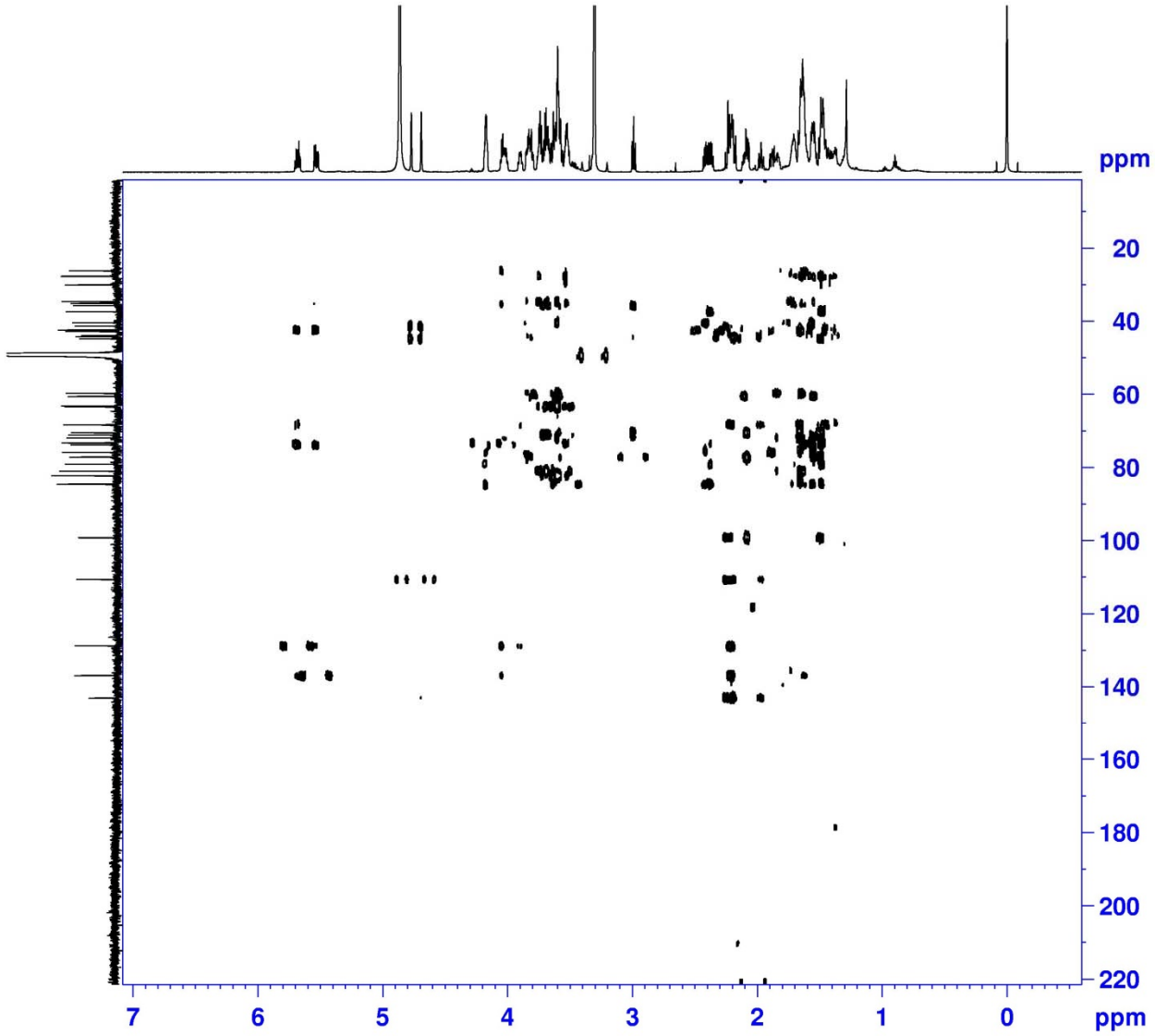

Figure S61. HMBC (700 MHz) spectrum of the fragment **1A** in CD_3OD

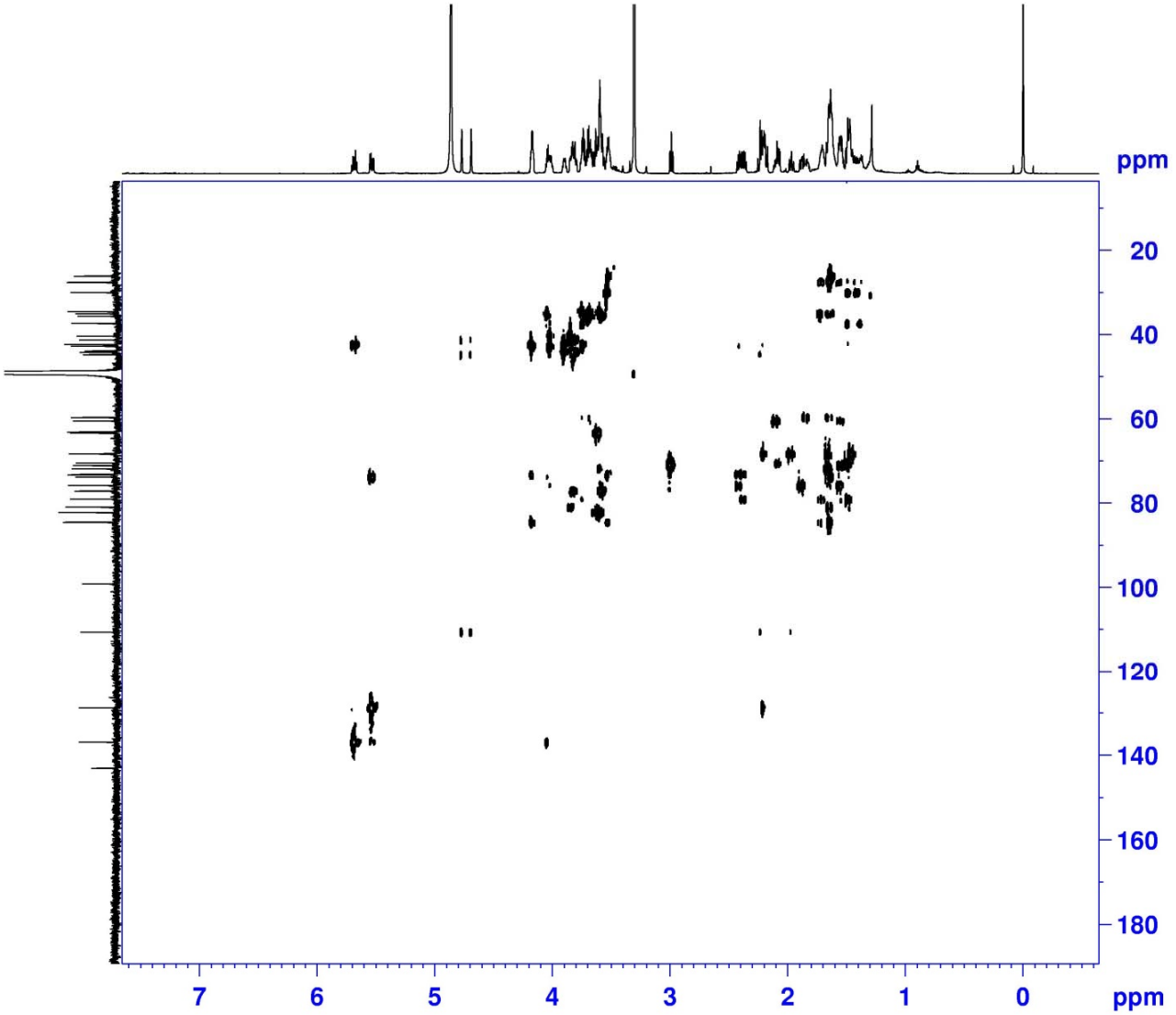

Figure S62. H2BC (700 MHz) spectrum of the fragment **1A** in CD_3OD

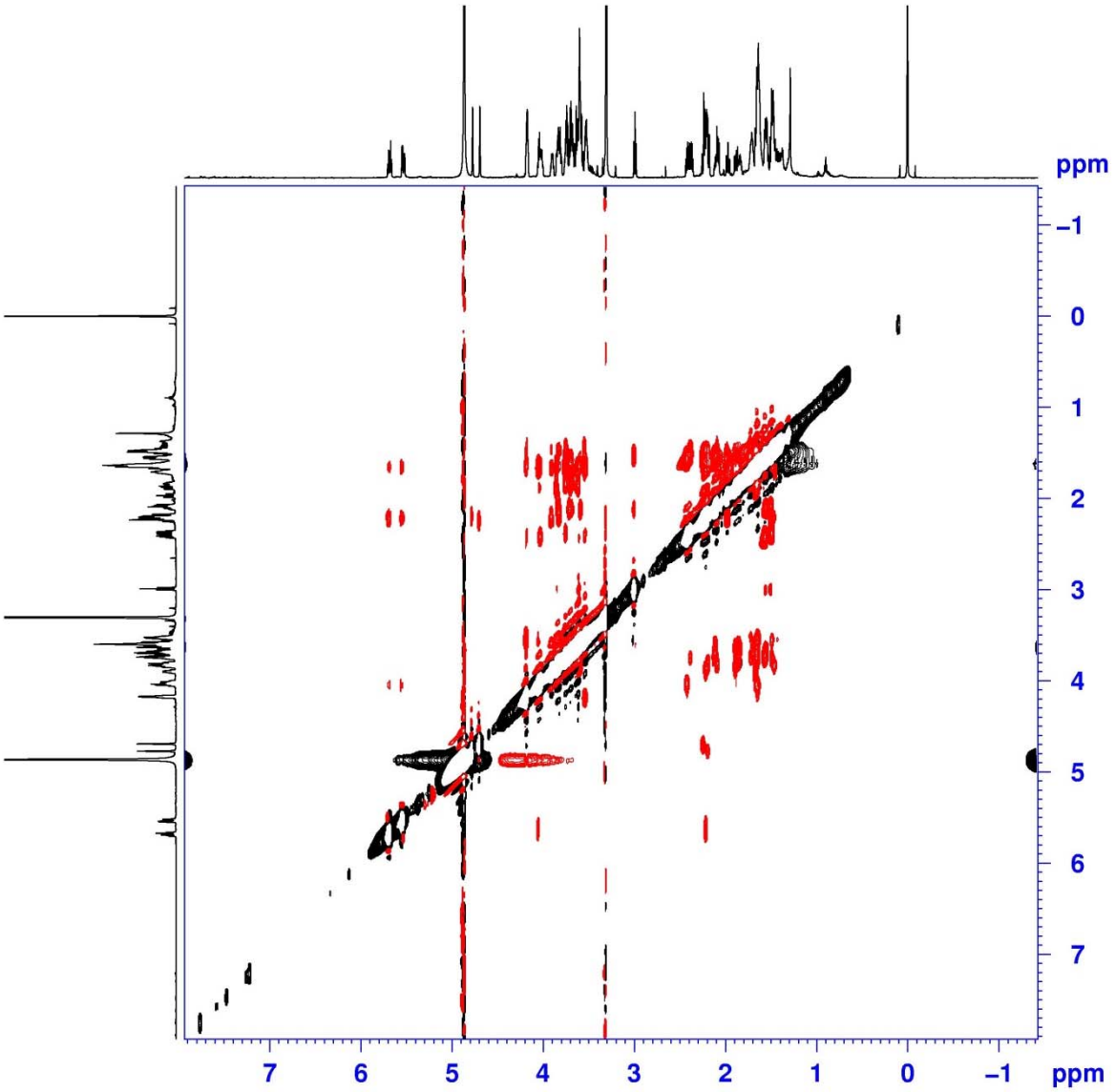

Figure S63. NOESY (700 MHz) spectrum of the fragment **1A** in CD_3OD

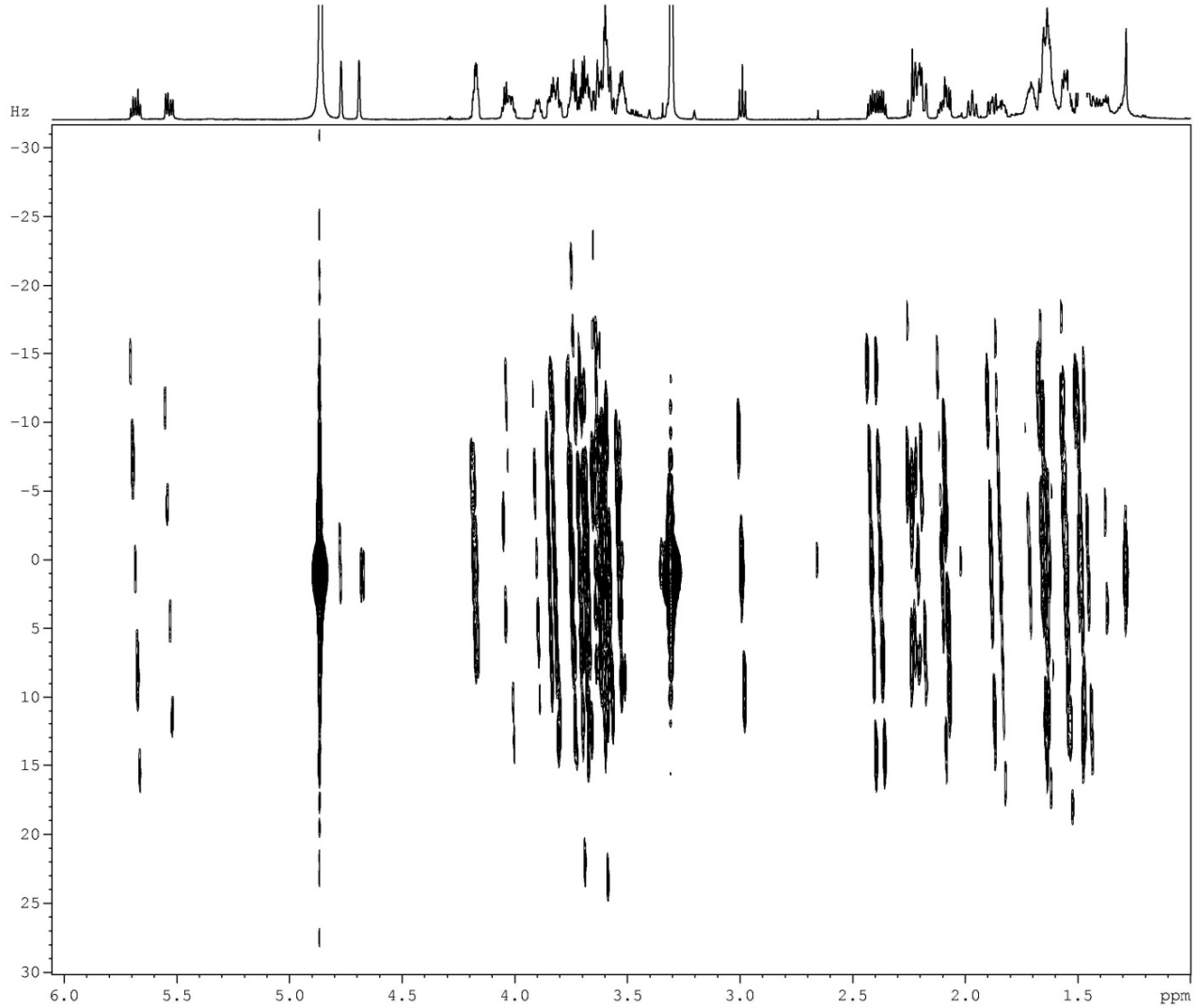

Figure S64. 2D *J*RES (700 MHz) spectrum of the fragment **1A** in CD_3OD

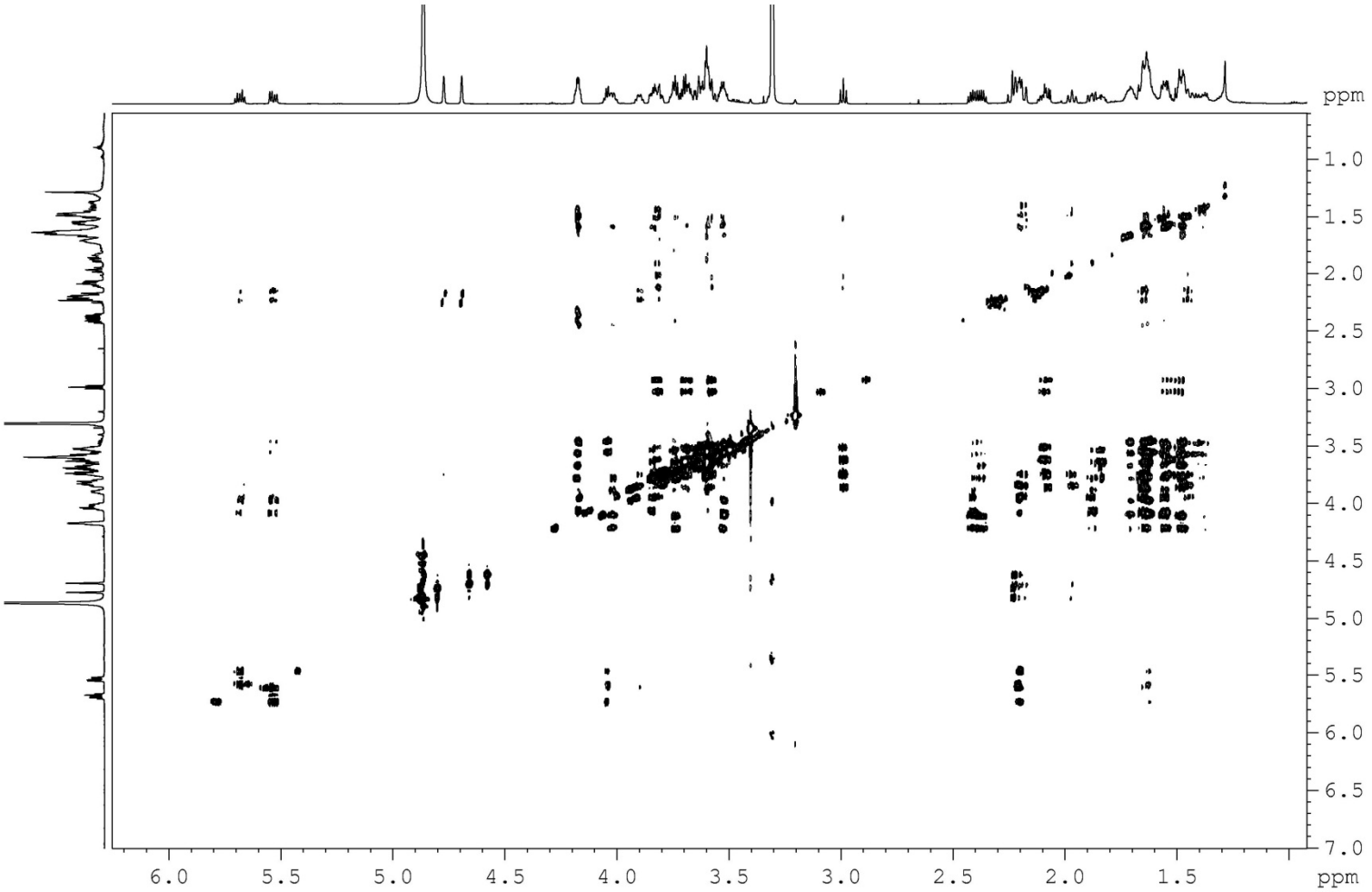

Figure S65. HETLOC (700 MHz) spectrum of the fragment **1A** in CD_3OD

Mass Spectrum SmartFormula Report

Analysis Info

Analysis Name	H:\data2015-2017\201703\liwanshan_AX-1-b_pos_33_01_2762.d	Acquisition Date	3/23/2017 4:26:15 PM
Method	LC_Direct Infusion_pos_70-500mz.m	Operator	SCSIO
Sample Name	liwanshan_AX-1-b_pos	Instrument	maXis 255552.00029
Comment			

Acquisition Parameter

Source Type	ESI	Ion Polarity	Positive	Set Nebulizer	0.4 Bar
Focus	Active	Set Capillary	4500 V	Set Dry Heater	180 °C
Scan Begin	70 m/z	Set End Plate Offset	-500 V	Set Dry Gas	4.0 l/min
Scan End	1500 m/z	Set Charging Voltage	0 V	Set Divert Valve	Waste
		Set Corona	0 nA	Set APCI Heater	0 °C

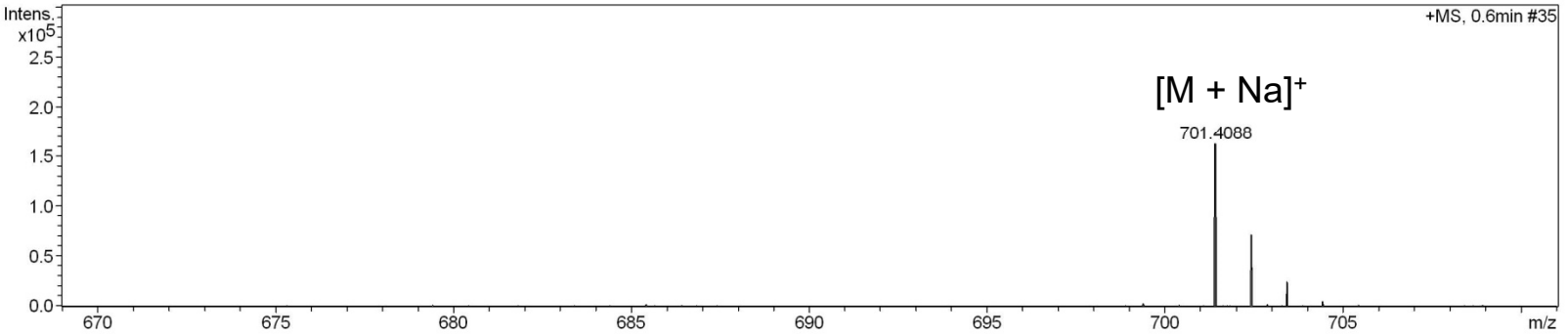

Meas. m/z	#	Ion Formula	Score	m/z	err [ppm]	err [mDa]	mSigma	rdb	e⁻ Conf	N-Rule
679.4231	1	C34H63O13	100.00	679.4263	-4.7	-3.2	52.7	3.5	even	ok
701.4088	1	C34H62NaO13	100.00	701.4083	0.7	0.5	40.8	3.5	even	ok

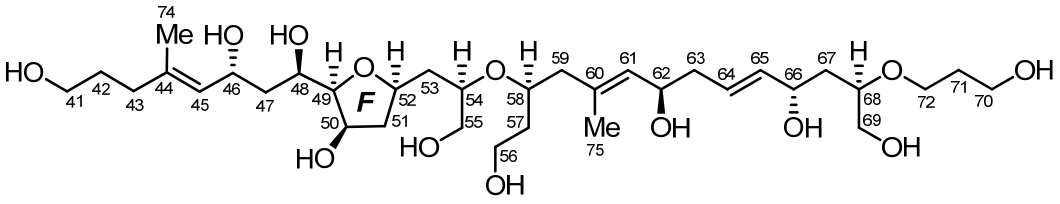

Figure S66. HR-ESIMS for the fragment **1B**

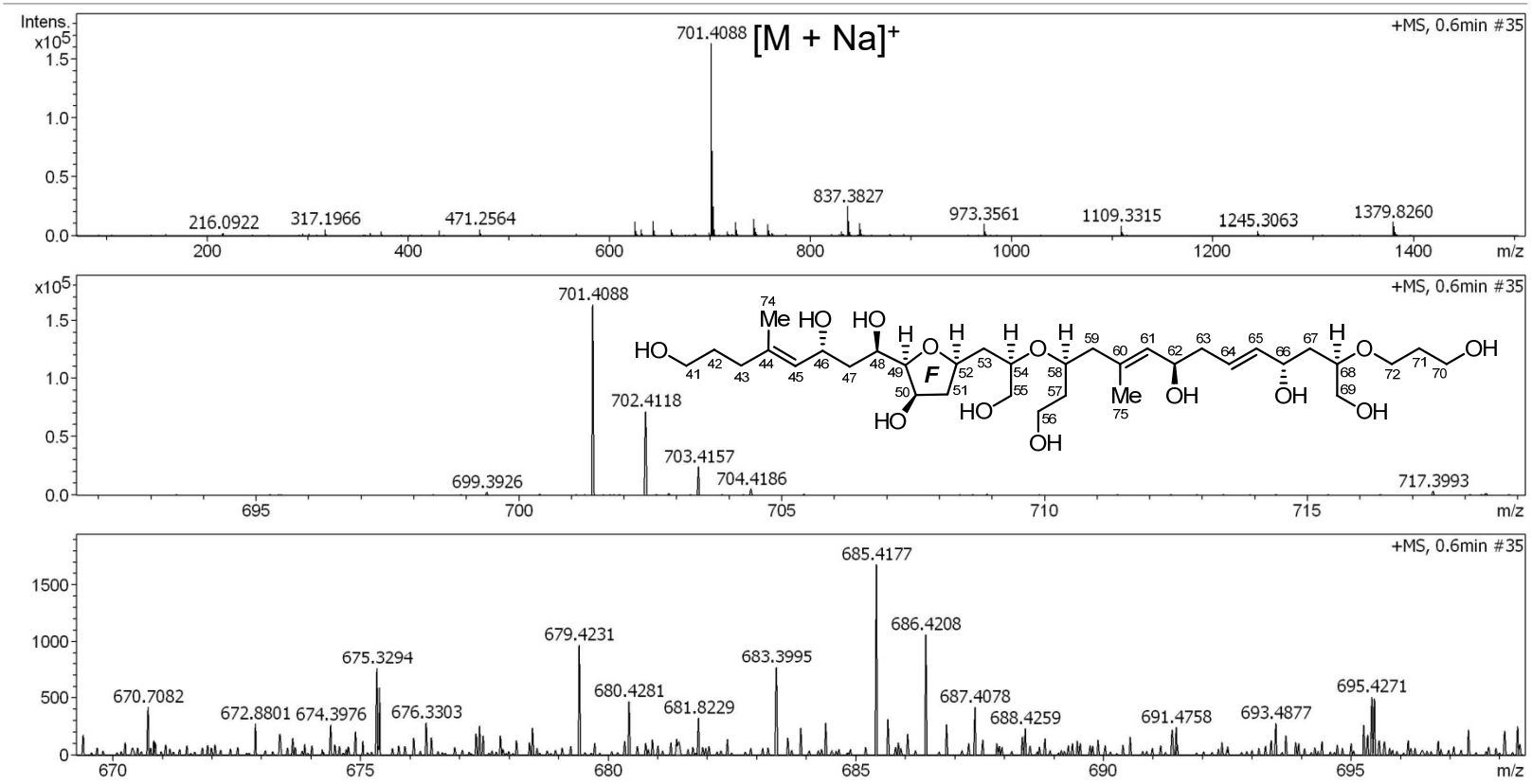

Figure S67. HR-ESIMS for the fragment **1B**

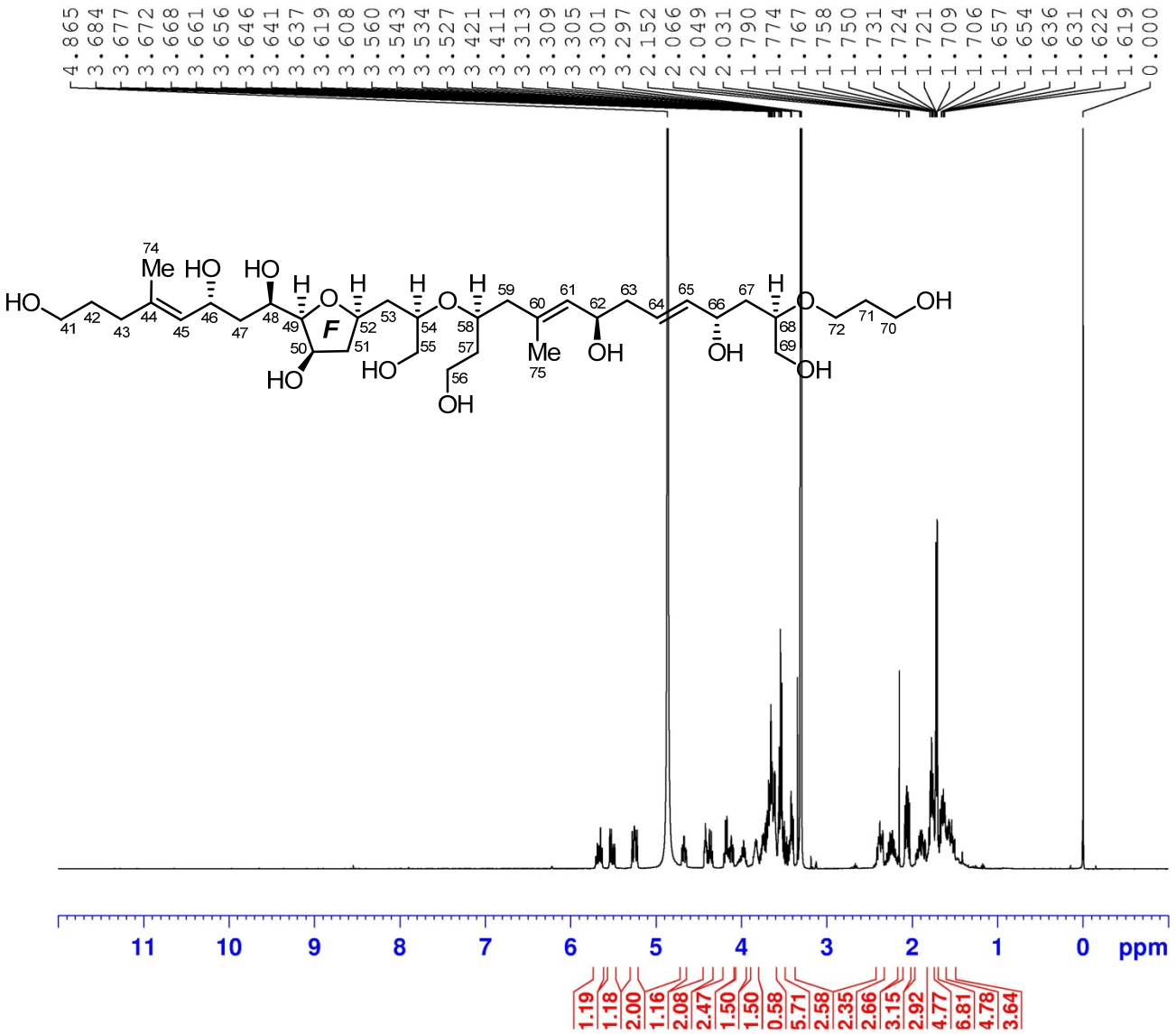

Figure S68. ^{1}H (400 MHz) NMR spectrum of the fragment **1B** in CD_3OD

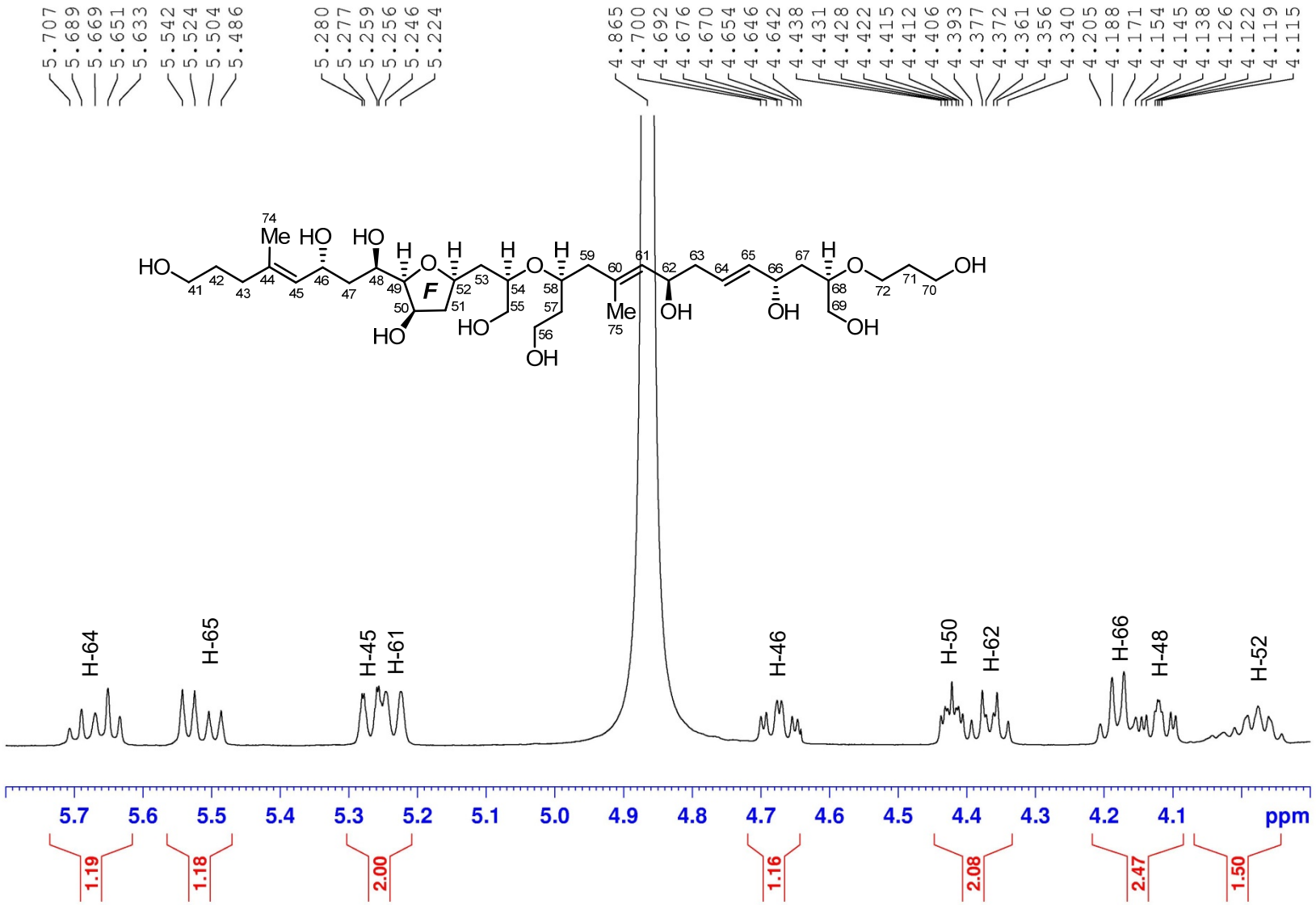

Figure S69. ^{1}H (400 MHz) NMR spectrum of the fragment **1B** in CD_3OD

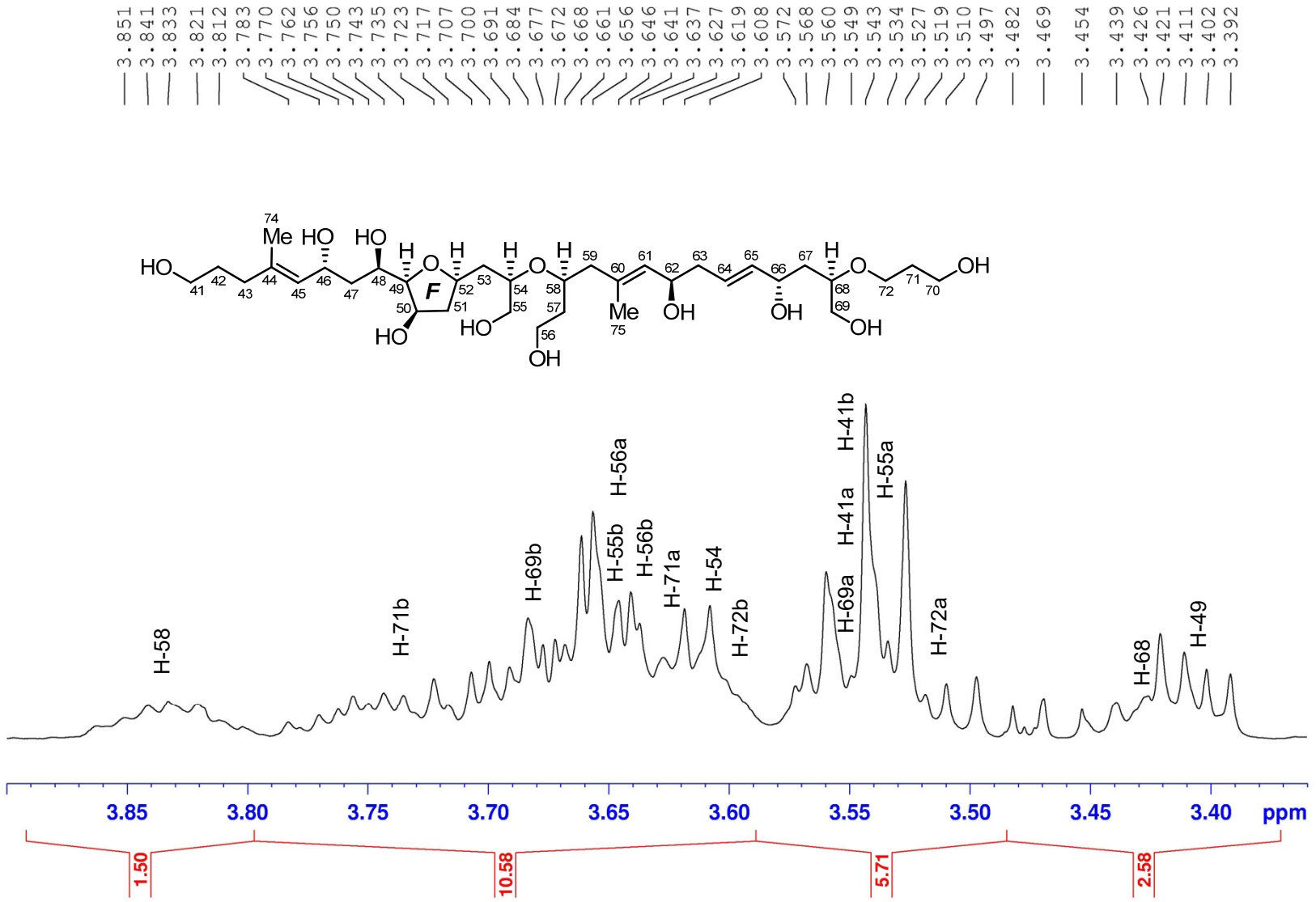

Figure S70. ^{1}H (400 MHz) NMR spectrum of the fragment **1B** in CD_3OD

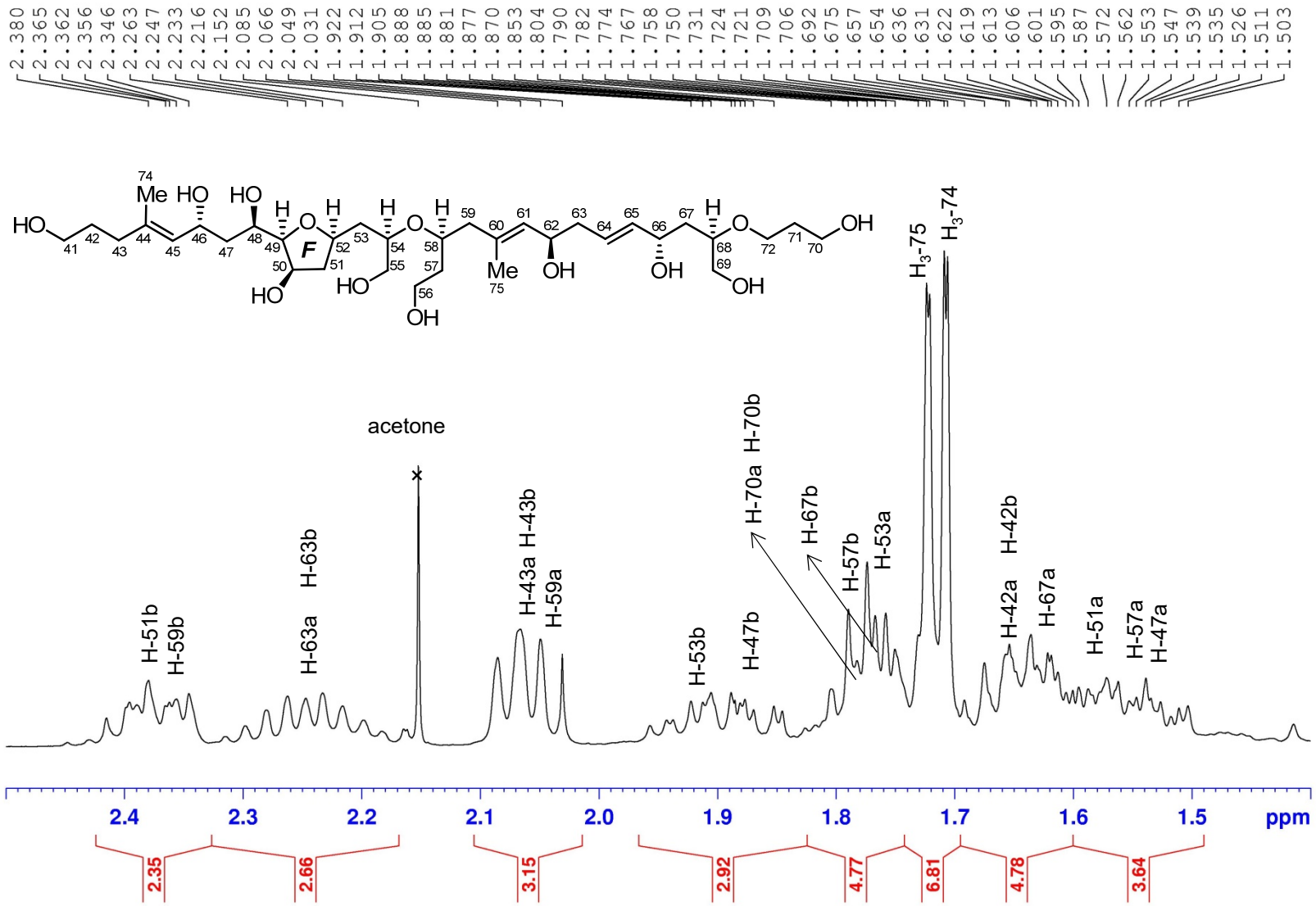

Figure S71. ^{1}H (400 MHz) NMR spectrum of the fragment **1B** in CD_3OD

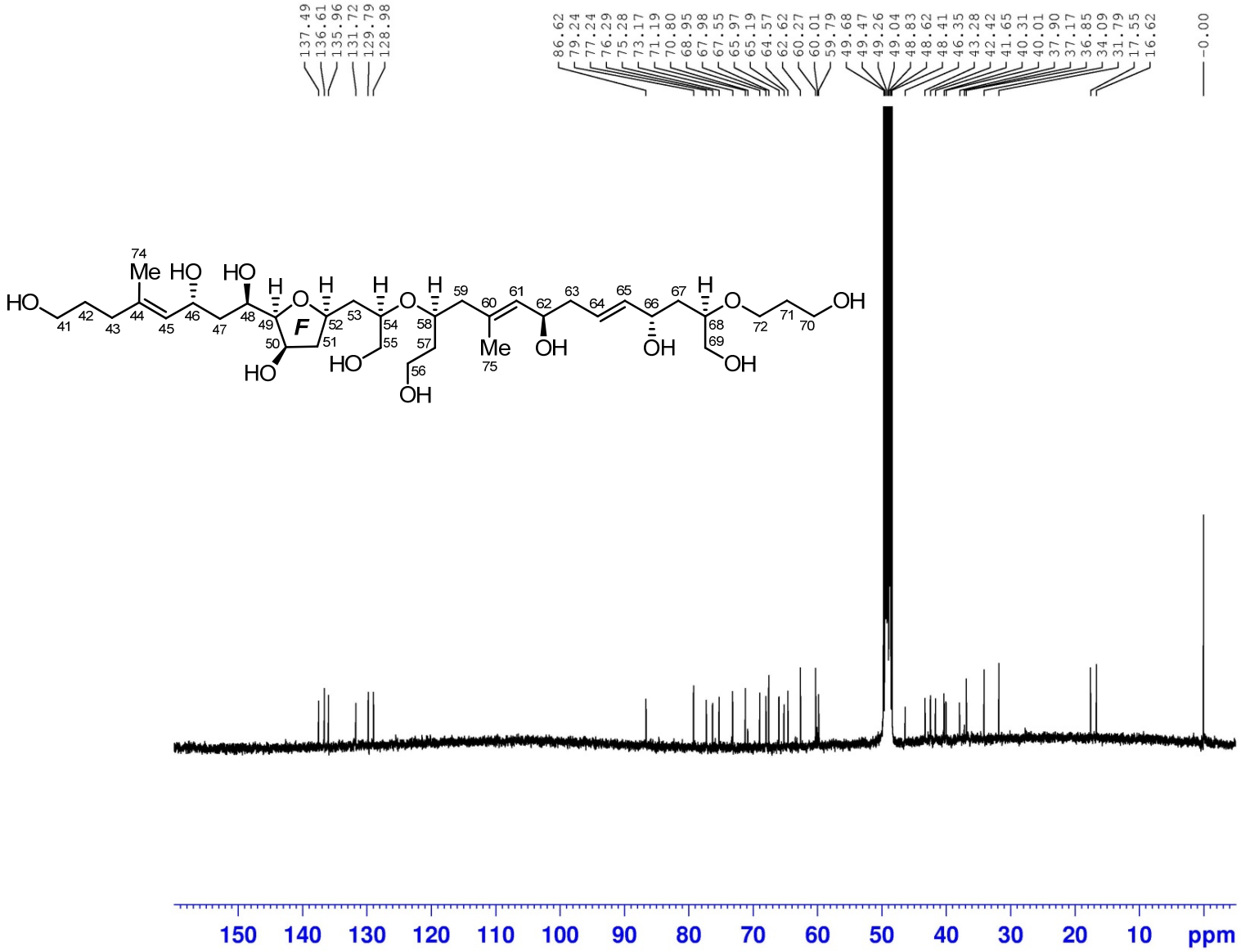

Figure S72. ^{13}C (100 MHz) NMR spectrum of the fragment **1B** in CD_3OD

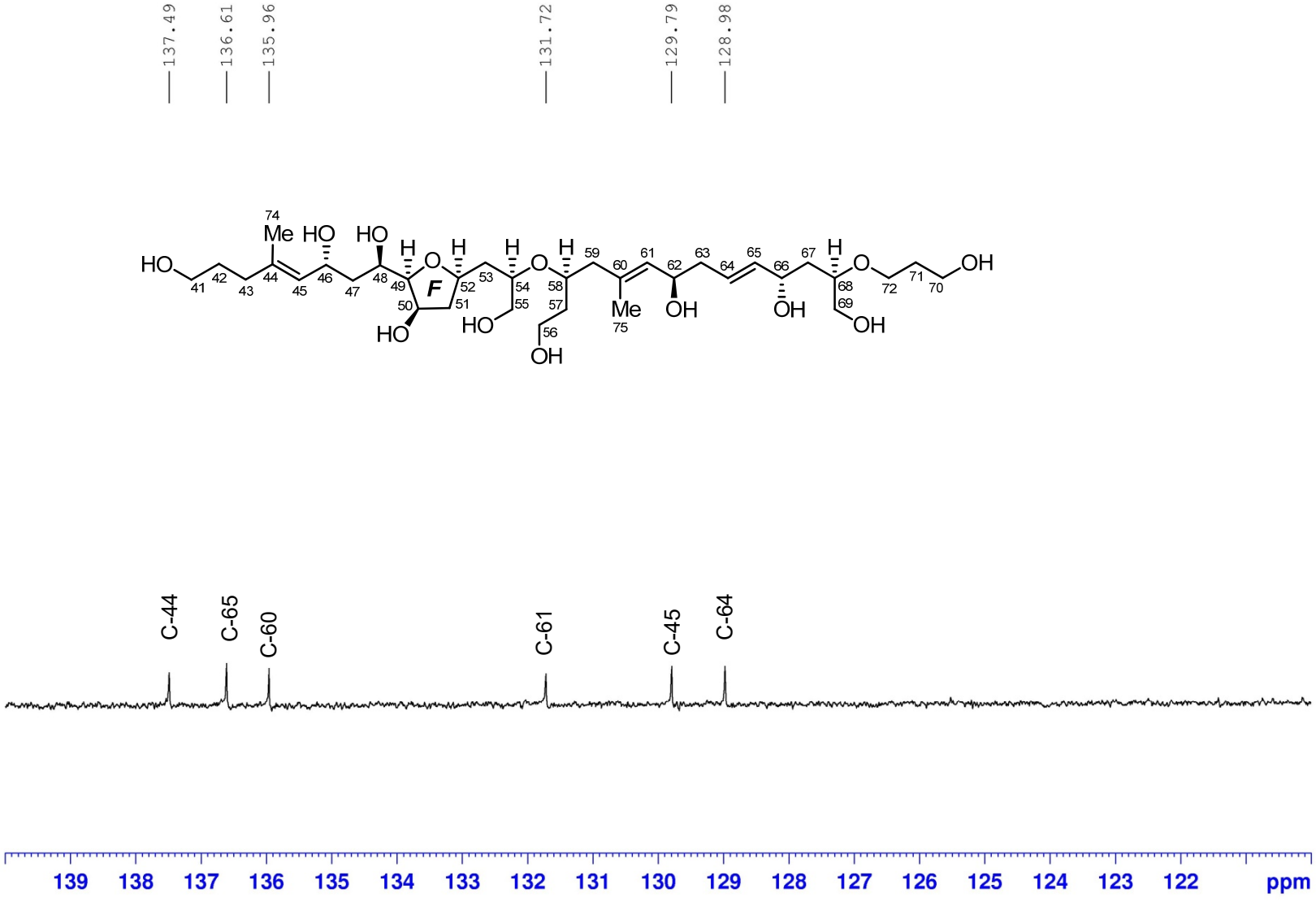

Figure S73. ^{13}C (100 MHz) NMR spectrum of the fragment **1B** in CD_3OD

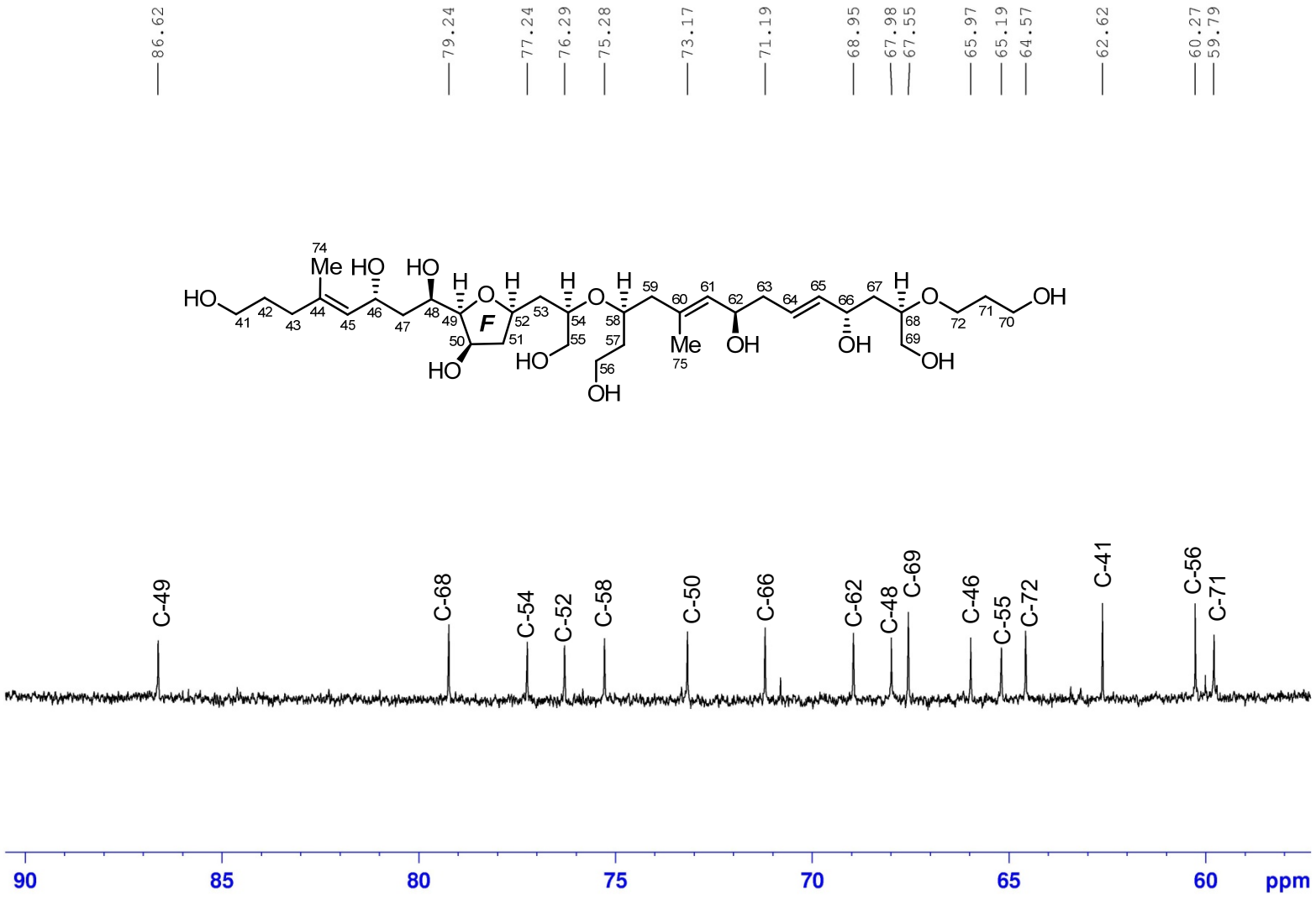

Figure S74. ^{13}C (100 MHz) NMR spectrum of the fragment **1B** in CD_3OD

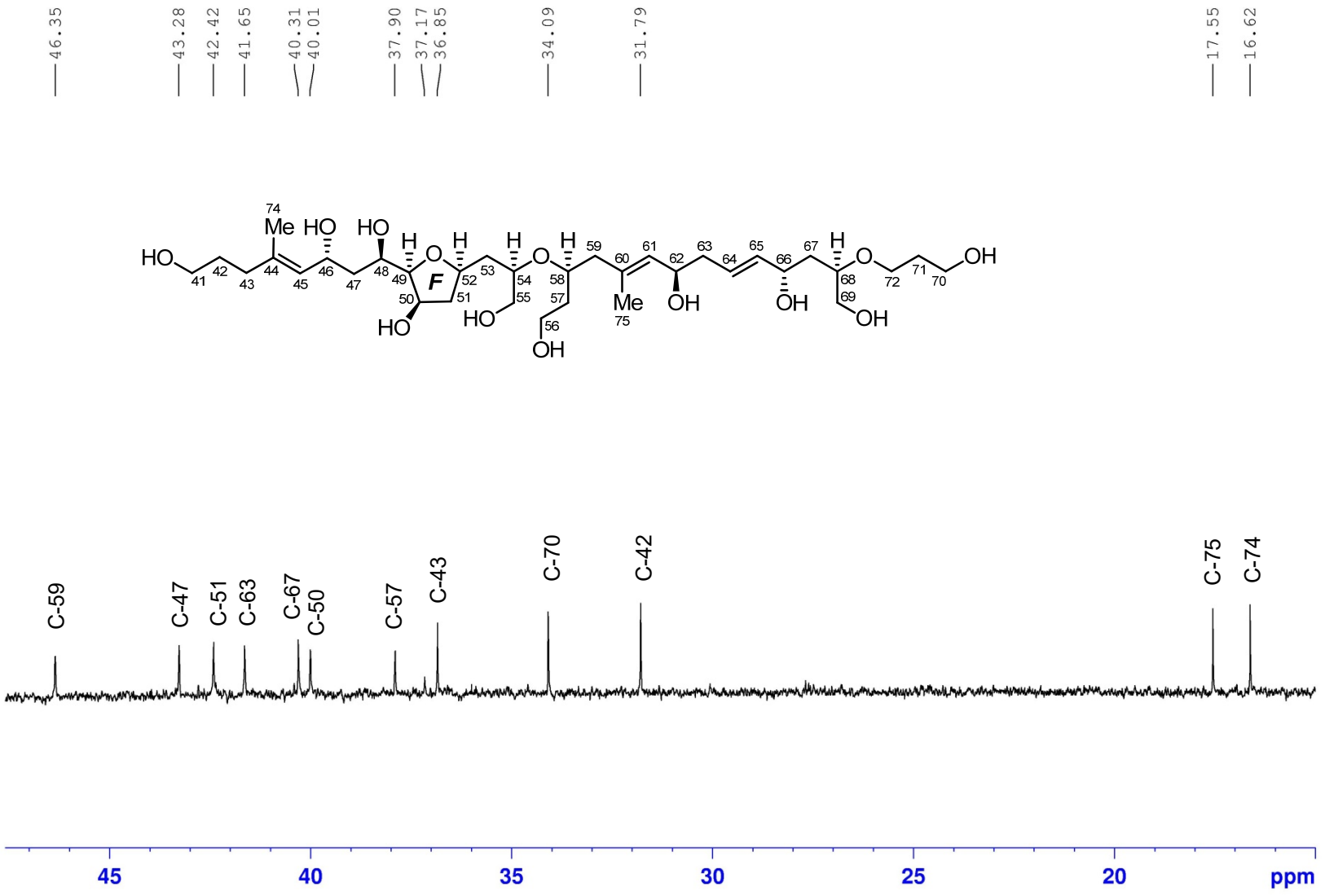

Figure S75. ^{13}C (100 MHz) NMR spectrum of the fragment **1B** in CD_3OD

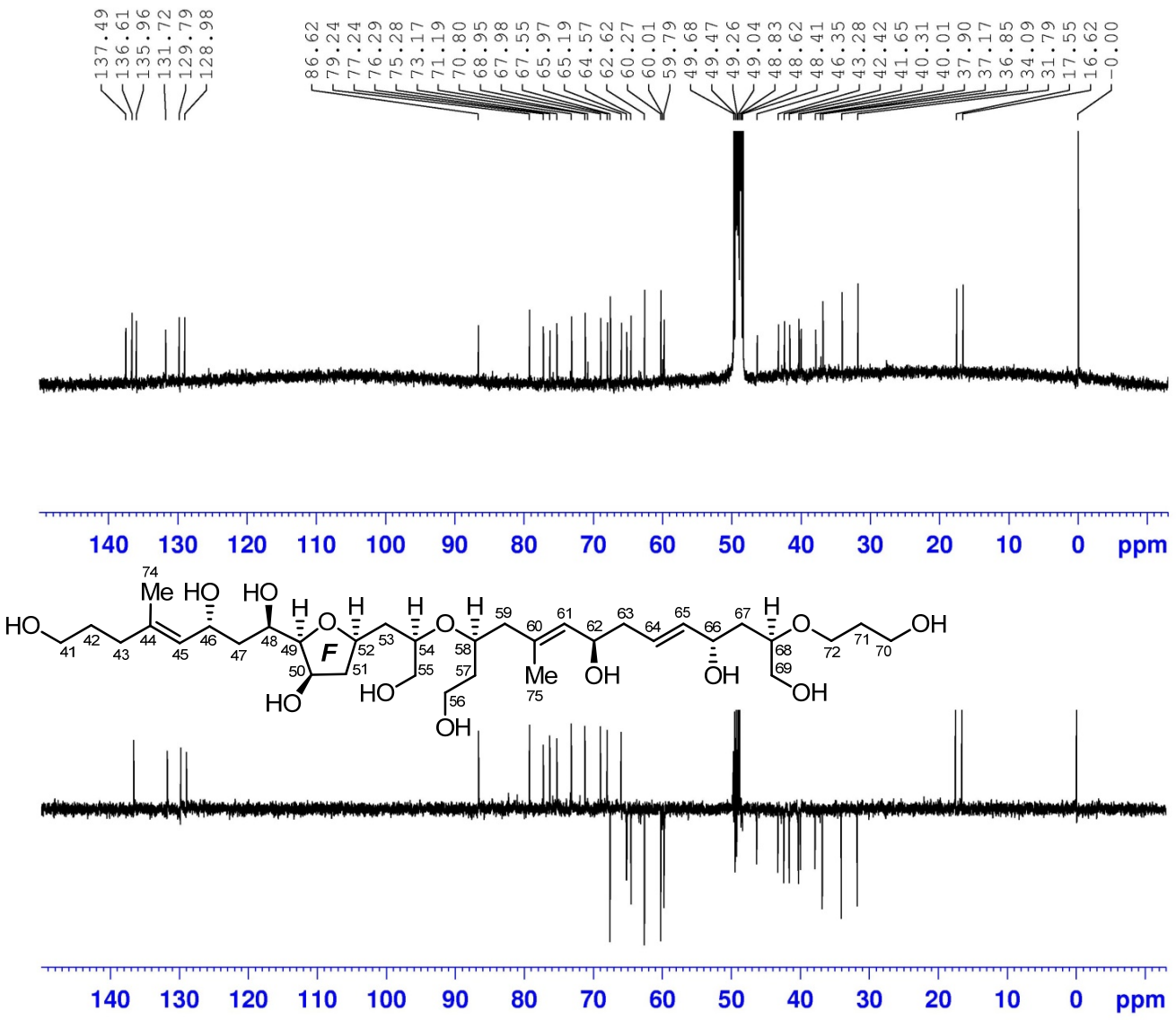

Figure S76. DEPT135 (100 MHz) spectrum of the fragment **1B** in CD_3OD

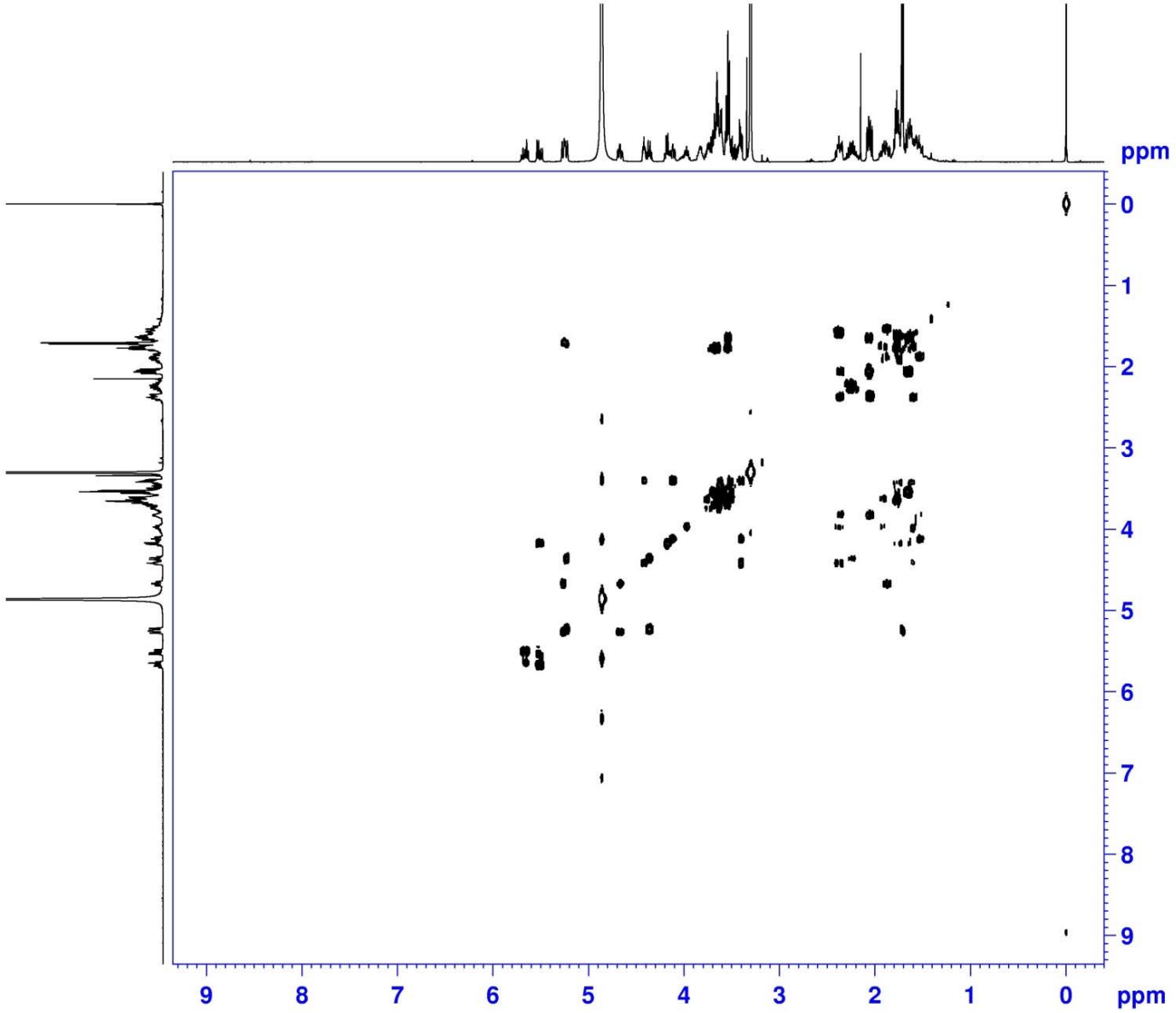

Figure S77. ^{1}H–^{1}H COSY (400 MHz) spectrum of the fragment **1B** in CD_3OD

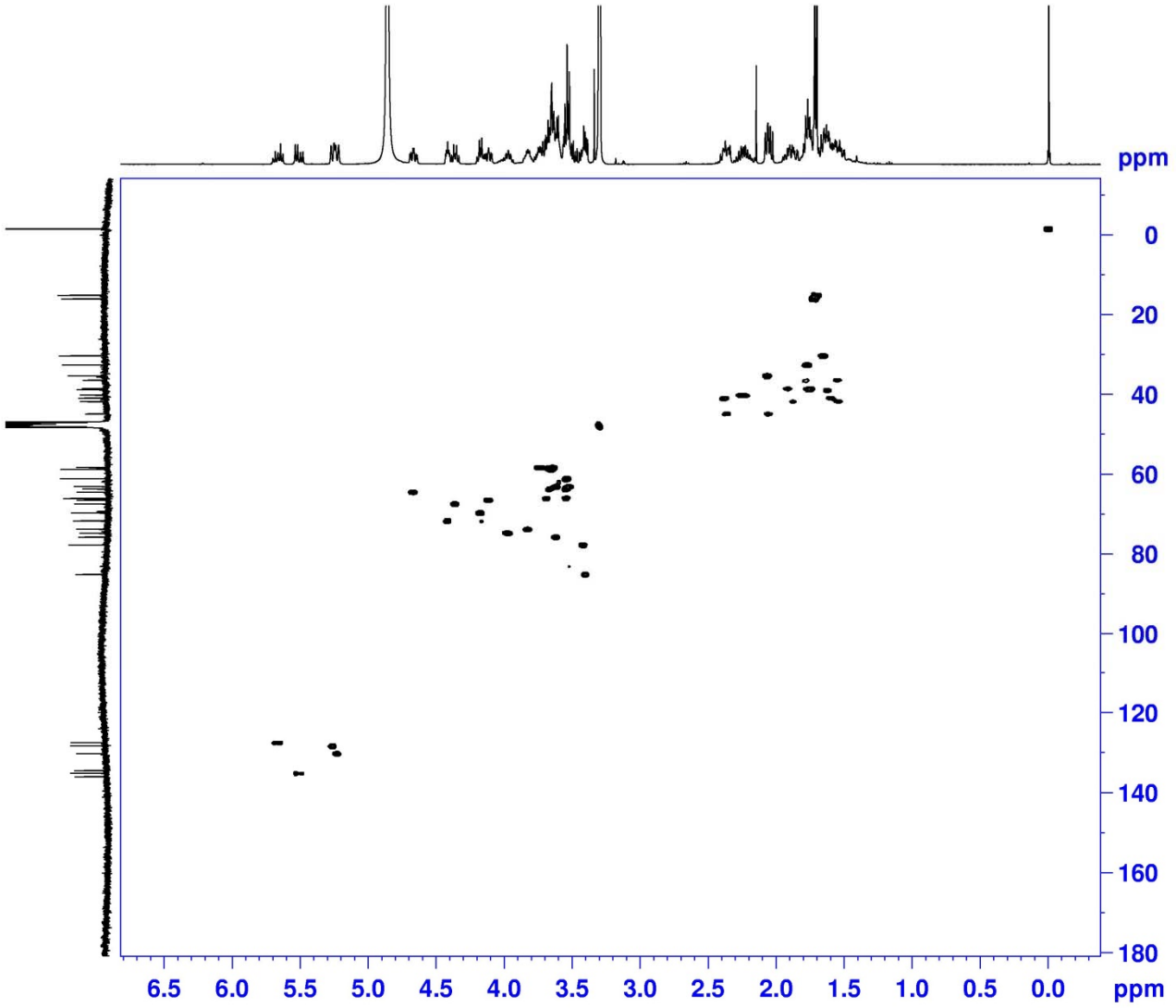

Figure S78. HSQC (400 MHz) spectrum of the fragment **1B** in CD_3OD

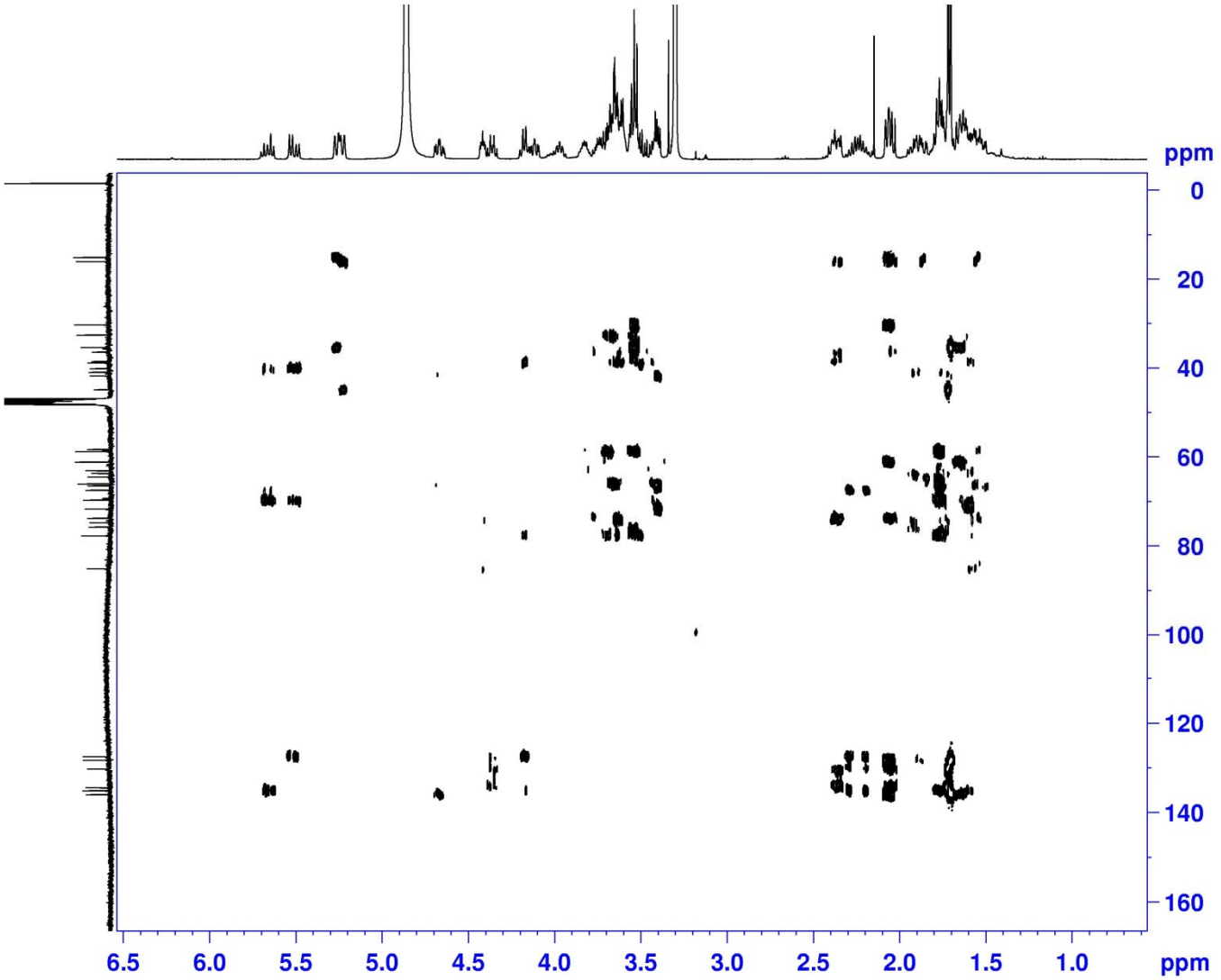

Figure S79. HMBC (400 MHz) spectrum of the fragment **1B** in CD_3OD

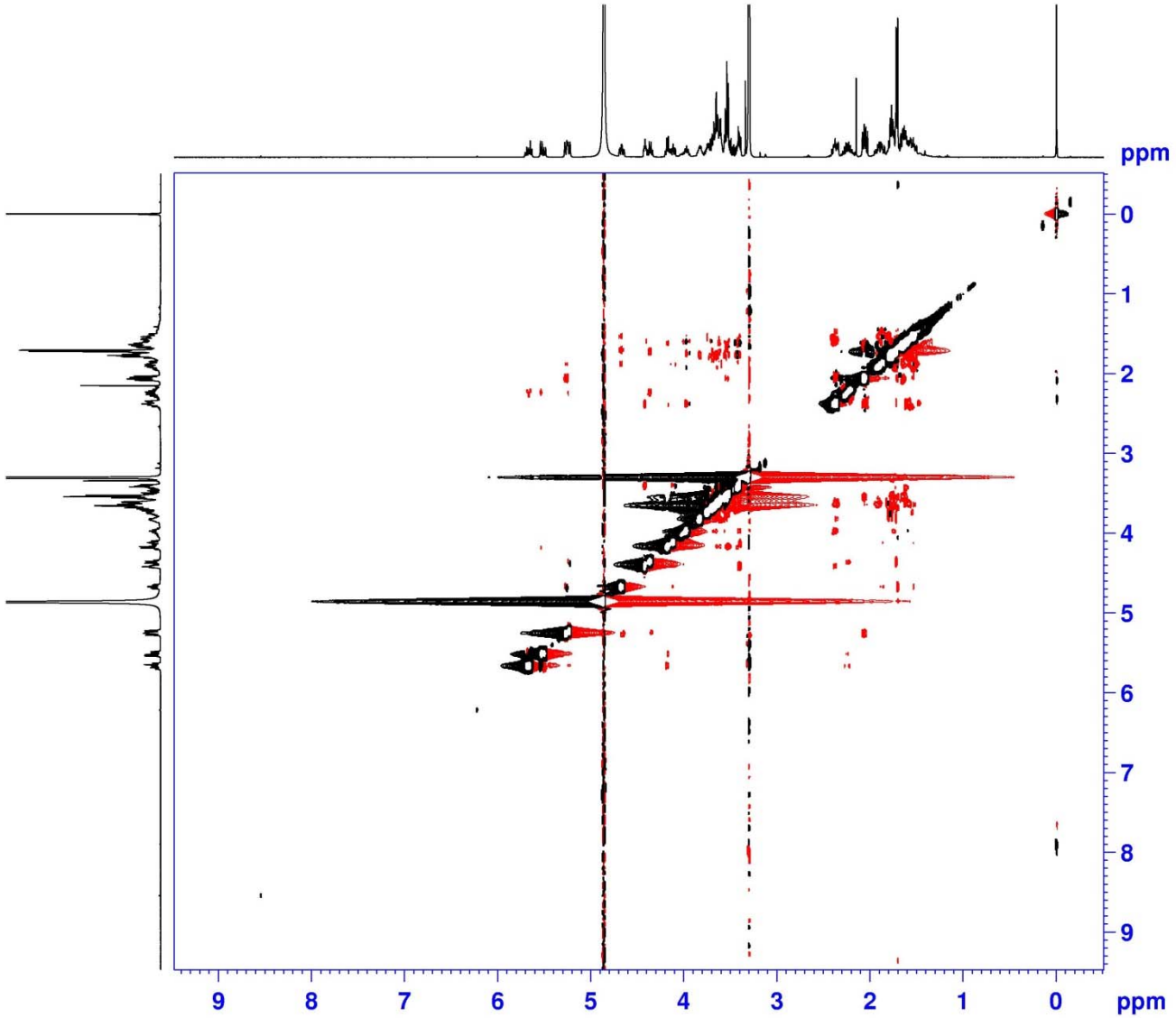

Figure S80. NOESY (400 MHz) spectrum of the fragment **1B** in CD_3OD

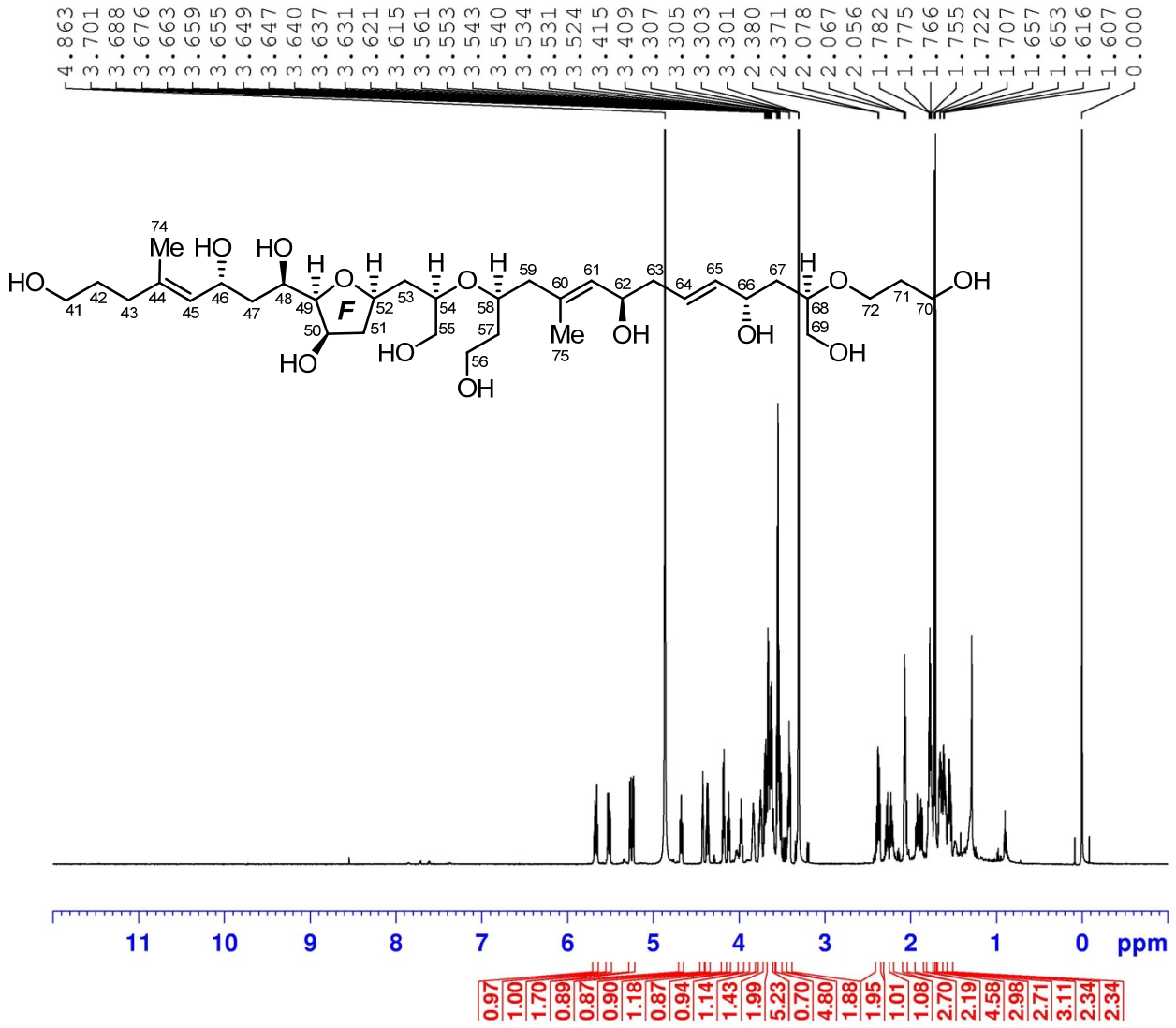

Figure S81. ^{1}H (700 MHz) NMR spectrum of the fragment **1B** in CD_3OD

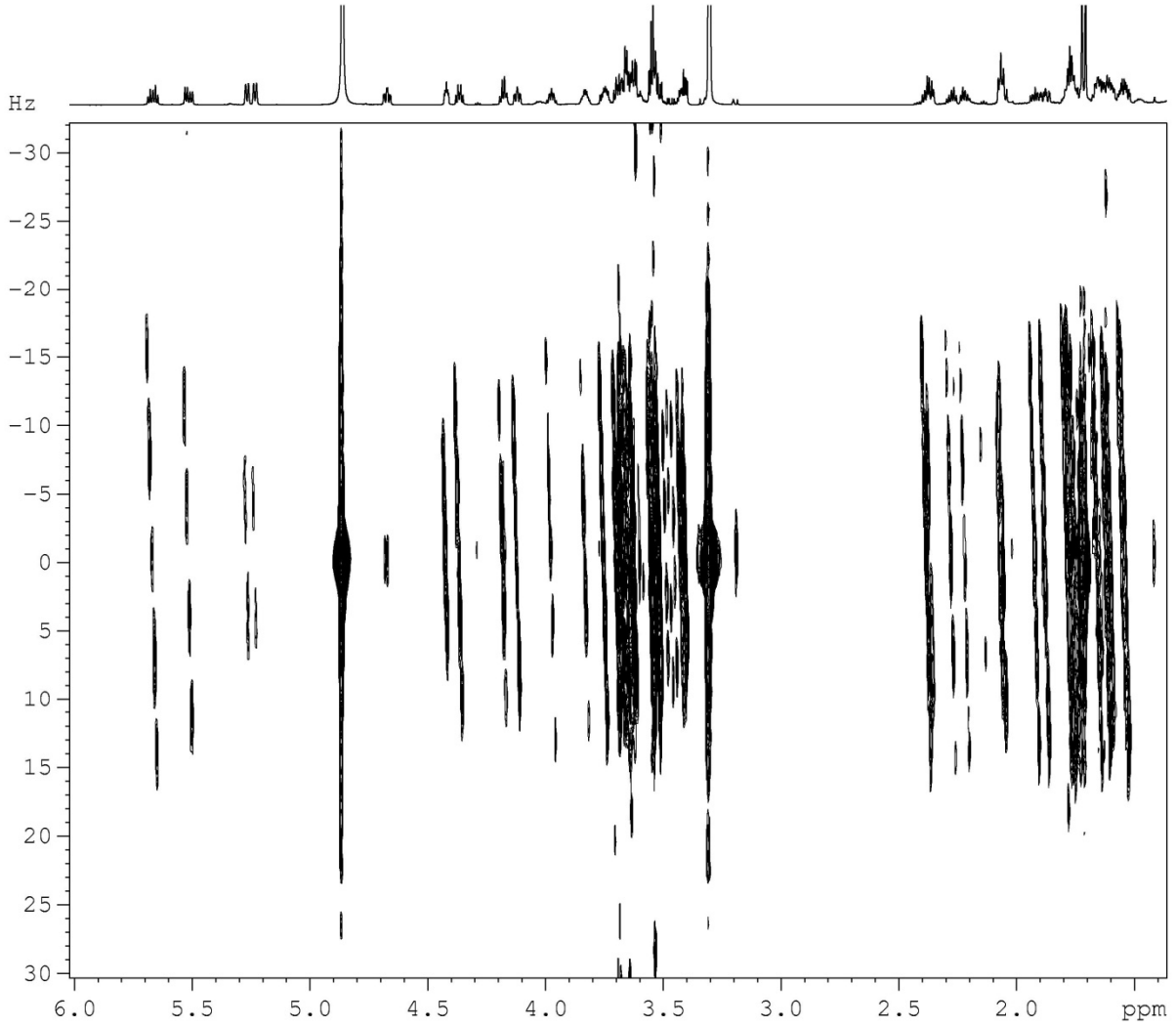

Figure S82. 2D *J*RES (700 MHz) spectrum of the fragment **1B** in CD_3OD

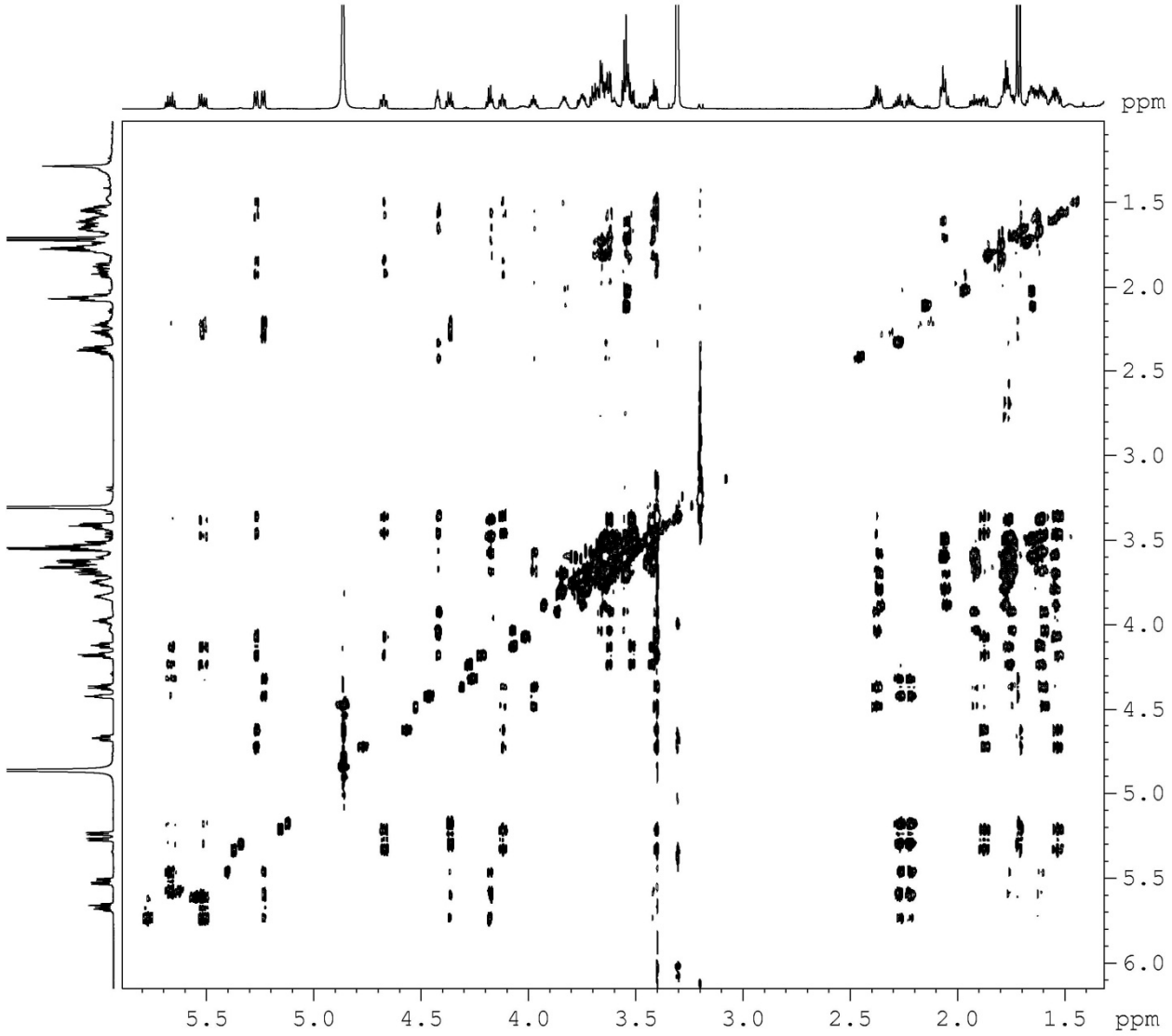

Figure S83. HETLOC (700 MHz) spectrum of the fragment **1B** in CD_3OD

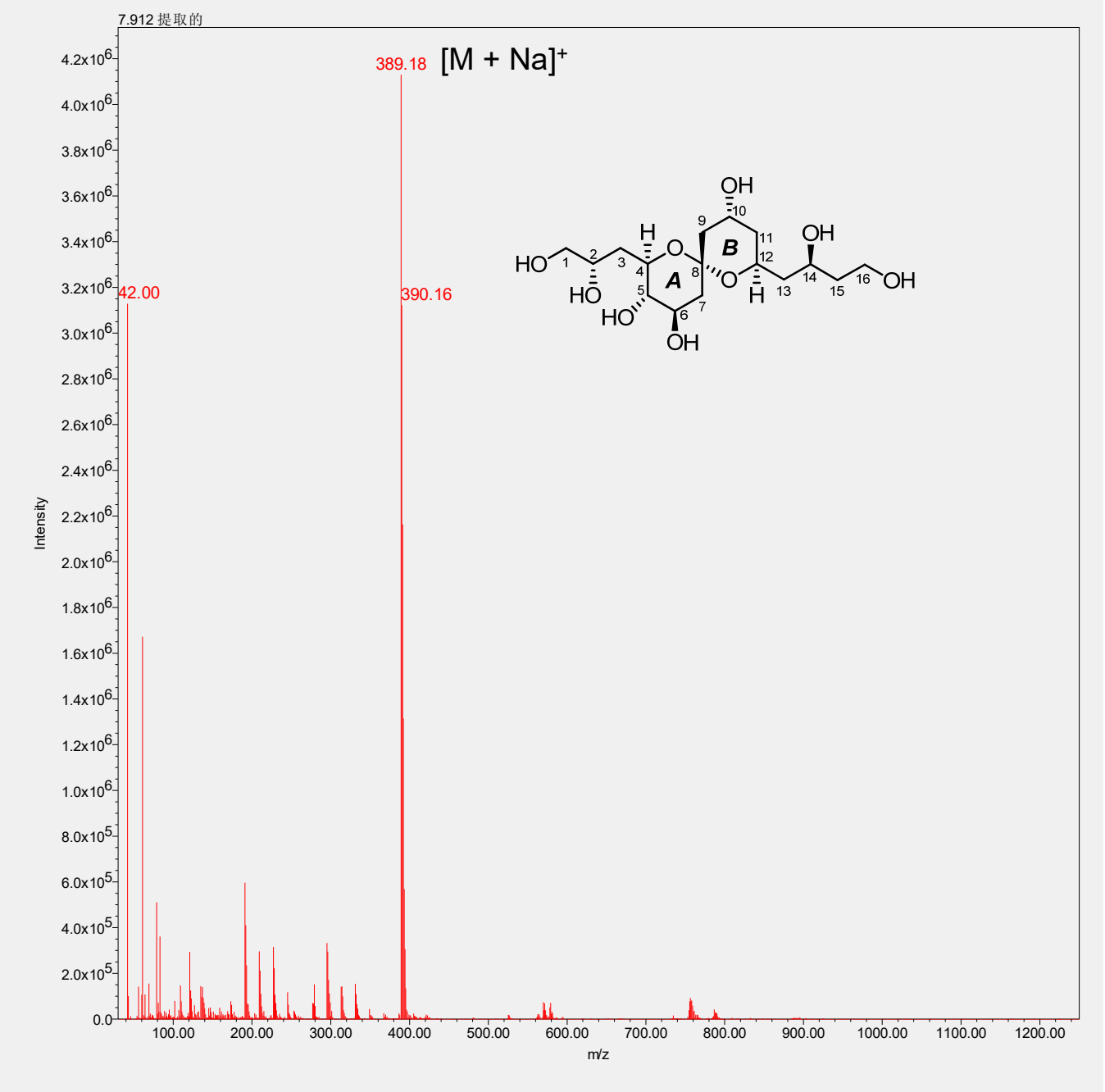

Figure S84. LR-ESIMS for the fragment **1a**

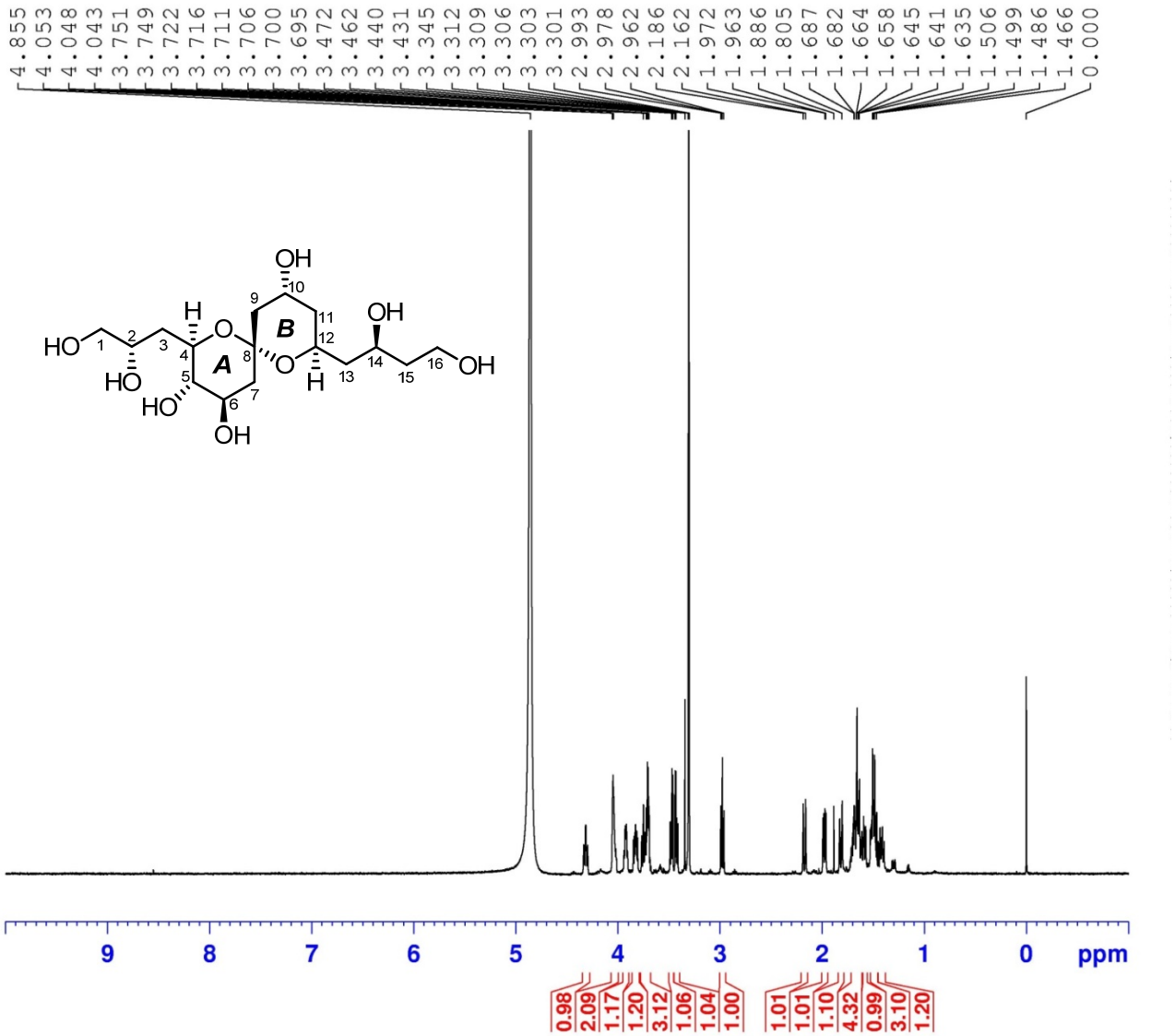

Figure S85. ^{1}H (600 MHz) NMR spectrum of the fragment **1a** in CD_3OD

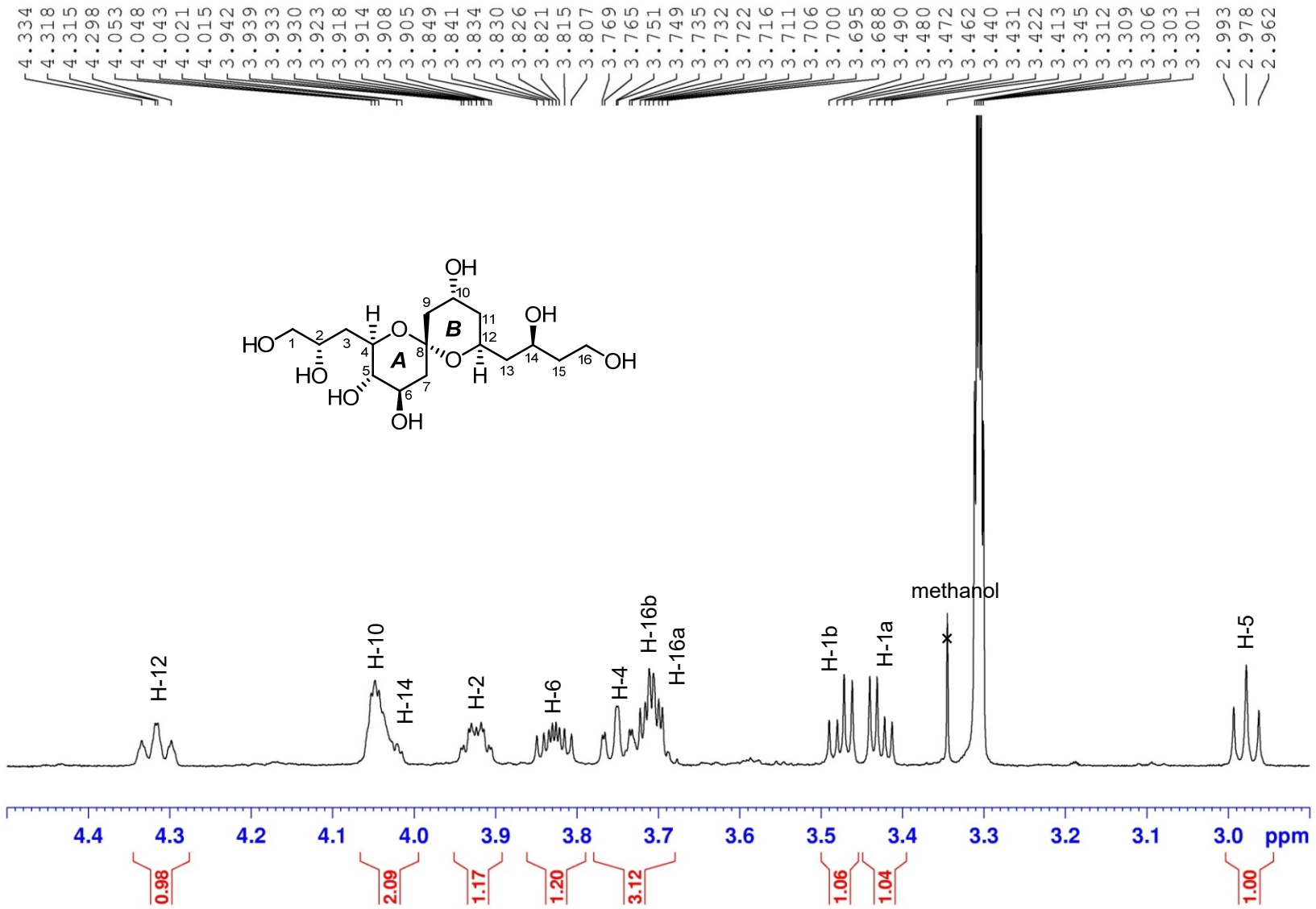

Figure S86. ^{1}H (600 MHz) NMR spectrum of the fragment **1a** in CD_3OD

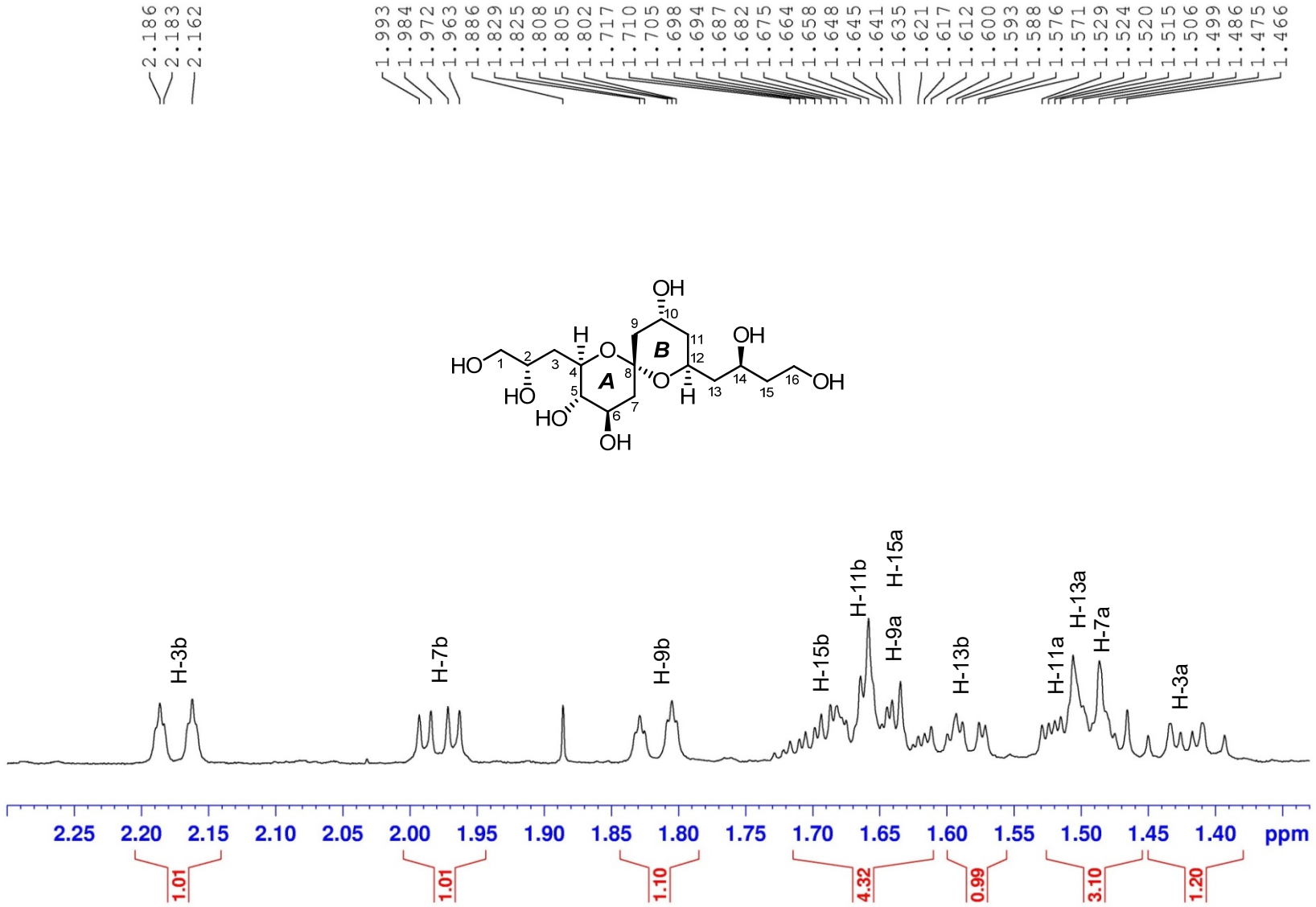

Figure S87. ^{1}H (600 MHz) NMR spectrum of the fragment **1a** in CD_3OD

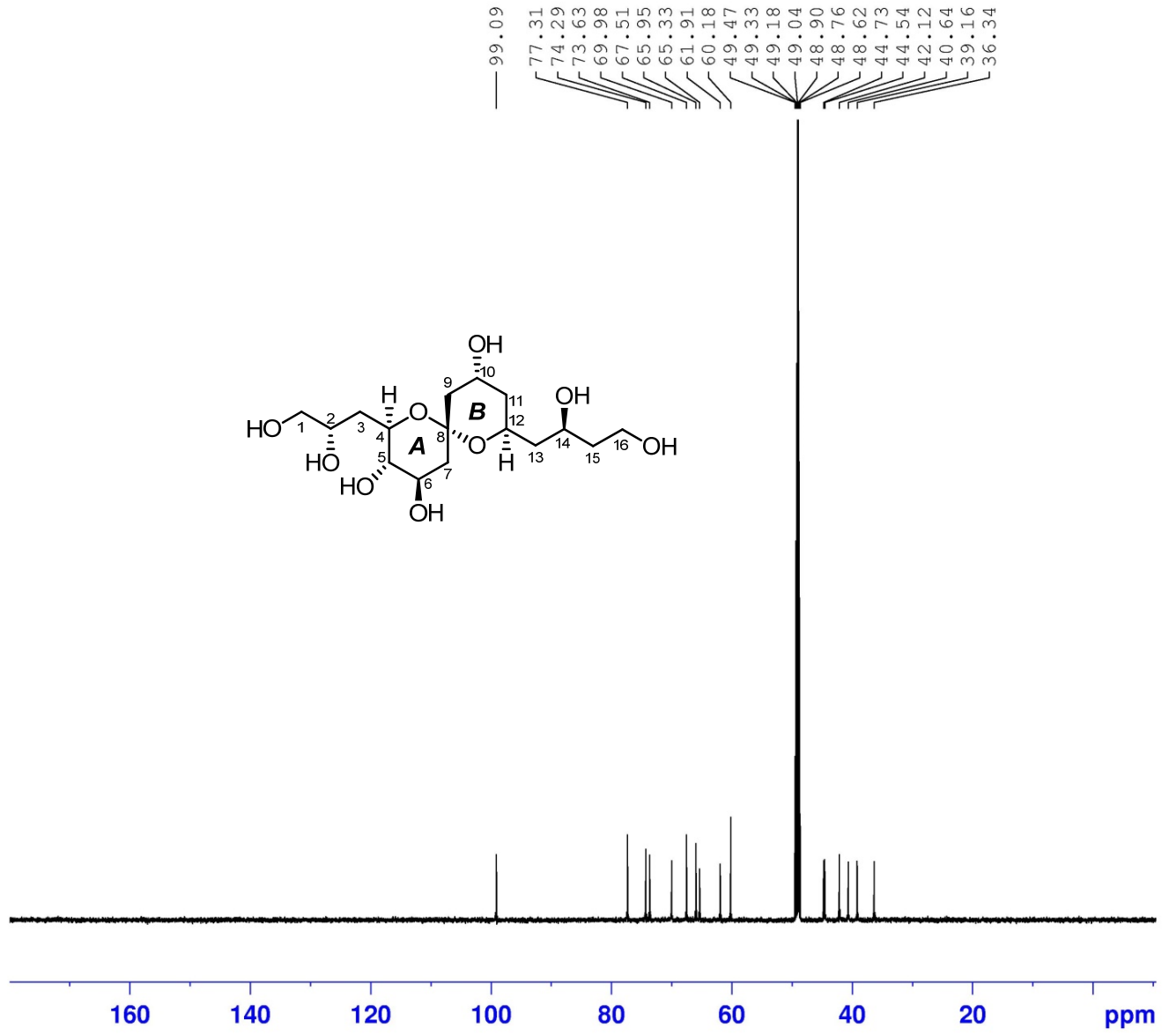

Figure S88. ^{13}C (150 MHz) NMR spectrum of the fragment **1a** in CD_3OD

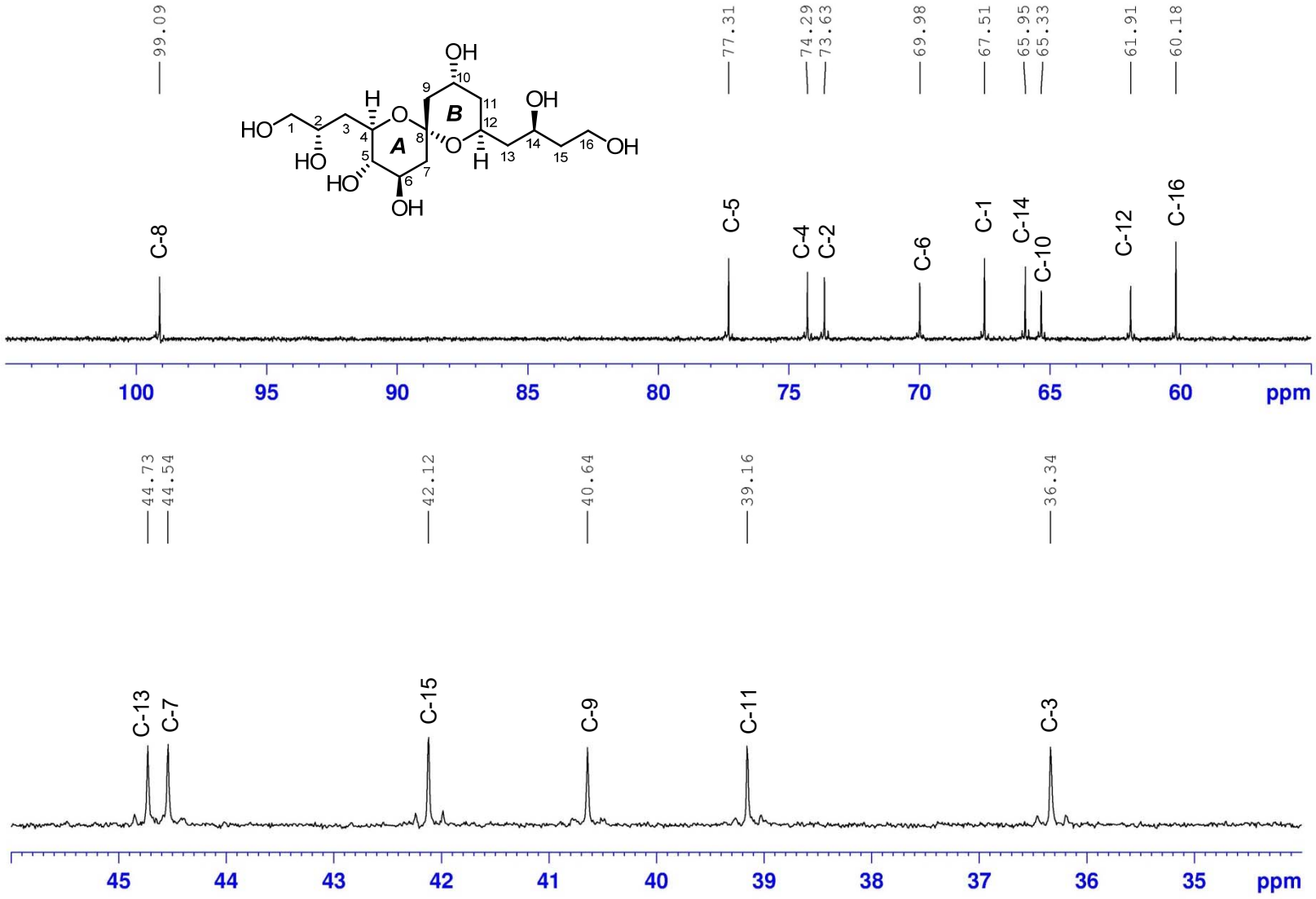

Figure S89. ^{13}C (150 MHz) NMR spectrum of the fragment **1a** in CD_3OD

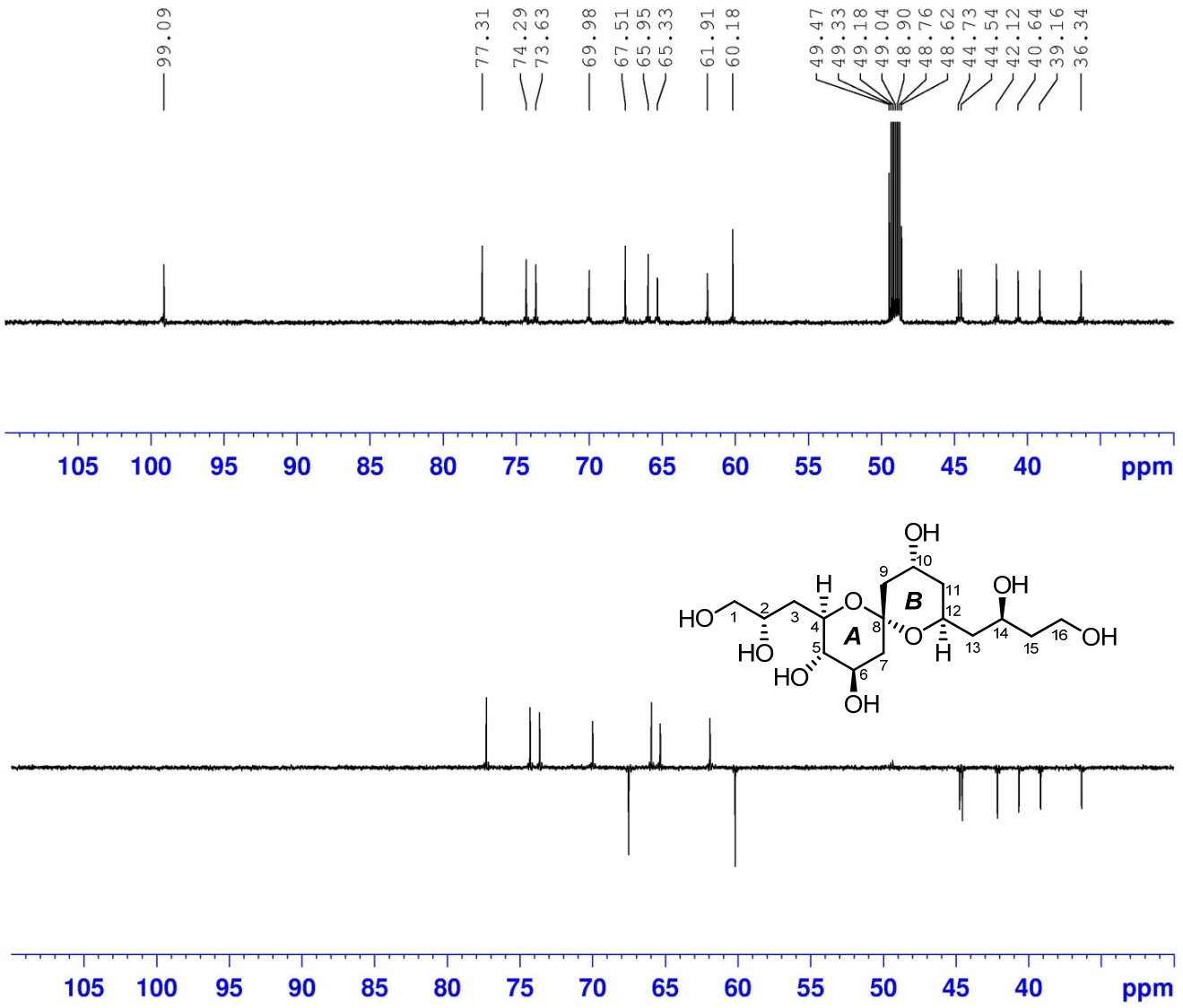

Figure S90. DEPT 135 (150 MHz) spectrum of the fragment **1a** in CD_3OD

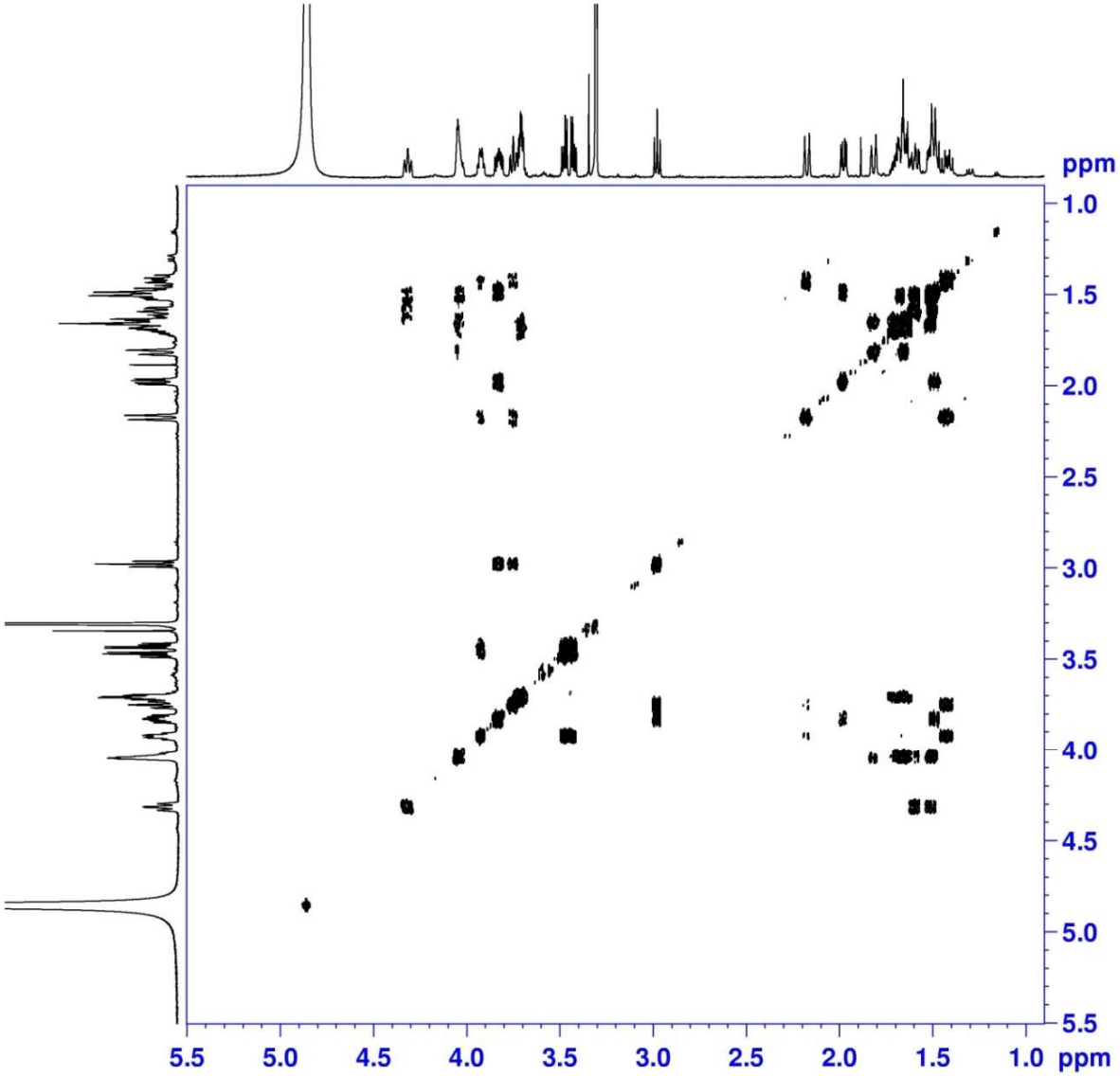

Figure S91. $^{1}H–^{1}H$ COSY (600 MHz) spectrum of the fragment **1a** in CD_3OD

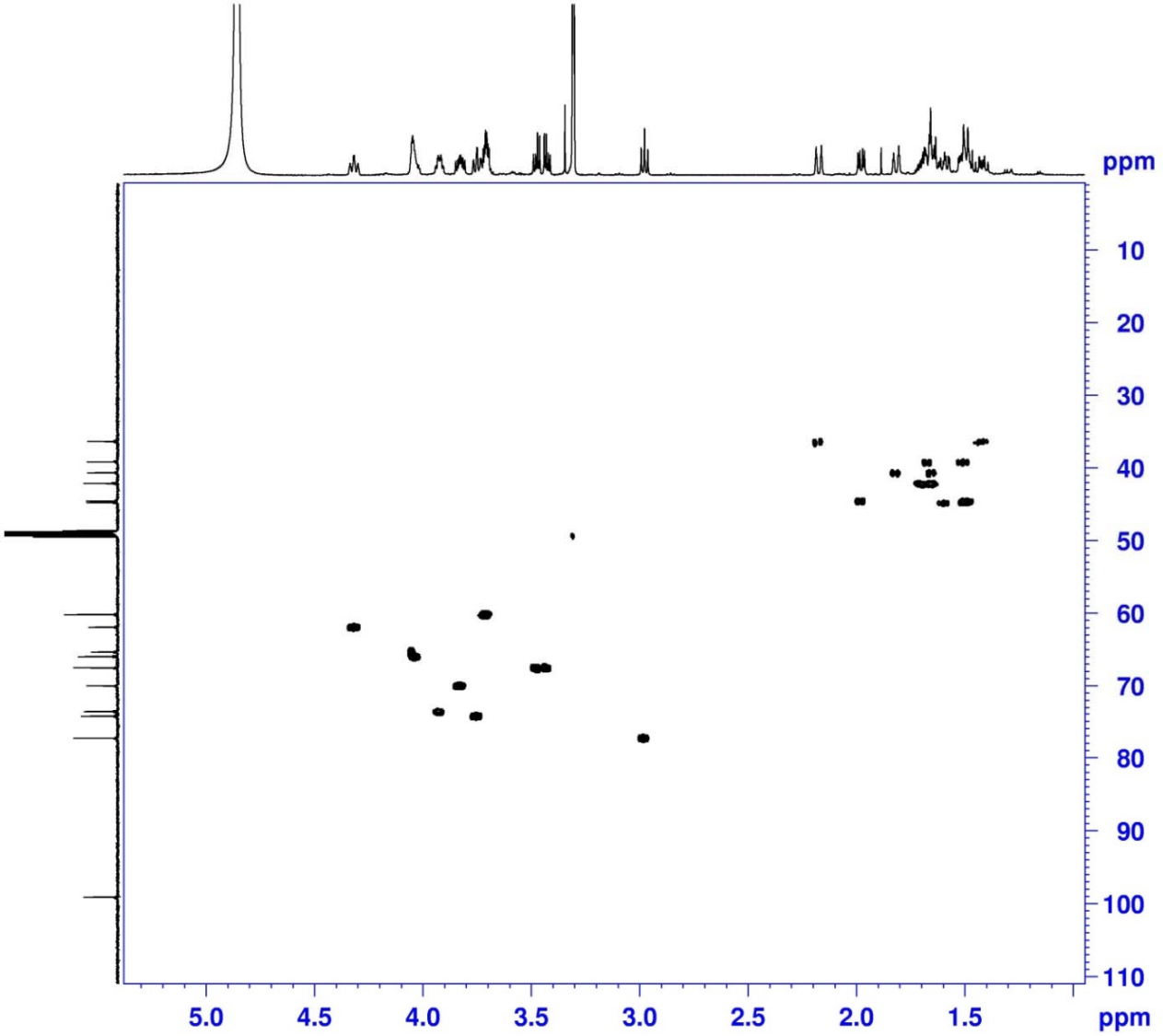

Figure S92. HSQC (600 MHz) spectrum of the fragment **1a** in CD_3OD

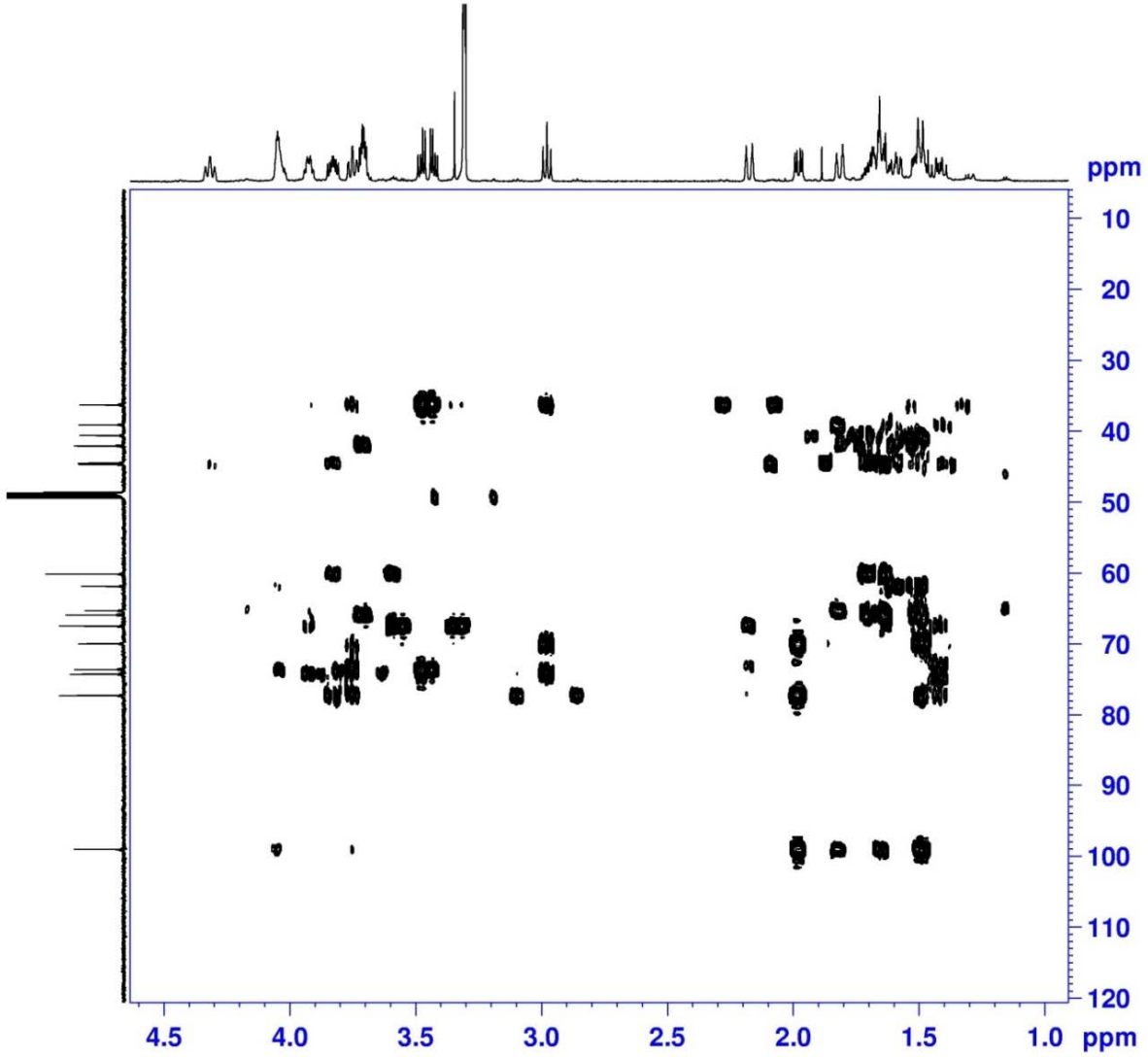

Figure S93. HMBC (600 MHz) spectrum of the fragment **1a** in CD_3OD

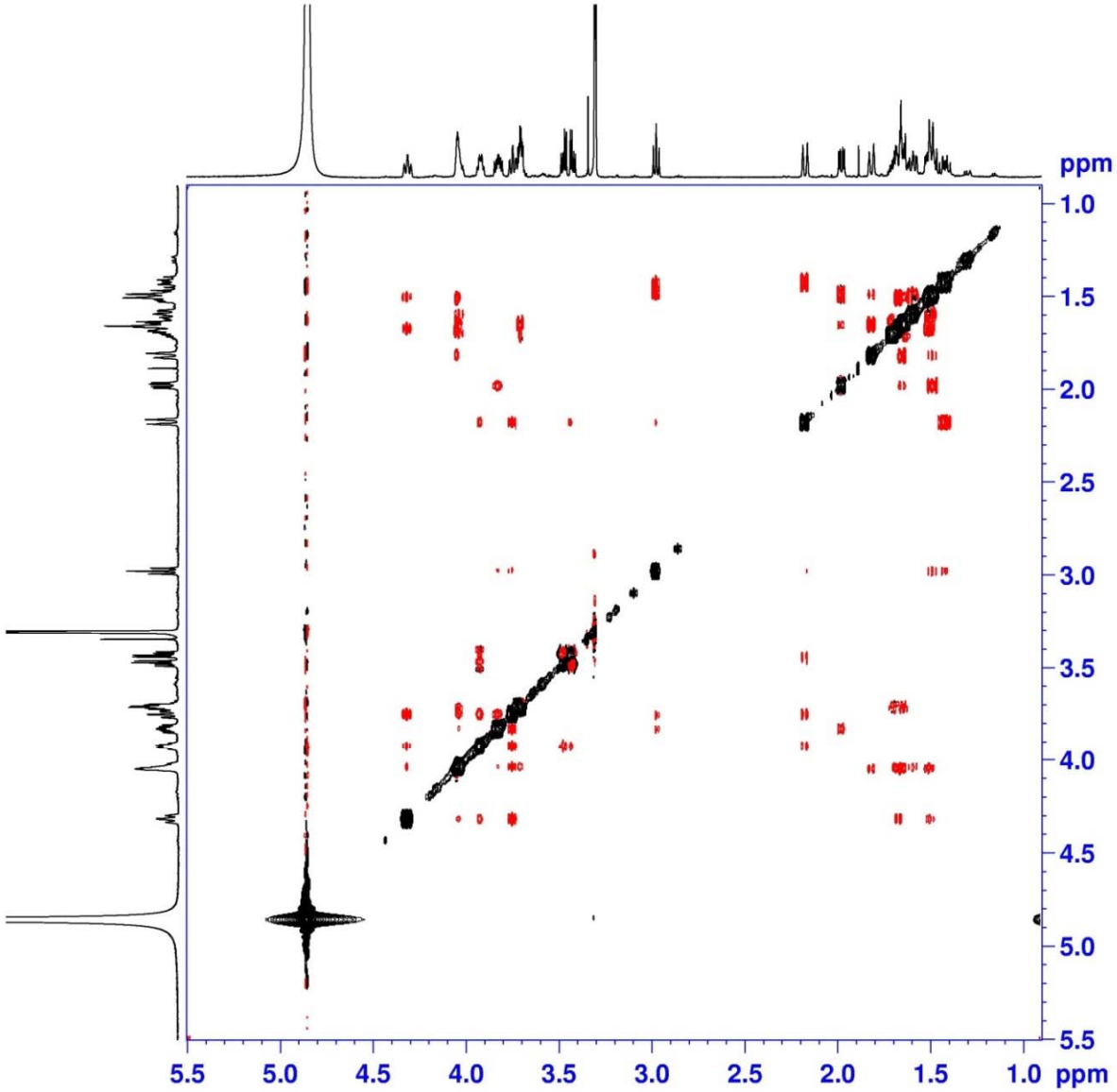

Figure S94. NOESY (600 MHz) spectrum of the fragment **1a** in CD_3OD

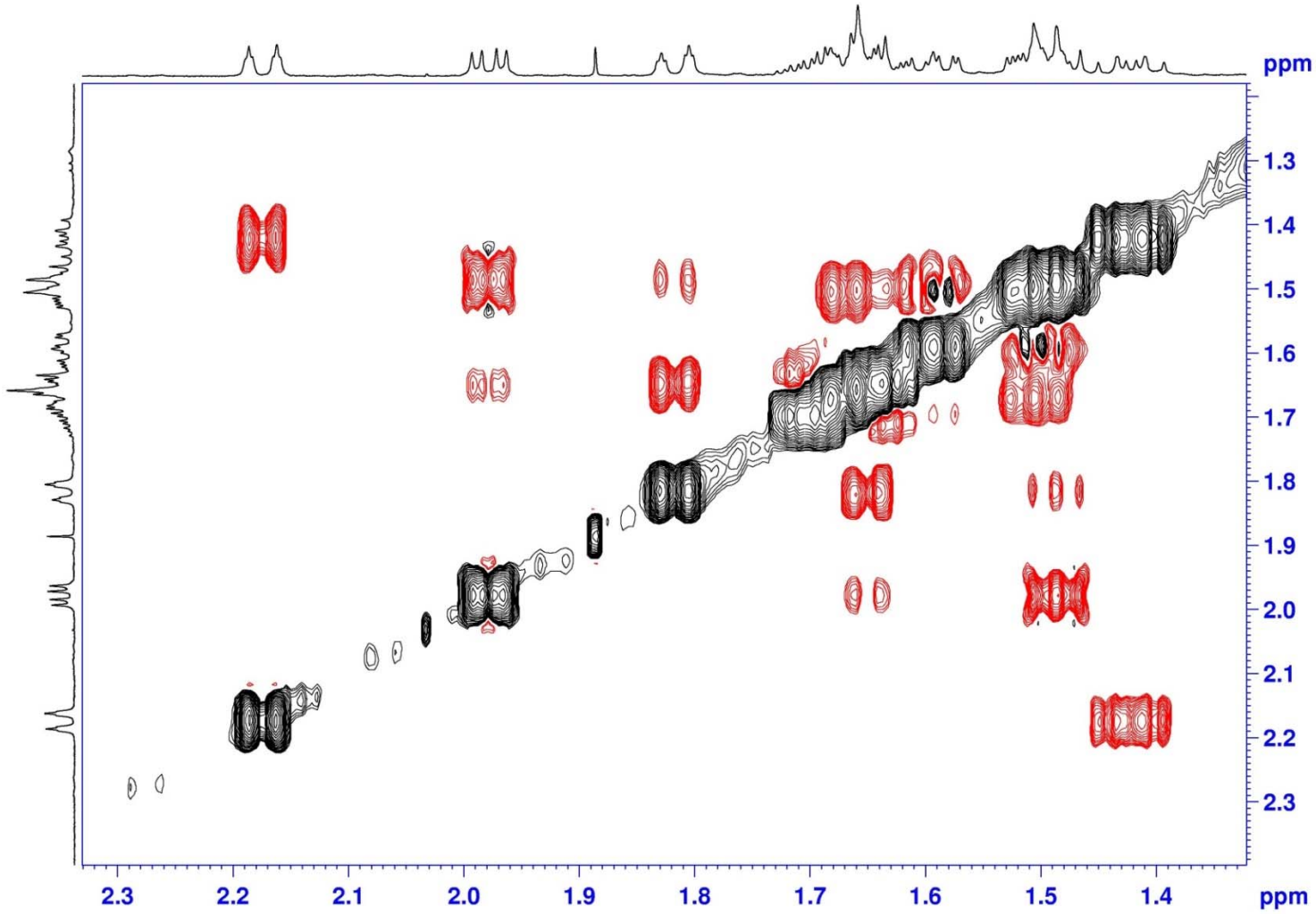

Figure S95. NOESY (600 MHz) spectrum of the fragment **1a** in CD_3OD

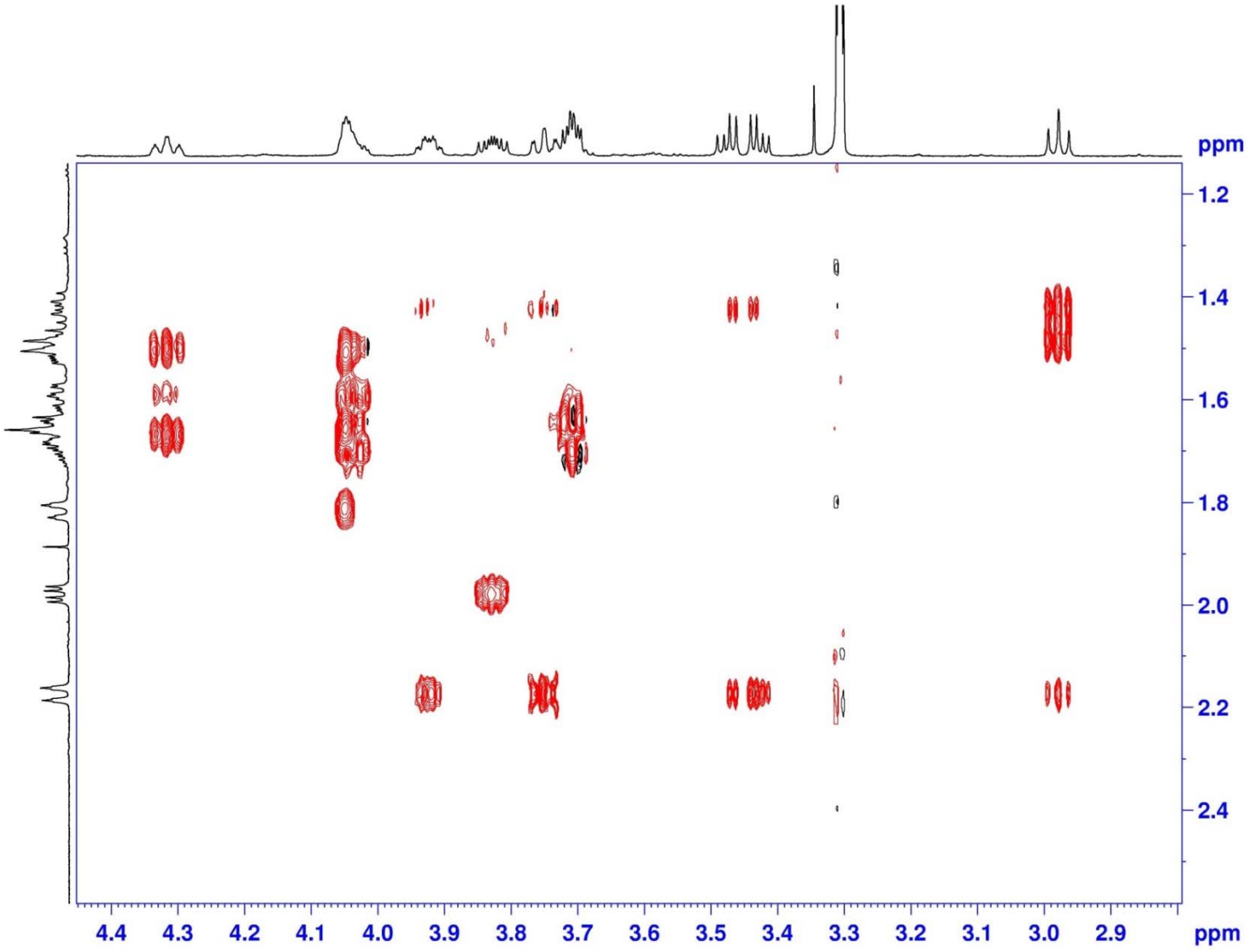

Figure S96. NOESY (600 MHz) spectrum of the fragment **1a** in CD_3OD

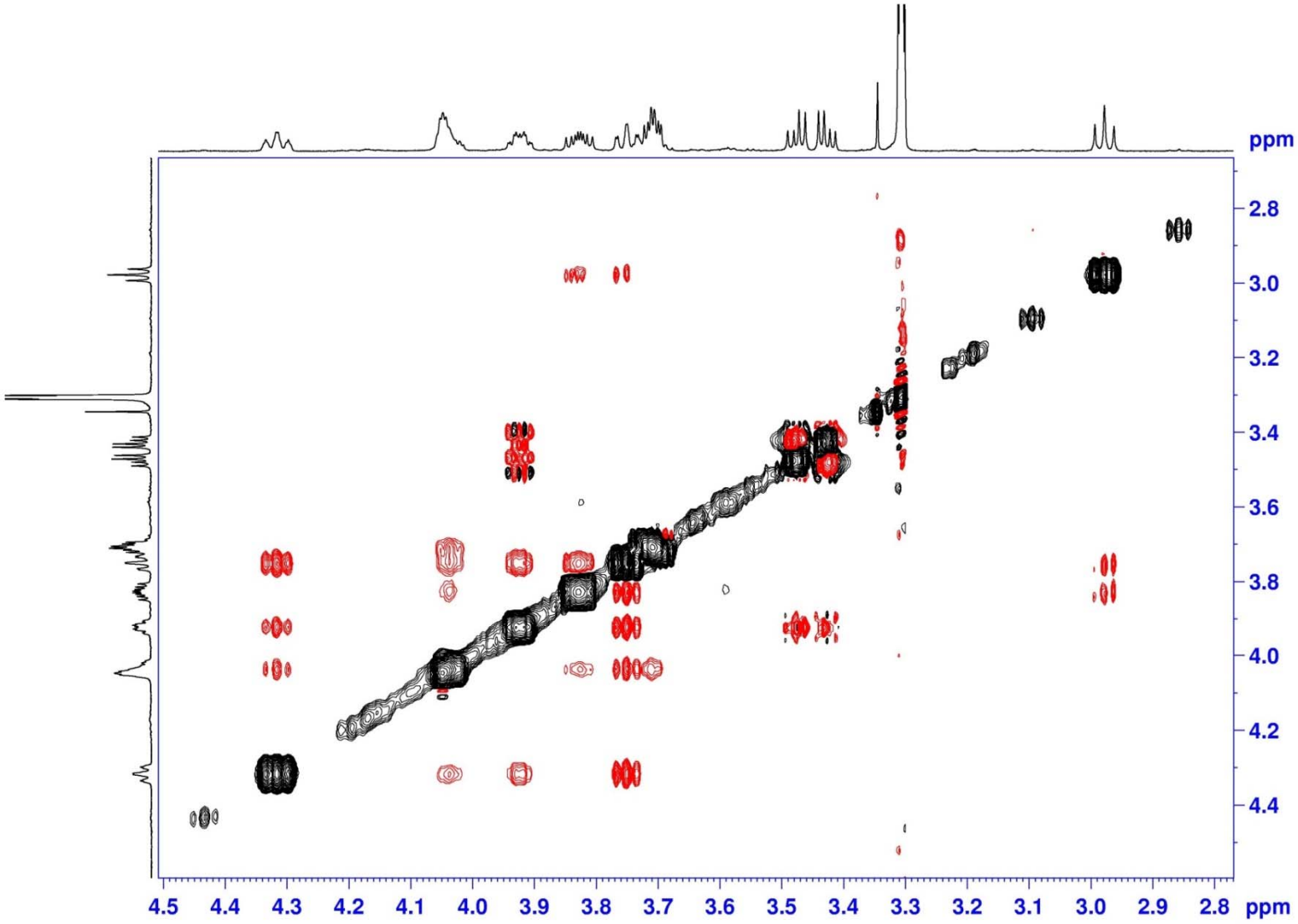

Figure S97. NOESY (600 MHz) spectrum of the fragment **1a** in CD_3OD

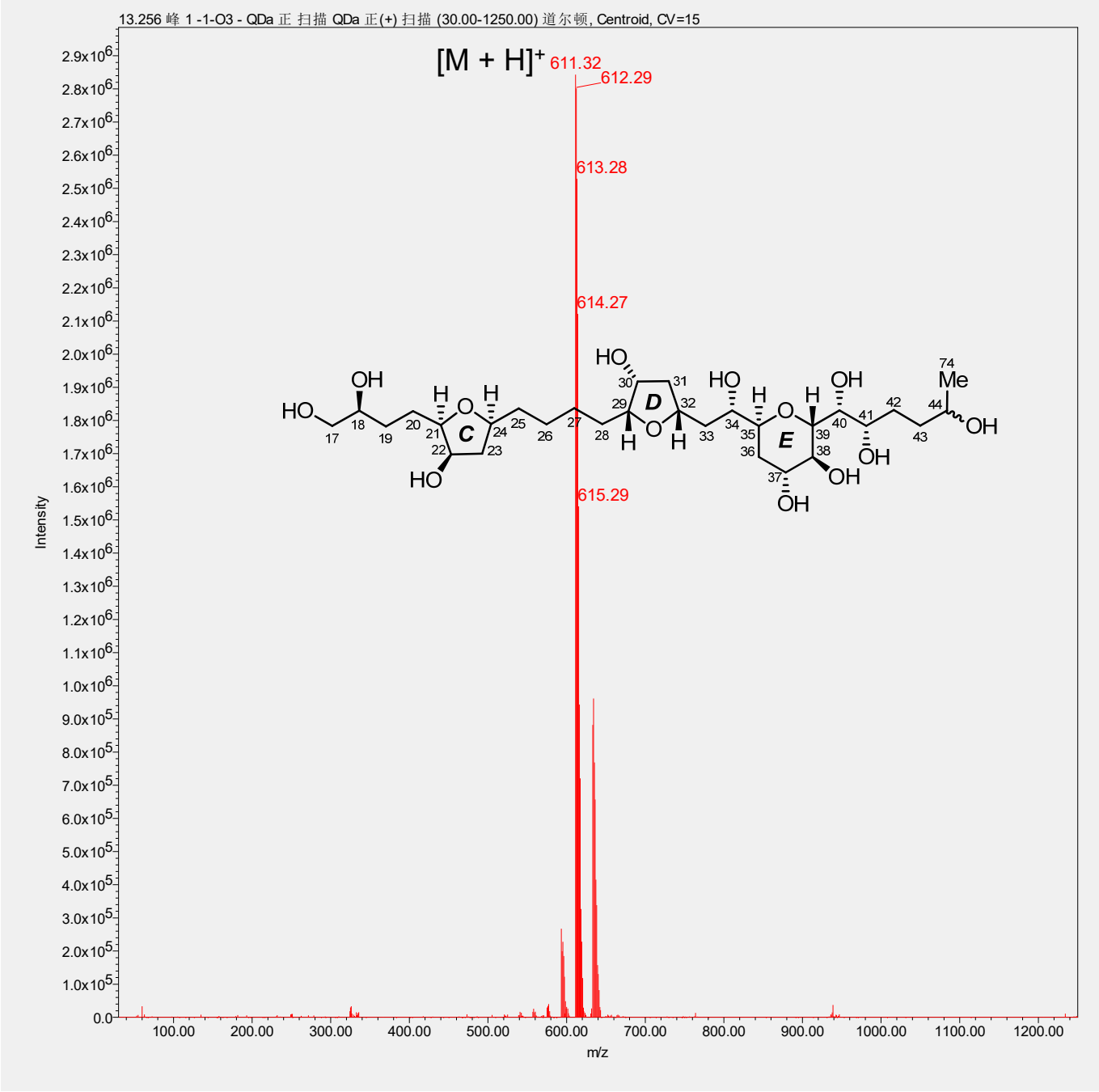

Figure S98. LR-ESIMS for the fragment **1b**

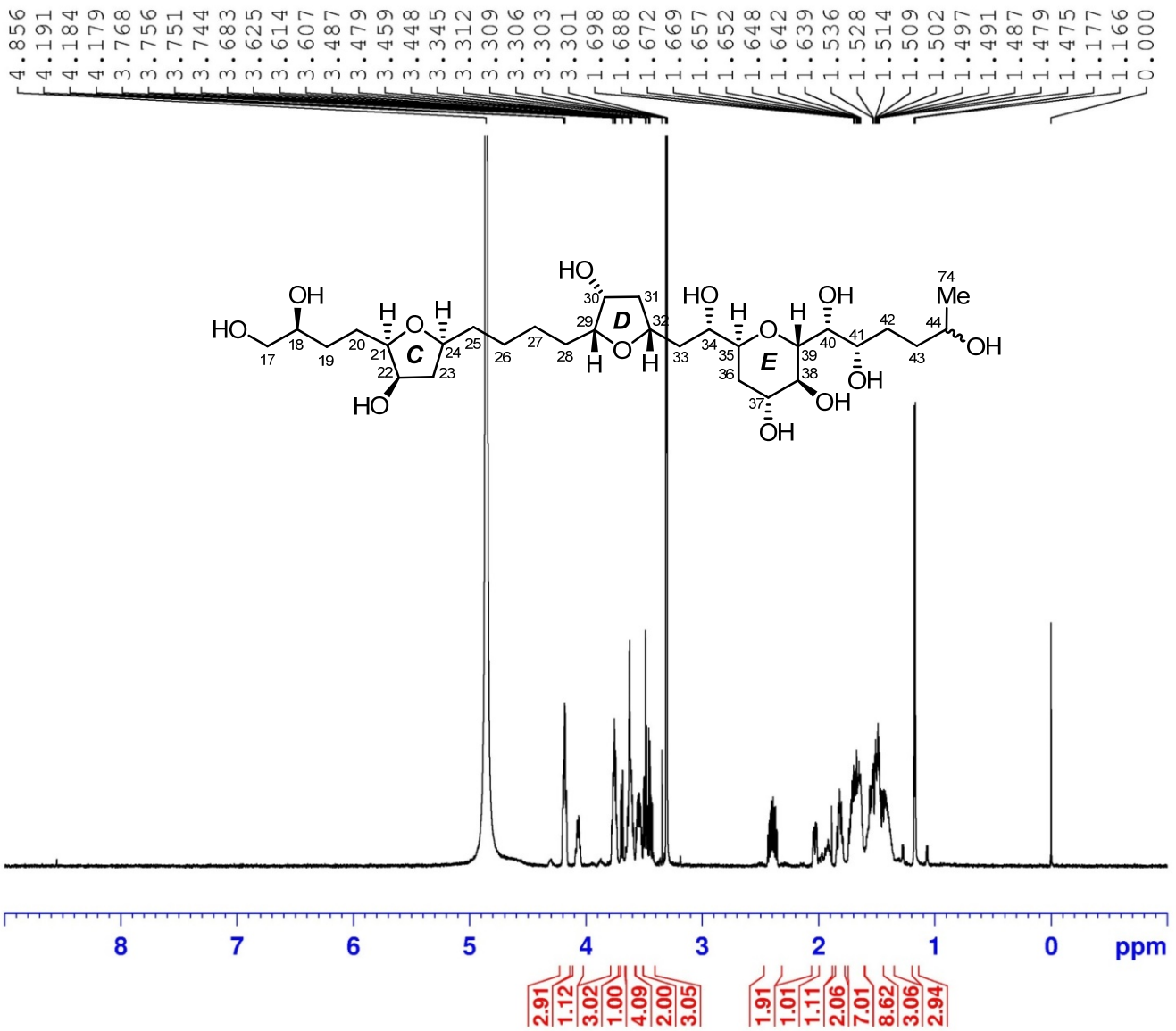

Figure S99. ^{1}H (600 MHz) NMR spectrum of the fragment **1b** in CD_3OD

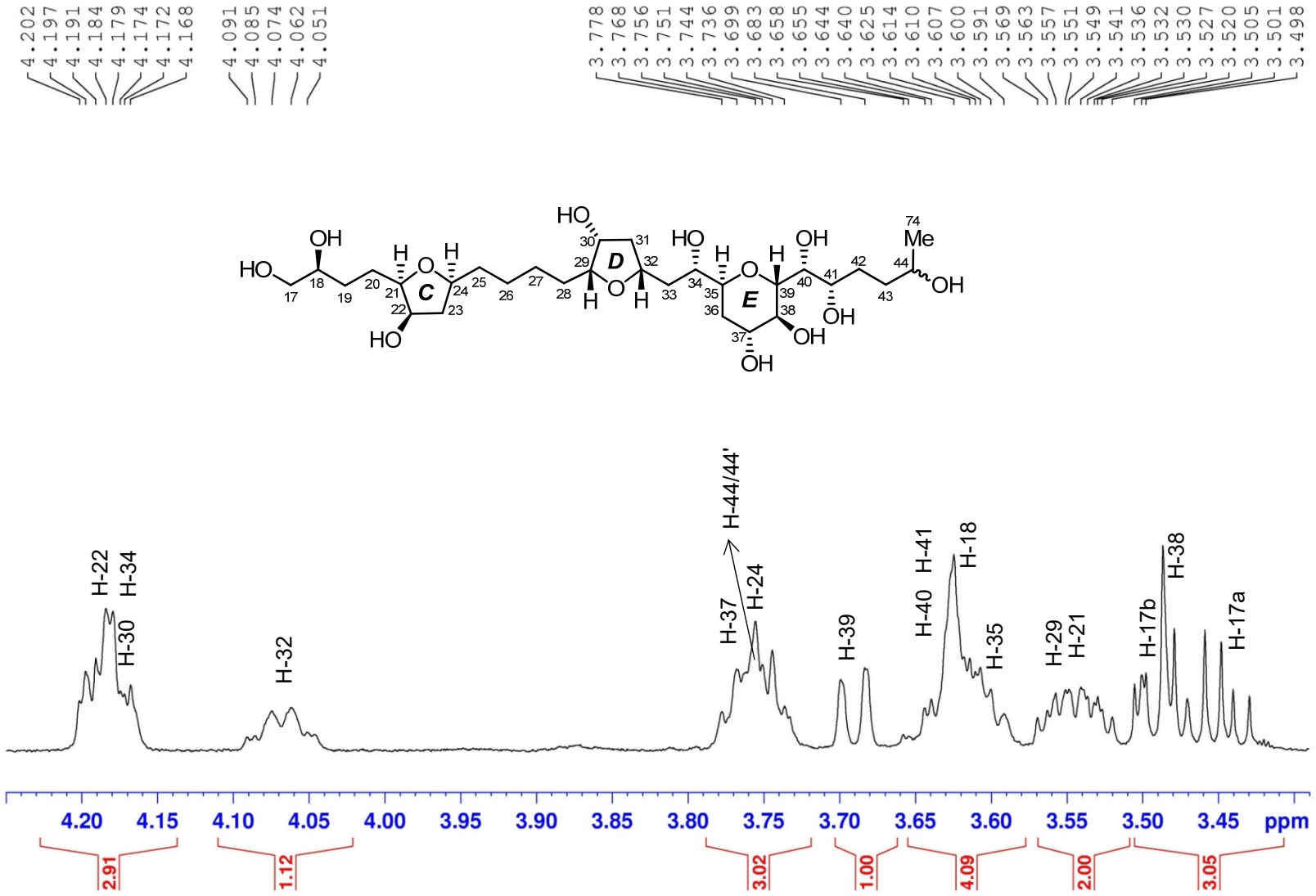

Figure S100. ^{1}H (600 MHz) NMR spectrum of the fragment **1b** in CD_3OD

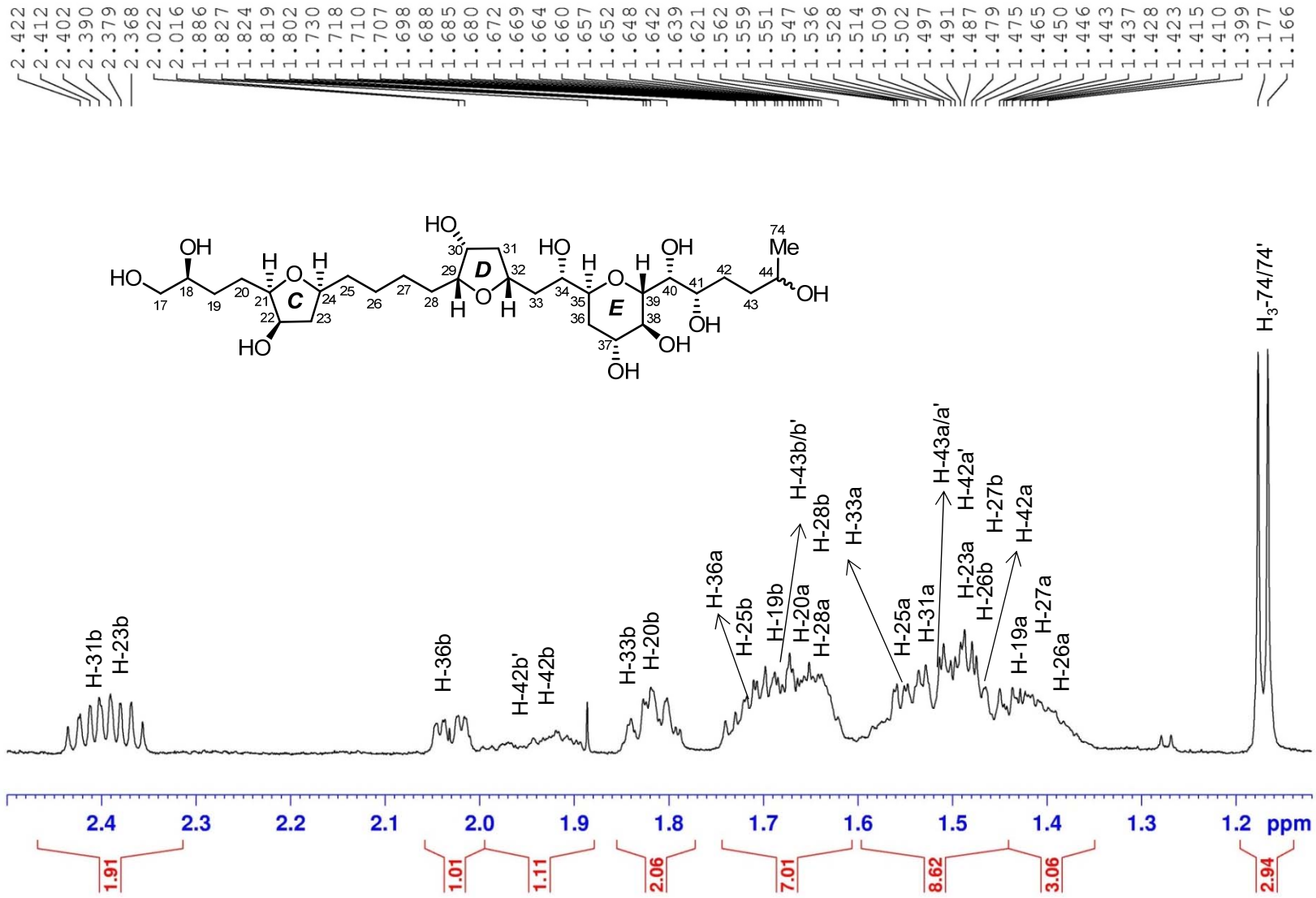

Figure S101. ^{1}H (600 MHz) NMR spectrum of the fragment **1b** in CD_3OD

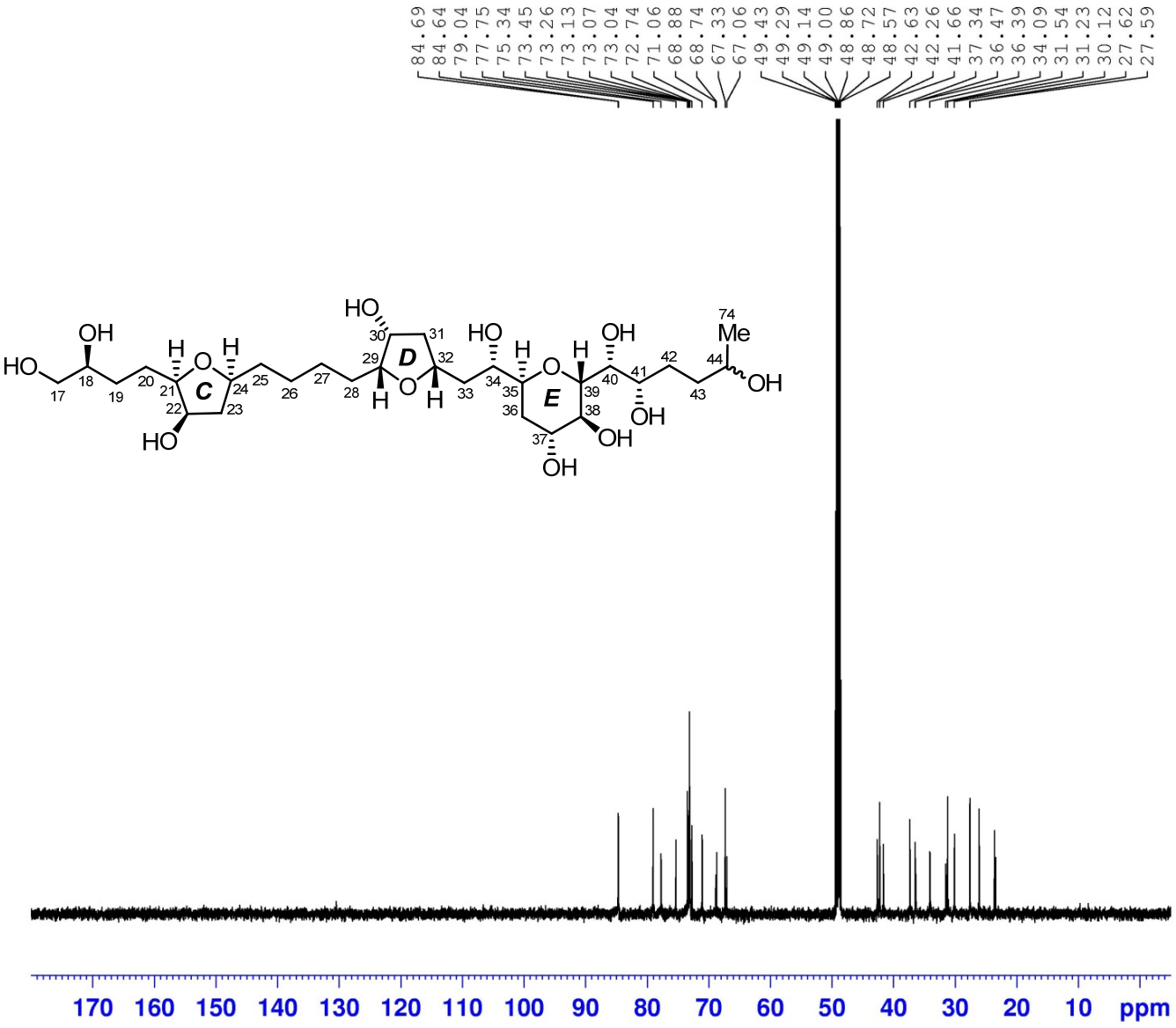

Figure S102. ^{13}C (150 MHz) NMR spectrum of the fragment **1b** in CD_3OD

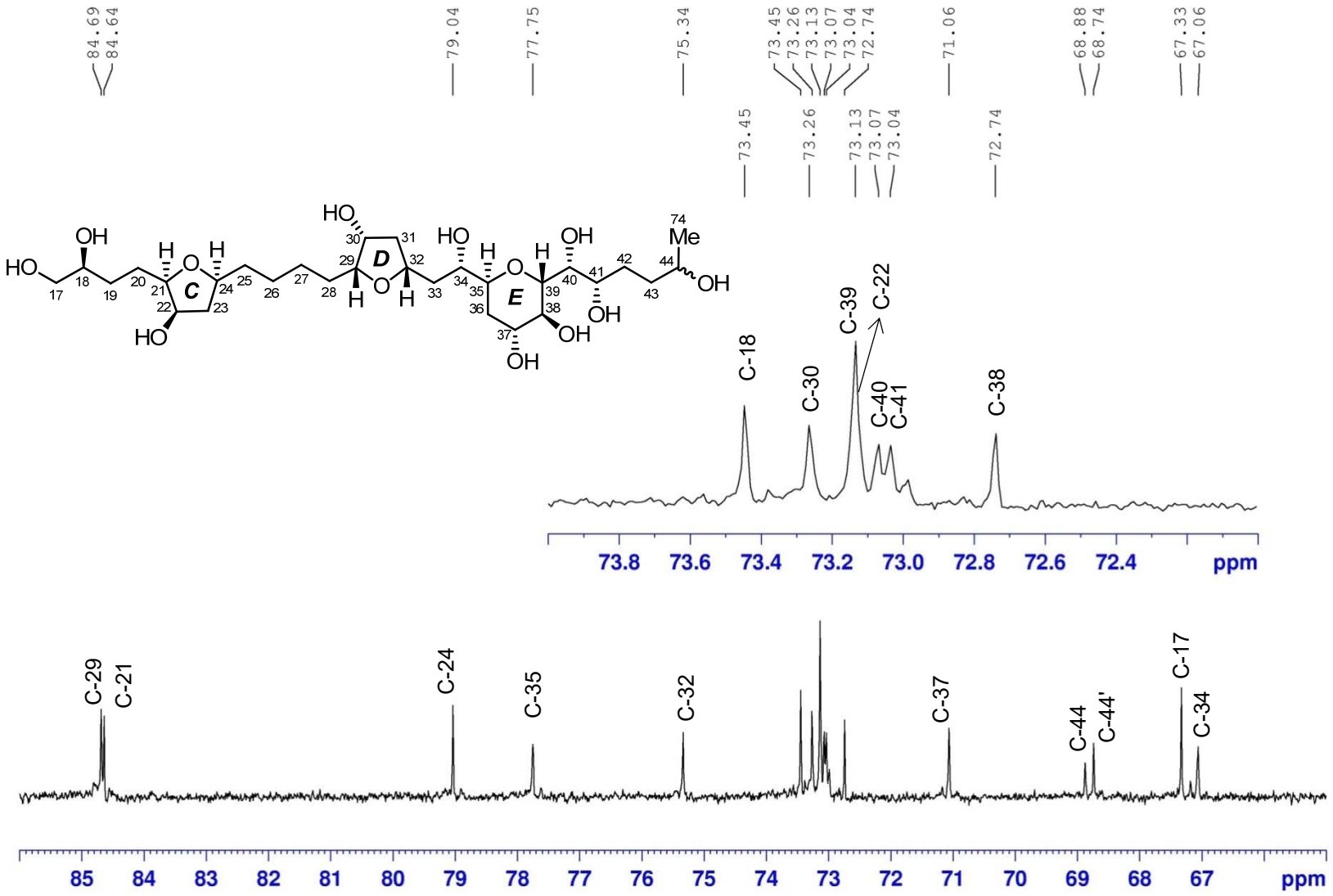

Figure S103. ^{13}C (150 MHz) NMR spectrum of the fragment **1b** in CD_3OD

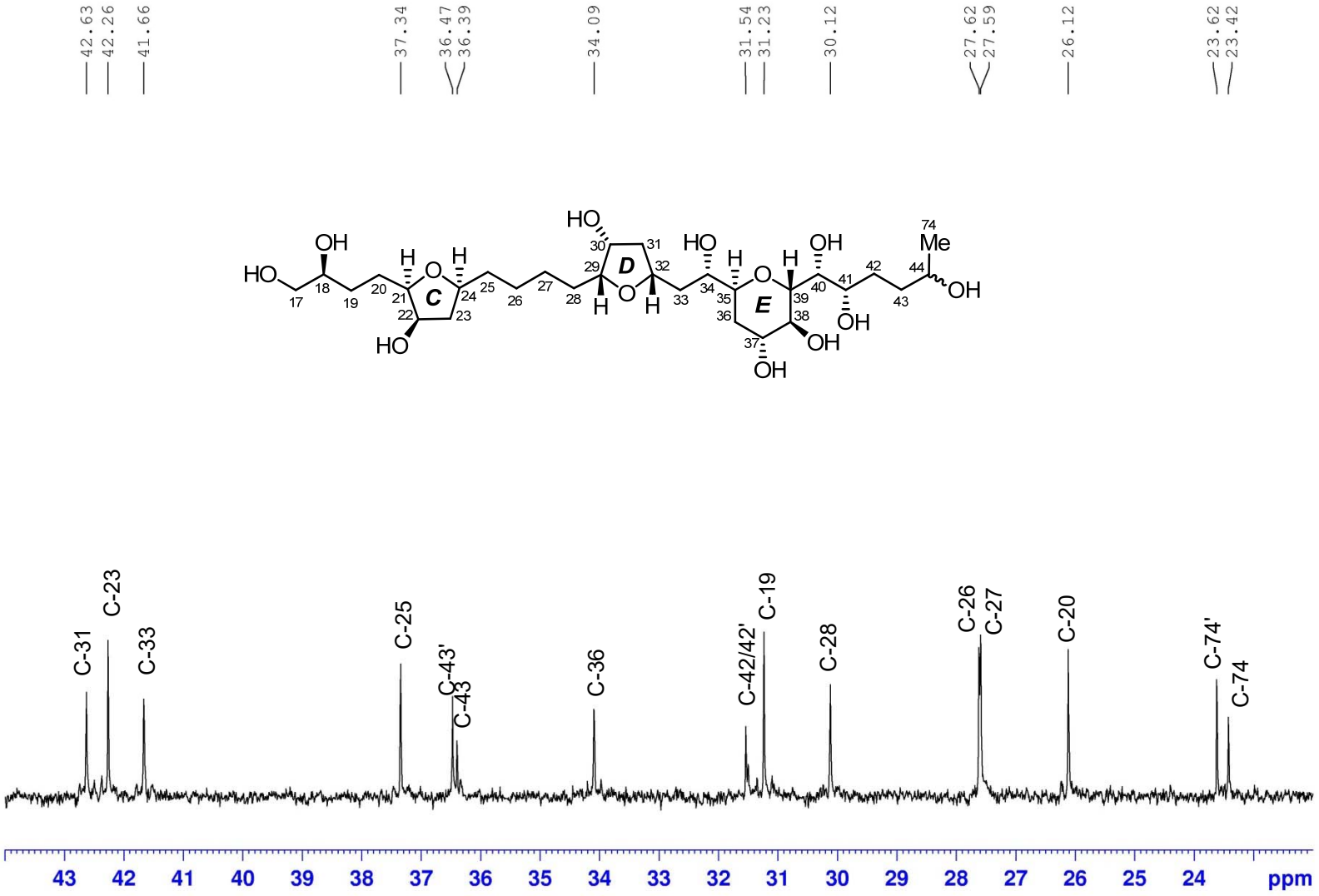

Figure S104. ^{13}C (150 MHz) NMR spectrum of the fragment **1b** in CD_3OD

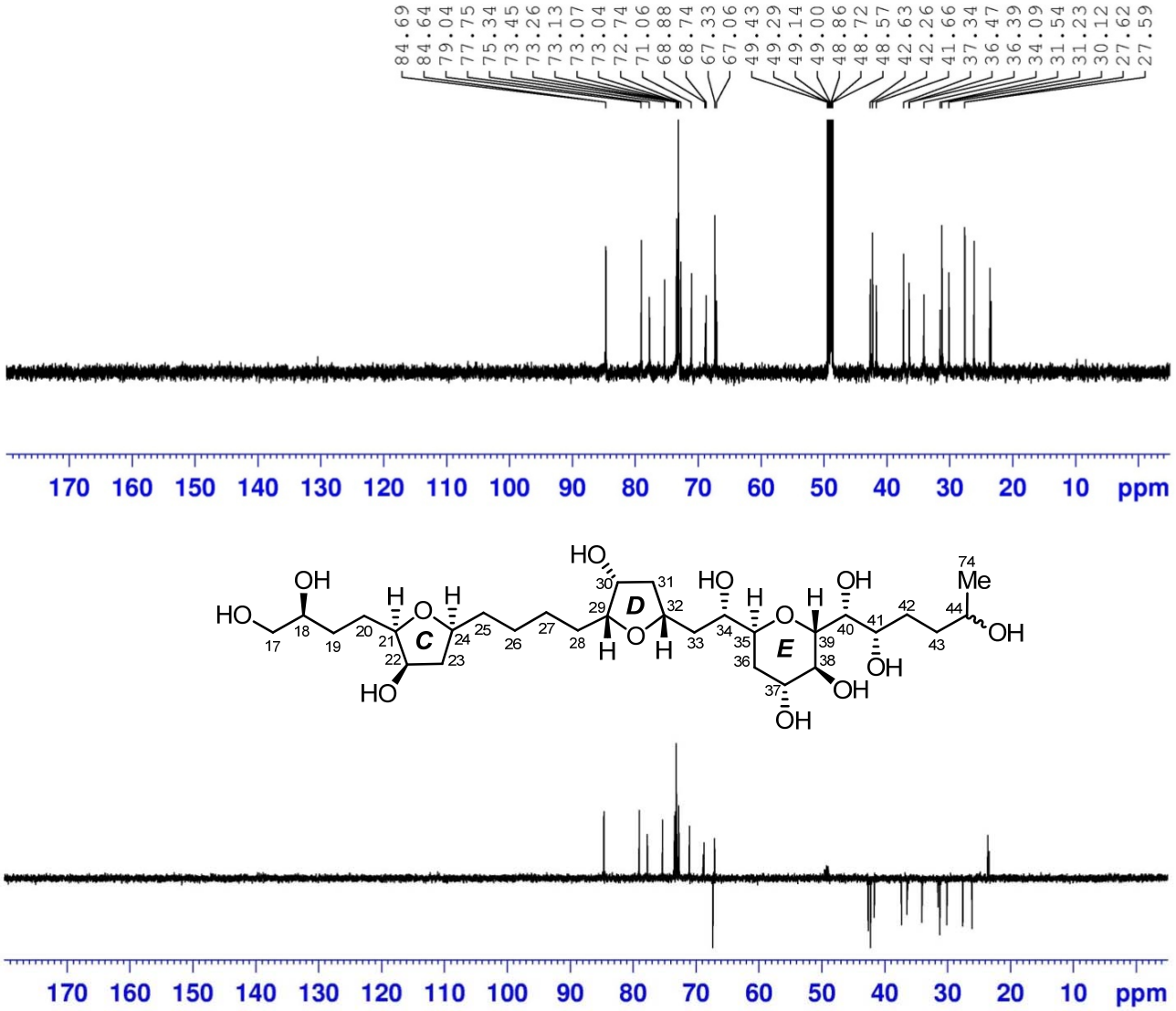

Figure S105. DEPT 135 (150 MHz) spectrum of the fragment **1b** in CD_3OD

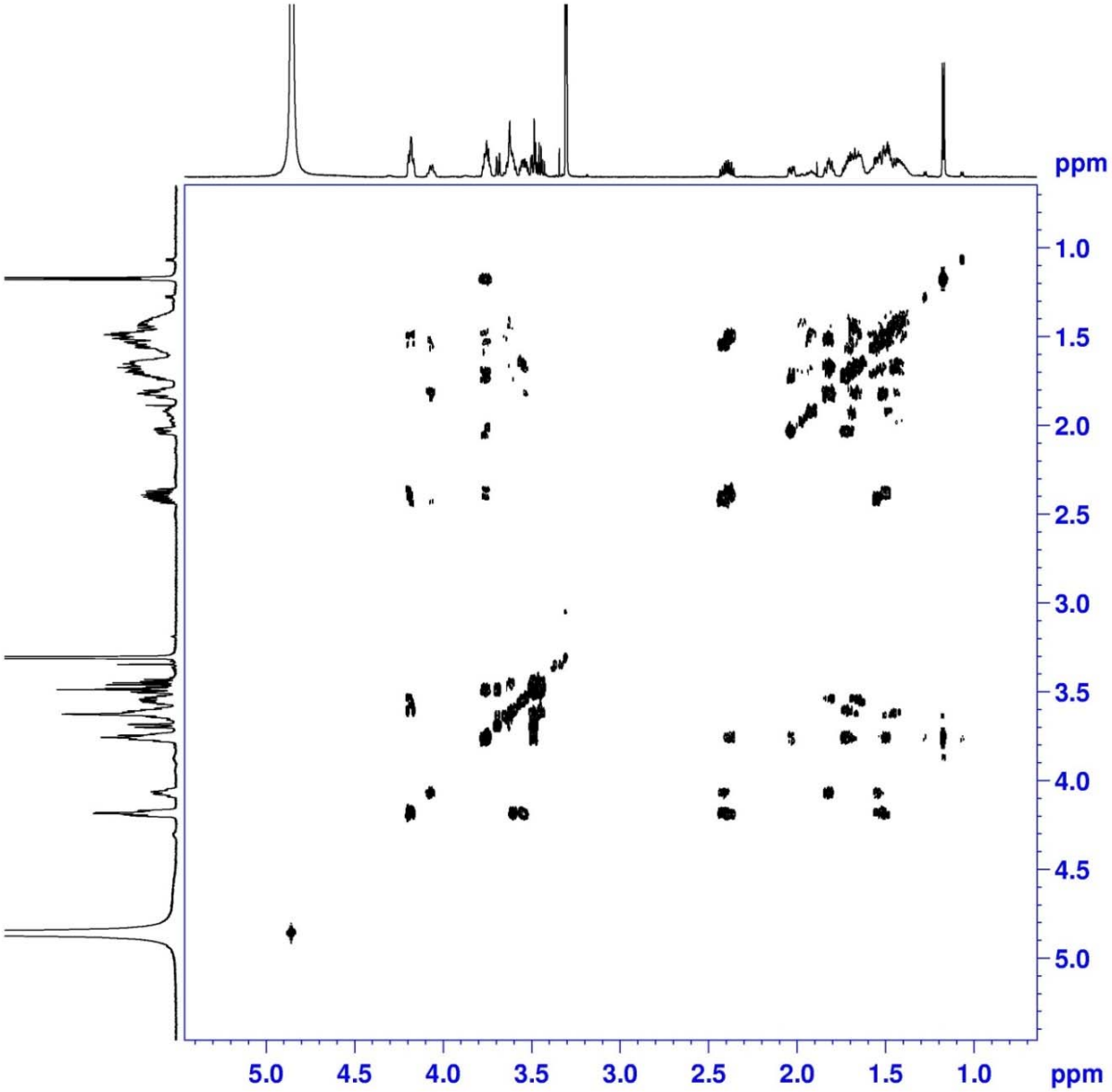

Figure S106. $^{1}H–^{1}H$ COSY (600 MHz) spectrum of the fragment **1b** in CD_3OD

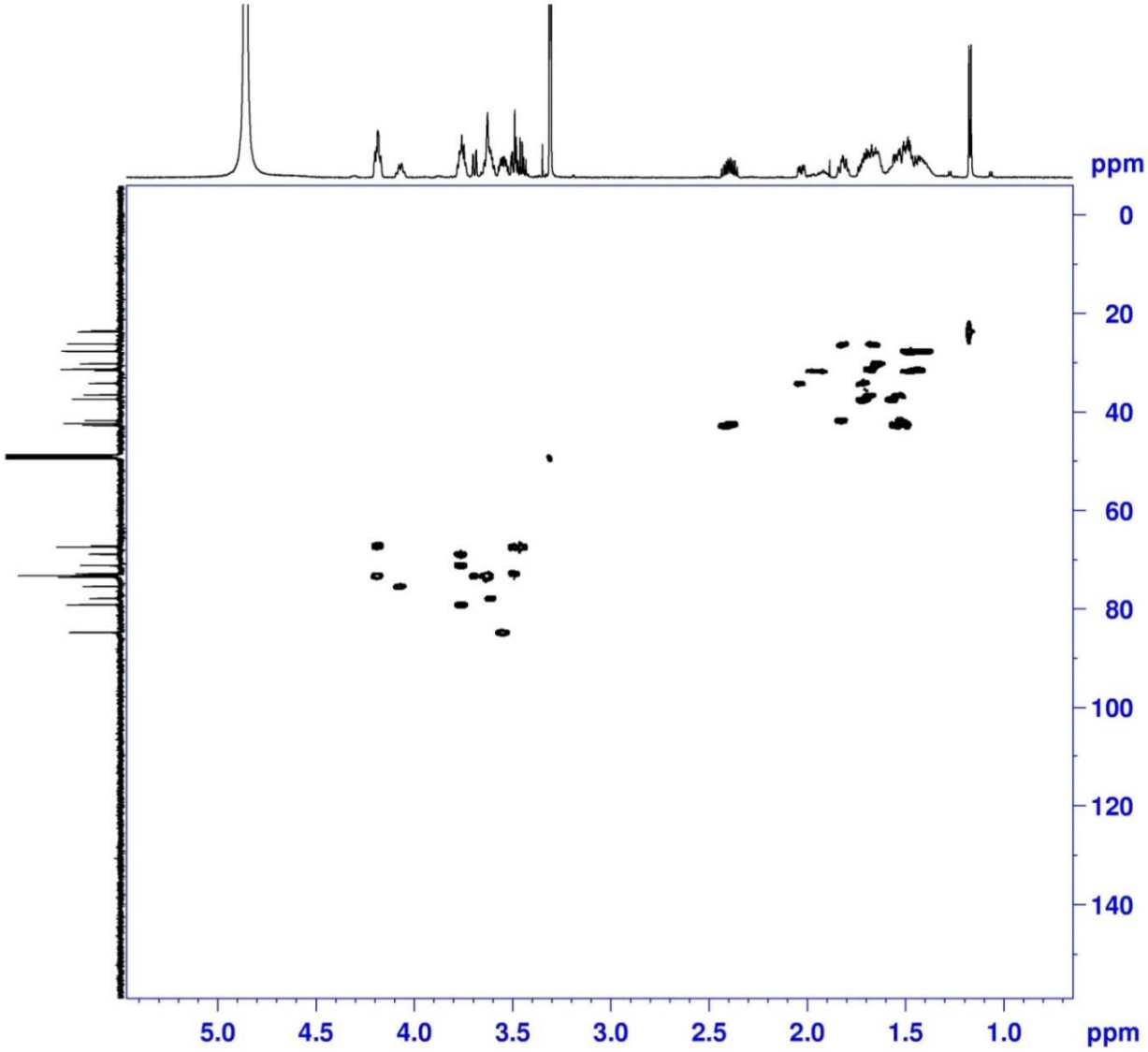

Figure S107. HSQC (600 MHz) spectrum of the fragment **1b** in CD_3OD

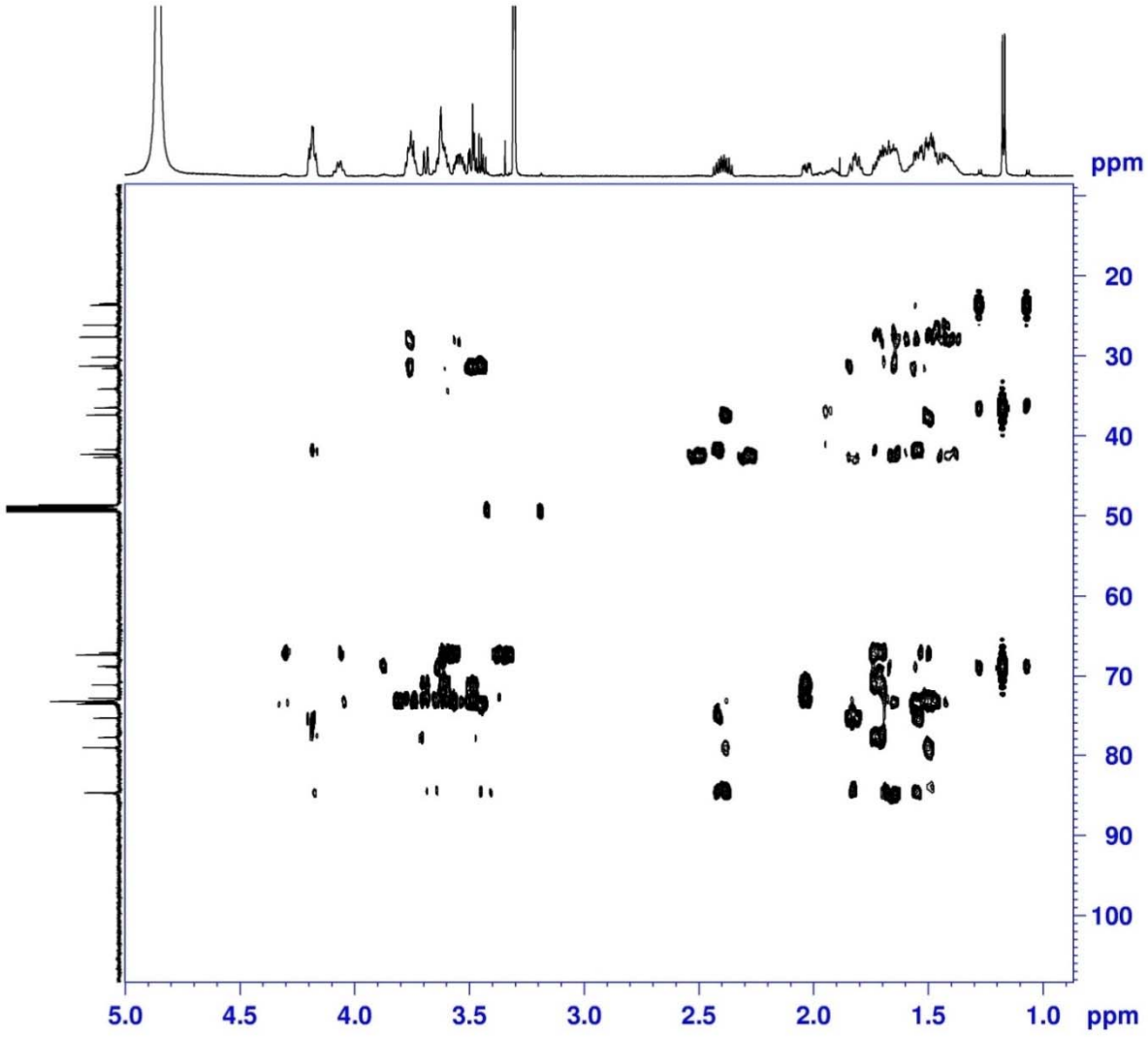

Figure S108. HMBC (600 MHz) spectrum of the fragment **1b** in CD_3OD

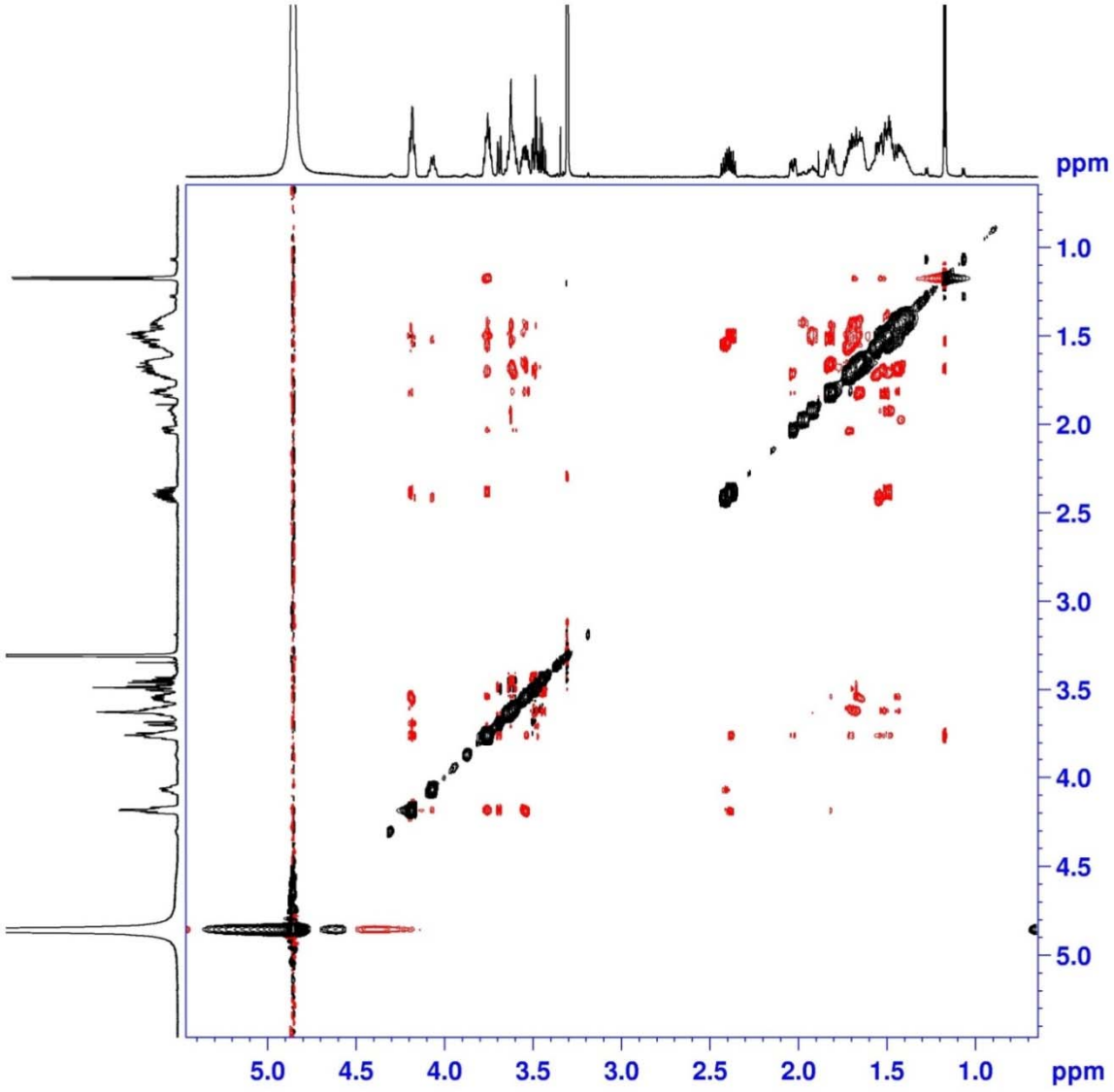

Figure S109. NOESY (600 MHz) spectrum of the fragment **1b** in CD_3OD

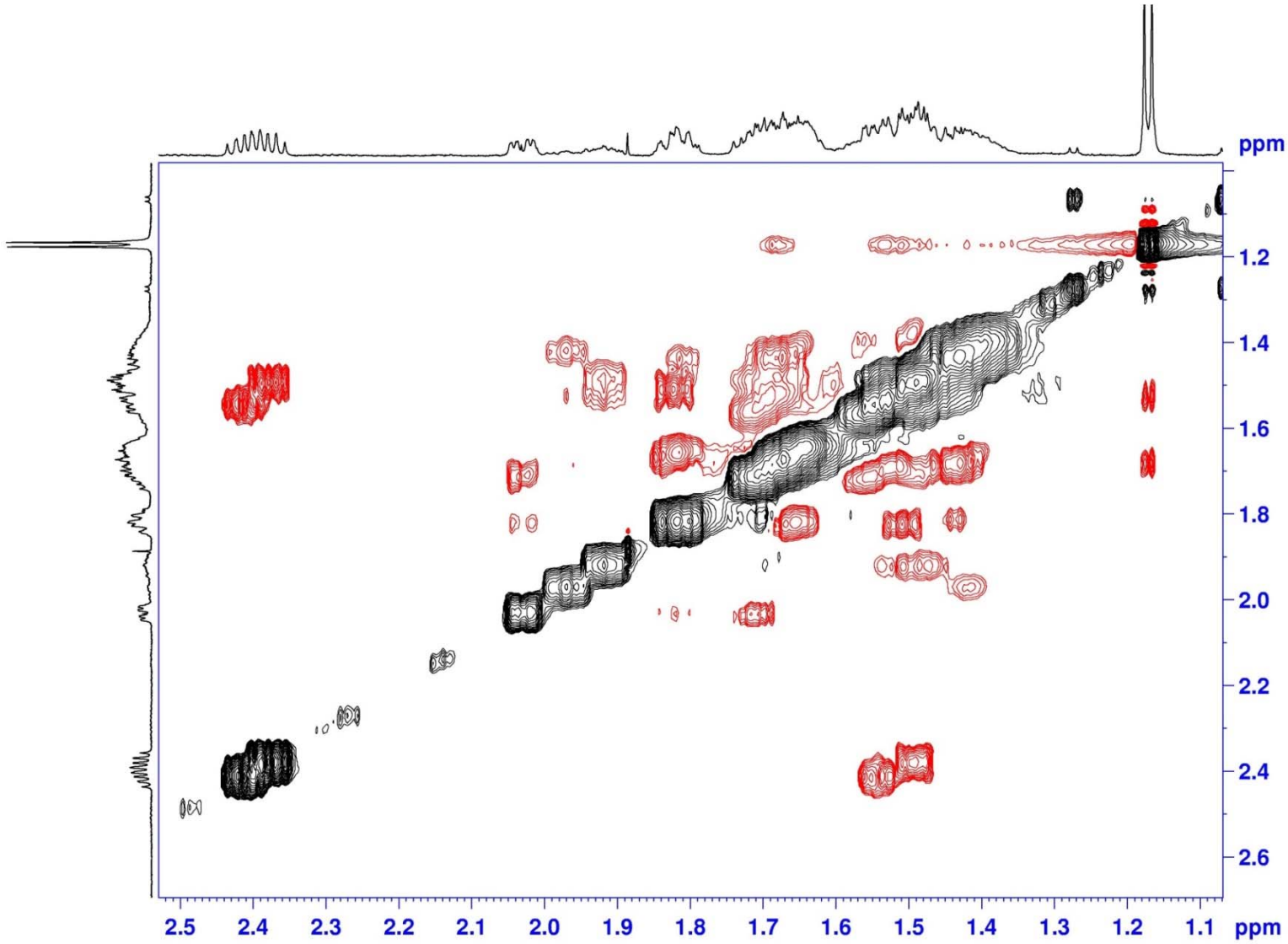

Figure S110. NOESY (600 MHz) spectrum of the fragment **1b** in CD_3OD

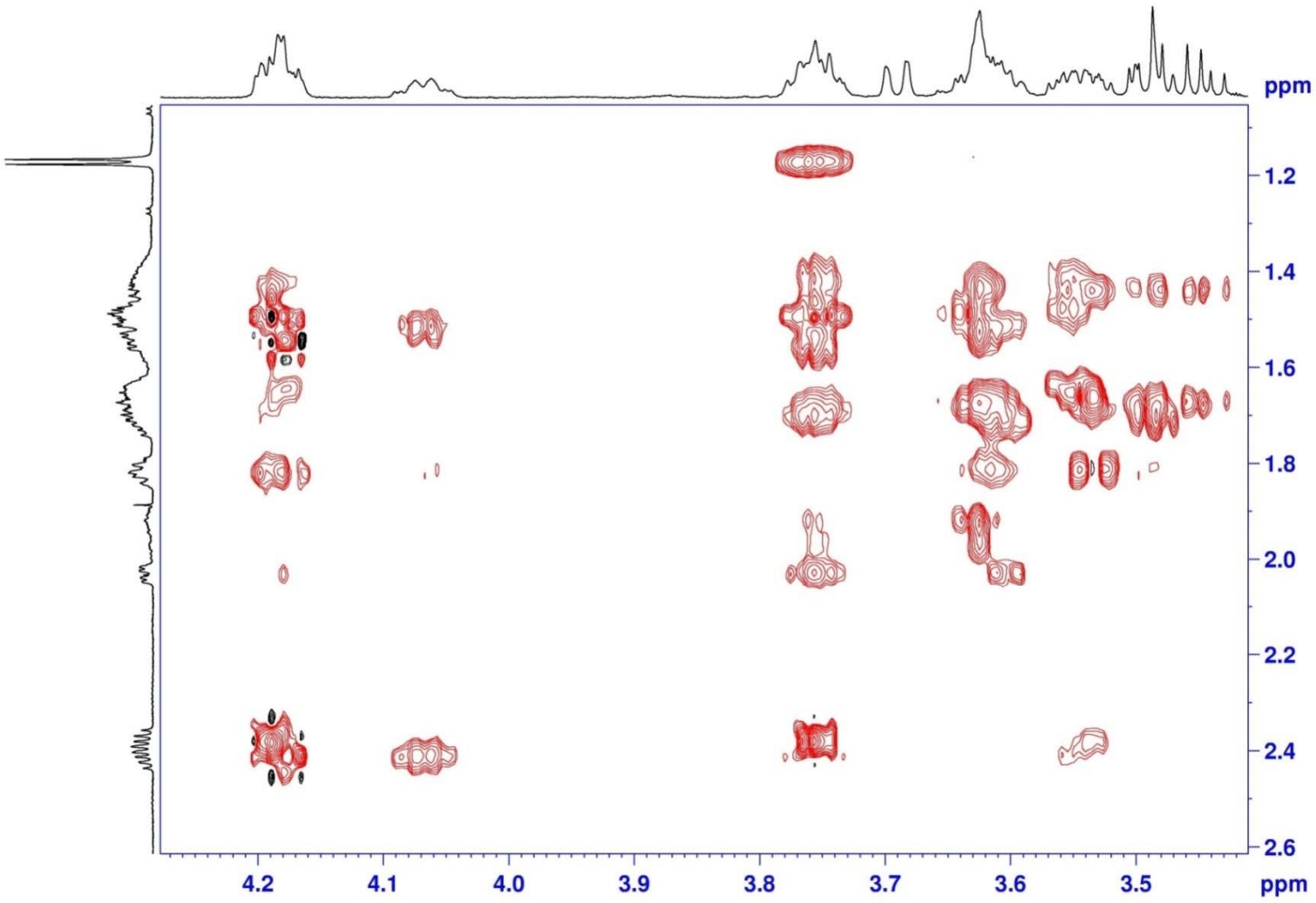

Figure S111. NOESY (600 MHz) spectrum of the fragment **1b** in CD_3OD

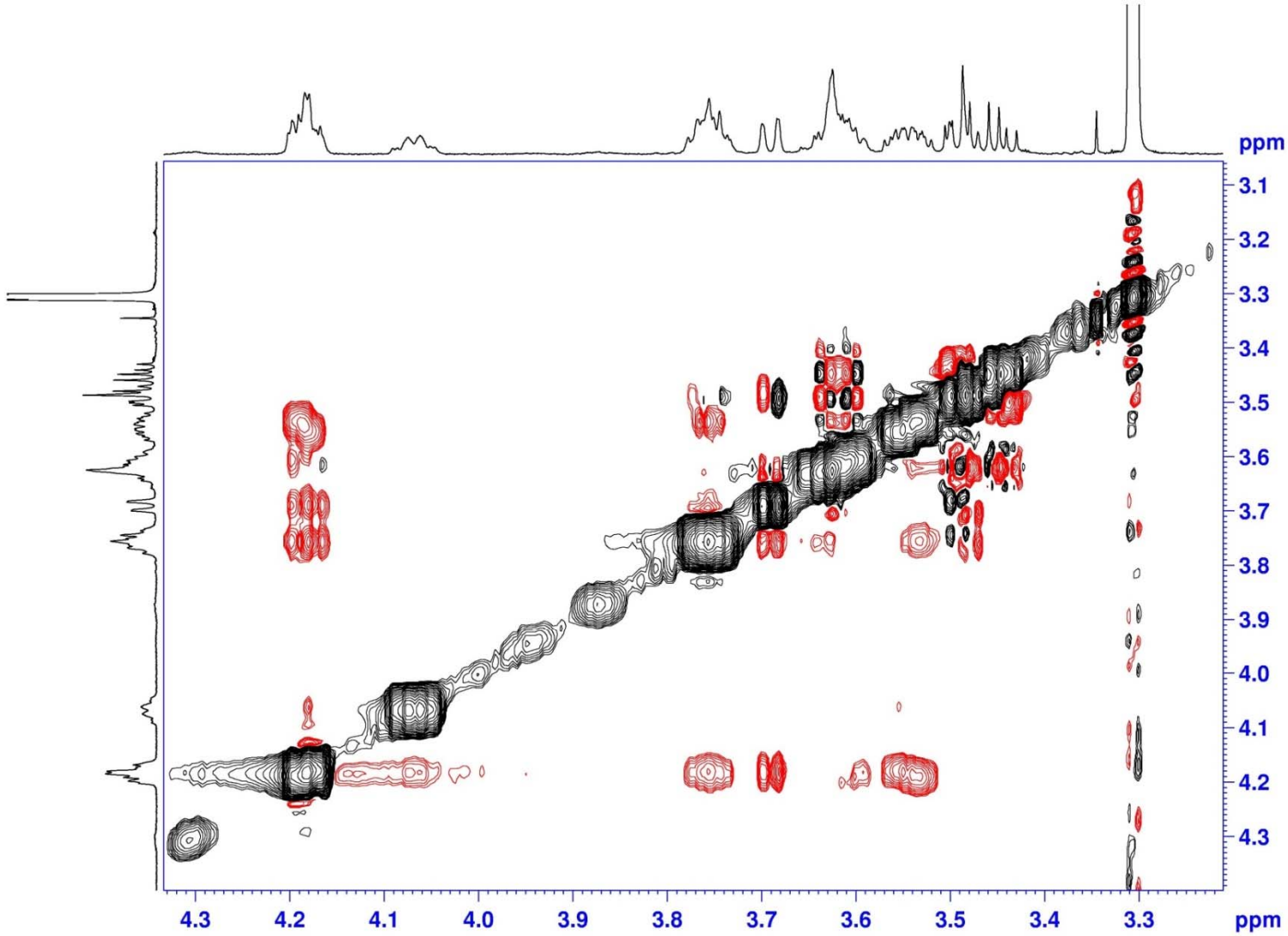

Figure S112. NOESY (600 MHz) spectrum of the fragment **1b** in CD_3OD

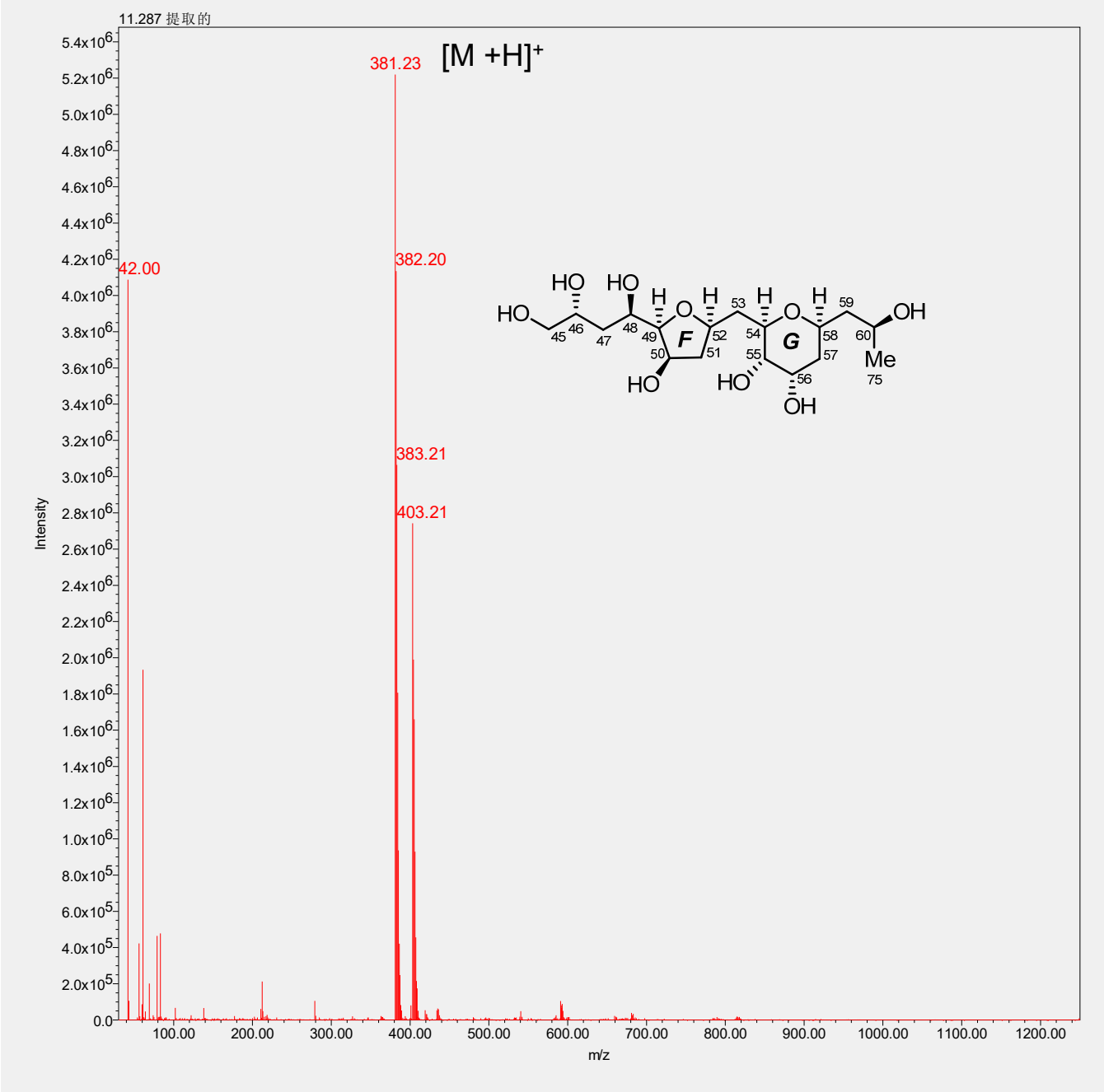

Figure S113. LR-ESIMS for the fragment **1c**

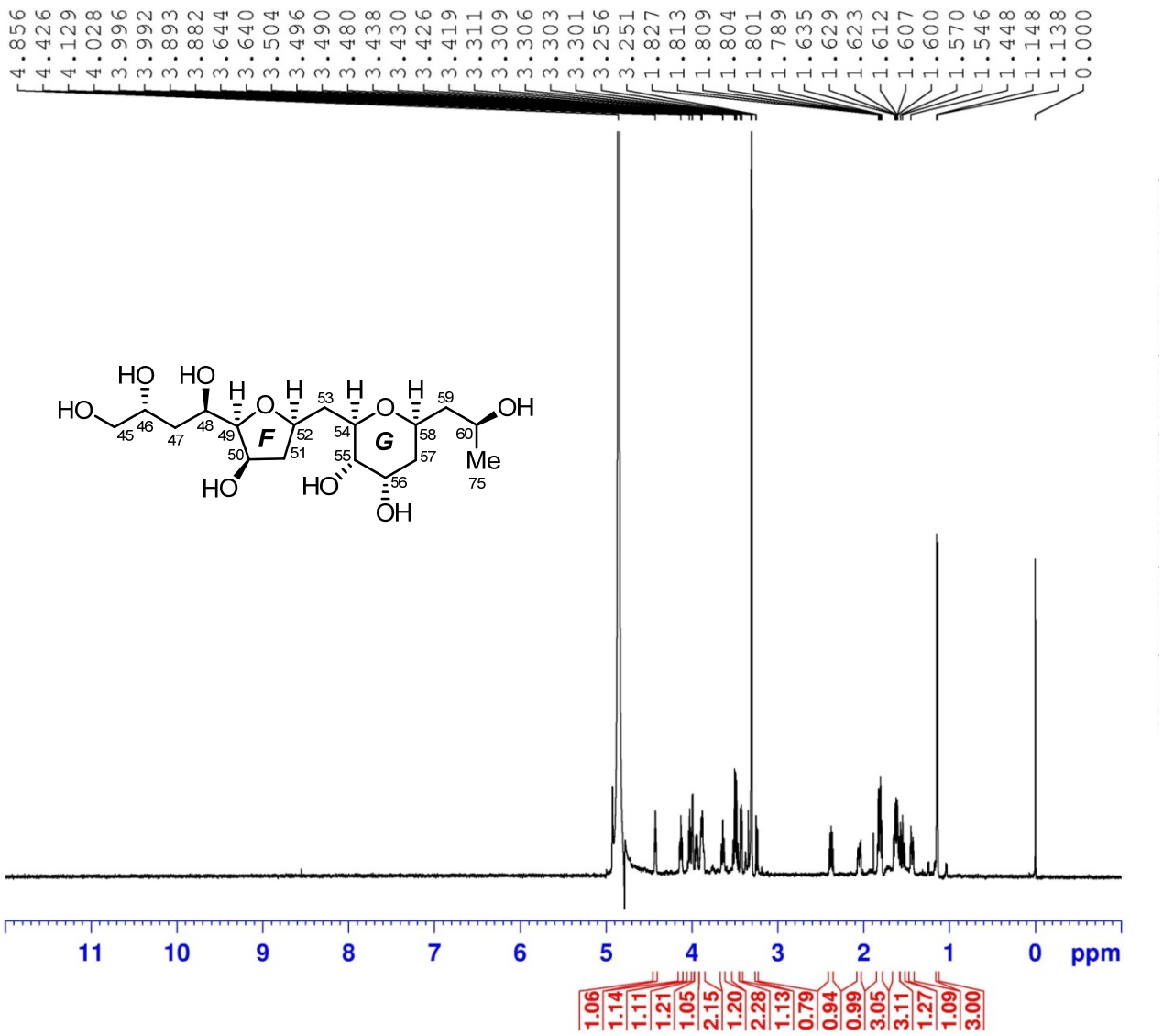

Figure S114. ^{1}H (600 MHz) NMR spectrum of the fragment **1c** in CD_3OD

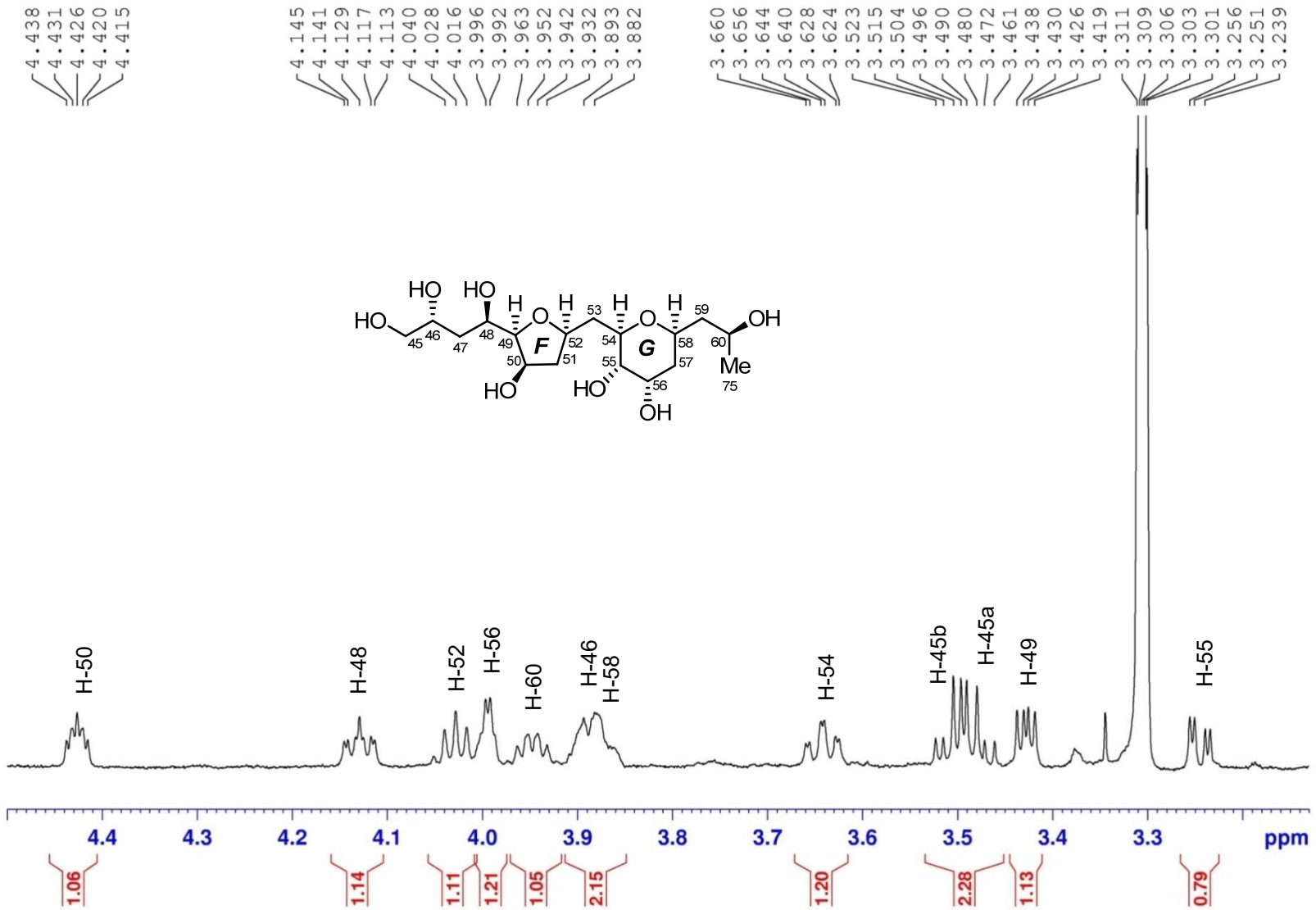

Figure S115. ^{1}H (600 MHz) NMR spectrum of the fragment **1c** in CD_3OD

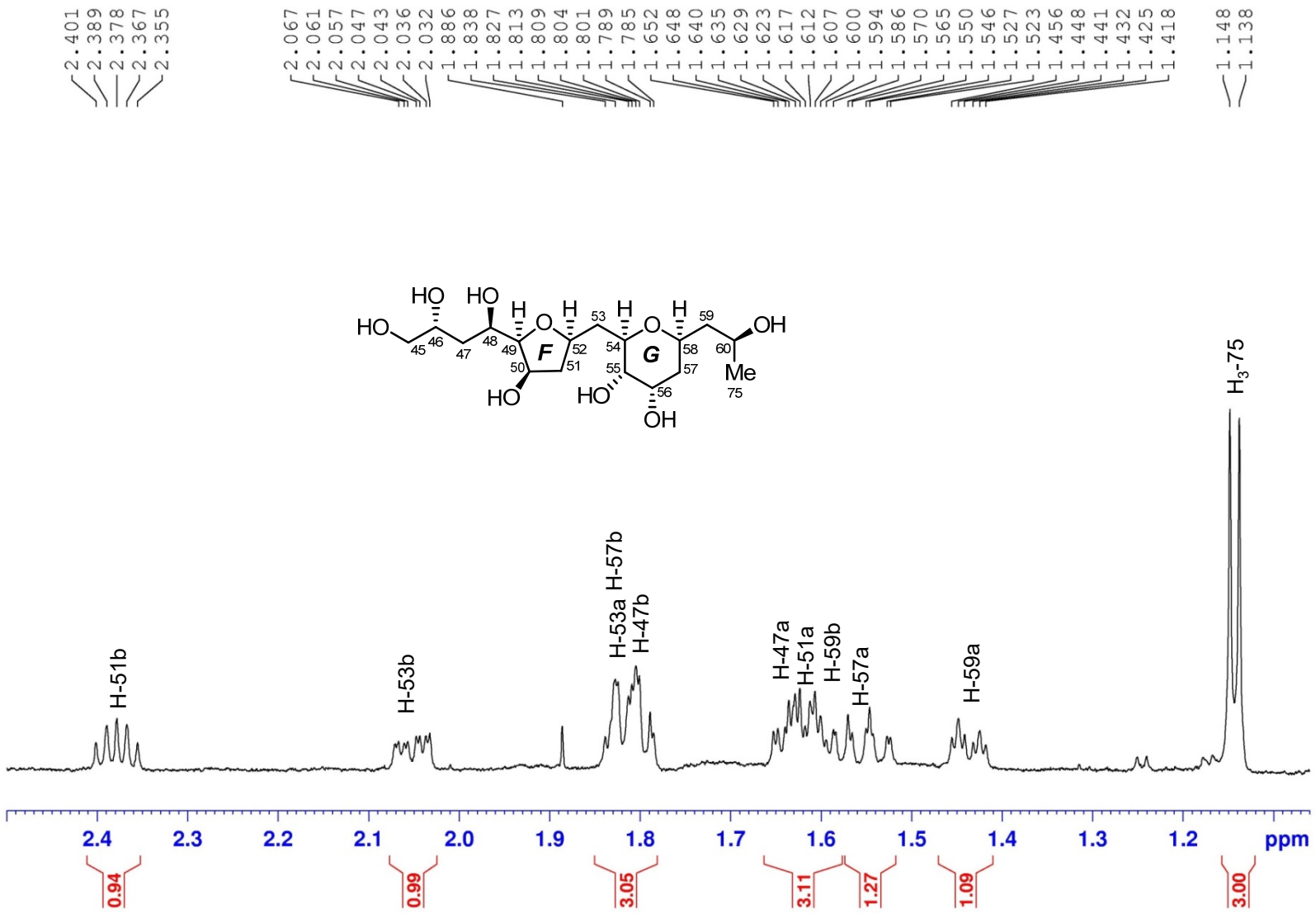

Figure S116. ^{1}H (600 MHz) NMR spectrum of the fragment **1c** in CD_3OD

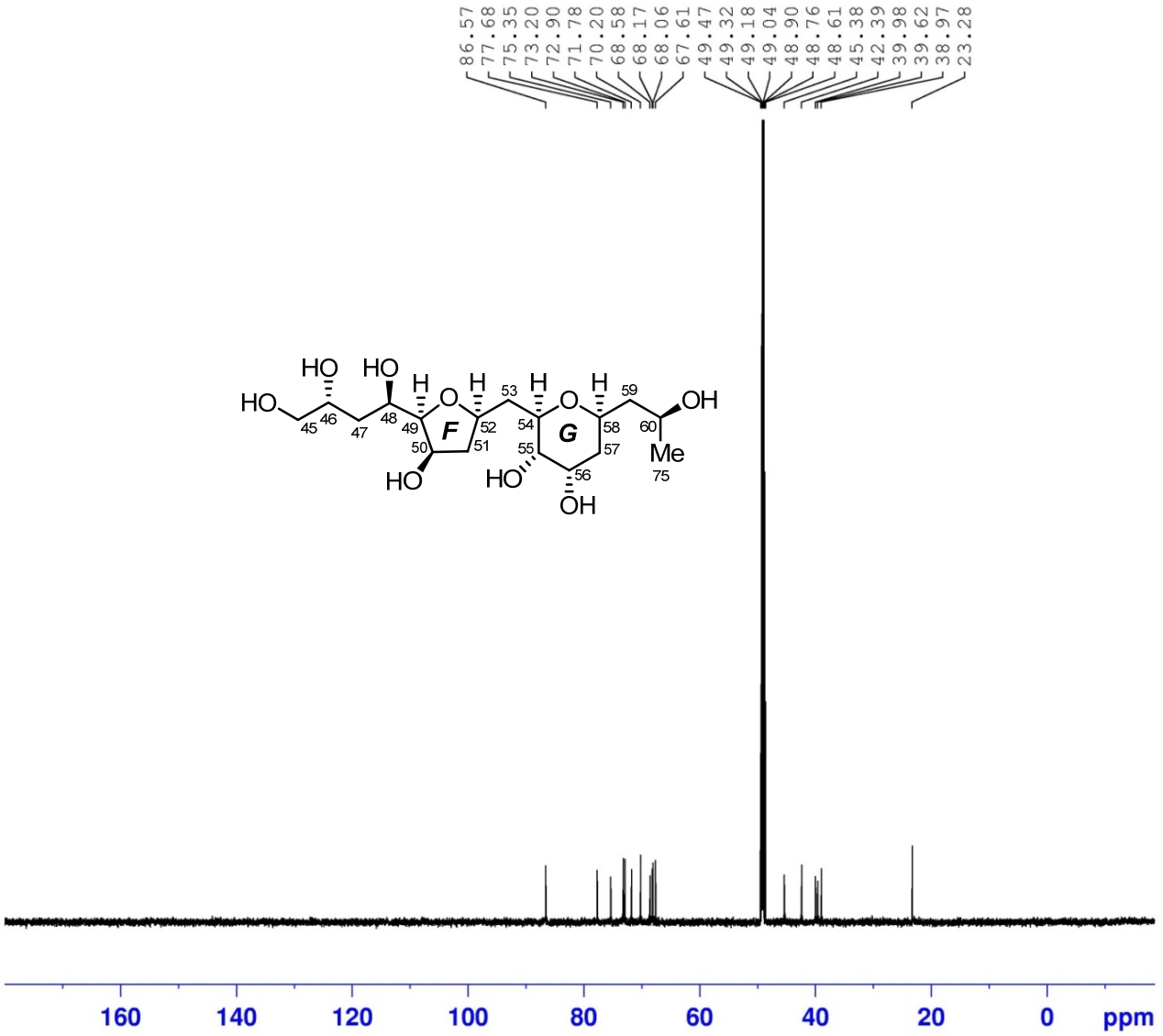

Figure S117. ^{13}C (150 MHz) NMR spectrum of the fragment **1c** in CD_3OD

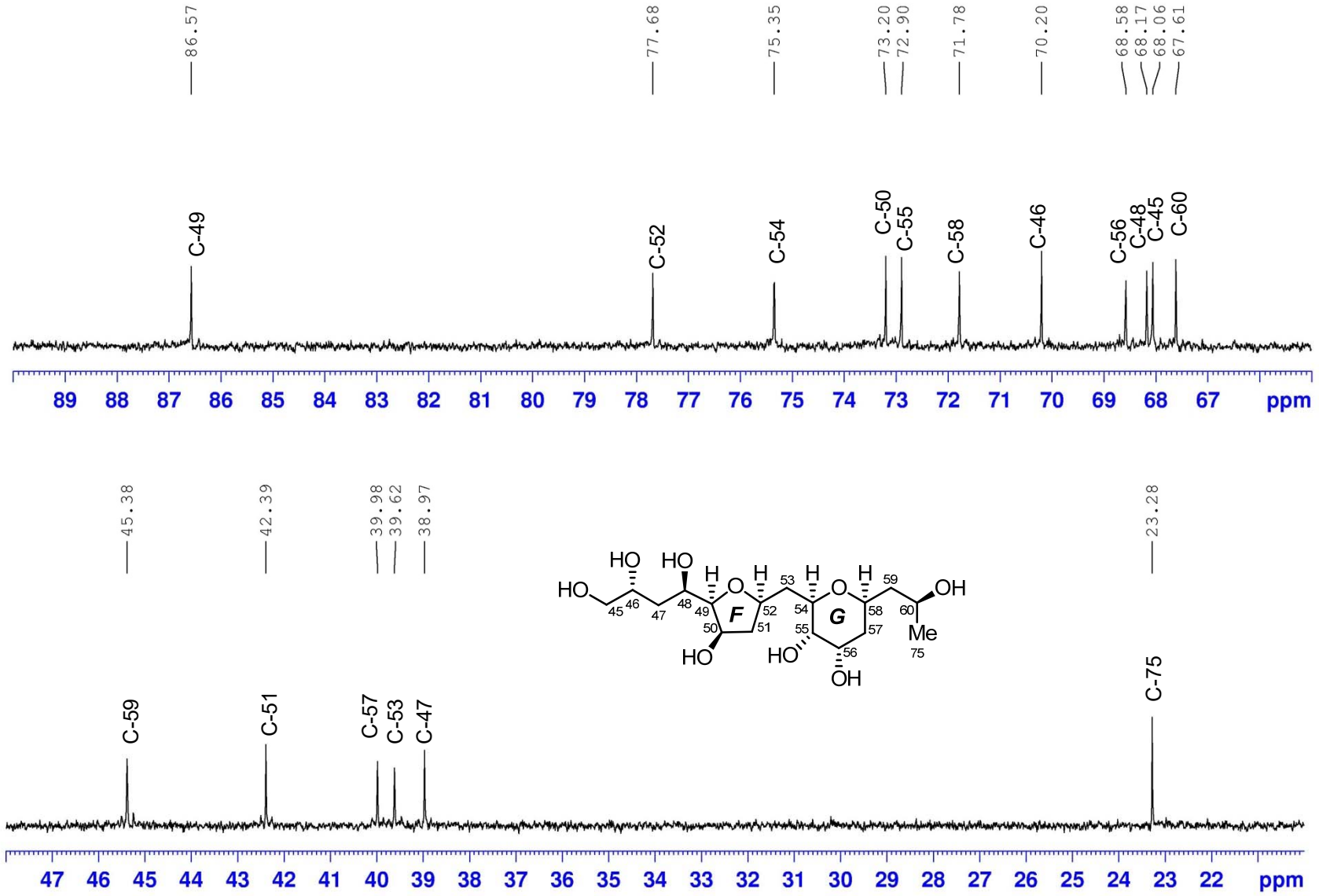

Figure S118. ^{13}C (150 MHz) NMR spectrum of the fragment **1c** in CD_3OD

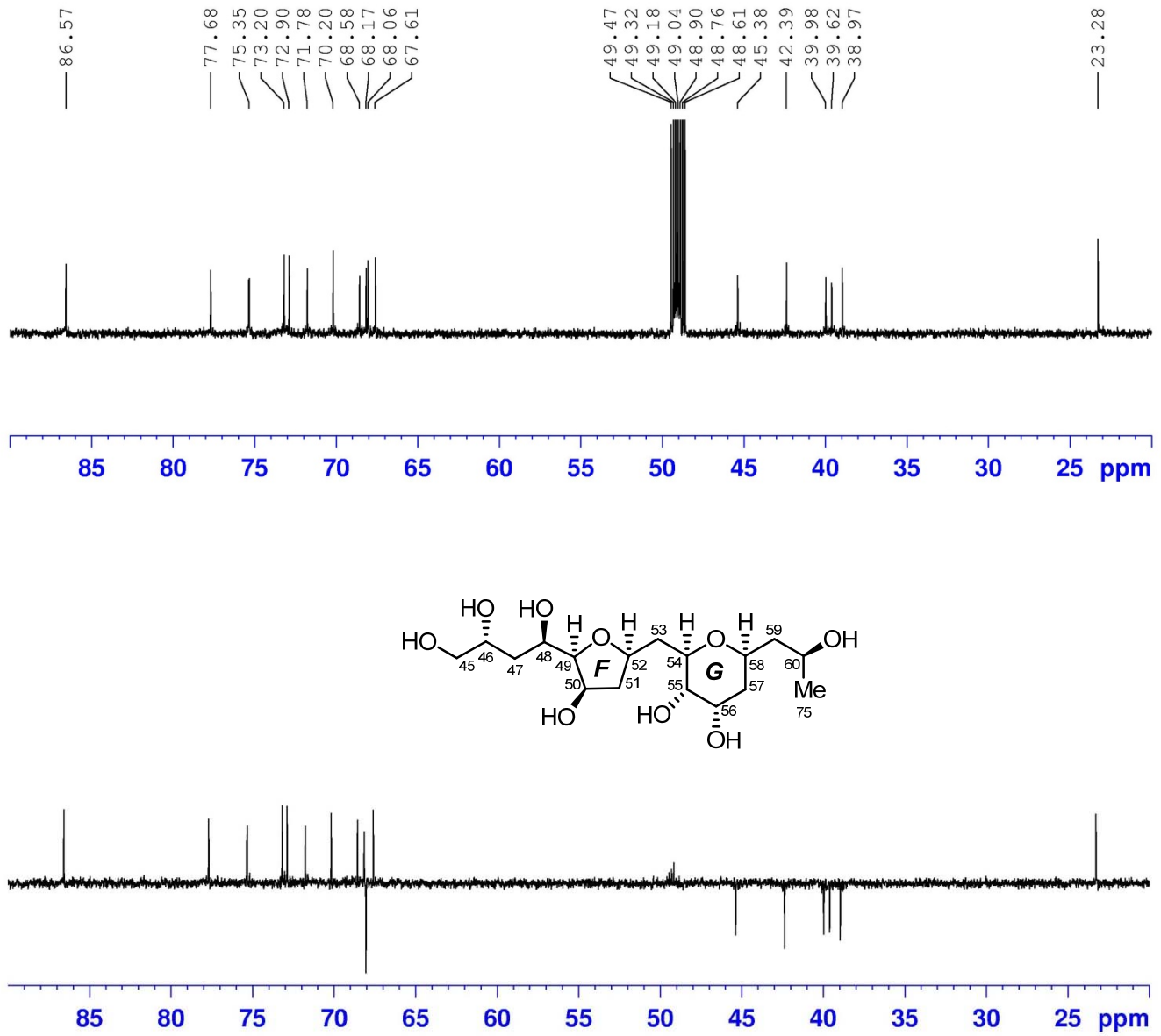

Figure S119. DEPT 135 (150 MHz) spectrum of the fragment **1c** in CD_3OD

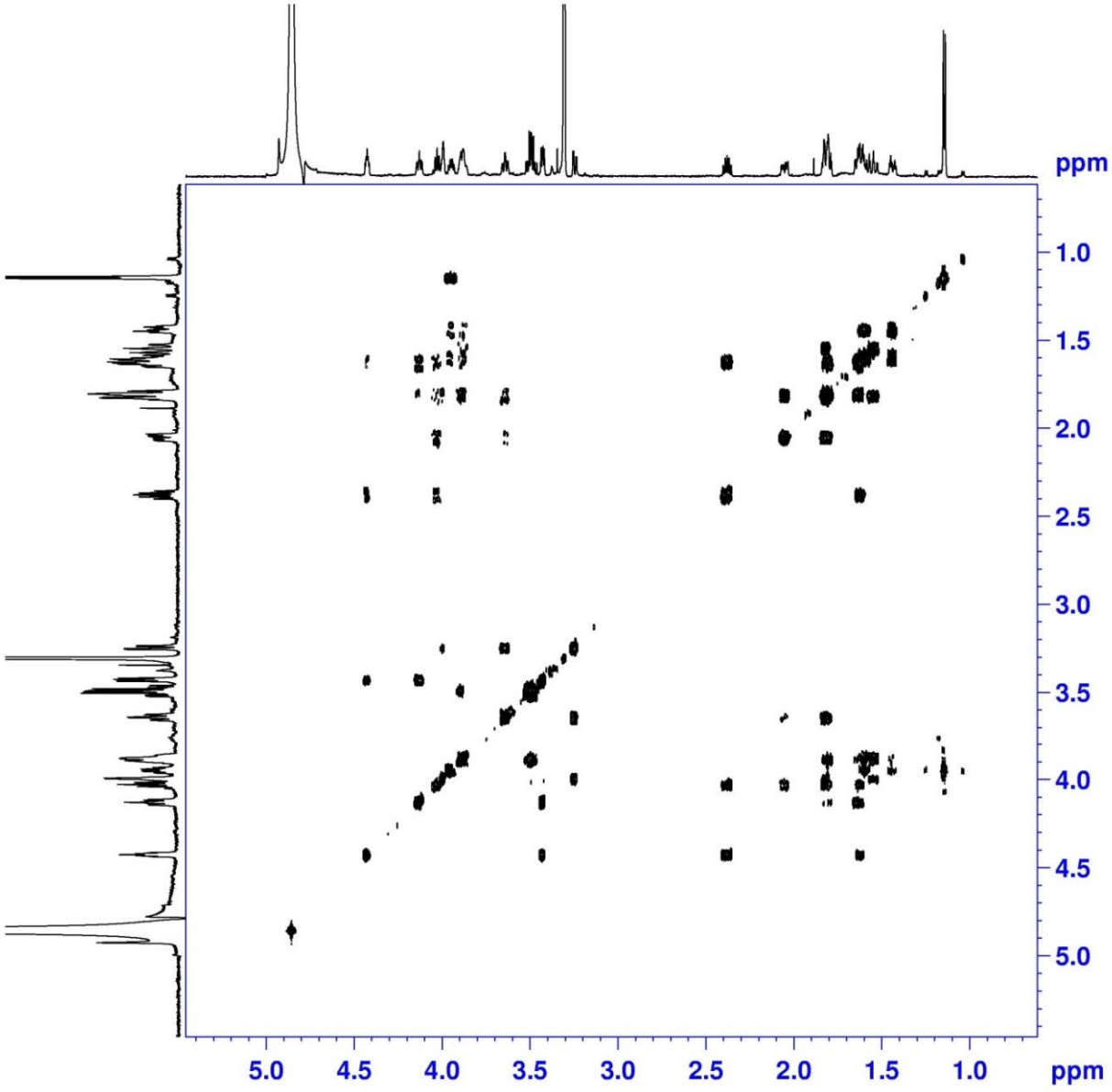

Figure S120. $^{1}H–^{1}H$ COSY (600 MHz) spectrum of the fragment **1c** in CD_3OD

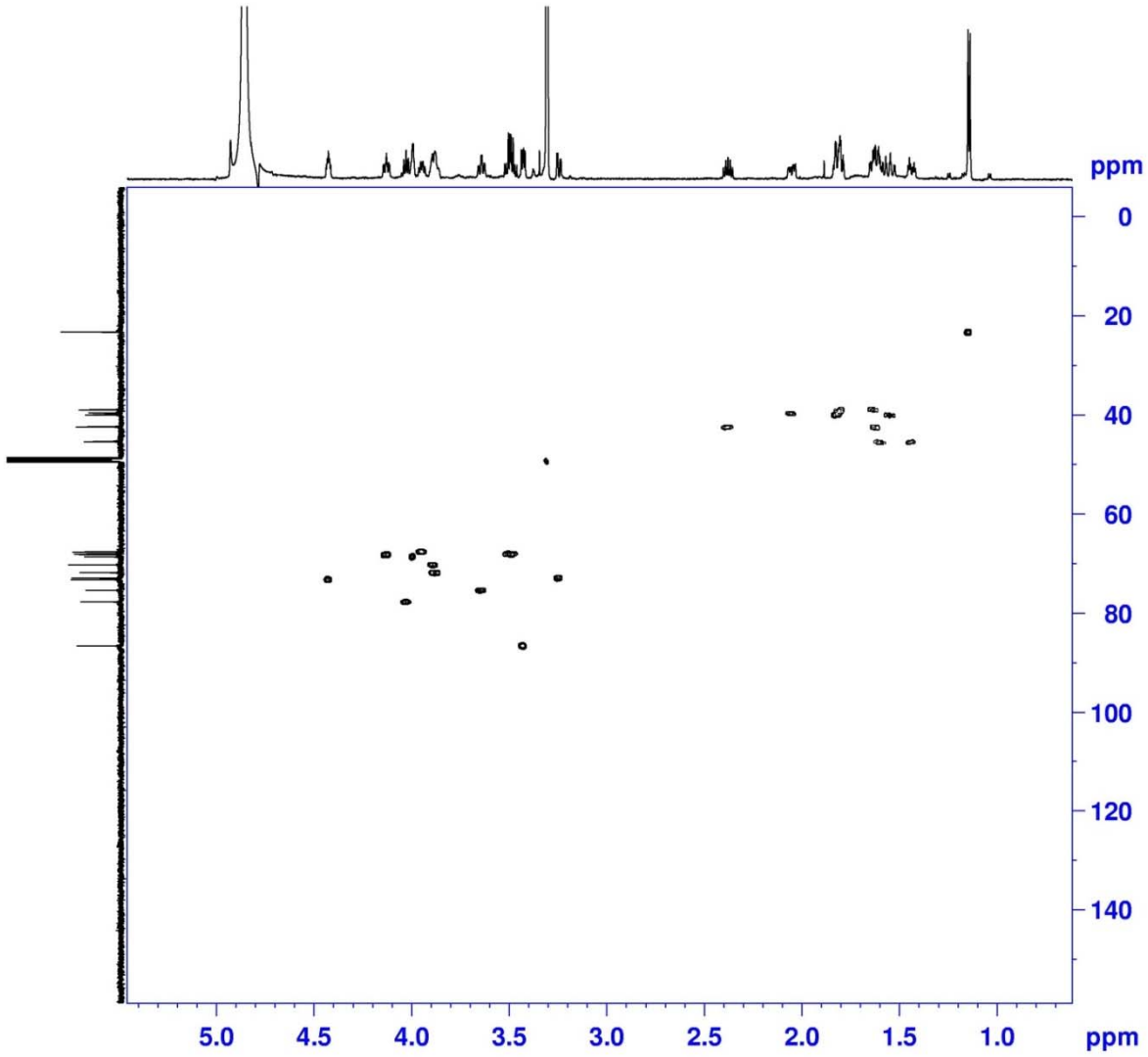

Figure S121. HSQC (600 MHz) spectrum of the fragment **1c** in CD_3OD

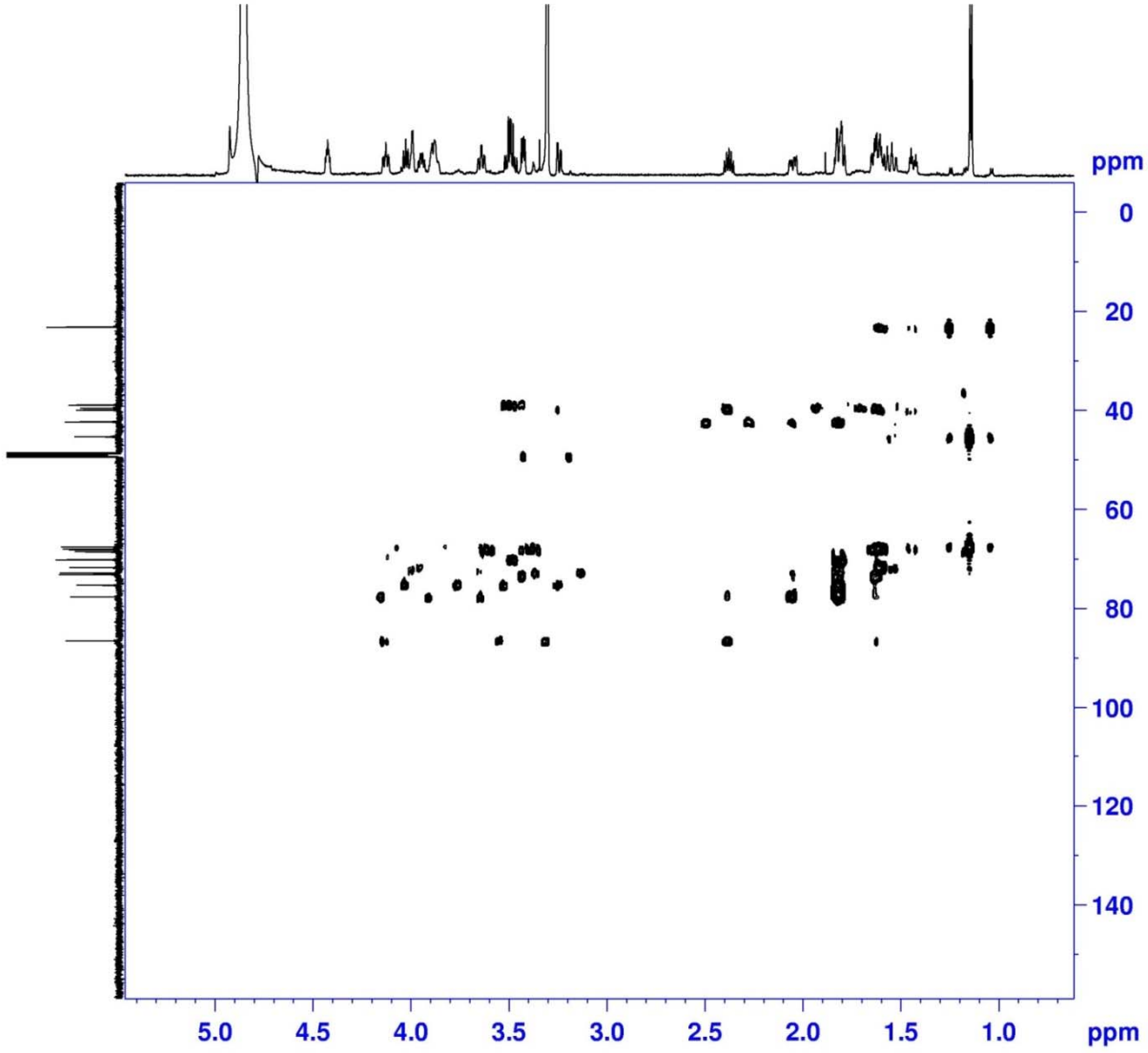

Figure S122. HMBC (600 MHz) spectrum of the fragment **1c** in CD_3OD

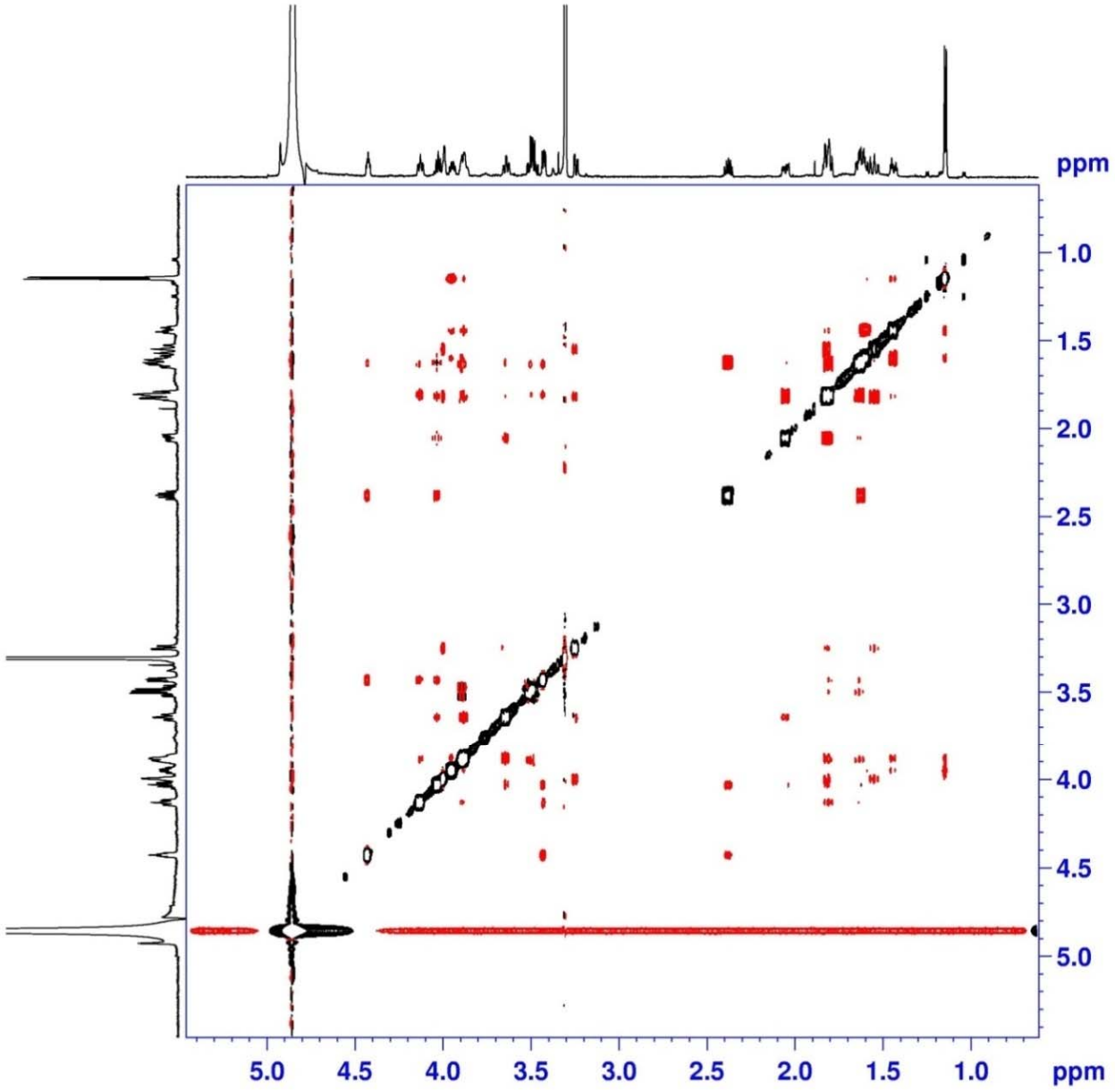

Figure S123. NOESY (600 MHz) spectrum of the fragment **1c** in CD_3OD

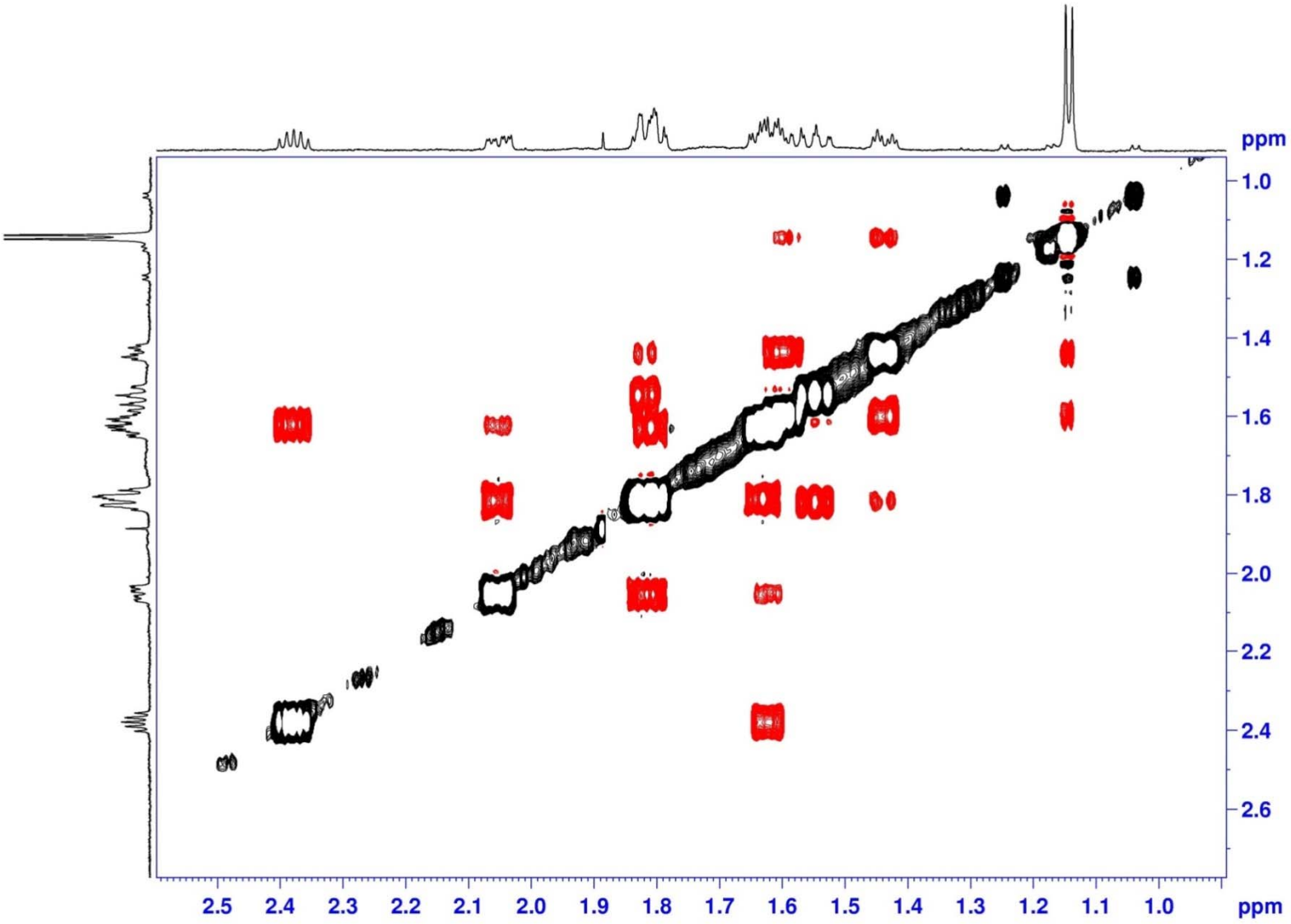

Figure S124. NOESY (600 MHz) spectrum of the fragment **1c** in CD_3OD

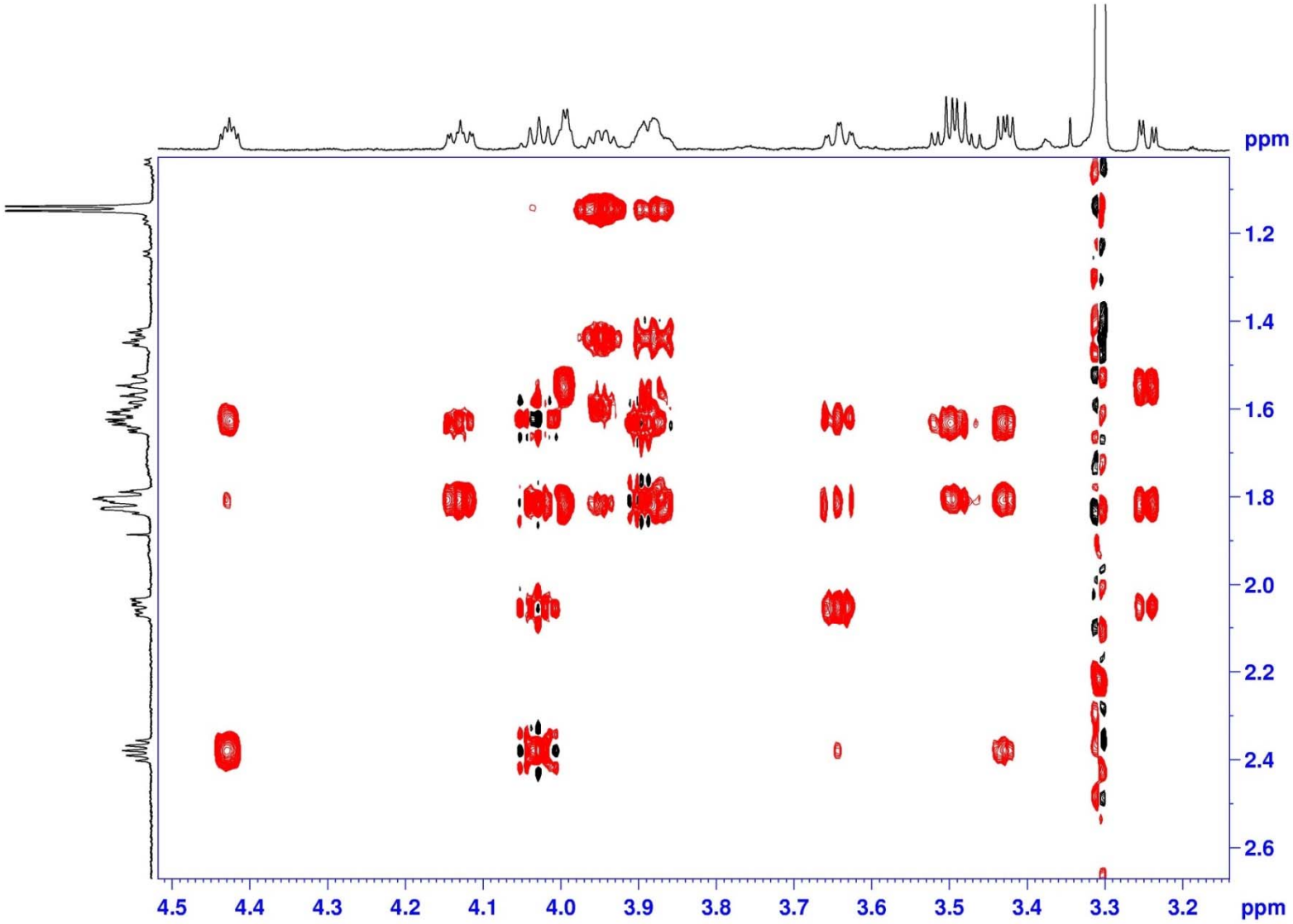

Figure S125. NOESY (600 MHz) spectrum of the fragment **1c** in CD_3OD

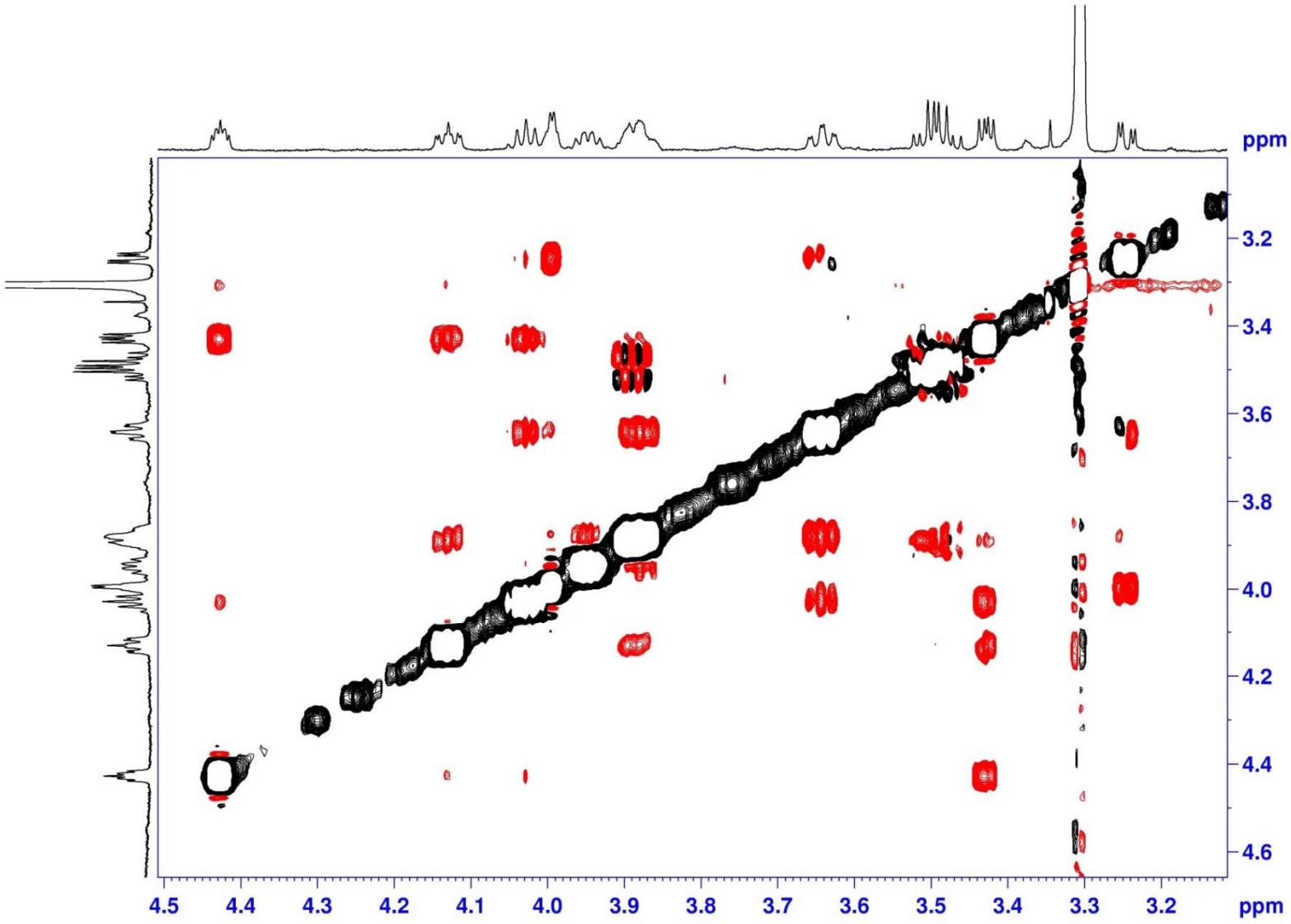

Figure S126. NOESY (600 MHz) spectrum of the fragment **1c** in CD_3OD

Mass Spectrum SmartFormula Report

Analysis Info

Analysis Name	D:\Data\MS\data\202102\yuyi_AX-1-O3-O_pos_15_01_9969.d	Acquisition Date	2/5/2021 5:02:58 PM
Method	LC_Direct Infusion_pos_70-500mz.m	Operator	SCSIO
Sample Name	yuyi_AX-1-O3-O_pos	Instrument	maXis 255552.00029
Comment			

Acquisition Parameter

Source Type	ESI	Ion Polarity	Positive	Set Nebulizer	0.4 Bar
Focus	Active	Set Capillary	4500 V	Set Dry Heater	180 °C
Scan Begin	70 m/z	Set End Plate Offset	-500 V	Set Dry Gas	4.0 l/min
Scan End	1500 m/z	Set Charging Voltage	0 V	Set Divert Valve	Waste
		Set Corona	0 nA	Set APCI Heater	0 °C

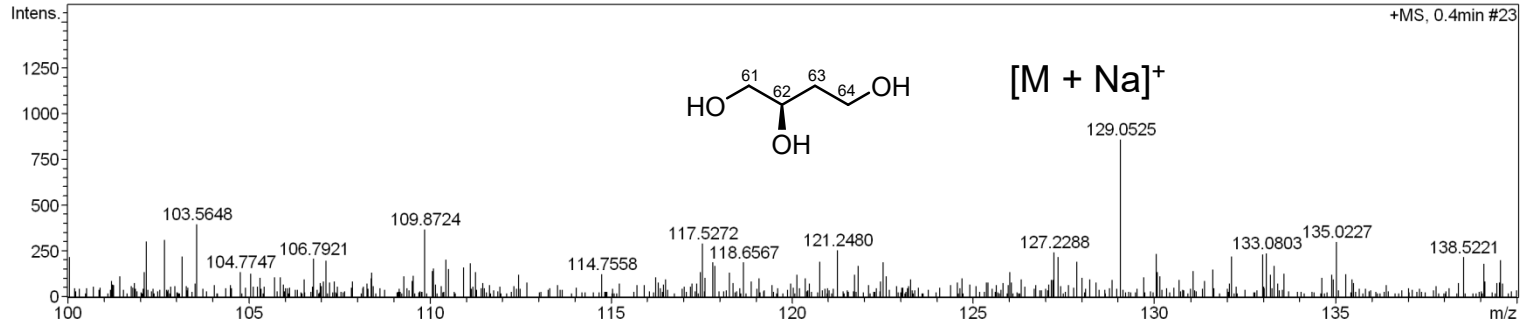

Meas. m/z	#	Ion Formula	Score	m/z	err [ppm]	err [mDa]	mSigma	rdb	e⁻ Conf	N-Rule
129.0525	1	C4H10NaO3	100.00	129.0522	-2.2	-0.3	160.7	-0.5	even	ok

yuyi_AX-1-O3-O_pos_15_01_9969.d

Bruker Compass DataAnalysis 4.1 printed: 2/5/2021 5:06:41 PM by: SCSIO Page 1 of 1

Figure S127. HR-ESIMS for the fragment **1d**

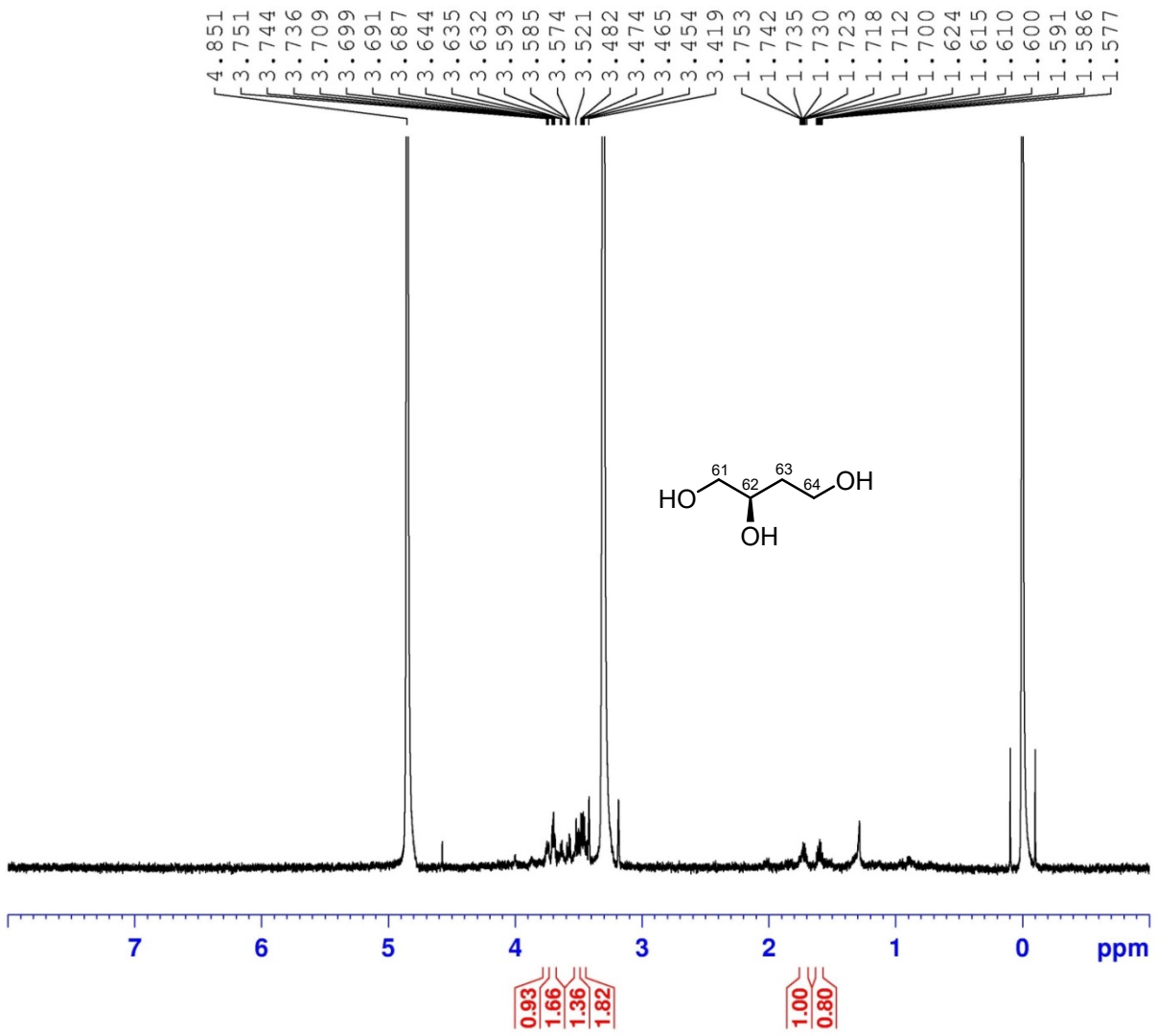

Figure S128. ^{1}H (600 MHz) NMR spectrum of the fragment **1d** in CD_3OD

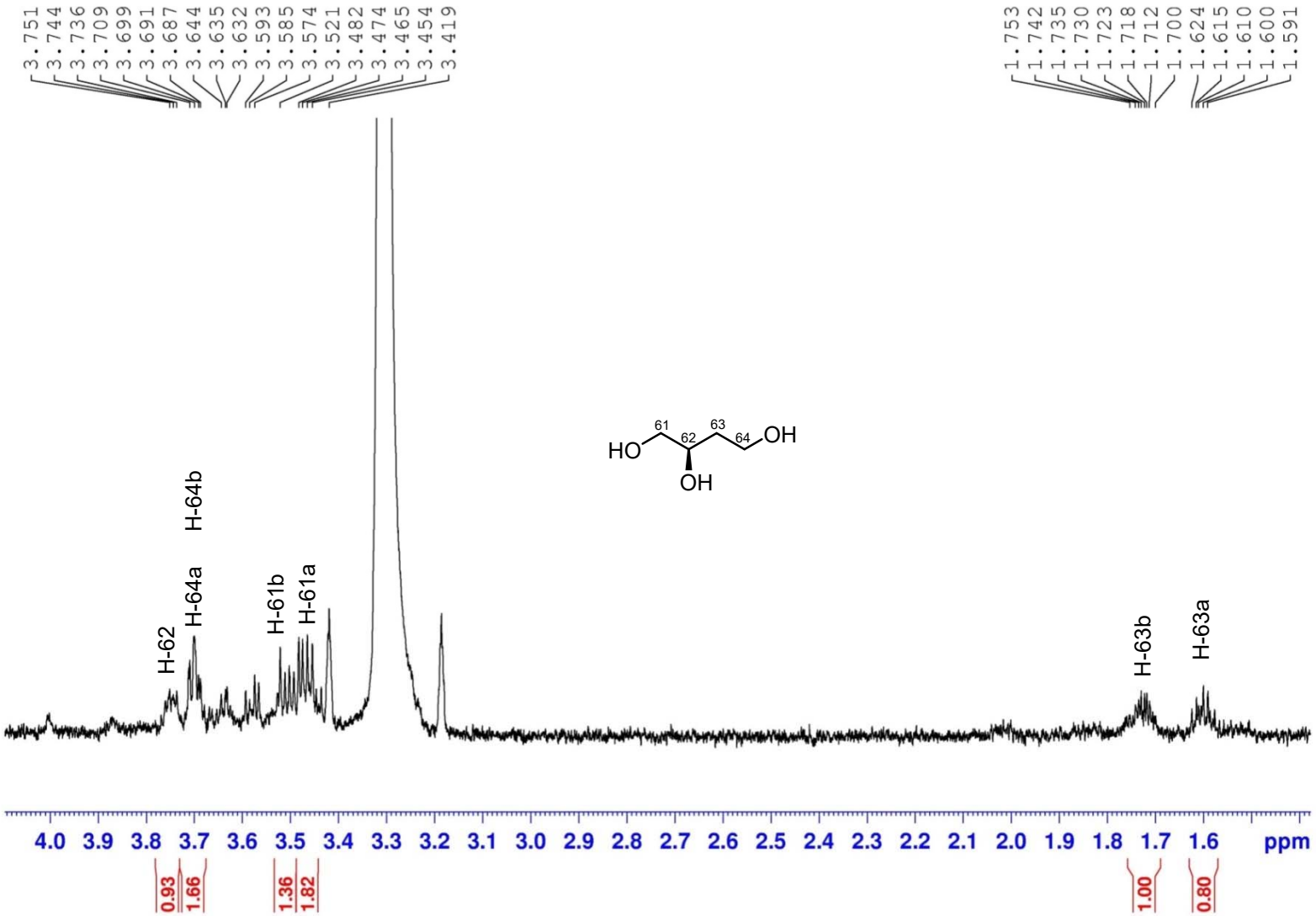

Figure S129. ^{1}H (600 MHz) NMR spectrum of the fragment **1d** in CD_3OD

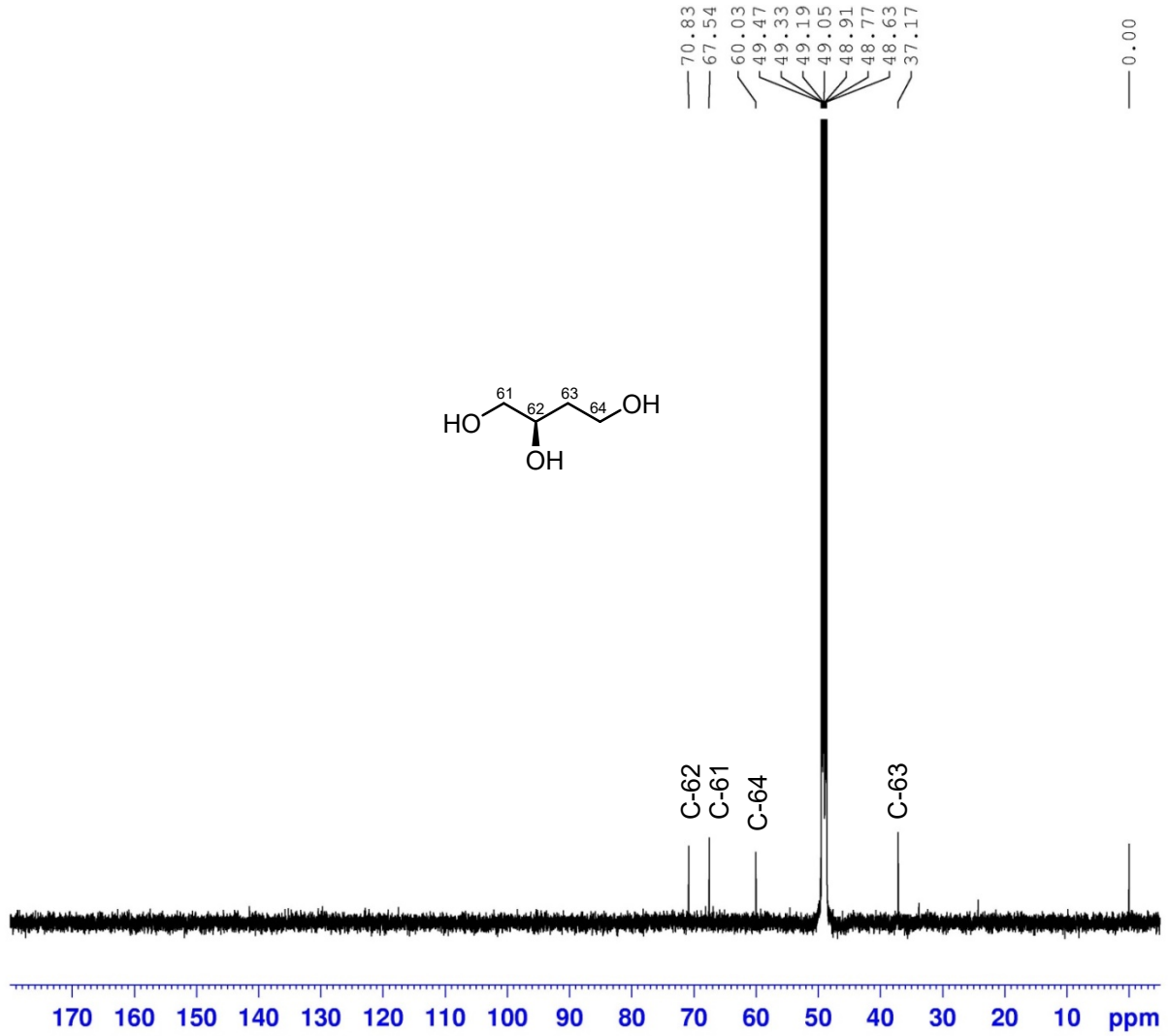

Figure S130. ^{13}C (150 MHz) NMR spectrum of the fragment **1d** in CD_3OD

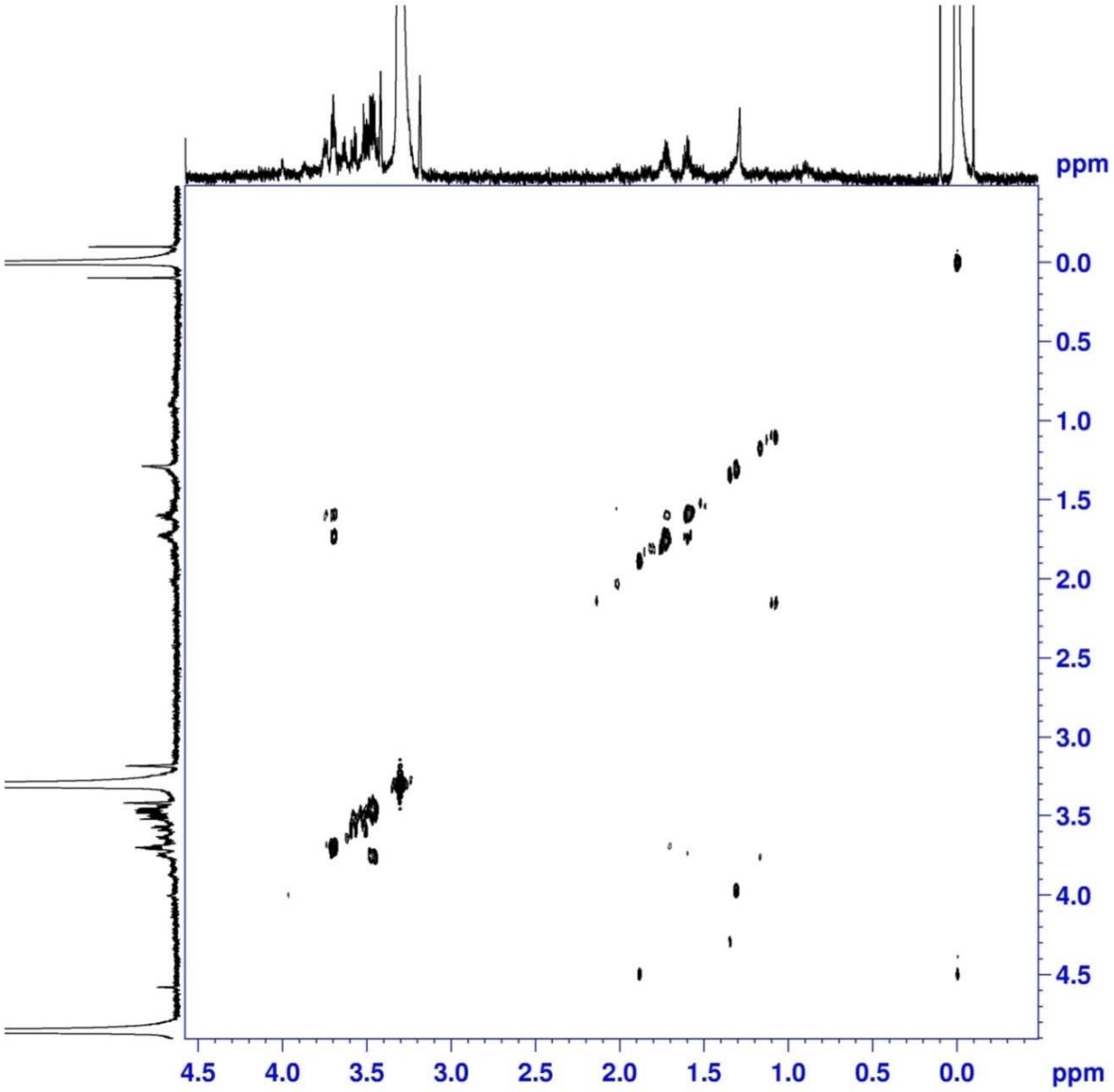

Figure S131. $^{1}H–^{1}H$ COSY (600 MHz) spectrum of the fragment **1d** in CD_3OD

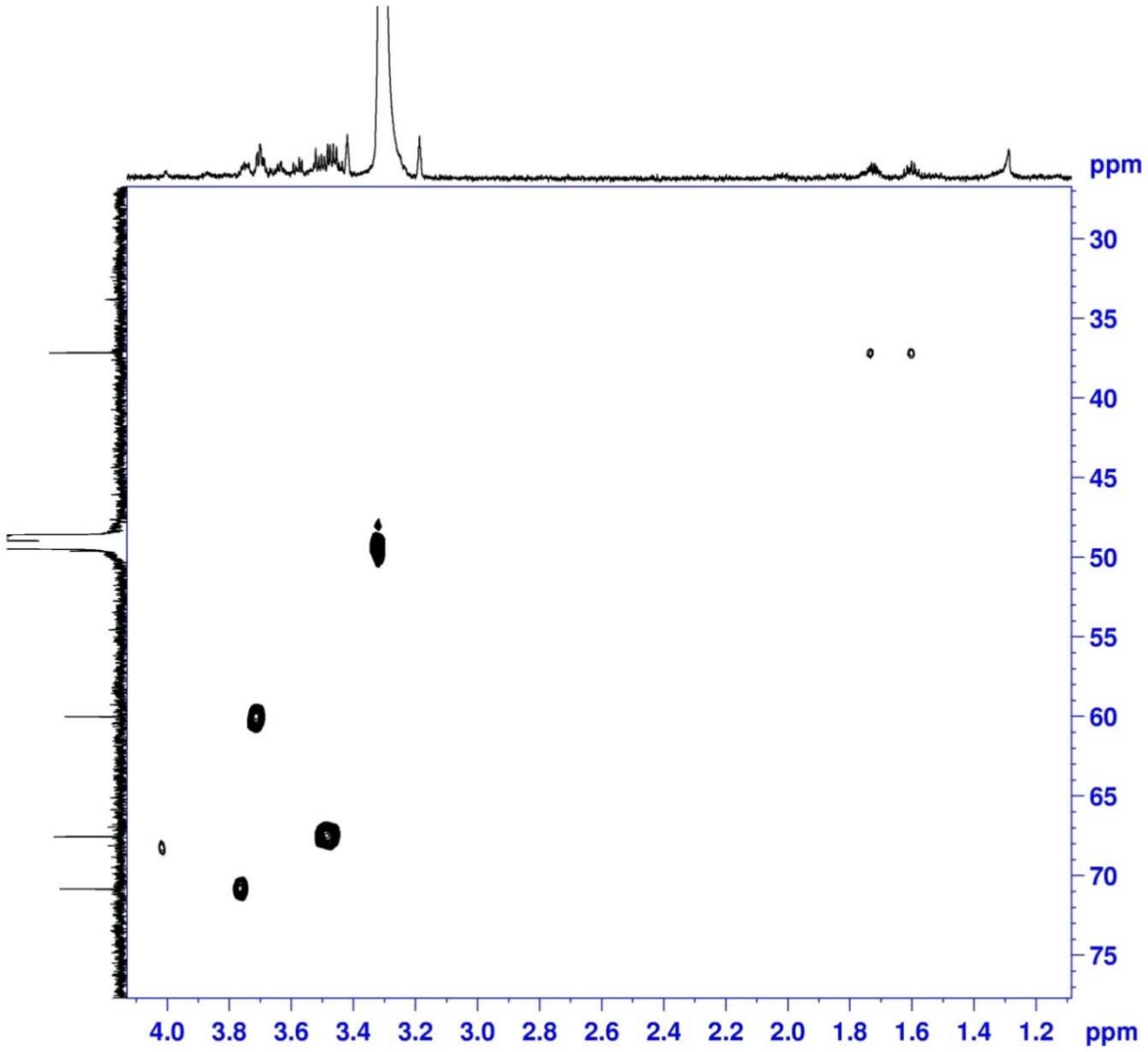

Figure S132. HSQC (600 MHz) spectrum of the fragment **1d** in CD_3OD

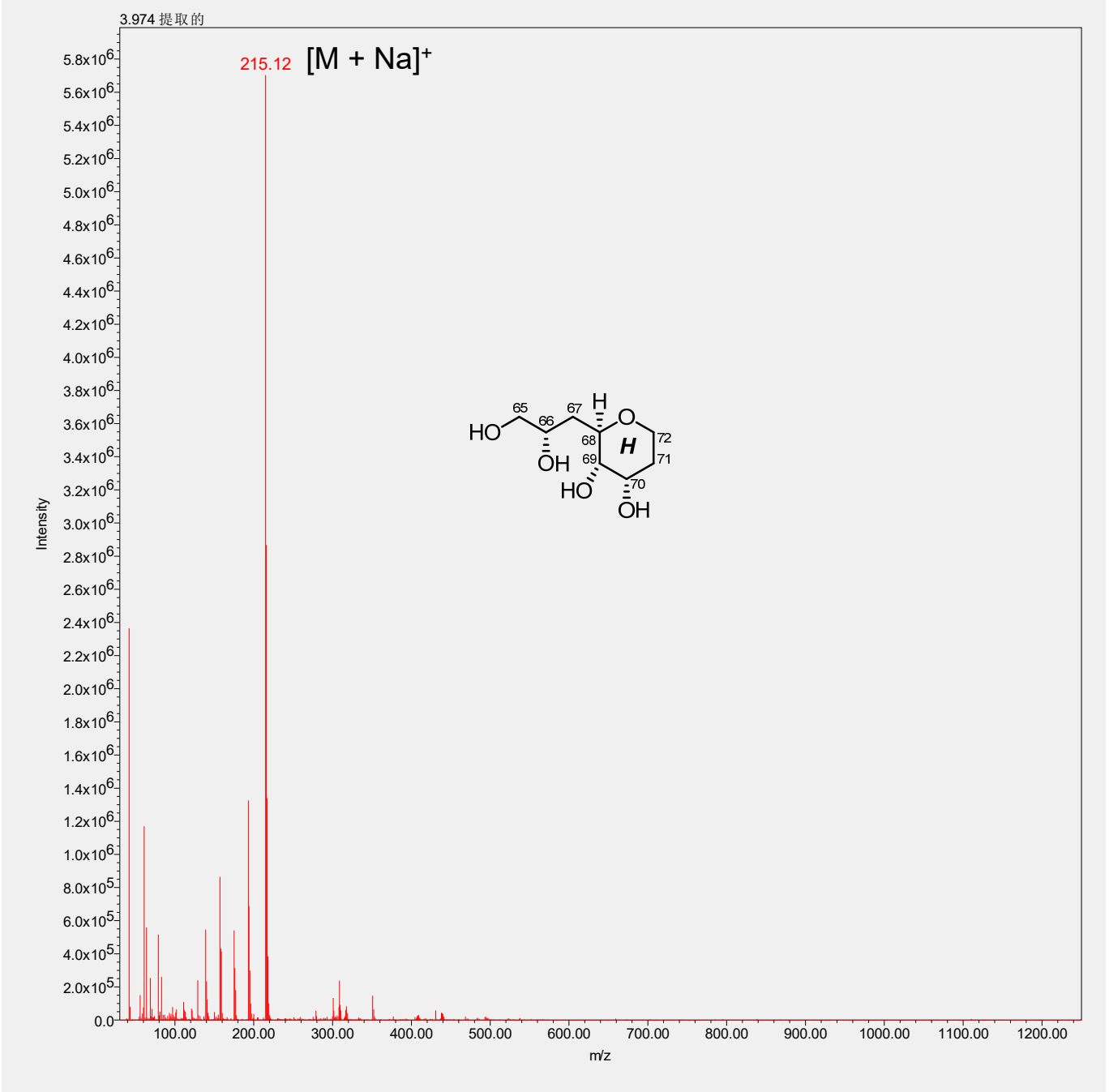

Figure S133. LR-ESIMS for the fragment **1e**

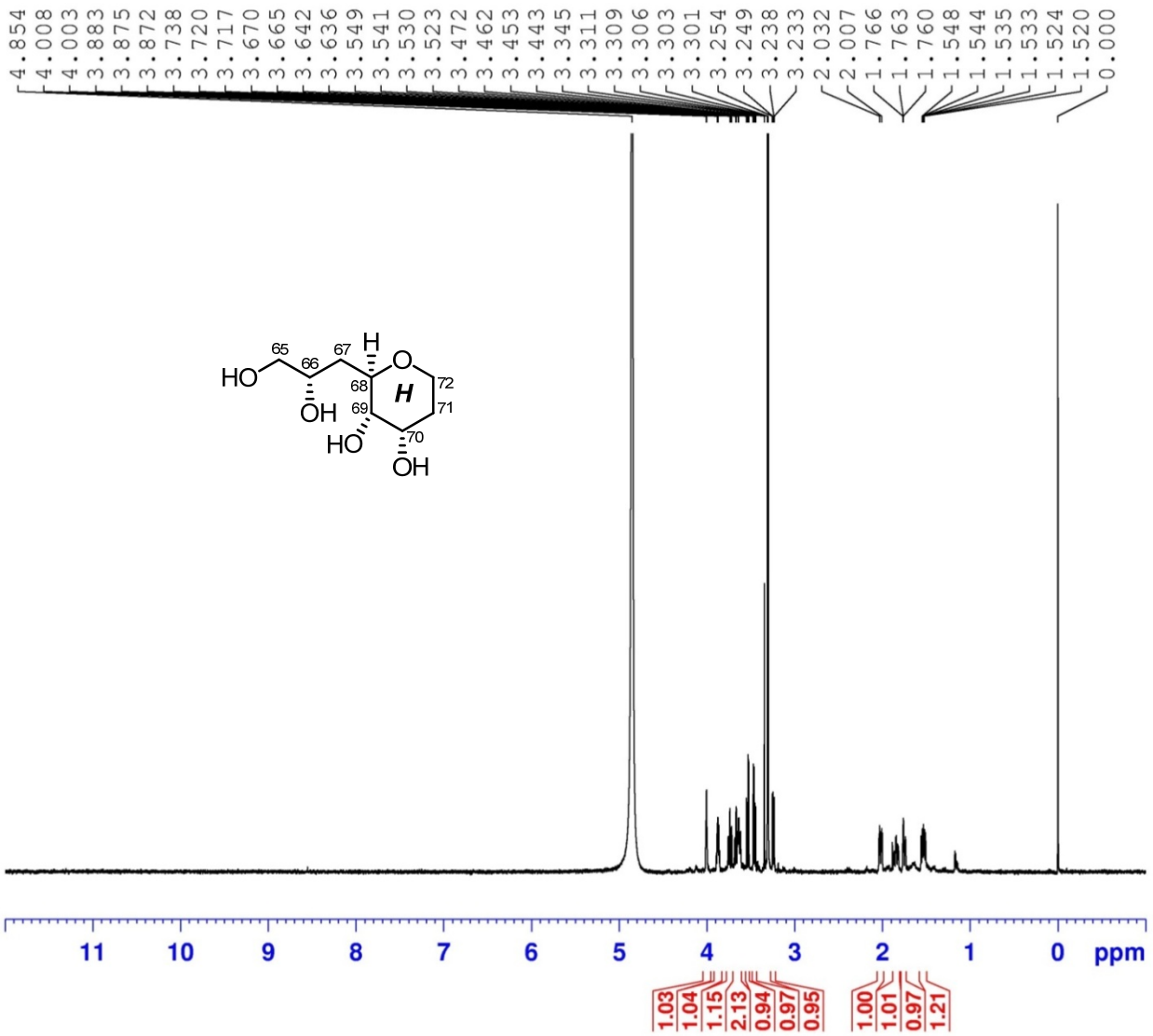

Figure S134. ^{1}H (600 MHz) NMR spectrum of the fragment **1e** in CD_3OD

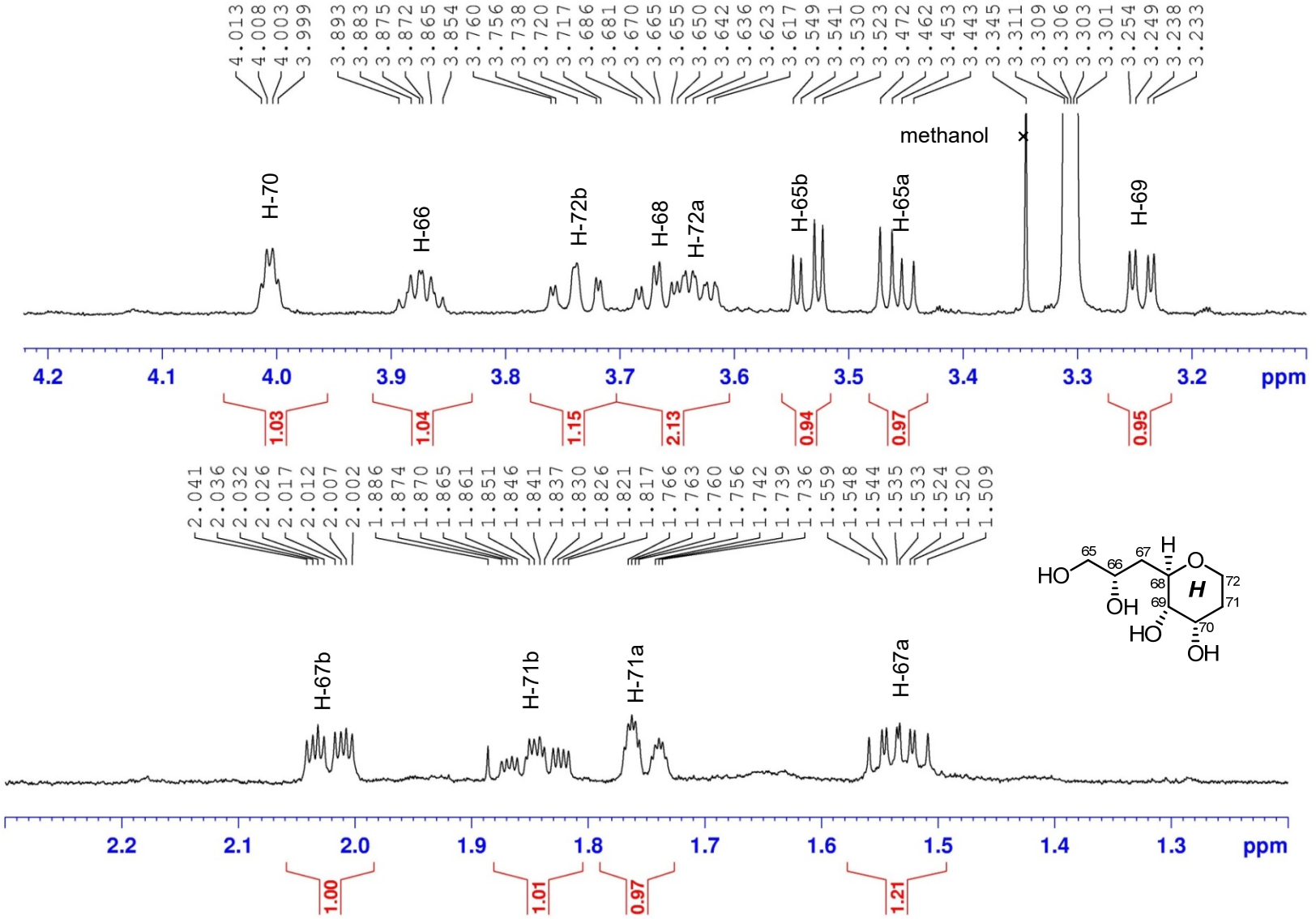

Figure S135. ^{1}H (600 MHz) NMR spectrum of the fragment **1e** in CD_3OD

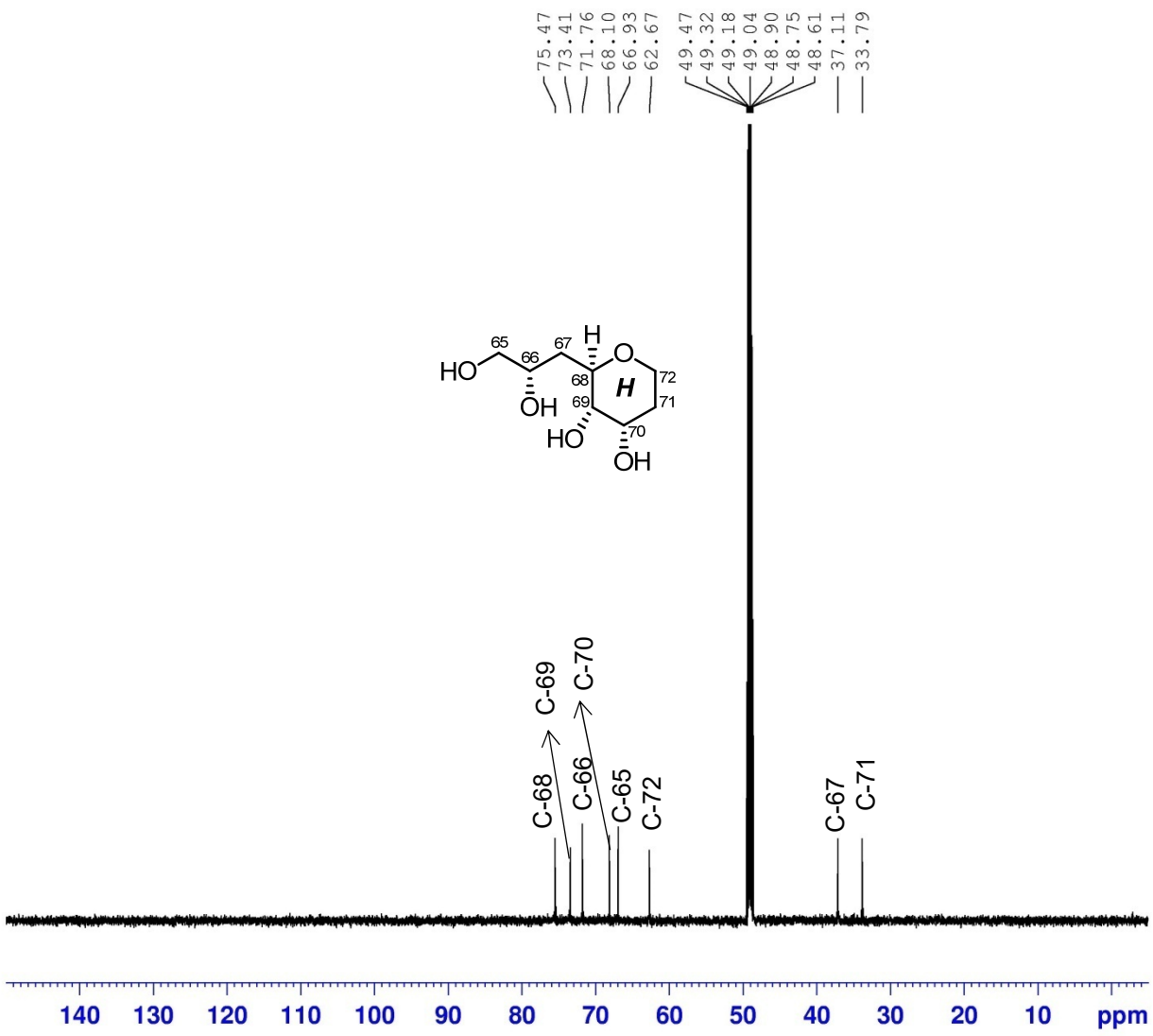

Figure S136. ^{13}C (150 MHz) NMR spectrum of the fragment **1e** in CD_3OD

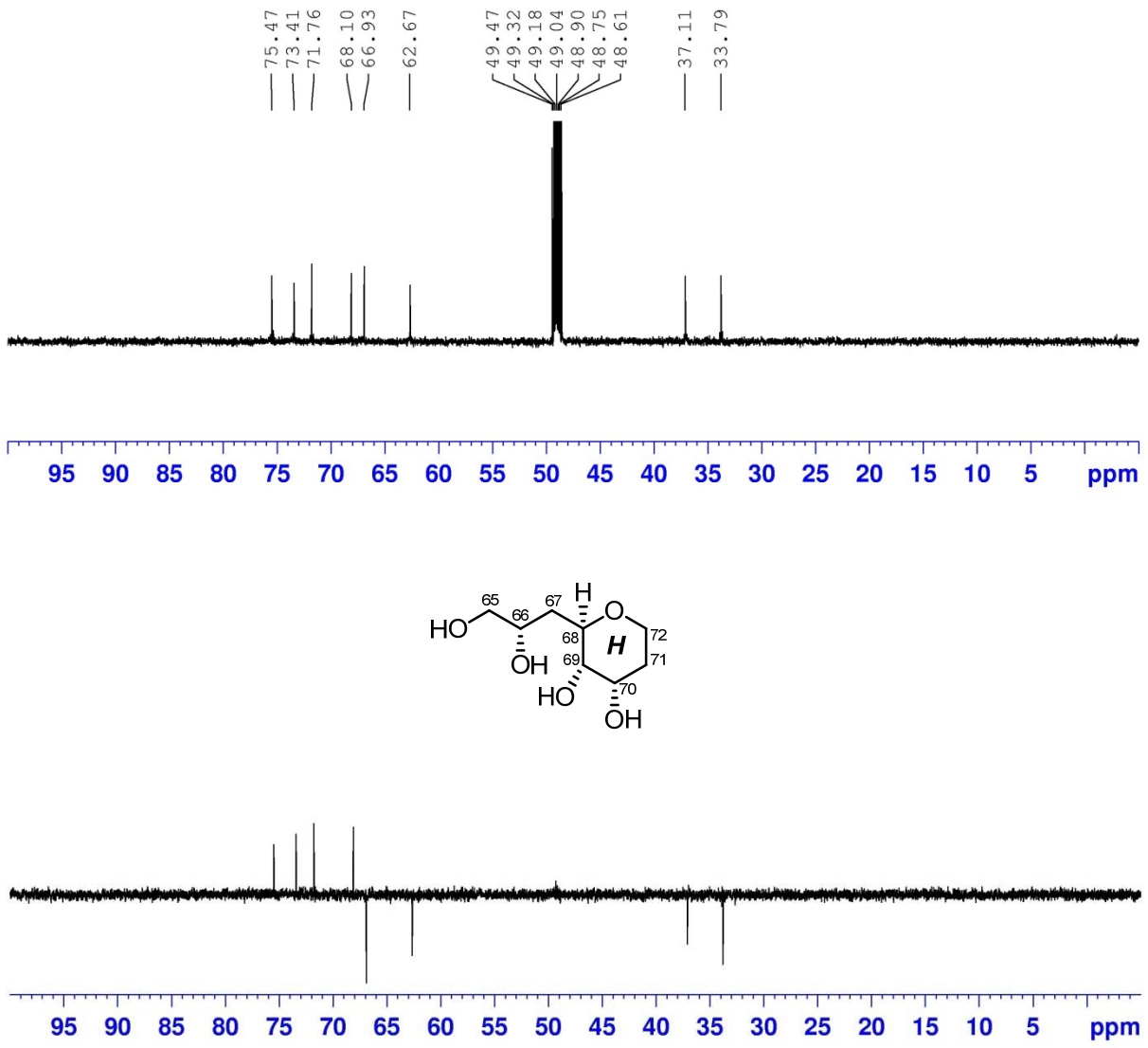

Figure S137. DEPT 135 (150 MHz) NMR spectrum of the fragment **1e** in CD_3OD

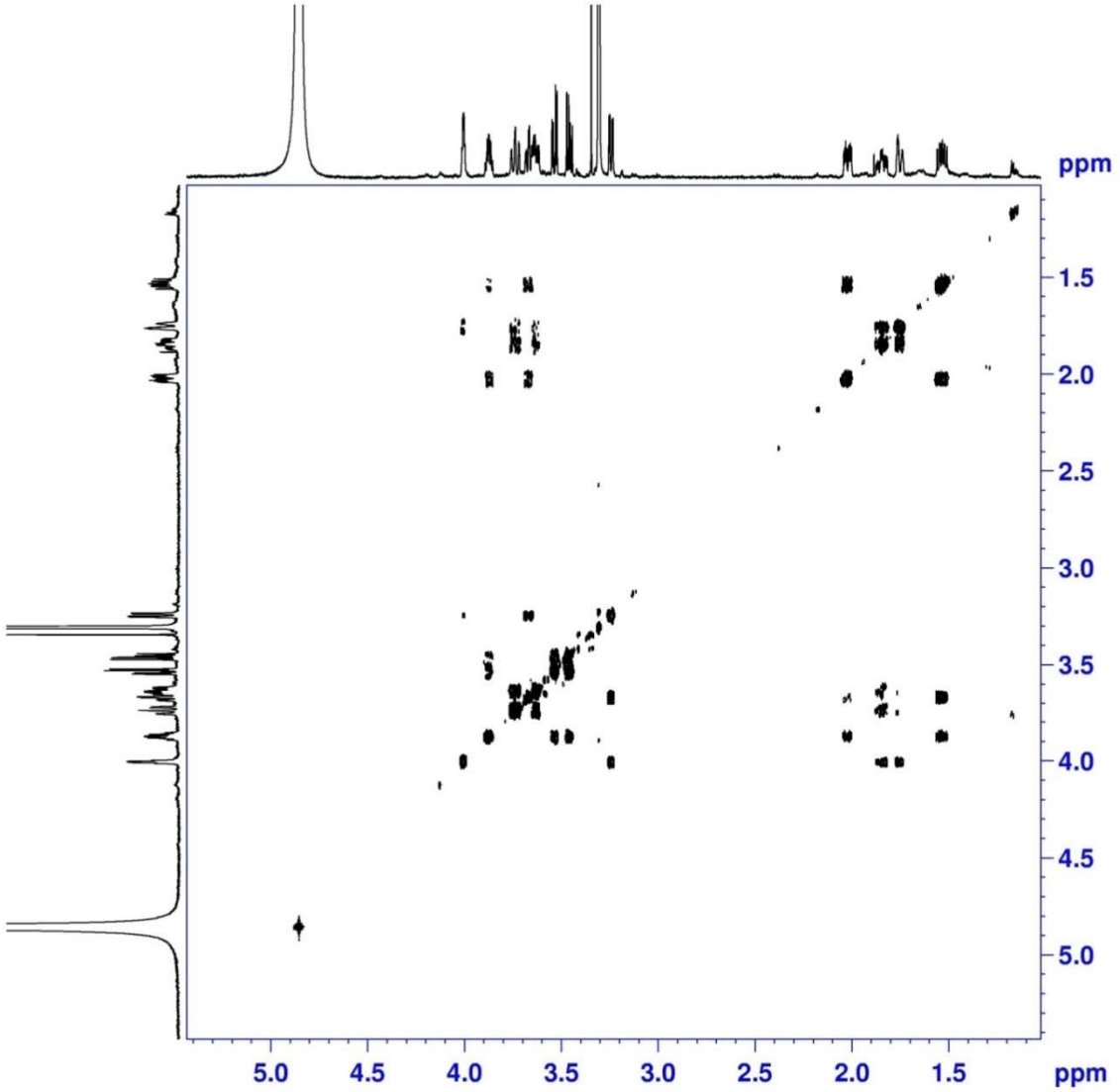

Figure S138. $^{1}H–^{1}H$ COSY (600 MHz) spectrum of the fragment **1e** in CD_3OD

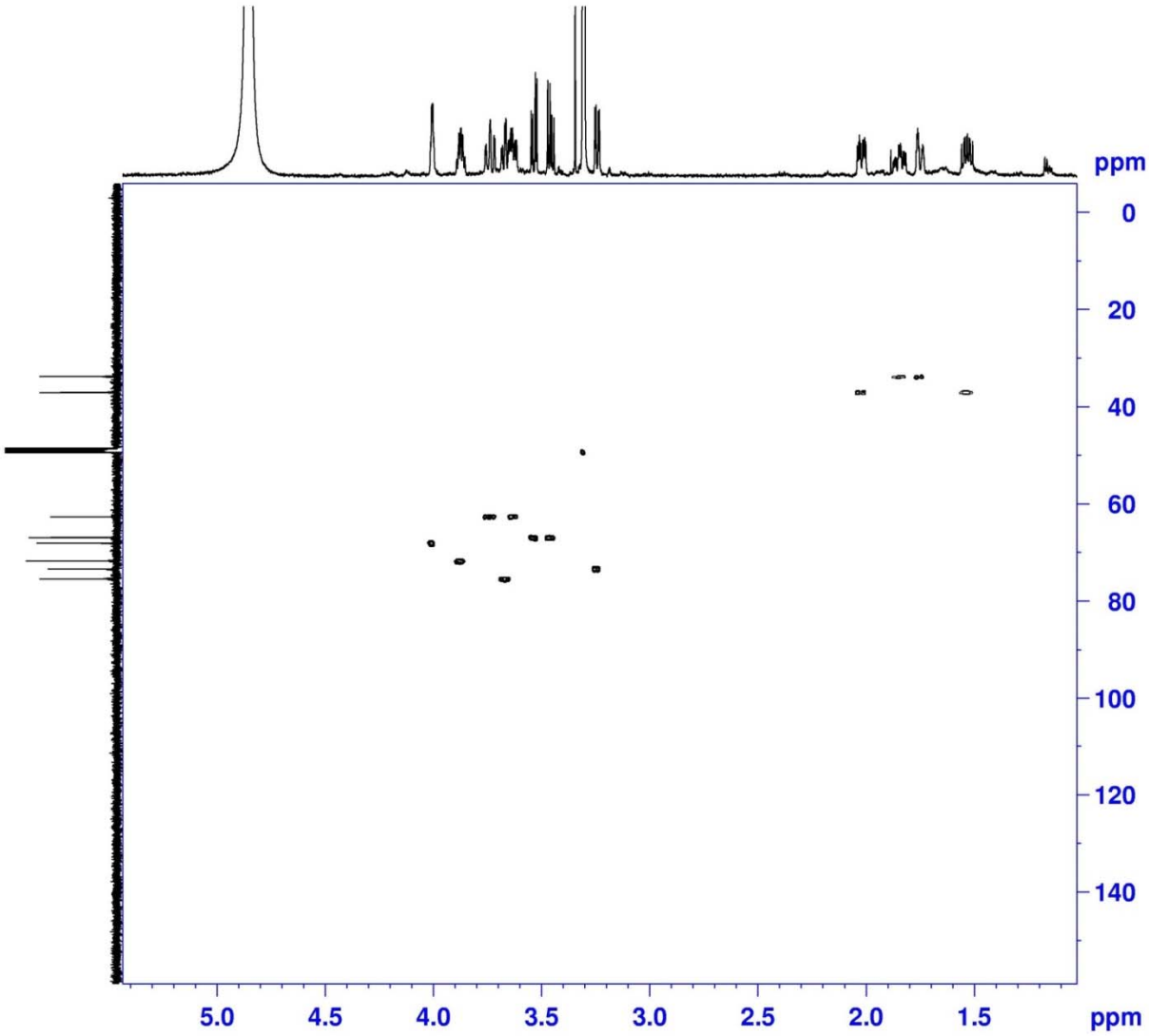

Figure S139. HSQC (600 MHz) spectrum of the fragment **1e** in CD_3OD

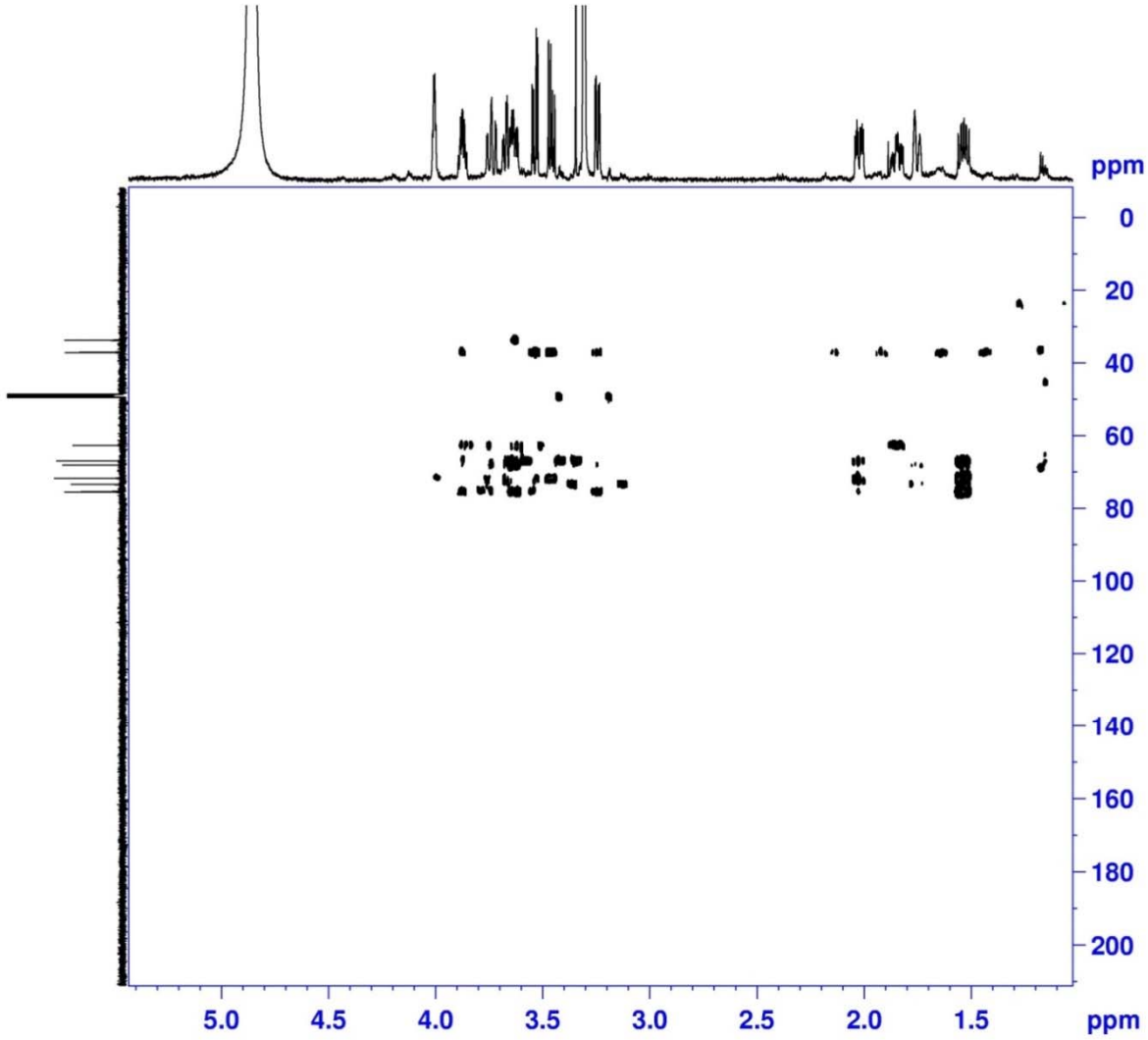

Figure S140. HMBC (600 MHz) spectrum of the fragment **1e** in CD_3OD

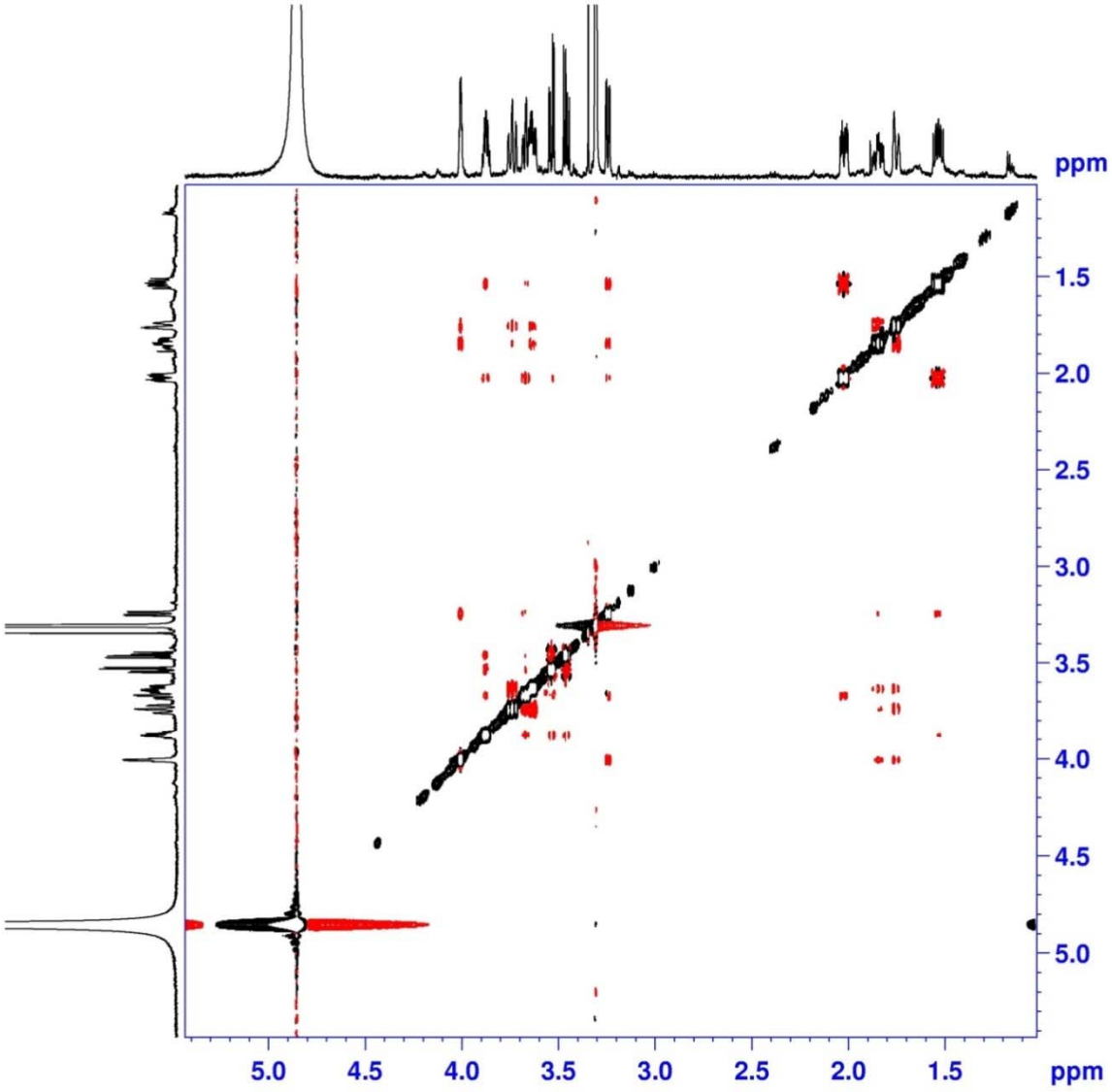

Figure S141. NOESY (600 MHz) spectrum of the fragment **1e** in CD_3OD

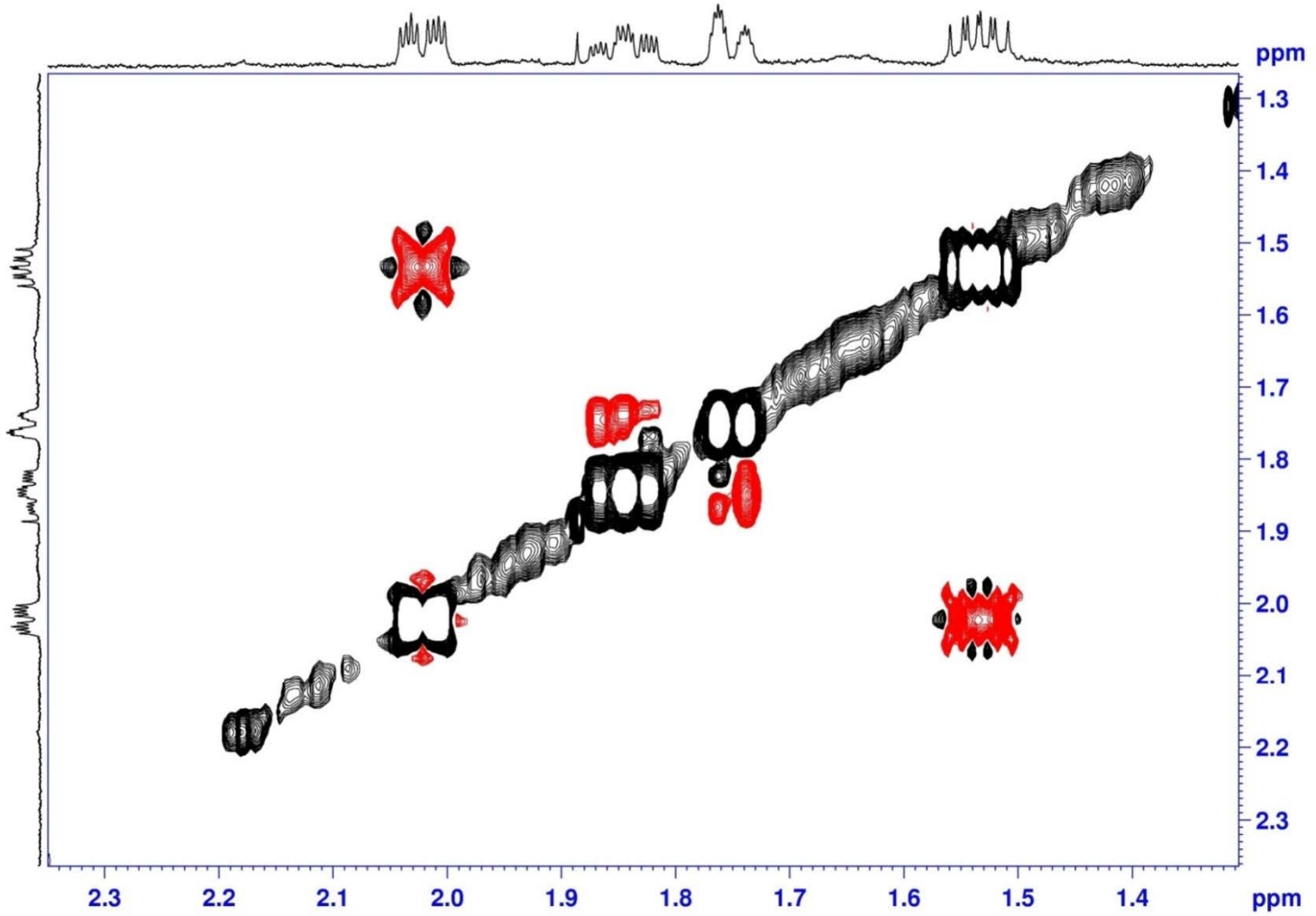

Figure S142. NOESY (600 MHz) spectrum of the fragment **1e** in CD_3OD

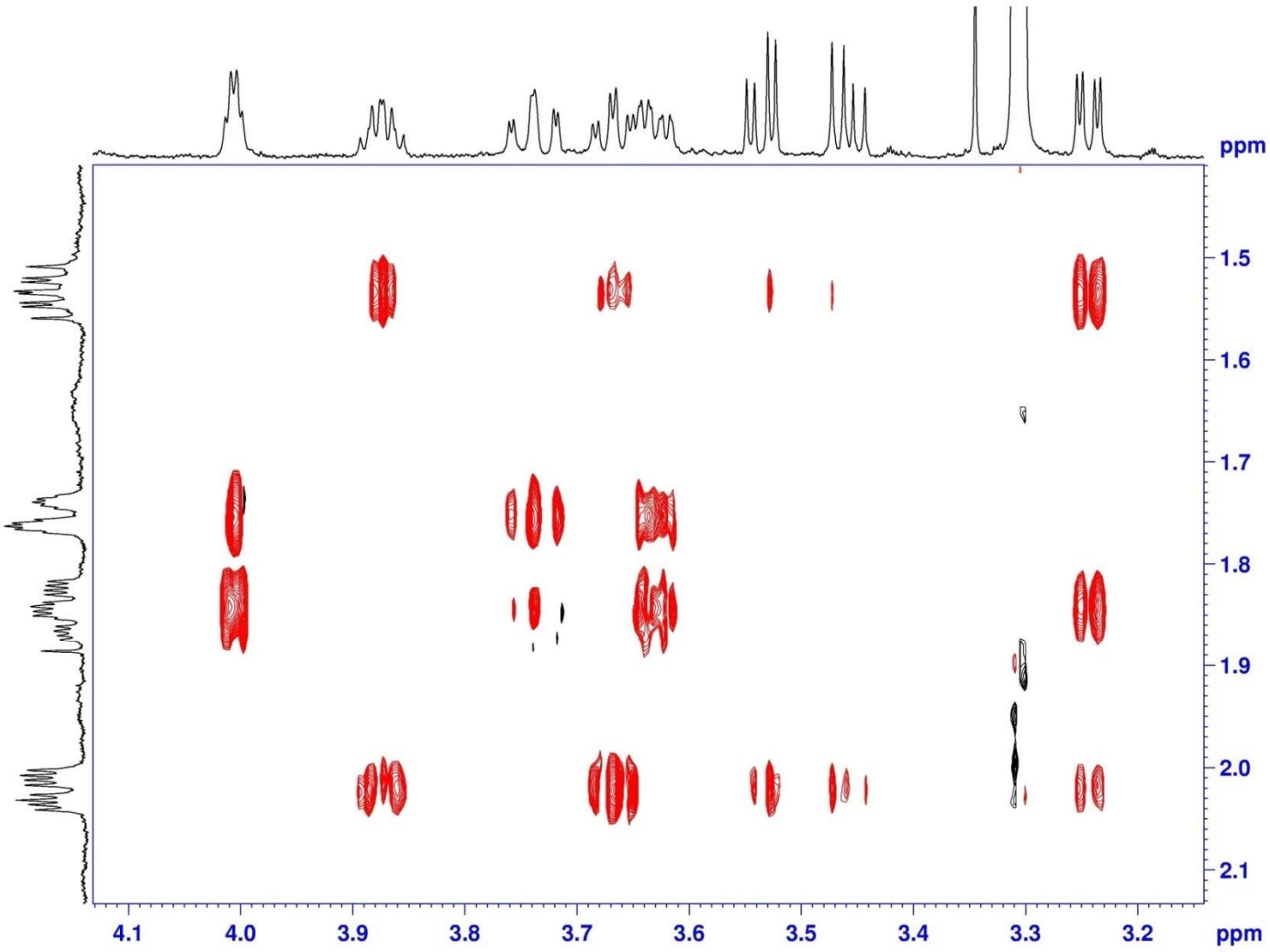

Figure S143. NOESY (600 MHz) spectrum of the fragment **1e** in CD_3OD

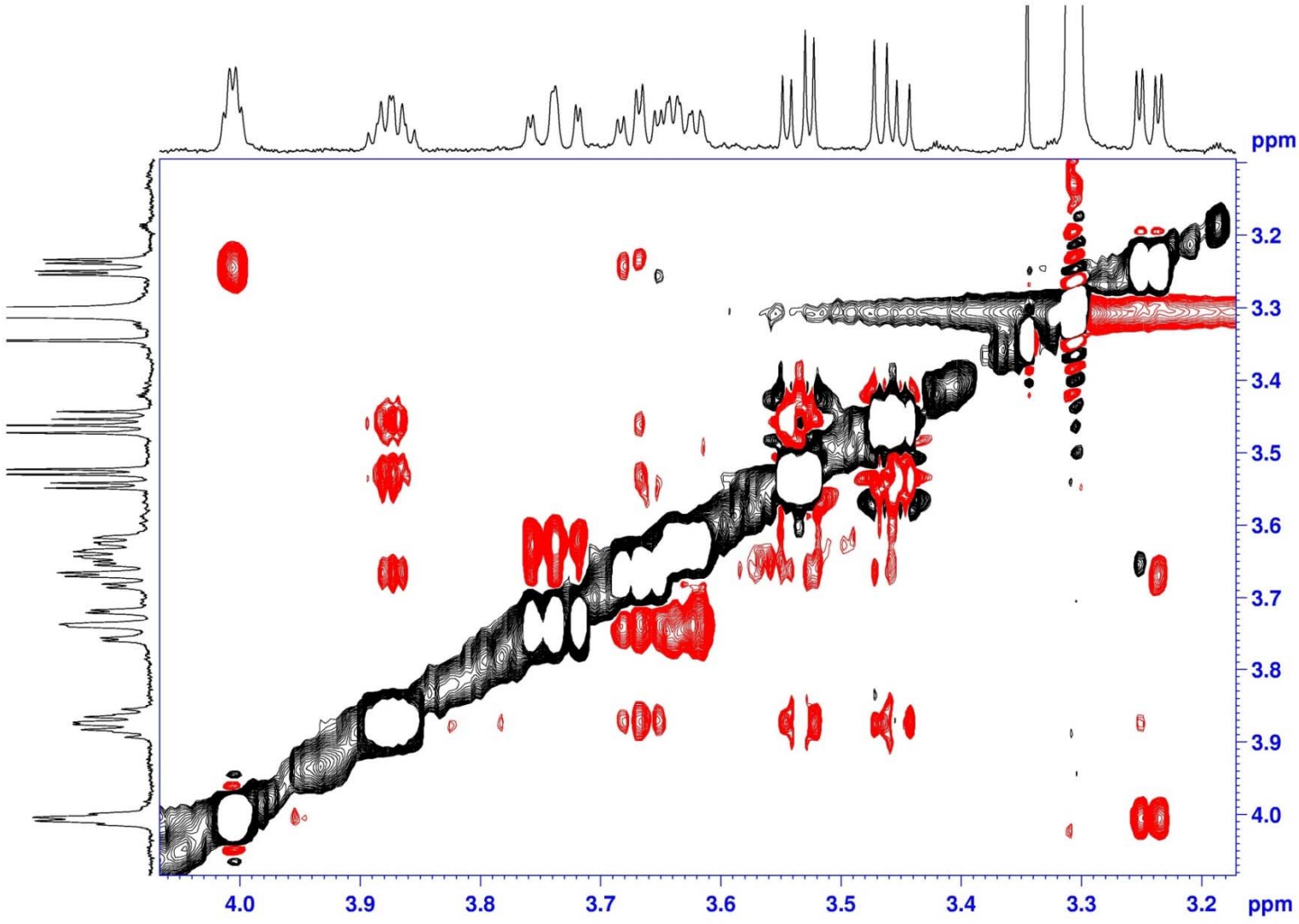

Figure S144. NOESY (600 MHz) spectrum of the fragment **1e** in CD_3OD

Mass Spectrum SmartFormula Report

Analysis Info

Analysis Name	D:\Data\MS\data\202008\liwanshan_AX-a-R-cl_pos_13_01_8656.d	Acquisition Date	8/12/2020 4:26:56 PM
Method	LC_Direct Infusion_pos_100-3000mz.m	Operator	SCSIO
Sample Name	liwanshan_AX-a-R-cl_pos	Instrument	maXis 255552.00029
Comment			

Acquisition Parameter

Source Type	ESI	Ion Polarity	Positive	Set Nebulizer	0.4 Bar
Focus	Active	Set Capillary	4500 V	Set Dry Heater	180 °C
Scan Begin	100 m/z	Set End Plate Offset	0 V	Set Dry Gas	4.0 l/min
Scan End	3500 m/z	Set Charging Voltage	0 V	Set Divert Valve	Waste
		Set Corona	0 nA	Set APCI Heater	0 °C

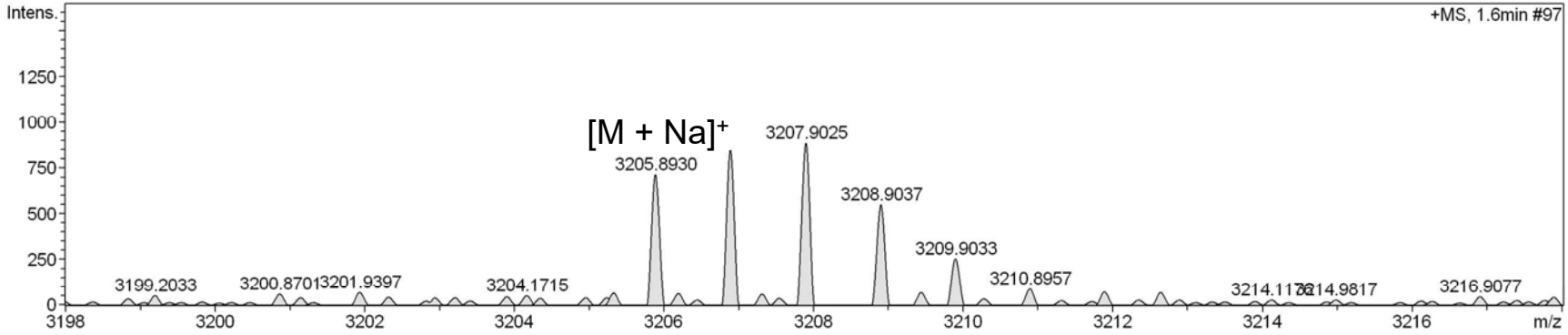

Meas. m/z	#	Ion Formula	Score	m/z	err [ppm]	err [mDa]	mSigma	rdb	e⁻ Conf	N-Rule
3205.8930	1	C150H147F33NaO38	100.00	3205.8936	-0.2	-0.6	95.0	60.5	even	ok

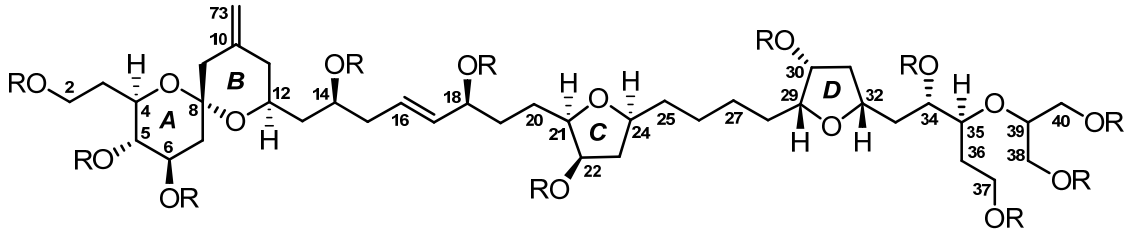

Figure S145. HR-ESIMS for the fragment **1As**

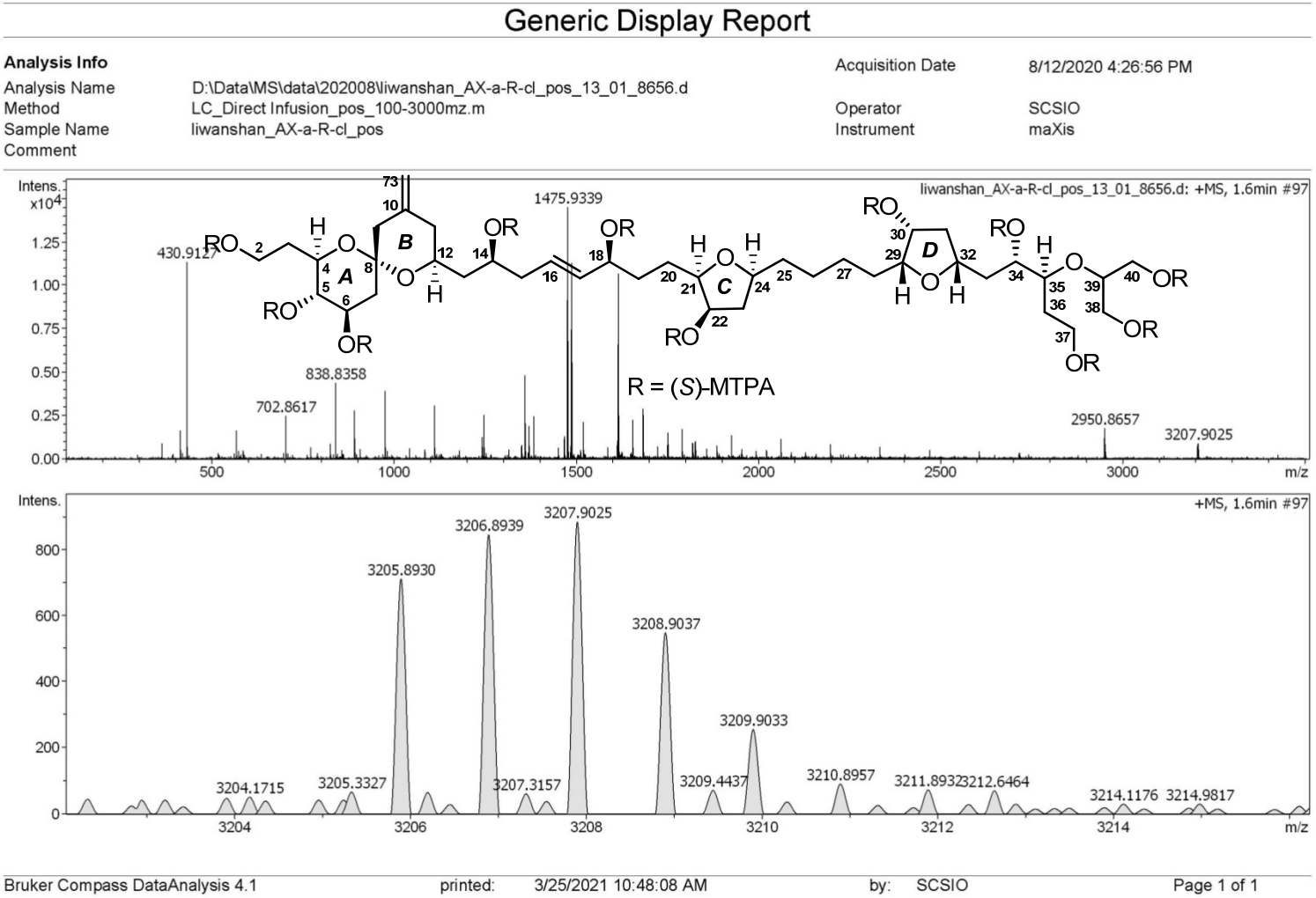

Figure S146. HR-ESIMS for the fragment **1As**

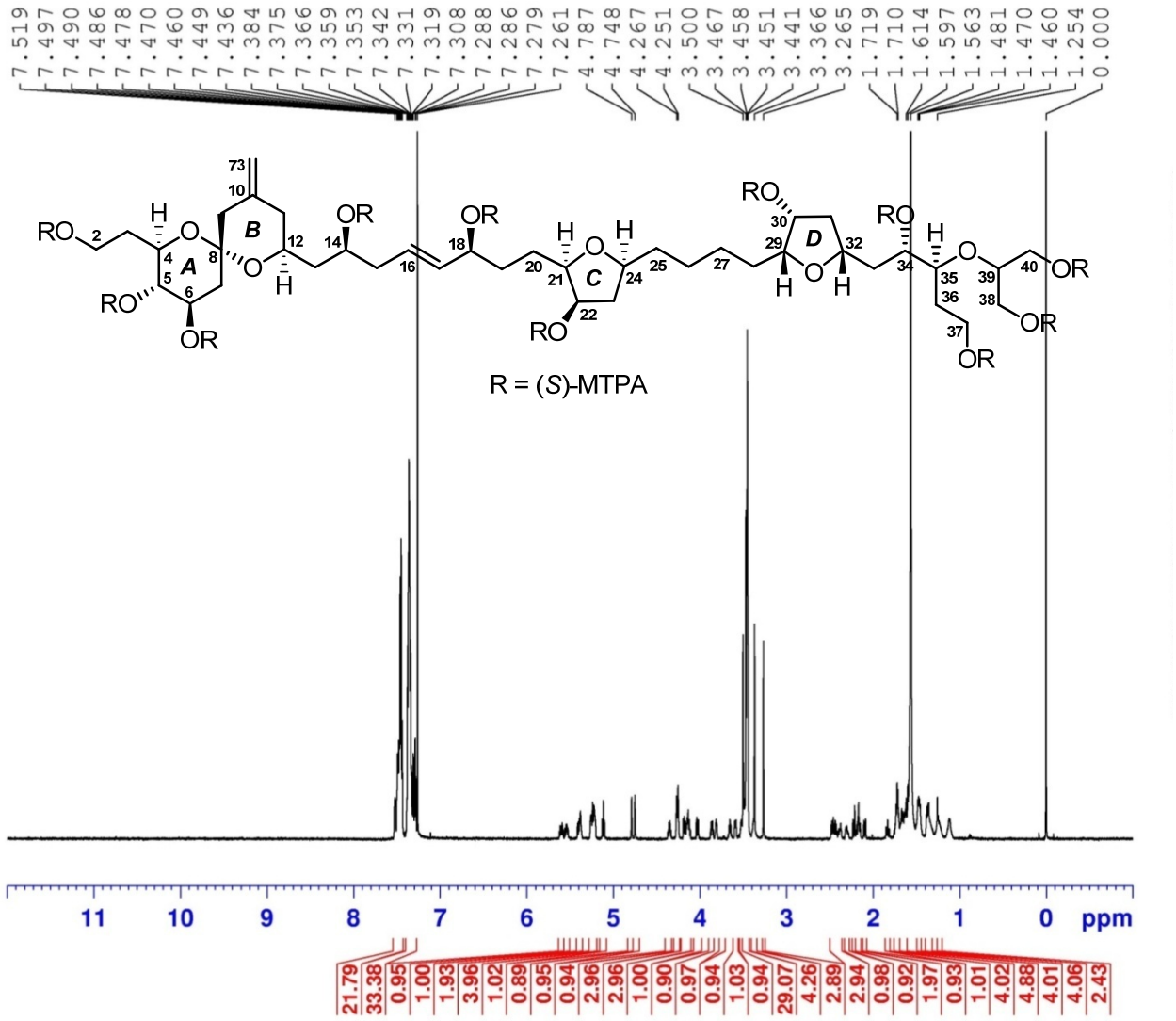

Figure S147. ^{1}H (700 MHz) NMR spectrum of the fragment **1As** in $CDCl_3$

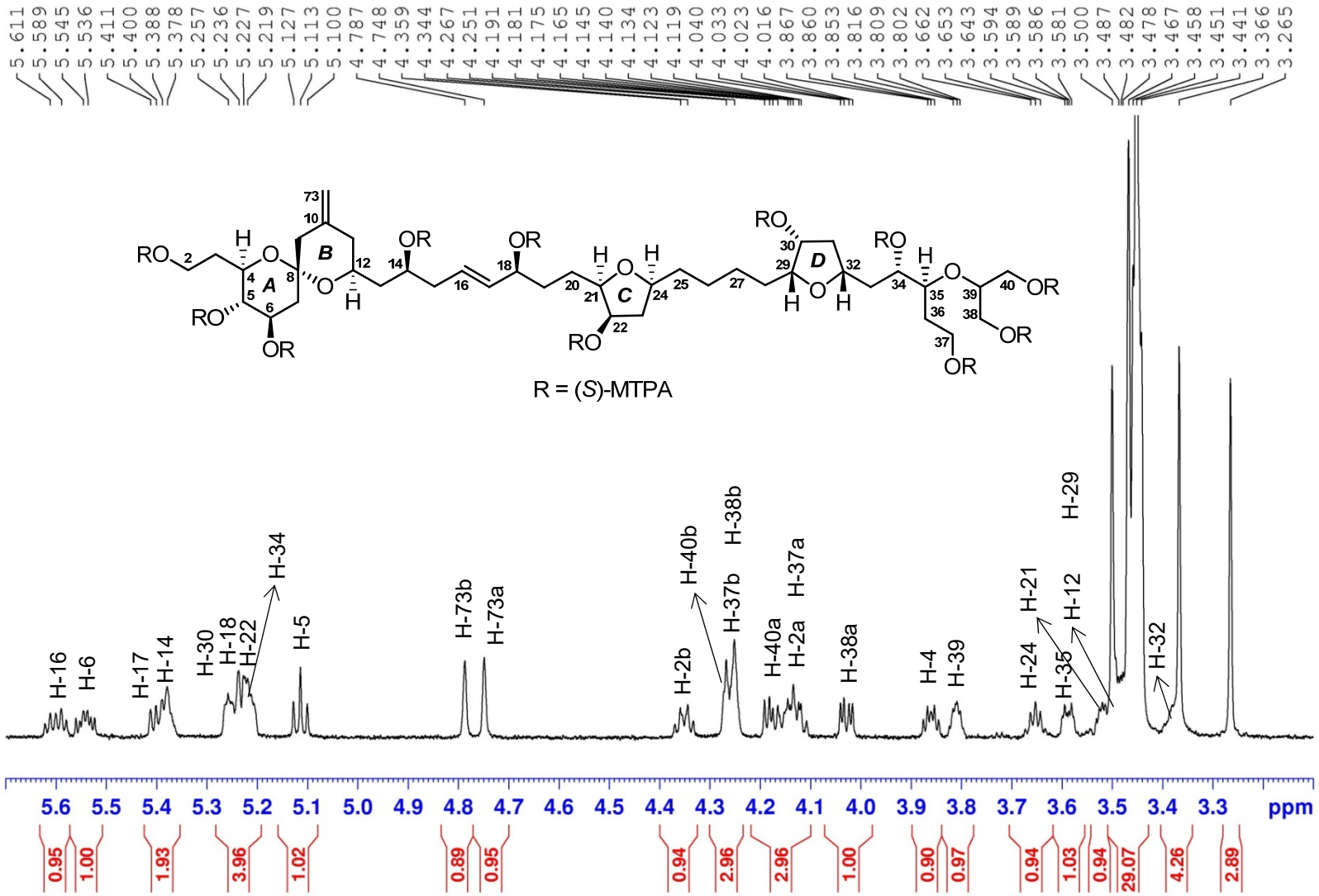

Figure S148. ^{1}H (700 MHz) NMR spectrum of the fragment **1As** in $CDCl_3$

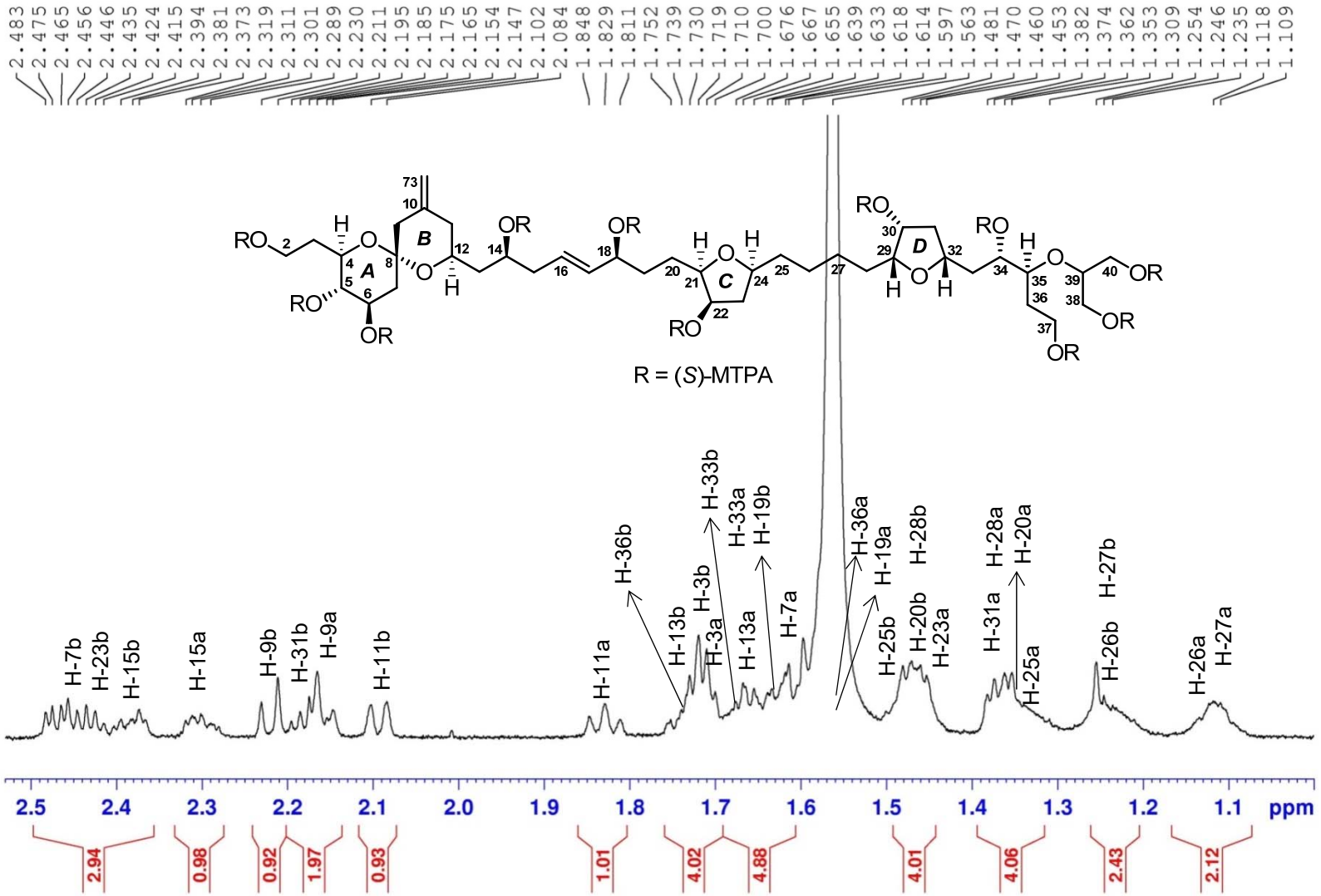

Figure S149. ^{1}H (700 MHz) NMR spectrum of the fragment **1As** in $CDCl_3$

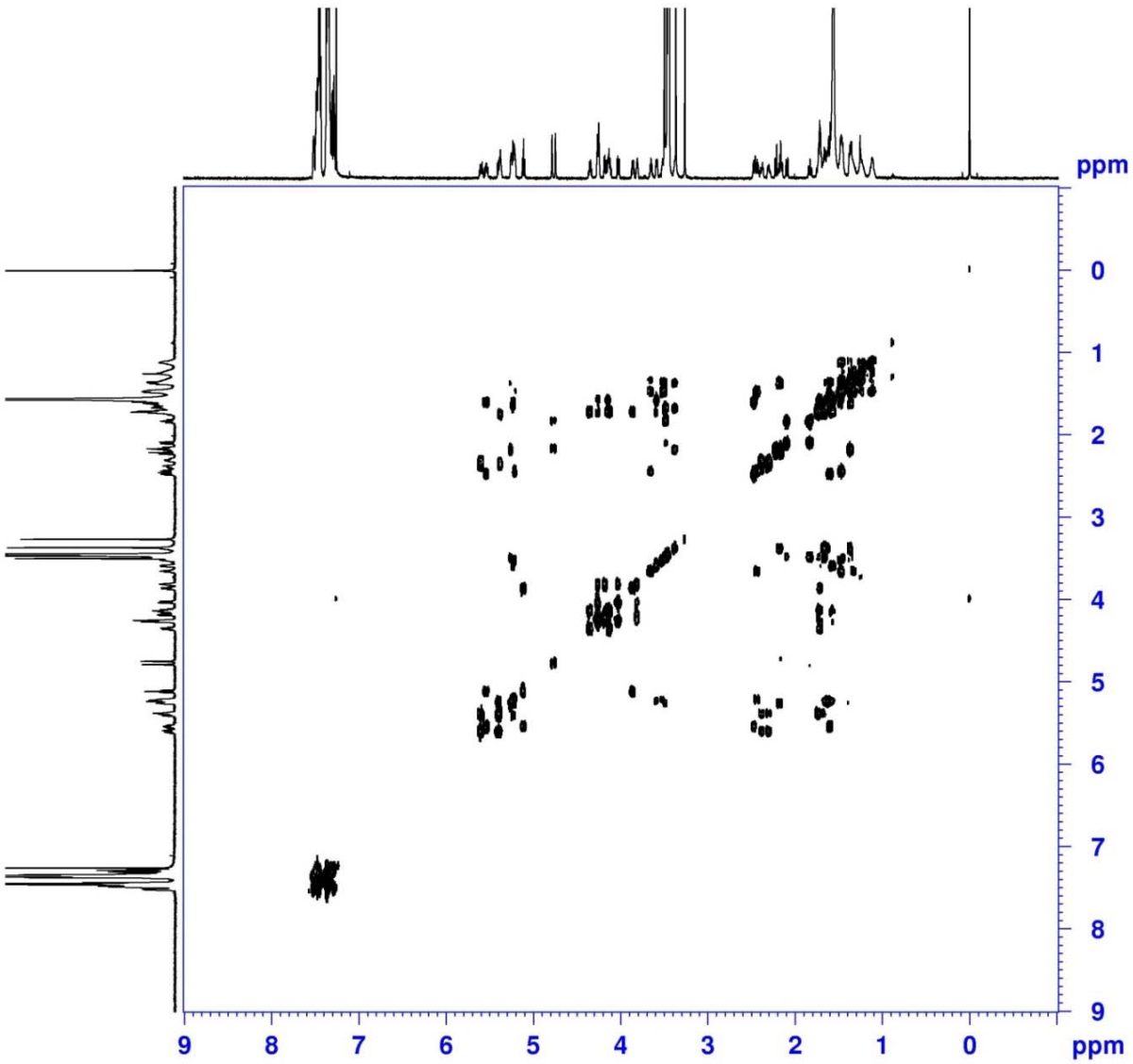

Figure S150. ^{1}H–^{1}H COSY (700 MHz) spectrum of the fragment **1As** in $CDCl_3$

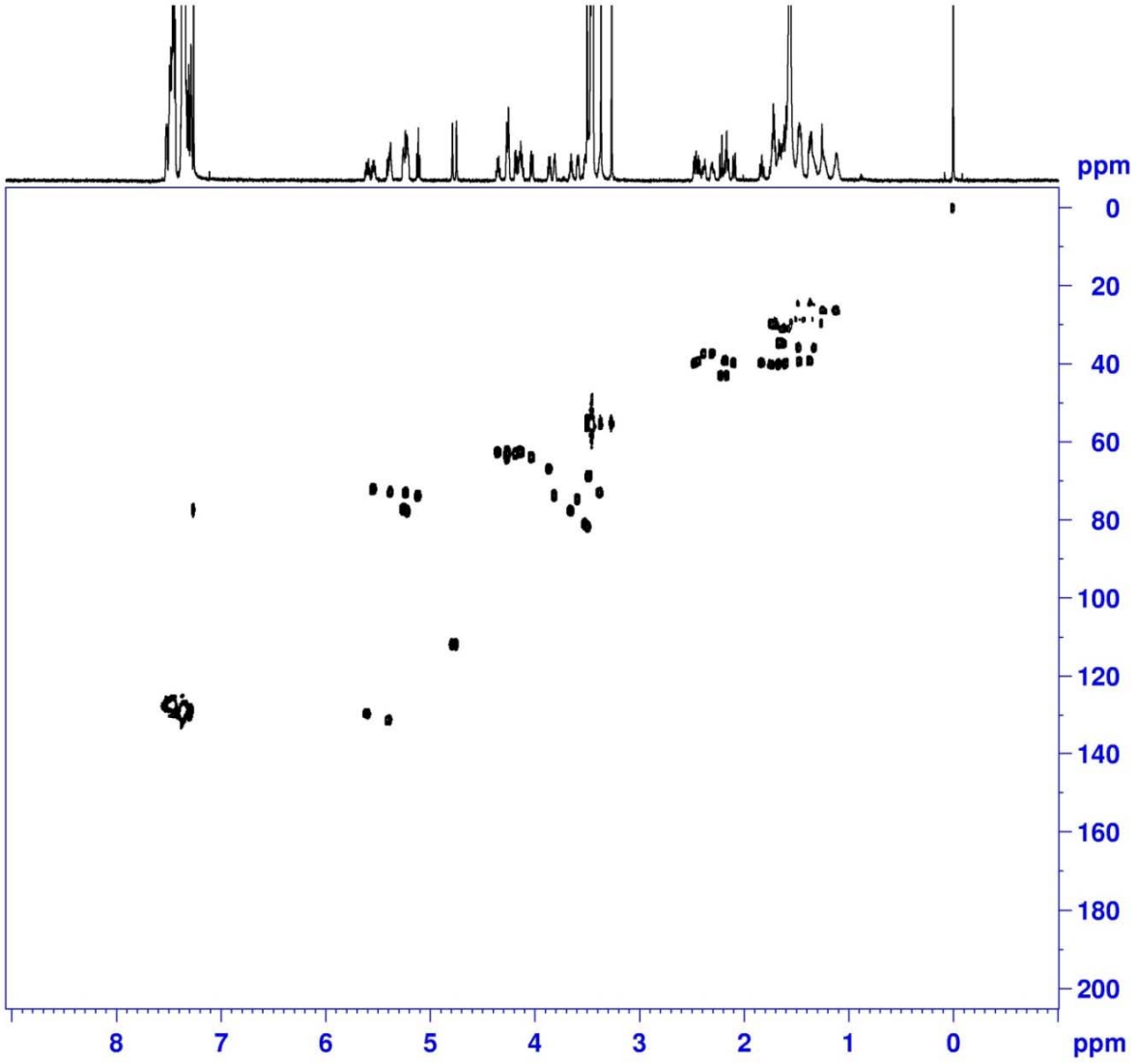

Figure S151. HSQC (700 MHz) spectrum of the fragment **1As** in $CDCl_3$

Mass Spectrum SmartFormula Report

Analysis Info

Analysis Name	D:\Data\MS\data\202008\liwanshan_AX-a-S-cl_pos_12_01_8655.d	Acquisition Date	8/12/2020 4:23:30 PM
Method	LC_Direct Infusion_pos_100-3000mz.m	Operator	SCSIO
Sample Name	liwanshan_AX-a-S-cl_pos	Instrument	maXis 255552.00029
Comment			

Acquisition Parameter

Source Type	ESI	Ion Polarity	Positive	Set Nebulizer	0.4 Bar
Focus	Active	Set Capillary	4500 V	Set Dry Heater	180 °C
Scan Begin	100 m/z	Set End Plate Offset	0 V	Set Dry Gas	4.0 l/min
Scan End	3500 m/z	Set Charging Voltage	0 V	Set Divert Valve	Waste
		Set Corona	0 nA	Set APCI Heater	0 °C

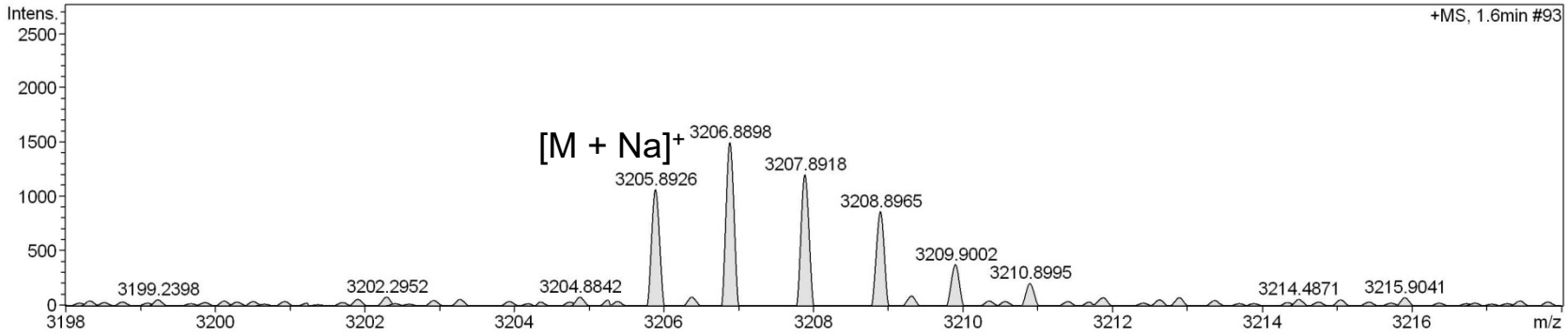

Meas. m/z	#	Ion Formula	Score	m/z	err [ppm]	err [mDa]	mSigma	rdb	e⁻ Conf	N-Rule
3205.8926	1	C150H147F33NaO38	100.00	3205.8936	0.3	0.9	51.1	60.5	even	ok

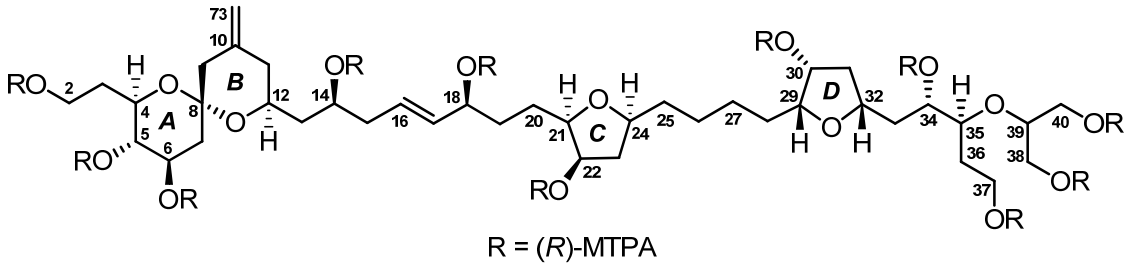

Figure S152. HR-ESIMS for the fragment **1Ar**

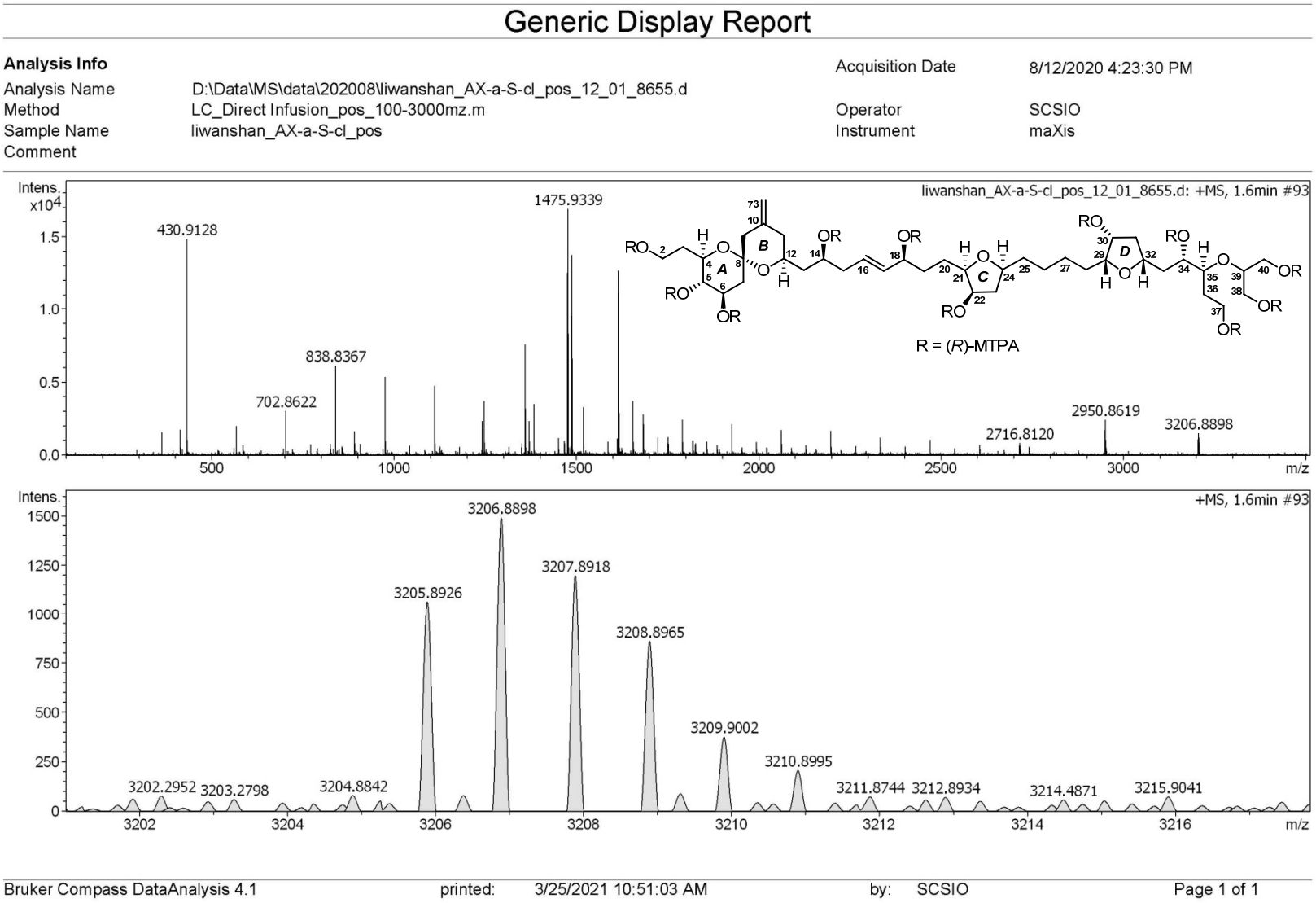

Figure S153. HR-ESIMS for the fragment **1Ar**

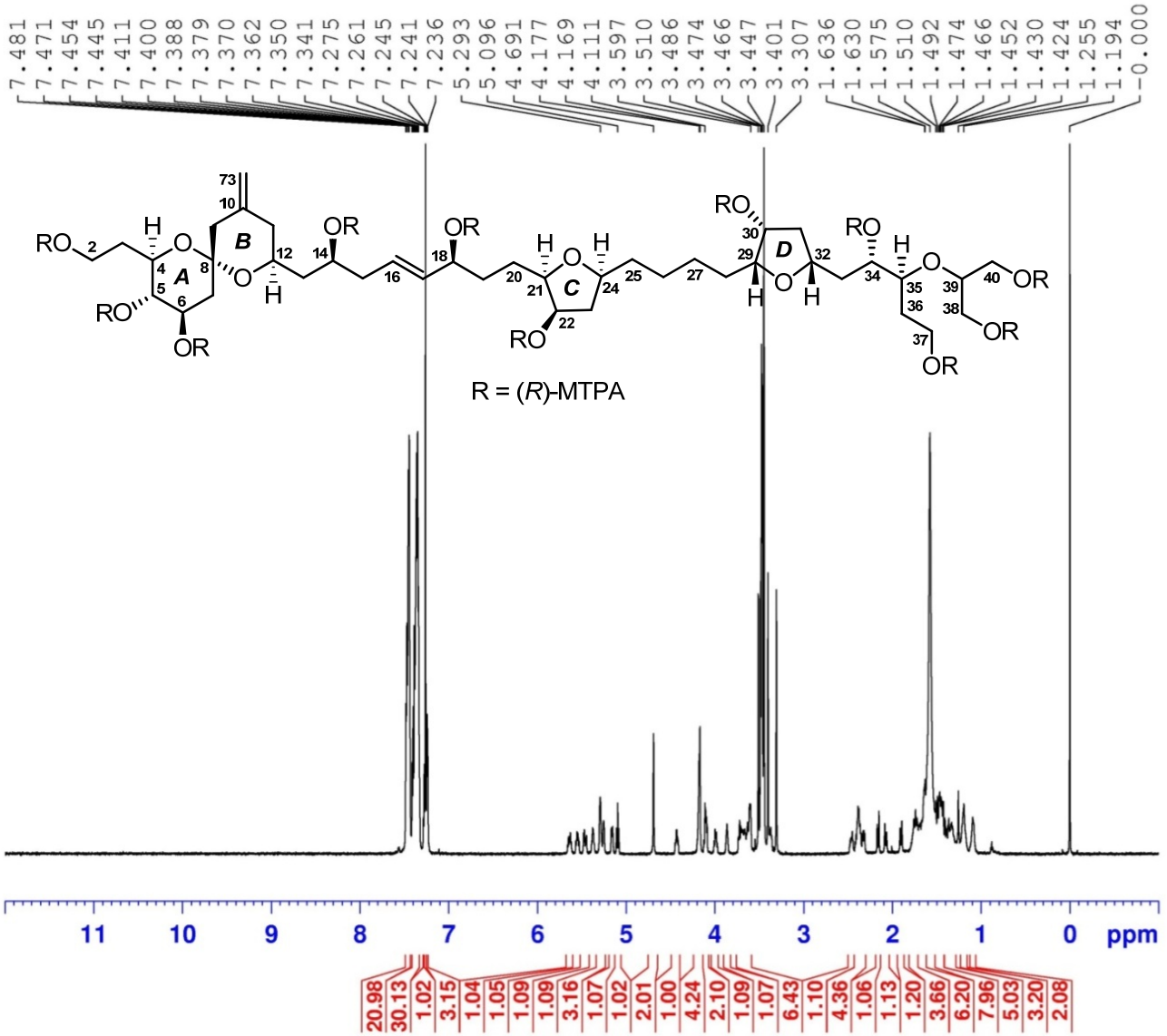

Figure S154. ^{1}H (700 MHz) NMR spectrum of the fragment **1Ar** in $CDCl_3$

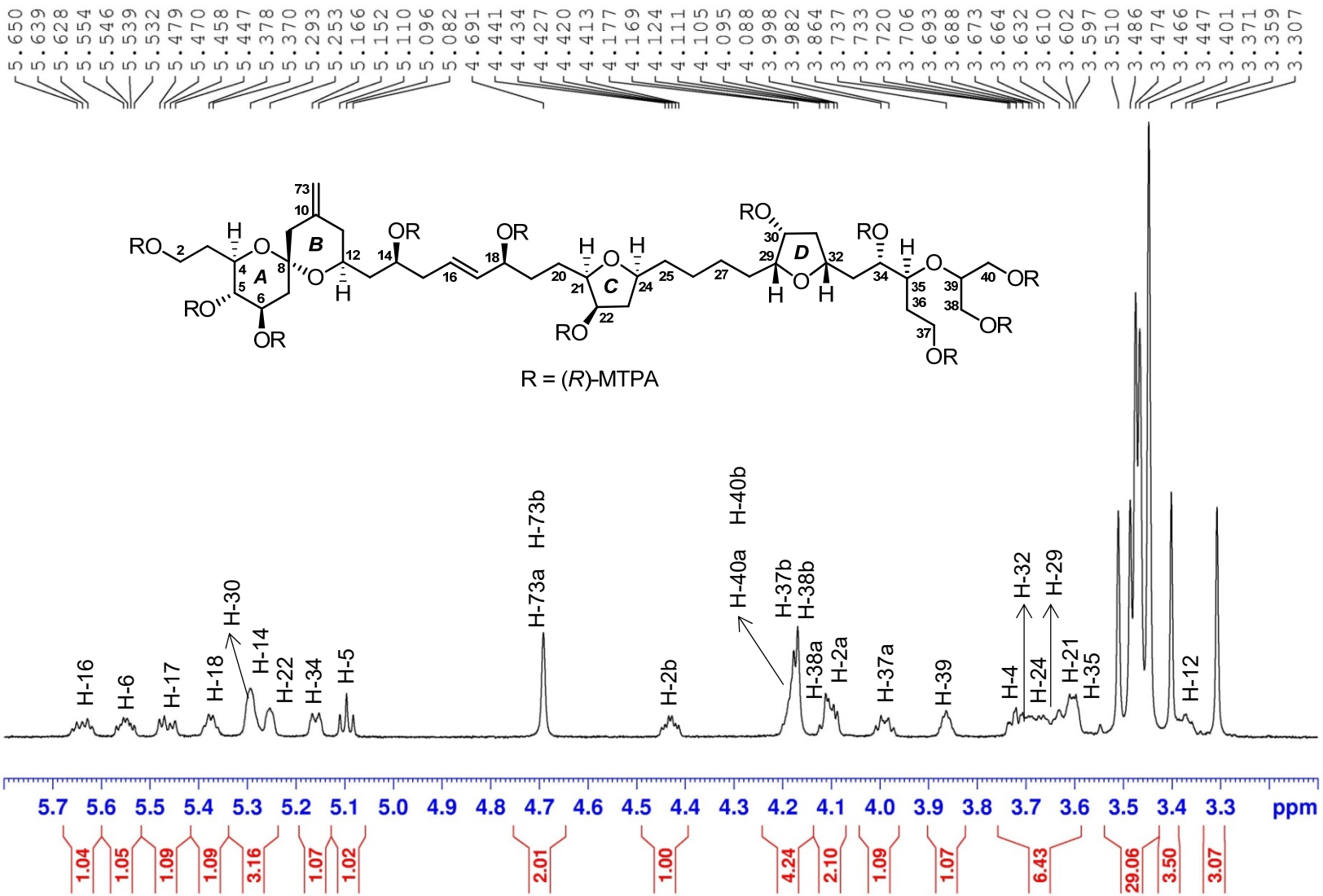

Figure S155. ^{1}H (700 MHz) NMR spectrum of the fragment **1Ar** in $CDCl_3$

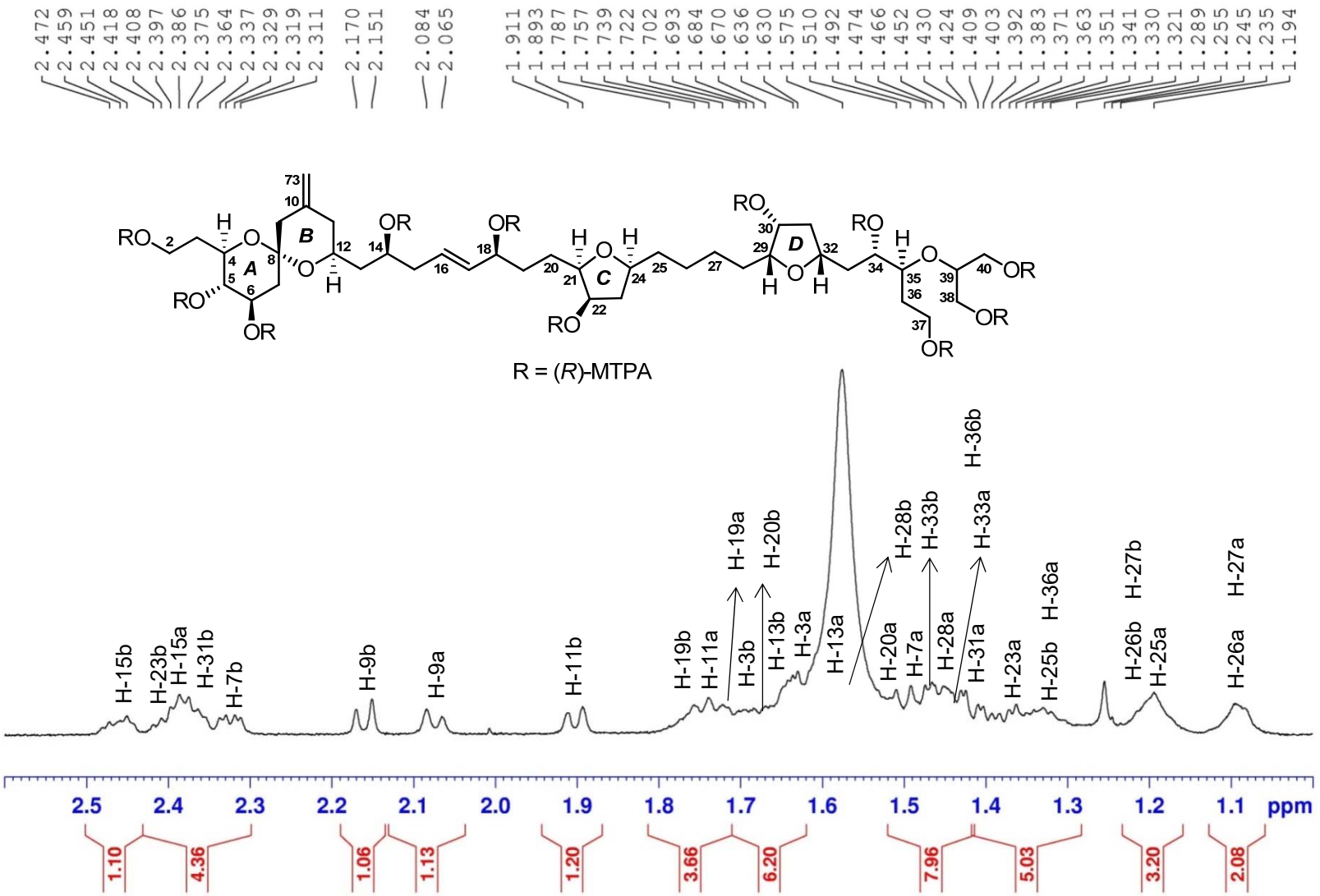

Figure S156. ^{1}H (700 MHz) NMR spectrum of the fragment **1Ar** in $CDCl_3$

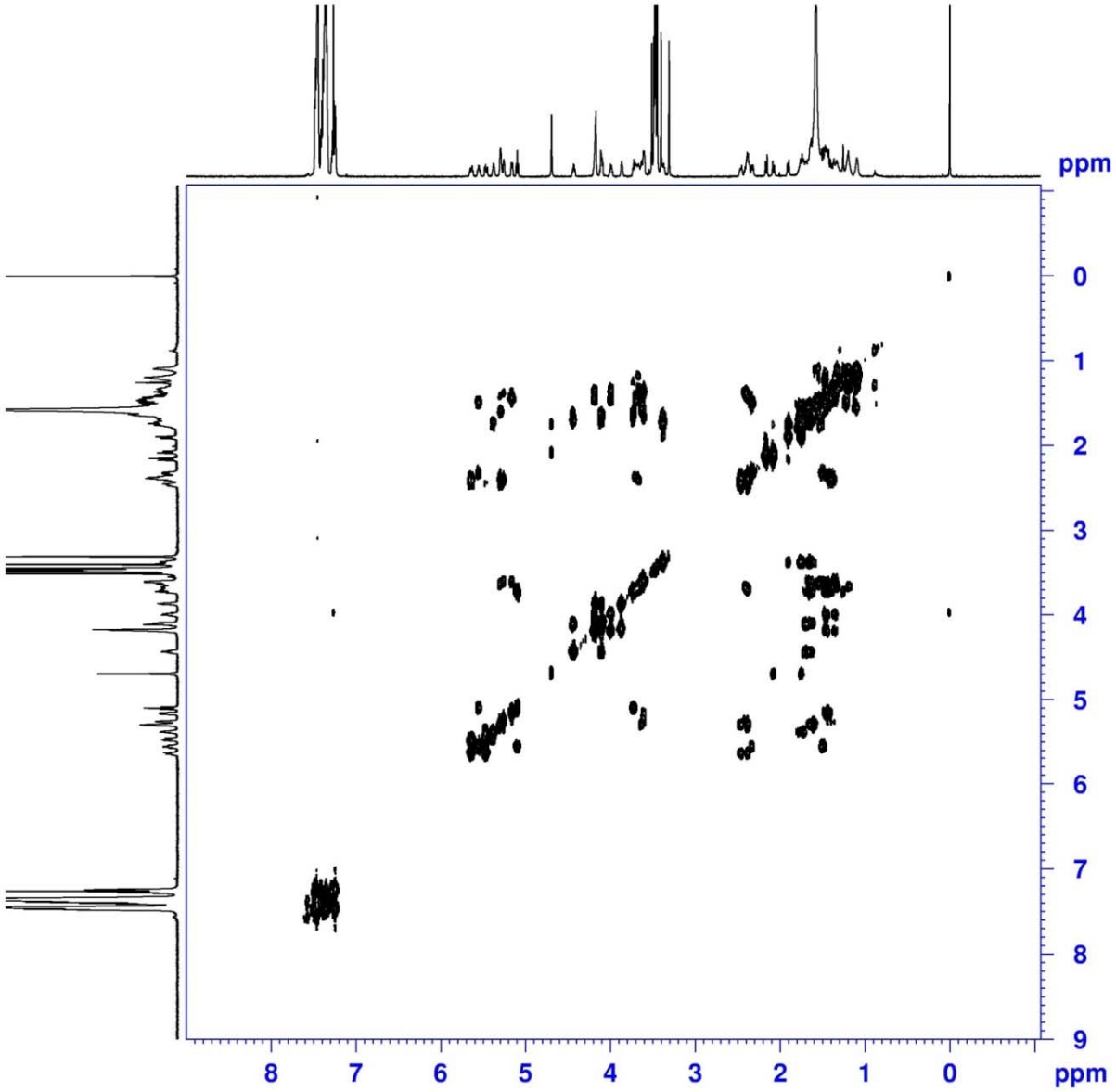

Figure S157. ^{1}H–^{1}H COSY (700 MHz) spectrum of the fragment **1Ar** in $CDCl_3$

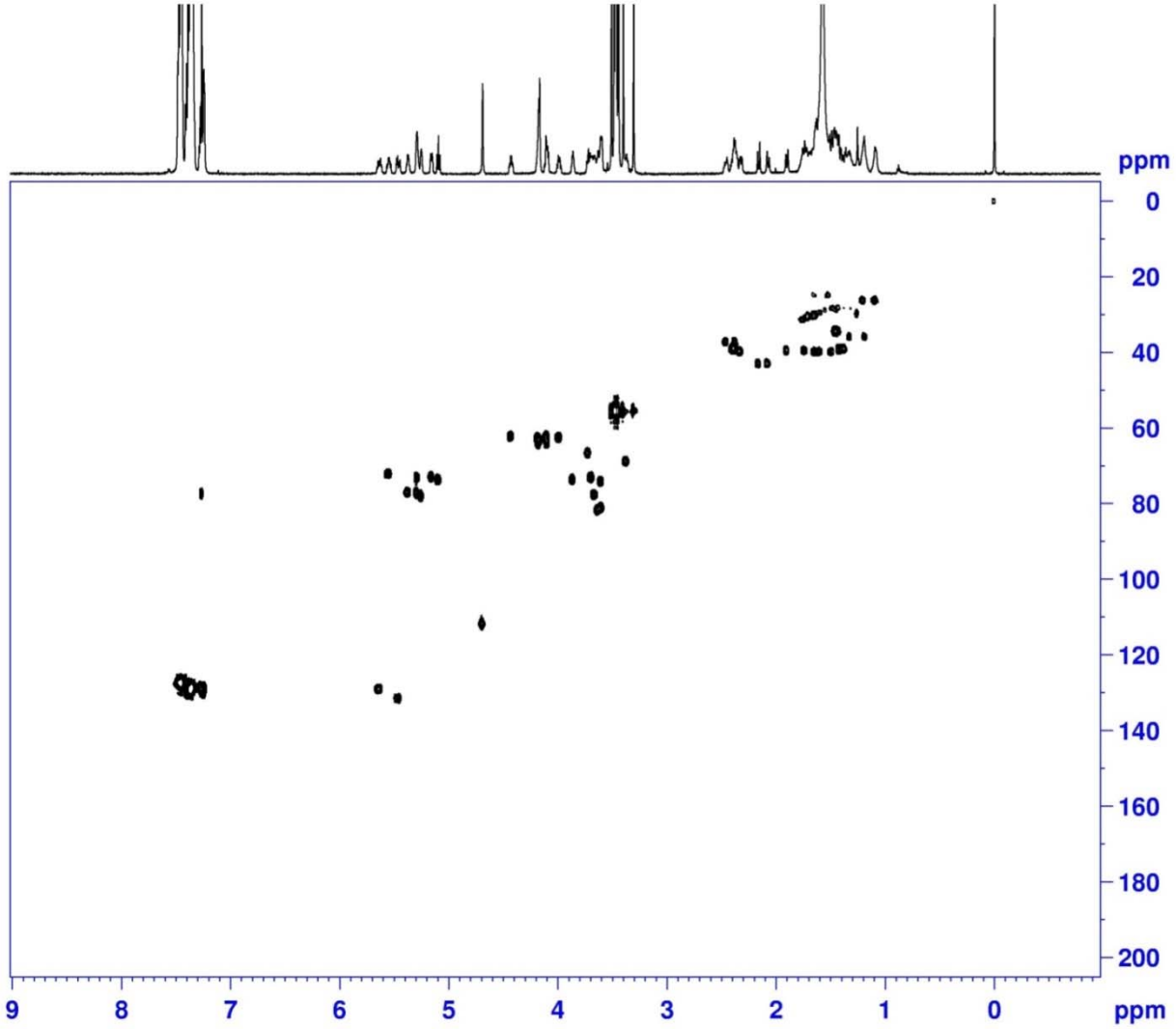

Figure S158. HSQC (700 MHz) spectrum of the fragment **1Ar** in $CDCl_3$

Mass Spectrum SmartFormula Report

Analysis Info

Analysis Name	D:\Data\MS\data\202008\liwanshan_b-R-cl_pos_15_01_8658.d	Acquisition Date	8/12/2020 4:33:49 PM
Method	LC_Direct Infusion_pos_100-3000mz.m	Operator	SCSIO
Sample Name	liwanshan_b-R-cl_pos	Instrument	maXis 255552.00029
Comment			

Acquisition Parameter

Source Type	ESI	Ion Polarity	Positive	Set Nebulizer	0.4 Bar
Focus	Active	Set Capillary	4500 V	Set Dry Heater	180 °C
Scan Begin	100 m/z	Set End Plate Offset	0 V	Set Dry Gas	4.0 l/min
Scan End	3500 m/z	Set Charging Voltage	0 V	Set Divert Valve	Waste
		Set Corona	0 nA	Set APCI Heater	0 °C

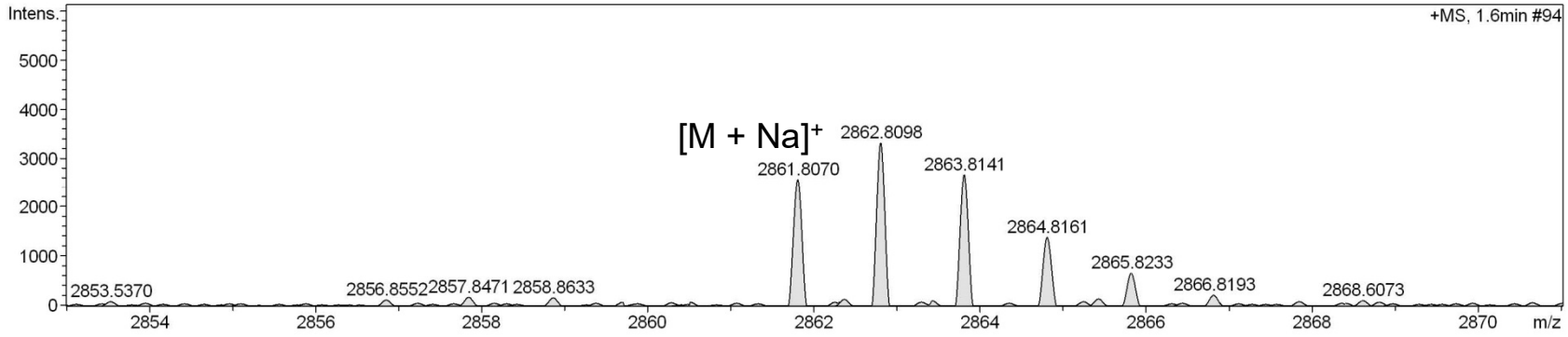

Meas. m/z	#	Ion Formula	Score	m/z	err [ppm]	err [mDa]	mSigma	rdb	e⁻ Conf	N-Rule
2861.8070	1	C134H132F30NaO33	100.00	2861.8064	0.2	0.6	36.9	53.5	even	ok

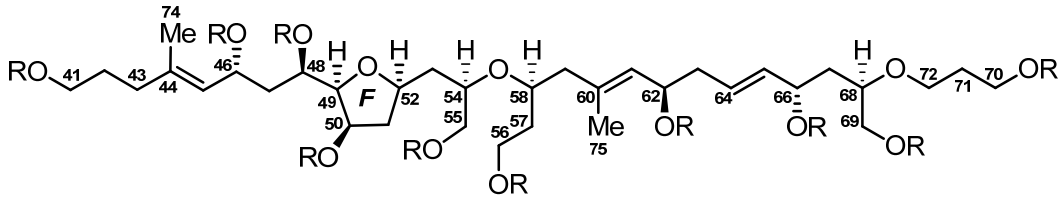

R = (*S*)-MTPA

Figure S159. HR-ESIMS for the fragment **1Bs**

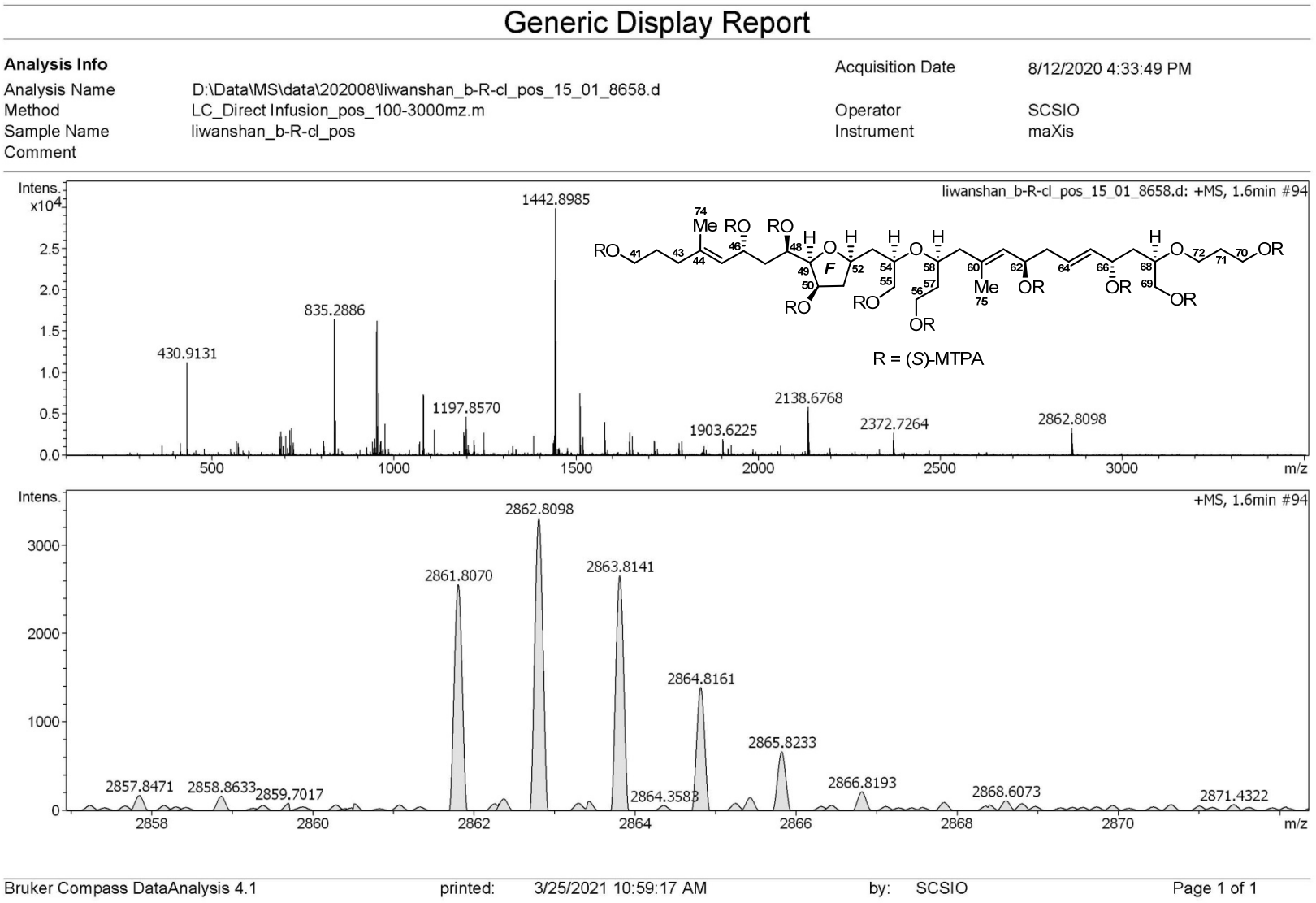

Figure S160. HR-ESIMS for the fragment **1Bs**

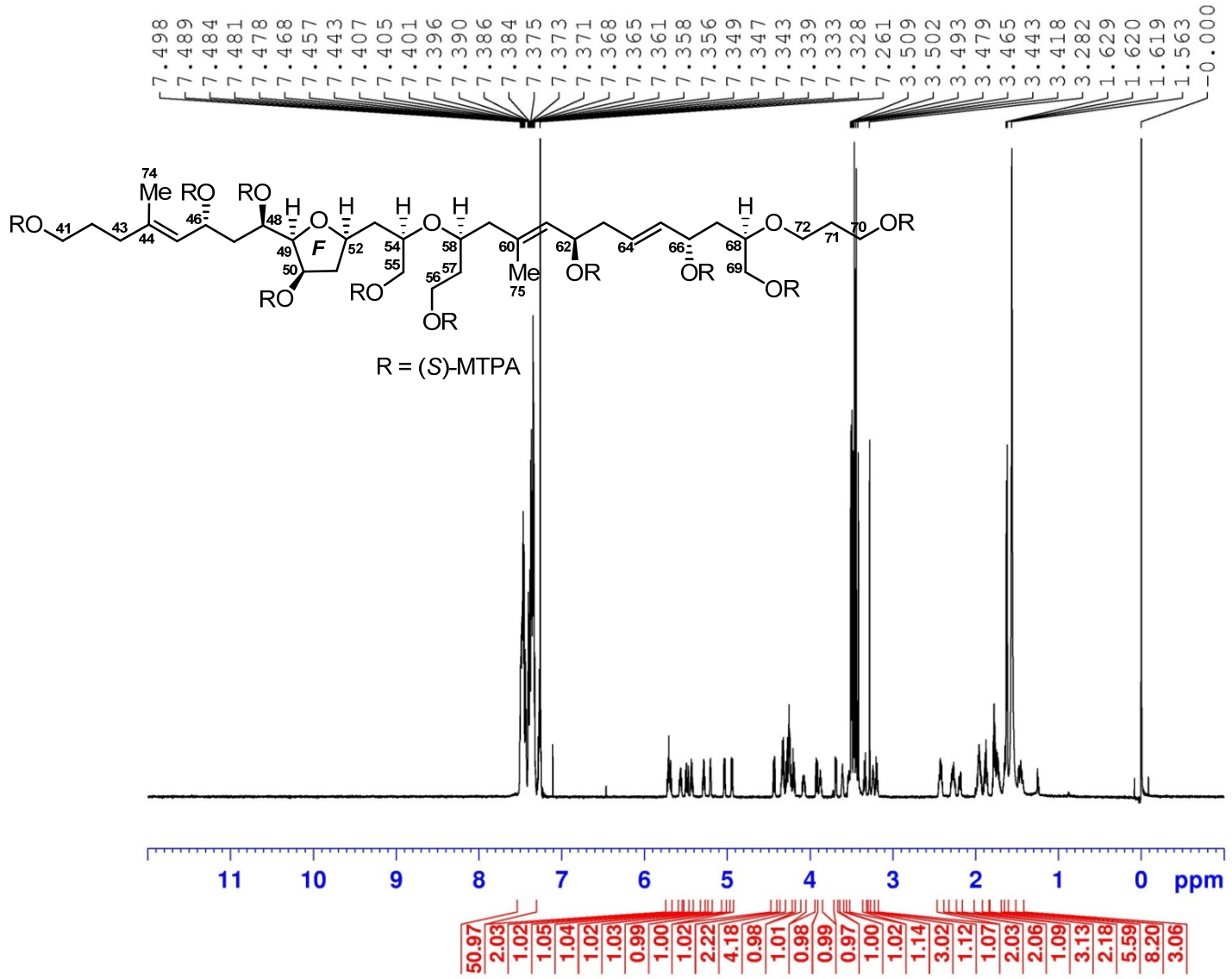

Figure S161. ^{1}H (700 MHz) NMR spectrum of the fragment **1Bs** in $CDCl_3$

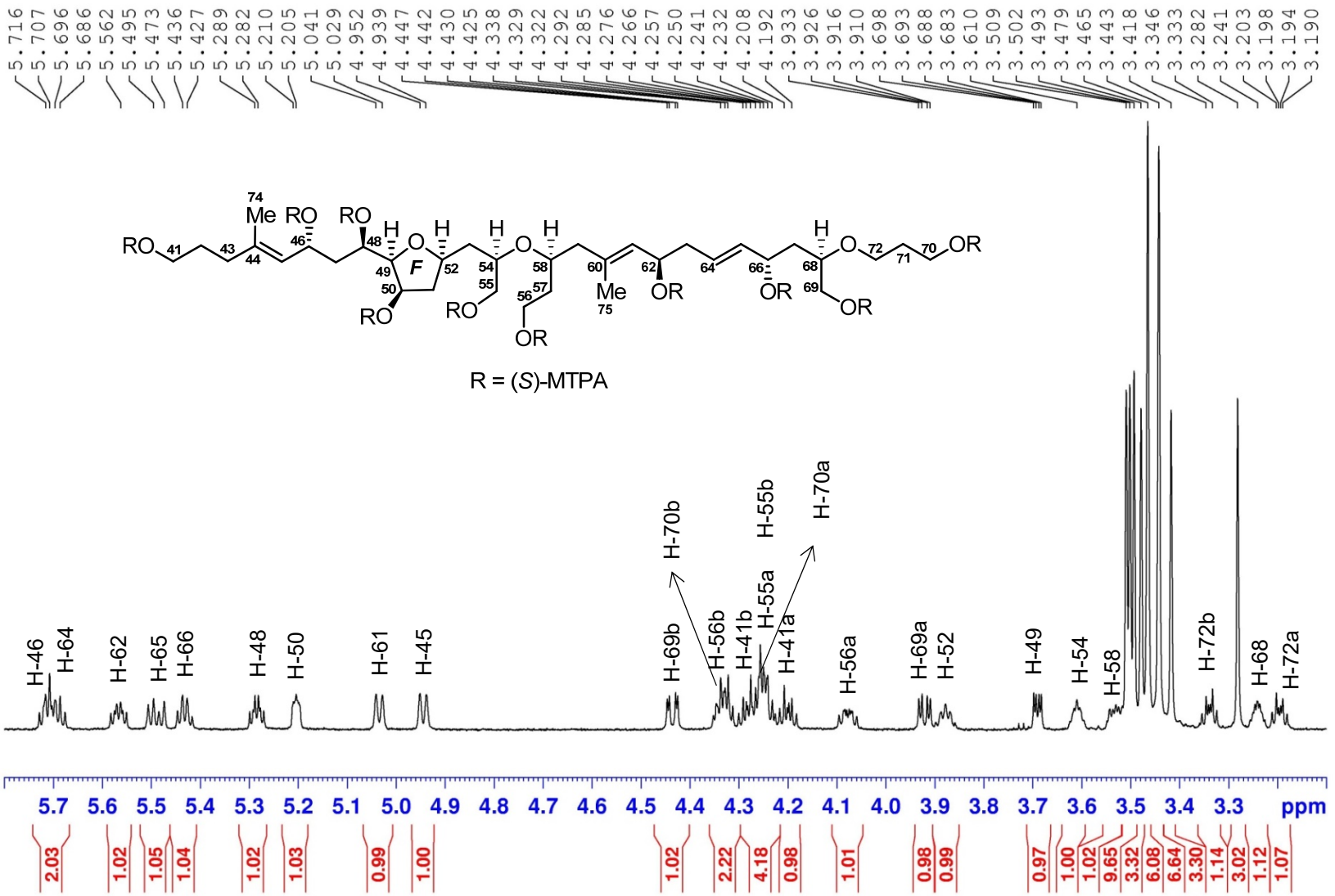

Figure S162. ^{1}H (700 MHz) NMR spectrum of the fragment **1Bs** in $CDCl_3$

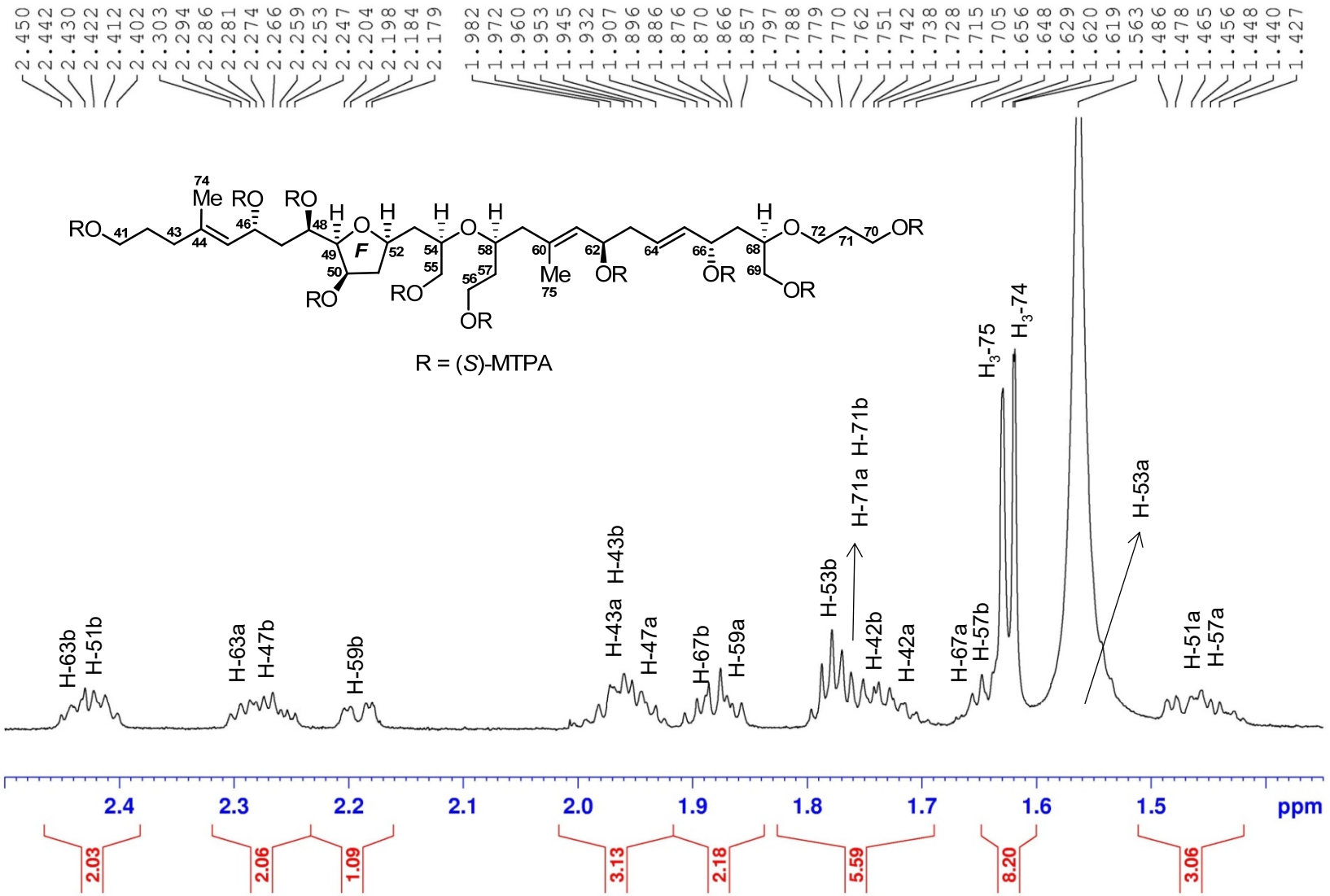

Figure S163. ^{1}H (700 MHz) NMR spectrum of the fragment **1Bs** in $CDCl_3$

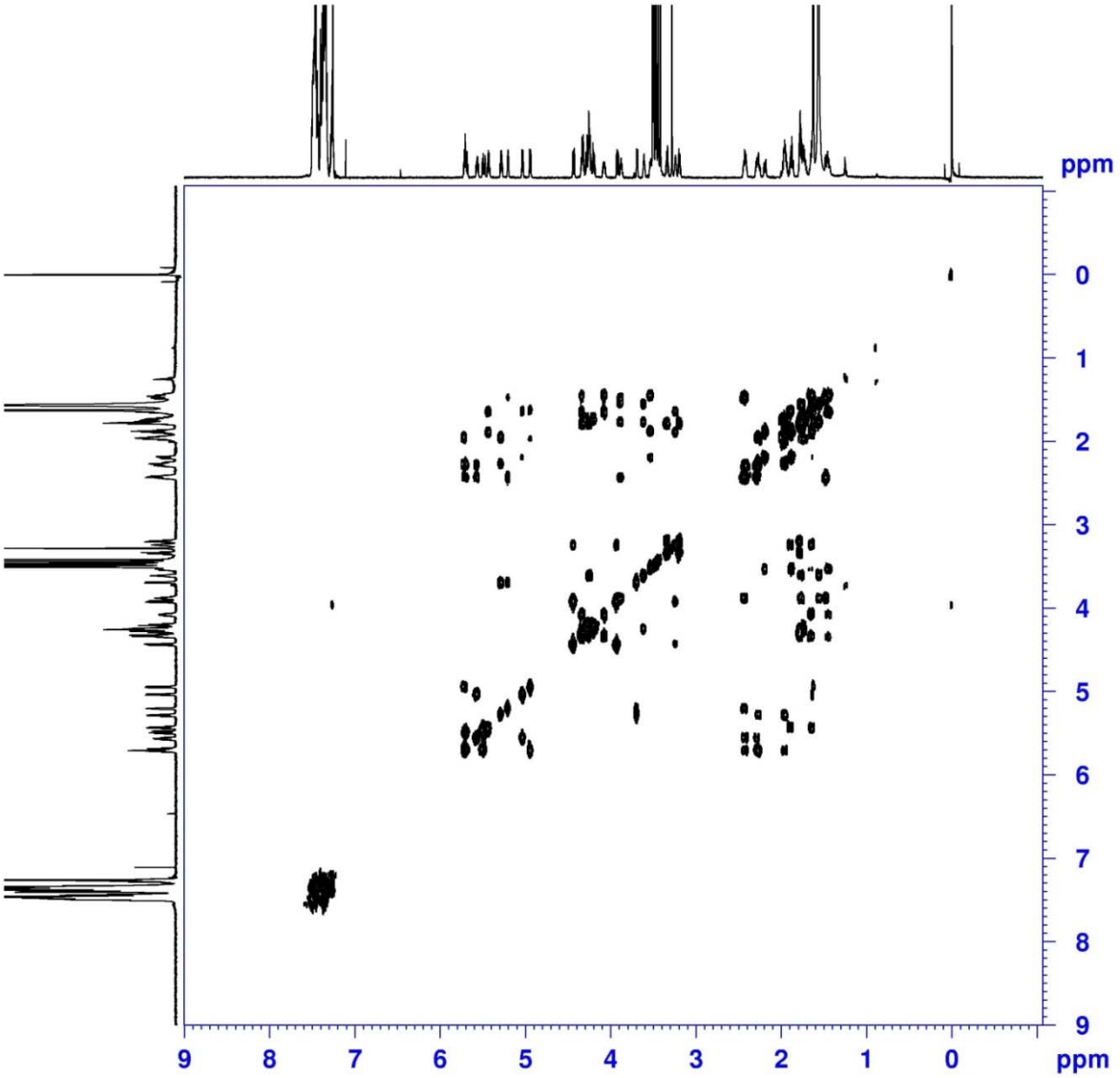

Figure S164. ^{1}H–^{1}H COSY (700 MHz) spectrum of the fragment **1Bs** in $CDCl_3$

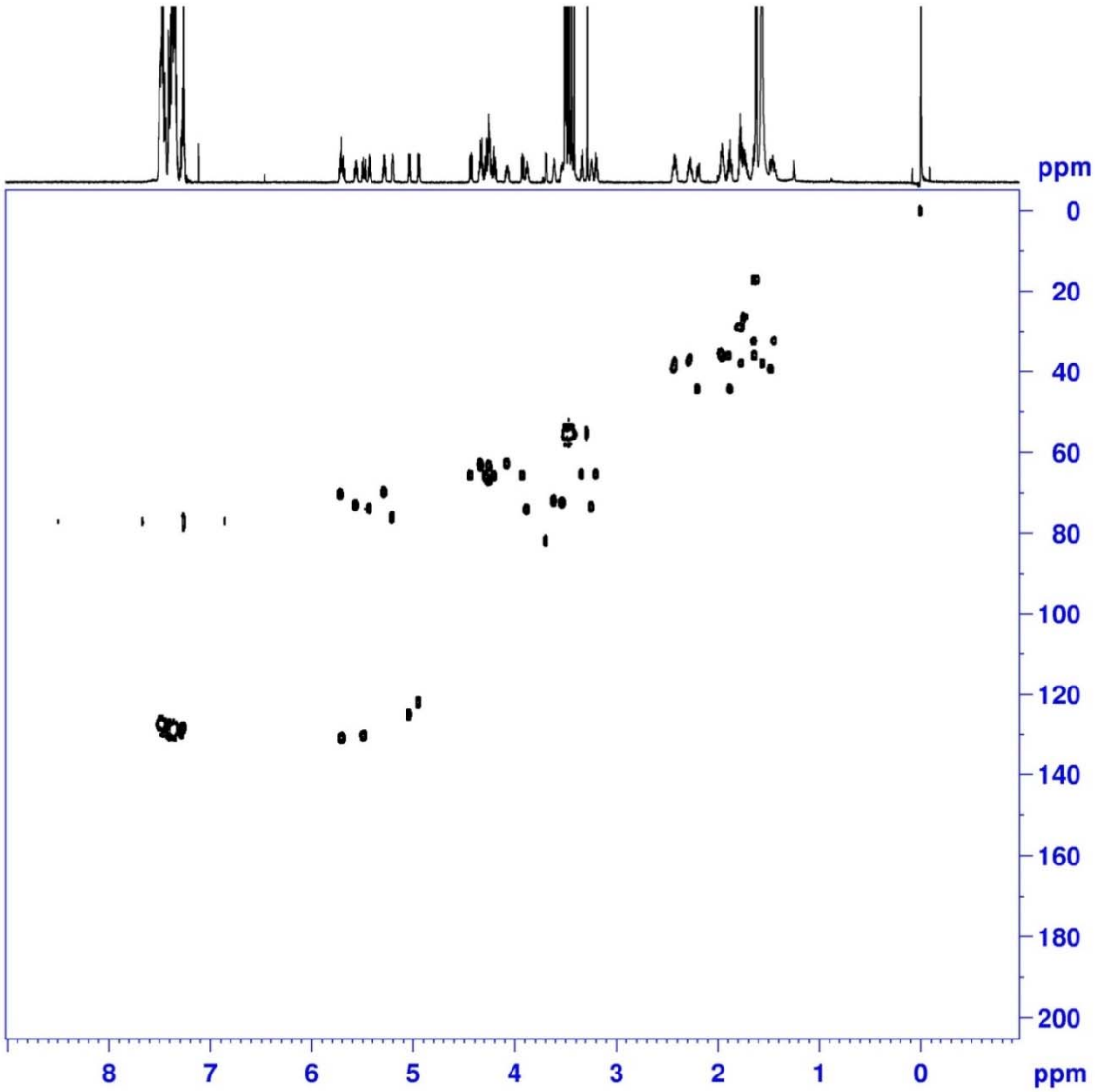

Figure S165. HSQC (700 MHz) spectrum of the fragment **1Bs** in $CDCl_3$

Mass Spectrum SmartFormula Report

Analysis Info

Analysis Name	D:\Data\MS\data\202008\liwanshan_b-S-cl_pos_14_01_8657.d	Acquisition Date	8/12/2020 4:30:22 PM
Method	LC_Direct Infusion_pos_100-3000mz.m	Operator	SCSIO
Sample Name	liwanshan_b-S-cl_pos	Instrument	maXis 255552.00029
Comment			

Acquisition Parameter

Source Type	ESI	Ion Polarity	Positive	Set Nebulizer	0.4 Bar
Focus	Active	Set Capillary	4500 V	Set Dry Heater	180 °C
Scan Begin	100 m/z	Set End Plate Offset	0 V	Set Dry Gas	4.0 l/min
Scan End	3500 m/z	Set Charging Voltage	0 V	Set Divert Valve	Waste
		Set Corona	0 nA	Set APCI Heater	0 °C

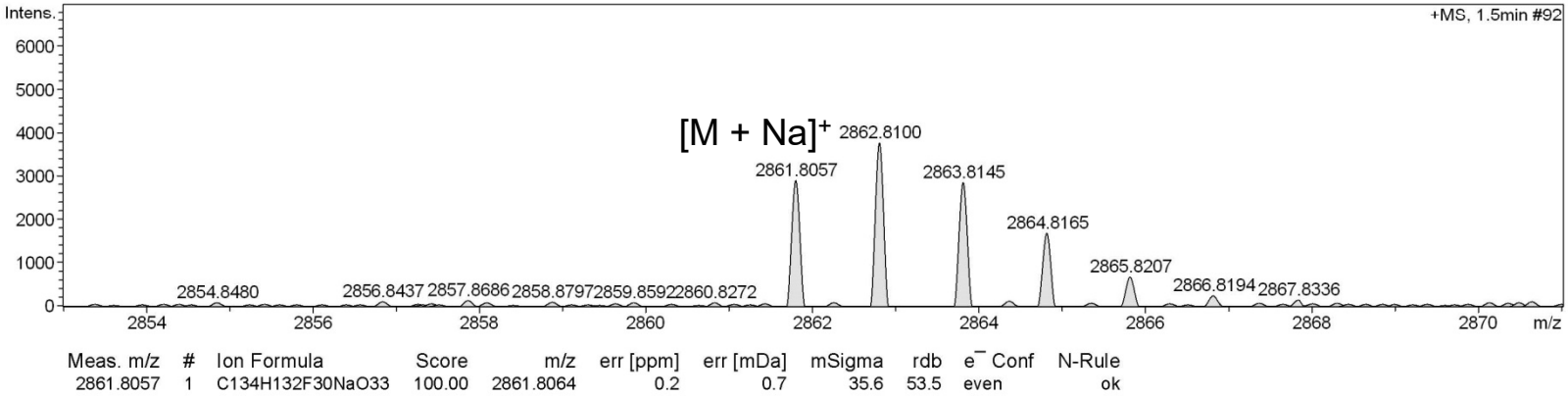

Meas. m/z	#	Ion Formula	Score	m/z	err [ppm]	err [mDa]	mSigma	rdb	e⁻ Conf	N-Rule
2861.8057	1	C134H132F30NaO33	100.00	2861.8064	0.2	0.7	35.6	53.5	even	ok

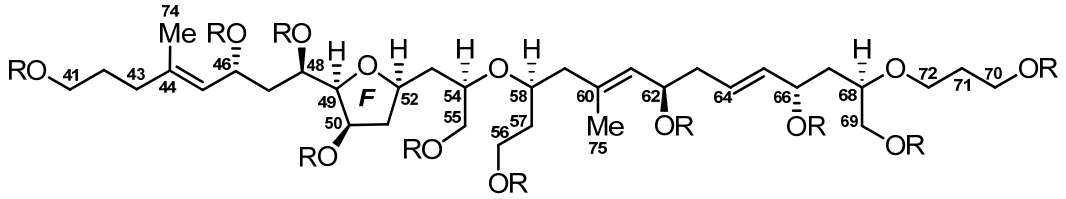

R = (*R*)-MTPA

Figure S166. HR-ESIMS for the fragment **1Br**

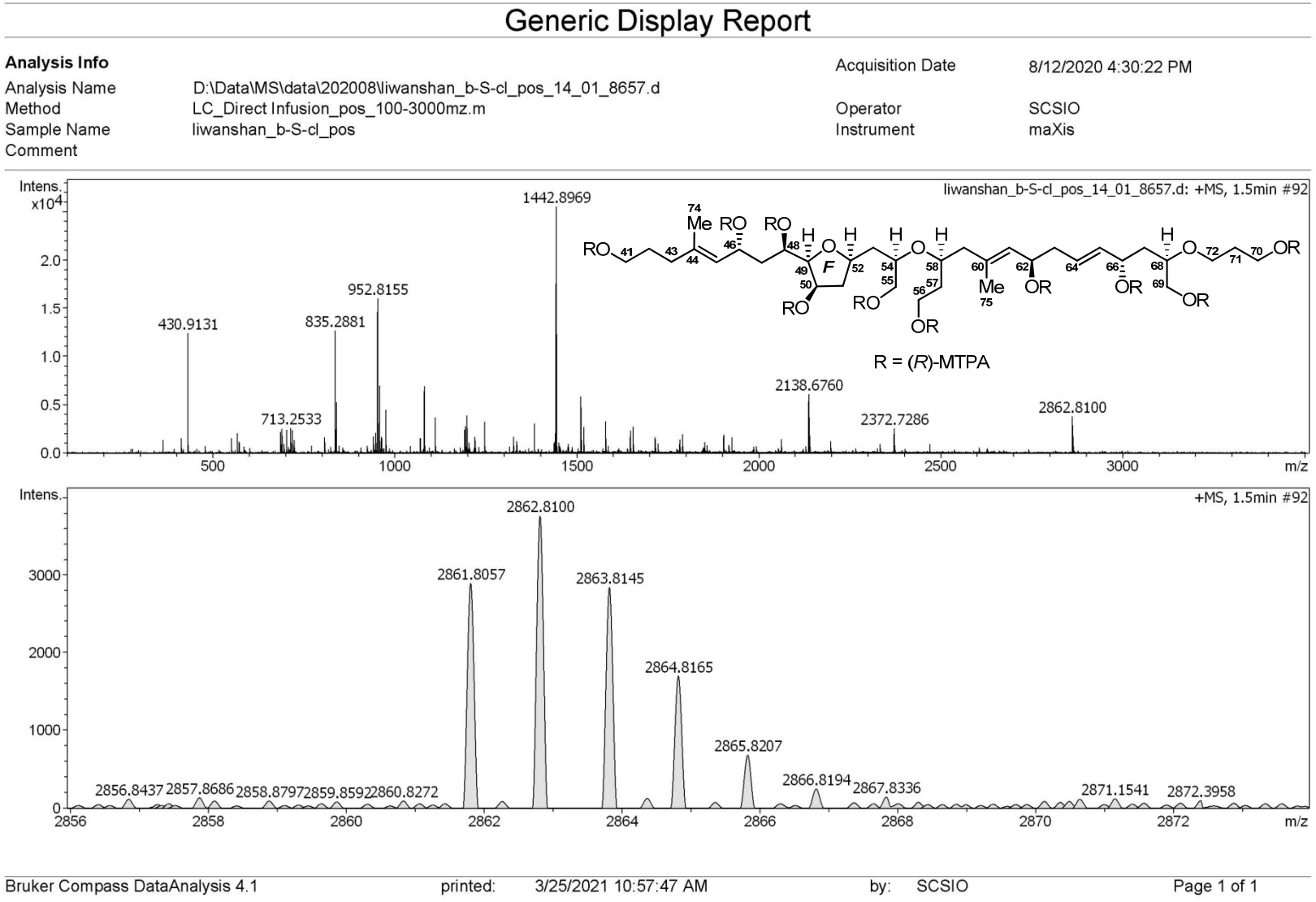

Figure S167. HR–ESIMS for the fragment **1Br**

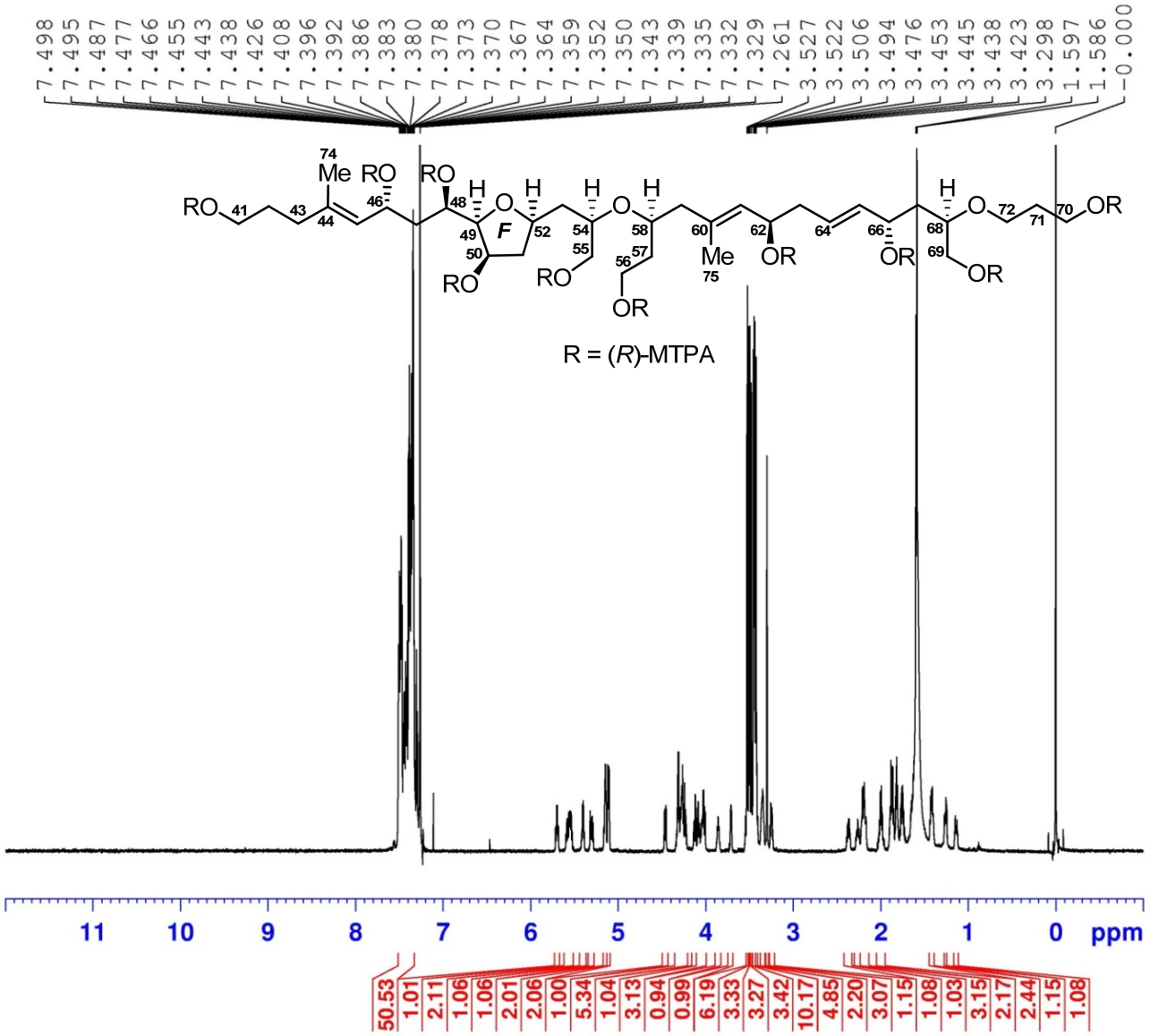

Figure S168. ^{1}H (700 MHz) NMR spectrum of the fragment **1Br** in $CDCl_3$

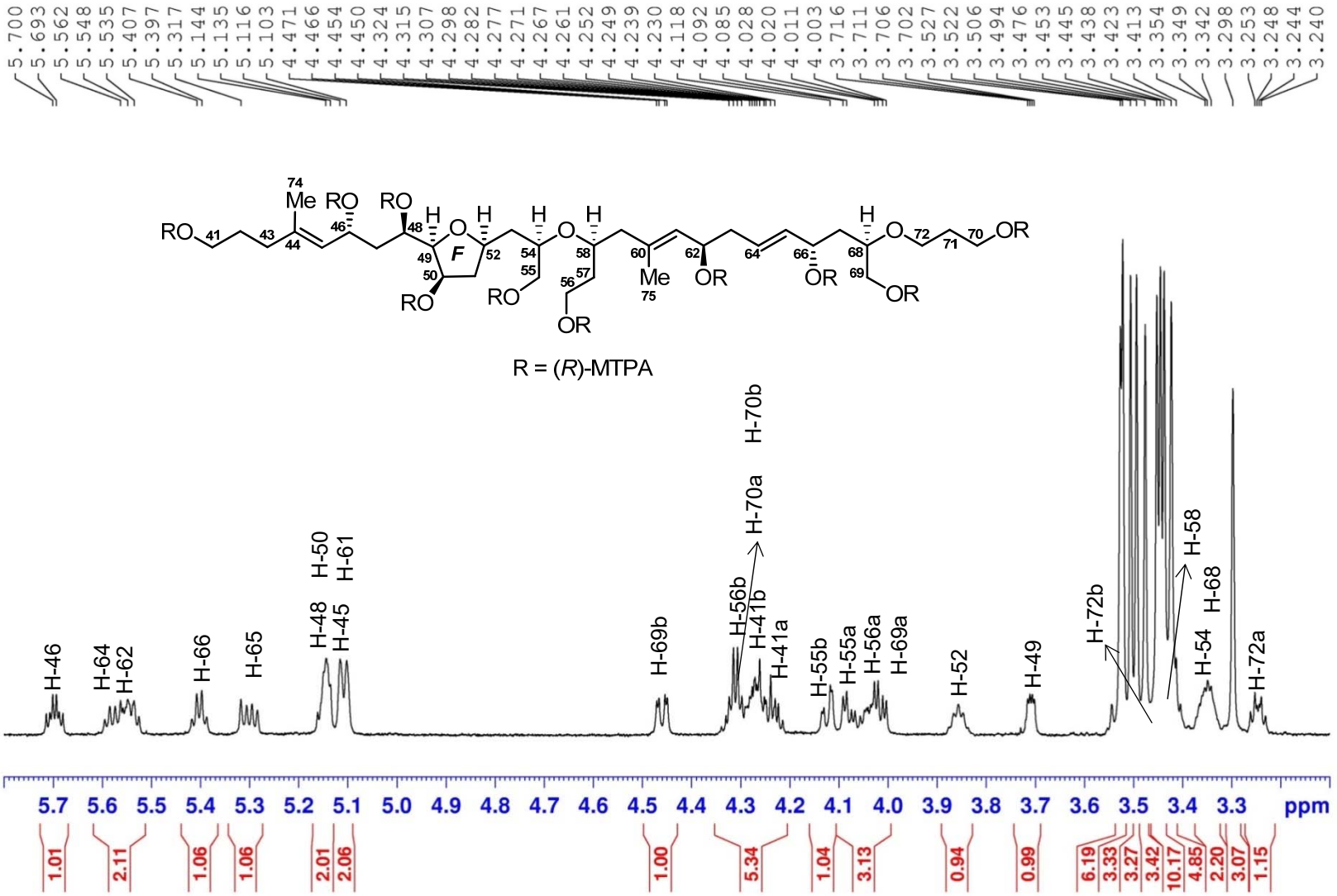

Figure S169. ^{1}H (700 MHz) NMR spectrum of the fragment **1Br** in $CDCl_3$

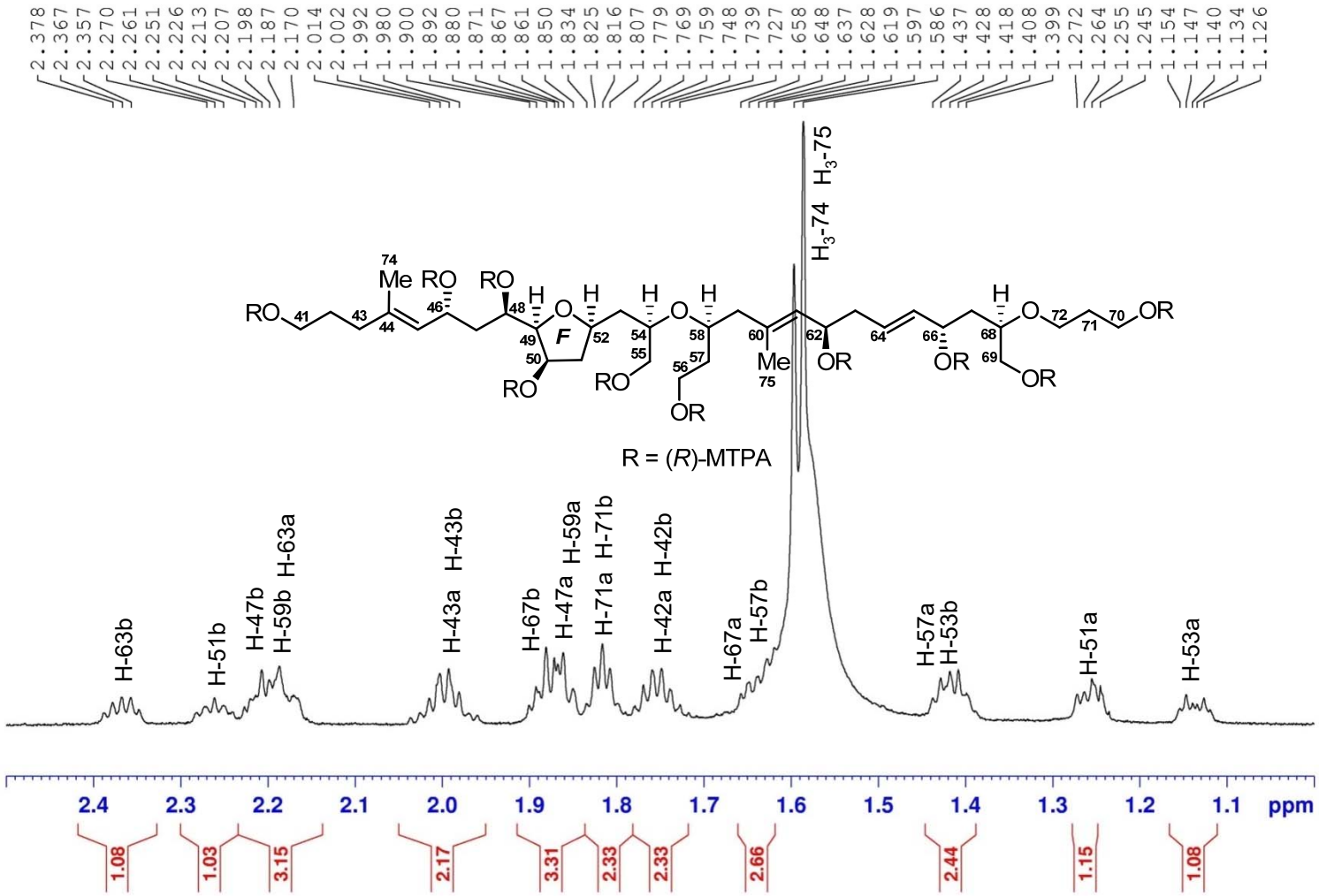

Figure S170. ^{1}H (700 MHz) NMR spectrum of the fragment **1Br** in $CDCl_3$

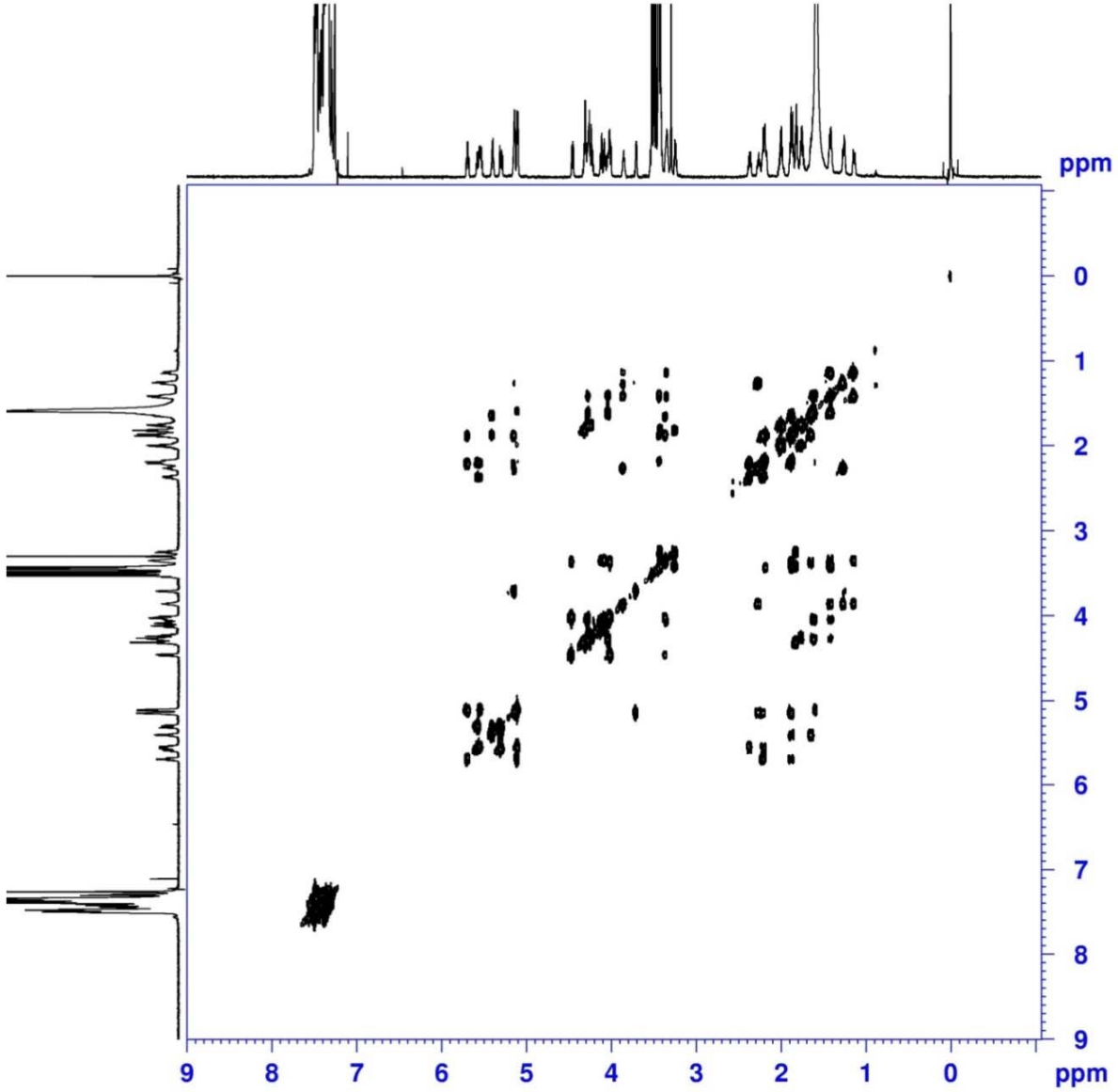

Figure S171. ^{1}H–^{1}H COSY (700 MHz) spectrum of the fragment **1Br** in $CDCl_3$

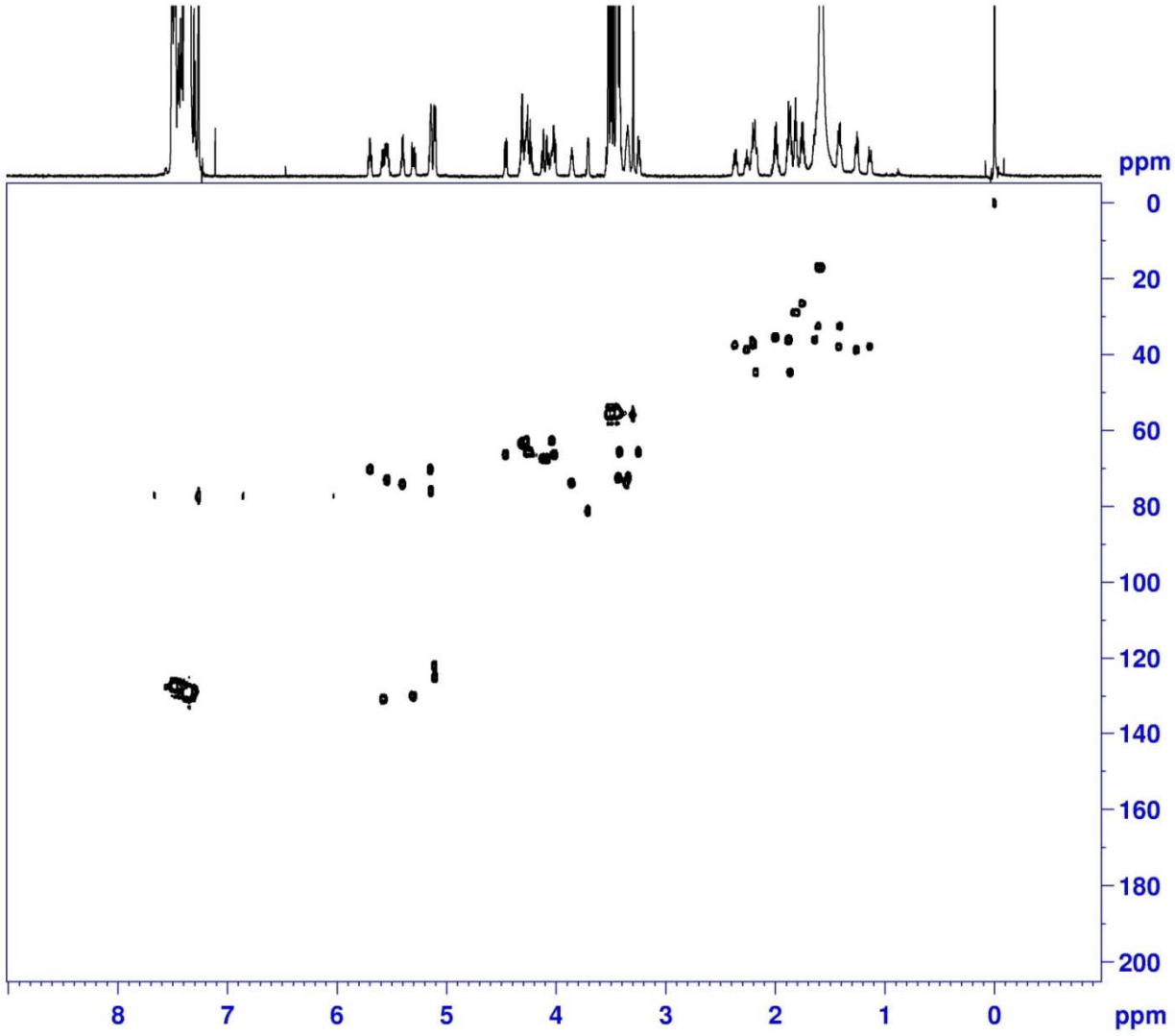

Figure S172. HSQC (700 MHz) spectrum of the fragment **1Br** in $CDCl_3$

Mass Spectrum SmartFormula Report

Analysis Info

Analysis Name	D:\Data\MS\data\202103\yuyi_AX-1-03-3-R_pos_4_01_10273.d	Acquisition Date	3/29/2021 3:14:17 PM
Method	LC_Direct Infusion_pos_100-3000mz.m	Operator	SCSIO
Sample Name	yuyi_AX-1-03-3-R_pos	Instrument	maXis 255552.00029
Comment			

Acquisition Parameter

Source Type	ESI	Ion Polarity	Positive	Set Nebulizer	0.4 Bar
Focus	Active	Set Capillary	4500 V	Set Dry Heater	180 °C
Scan Begin	100 m/z	Set End Plate Offset	0 V	Set Dry Gas	4.0 l/min
Scan End	3500 m/z	Set Charging Voltage	0 V	Set Divert Valve	Waste
		Set Corona	0 nA	Set APCI Heater	0 °C

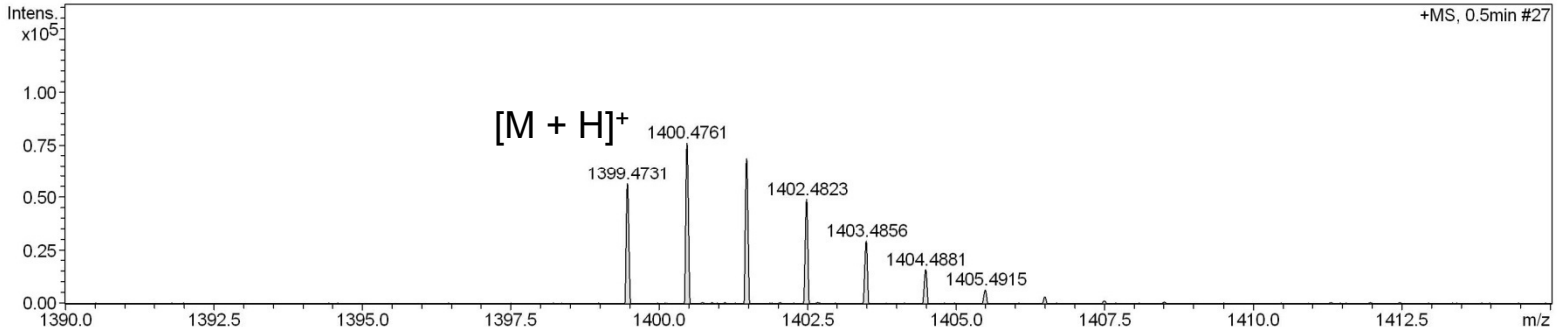

Meas. m/z	#	Ion Formula	Score	m/z	err [ppm]	err [mDa]	mSigma	rdb	e⁻ Conf	N-Rule
1399.4731	1	C66H75F12O19	100.00	1399.4705	1.8	2.6	405.8	23.5	even	ok

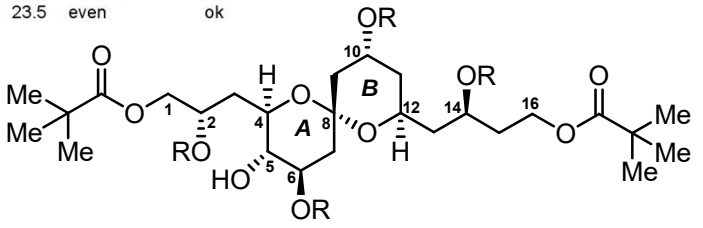

R = (*S*)-MTPA

yuyi_AX-1-03-3-R_pos_4_01_10273.d

Bruker Compass DataAnalysis 4.1 printed: 3/29/2021 3:20:44 PM by: SCSIO Page 1 of 1

Figure S173. HR-ESIMS for the fragment **1as**

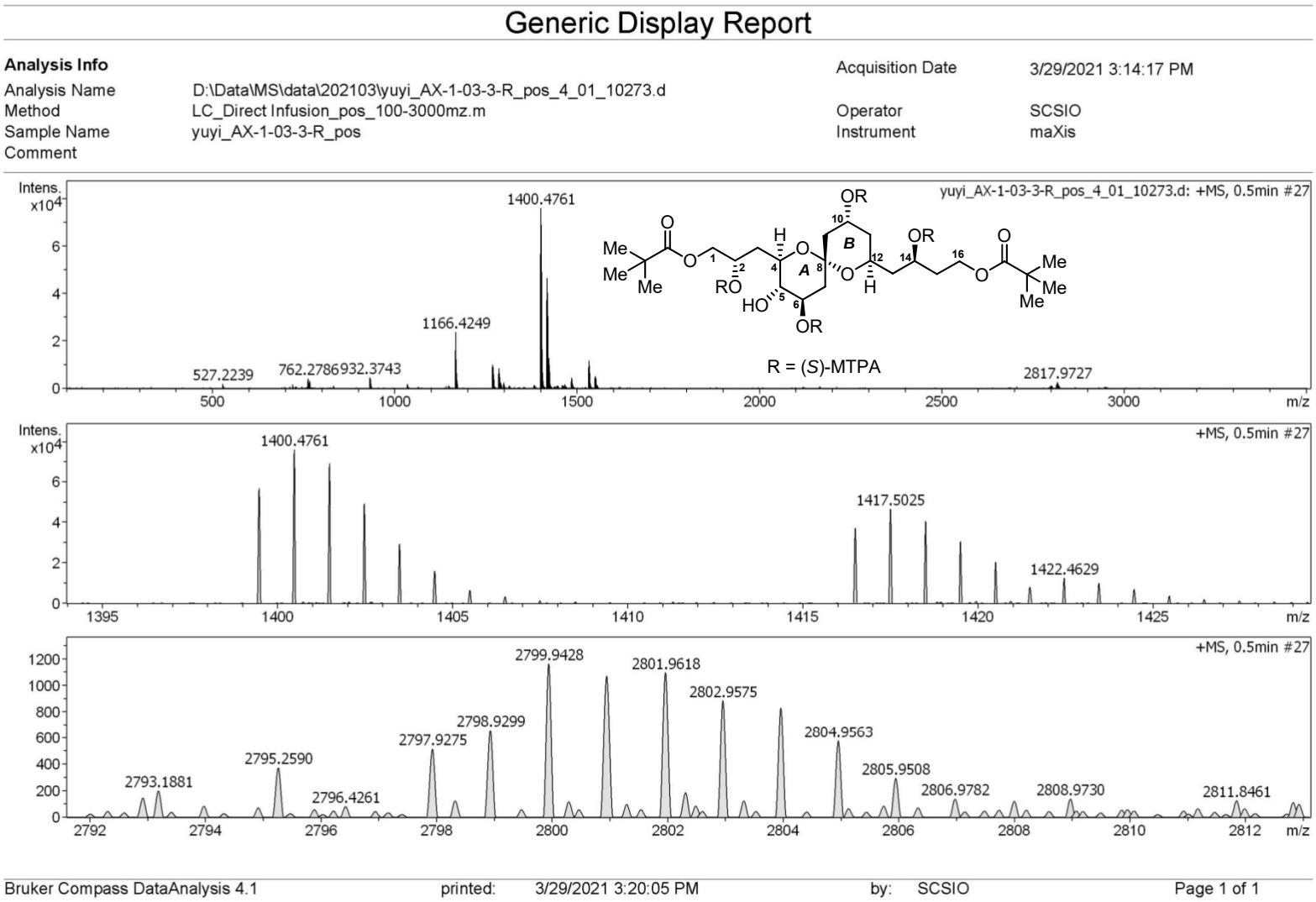

Figure S174. HR-ESIMS for the fragment **1as**

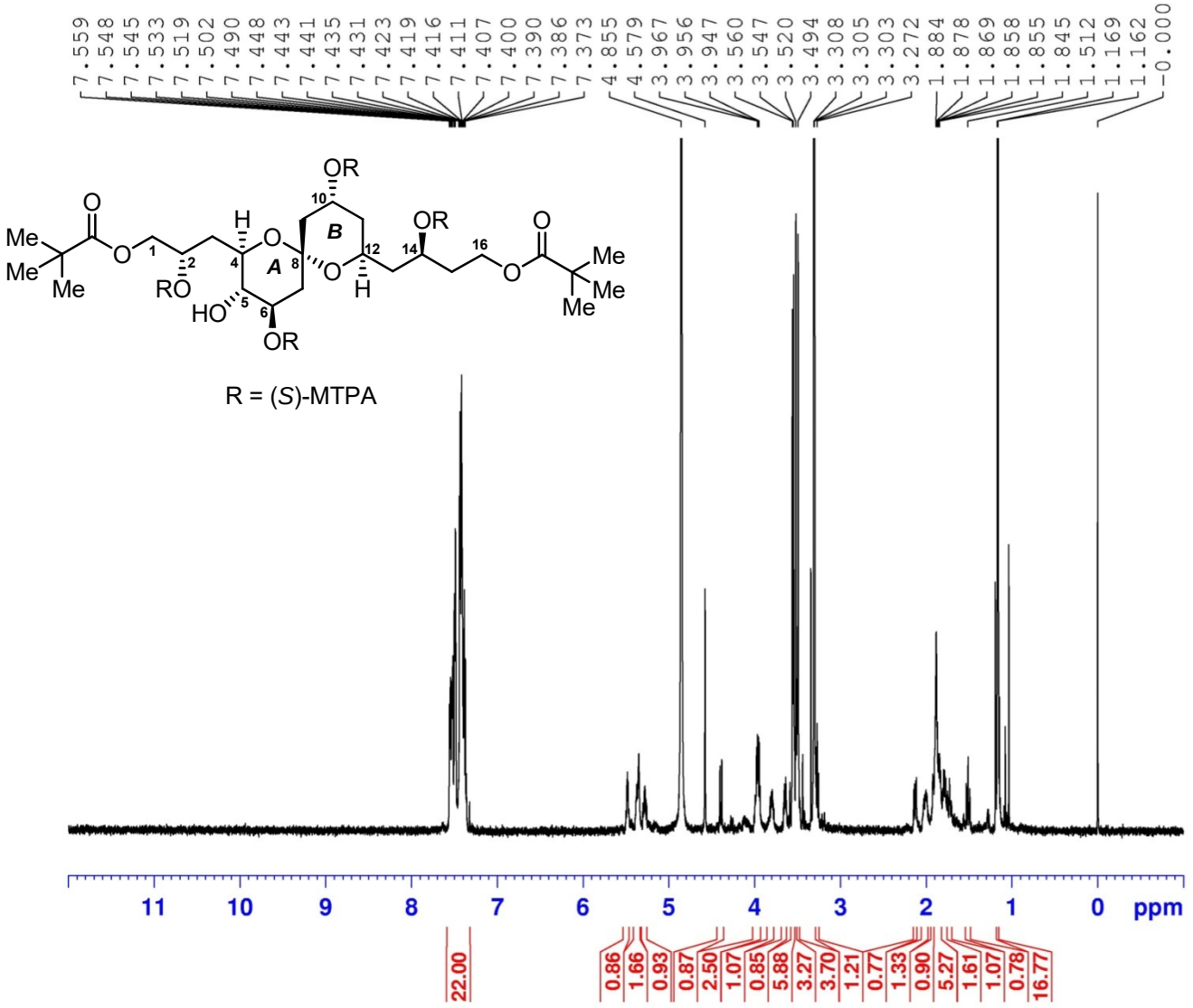

Figure S175. ^{1}H (600 MHz) NMR spectrum of the fragment **1as** in CD_3OD

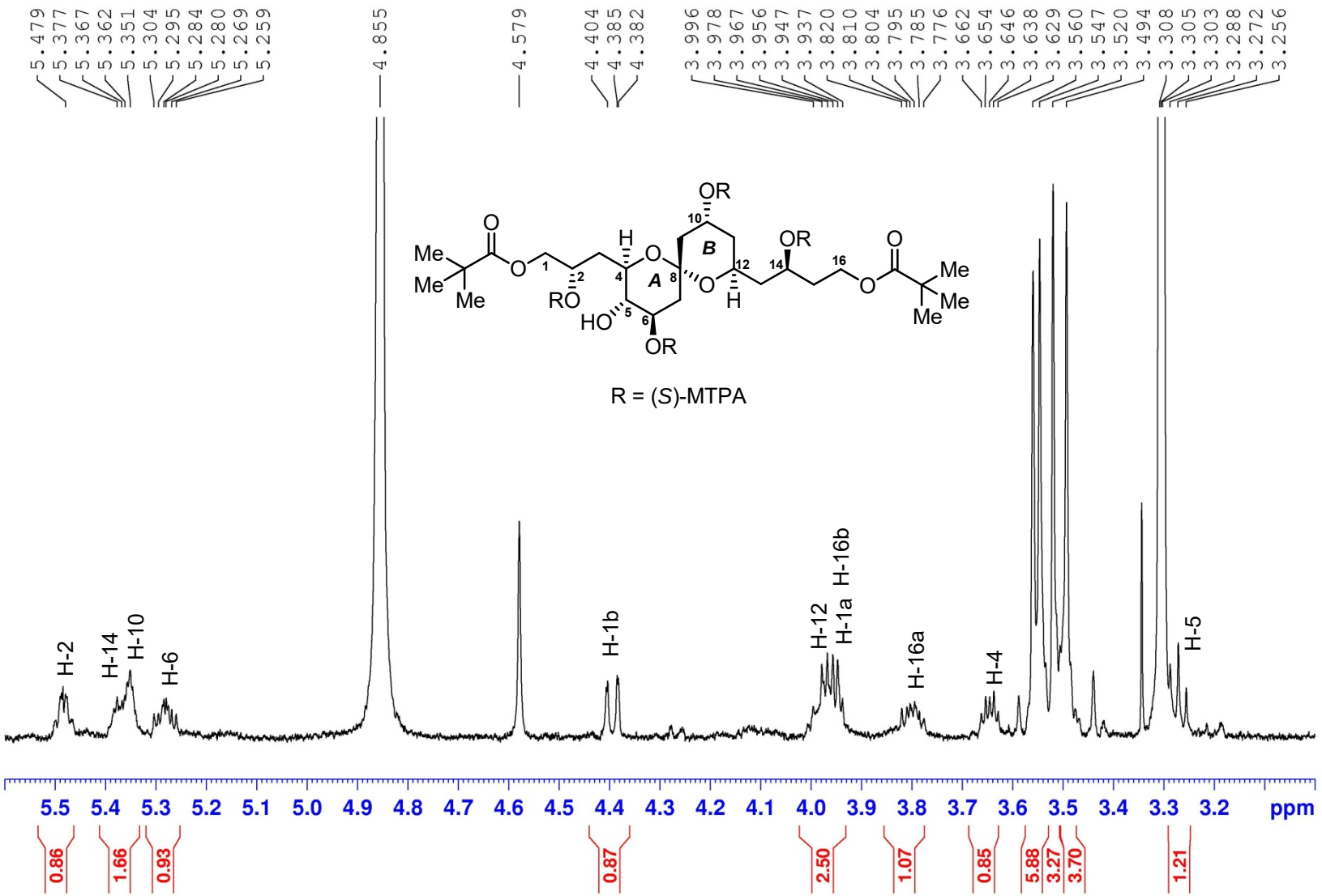

Figure S176. ^{1}H (600 MHz) NMR spectrum of the fragment **1as** in CD_3OD

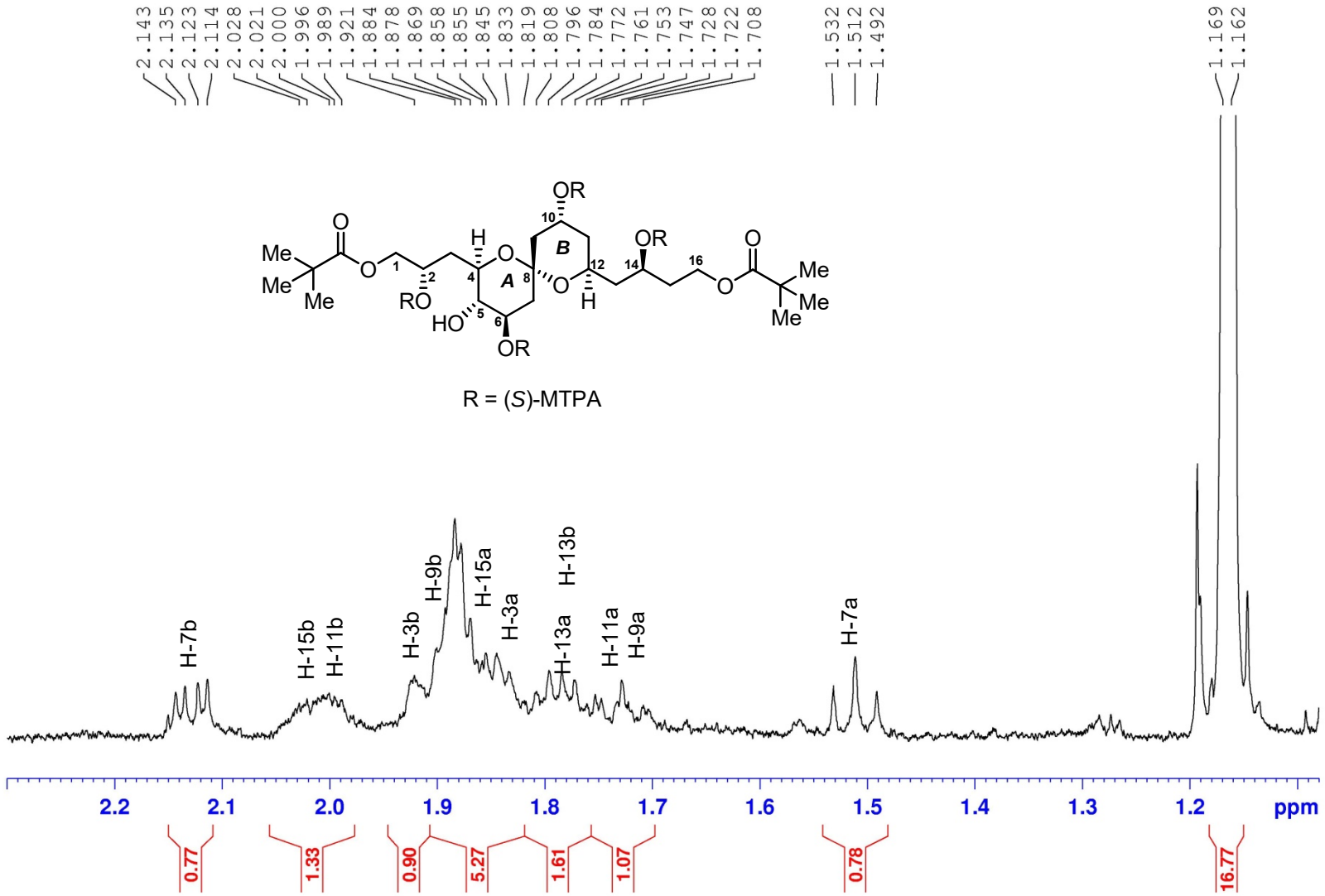

Figure S177. ^{1}H (600 MHz) NMR spectrum of the fragment **1as** in CD_3OD

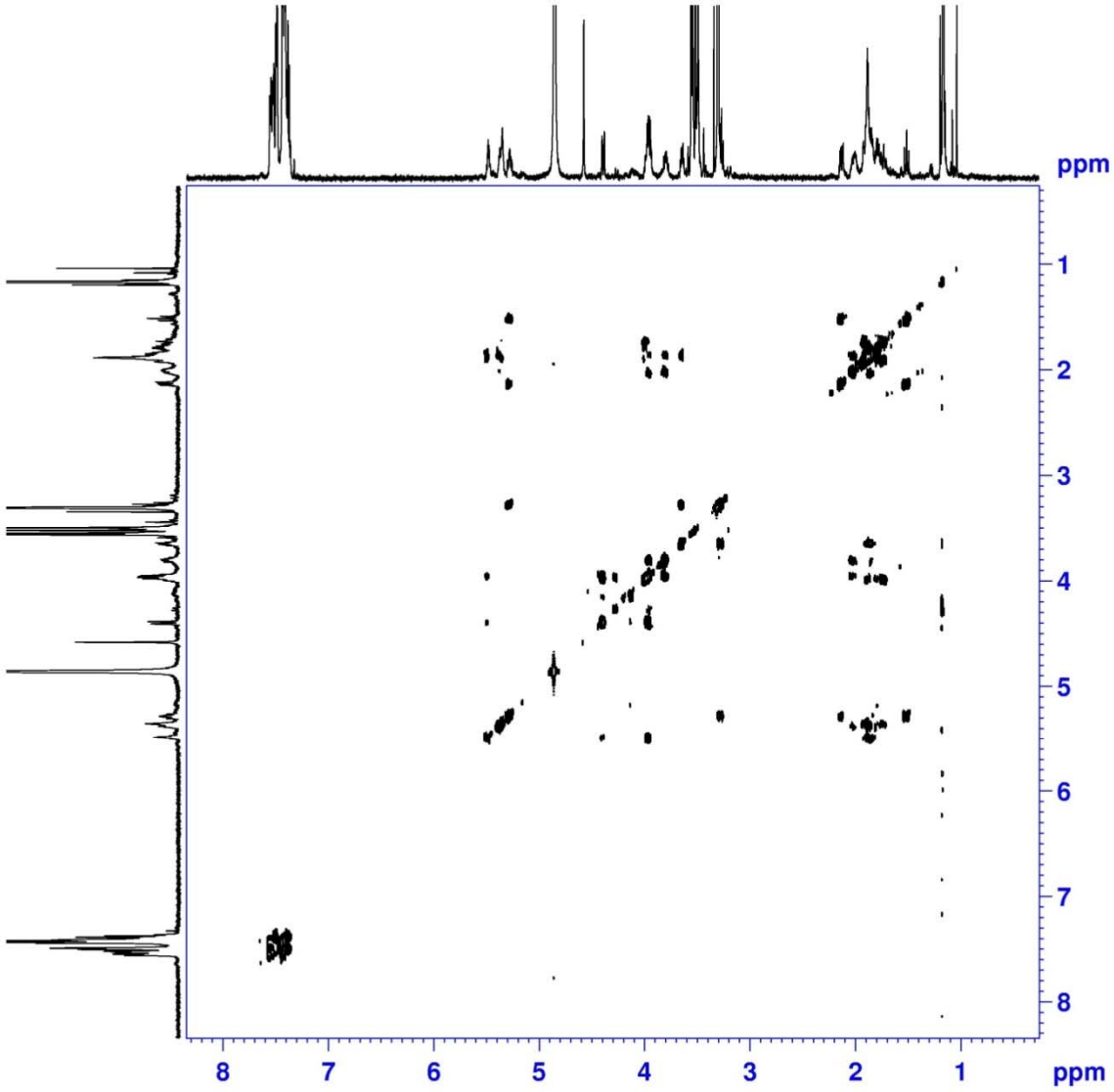

Figure S178. $^{1}H–^{1}H$ COSY (600 MHz) spectrum of the fragment **1as** in CD_3OD

Mass Spectrum SmartFormula Report

Analysis Info

Analysis Name	D:\Data\MS\data\202103\yuyi_AX-1-03-3-S_pos_5_01_10274.d	Acquisition Date	3/29/2021 3:17:46 PM
Method	LC_Direct Infusion_pos_100-3000mz.m	Operator	SCSIO
Sample Name	yuyi_AX-1-03-3-S_pos	Instrument	maXis 255552.00029
Comment			

Acquisition Parameter

Source Type	ESI	Ion Polarity	Positive	Set Nebulizer	0.4 Bar
Focus	Active	Set Capillary	4500 V	Set Dry Heater	180 °C
Scan Begin	100 m/z	Set End Plate Offset	0 V	Set Dry Gas	4.0 l/min
Scan End	3500 m/z	Set Charging Voltage	0 V	Set Divert Valve	Waste
		Set Corona	0 nA	Set APCI Heater	0 °C

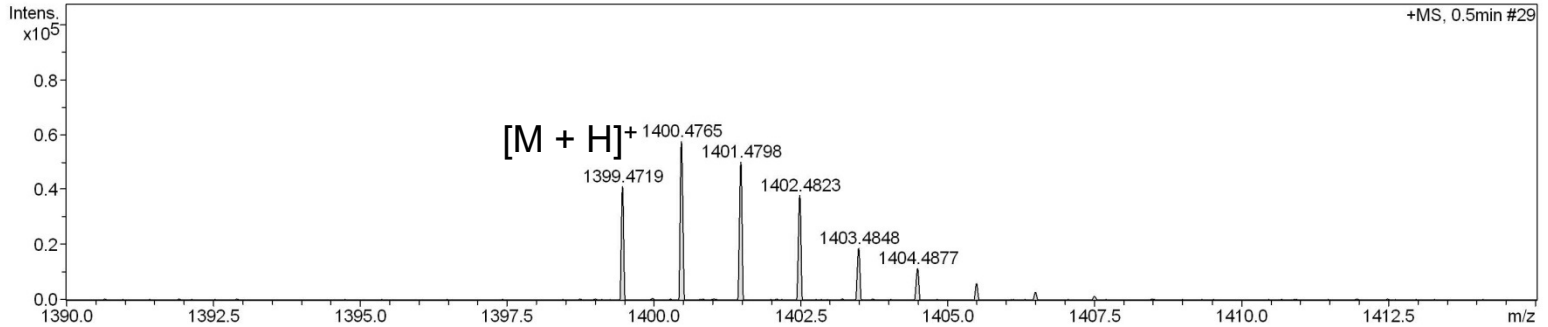

Meas. m/z	#	Ion Formula	Score	m/z	err [ppm]	err [mDa]	mSigma	rdb	e⁻ Conf	N-Rule
1399.4719	1	C66H75F12O19	100.00	1399.4705	-1.0	-1.4	393.2	23.5	even	ok

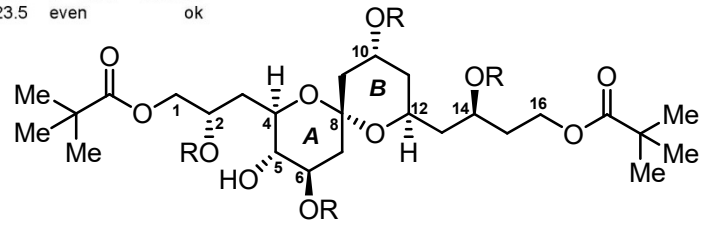

R = (*R*)-MTPA

Figure S179. HR-ESIMS for the fragment **1ar**

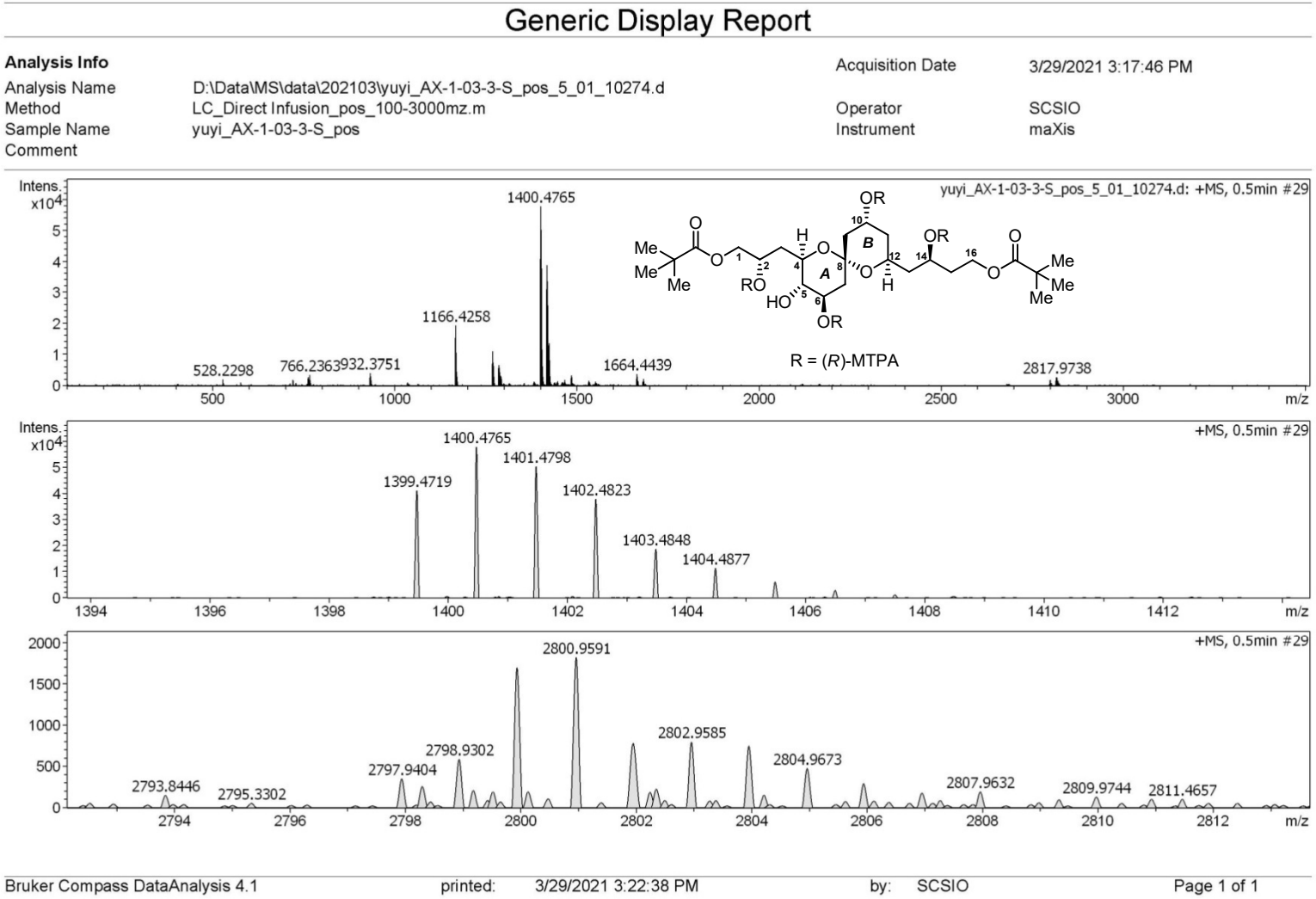

Figure S180. HR-ESIMS for the fragment **1ar**

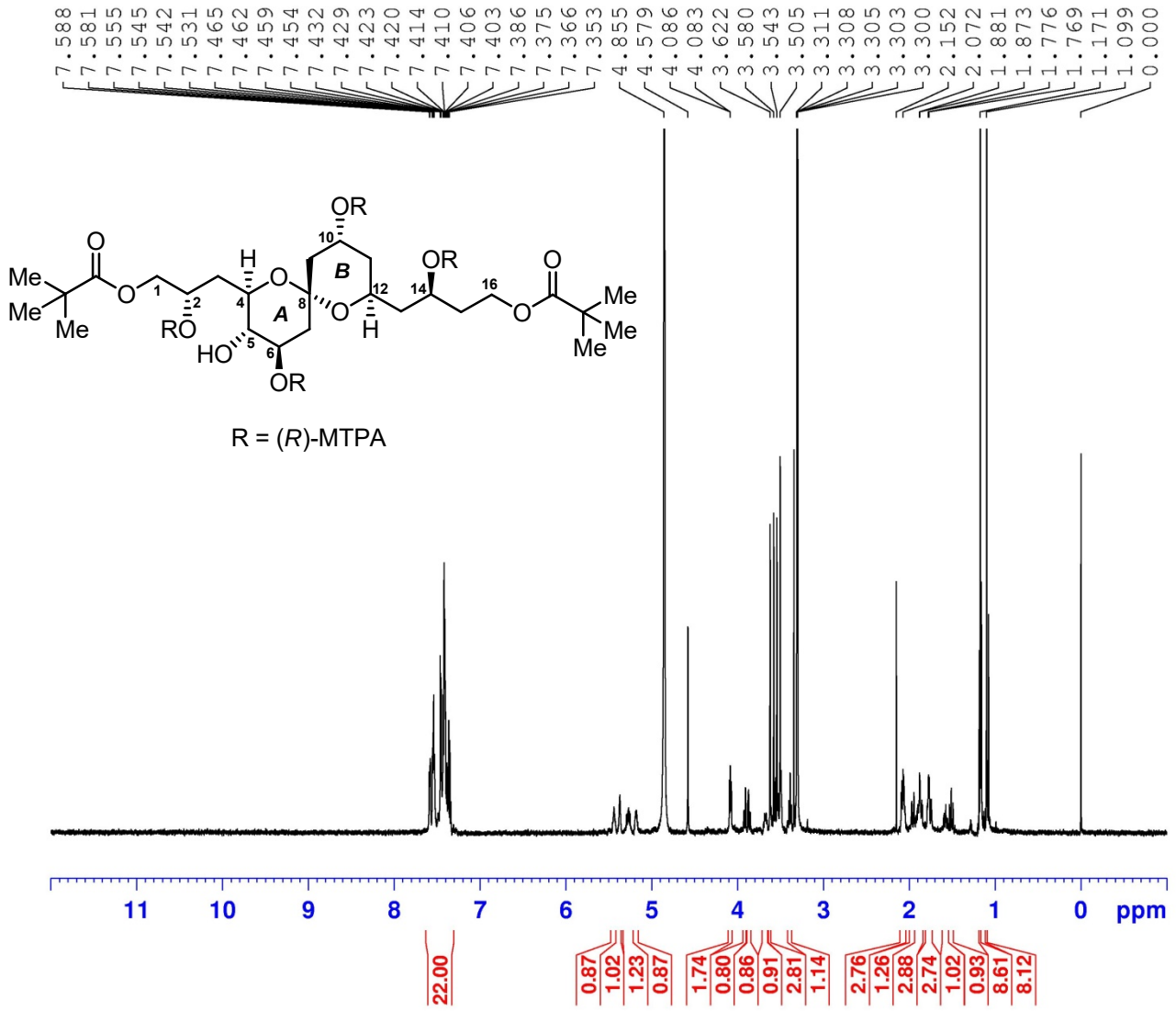

Figure S181. ^{1}H (600 MHz) NMR spectrum of the fragment **1ar** in CD_3OD

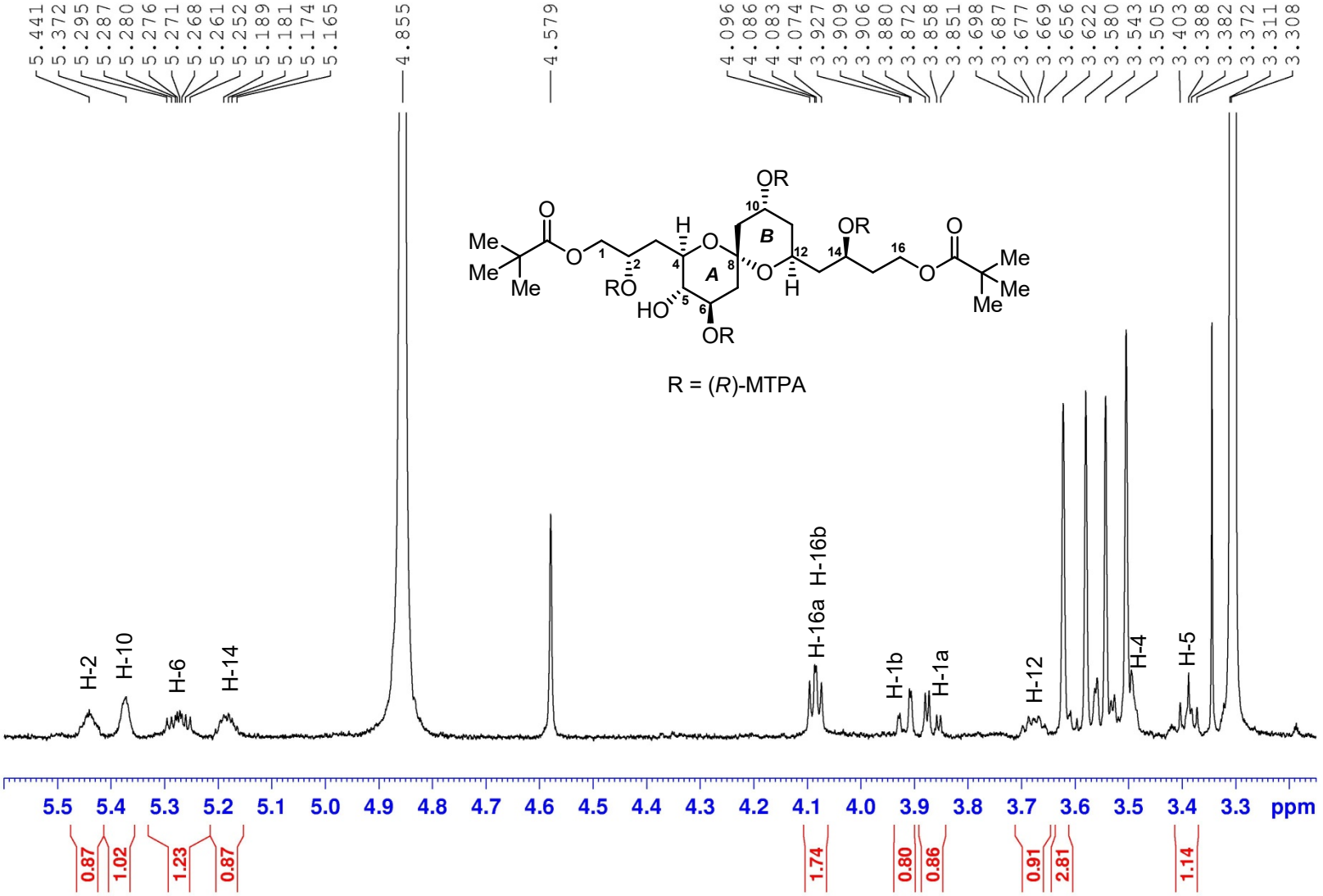

Figure S182. ^{1}H (600 MHz) NMR spectrum of the fragment **1ar** in CD_3OD

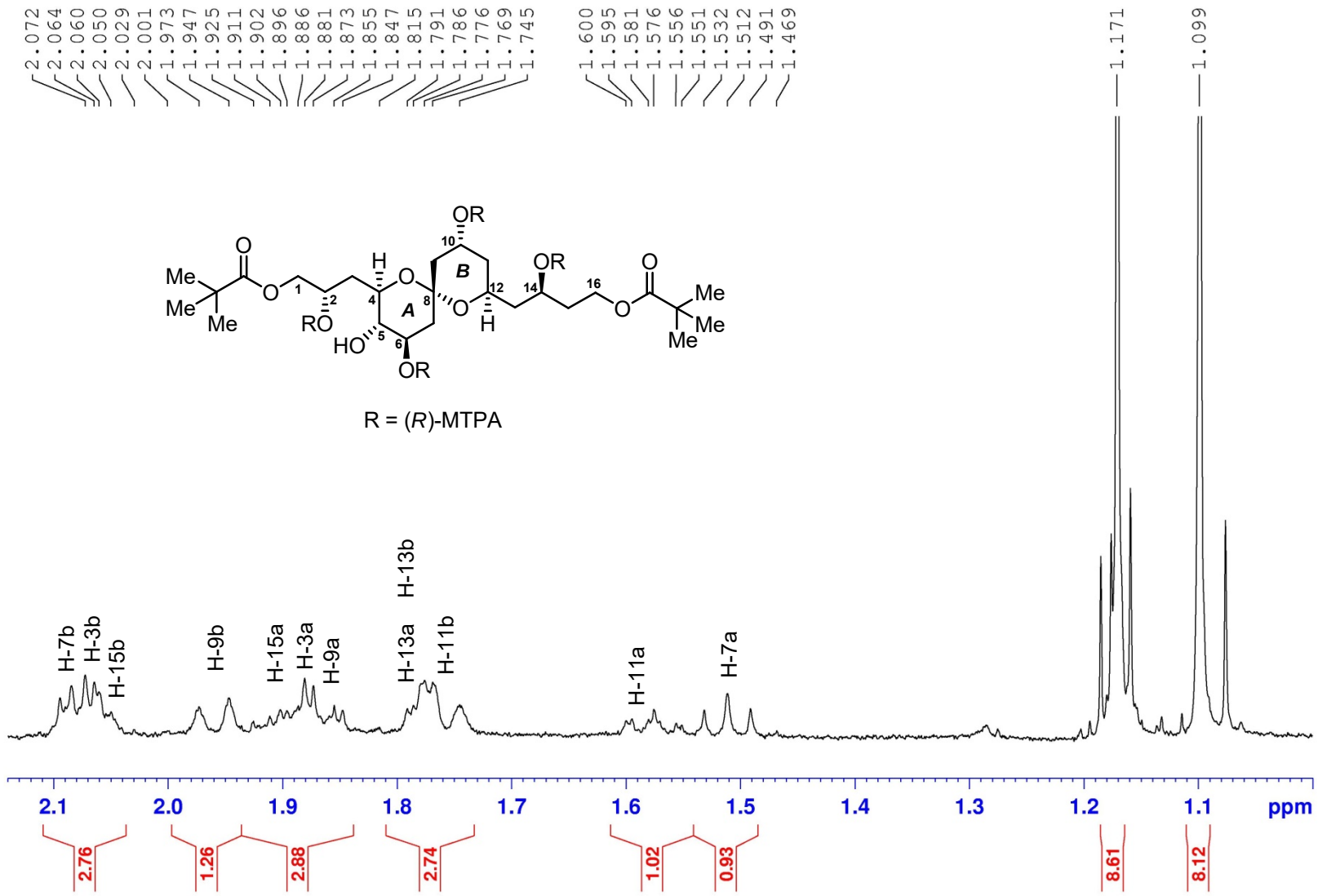

R = (*R*)-MTPA

Figure S183. ^{1}H (600 MHz) NMR spectrum of the fragment **1ar** in CD_3OD

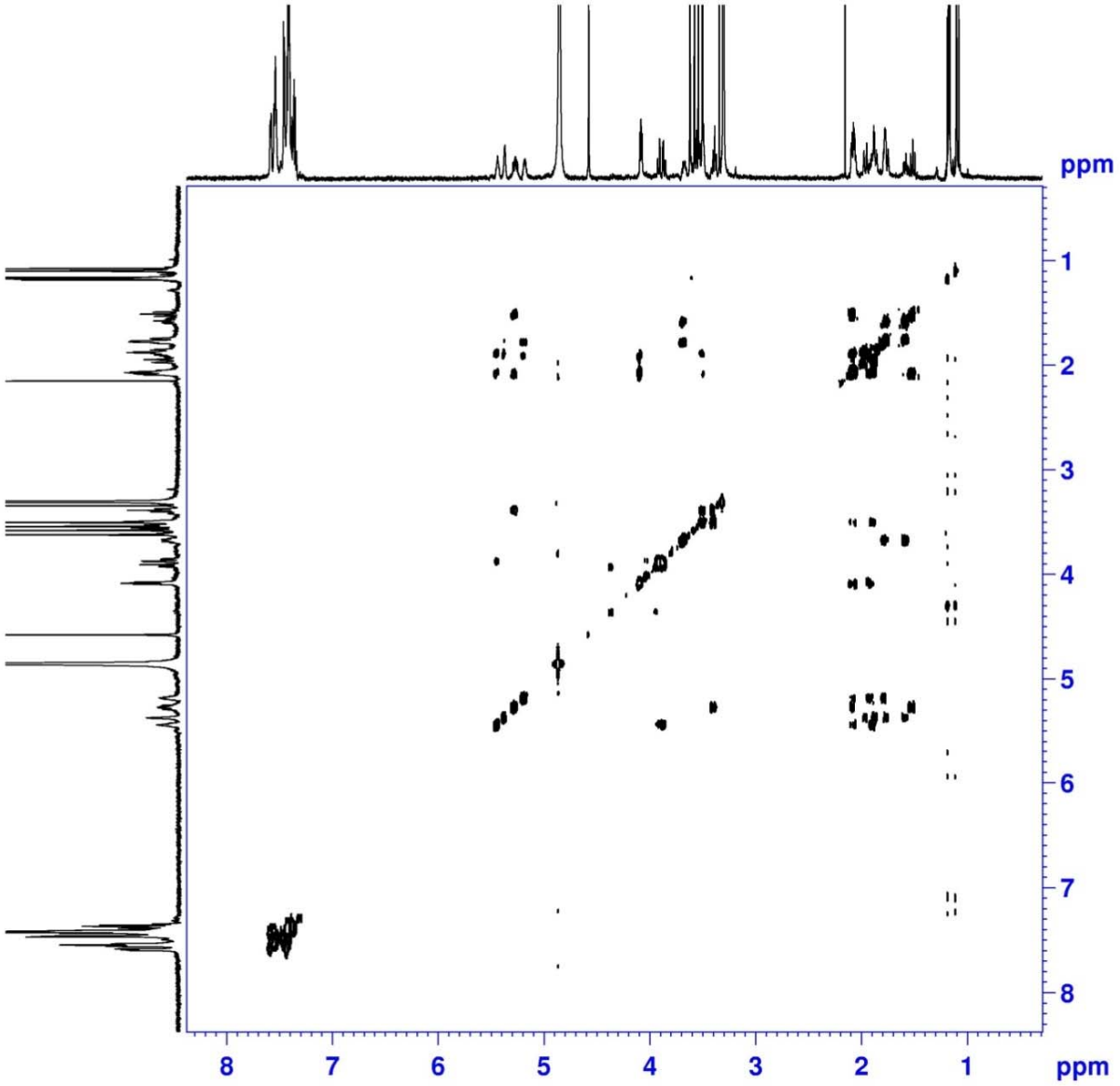

Figure S184. ^{1}H–^{1}H COSY (600 MHz) spectrum of the fragment **1ar** in CD_3OD

Mass Spectrum SmartFormula Report

Analysis Info

Analysis Name	D:\Data\MS\data\202102\yuyi_AX-1-O3-7-R_pos_14_01_9967.d	Acquisition Date	2/5/2021 4:49:57 PM
Method	LC_Direct Infusion_pos_100-3000mz.m	Operator	SCSIO
Sample Name	yuyi_AX-1-O3-7-R_pos	Instrument	maXis 255552.00029
Comment			

Acquisition Parameter

Source Type	ESI	Ion Polarity	Positive	Set Nebulizer	0.4 Bar
Focus	Active	Set Capillary	4500 V	Set Dry Heater	180 °C
Scan Begin	100 m/z	Set End Plate Offset	0 V	Set Dry Gas	4.0 l/min
Scan End	3500 m/z	Set Charging Voltage	0 V	Set Divert Valve	Waste
		Set Corona	0 nA	Set APCI Heater	0 °C

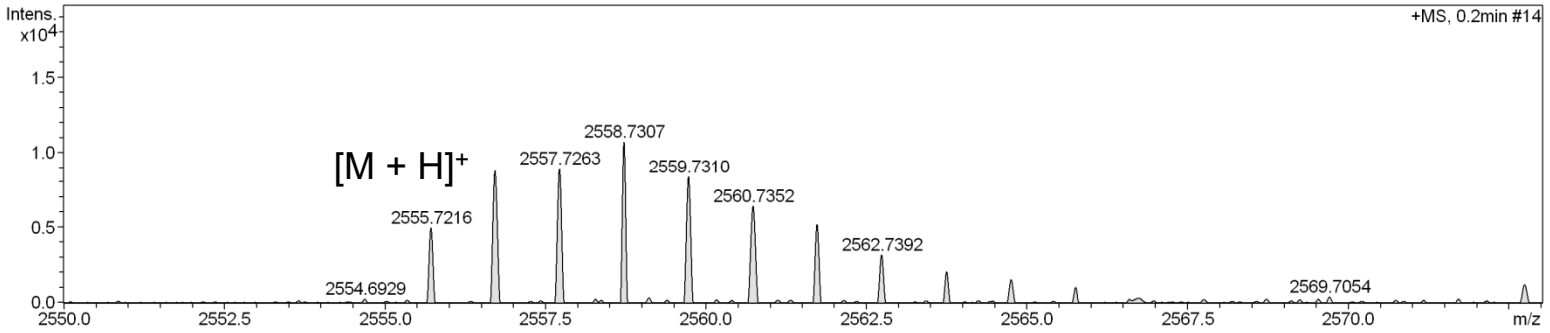

Meas. m/z	#	Ion Formula	Score	m/z	err [ppm]	err [mDa]	mSigma	rdb	e⁻ Conf	N-Rule
2555.7216	1	C119H118F27O31	100.00	2555.7220	-0.2	-0.5	467.1	47.5	even	ok
2577.7161	1	C119H117F27NaO31	0.00	2577.7040	4.7	12.1	379.1	47.5	even	ok

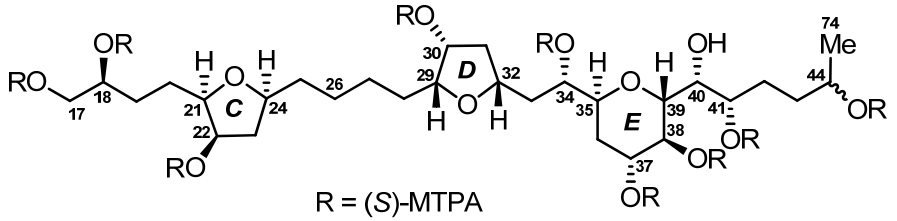

Figure S185. HR-ESIMS for the fragment **1bs**

Generic Display Report

Analysis Info

Analysis Name	D:\Data\MS\data\202102\yuyi_AX-1-O3-7-R_pos_14_01_9967.d	Acquisition Date	2/5/2021 4:49:57 PM
Method	LC_Direct Infusion_pos_100-3000mz.m	Operator	SCSIO
Sample Name	yuyi_AX-1-O3-7-R_pos	Instrument	maXis
Comment			

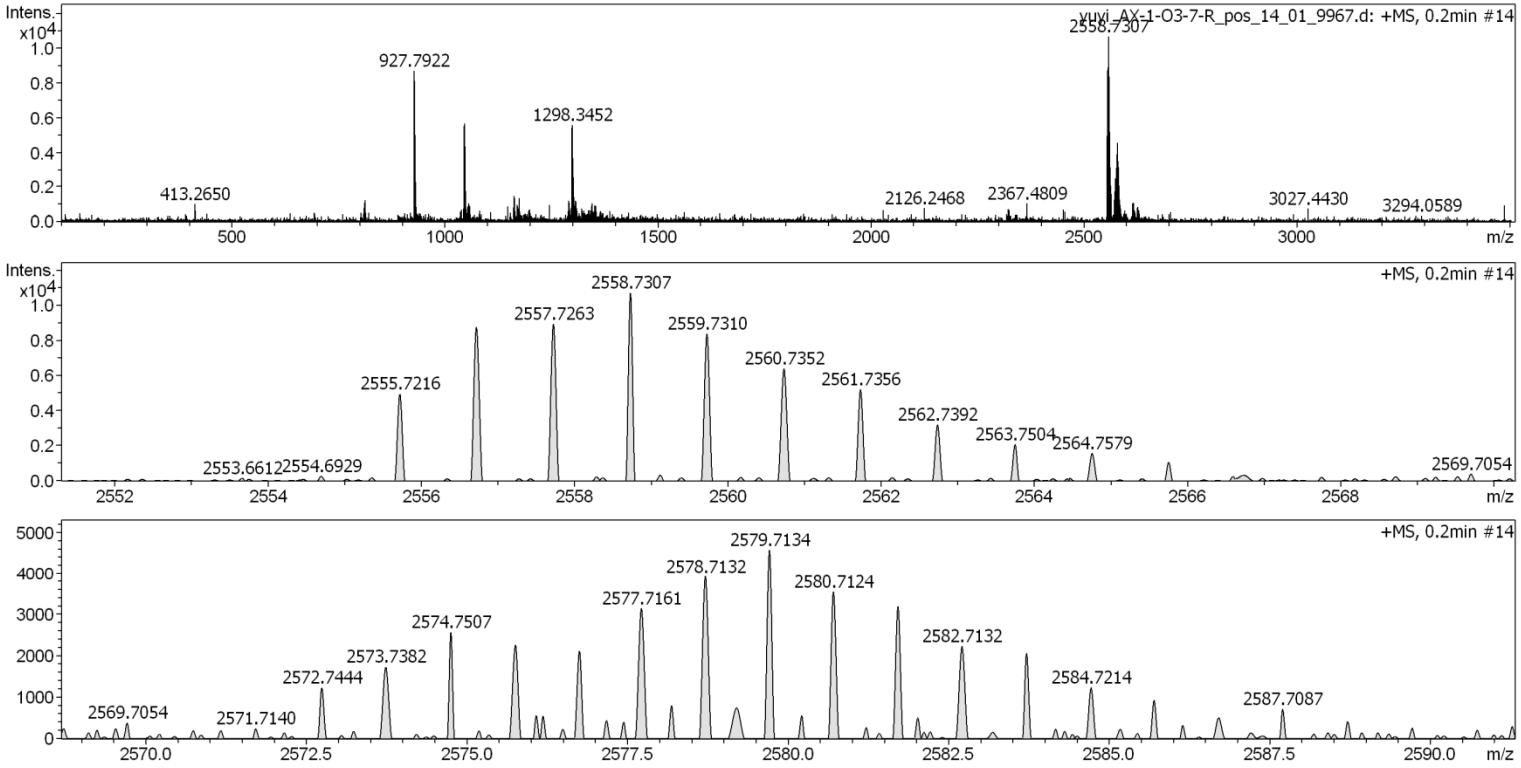

Bruker Compass DataAnalysis 4.1 printed: 2/5/2021 5:01:34 PM by: SCSIO Page 1 of 1

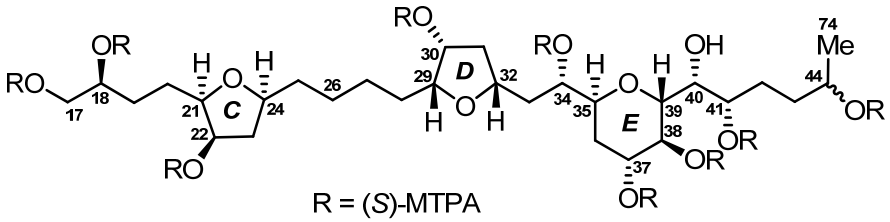

R = (*S*)-MTPA

Figure S186. HR-ESIMS for the fragment **1bs**

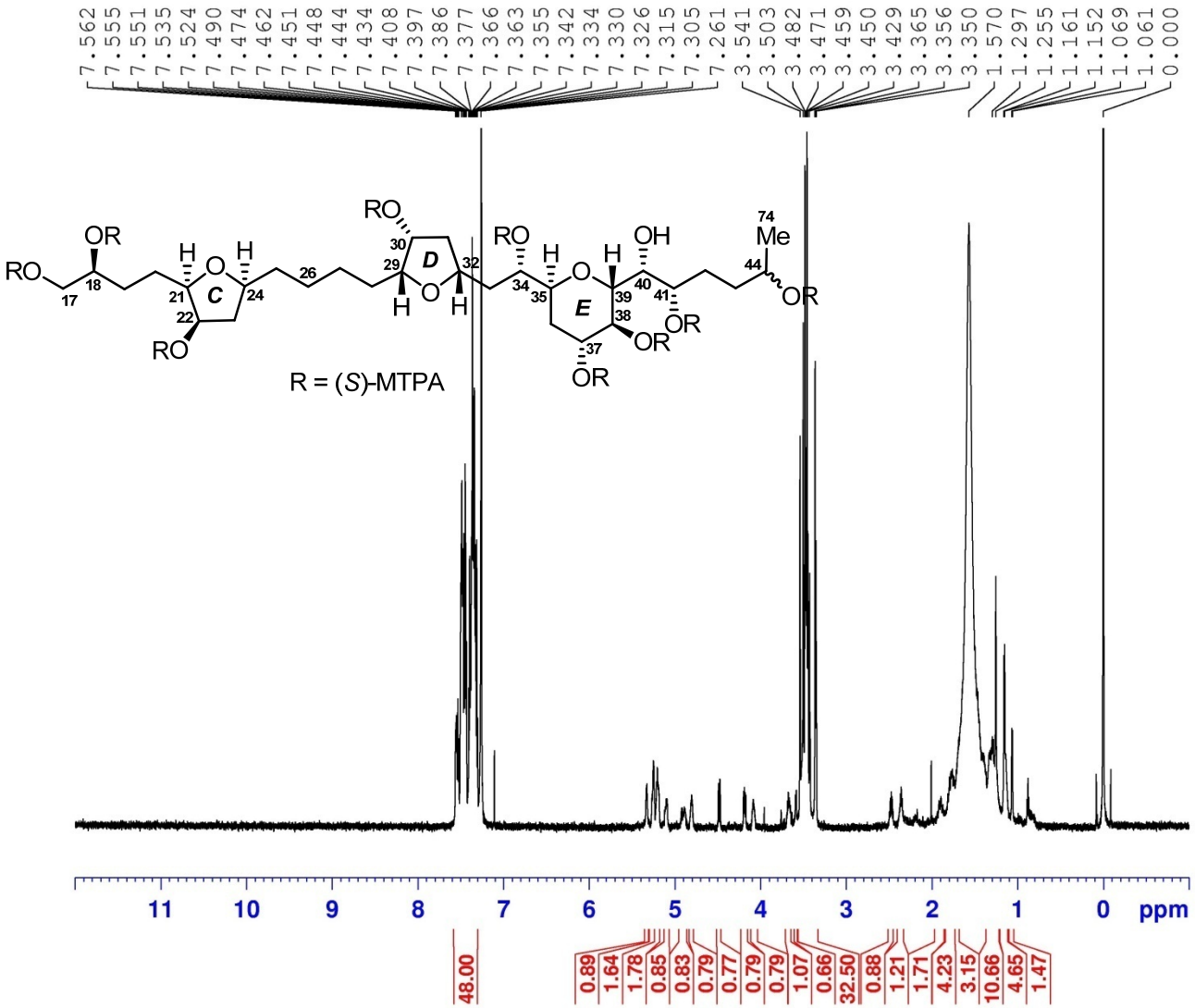

Figure S187. ^{1}H (700 MHz) NMR spectrum of the fragment **1bs** in $CDCl_3$

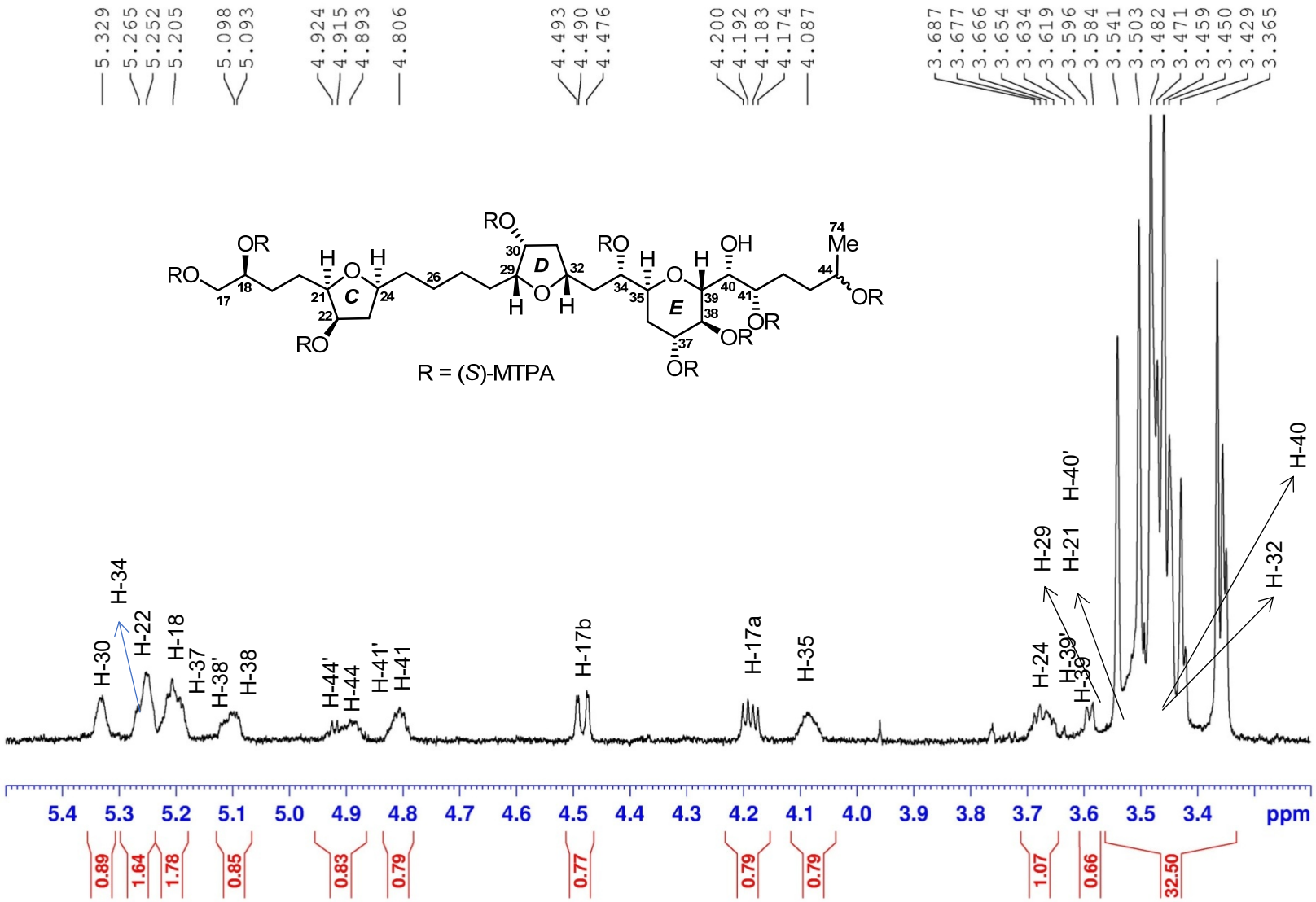

Figure S188. ^{1}H (700 MHz) NMR spectrum of the fragment **1bs** in $CDCl_3$

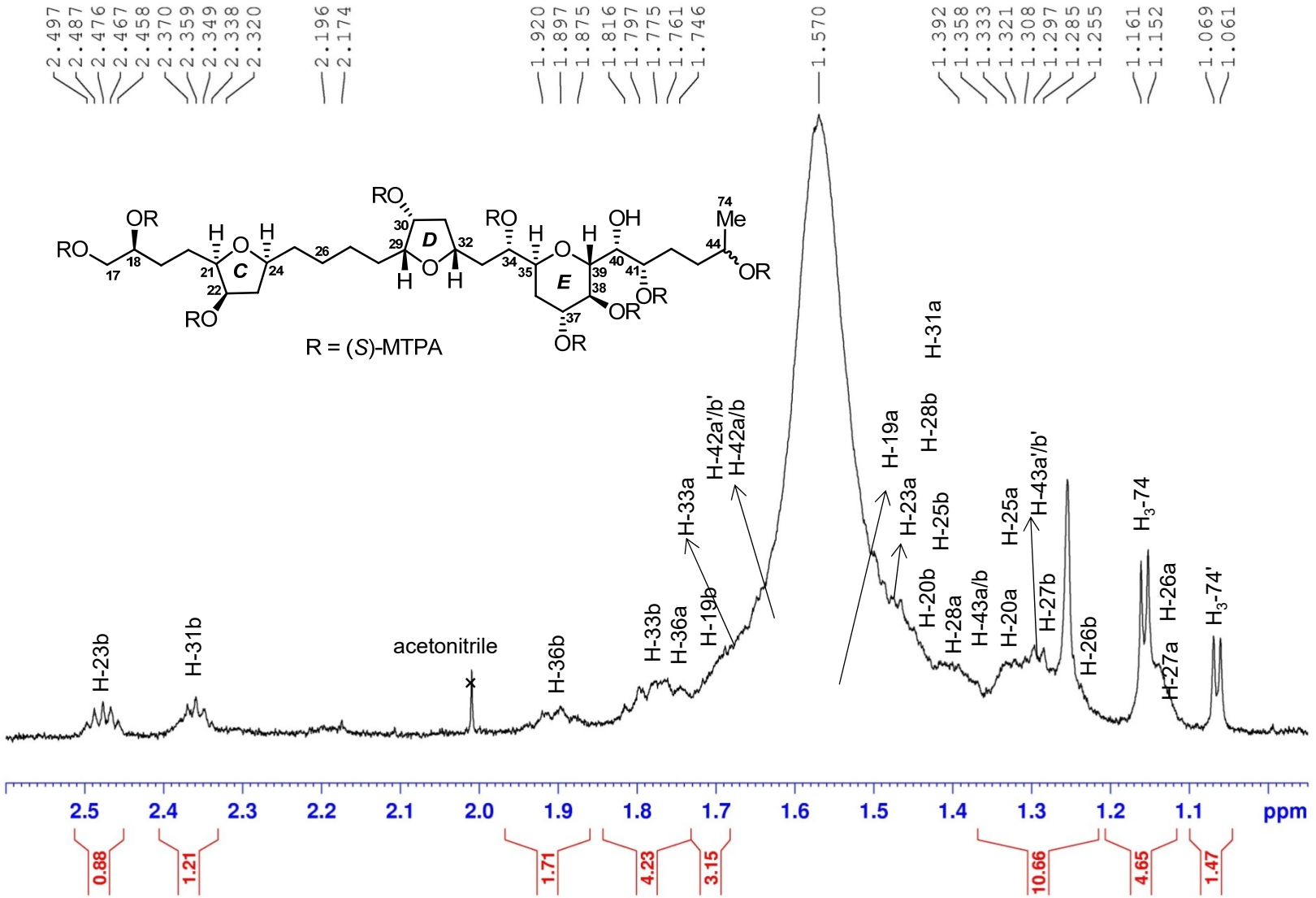

Figure S189. ^{1}H (700 MHz) NMR spectrum of the fragment **1bs** in $CDCl_3$

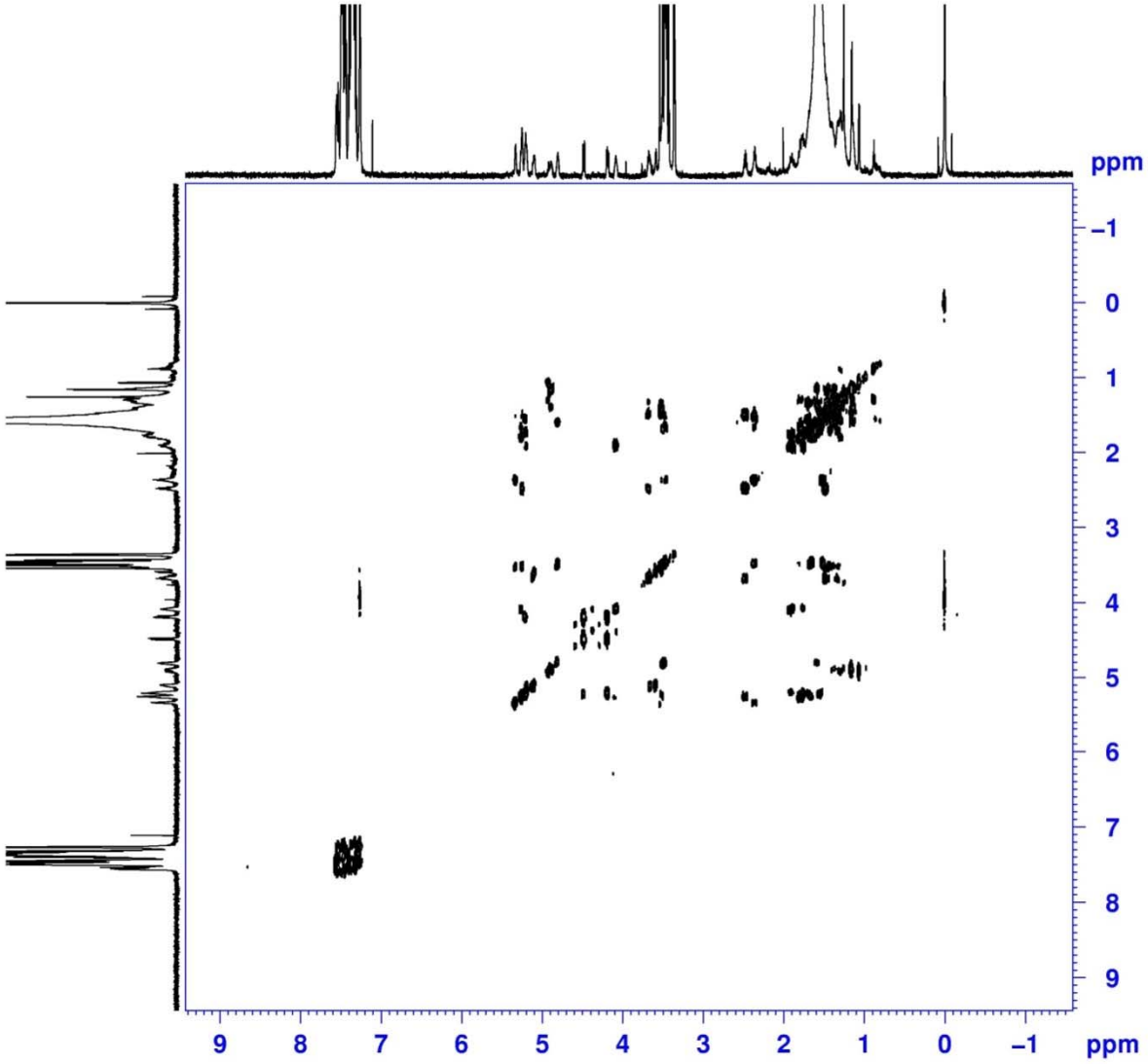

Figure S190. ^{1}H–^{1}H COSY (700 MHz) spectrum of the fragment **1bs** in $CDCl_3$

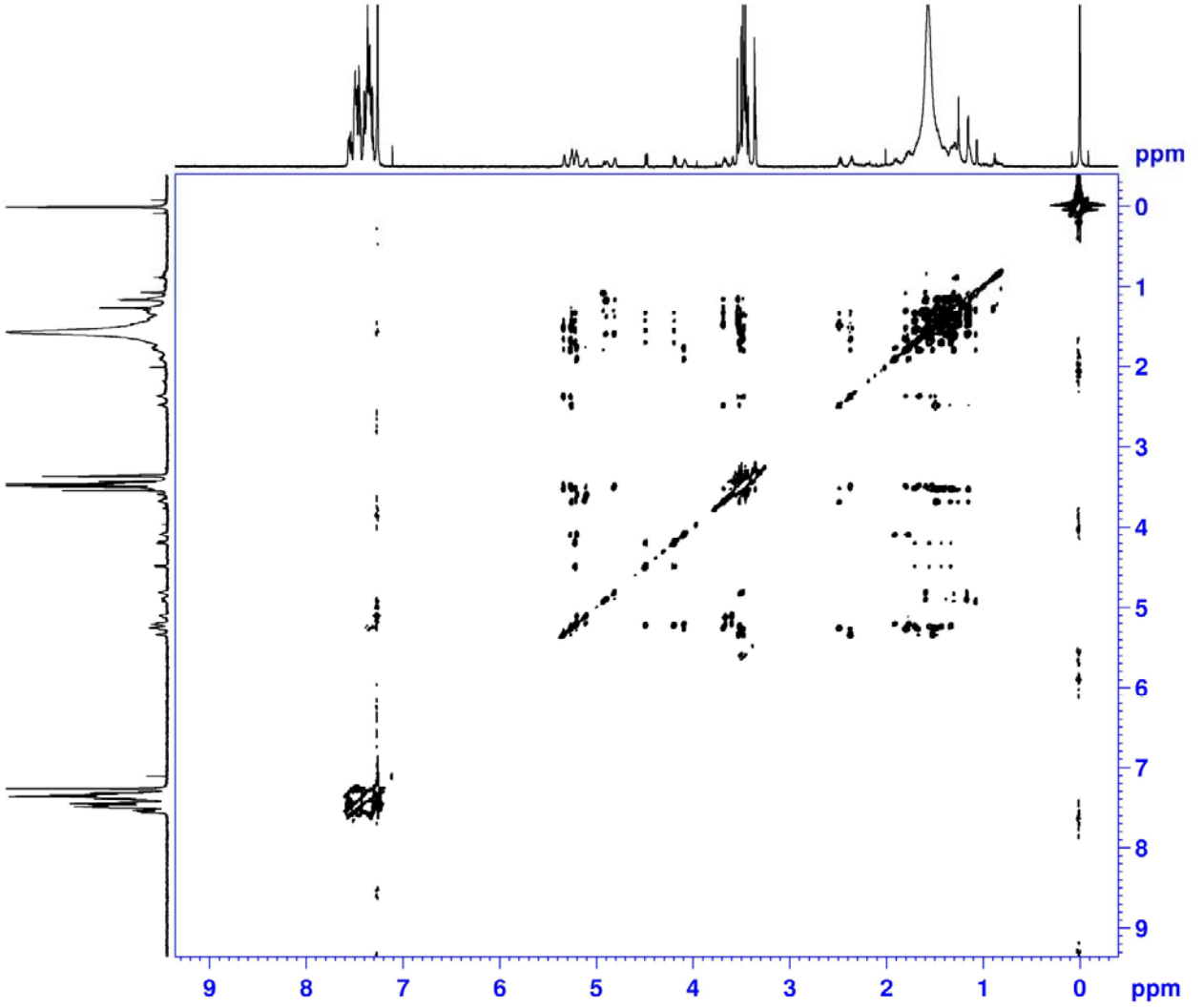

Figure S191. TOCSY (700 MHz) spectrum of the fragment **1bs** in $CDCl_3$

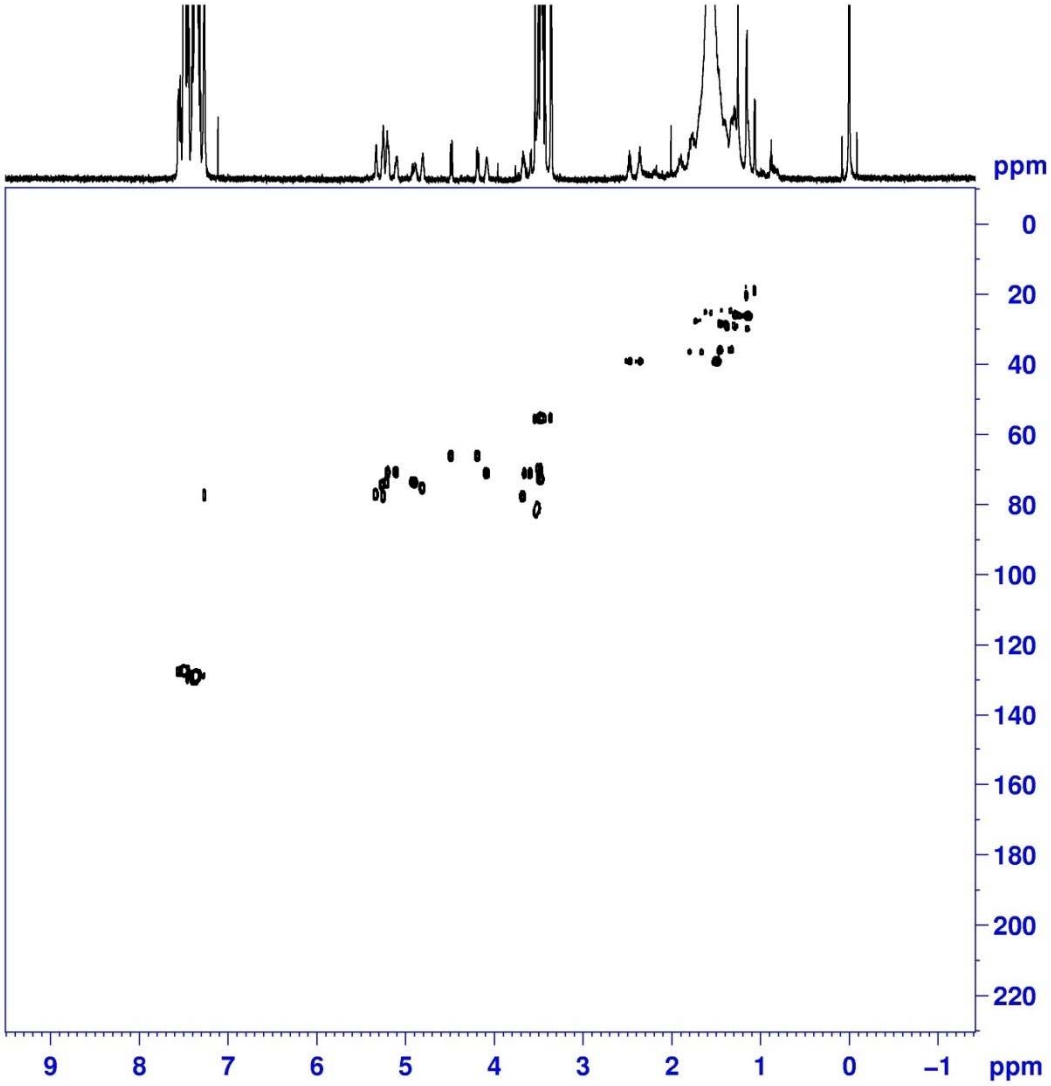

Figure S192. HSQC (700 MHz) spectrum of the fragment **1bs** in $CDCl_3$

Mass Spectrum SmartFormula Report

Analysis Info

Analysis Name	D:\Data\MS\data\202102\yuyi_AX-1-O3-7-S_pos_13_01_9968.d	Acquisition Date	2/5/2021 4:53:23 PM
Method	LC_Direct Infusion_pos_100-3000mz.m	Operator	SCSIO
Sample Name	yuyi_AX-1-O3-7-S_pos	Instrument	maXis 255552.00029
Comment			

Acquisition Parameter

Source Type	ESI	Ion Polarity	Positive	Set Nebulizer	0.4 Bar
Focus	Active	Set Capillary	4500 V	Set Dry Heater	180 °C
Scan Begin	100 m/z	Set End Plate Offset	0 V	Set Dry Gas	4.0 l/min
Scan End	3500 m/z	Set Charging Voltage	0 V	Set Divert Valve	Waste
		Set Corona	0 nA	Set APCI Heater	0 °C

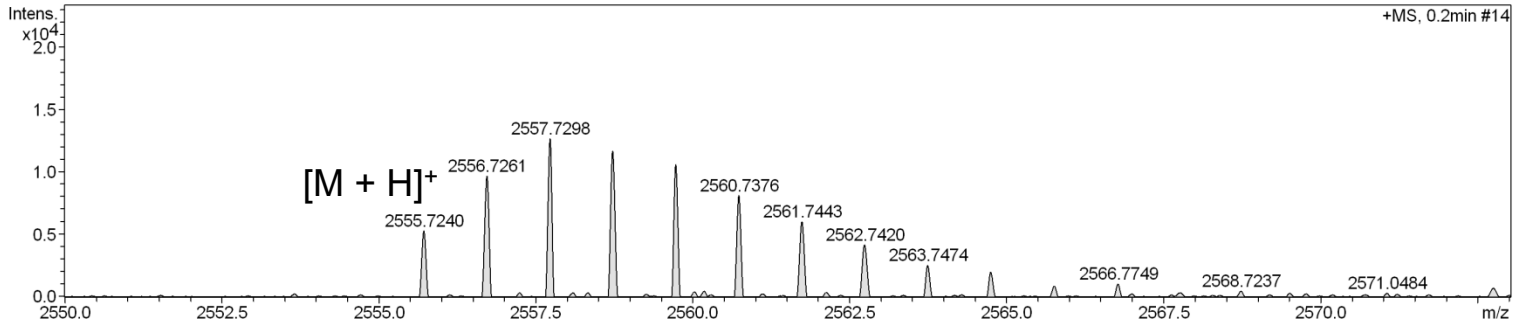

Meas. m/z	#	Ion Formula	Score	m/z	err [ppm]	err [mDa]	mSigma	rdb	e⁻ Conf	N-Rule
2555.7240	1	C119H118F27O31	100.00	2555.7220	0.8	1.9	488.4	47.5	even	ok
2577.7142	1	C119H117F27NaO31	0.00	2577.7040	4.0	10.2	510.2	47.5	even	ok

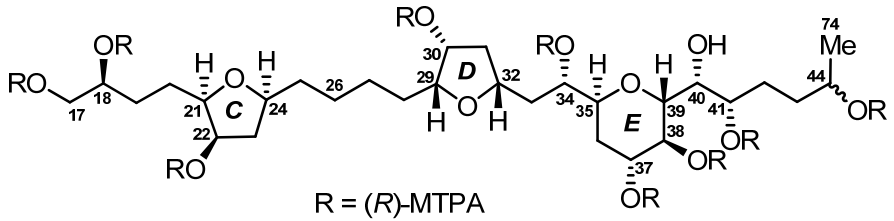

R = (*R*)-MTPA

yuyi_AX-1-O3-7-S_pos_13_01_9968.d

Bruker Compass DataAnalysis 4.1 printed: 2/5/2021 5:04:38 PM by: SCSIO Page 1 of 1

Figure S193. HR-ESIMS for the fragment **1br**

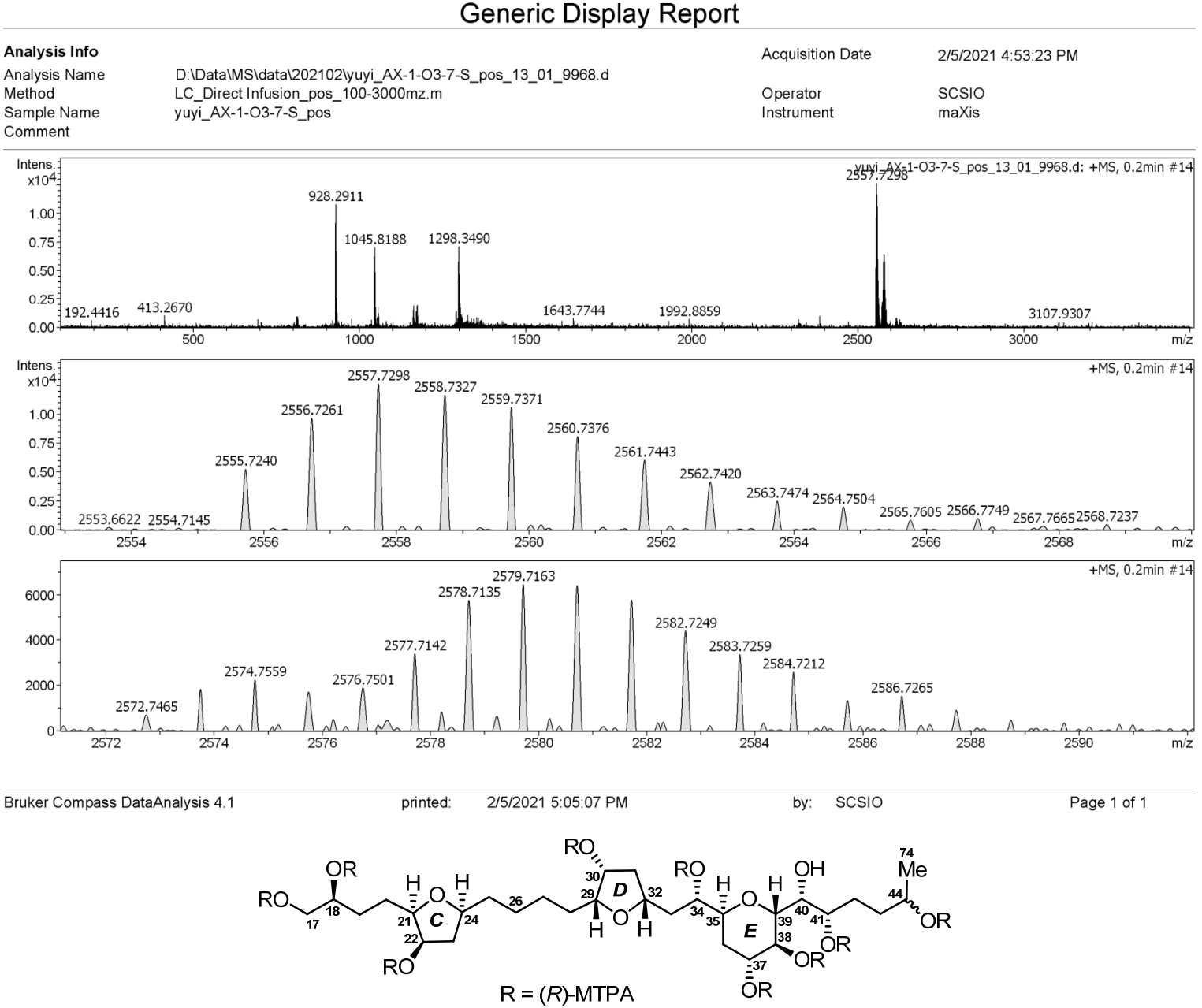

Figure S194. HR-ESIMS for the fragment **1br**

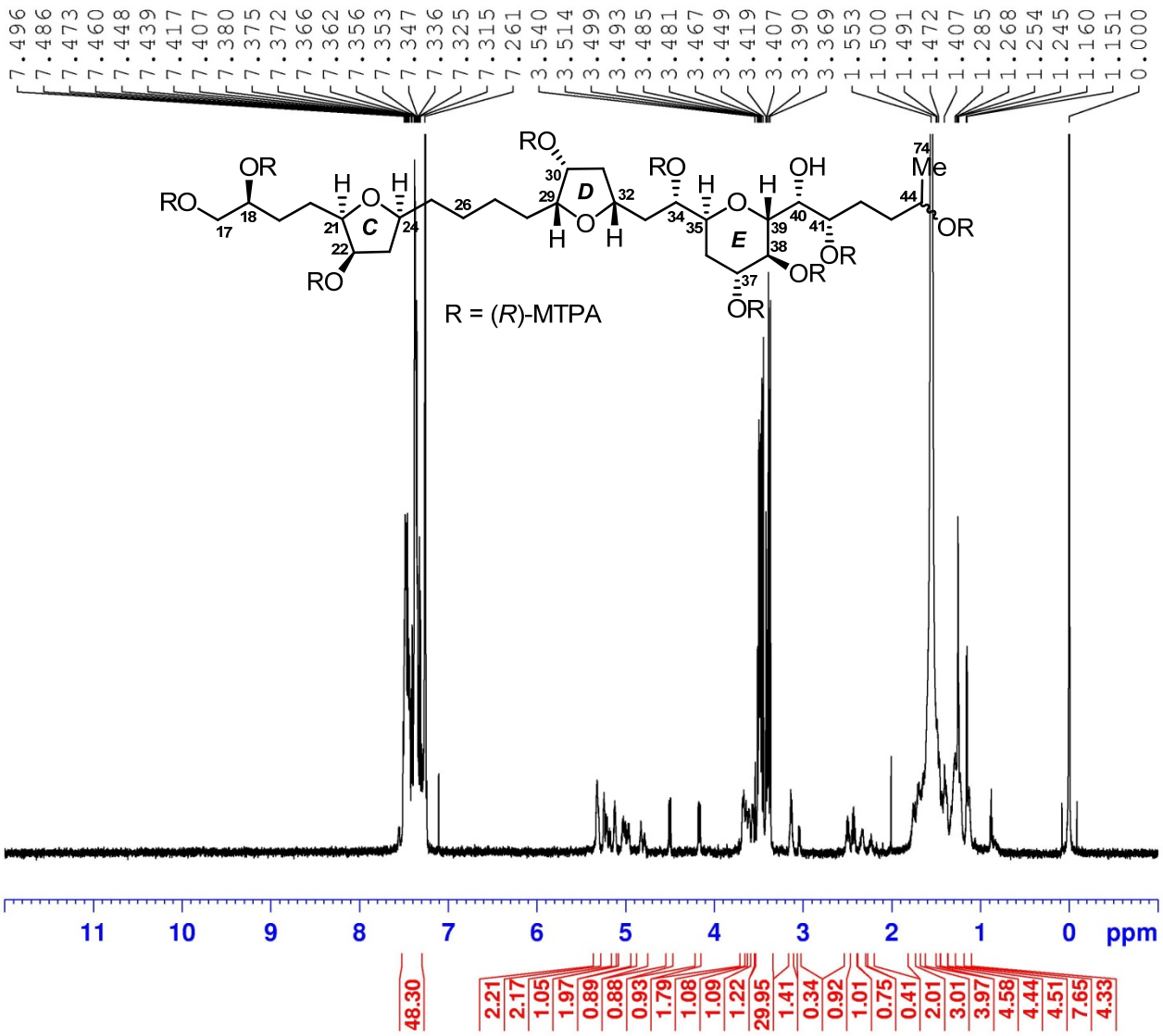

Figure S195. ^{1}H (700 MHz) NMR spectrum of the fragment **1br** in $CDCl_3$

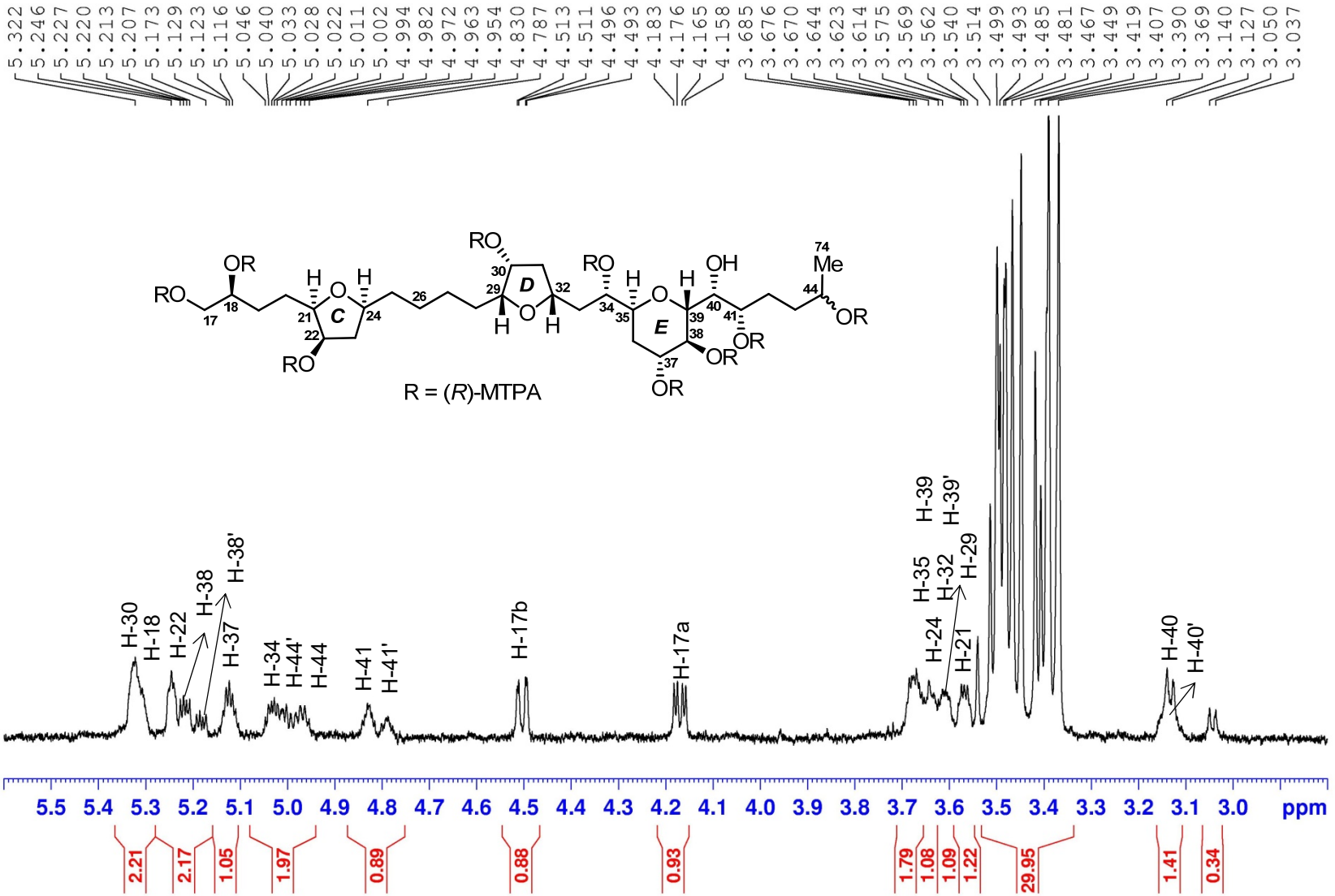

Figure S196. ^{1}H (700 MHz) NMR spectrum of the fragment **1br** in $CDCl_3$

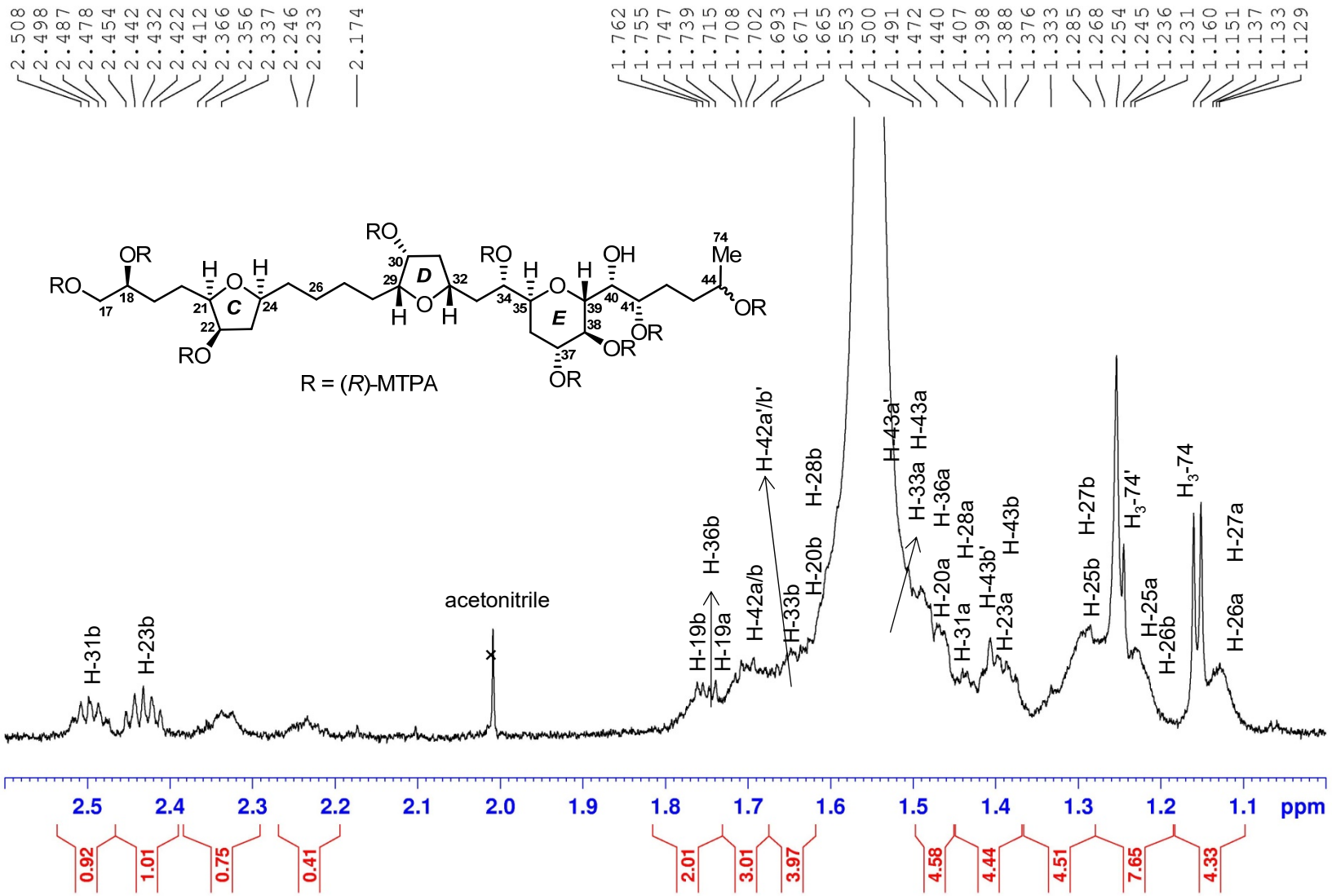

Figure S197. ^{1}H (700 MHz) NMR spectrum of the fragment **1br** in $CDCl_3$

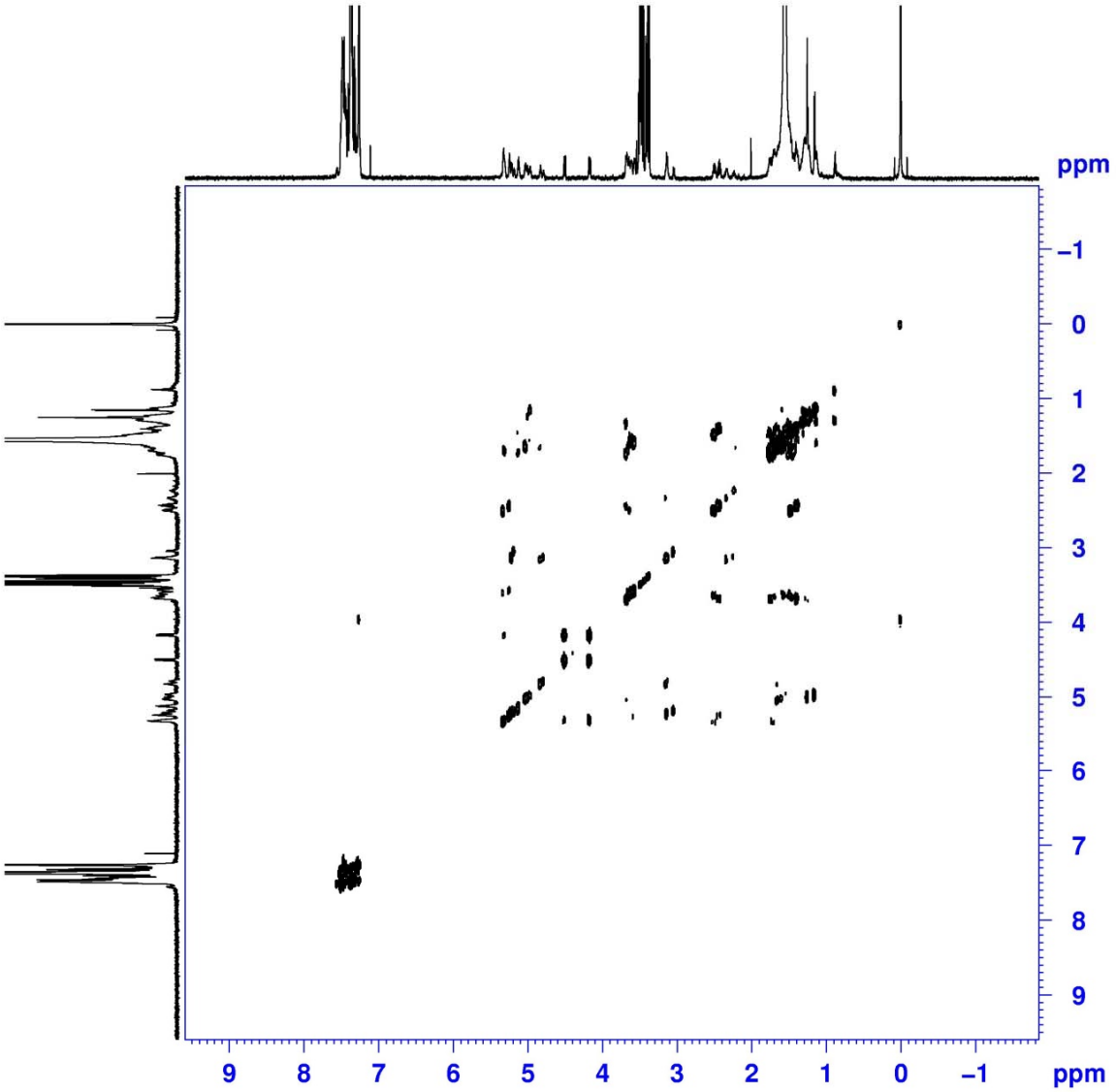

Figure S198. $^{1}H–^{1}H$ COSY (700 MHz) spectrum of the fragment **1br** in $CDCl_3$

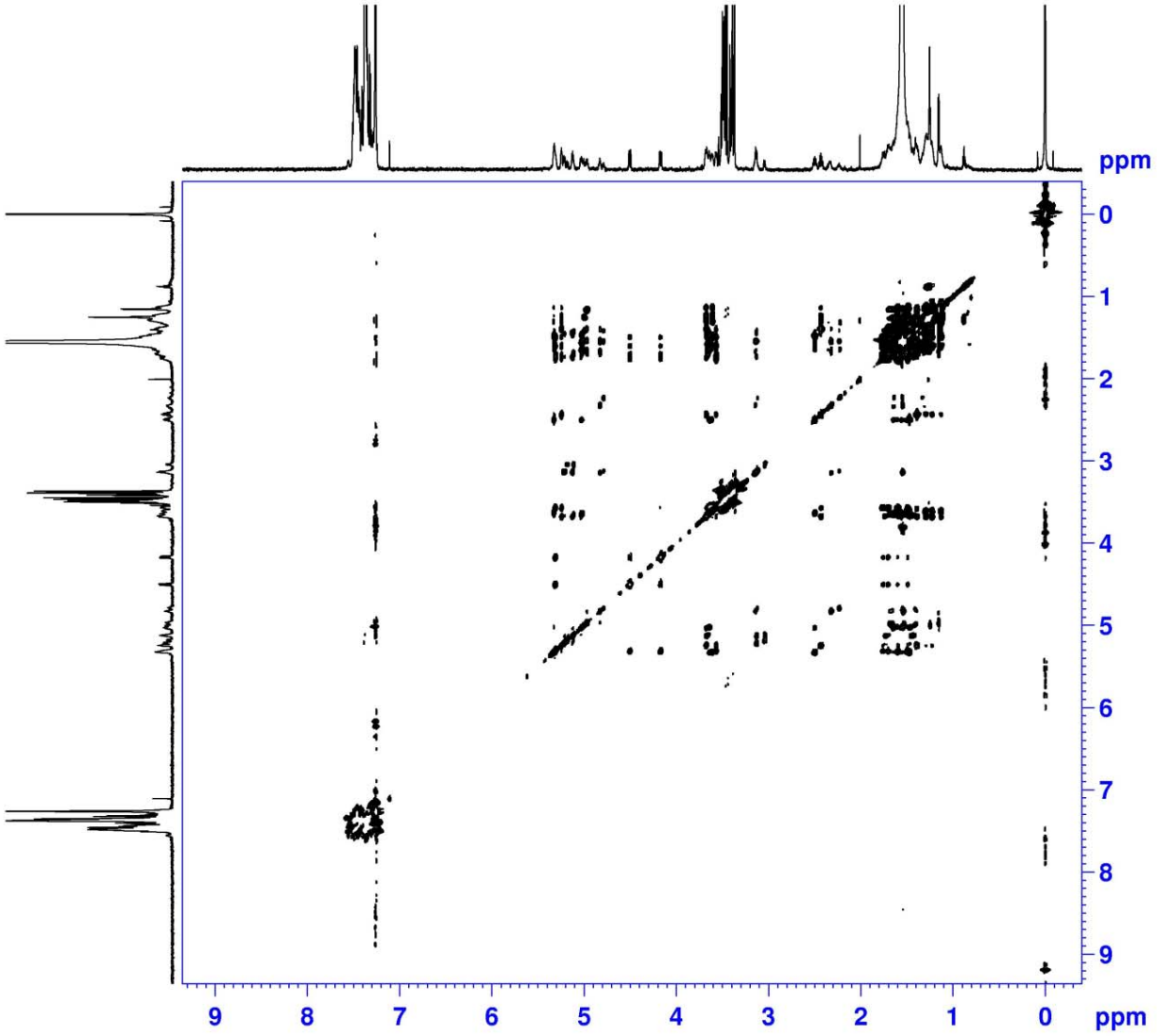

Figure S199. TOCSY (700 MHz) spectrum of the fragment **1br** in $CDCl_3$

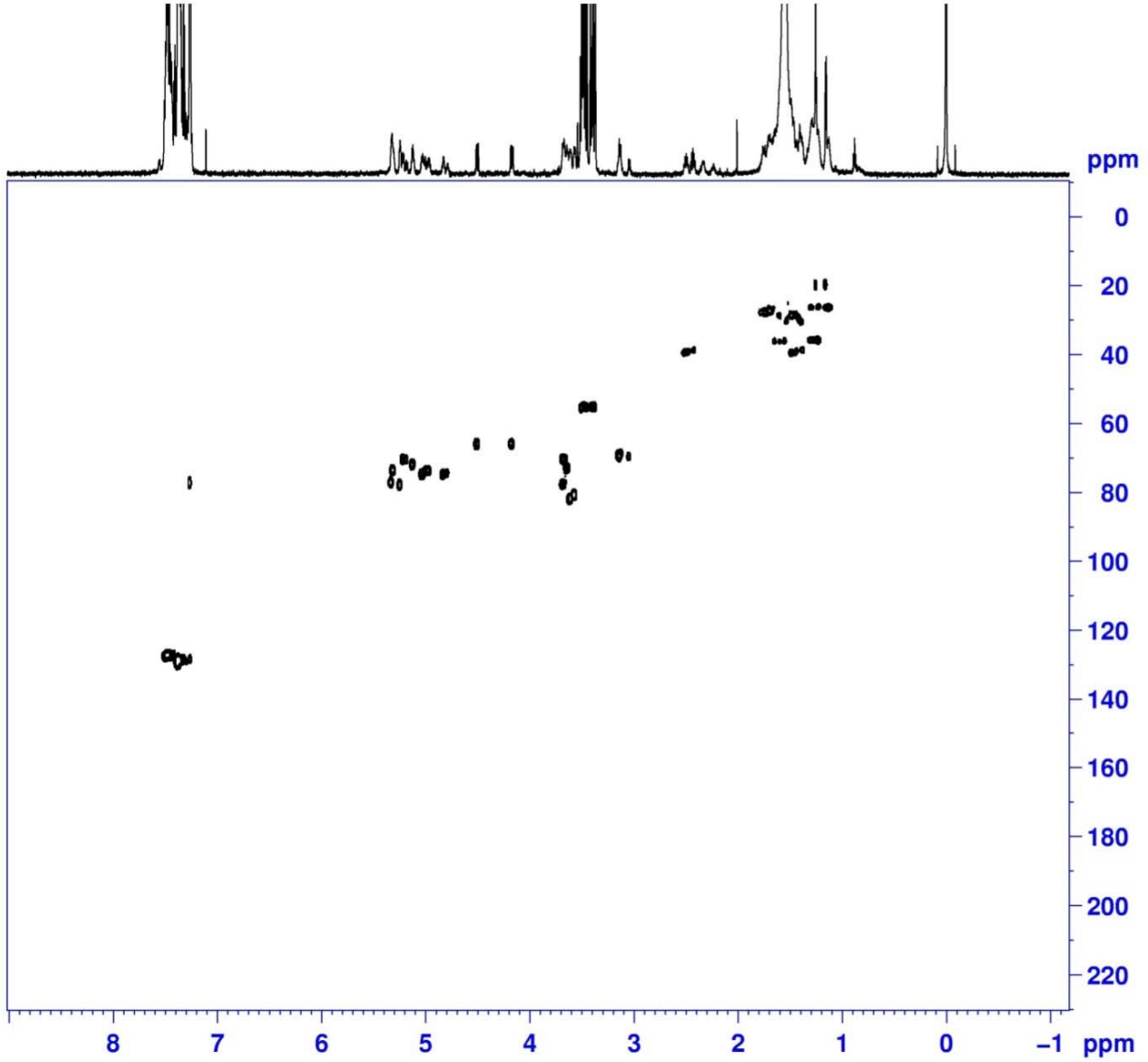

Figure S200. HSQC (700 MHz) spectrum of the fragment **1br** in $CDCl_3$

Mass Spectrum SmartFormula Report

Analysis Info

Analysis Name	D:\Data\MS\data\202103\yuyi_AX-1-03-4-R_pos_6_01_10275.d	Acquisition Date	3/29/2021 3:21:11 PM
Method	LC_Direct Infusion_pos_100-3000mz.m	Operator	SCSIO
Sample Name	yuyi_AX-1-03-4-R_pos	Instrument	maXis 255552.00029
Comment			

Acquisition Parameter

Source Type	ESI	Ion Polarity	Positive	Set Nebulizer	0.4 Bar
Focus	Active	Set Capillary	4500 V	Set Dry Heater	180 °C
Scan Begin	100 m/z	Set End Plate Offset	0 V	Set Dry Gas	4.0 l/min
Scan End	3500 m/z	Set Charging Voltage	0 V	Set Divert Valve	Waste
		Set Corona	0 nA	Set APCI Heater	0 °C

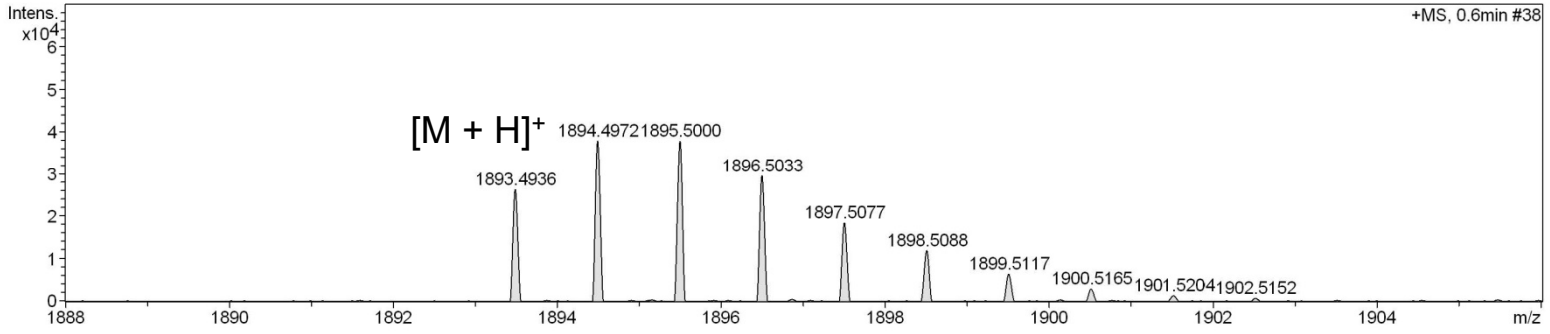

Meas. m/z	#	Ion Formula	Score	m/z	err [ppm]	err [mDa]	mSigma	rdb	e⁻ Conf	N-Rule
1893.4936	1	C87H82F21O23	100.00	1893.4906	-1.6	-3.0	403.2	36.5	even	ok

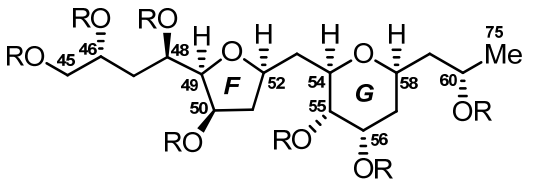

R = (*S*)-MTPA

yuyi_AX-1-03-4-R_pos_6_01_10275.d

Bruker Compass DataAnalysis 4.1 printed: 3/29/2021 5:31:58 PM by: SCSIO Page 1 of 1

Figure S201. HR-ESIMS for the fragment **1cs**

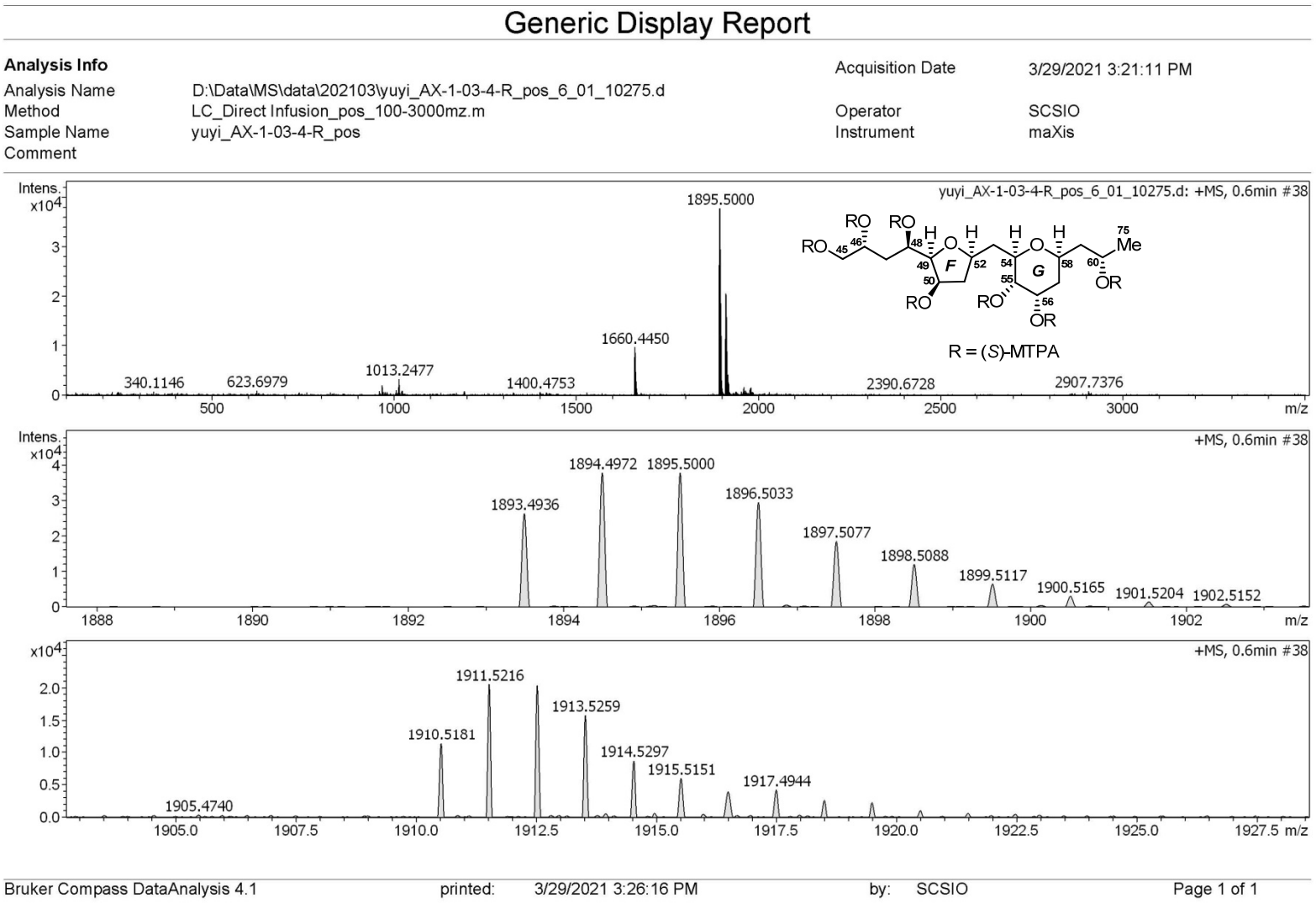

Figure S202. HR-ESIMS for the fragment **1cs**

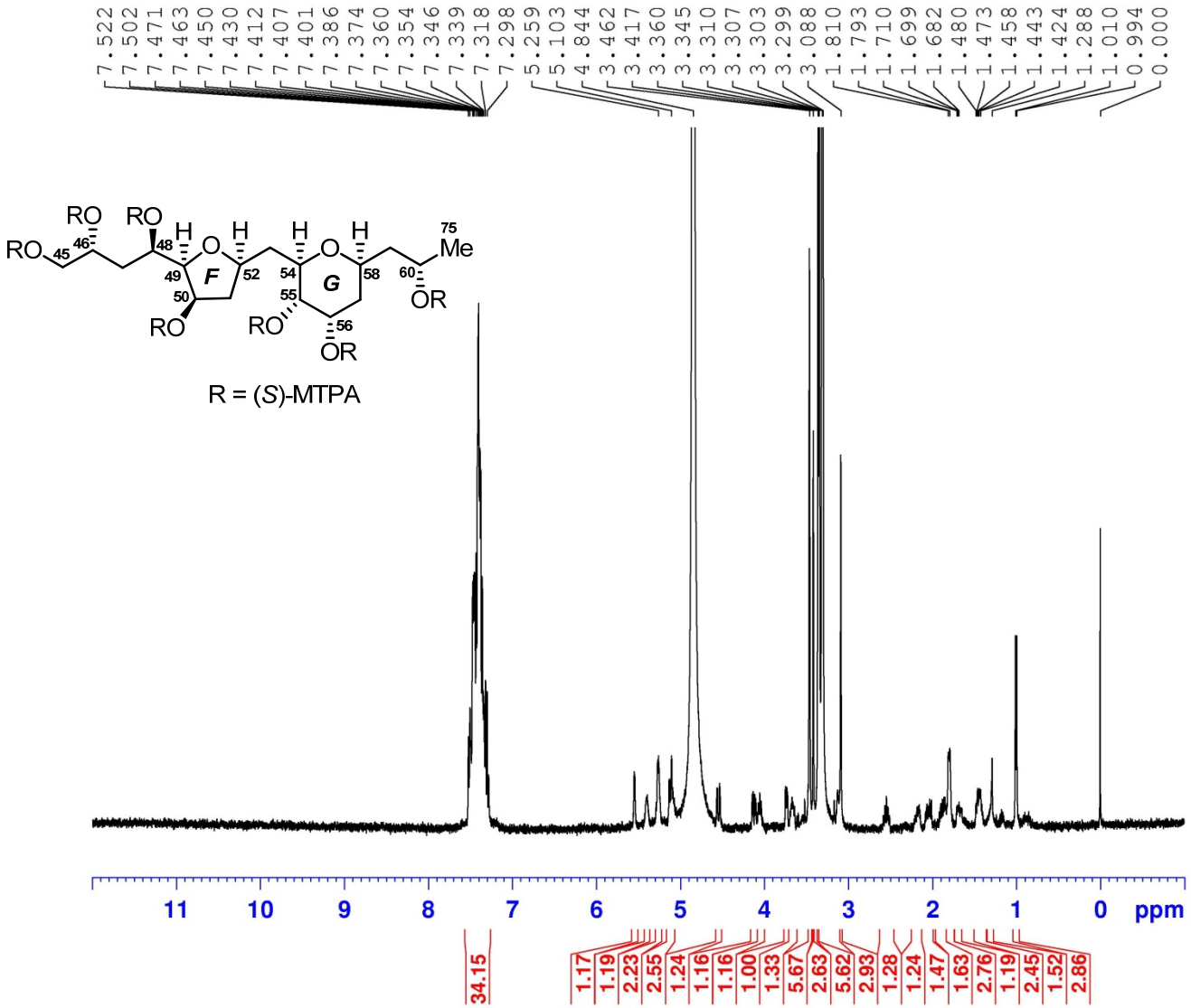

Figure S203. ^{1}H (400 MHz) NMR spectrum of the fragment **1cs** in CD_3OD

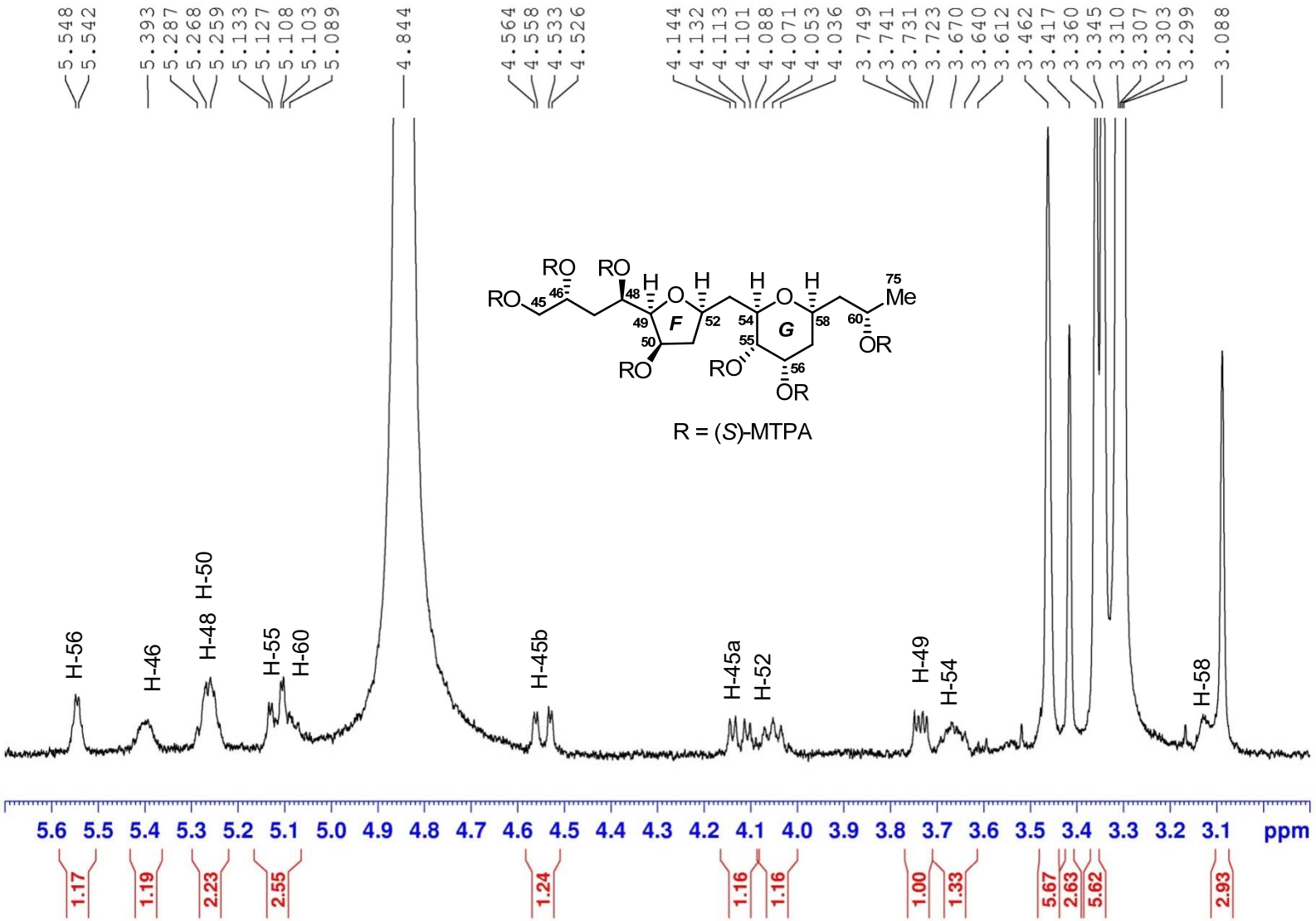

Figure S204. ^{1}H (400 MHz) NMR spectrum of the fragment **1cs** in CD_3OD

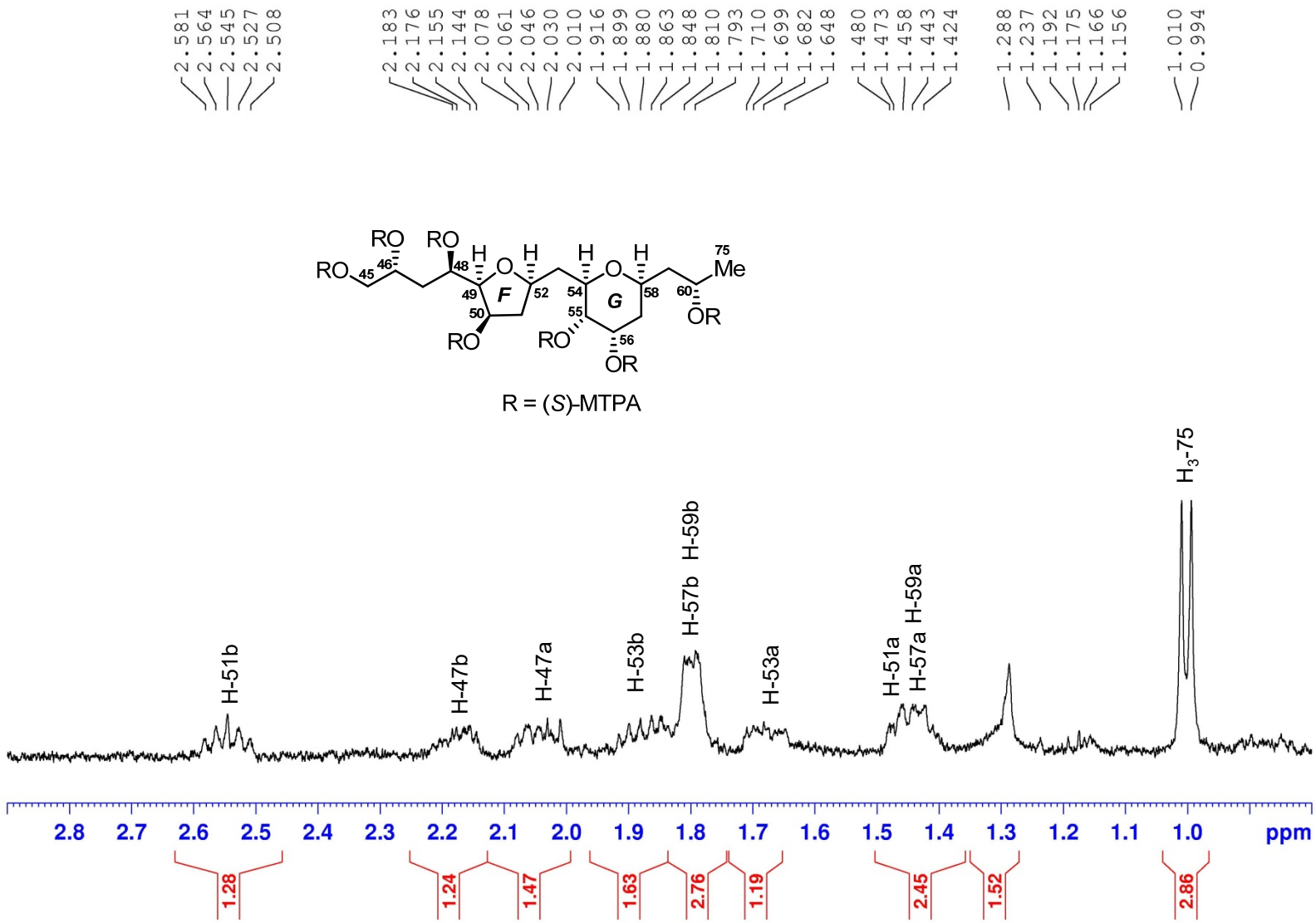

Figure S205. ^{1}H (400 MHz) NMR spectrum of the fragment **1cs** in CD_3OD

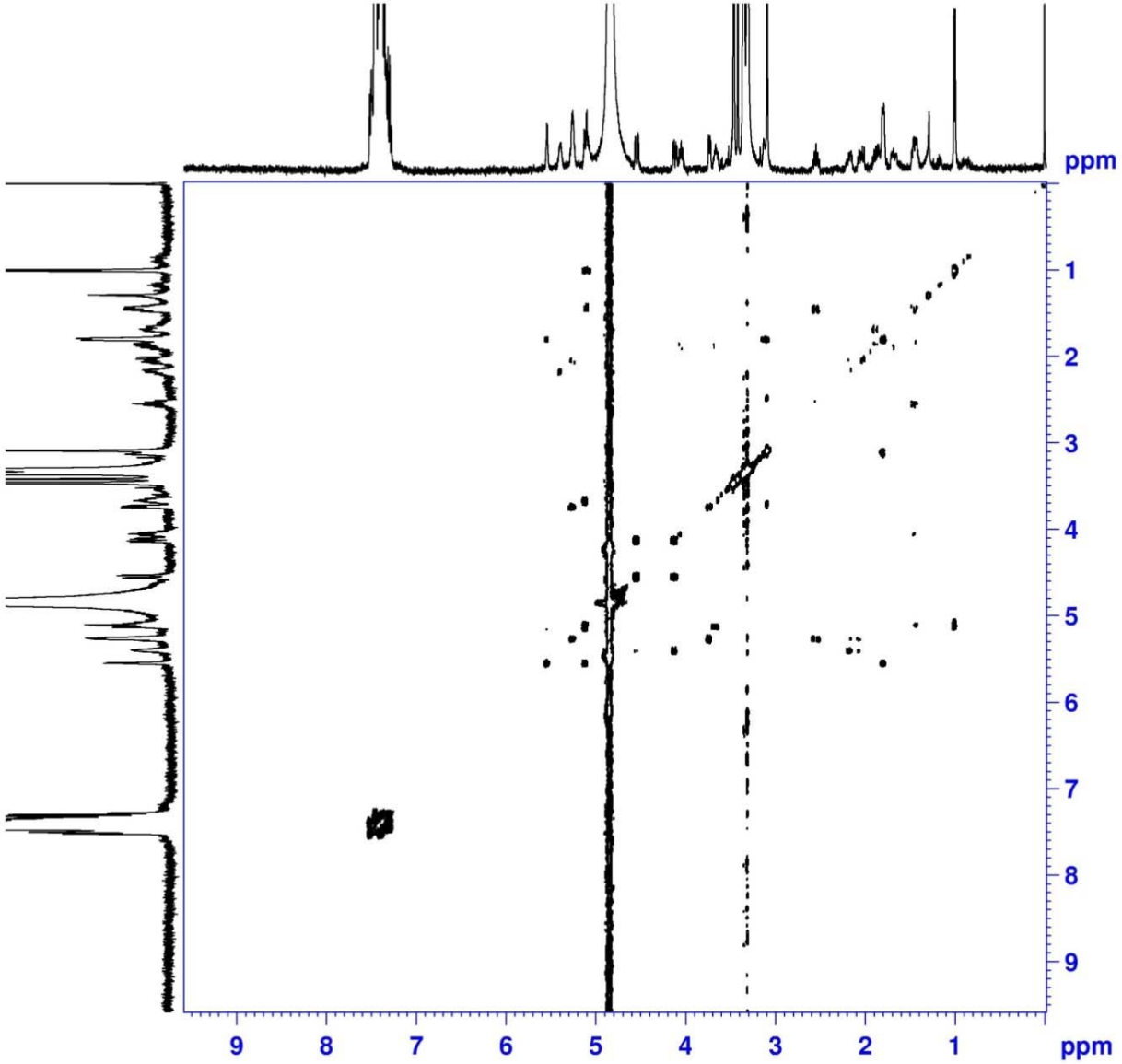

Figure S206. ^{1}H–^{1}H COSY (400 MHz) spectrum of the fragment **1cs** in CD_3OD

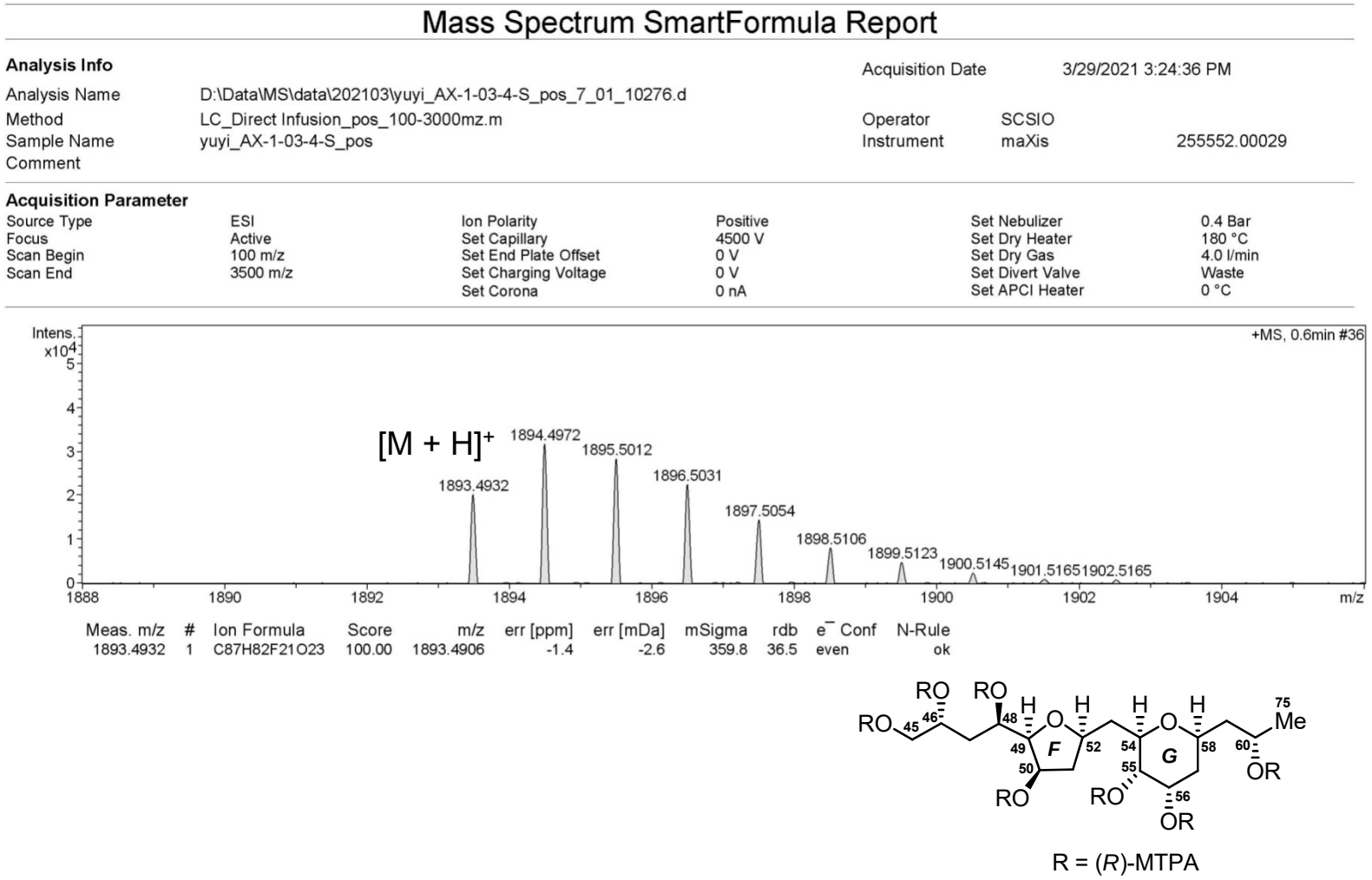

Figure S207. HR-ESIMS for the fragment **1cr**

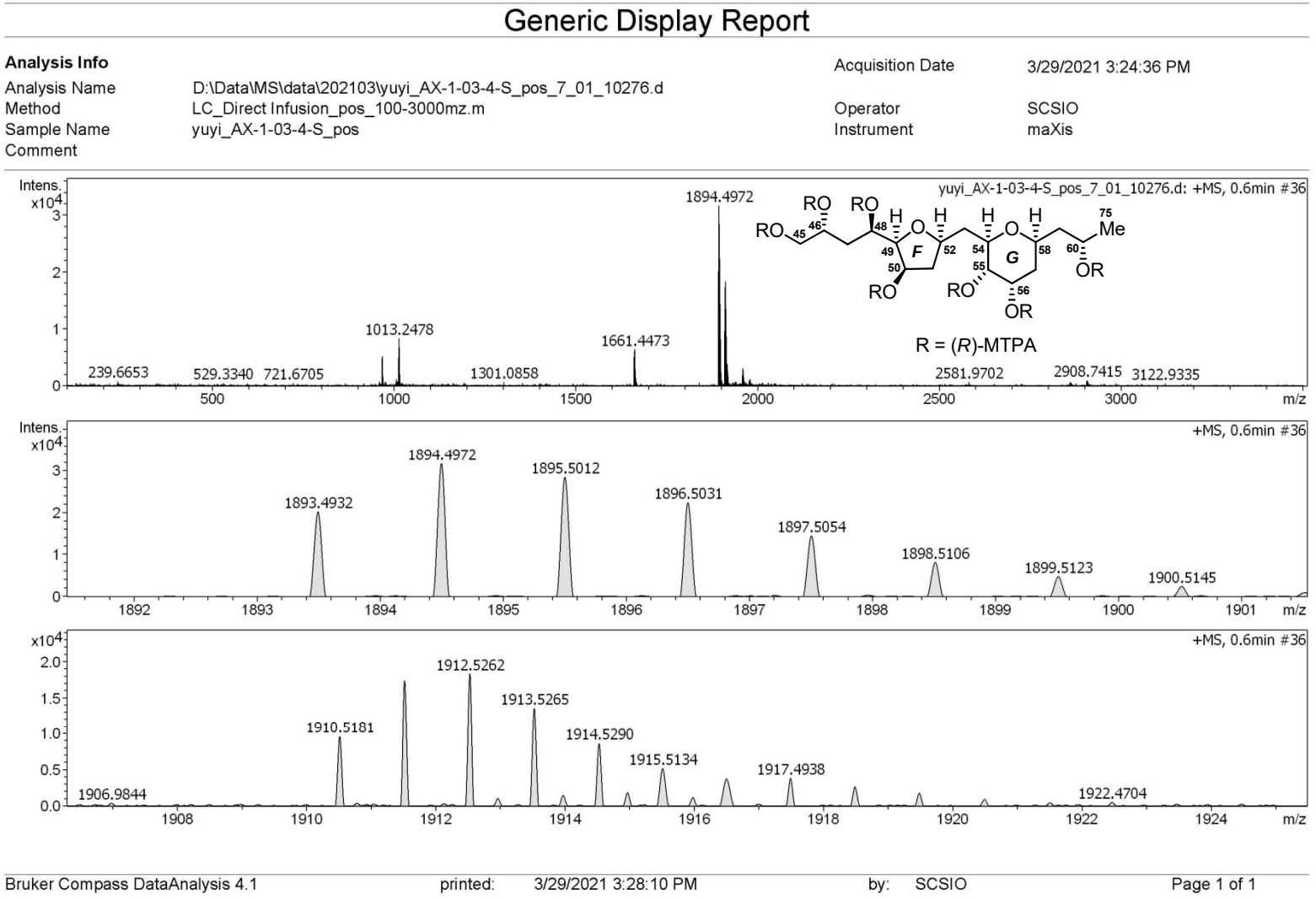

Figure S208. HR-ESIMS for the fragment **1cr**

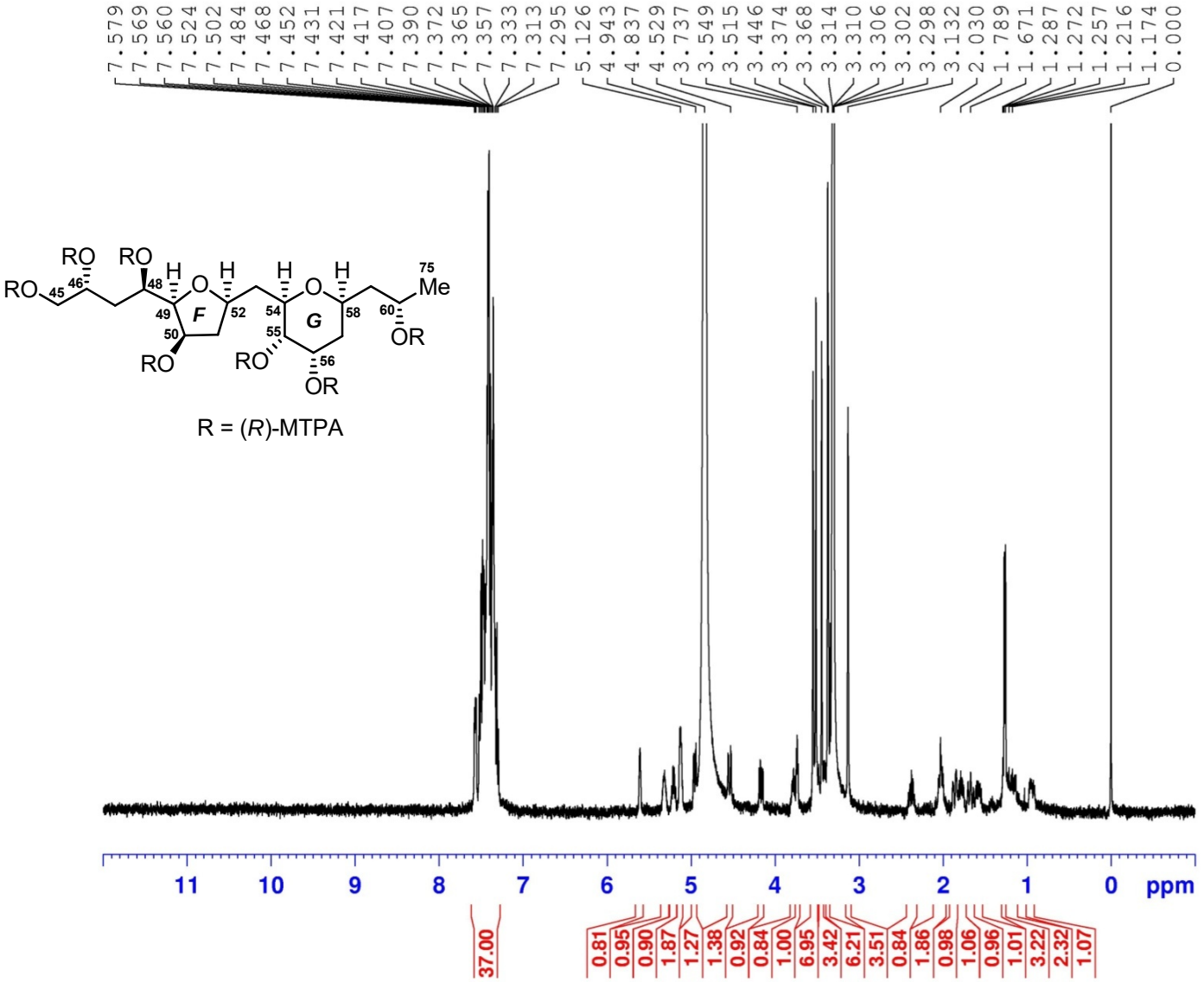

Figure S209. ^{1}H (400 MHz) NMR spectrum of the fragment **1cr** in CD_3OD

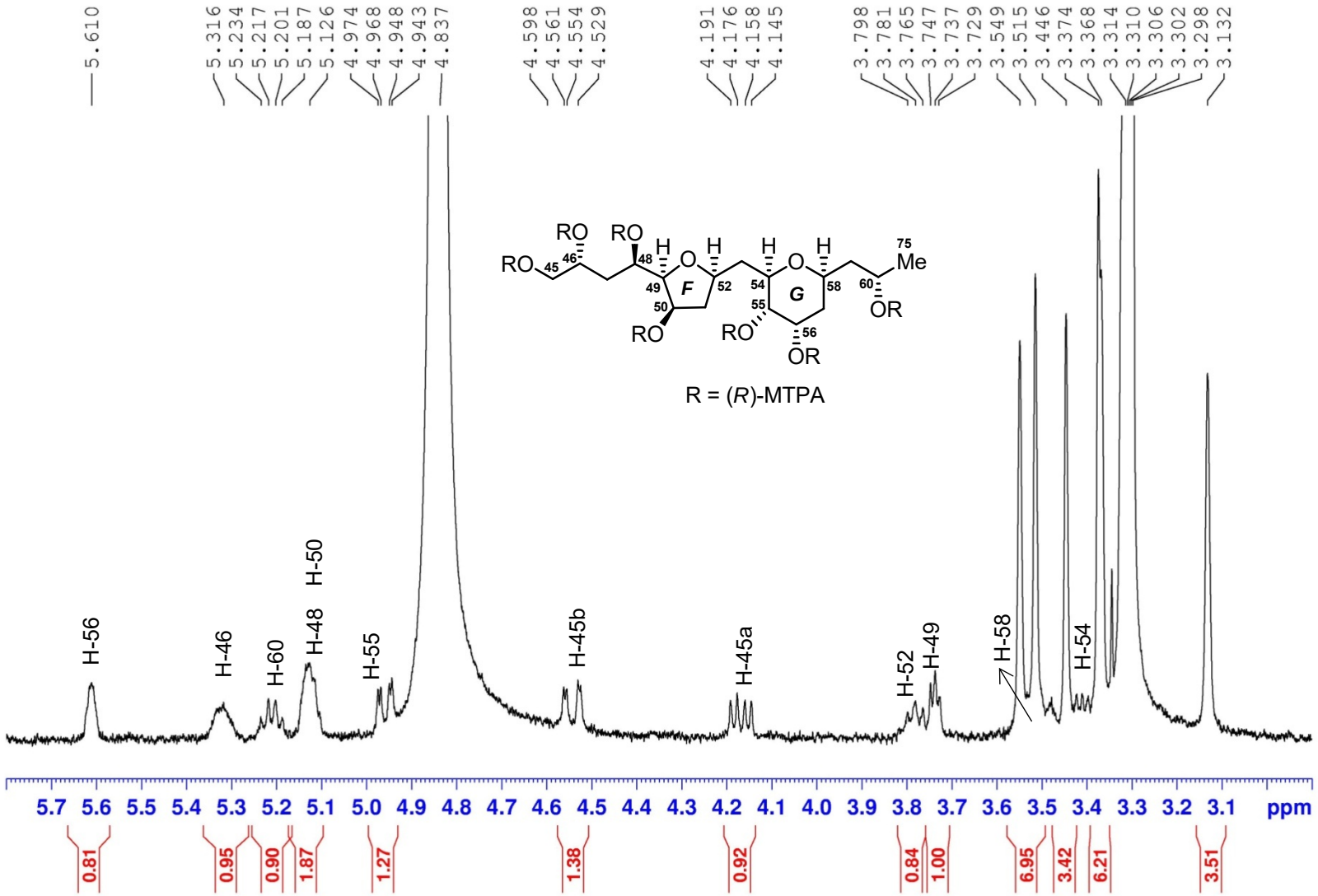

Figure S210. ^{1}H (400 MHz) NMR spectrum of the fragment **1cr** in CD_3OD

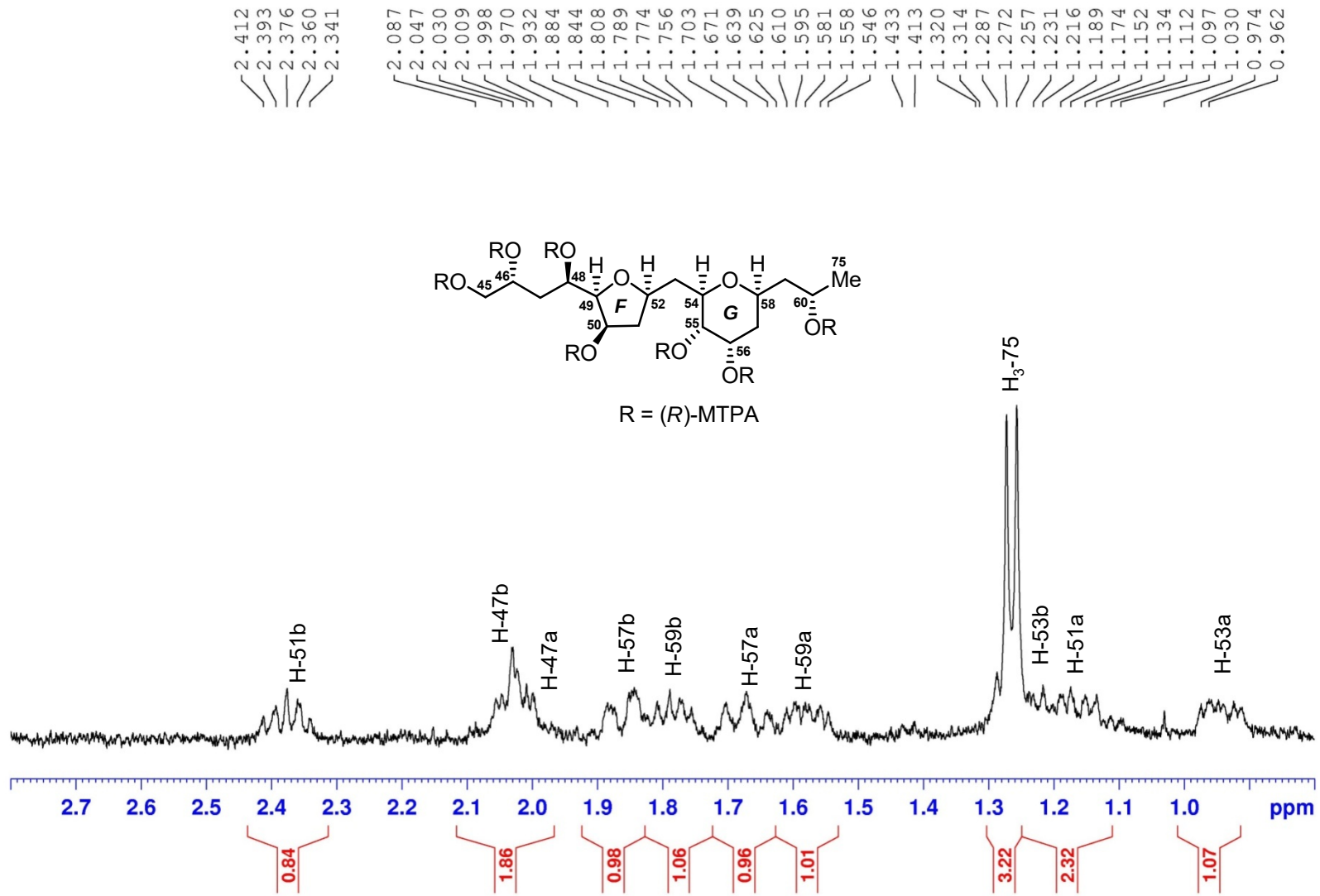

Figure S211. ^{1}H (400 MHz) NMR spectrum of the fragment **1cr** in CD_3OD

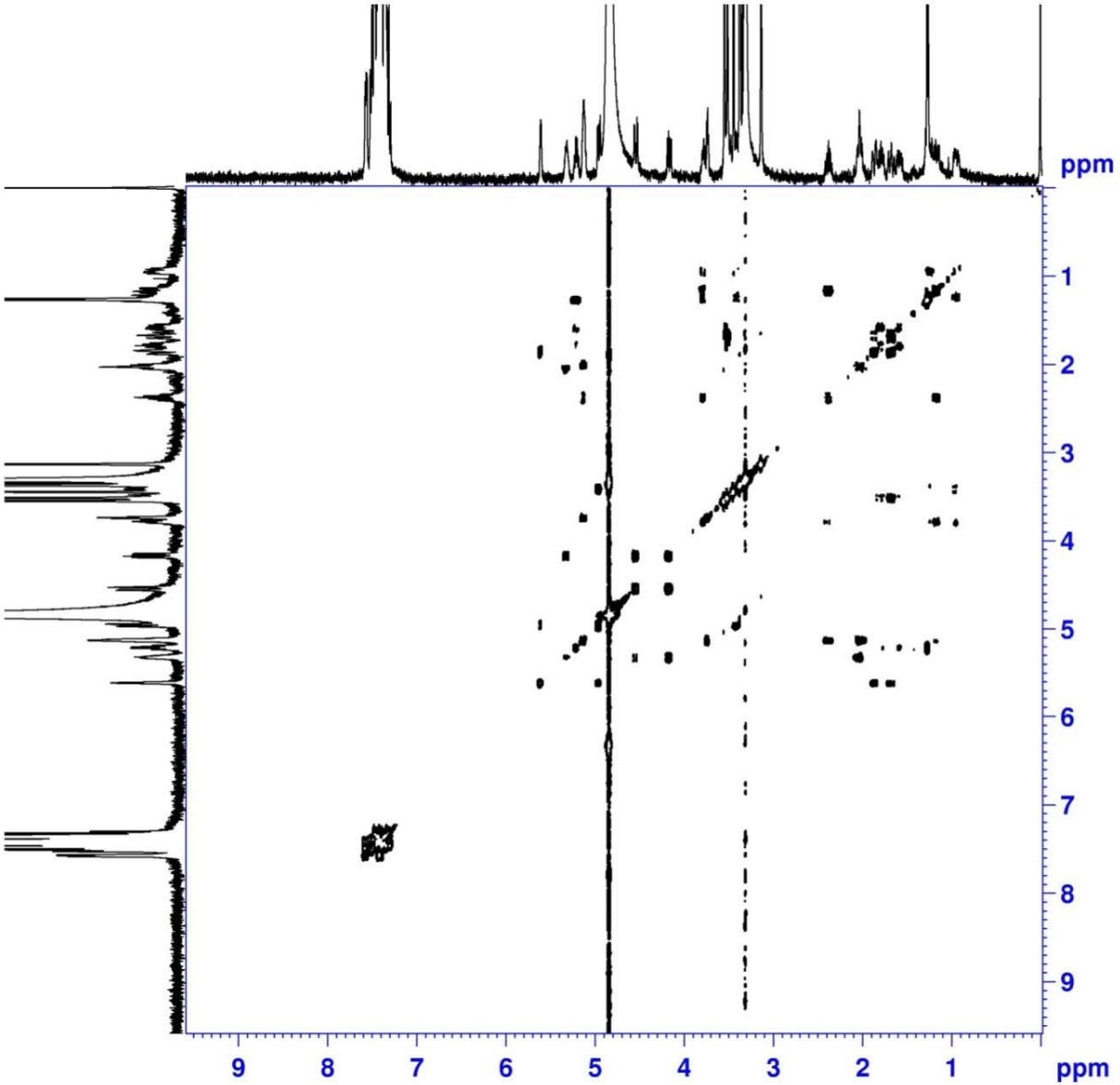

Figure S212. ^{1}H–^{1}H COSY (400 MHz) spectrum of the fragment **1cr** in CD_3OD

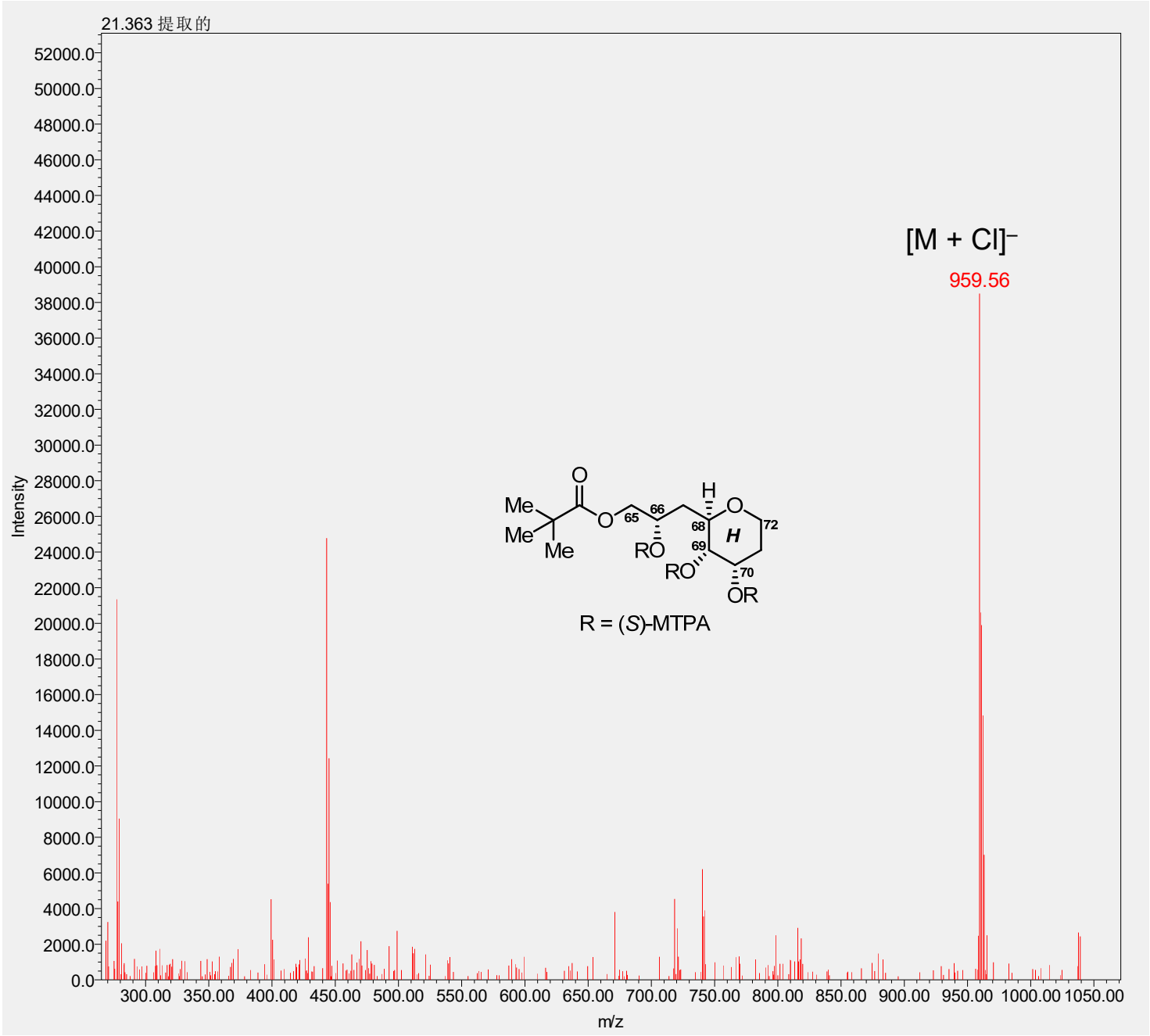

Figure S213. LR-ESIMS for the fragment **1es**

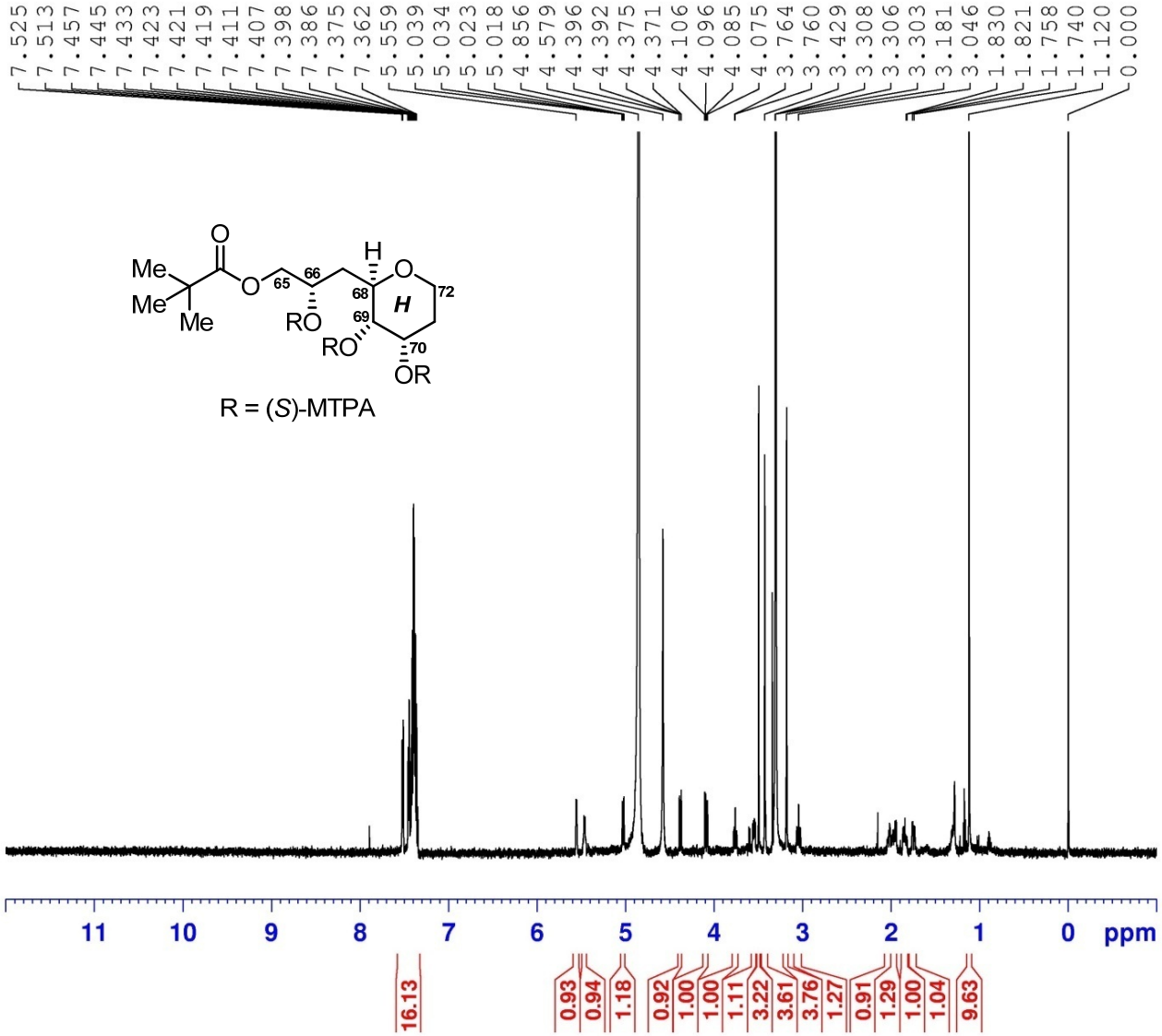

Figure S214. ^{1}H (600 MHz) NMR spectrum of the fragment **1es** in CD_3OD

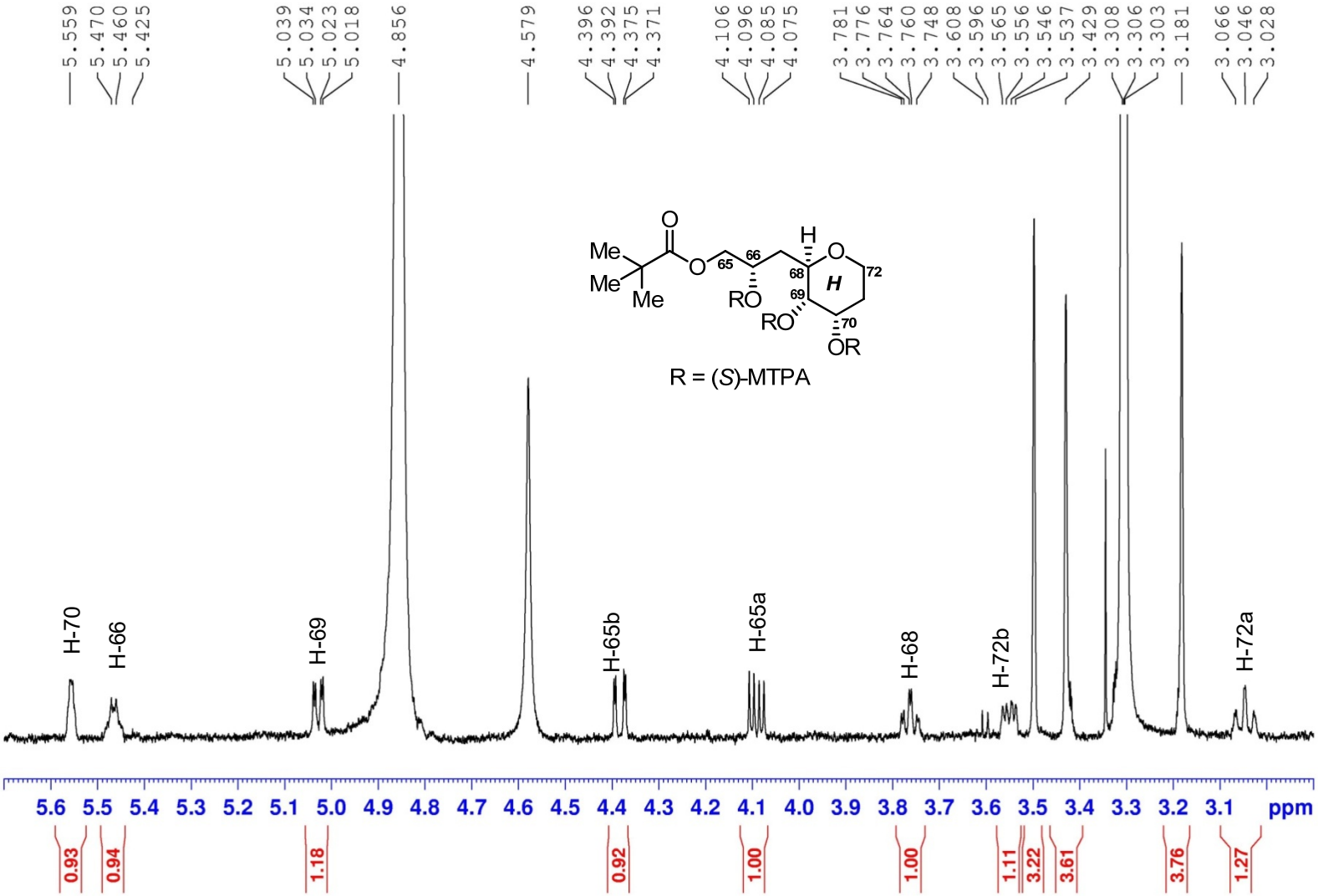

Figure S215. ^{1}H (600 MHz) NMR spectrum of the fragment **1es** in CD_3OD

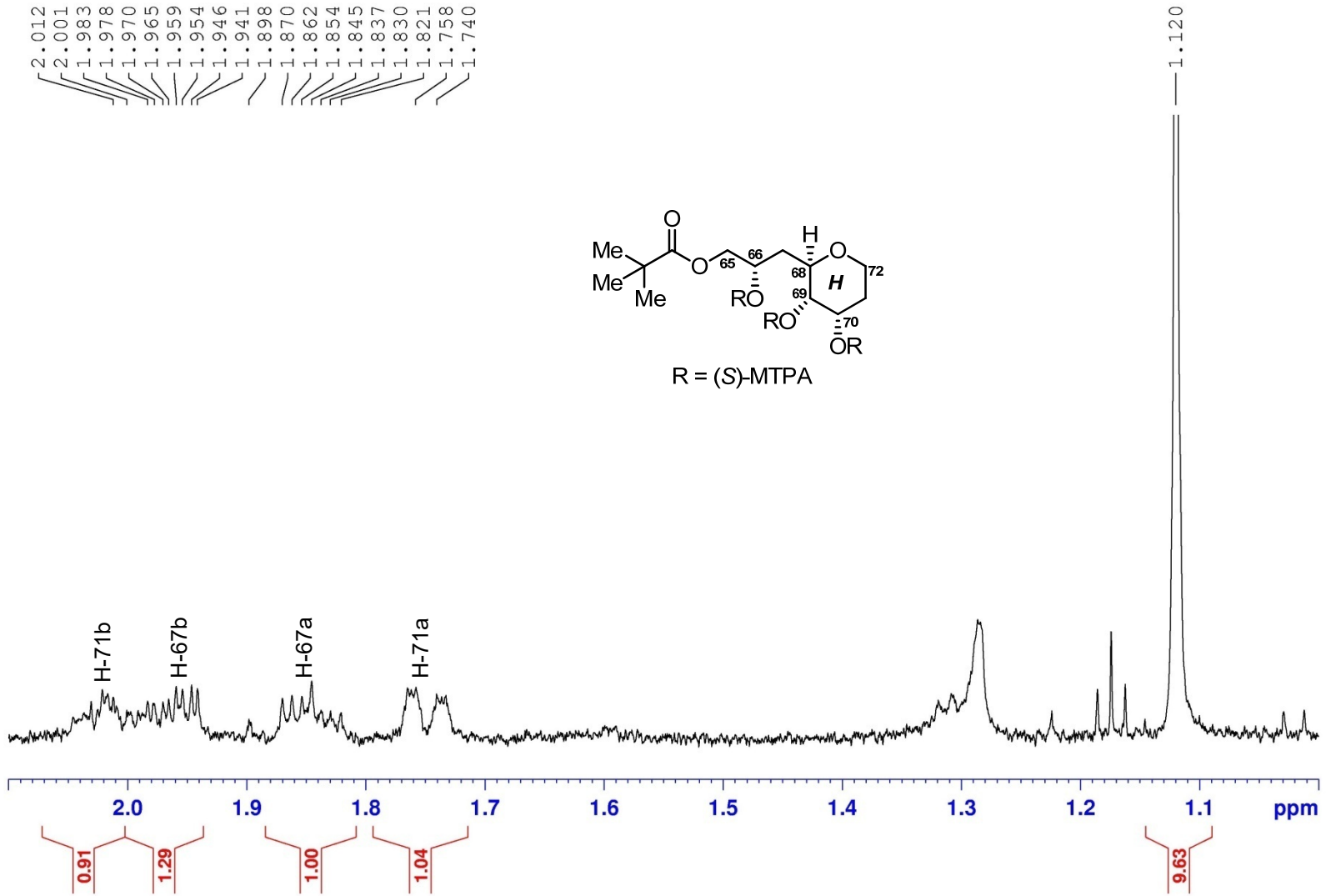

Figure S216. ^{1}H (600 MHz) NMR spectrum of the fragment **1es** in CD_3OD

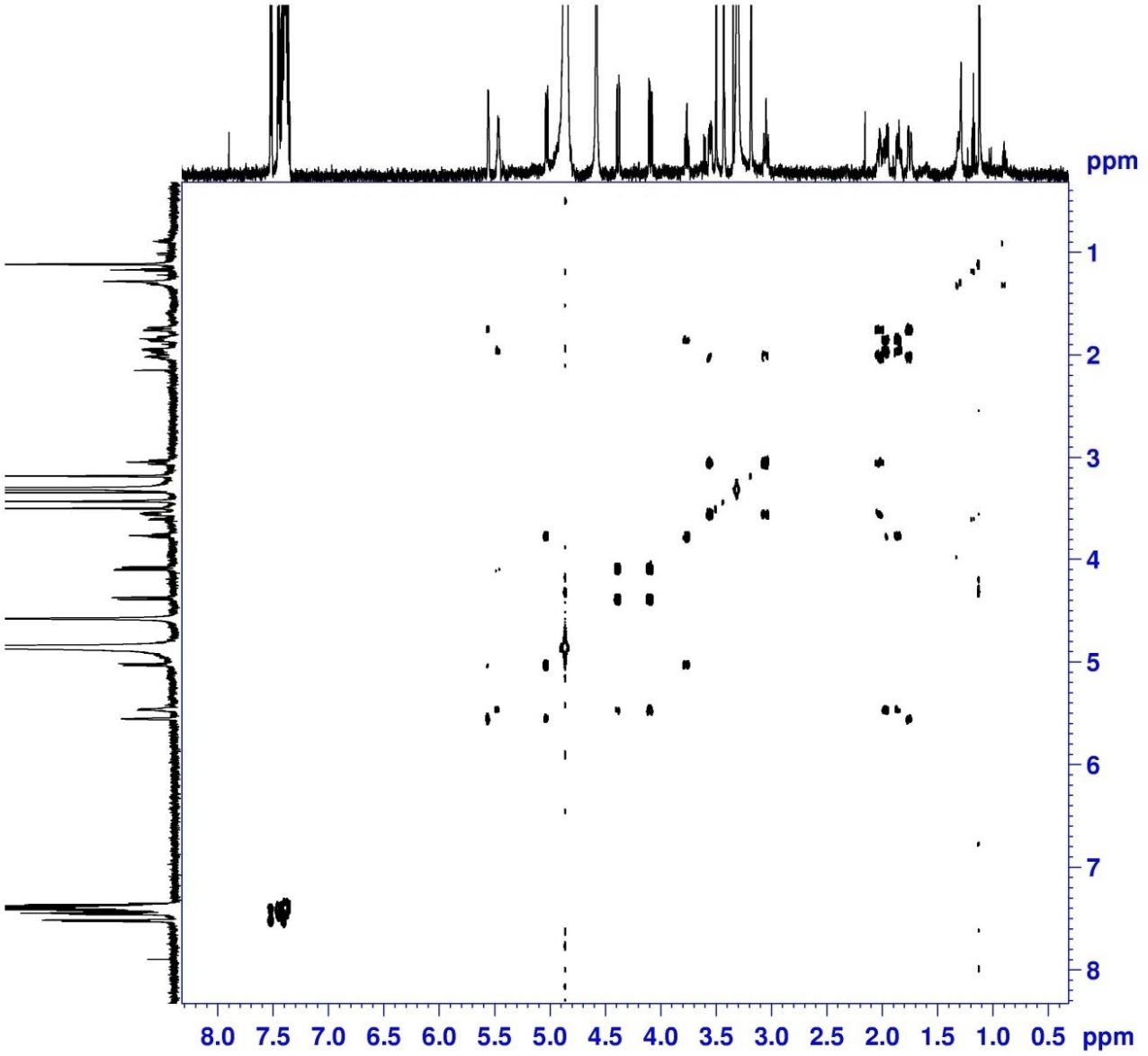

Figure S217. $^{1}H–^{1}H$ COSY (600 MHz) spectrum of the fragment **1es** in CD_3OD

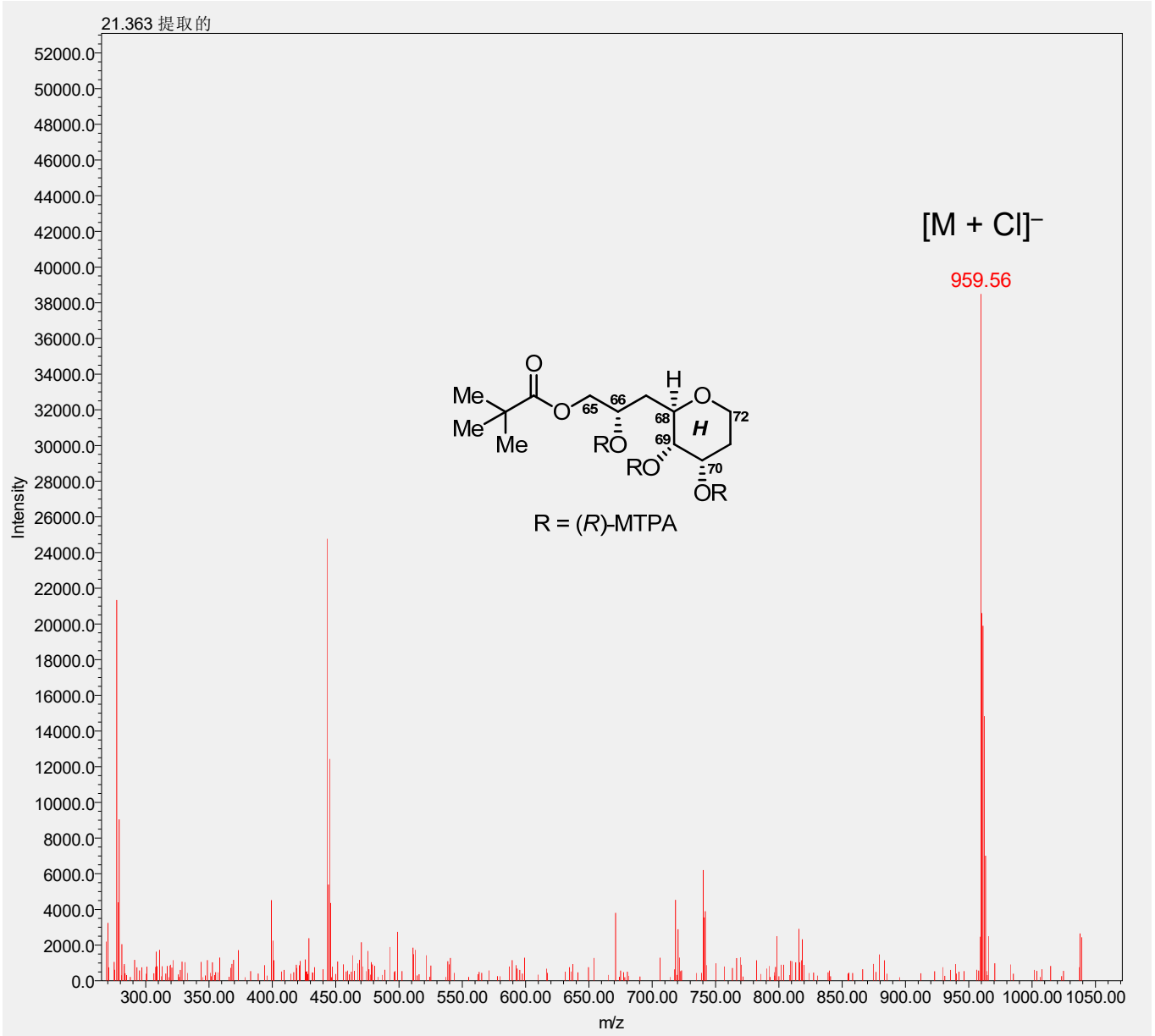

Figure S218. LR-ESIMS for the fragment **1er**

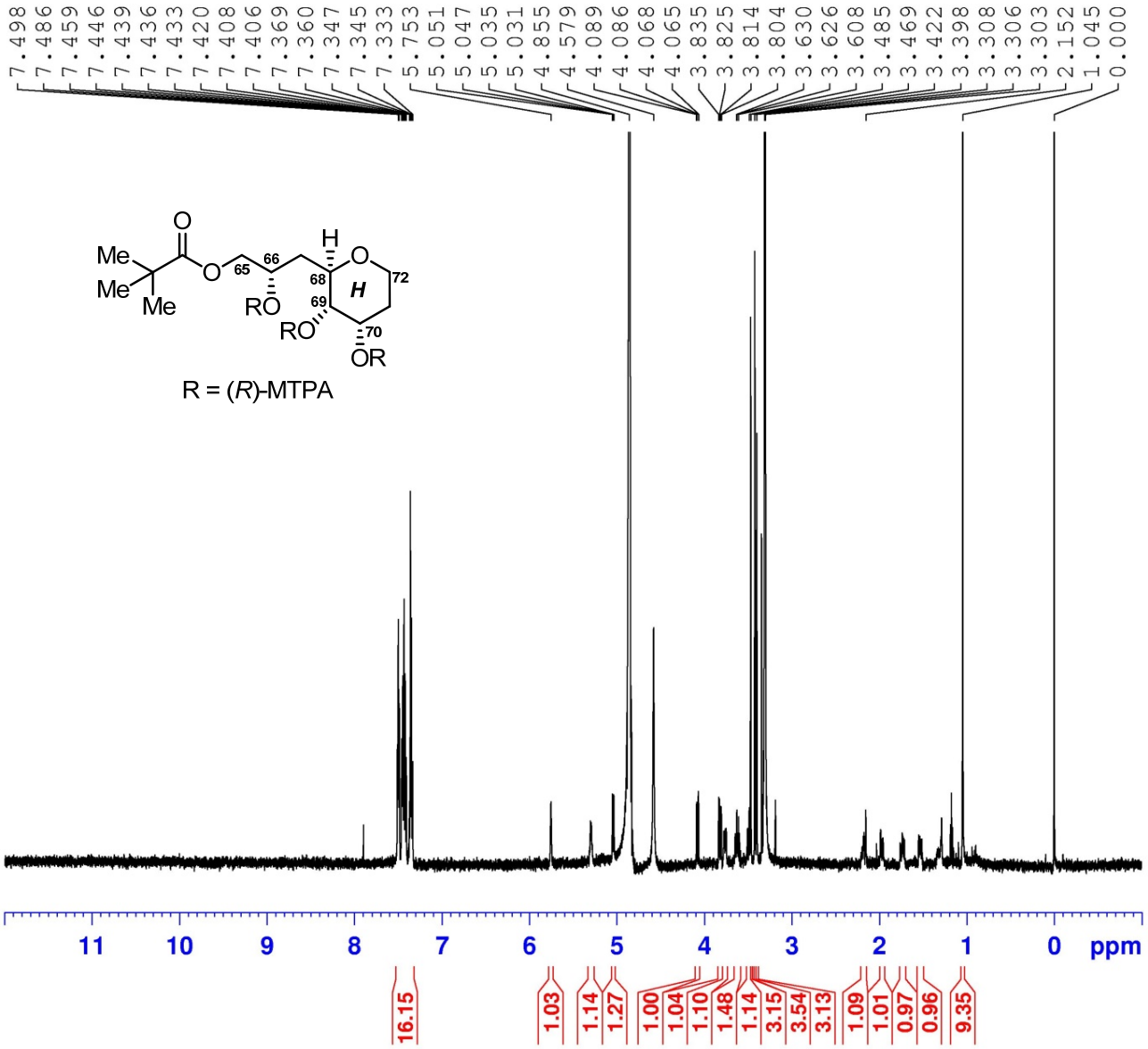

Figure S219. ^{1}H (600 MHz) NMR spectrum of the fragment **1er** in CD_3OD

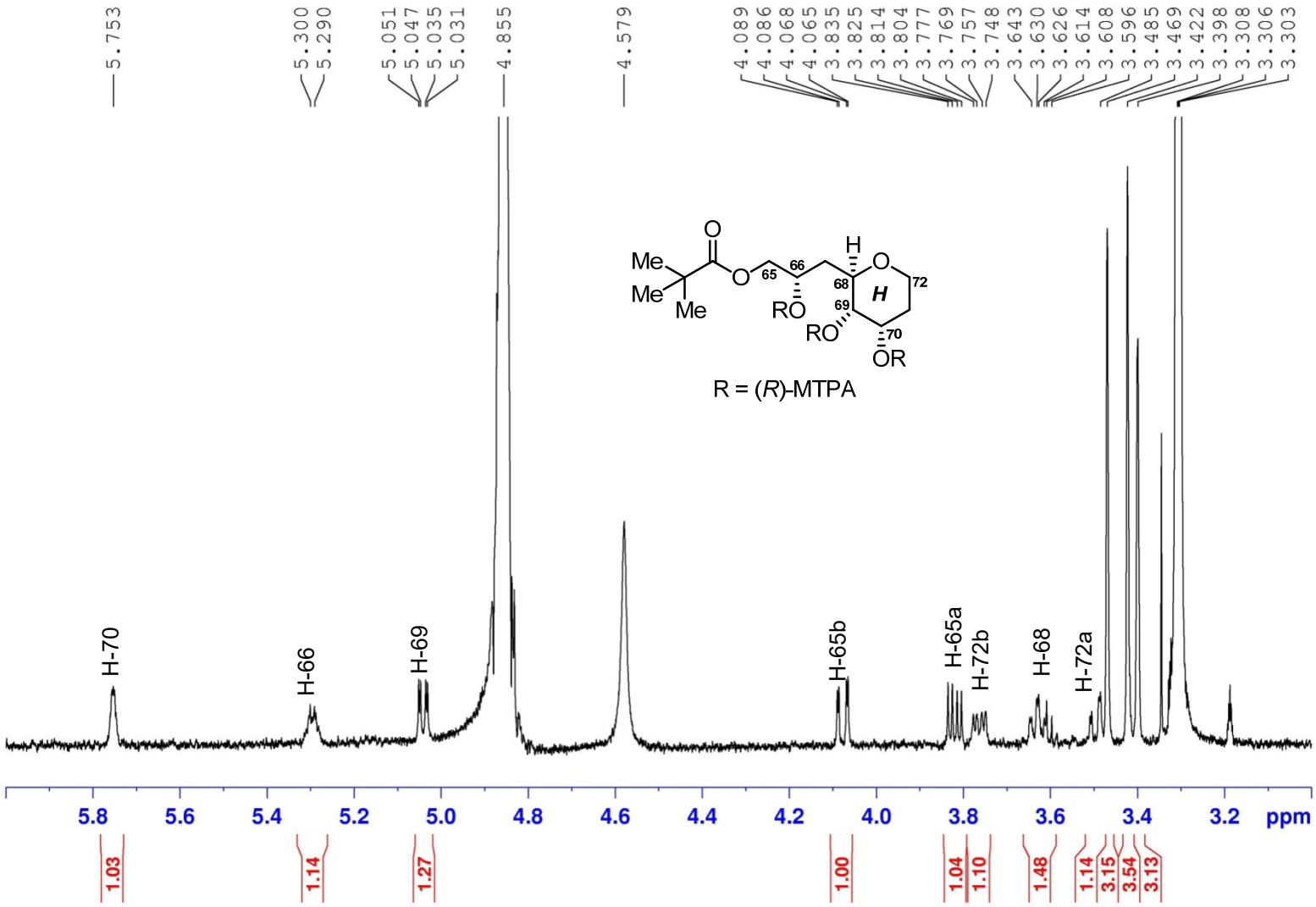

Figure S220. ^{1}H (600 MHz) NMR spectrum of the fragment **1er** in CD_3OD

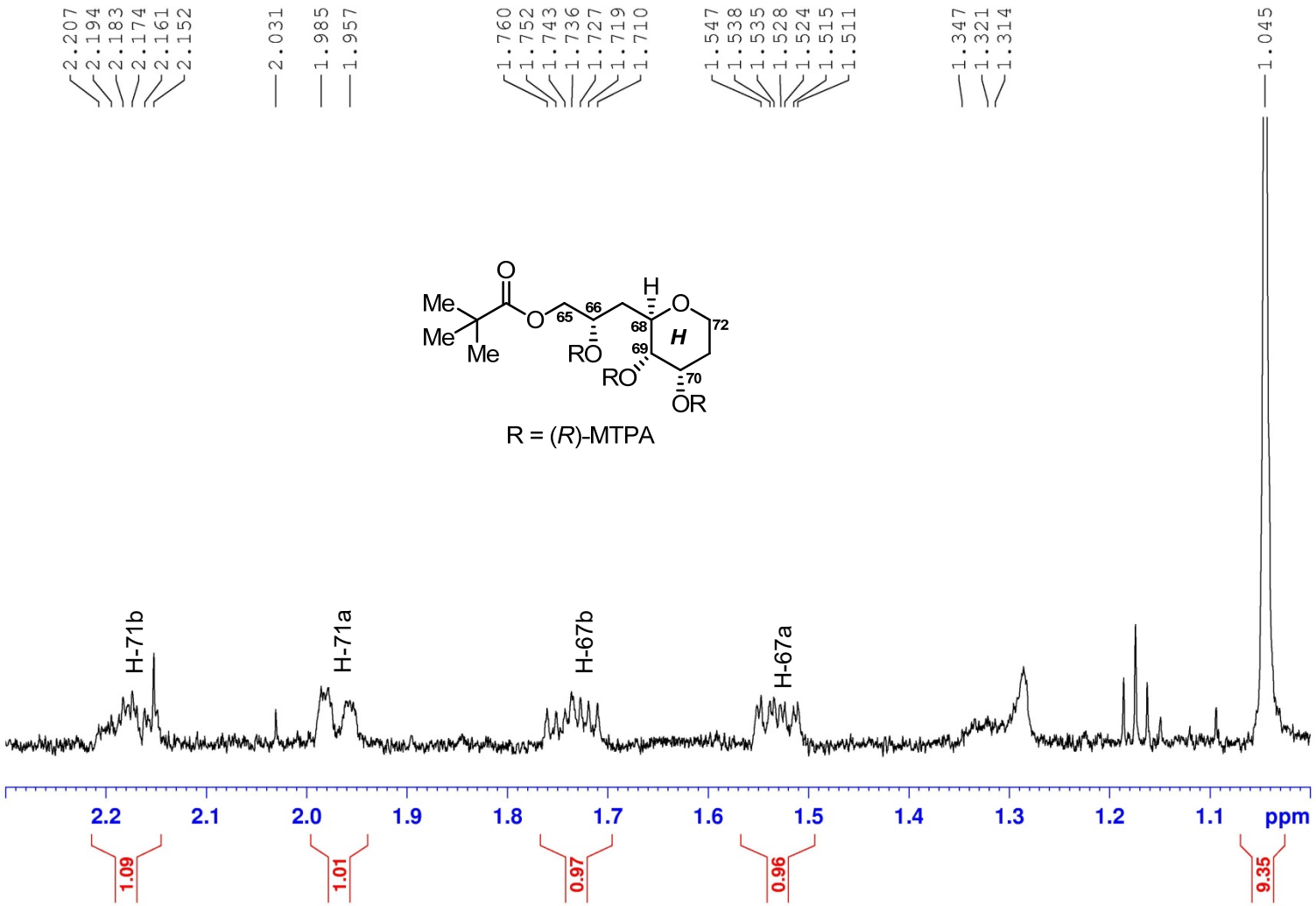

Figure S221. ^{1}H (600 MHz) NMR spectrum of the fragment **1er** in CD_3OD

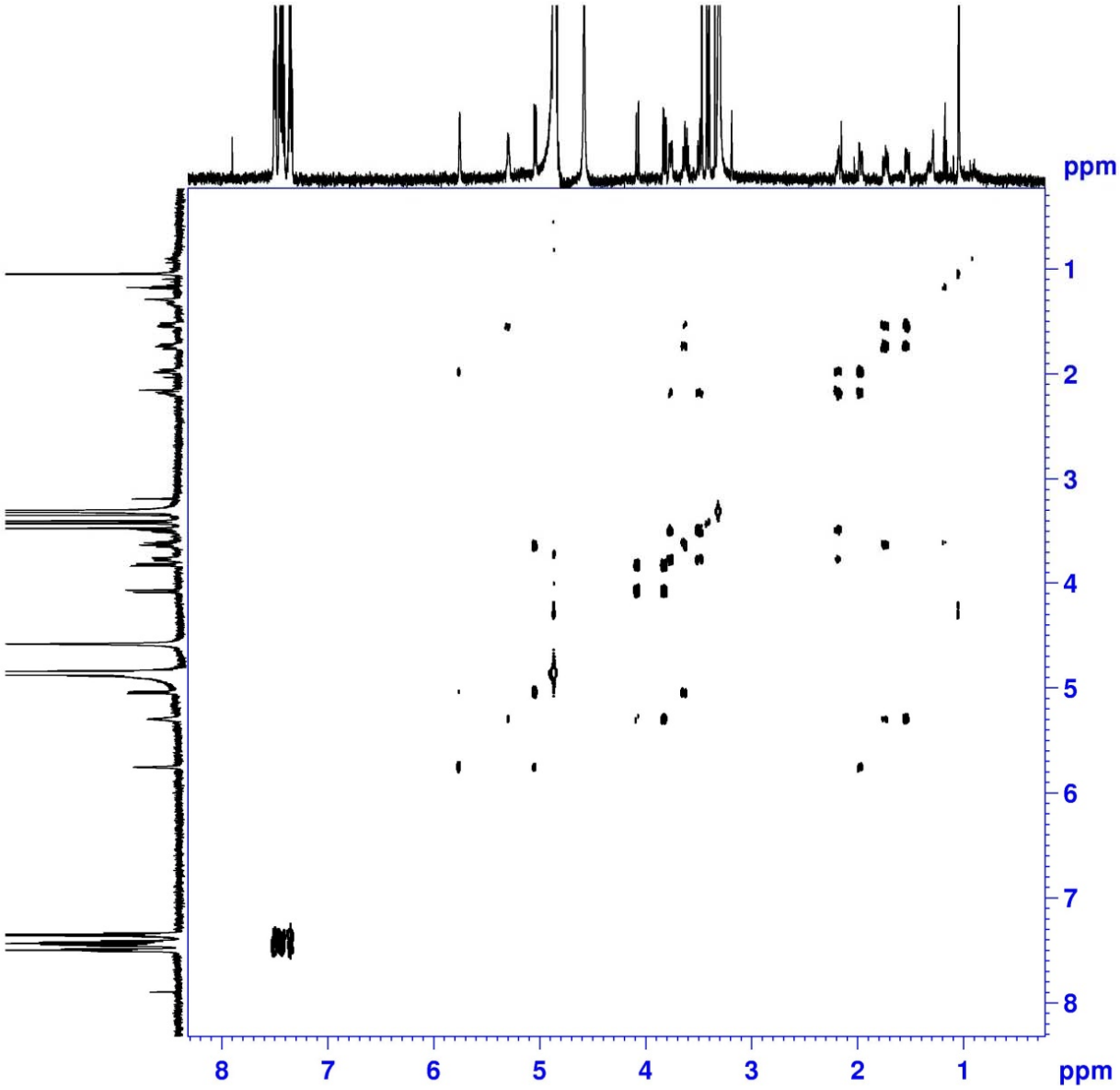

Figure S222. ^{1}H–^{1}H COSY (600 MHz) spectrum of the fragment **1er** in CD_3OD